UNIVERSIDAD COMPLUTENSE DE MADRID

FACULTAD DE FARMACIA
Departamento de Química Orgánica y Farmacéutica

TESIS DOCTORAL

New molecular scaffolds for antineurodegenerative drug discovery

Nuevos esqueletos moleculares para el descubrimiento de fármacos antineurodegenerativos

MEMORIA PARA OPTAR AL GRADO DE DOCTOR

PRESENTADA POR

Matteo Staderini

Directores

José Carlos Menéndez Ramos
Maria Laura Bolognesi

Madrid, 2015

FACULTAD DE FARMACIA
DEPARTAMENTO DE QUÍMICA ORGÁNICA Y FARMACÉUTICA

New molecular scaffolds for anti-neurodegenerative drug discovery

Nuevos esqueletos moleculares para el descubrimiento de fármacos antineurodegenerativos

DOCTORAL THESIS

MATTEO STADERINI

Supervisors: José Carlos Menéndez Ramos
Maria Laura Bolognesi

Madrid, February 2015

Table of contents

List of publications 3
English summary 5
Resumen 11

1. Introduction 17
   1.1. Alzheimer's and prion diseases: two examples of protein misfolding diseases 19
   1.2. Modulation of prion by small molecules: from monovalent to bivalent ligands 22
      1.2.1. Modulators of PPIs: symmetric benzoquinone derivatives 24
      1.2.2. Dimeric acridine and quinoline compounds 26
      1.2.3. GN8, a chemical chaperone 29
   1.3. Theranostics in neurodegenerative diseases 32
   1.4. Imaging of amyloid plaques by near infrared fluorescent tracers 36
      1.4.1. Molecular design for emission in the NIR region 40
      1.4.2. NIR tracers imaging amyloid plaques *in vivo* 46
   1.5. Privileged structures common to neurodegenerative and protozoan disease drugs 54

2. Objectives 57

3. Development of general methods for the functionalization of πa deficient heterocyclic substrates of pharmacological interest 65
   3.1. Introduction 67
   3.2 Amination of π-deficient nitrogen heterocycles under MW irradiation in the presence of phenol 71
   3.3. Lewis acid–catalyzed generation of C-C and C-N bonds on nitrogen heterocycles 79

4. Diketopiperazine baseda ligands of prion protein 93
   4.1. Design rationale 95

4.2. Library synthesis 98
4.3. Screening methodology 106
4.4. Biological activity results and SAR 107
4.5. Modeling studies 111
4.6. Mechanism of action 113

5. Synthesis of GN8 fluorescent analogues and evaluation of their antiprion activity 115
5.1. Synthesis of GN8 and their fluorene and carbazole based analogues 117
5.2. Fluorescence studies 123
5.3. Antiprion activity evaluation in a cell-based model 127
5.4. Fluorescent staining in ScN2A cells 130
5.5. Proposed mechanism of action 133

6. Fluorescent styrylquinolines as innovative therapeutic and diagnostic tools to combat protein misfolding diseases 135
6.1. Styryl compounds to detect and treat amyloid aggregates 137
6.2. A fluorescent styrylquinoline with combined therapeutic and diagnostic activities against Alzheimer's and prion diseases 139
6.2.1. Synthesis of 2-styrylquinolines 139
6.2.2. Native fluorescence study of styrylquinolines 142
6.2.3. Prediction of brain penetration 144
6.2.4. Antiaggregating potency towards Aβ 145
6.2.5. Antiprion evaluation 149
6.2.6. Fluorescent staining of PrP^{Sc} in ScGT1 cells 151
6.3. Second styrylquinoline library 154
6.3.1 Synthetic approaches 154
6.3.2. Preliminary biological evaluation in ScN2a cells 167
6.3.3. Preliminary antiprion assessment *in vitro* by using PMCA 168

7. Hybrid styrylquinolinea polyamine scaffolds 171
7.1. Introduction 173
7.2. Styrylquinolines and polyamines against leishmaniasis 174

7.3. Synthesis of 4-(polyamino)styrylquinoline compounds 178
7.4. Biological study 184
7.5. Synthesis of 8-aminostyrylquinolines 194

8. Nanoparticles as promising tools for the development of theranostics 197
8.1. Introduction 199
8.2. SPION coating and purification 201
8.3. Functionalization of polystyrene NPs with PEG 204
8.4. Synthesis of an analogue of the MSH peptide 206
8.5. Covalent coupling between the specific ligand (MSH) and PEG 207

9. Experimental section 209

10. Conclusions 393

Appendix: Representative spectra 401

List of publications

The work carried out during my doctoral studies has led so far to the following publications:

1. Bolognesi ML, Tran HNA, **Staderini M**, Monaco A, López-Cobeñas A, Bongarzone S, Biarnés X, López-Alvarado P, Cabezas N, Caramelli M, Carloni P, Menéndez JC, Legname G. Discovery of a class of diketopiperazines as antiprion compounds.
   ChemMedChem **2010**, *5*, 1324-1334.
   Front cover of the *ChemMedChem* issue **2010**, *5* (8).

2. **Staderini M**, Cabezas N, Bolognesi ML, Menéndez JC. General protocol for the solvent- and catalyst-free synthesis of 2-styrylquinolines under focused microwave irradiation.
   Synlett, **2011**, *17*, 2577-2579.

3. **Staderini M**, Cabezas N, Bolognesi ML, Menéndez JC. Solvent- and chromatography-free amination of π-deficient nitrogen heterocycles under microwave irradiation. A fast, efficient and green route to 9-aminoacridines, 4-aminoquinolines and 4-aminoquinazolines and its application to the synthesis of the drugs amsacrine and bistacrine.
   Tetrahedron, **2013**, *69*, 1024-1030.

4. González-Ruiz V, **Staderini M**, Bartolini M, Andrisano V, Bolognesi ML, Cabezas N, Menéndez JC, Olives A, Martín MA. Searching for new fluorescent probes to detect beta-amyloid proteins involved in Alzheimer's disease.
   Luminescence, **2012**, 27, 539-540.

5. **Staderini M**, Aulić S, Bartolini M, Tran HNA, González-Ruiz V, Pérez DI, Cabezas N, Martínez A, Martín MA, Andrisano V, Legname G, Menéndez JC, Bolognesi ML. A fluorescent styrylquinoline with combined therapeutic and diagnostic activities against Alzheimer's and prion diseases.
ACS Med. Chem. Lett., **2013**, *4*, 225-229.

6. **Staderini M**, Legname G, Bolognesi ML, Menéndez JC. Modulation of prion by small molecules: from monovalent to bivalent and multivalent ligands.
Curr. Top. Med. Chem. **2013**, *13*, 2491-2503

7. Bongarzone S, **Staderini M,** Bolognesi ML. Multitarget ligands and theranostics: sharpening the medicinal chemistry sword against prion diseases.
Future Med. Chem. **2014**, *6*, 1017-1029.

8. **Staderini M**, Bolognesi ML, Menéndez JC. Lewis acid–catalyzed generation of C-C and C-N bonds on π-deficient heterocyclic substrates.
Adv. Synth. Cat. **2015**, *357*, 185-195.

9. **Staderini M**, Martín MA, Bolognesi ML, Menéndez JC. Imaging of β-amyloid plaques by near infrared fluorescent tracers: A new frontier for chemical neuroscience.
Chem. Soc. Rev. **2015**, *44*, DOI: 10.1039/c4cs00337c.

Summary of the thesis "New molecular scaffolds for anti-neurodegenerative drug discovery"

1. Introduction

Alzheimer's (AD) and prion diseases (PrDs) are characterized by a conformational change of normally expressed proteins that leads to the formation of fibrillar aggregates, causing neuronal damages. In both maladies, amyloid-β protein (Aβ) or cellular prion protein (PrP^{C}), respectively, are converted into β-sheet toxic isoforms termed β-amyloid (Aβ) and scrapie prion protein (PrP^{Sc}) that represent the main neuropathological hallmarks of these protein-misfolding diseases (PMDs) for diagnosis and therapy.

Despite the many advances occurred so far, PrDs and AD remain incurable. However, in the context of PrDs, compounds consisting of two identical moieties joined *via* an appropriate spacer (*i.e.* bivalent compounds) have proved to be effective tools to prevent prion fibril formation. Among them, GN8 is of great importance because for the first time the mechanism of action of an antiprion ligand was clarified.

Another option is the exploitation of theranostics, *i.e.* single agents with concomitant therapeutic and diagnostic properties, with the aim of optimizing the efficacy and safety of therapy. In the field of neurodegenerative diseases, imaging of fibrillar aggregates is particularly suitable to diagnose the onset of these maladies in their early stage and monitor their progression. On the other hand, interference with amyloid fibril formation is well known to have therapeutic implications.

As regard bioimaging techniques, there is a growing interest in fluorescence spectroscopy as non-invasive alternatives for studying fibrillar aggregates. It is

relevant to note that a critical feature for an ideal fluorescent tracer is the ability to absorb and emit light in the near-infrared (NIR) region (600-900 nm), where tissue scattering and absorption is lowest.

Intriguingly, a connection between neurodegenerative and protozoan diseases has been hypothesized due to the fact that several privileged heterocyclic motifs, most notably acridine and quinoline, are particularly recurrent in compounds active against these quite different pathologies.

2. Objectives

In our drug discovery project devoted to the identification of novel scaffolds towards neurodegenerative diseases, the present thesis has the following specific objectives:

1. Development of a general protocol for the amination and (hetero)arylation of halogenated nitrogen heterocycles of importance in the field of neurodegenerative diseases.
2. Building on the bivalent approach, we planned to generate a chemical library of bifunctional molecules focusing on 2,5-diketopiperazine as the central nucleus due to its peptidic nature.
3. Generation a new class of bifunctional carbazole and fluorene GN8-based analogues that, due to their fluorescent properties, offer the potential to act as therapeutic tools and chemical sensors for prion protein.
4. Exploration of fluorescent styrylquinolines designed with the aim of staining amyloid fibrils, and simultaneously blocking their aggregation, acting as theranostic small molecules.
5 We also planned to explore further stryrylquinolines endowed with different polyamino chains to face AD and PrDs. Based on the concept of

privileged structure, we explored this new series of compounds against protozoan diseases.

6. To better explore the theranostic field, we focused our work during the three-month stay required for the European Mention for the Ph. D. title on nanomedicine and nanoparticle chemistry.

3. Results and discussion

The main results obtained are summarized below:

- Focused MW irradiation of equimolecular mixtures of halogenated nitrogen heterocycles with amines in the presence of 2 equiv of phenol allows the synthesis of aminated compounds. Interestingly, replacement of phenol with a catalytic amount of $InCl_3$ led to the development of an efficient, transition metal-free method for aromatic C-N and C-C bond generation.

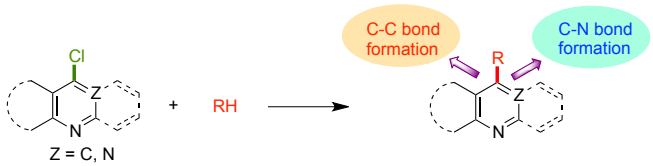

- A library of bifunctional prion ligands was generated by condensing 1,4-diacetyl-2,5-piperazinedione with aromatic aldehydes. The antiprion activity of all these DKPs was evaluated in a cell-based model.

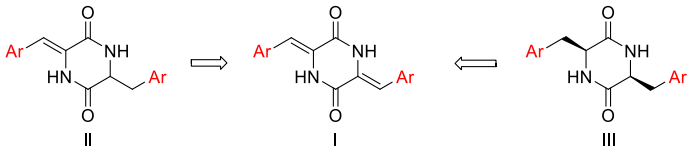

- Fluorene and carbazole-based analogues of GN8 were studied on a cellular model to test their antiprion potency. Their native fluorescence and their possible use to stain fibrillar plaques was also evaluated.

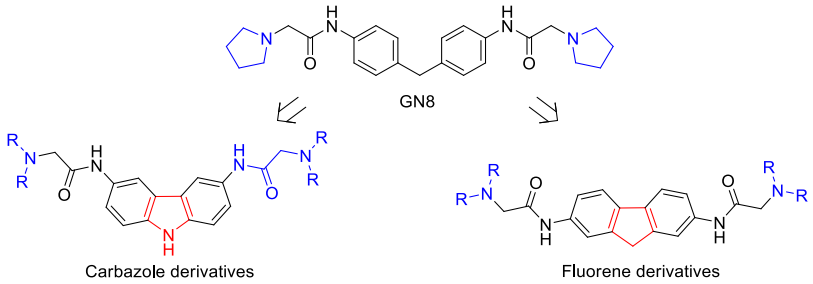

- The styrylquinoline **139** showed an emission maxima above 600 nm, in the NIR region, and was able to stain both Aβ and prion fibrils and to inhibit Aβ self-aggregation and prion replication in infected cells. In the light of these results, we generated a large library of styrylquinoline derivatives to detect, and potentially treat, fibrillar amyloidogenic aggregates. A preliminary screening *in vitro* was carried out to evaluate their antiprion potential.

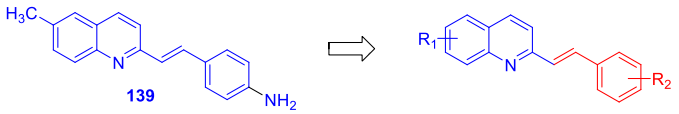

- We designed two new chemical libraries using the styrylquinoline moiety as the central scaffold with polyamino chains at the quinoline C-4 and C-8 positions. We tested the C-4 functionalized compounds against leishmaniasis.

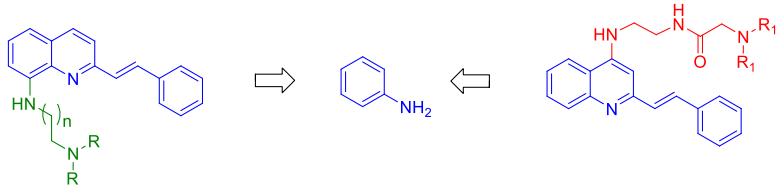

- We prepared polymer-coated magnetite (Fe_3O_4) nanoparticles and conjugated adducts between a peptide that specifically binds a receptor overexpressed on the melanoma cells (MC1R) and PEG.

4. Conclusions

1. We developed two general protocols that solve a long-standing synthetic problem related to the functionalization of heterocyclic frameworks. Besides their application to the objectives of this thesis, these methods will facilitate the generation of compound libraries of great significance in many areas of medicinal chemistry and drug discovery.
2. We identified a DKP compound (**83**) that is able to perturb *in vitro* PrP amyloid fibril formation. Moreover, it has also been shown to inhibit prion replication in a cellular context.
3. Some carbazole compounds turned out to be more active and less toxic that GN8. These compounds, exemplified by **128**, have been shown to interact selectively with PrP^{Sc}, which represents a change in mechanism for preventing prion replication with regard to the reference compound.
4. We showed that the styrylquinoline compound **139** was potentially useful to diagnose, treat and monitor response to therapy in PMDs. Among the additional styrylquinoline derivatives generated, six molecules have a higher antiprion activity than that of **139**, and further studies on these compounds are in progress.
5. 4-(Polyamino)styrylquinolines showed good activity as anti-leishmanial agents, interacting with the parasite mitochondrial metabolism. The polyamino chain was shown to be critical for their activity.
6. With the preparation of coated SPIONs, we paved the way to the final synthetic step that will allow their combination with the targeting ligand (PEG-MSH) to obtain new innovative tools against metastatic melanoma.

Resumen de la tesis "Nuevos esqueletos moleculares para el descubrimiento de fármacos antineurodegenerativos"

1. Introducción

Las enfermedades de Alzheimer (AD) y priónicas (PrDs) se caracterizan por un cambio conformacional de ciertas proteínas que conduce a la formación de agregados fibrilares y causa daños neuronales. En estas enfermedades, la proteína β-amiloide (Aβ) y la proteína priónica celular (PrP^{C}), respectivamente, se transforman en isoformas tóxicas, con un gran predominio de lámina β, que se llaman proteína β-amiloide (Aβ) proteína priónica celular scrapie (PrP^{Sc}), que son las principales características neuropatológicas de estas enfermedades asociadas al plegamiento anómalo de proteínas (PMDs) desde los puntos de vista diagnóstico y terapéutico.

A pesar de los muchos avances registrados, las enfermedades priónicas y de Alzheimer continúan siendo incurables. En el contexto de las enfermedades priónicas, han demostrado ser prometedores los llamados compuestos divalentes, poseedores de dos unidades idénticas enlazadas por un espaciador. Entre ellos, es especialmente importante desde el punto de vista del descubrimiento de fármacos GN8, que fue el primer compuesto para el que se estableció un mecanismo de acción antipriónica.

Otra opción consiste en el desarrollo de agentes teranósticos, es decir, compuestos que poseen simultáneamente propiedades terapéuticas y capacidad de dar lugar a imágenes de las fibrillas proteicas con fines diagnósticos. En el campo de las enfermedades neurodegenerativas, es especialmente importante el diagnóstico temprano.

En relación con las técnicas de imagen, hay cada vez más interés en la fluorimetría como técnica no invasiva de detección de agregados fibrilares. El

marcador fluorescente ideal debería emitir en una region del espectro electromagnético en la que sea mínima la absorción por los tejidos, siendo prometedor en ese sentido el infrarrojo cercano (NIR), entre 600 y 900 nm.

2. Objetivos

Dentro de un proyecto orientado a la identificación de nuevos esqueletos moleculares útiles en el descubrimiento de fármacos para enfermedades neurodegenerativas, esta tesis tiene los siguientes objetivos concretos:

1. Desarrollo de un método general para la aminación y (hetero)arilación de heterociclos halogenados nitrogenados de relevancia en la terapia contra enfermedades neurodegenerativas.
2. Estudio como agentes antipriónicos de una quimioteca de derivados de 2,5-dicetopiperazina, planificada mediante la combinación de la “aproximación divalente" con el empleo de un espaciador peptídico.
3. Síntesis y estudio de quimiotecas de análogos bifuncionales de GN8 con núcleos de carbazol y fluoreno, capaces de inhibir la agregación de los priones y cuya fluorescencia los convierte en marcadores potenciales de los agregados fibrilares.
4. Estudio de los derivados de estirilquinolina como agentes teranósticos potenciales frente a proteína priónica y β-amiloide.
5. Estudio de los derivados de (poliamino)estirilquinolina frente a enfermedades asociadas a plegamientos anómalos de proteínas, así como su estudio frente a enfermedades protozoarias, basada en el concepto de estructuras privilegiadas.
6. Dentro del campo de la teranóstica y durante la estancia conducente a la Mención Europea en el título de doctor se ha hecho un estudio

correspondiente al campo de la nanomedicina, enfocado a la síntesis de nanopartículas para vectorización selectiva de fármacos.

3. Resultados y discusión

Los principales resultados obtenidos se resumen a continuación:

- La irradiación con microondas focalizadas de mezclas equimoleculares de heterociclos halogenados nitrogenados y aminas en presencia de fenol (2 equiv) permite la síntesis de productos de aminación. También se demostró la posibilidad de reemplazar el fenol por un ácido de Lewis ($InCl_3$), lo que condujo a un método general para la generación de enlaces C-N y C-C en ausencia de metales de transición.

- Se sintetizó una quimioteca de ligandos bifuncionales de proteína priónica por doble condensación aldólica de 1,4-diacetil-2,5-piperazinadiona con aldehídos aromáticos. Estos compuestos se evaluaron en un modelo celular.

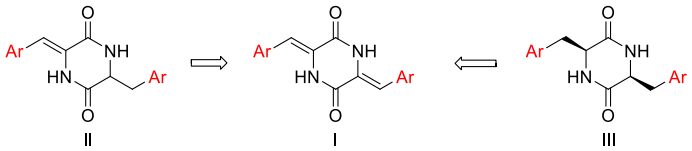

- Se sintetizaron quimiotecas de análogos de GN8 derivados de fluoreno y carbazol y se evaluaron en un modelo cellular para investigar su potencia como agentes antipriónicos. También se estudiaron su fluorescencia nativa y su capacidad de marcar placas fibrilares.

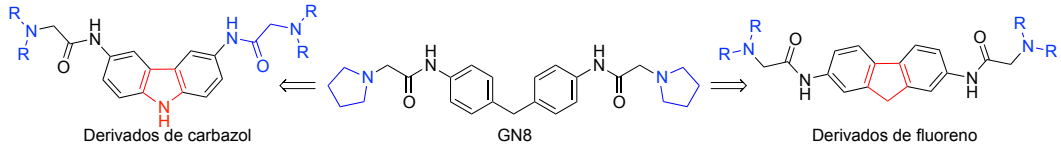

- La estirilquinolina **139** mostró un máximo de emisión fluorescente por encima de 600 nm. Este compuesto es capaz de marcar tanto las fibrillas Aβ como las priónicas y de inhibir la autoagregación de Aβ y la replicación de priones. A la vista de estos resultados, se sintetizó una quimioteca de más de 50 compuestos y se llevó a cabo un ensayo preliminar *in vitro* de su actividad como agentes antipriónicos.

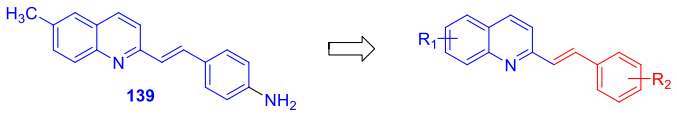

- Se han diseñado quimiotecas de estirilquinolinas portadoras de cadenas de poliamina en C-4 y C-8. Las derivados sustituidos en C-4 se han estudiado como agentes anti-leishmania.

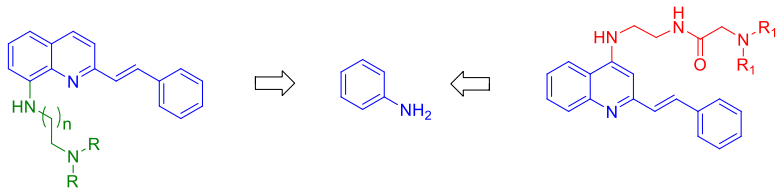

  - Hemos sintetizado nanopartículas de magnetita (Fe_3O_4) recubierta de un polímero, así como sus productos de conjugación con PEG y con péptidos que actúan como ligandos de un receptor sobreexpresado en células de melanoma (MC1R).

4. Conclusiones

1. Hemos desarrollado dos protocolos generales que resuelven un antiguo problema sintético relacionado con la funcionalización de esqueletos heterocíclicos. Estos métodos, además de su aplicación a los objetivos de esta tesis, permitirán la generación de quimiotecas de interés en muchas áreas de la química farmacéutica y el descubrimiento de fármacos.

2. Hemos descubierto un derivado de dicetopiperazina (compuesto **83**) que presenta una buena capacidad de interferir el proceso de formación de fibrillas amiloides priónicas *in vitro*. Además, este compuesto es activo en ensayos celulares.
3. Algunos de los derivados bifuncionales portadores de anillos de carbazol han resultado ser más activos y menos tóxicos que GN8. El estudio mecanístico de estos compuestos, llevado a cabo en **128**, ha demostrado que interaccionan selectivamente con la proteína PrP^{Sc}, lo que supone un cambio de mecanismo respecto al compuesto de referencia.
4. Hemos descubierto un derivado de estirilquinolina (compuesto **139**) con utilidad potencial para el diagnóstico, tratamiento y monitorización de la respuesta a la terapia de PMDs. De entre una amplia quimioteca de estirilquinolinas, al menos 6 moléculas presentan una actividad antipriónica superior a la de **139**, y algunos de estos compuestos continúan en estudio.
5. Algunos derivados de 4-(poliamino)estirilquinolina muestran buena actividad como agentes anti-leishmania, y actúan por interferencia con el metabolismo mitochondrial del parásito. Se ha demostrado que la cadena de poliamina es crucial para esta actividad.
6. Se ha logrado la preparación de nanopartículas magnéticas (SPIONs) y del conjugado PEG-MSH, lo que permitirá en el futuro el estudio de nuevos agentes de distribución selectiva para el tratamiento del melanoma.

1. Introduction

1.1. Alzheimer's and prion diseases: two examples of protein misfolding diseases

In the last decades protein misfolding diseases (PMDs), characterized by the structural change of normally expressed proteins to amyloidogenic conformations, have come to public and scientific attention due to the fact that they are increasing enormously in developed countries and becoming a serious problem in terms of health and economic costs.[1] Alzheimer's disease (AD), prion diseases (PrDs), Parkinson's disease (PD) and amyotrophic lateral sclerosis are prominent examples of PMDs, in which the misfolded proteins are responsible for the neurodegeneration.

Among them, AD is the most common type of dementia, characterized by a progressive cognitive decline and loss of the ability to learn, reason and communicate. One of the main hallmarks of AD is the formation and accumulation of fibrillar aggregates known as β-amyloid (Aβ) plaques that lead to neuronal death and to the disruption of memory. These amyloidogenic deposits consist mainly of two peptides, $A\beta_{40}$ and $A\beta_{42}$, resulting from the proteolytic cleavage of the transmembrane glycoprotein amyloid precursor protein (APP). Aβ peptides are rich in β-sheet secondary structures, which are insoluble and resistant to proteolytic digestion and tend to aggregate in plaques.[2]

On the other hand, prion diseases (PrDs) or transmissible spongiform encephalopathies (TSEs), are a family of neurological disorders that include Creutzfeldt-Jakob disease (CJD) and Gerstmann-Sträussler-Scheinker disease (GSS) in humans, chronic wasting disease in deer, and scrapie in sheep.[3,4]

1 Chiti, F.; Dobson, C. M. *Annu. Rev. Biochem.* **2006**, *75*, 333.
2 Mucke, L.; Selkoe, D. J. *Cold Spring Harb. Perspect. Med*. **2012**, *2*, a006338.
3 Aguzzi, A. *J. Neurochem*. **2006**, *97*, 1726.

Although CJD is a rare human malady, it affects approximately one in one million people worldwide and invariably proves fatal.[4]

Scientific and public interest in PrDs has increased dramatically in recent years, transforming them from rare, enigmatic infectious diseases to a sort of emblem of neurodegeneration.[5] Initially, what made them so unique and fascinating to scientists was the growing understanding that the infectious agent responsible for PrDs was different from conventional microorganisms.[6] Over the years, many discoveries provided compelling evidence in favor of Prusiner's revolutionary *prion only hypothesis*, *i.e.* that a misfolded protein is the main (and perhaps the sole) component of the prion infectious agent.[7] In PrDs, the key pathological event is a conformational change of the normally expressed protein, known as cellular prion protein (PrP^{C}), into its abnormal amyloidogenic isoform, the scrapie prion protein (PrP^{Sc}) which features the same characteristics of Aβ including insolubility, resistance to proteolytic digestion and a high content of β-sheet secondary structures.[8,9] Through an autocatalytic replication process, PrP^{Sc} accumulates in proteinaceous aggregates, resulting in the diffuse neuronal degeneration and the spongiform brain lesions typical of the disease.[10] Although the exact molecular mechanism of PrP^{C} to PrP^{Sc} conversion is still not clear, it has been proposed that the misfolded PrP^{Sc} acts as a template that induces the normally folded proteins to change their conformation (Figure 1.1).[11]

4 Collinge J. *Annu. Rev. Neurosci.* **2001**, *24*, 519.
5 Legname, G.; Bolognesi, M. L.*Curr. Top. Med. Chem.* **2013**, *13*, 2395.
6 Soto C. *Trends Biochem. Sci.* **2011**, *36*, 151.
7 Prusiner, S. B. *Proc. Natl. Acad. Sci. U. S. A.* **1998**, *95*, 13363.
8 Kovacs, G. G.; Budka, H.*Am. J. Pathol.* **2008**, *172*, 555.
9 Lloyd, S.; Mead, S.; Collinge, J. *Top. Curr. Chem.* **2011**, *305*, 1.
10 Aguzzi, A.; Calella, A. M. *Physiol. Rev.* **2009**, *89*, 1105.
11 Aguzzi, A.; Steele, A. D. *Cell* **2009**, *137*, 994.

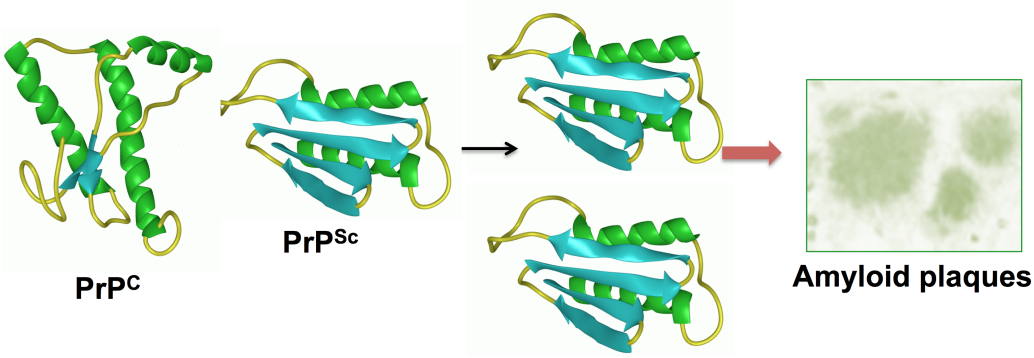

Figure 1.1. The scrapie prion protein (PrP^{Sc}) acts as a template for the misfolding of the normal cellular PrP^{C}

Recent studies suggest that Aβ and α-synuclein proteins, involved in AD and PD, respectively, could also have a prion-like mechanism of propagation.[12,13] On the basis of these findings, Prusiner claimed that proteins causing neurodegeneration are all prions, in the sense that folded and aggregated molecules are able to catalyze the transformation of normal proteins and thus propagate the disease.[14] If confirmed, this hypothesis would profoundly influence the development of therapeutic tools. Nevertheless, Prusiner's hypothesis seems to be somewhat premature and it has been pointed out that, at least in the case of AD, it ignores a great deal of evidence about the etiology of this disorder.[15]

12 Frost, B.; Diamond, M. I. *Nat. Rev. Neurosci.* **2010**, *11*, 155.
13 Miller, G. *Science* **2009**, *326*, 1137.
14 Prusiner, S. B. *Science* **2012**, *336*, 1511.
15 Lahiri, D. K. *Science* **2012**, *337*, 1172.

1.2. Modulation of prion by small molecules: from monovalent to bivalent ligands

As mentioned above, PrP^{Sc} plays a pivotal role in the onset and propagation of PrDs.[6]

Several reports have suggested that small molecules that directly target the proteins involved in the fibrillization process represent valid therapeutic tools against prion replication.[16] In this regard, drug discovery approaches that have been widely employed consisted in developing molecules able to interfere with protein-protein interactions (PPIs) between PrP^{Sc} and PrP^{C}, to avoid prion propagation, or to directly prevent fibril formation.[17] On the other hand, the modulation of these PPIs using small molecules is currently regarded as very challenging, for several reasons:

(i) It does not present defined active sites or pockets as in the case of enzymes and receptors, since in PPIs large and extended surfaces are involved, and a complex network of weak interactions takes place.[18]

(ii) High-resolution structural information on amyloid fibrils and aggregates is very scarce. This is mostly due to the inability of crystallography and NMR to address proteins that are by nature insoluble and non-crystalline. Furthermore, characterization of the transient states of such proteins remains challenging because these techniques are not even suitable for studying short-lived protein states.[17]

16 Trevitt, C. R.; Collinge, J. *Brain* **2006**, *129*, 2241.
17 Gavrin, L. K.; Denny, R. A.; Saiah, E. *J. Med. Chem.* **2012**, *55*, 10823.
18 Kranjc, A.; Bongarzone, S.; Rossetti, G.; Biarnés, X.; Cavalli, A.; Bolognesi, M. L.; Roberti, M.; Legname, G.; Carloni, P. *J. Chem. Theory Comput*. **2009**, *5*, 2565.

Based on these considerations, it clearly emerges that the rational design of antiprion compounds represents a big challenge for medicinal chemists. However, considering the oligomeric and repetitive structure of fibrillar aggregates, it has been deemed convincible that bivalent molecules, endowed with two identical protein recognition motifs (PRMs) connected by a spacer, could interact simultaneously with two prion binding surfaces (hot spots), which are regions of the protein that contribute a disproportionate percentage of the binding energy and can serve as crucial point for chemical intervention.[19] The protein recognition motifs can, at least initially, be designed from the structure of known prion inhibitors (Figure 1.2).

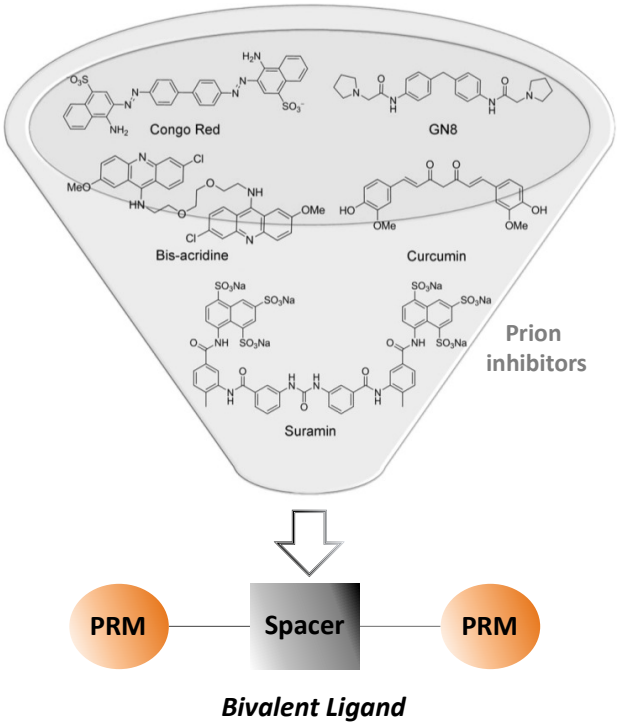

Figure 1.2. Design strategy leading to bifunctional derivatives able to modulate PPIs in PrDs

19 Xu, Y.; Shi, J.; Yamamoto, N.; Moss, J. A.; Vogt, P. K.; Janda, K. D. *Bioorg. Med. Chem.***2006**, *14*, 2660.

The synergy between two PRMs connected by a spacer is due to two factors:

(i) An increase in the local concentration of the active moiety.

(ii) Since a bivalent ligand must first undergo univalent binding, in this bound-state the binding of the second pharmacophore to a neighboring recognition site is favored owing to entropic factors.[20]

This type of binding allows achieving a higher potency and enhancing significantly the recognition process.[21] In the light of the considerations outlined above, many libraries of bifunctional molecules have been generated by synthetic approaches in order to identify novel ligands to combat PrDs. The most relevant ones will be reviewed in the following Sections.

1.2.1. Modulators of PPIs: benzoquinone derivatives

Several lines of evidences suggest that lipophilic and aromatic residues able to provide van der Waals and π–π stacking interactions, connected by a central core, might modulate PPIs. With this in mind, Bolognesi et al. developed a small library of bivalent ligands by attaching seven amino acids methyl esters to two different 2,5-bis-diaminobenzoquinone (BQ, Figure 1.2).[22,] The choice of the BQ system as the central spacer was motivated by the fact that it is a planar system that should be able to interfere, through hydrophobic interactions, with the aromatic residues involved in the fibril formation. Furthermore, BQ derivatives have been demonstrated to be able to bind Aβ and interfere with the native

20 Portoghese, P. S. *J. Med. Chem.***2001**, *44*, 2259.

21 **Staderini, M.**; Legname, G.; Bolognesi, M. L.; Menéndez, J. C. *Curr. Top. Med. Chem.* **2013**, *13*, 2491.

22 Tran, H. N. A.; Bongarzone, S.; Carloni, P.; Legname, G.; Bolognesi, M. L. *Bioorg. Med. Chem. Lett*. **2010**, *20*, 1866.

ability of Aβ to self-assemble by disrupting PPIs.[23] On the other hand, aromatic amino acid fragments, such as Trp, Phe and Tyr, could act as PRMs and promote the molecular recognition process providing hydrogen bonds, van der Waals and π-π stacking interactions. As expected, in a prion cell culture model the phenylalanine derivatives **BQ-1** and **BQ-2** (Figure 1.3) showed the best anti-prion activity, displaying EC_{50} values of 0.9 and 3.6 μM, respectively. In addition, a chemoinformatic analysis confirmed that a BQ central scaffold connected to two aromatic rings is a suitable motif for designing novel antiprion compounds.

Considering the BQ nucleus as particularly suitable for perturbing PPIs, the same authors developed a further series of bivalent ligands.[24] Thus, two active terminal moieties were attached at the positions 2 and 5 of the central BQ core through proper linkers. As PRMs acridine, quinoline, and 1,2,3,4-tetrahydroacridine systems were chosen due to the fact that these aromatic heterocycles had been shown to have anti-prion potential.[25] On the other hand, three different polyamine chains linkers were selected to explore different lengths and chemical compositions.[24] Compounds **BQ-3** – **BQ-6** (Figure 1.2) showed remarkably potency against prion replication in cell culture, with EC_{50} values ranging from 0.2 to 0.7 μM. The obtained results suggested that a specific length of the linker and the presence of a chlorine atom on the terminal residues are critical for the anti-prion activity. Furthermore, to elucidate the mechanism of action of these ligands, the capability of inhibiting prion fibril formation was studied *in vitro* by using an amyloid seeding assay (ASA).[26] Interestingly, only **BQ-**

23 Bartolini, M.; Bertucci, C.; Bolognesi, M. L.; Cavalli, A.; Melchiorre, C.; Andrisano, V. *ChemBioChem* **2007**, *8*, 2152.

24 Bongarzone, S.; Tran, H. N. A.; Cavalli, A.; Roberti, M.; Carloni, P.; Legname, G.; Bolognesi, M. L. *J. Med. Chem.* **2010**, *53*, 8197.

25 Bongarzone, S.; Bolognesi M. L. *Expert Opin. Drug Discov*. **2011**, *6*, 251.

26 Colby, D. W.; Zhang, Q.; Wang, S.; Groth, D.; Legname, G.; Riesner, D.; Prusiner, S. B. *Proc. Natl. Acad. Sci. USA* **2007**, *104*, 20914.

4 and **BQ-6** delayed fibril formation, and it was proposed that the active molecules probably interact with the recombinant PrP^{C} and avoid its folding into PrP^{Sc}.

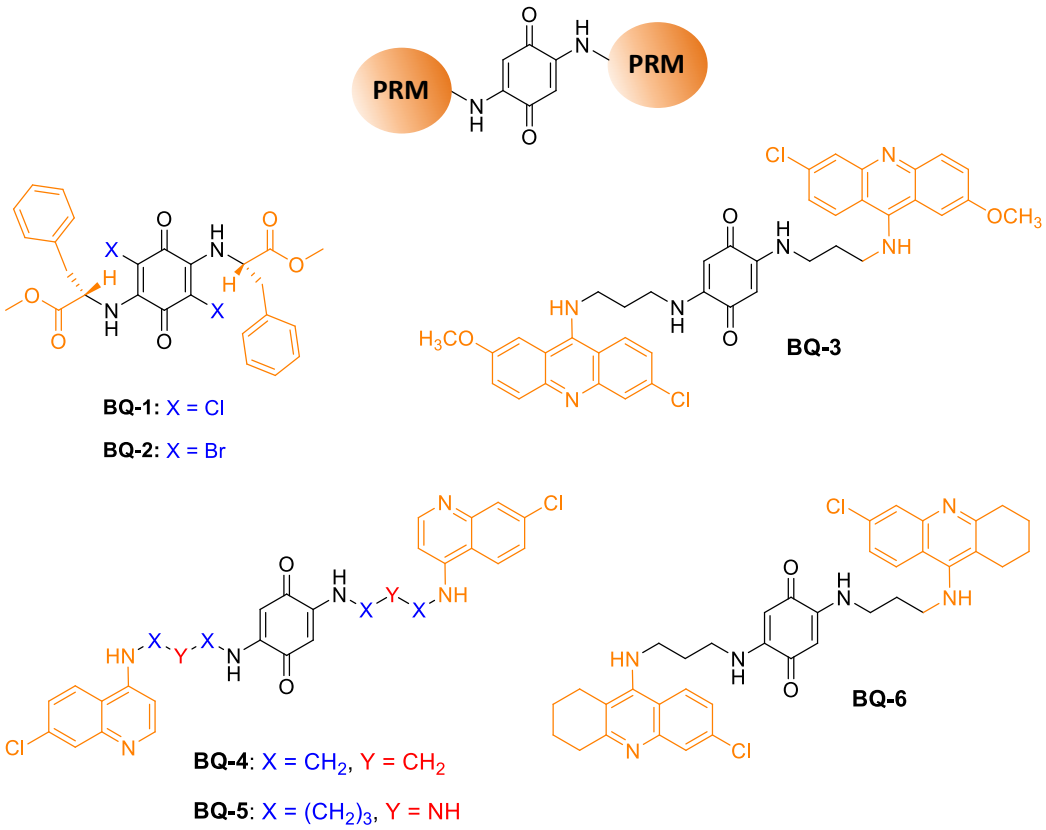

Figure 1.3. Chemical structure of benzoquinone-based (**BQ-1** -**BQ-6**) bivalent ligands.

1.2.2. Dimeric acridine and quinoline compounds

Quinacrine, an acridine-based compound, is a well-known antimalarial drug. Interestingly, quinacrine and its analogues were found to inhibit PrP^{Sc} formation in cell cultures.[27,28] In addition, due to its good pharmacokinetic properties, low

27 Korth, C.; May, B. C. H.; Cohen, F. E.; Prusiner, S. B. *Proc. Natl. Acad. Sci. U. S. A.* **2001**, *98*, 9836.

toxicity and ability to cross the BBB, its efficacy and safety were explored *in vivo*.[29] In an effort to shed some light on the mechanism of action of these derivatives, Vogtherr *et al.* used nuclear magnetic resonance (NMR) to map the binding site of quinacrine to recombinant human prion protein. Although the precise mechanism by which quinacrine hinders the conversion of PrP^{C} into the scrapie pathogenic form remains unclear, the identification of its binding site influenced profoundly the development of new strategies to combat PrDs.[30]

Considering the propensity of PrP^{Sc} to assemble into multimers, May and co-workers envisaged that dimers of quinacrine could be more potent inhibitors of prion replication by increasing the local concentration of the active moiety.[31] Thus, bis-acridine compounds were generated and, as expected, they turned out to be ten-fold more active than quinacrine in cell models. For instance, compound **ACR-1**, consisting of two quinacrine nucleus linked by an alkyl ether chain, showed activity in a nanomolar range (Figure 1.4 A). In the literature are reported other examples of bis-acridines, *i.e.* compound **ACR-2** (Figure 1.4A), that exhibited higher antiprion potency than monomeric acridines in infected neuroblastoma cells offering a valid starting point to study the mechanism of prion replication.[32]

---

28 a) Nguyen Thi, H. T.; Lee, C. Y.; Teruya, K.;Ong, W.Y.; Doh-ura, K.; Go, M. L. *Bioorg. Med. Chem.* **2008**, 16, 6737; b) Nguyen, T.; Sakasegawa, Y.; Ong, W. Y.; Doh-ura, K.;Go, M. L. *Eur. J. Med. Chem.* **2011**, *46*, 2917; c) May, B. C.; Witkop, J.; Sherrill, J. et al. *Bioorg. Med. Chem. Lett.* **2006**, *16*, 4913.

29 Collinge, J.; Gorham, M.; Hudson, F.; Kennedy, A.; Keogh, G.; Pal, S.; Rossor, M.; Rudge, P.; Siddique, D.; Spyer, M.; Thomas, D.; Walker, S.; Webb, T.; Wroe, S.; Darbyshire, J. *Lancet Neurol.* **2009**, *8*, 334.

30 Vogtherr, M.; Grimme, S.; Elshorst, B.; Jacobs, D. M.; Fiebig, K.; Griesinger, C.; Zahn, R. *J. Med. Chem.* **2003**, *46*, 3563.

31 May, B. C.; Fafarman, A. T.; Hong, S. B.; Rogers, M.; Deady, L. W.; Prusiner, S. B; Cohen, F. E. *Proc. Natl. Acad. Sci. U. S. A.* **2003**, *100*, 3416.

32 Csuk, R.; Barthel, A.; Raschke, C.;Kluge, R.; Strohl, D.; Trieschmann, L.; Bohm, G. *Arch. Pharm.* **2009**, *342*, 699.

Quinine, chloroquine and other antimalarial drugs were found to be effective for inhibition of PrP^{Sc} formation in scrapie-infected cells.[33] Since these compounds have a quinoline ring in their structures, Mukarami-Kubo *et al.* decided to focus on quinoline derivatives to explore the structure-activity

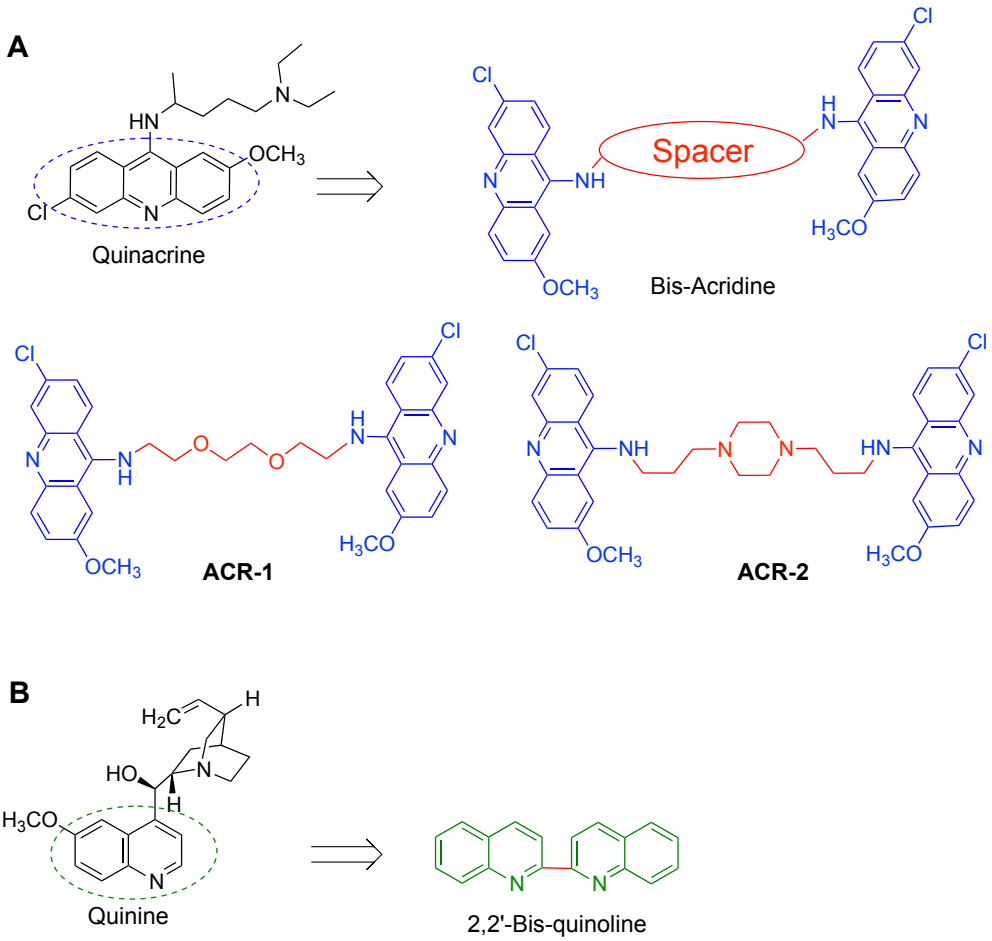

Figure 1.4. (**A**) Quinacrine and bis-acridine compounds (**ACR-1** and **ACR-2**) with high inhibitory effect against PrP^{Sc} formation. (**B**) 2,2'-Biquinoline was 1000 times more effective than quinine in inhibiting PrP^{Sc} formation in infected cell cultures.

33 a) Kocisko, D. A.; Baron, G. S.; Rubenstein, R.; Chen, J.; Kuizon, S.; Caughey, B. *J. Virol.* **2003**, *77*, 10288; b) Klingenstein, R.; Melnyk, P.; Leliveld, S. R.; Ryckebusch, A.; Korth, C. *J. Med. Chem.* **2006**, *49*, 5300; c) Macedo, B.; Kaschula, C. H.; Hunter, R.; Chaves, J. A.; van der Merwe, J. D.; Silva, J. L.; Egan, T. J.; Cordeiro, Y. *Eur. J. Med. Chem.* **2010**, *45*, 5468.

relationships involved in prion replication process. Interestingly, the symmetrical bisquinoline (Figure 1.4B) inhibited PrP^{Sc} formation with an impressive EC_{50} of 0.003 μM, being 1000 times more effective than quinine.[34]

As regards the mechanism behind the inhibitory action of 2,2'-bis-quinoline, the authors demonstrated that no alterations in the protein biosynthesis or in the metabolic labeling of PrP^{C} were involved, whereas 2,2'-bis-quinoline was able to exert a strong binding with recombinant cellular prion protein. In the light of these evidences, the authors suggested that bisquinoline might inhibit the conversion of PrP^{C} to PrP^{Sc} interacting directly with PrP^{C} molecule, even if the binding site remains to be determined. Furthermore, it also prolonged the incubation periods in infected mice.[34]

1.2.3. GN8, a chemical chaperone

In 2007, a Japanese group headed by K. Kuwata used a virtual screening protocol based on the NMR-elucidated structure of PrP^{C} to discover a compound named GN8, able to inhibit PrP^{Sc} formation in cell-based models and prolong survival time of TSE-infected mice.[35] Furthermore, the toxicological and pharmacological profile of GN8 was characterized in rats and dogs, and no severe adverse effects were found at doses sufficient for antiprion activity.[36] On its own, this finding was important although not exceptional, but what made this discovery unique was that for the first time the mechanism of action of an antiprion compound

34 Murakami-Kubo, I.; Doh-ura, K.; Ishikawa, K.; Kawatake, S.; Sasaki, K.; Kira, J. I.; Ohta, S.; Iwaki, T. *J. Virol.* **2004**, *78*, 1281.

35 Kuwata, K.; Nishida, N.; Matsumoto, T.; Kamatari, Y. O.; Hosokawa-Muto, J.; Kodama, K.; Nakamura, H. K.; Kimura, K.; Kawasaki, M.; Takakura, Y.; Shirabe, S.; Takata, J.; Kataoka, Y.; Katamine, S. *Proc. Natl. Acad. Sci. U. S. A.* **2007**, *104*, 11921.

36 Hosokawa-Muto, J.; Kimura, T.; Kuwata, K. *Drug. Chem. Toxicol.* **2012**, *35*, 264.

was clarified. Thus, it was proposed that GN8 acts as chemical chaperone interacting with hot spot regions at the helix B of PrP^{C} forming a stable complex PrP^{C}-GN8 that blocks its conformational change into PrP^{Sc} (Figure 1.5).

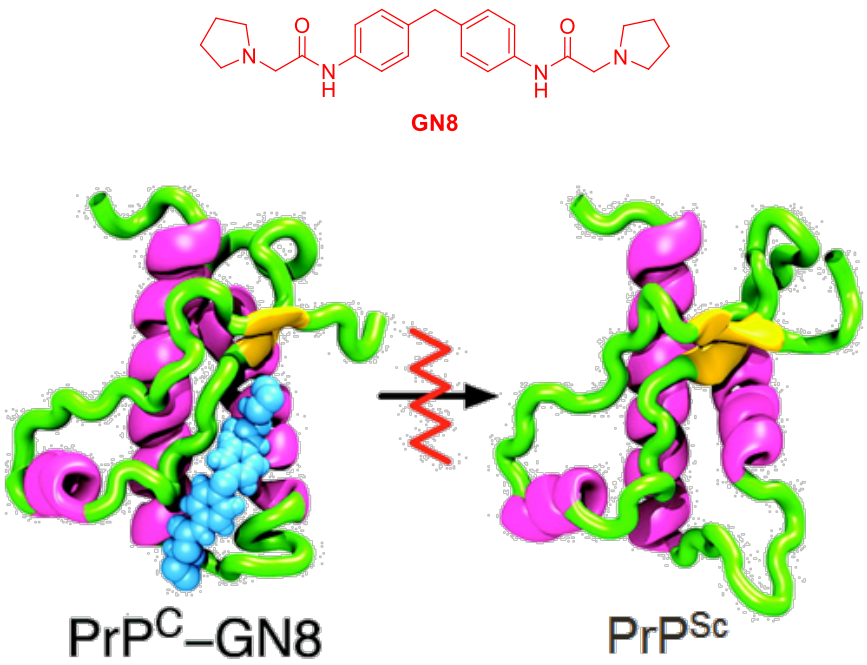

Figure 1.5. GN8 interacts with a hot spot region of PrP^{C} forming a stable complex PrP^{C}-GN8 that blocks its conformational change into PrP^{Sc}

GN8 is composed of two 2-(1-pyrrolidinyl)acetylamino groups attached to a diphenylmethane scaffold. In an effort to study the SAR and optimize the lead compound, a large library of GN8 derivatives was generated. The evaluation of the antiprion activity in infected cell culture across the synthetized compounds showed that the bivalent character of GN8 is essential for its action against prion

replication.[37] Indeed, truncation of one or two tetramethylene units, pyrrolidine units, or 2-(1-pyrrolidinyl)acetyl units resulted in a significant decrease in terms of activity. Furthermore, other chemical manipulations suggested that, more in general, the overall structure of GN8 contributes to the activity including the amide N–H and nitrogen atoms of the pyrrolidine rings that act as H-bond donors and acceptors, respectively. The hydrophobicity of the substituents on the nitrogen atoms of both terminal amino groups also plays a crucial role in the ligand–protein interaction. Moreover, the introduction of one or two substituents at the benzylic position of GN8 restricts the conformational variability of the diphenylmethane unit leading to an increased stability of the prion protein upon binding, and consequently to an improvement of antiprion activity (Figure 1.6).

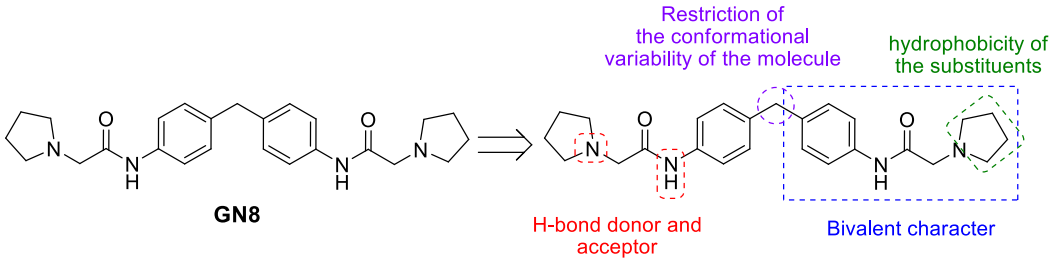

Figure 1.6. From a large library of GN8 derivatives the SAR was studied highlighting the chemical properties of the molecules critical for the antiprion activity

37 Kimura, T.; Hosokawa-Muto, J.; Kamatari, Y. O.; Kuwata, K. *Bioorg. Med. Chem. Lett.* **2011**, *21*, 1502.

1.3. Theranostics in neurodegenerative diseases

Despite the great advances achieved so far and their potential impact in future therapies, PrDs, AD and other neurodegenerative diseases, remain incurable and are extremely challenging for medicinal chemists.[5,38] Paradoxically, in the last decades we seem to have witnessed an inverse relationship between investments in research on CNS drug discovery and the development of successful new drugs. As a result, treatments able to definitely arrest the course of disease do not yet exist for any of these disorders.[39] This situation has been attributed to several hurdles that apply to neurodegenerative diseases in general:

(i) Their etiology is not well understood and consequently no therapeutic target has been truly validated. Furthermore, drug discovery in this area appears less amenable to target-based approaches than it seems for other types of therapeutics.[40]

(ii) Another reason for the high attrition rate of drugs in the clinic has been the poor predictive power of animal models for efficacy in humans.[41]

(iii) Furthermore, the failure of many drug candidates has been related to their late administration when the pathology is too advanced.[42]

All these inherent difficulties have somehow led medicinal chemists to neglect rational approaches and consider screening approaches as the method of

38 Chen, B.; Thompson, M.; Louth, J.; Guo, K. *Curr. Top. Med. Chem.* **2013**, *13*, 2441.
39 Pangalos, M. N.; Schechter, L. E.; Hurko, O. *Nat. Rev. Drug Discov.* **2007**, *6*, 521.
40 Enna, S. J.; Williams, M. *J. Pharmacol. Exp. Ther.* **2009***, 329*, 404.
41 Markou, A.; Chiamulera, C.; Geyer, M. A.; Tricklebank, M.; Steckler, T. *Neuropsychopharmacology* **2009**, *34*, 74.
42 Becker, R. E.; Greig, N. H. *Expert Opin. Drug Discov.* **2012**, *7*, 367.

election when looking for new drugs. Nevertheless, there is still a multitude of intriguing ideas in the med-chem toolbox on how to potentially target PrDs and AD and eventually overcome the challenges summarized above. One such option is the exploitation of theranostics, *i.e.* the use of single agents with concomitant therapeutic and diagnostic properties in order to optimize the efficacy and safety of therapy, as well as to streamline the whole drug discovery process (Figure 1.7.).[43,44] Theranostic agents seem particularly suitable towards neurodegenerative diseases[45,46] because in the case of both PrDs and AD, brain amyloidogenic deposition is the main pathological hallmark, which is believed to precede clinical symptoms by several years.[47,48] Therefore, the imaging of fibrillar

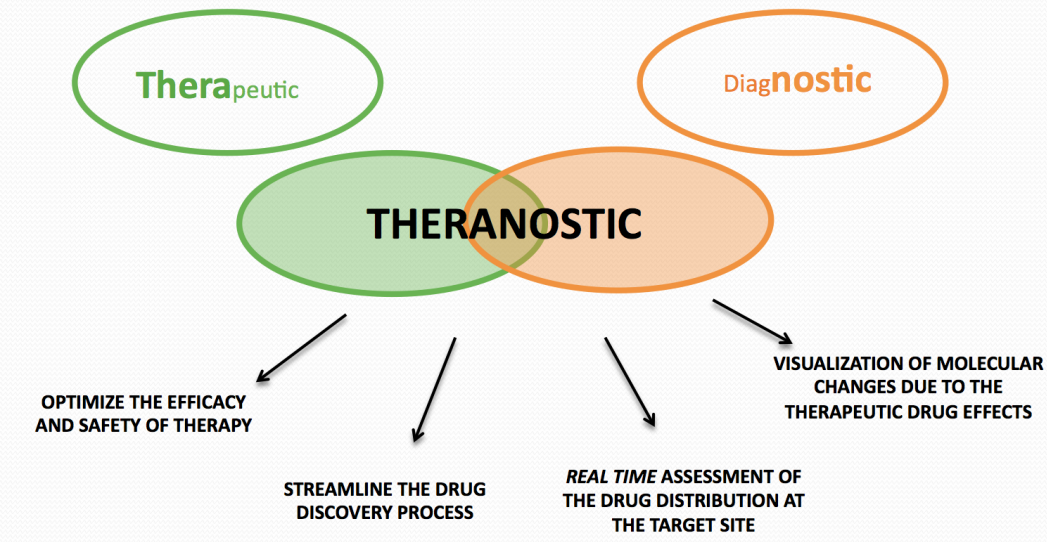

Figure 1.7. The concept of theranostic in biomedicine: a single agent that can be used as diagnostic and for therapeutic intervention

43 Kelkar, S. S.; Reineke, T. M. *Bioconjug. Chem*. **2011**, *22*, 1879.
44 Lammers, T.; Aime, S.; Hennink, W. E.; Storm, G.; Kiessling, F.*Acc. Chem. Res.* **2011**, *44*, 1029.
45 Bolognesi, M. L. Lackey K,Roth BD (Ed.), *Wiley-VCH Verlag GmbH & Co. KGaA*, **2013**, 211.
46 Bongarzone, S.; **Staderini, M.**; Bolognesi, M. L. *Future Med. Chem*. **2014**, *6*, 1017.
47 Tateishi, J.; Kitamoto, T. *Br. Med. Bull.* **1993**, 49, 971.
48 Schulz-Schaeffer, W. J.; Tschoke, S.; Kranefuss, N. et al. *Am. J. Pathol.* **2000**, *156*, 51.

aggregates is particularly suitable to diagnose the onset of the disease in its early stage and monitor its progression.[49]

Theranostics raises fascinating questions about the possibility to devise common strategies for monitoring the aggregation process and for therapeutic intervention.[46] These agents, if properly designed, would have the ability to simultaneously allow the *real time* assessment of the amount of drug reaching a pathological district and the visualization of molecular changes due to the therapeutic effects of the drug itself.

Although research in the theranostic area poses many difficulties because of the sophisticated technology and the novel challenges involved, it offers concrete alternatives to the current paradigm of drug discovery. In this regard, examples of nanoparticles (NPs) for improving diagnosis and therapy of AD already exist and have been recently reviewed by Andrieux and Couvreur.[50] NPs seem particularly suitable for the development of theranostic agents by combining diagnostic and therapeutic components in a unique particle. Furthermore, NPs are currently used as drug delivery systems to improve the pharmacokinetic and pharmacodynamic properties of existing drugs,[51] although they do pose a number of health risks.[52] For this reason, the use of small molecules as theranostics is an attractive alternative. In the context of PrDs, many molecules staining scrapie fibrils with high affinity turned out to be also capable of blocking their aggregation. Ishikawa *et al.* provided two representative examples: a thioflavin (BTA-1) and a styrylbenzene (BSB)

49 Aulić, S.; Bolognesi, M. L.; Legname, G. *Int. J. Cell Biol.* **2013**, 150952.
50 Andrieux, K.; Couvreur, P. *Ann. Pharm. Fr.* **2013**, *71*, 225.
51 Desai, N. *AAPS J*. **2012**, *14*, 282.
52 **Staderini, M.**; Martín, M. A.; Bolognesi, M. L.; Menéndez, J. C. *Chem. Soc. Rev.* **2015**, *44*, DOI: 10.1039/c4cs00337c.

derivative (Figure 1.8).[53] Both fluorescent probes, known to image Aβ plaques, were shown to stain prion fibrils *ex vivo* and to prevent abnormal PrP formation in a cellular model. In addition, the incubation time of an experimental prion mouse model was prolonged when BSB was injected intravenously.[53] In the same vein, amyloid ligands that showed the concomitant capability of staining abnormal prion deposits and inhibiting prion replication were recently reviewed.[49,54] Thus, it seems conceivable that PrP^{Sc} binding compounds represent attractive candidates for monitoring the aggregation process and at the same time for therapeutic intervention.

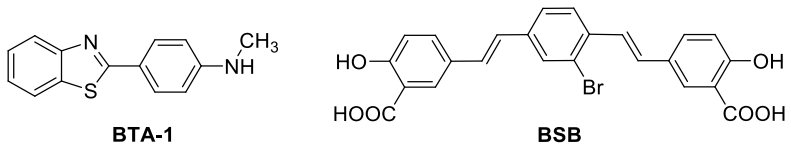

Figure 1.8. Chemical structures of BTA-1 and BSB

53 Ishikawa, K.; Doh-ura, K.; Kudo, Y.; Nishida, N.; Murakami-Kubo, I.; Ando, Y.; Sawada, T.; Iwaki, T. *J. Gen. Virol.* **2004**, *85*, 1785.

54 Teruya, K.; Doh-Ura, K.*Curr. Top. Med. Chem*. **2013**, *13*, 2522.

1.4. Imaging of amyloid plaques by near infrared fluorescent tracers

In the last decade, great strides forward have been made in the field of molecular imaging with the aim of detecting abnormal proteinaceous deposits *in vivo*. Generally speaking, MRI (magnetic resonance imaging) and PET (positron emission tomography) are the most used imaging techniques in clinical settings.[55] However, MRI has too low a sensitivity for amyloid imaging, and PET has some serious limitations due to its high cost, the scarcity of the required isotopes and practical limitations in their use associated to the need to prepare and use them within the short half-lives of the radioactive atomic species (20 min in the case of ^{14}C and 110 min for ^{18}F).[56] In addition, PET has not found practical application for monitoring drug effectiveness in mice because of the complexity of the experimental procedure and data analysis protocols required for small animals. On the other hand, fluorescence spectroscopy has proven suitable for studying fibrillar aggregates.

There is a growing interest in fluorescence spectroscopy as a non-invasive alternative for early diagnosis that enables the real-time visualization of biomolecules in living systems. It is a versatile and sensitive method that leads to a rapid, inexpensive and non-radioactive imaging system.[57] It is important to remark that for their *in vivo* application, fluorescent probes have to possess proper features including the ability to emit fluorescence in the far-red or near-infrared (NIR) region (600-900 nm). In fact, NIR light is particularly suitable to be used for *in vivo* imaging of molecular processes due its acceptable depth of penetration, non-invasive operation, minimal interferences from the auto-

55 Raji, C. A.; Becker, J. T.; Tsopelas, N. D. et al. *J. Neurosci. Methods* **2008***, 172*, 277; (b) Rowe, C. C.; Ackerman, U.; Browne, W. et al. *Lancet Neurol.* **2008**, 7, 129; (c) Choi, S. R.; Golding, G.; Zhuang, Z. et al. *J. Nucl. Med.* **2009**, *50*, 1887.

56 Skoch, J.; Dunn, A.; Hyman, B. T.; Bacskai, B. J. *J. Biomed. Opt.* **2005**, *10*, 11007.

57 Bertoncini, C. W.; Celej. M. S. *Curr. Protein Pept. Sci*. **2011**, *12*, 206.

fluorescence of biological matter and minimal photo-damage to biological samples.[58] Furthermore, in this spectral range the absorption of fluorescence signals by body tissues are minimal.

Although, so far, NIR fluorescent probes have been mainly used in the oncology field for imaging tumors, both *in vivo* and *in vitro*, they are also extremely useful to visualize and monitor amyloid plaque formation and to evaluate the effectiveness of drug treatment in animal models and they are therefore considered an attractive and promising tool for the early diagnosis of AD and PrDs (Figure 1.9).[52]

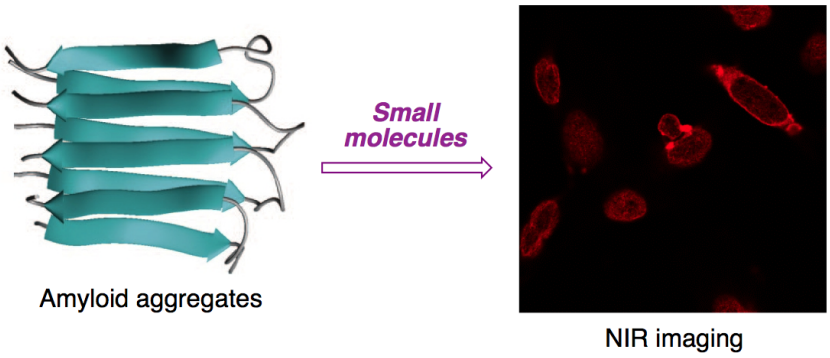

Figure 1.9. Near infrared fluorescent tracers have shown to be suitable to image amyloid aggregates *in vivo*

The application of NIR imaging in neurodegenerative diseases is challenging due to the fact that Aβ plaques are located inside the skull-shielded brain. Indeed, fluorescence-based optical imaging of the brain of small animals in traditional near-infrared regions has previously relied on craniotomy, cranial windows and skull-thinning techniques. Since the resolution of optical imaging

58 Liebert, A.; Wabnitz, H.; Obrig, H.; Erdmann, R.; Möller, M.; Macdonald, R.; Rinneberg, H.; Villringer, A.; Steinbrink, J. *NeuroImage* **2006**, *31*, 600.

decreases with increasing depth of the source of fluorescence emission because of fluorescence scattering in the biological environment, quantification of the amyloid load by NIR imaging is limited to the surface area of the brain.

The development of modern and efficient optical imaging systems, such as fluorescent molecular tomographic (FMT) imaging and the hybrid technique known as FMT-CT (X-ray computed tomography) imaging, has enabled the *in vivo* visualization of Aβ plaque distribution in AD mice with an intact cranium. Nevertheless, mice do not develop the same neuropathological or clinical characteristics seen in humans, and therefore amyloid aggregates in transgenic mouse models are different to those observed in AD patients, thereby hampering the translation into clinics of diagnostic or therapeutic findings done in these models.[59] Although further technological improvements are needed and it is not likely that the entire human brain can be visualized using optical methods, it has been proposed that it will be feasible in the near future to probe the brain cortex at depths up to 3–5 cm.[60] This should be sufficient for obtaining diagnostic information on AD patients, taking into account that most of the amyloid depositions are placed on the neo-cortical surface, although the problem of non-specific binding to white matter has to be taken into account as well.[61]

Another possible approach to NIR AD imaging could be based on the use of parts of the central nervous system (CNS) that are not shielded by the skull and can therefore be considered physiological skull windows. For instance, the retina, which is easily accessible for direct and non-invasive imaging, could provide a

59 Jucker, M. *Nature Medicine* **2010**, *16*, 1210.

60 a) Hyde, D.; de Kleine, R.; MacLaurin, S. A.; Miller, E.; Brooks, D. H.; Krucker, T.; Ntziachristos, V. *Neuroimage.* **2009**, *44*, 1304; b) Ntziachristos, V. *Nature Methods* **2010**, *7*, 603.

61 Fodero-Tavoletti, M. T.; Rowe, C. C.; McLean, C. A.; Leone, L.; Li, Q. X.; Masters, C. L.; Cappai R. and Villemagne, V. L. *J. Nucl. Med.* **2009**, *50*, 198.

unique opportunity for early diagnosis of AD in animal models and humans by exploiting NIR imaging. Thus, recent findings demonstrated the presence of Aβ plaques in the retina, of AD patients with similar biochemical properties of those observed in their brains,[62] and curcumin was shown to bind these plaques and allow their visualization in vivo at high resolution.[62] Unfortunately, Schon et al. could not find any evidence for the presence of Aβ plaques in retina of transgenic mice or AD patients, challenging the results of the previous work.[63] On the other hand, they were able to detect fibrillar tau aggregates in vivo in transgenic mice retina, whereas only hyperphosphorylated (but not fibrillar) tau was observed in AD human retina.[63] The olfactory epithelium, being also an extension of the brain, can be viewed as an optimum target for NIR imaging. It is interesting to note that the presence of neurofibrillary tangles was confirmed by staining, whereas no Aβ deposits could be observed in this region.[64]

Since the discovery of amyloid depositions more than a century ago, several fluorescent dyes with high affinity for the amyloid species have been generated for the post-mortem diagnosis of PrDs, AD and other PMDs.[65,66] Nevertheless, most conventional dyes cannot translate into clinical diagnostic tools because of their low specificity, poor sensitivity, inability to cross the blood brain barrier (BBB) and marked toxicity.[67] Many efforts have been done to overcome these drawbacks with the purpose of obtaining an optical marker to be used for in vivo

62 Koronyo, Y.; Salumbides, B. C.; Black, K. L.; Koronyo-Hamaoui, M. *Neurodegener. Dis.* **2012**, *10*, 285.

63 Schon, C.; Hoffmann, N. A.; Ochs, S. M.; Burgold, S.; Filser, S.; Steinbach, S.; Seeliger, M. W.; Arzberger, T.; Goedert, M.; Kretzschmar, H. A.; Schmidt, B.; Herms, J. *Plos One* **2012**, *7*, e53547.

64 Gu, J.; Anumala, U. R.; Heyny-von Haußen, R.; Hölzer, J.; Goetschy-Meyer, V.; Mall, G.; Hilger, I.; Czech, C.; Schmidt, B. *ChemMedChem* **2013**, *8*, 891.

65 Klunk, W. E.; Engler, H.; Nordberg, A.;Wang, Y. et al. *Ann. Neurol.* **2004**, *55*, 306.

66 Li, Q.; Lee, J. S.; Ha, C.; Park, C. B.; Yang, G.; Gan, W. B.; Chang,Y. T. *Angew. Chem. Int. Ed.* **2004**, *43*, 6331.

67 Hong, Y.; Meng, L.; Chen, S.; Leung, C. W.; Da, L. T. et al. *J. Am. Chem. Soc.* **2012**, *134*, 1680.

imaging of amyloid plaques. To this end, NIR probes have been proposed as ideal candidates. Apart from the ability to emit fluorescence in the NIR region,[68] these probes must possess additional features including: (1) specificity to amyloid plaques, (2) ability to change fluorescence properties upon binding to fibrils, (3) high-affinity binding, (4) high fluorescence quantum yield, (5) large Stokes shift, (6) minimum interference from human serum albumin (HSA) binding, (7) a small molecular size and a suitable lipophilicity, enabling the molecule to cross the BBB, and (8) low toxicity.[69]

1.4.1. Molecular design for emission in the NIR region

If the suitable amount of energy is given to a molecule, electrons can be promoted from an occupied, low-energy molecular orbital to an empty, higher-energy one, giving rise to an absorption transition that corresponds to an absorption band in the spectrum. For a large number of organic compounds, energy is then dissipated by collision with solvent molecules. However, in the case of fluorescent compounds, electrons from the excited state return to the ground state by emission of photons, the latter phenomenon being known as fluorescence, because the electrons of the excited and ground states are paired (singlet state). The smallest possible difference in energy between a full and an empty orbital is the one existing between the highest occupied molecular orbital (HOMO) and lowest unoccupied molecular orbital (LUMO), called the HOMO-LUMO gap, which is closely correlated to the absorption and emission wavelengths. In fact, for a low energy gap a red shift in absorption and emission

68 Raymond, S. B.; Kumar, A. T.; Boas, D. A.; Bacskai, B. J. *Phys. Med. Biol.* **2009**, *54*, 6201.

69 Ran, C.; Xu, X.; Raymond, S. B.; Ferrara, B. J.; Neal, K.; Bacskai, B. J.; Medarova, Z.; Moore, A. *J. Am. Chem. Soc.* **2009**, *131*, 15257.

spectra would be expected. In line with these considerations, NIR probes have been designed and engineered with the aim of reducing the HOMO-LUMO gap of existing amyloid dyes.

It is well known that two double bonds connected by one single bond form a conjugated system in which electrons are delocalized over the entire molecule

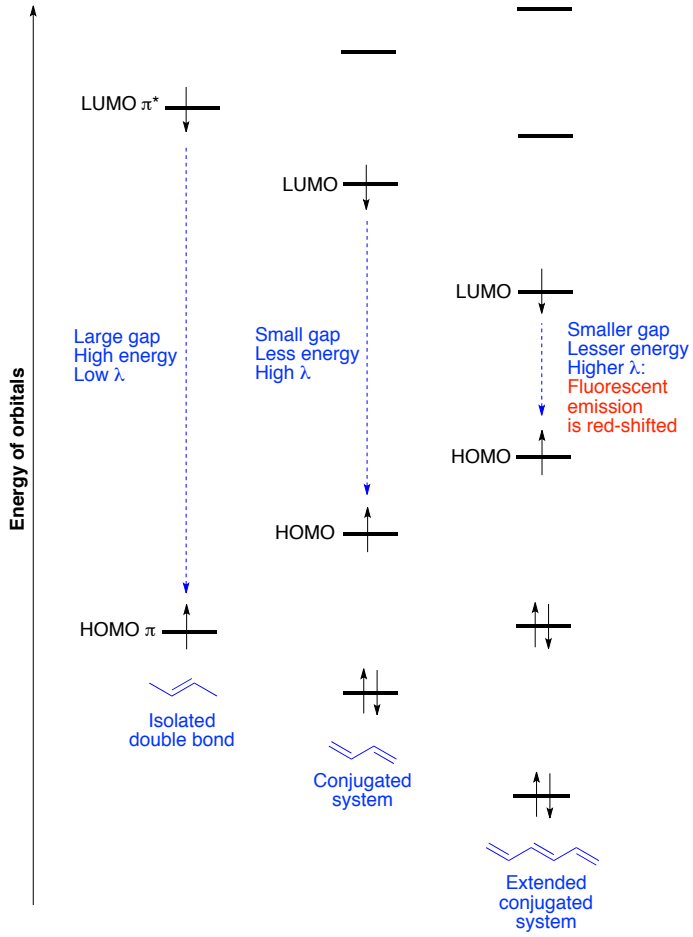

Figure 1.10. Schematic representation of the HOMO-LUMO gap of an isolated double bond and an extended conjugated system. The more conjugated a molecule is, the smaller the energy transition between its HOMO-LUMO and hence the longer wavelength of light it can absorb/emit.

through π-molecular orbitals that result from combining the 2p orbitals of the separate atoms. In this simple conjugated system model, fluorescent emission is due to the transition of electrons from the antibonding π* LUMO orbital to the bonding π HOMO orbital (π* → π transition), whose energy difference is lower than the HOMO-LUMO gap of an isolated double bond. Therefore, the conjugated system absorbs and emits light of a longer wavelength than a non-conjugated system. In addition, if the conjugation is extended further, the gap between HOMO and LUMO will decrease and consequently the fluorescent emission will be red-shifted (Figure 1.10).[70] Therefore, a conjugated π system is the ideal scaffold for the construction of NIR probes and a change of the conjugation length represents an effective way to tune the energy gap level.

Achieving NIR emission by conjugation alone would require the construction of prohibitively big molecules. A very common strategy used to lower the HOMO-LUMO gap of a conjugated π system is based upon the presence of electron-donor (D) and electron-acceptor (A) groups as terminal moieties in order to generate a "push-pull molecule". In its ground state, such a molecule can be described by two resonance forms, one of which is neutral and the other one is zwitterionic (Figure 1.11), with the latter form being a better representation of the excited state. Due to the presence of the A and D groups, the whole conjugated system is more polarized and, in terms of energy, the ground state is closer to the excited state. Therefore, less energy is needed to absorption and emission transitions and thus a longer wavelength (bathochromic shift) is observed. It is important to remark that obtaining the desired shift depends on the electronic features of D and A. The electron donor group must possess a lone pair of electrons in a π orbital able to interact with the π-

70 Qian, G. and Wang, Z. Y.*Chem. Asian J.* **2010**, *5*, 1006.

molecular orbitals of the conjugated system increasing the HOMO energy. On the other hand, the LUMO orbitals are made more stable by the interaction with the antibonding orbitals of the π electron-withdrawing group. Both concomitant effects lead to reduction of the HOMO-LUMO gap. Among the π-electron donor groups, dimethylamino (NMe_2) is widely regarded as the best red-shift absorption-pushing group, whereas the formyl (CHO) and cyano (CN) moieties are considered optimum acceptors. Moreover, pH can also influence the bathochromic shift of push-pull molecules. In fact, in a medium with pH around 7 the neutral form is generally dominant, often showing short absorption/emission wavelengths due to the weak push-pull system. In acid conditions, an ionic form having a strong push-pull system becomes dominant and a red-shift in absorption/emission is observed.[71]

A donor-acceptor-donor (D-A-D) architecture (Figure 1.11) is preferred when two photon microscopy (TPM) bioimaging is applied.[72] TPM has some advantages compared to one photon microscopy including increased depth penetration by exciting at a longer wavelength, enhanced 3D resolution and reduced photodamage. Unfortunately, the technique is invasive *in vivo* and cannot be used in the clinic.[73] TPM features a nonlinear dependence between absorbed light and incident light intensity, since in two-photon absorption (TPA) processes two photons are absorbed with a probability that is proportional to the square of the incident light intensity.[72] Considering that TPA efficiency depends on the conjugation length and D/A strength, a D-A-D system furnishes higher TPA cross

71 Yuan, L.; Lin, W.; Zhao, S.; Gao, W.; Chen, B.; He, L. and Zhu, S. *J. Am. Chem. Soc.* **2012**, *134*, 13510

72 Yao, S.; Ahn, H. Y.; Wang, X.; Fu, J.; Van Stryland, E. W.; Hagan, D. J. and Belfield, K. D. *J. Org. Chem.* **2010**, *75*, 3965.

73 Dong, J.; Revilla-Sánchez, R.; Moss, S. and Haydon, P. G. *Neuropharmacology*, **2010**, *59*, 268.

sections (a measure for the probability of an absorption process) than a D-A molecule.[72]

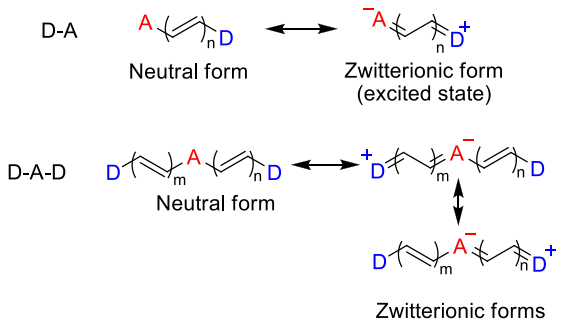

Figure 1.11. A push-pull molecule and a donor-acceptor-donor molecule, showing their neutral and zwitterionic forms.

Another important factor that must be considered for the reduction of the energy gap is the bond length alternation (BLA). BLA is the length difference between consecutive single and double bonds and its value quantifies the delocalization of electrons across the whole molecule.[74] In fact, in a conjugated system a single C-C bond has a partial double bond character due to the overlap of the π orbitals, and hence its length is slightly shorter than a standard single bond (154 pm) and closer to a double one (134 pm). Furthermore, because of this overlap such "formal single bond" becomes harder to rotate and the molecular structure tends to adopt a planar conformation. Based on these considerations, if the BLA is close to zero it means that there is a great overlap among the π orbitals and consequently the system is highly conjugated and the electrons very delocalized, leading to a reduction of the HOMO-LUMO gap. In push-pull molecules, the presence of D and A leads to an increase of the double-

74 Marder, S. R.; Gorman, C. B.; Meyers, F.; Perry, J. W.; Bourhill, G.; Brédas, J. L.; Pierce, B. M. *Science*, **1994**, *265*, 632.

bond character of the C-C bonds, resulting in a reduction of the BLA value as well as the energy gap.

As mentioned above, π orbitals overlap and combine better if the molecule is planar. In this way, a big molecular orbital over the whole molecule is generated that allows a strong π conjugation and a great delocalization of the electrons. This effect explains why the fluorescent emission maximum of compounds in their solid state is observed at longer wavelengths with regard to those obtained in solution. Indeed, in the solid state the free movements of a molecule are restricted resulting in a more rigid conformation, whereas in solution it possesses a substantial degree of conformational freedom.

Planarity is a common structural feature of fluorescent molecules, but it is not a requirement, and excited states have been proved to be non-planar in many cases, such as thioflavin T, and to have a different geometry from the ground state.[75] In the case of molecules containing aromatic rings linked by ethylene chains, which is the most common structure for amyloid probes, a change in the geometry of the molecule from the ground to the excited state is accompanied by a red shift in the fluorescent emission, together with a broadening of the spectrum. Furthermore, the donor-acceptor energy transfer effects may be enhanced by such changes in the excited state geometry.

Upon binding to aggregated Aβ proteins, fluorescent probes normally show shifts of their emission maxima and an increase in the fluorescent quantum yield. These effects are similar to those found upon an increase of viscosity of the medium and are due to conformational changes, since when the molecule is in unbound condition, *e.g.* in solution, free rotation around the single bonds is allowed, whereas upon binding to fibrils, where these movements are restricted

75 Sulatskaya, A. I.; Maskevich, A. A.; Kuznetsova, I. M.; Uversky, V. N.; Turoverov, K. K. *Plos One* **2010**, *5*, e15385.

and its rings are held rigidly, it becomes more planar, triggering a change in the HOMO-LUMO gap reduction and a concomitant red-shift in the absorption maximum. In addition, in such a rigid system the vibrational-rotational processes that couple the excited and the ground state are reduced and therefore the radiationless decay rate decreases, giving rise to an enhancement of the fluorescent yield. As previously mentioned, fluorescence quantum yield enhancement upon binding to fibrils is a desirable feature for a probe, in order for its fluorescence to be clearly distinguished from that of the background.

In summary, different factors influence the $\pi^* \rightarrow \pi$ transition reducing the energy gap between HOMO-LUMO including the extension of the conjugated system, the introduction of electron donor and acceptor moieties, the bond length alternation and the degree of planarity. Building on this knowledge, several fluorescent NIR probes have been designed to stain amyloid plaques.

1.4.2. NIR tracers imaging amyloid plaques *in vivo*

NIAD-4 is considered a milestone, as it was one of the first NIR probes used to image Aβ plaques *in vivo.*[76] NIAD-4 presents the classical push-pull architecture in which a *p*-hydroxyphenyl group (D) and a dicyanomethylene group (A) are connected by a dithienylethenyl π-conjugated bridge making the whole molecule highly polarizable. Interestingly, this biomarker changes its fluorescent properties upon binding to fibrils. Indeed, in the presence of synthetic aggregated Aβ proteins, the dye showed a noteworthy red shift (absorption above 600 nm) and the binding was accompanied by a strong enhancement (400

76 Nesterov, E. E.; Skoch, J.; Hyman, B. T.; Klunk, W. E.; Bacskai, B. J.; Swager, T. M. *Angew. Chem. Int. Ed.* **2005**, *44*, 5452.

fold) of the fluorescent intensity (Figure 1.12). Furthermore, NIAD-4 showed higha ffinity (K_i = 580 nM) to Aβ, thereby it was tested *in vivo* in transgenic AD mice with a cranial window to allow direct monitoring of the brain surface by multiphoton microscopy. The biomarker turned out to be able to cross the blood brain barrier (BBB) after intravenous injection and bound with high specificity to Aβ plaques in the living brain, allowing their easy detection due to its intense red fluorescence, even if the method used was invasive.

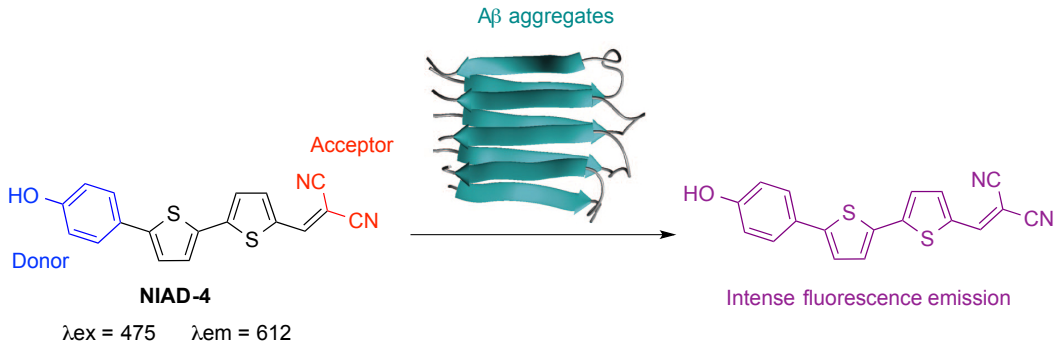

Figure 1.12. NIAD-4 features a push-pull architecture. A strong enhancement of the fluorescent signal is observed when it binds the Aβ fibrillar aggregates.

In an effort to overcome this limit, other NIR tracers were generated with improved optical properties. For example, AOI-987 (see its chemical structure in Figure 1.13) allowed the visualization of Aβ plaques *in vivo* in a non-invasive way.[77] AOI-987 is an oxazine dye characterized by its relatively low molecular weight (427 Da) and high lipophilicity that enables the compound to cross the BBB. Due to its conjugated structure, it showed good spectral properties with both absorption and emission maximum in the NIR region, at 650 and 670 nm respectively. Because its good spectroscopic characteristics and ability to

77 Hintersteiner, M.; Enz, A.; Frey, P.; Jaton, A. L.; Kinzy, W.; Kneuer, R.; Neumann, U.; Rudin, M.; Staufenbiel, M.; Stoeckli, M.; Wiederhold, K. H.; Gremlich, H. U. *Nat. Biotechnol.* **2005**, *23*, 577.

specifically bind Aβ fibrils, AOI-987 was used to visualize amyloid plaques in living APP23 transgenic mice that overexpressed amyloidogenic deposits. Following *i.v.* administration of AOI-987 into APP23 mice, an intense fluorescence signal was detected in the brain, significantly higher than that observed in wild type mice validating the feasibility of specific plaque labeling *in vivo* (Figure 1.13). It is important to note that amyloid plaques were observed without the need for any cranial windows.

The NIR technique used to capture mice images is known as reflectance fluorescence imaging (RFI), a system that has been shown to be particularly suitable for fast imaging but has limited depth resolution beyond (3–5 mm from the surface) and is not quantitative.[60] Despite these limitations, AOI-987 was the first successful NIR probe for non-invasive *in vivo* detection of Aβ plaque formation in AD animal models. Using a NIR device, it was demonstrated that this compound was able to distinguish transgenic mice from wild type mice as well as monitor disease progression.

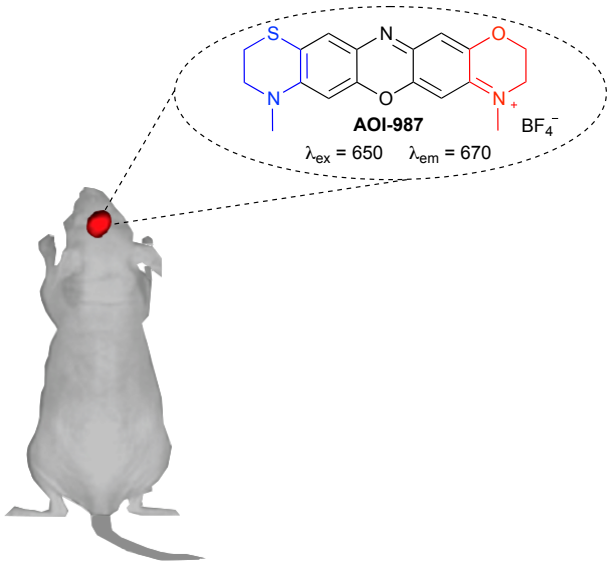

Figure 1.13. AOI-987 allowed the *in vivo* visualization of Aβ plaques in transgenic mice using NIR imaging.

Another important achievement in this field was the generation of a curcumin derivative named CRANAD-2 (Figure 1.14).[69] This compound was prepared by introducing a difluoroboronate moiety into curcumin that provided a favorable bathochromic shift of the absorption and emission wavelength. This effect was further reinforced by replacing the phenolic hydroxyl groups of curcumin with an *N,N'*-dimethylamino group that is regarded as one of the best groups for red-shifting the absorption. As expected, both absorption (λ_{ex} = 640 nm) and emission (λ_{em} = 805 nm) maxima, measured in PBS, fell in the NIR region (Figure 1.14). Remarkably, the molecule "turned on" in presence of amyloid fibrils showing a significant enhancement of its fluorescent intensity (70-fold), a

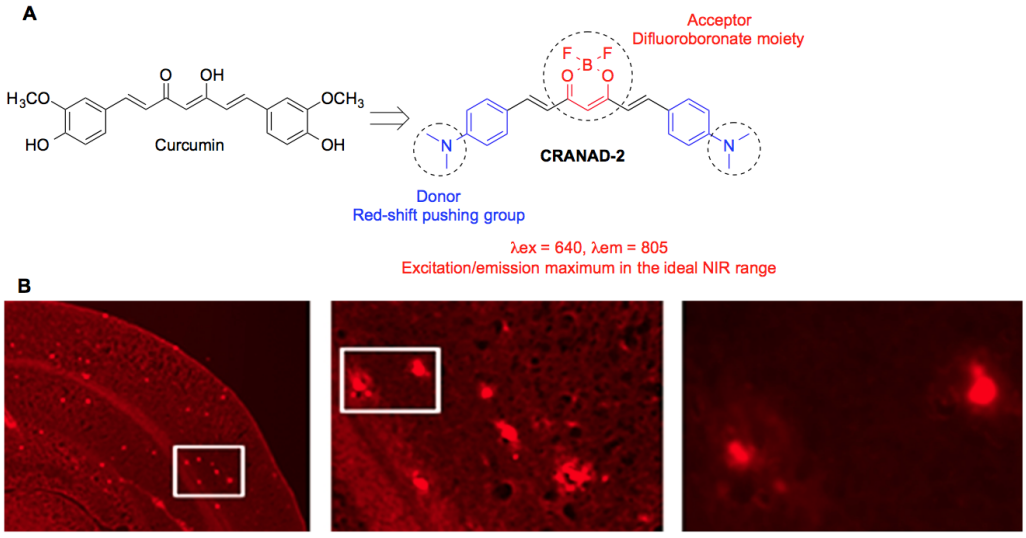

Figure 1.14. (**A**) Chemical structure and fluorescent properties of curcumin and CRANAD-2. It exhibited excitation and emission maximum in the ideal NIR spectral region. (**B**) CRANAD-2 was used to stain brain sections from transgenic mice. Amplification from left to right: 2x, 10x, 40x. Reprinted (adapted) with permission from Ran, C.; Xu, X.; Raymond, S. B.; Ferrara, B. J.; Neal, K.; Bacskai, B. J.; Medarova, Z.; Moore, A. *J. Am. Chem. Soc.* **2009**, *131*, 15257. Copyright (2009) American Chemical Society.

critical requirement for an ideal NIR tracer. On the other hand, its binding affinity to Aβ aggregates was much higher than that of AOI-987 and similar to that of NIAD-4. Then, CRANAD-2 was finally investigated *in vivo* and it was injected into transgenic mice that expressed significant concentration of Aβ fibrils. More intense fluorescent signals were observed in these transgenic mice with regard of those found in control mice. These data were confirmed by *ex vivo* staining of transgenic mice brain slices (Figure 1.14). Nevertheless, also in this case the NIR imaging technique employed was fluorescence reflectance, which is characterized by a low penetrating depth (< 1 cm) and a low resolution.

Another important breakthrough in the search for novel NIR tracers to be used *in vivo* was achieved with the discovery of THK-265.[78] This compound was identified through a virtual screening of NIR candidates and has the advantage of being commercially available. THK-265 (see its chemical structure in Figure 1.15A) is formed by two thiobarbituric acid units connected by a pentadienylidene chain, forming an extended conjugated system after oxo-enol tautomerism at one of the lactam groups. It showed suitable spectroscopic properties, with an emission maximum at $\lambda > 650$ nm and a high fluorescent quantum yield (38.5% in methanol). Importantly, a fluorescent binding assay revealed a strong affinity to Aβ aggregates, higher than that of ThT and AOI-1987, which was confirmed by a fluorescent staining on AD brain slices. Since the dye THK-265 also exhibited a low toxicity and a good brain uptake, its capability of visualizing Aβ plaques was explored *in vivo*. Thus, the compound was intravenously injected into AβPP-transgenic mice that overexpressed senile plaques and the fluorescent signal intensity observed was significantly higher than that detected in wild type mice.

78 Okamura, N.; Mori, M.; Furumoto, S.; Yoshikawa, T.; Harada, R.; Ito, S.; Fujikawa, Y.; Arai, H.; Yanai, K. and Kudo, Y. *J. Alzheimers Dis.*, **2011**, *23*, 37.

In the light of these findings, Schmidt *et al.* developed a systematic protocol to image and quantify amyloid fibrils in transgenic mice at different disease stages using THK-265 as NIR probe.[79] All the experiments were carried out involving AβPP-transgenic mice that started to show senile plaques after 50 days. Considering that the number and size of the Aβ plaques increased with age, the mice were scanned at different ages: 50, 75, 100 and older than 200 days in order to monitor the amyloid accumulation. Importantly, *in vivo* results confirmed a direct correlation between the enhancement of the fluorescence intensity signal and the increasing age of the mice (Figure 1.15B). As expected, *ex vivo* experiments proved that fluorescent signal changes were due to the different Aβ loads. Nevertheless, higher sensitivity is needed to real-time

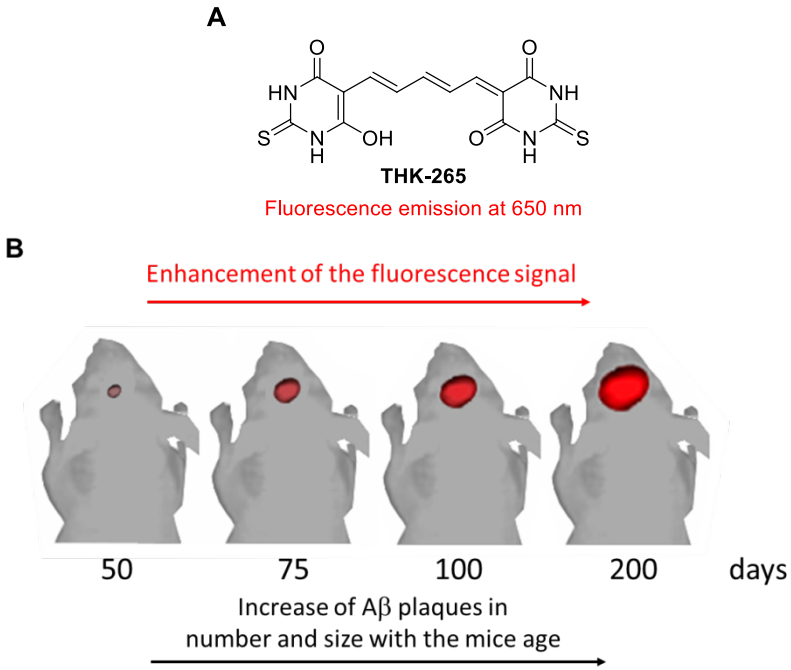

Figure 1.15. (**A**) Chemical structure of THK-265. (**B**) The fluorescence intensity signal of THK-265 enhances with the increasing age of the mice.

79 Schmidt A.; Pahnke, J. *J. Alzh. Dis.* **2012**, *30*, 651.

monitor cerebral amyloid deposits by using NIR imaging, even if THK-265 could represent a possible candidate to track AD progression and evaluate the efficacy of anti-AD drug.

Although all the NIR tracers for Aβ imaging discussed so far are able to cross the BBB and label selectively the amyloid plaques, they still show limitations that need to be overcome. For example, NIAD-4 could not be detected in mice with an intact cranium, AOI-1987 showed only moderate affinity for Aβ aggregates and CRANAD-2 displayed a low washout from the brain. In an effort to design improved NIR probes, Cui et al. developed a new series of fluorescent small molecules for *in vivo* detection of amyloid plaques.[80] The authors used the push-pull architecture to generate new compounds that consisted of a donor and acceptor connected by a conjugated π electron chain. The *N,N'*-dimethylamino group was selected as the electron donor because of its known ability to redshift light absorption, and a dicyanomethylene group was chosen as acceptor. The donor-acceptor system was separated by a polymethine moiety that was expected to further push both absorption and emission wavelength toward the NIR spectral region. Compound DANIR showed a red-shifted emission wavelength at 665 nm (Figure 1.16A). This biomarker was able to bind Aβ plaques with great affinity, cross the BBB and could be quickly washed out from the brain. Thus, following administration of DANIR to APPswe/PSEN1 double transgenic mice, the fluorescent signal detected was remarkably higher than that for the wild-type control. Importantly, this specific labelling was confirmed *ex vivo* (Fig. 1.16B). Taken in the aggregate, these results confirmed that compound DANIR is close to meeting the requirements for an ideal NIR probe.

80 Cui, M.; Ono, M.; Watanabe, H.; Kimura, H.; Liu, B. and Saji, H. *J. Am. Chem. Soc.* **2014**, *136*, 3388.

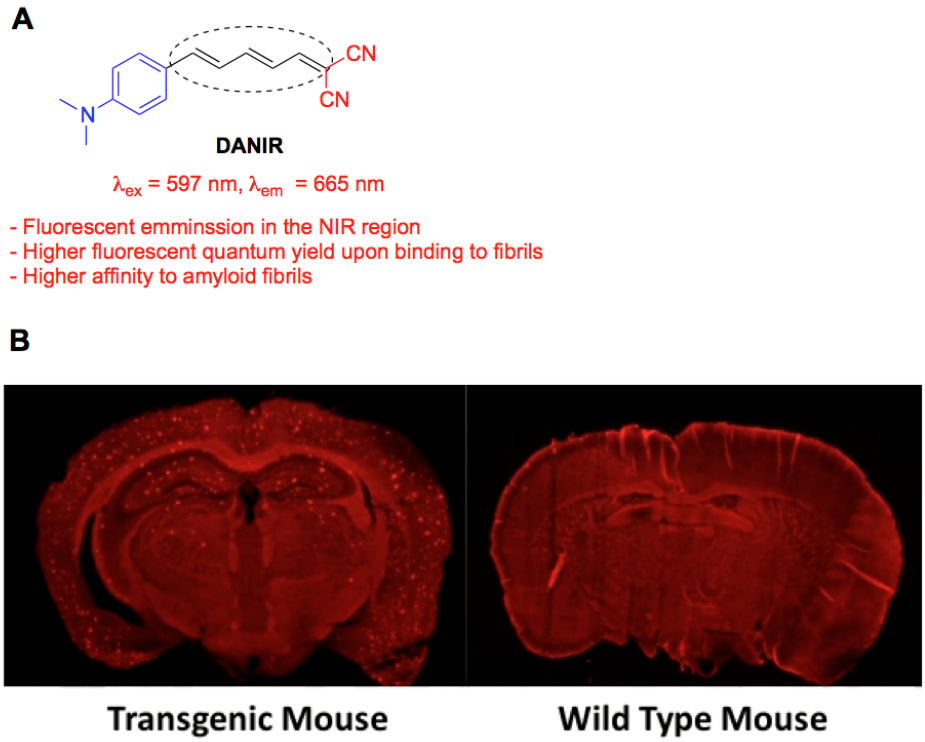

Figure 1.16. (**A**) Chemical structure and optical properties of DANIR. Due to its favourable florescent features and high affinity to amyloid fibrils, DANIR was selected for *in vivo* NIR imaging. (**B**) Fluorescence staining with DANIR of a brain section from a transgenic mouse compared with that from a wild type one. Reprinted (adapted) with permission from Cui, M.; Ono, M.; Watanabe, H.; Kimura, H.; Liu, B. and Saji, H. *J. Am. Chem. Soc.* **2014**, *136*, 3388. Copyright (2014) American Chemical Society.

1.5. Privileged structures common to neurodegenerative and protozoan disease drugss

From a medicinal chemistry point of view, a privileged structure consists in a single molecular fragment that can provide ligands for different targets.[81] Privileged structures have been widely used in drug discovery as they represent an ideal source of scaffolds and capping fragments to be used for the design of combinatorial libraries addressed to explore a broad spectrum of pharmacological targets. In few words, the privileged structure is supposed to be responsible for the affinity to a receptor, meanwhile structure modifications of the whole molecule provide the selectivity.[82]

Antimalarial quinolines[83] are represented by the 4-aminoquinoline derivatives amodiaquine, mefloquine and chloroquine and by the 8-substituted quinolines primaquine, pamaquine and sitamaquine.[84] Interestingly, some quinoline-derived antimalarial drugs including chloroquine, mefloquine and 2,2'-bis-quinoline were found to be also active against prion replication.[33] In this context, Klingenstein et al. reported a further 4-aminoquinoline compound that exhibited concomitant inhibitory potency in scrapie infected cells and against *P. falciparum* growth (Figure 1.17).[33b] Similarity, the acridine motif has been observed in many antiprion, antimalarial and antileishmanial ligands.[85] Acridine quinacrine is one of the earliest antimalarial drug that was found to inhibit PrP^{Sc} fibril formation.[27] Starting from this finding, many 9-aminoacridines were

81 Evans, B. E.; Rittle, K. E.; Bock, M. G. et al. *J. Med. Chem.* **1988**, *31*, 2235.
82 Muller, G. *Drug Discov. Today* **2003**, *8*, 681.
83 a) Ridley, R. G.; Hudson, A. T. *Expert Opin. Ther. Pat.* **1998**, 8, 121; b)O'Neill, P. M.; Ward, S. A.; Berry, N. G.; Jeyadevan, J. P.; Biagini, G. A.; Asadollaly, E.; Park, B. K.; Bray, P. G. *Curr. Top. Med. Chem.* **2006**, *6*, 479; c) Kaur, K.; Jain, M.; Reddy, R. P.; Jain, R. *Eur. J. Med. Chem*. **2010**, *45*, 3245.
84 Yeates, C.*Curr. Opin. Investig. Drugs* **2002**, *3*, 1446.
85 Gamage, S. A.; Figgitt, D. P.; Wojcik, S. J. et al. *J. Med. Chem.* **1997**, *40*, 2634.

generated and evaluated in scrapie infected cells revealing nanomolar actvity.[28] In particular, bis-acridines exhibited very high potency against prion replication as well as *Leishmania*, such as compound BiCappa (Figure 1.17).[24,31,86] In summary, it can be concluded that some molecular targets of antiprion and antiprotozoal ligands, including the acidic organelles or endosomal/lysosomal compartments and downstream molecular targets of lipid metabolism, could overlap.[25,33b]

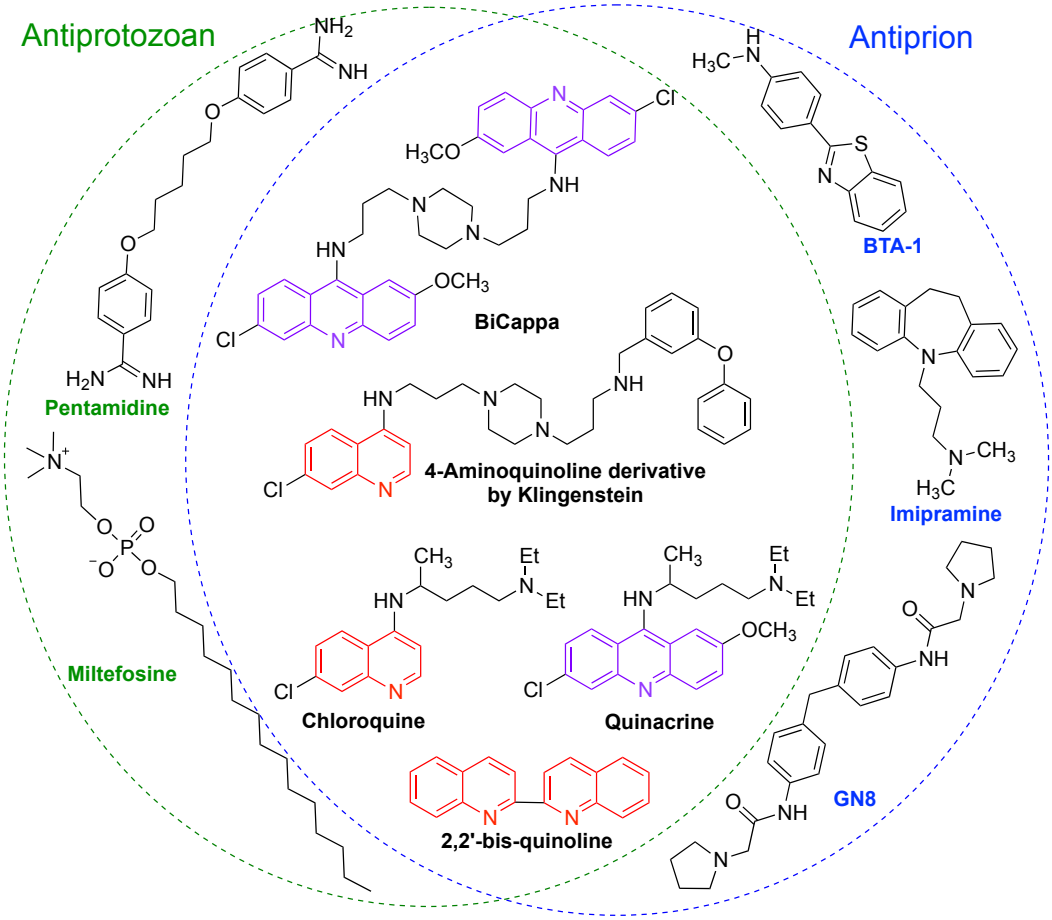

Figure 1.17. Quinoline and acridine cores are particularly recurrent in compounds active against two different pathologies, neurodegenerative and protozoan diseases

86 Girault, S.; Grellier, P.; Berecibar, A. et al. *J. Med. Chem.* **2000**, *43*, 2646.

In the light of these considerations, acridine, quinoline and other kinds of privileged structures represent a unique opportunity to improve the productivity of drug discovery projects in the field of neurodegenerative and protozoan diseases.

2. Objectives

In the context of our drug discovery project devoted to the identification of novel scaffolds towards neurodegenerative diseases, the present thesis has the following specific objectives:

1. We started our work with the development of synthetic methodology required for some parts of the project. More specifically, we needed a general and green protocol for the amination and (hetero)arylation of halogenated nitrogen heterocycles. We focused in particular on quinoline and acridine substrates, by exploiting focused microwave (MW) irradiation in order to provide a rapid access to molecular frameworks of relevance in the field of neurodegenerative diseases (Figure 2.1).

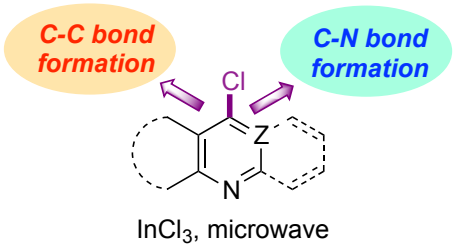

Figure 2.1. Generation of carbon-carbon (C-C) and carbon-nitrogen (C-N) bonds on heterocyclic substrates

2. Building on the bivalent approach, we planned to generate a chemical library of bifunctional molecules, consisting of two prion recognition moieties joined via an appropriate spacer.[21] In an effort to employ a spacer that might have an active role in the molecular recognition process, we focused on 2,5-diketopiperazine (DKP) due to its peptidic nature. Thus, a library was generated by condensing DKP with aromatic aldehydes (structure **I**, Scheme 2.1) bearing side chains that have been shown to be critical for the molecular recognition and self-assembly processes leading to fibrillar aggregate formation. Furthermore, to

study the importance of an appropriate planar conformation, some monoreduced (structure **II**, Scheme 2.1) and a saturated derivative (structure **III**, Scheme 2.1) were also synthesized.

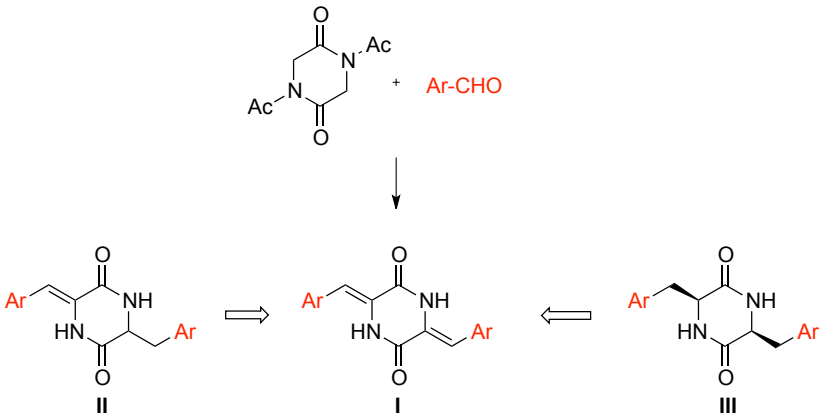

Scheme 2.1. Chemical structure of planned DKP derivatives

3. In our search for novel symmetrical small molecules to diagnose and treat PrDs, we focused on GN8, an antiprion compound, which acts as a chemical chaperone by binding PrP^{C}. We modified the diphenylmethane core of GN8 by linking its two phenyl rings in order to generate a new class of carbazole and fluorene derivatives (Scheme 2.2). Furthermore, additional modifications were carried out, such as the replacement of the pyrrolidine group on the side chains with several secondary amino moieties (cyclic, acyclic and heterocyclic amines). Such structural changes made the new compounds more planar and fluorescent, offering the opportunity to use them as therapeutic tools and also as chemical tracers to elucidate their antiprion mechanism of action.

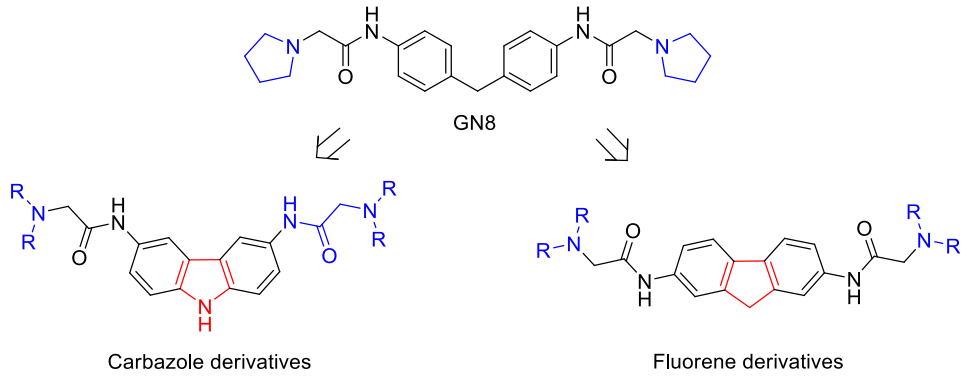

Scheme 2.2. Chemical modifications of GN8 to generate new libraries of fluorene and carbazole derivatives.

4. In an effort to identify novel fluorescent compounds capable of marking amyloid fibrils, and, ideally, of simultaneously blocking their aggregation, we turned our attention on styryl heterocycles. They have been widely used for amyloid staining, and some of them were also found to be active against prion replication. Therefore, it seemed conceivable that the styryl moiety is critical to recognize and interfere with the amyloidogenic processes. With this in mind, we generated some styrylquinoline derivatives by linking the styryl moiety to a quinoline nucleus, to detect, and potentially treat, fibrillar amyloidogenic aggregates. The synthesis was achieved via a vinylogous variation of the Povarov reaction to afford 2-styryl-1,2,3,4-tetrahydroquinolines followed by their dehydrogenation or, alternatively, by microwave-assisted aldol condensation between substituted quinaldines and aromatic aldehydes (Scheme 2.3).

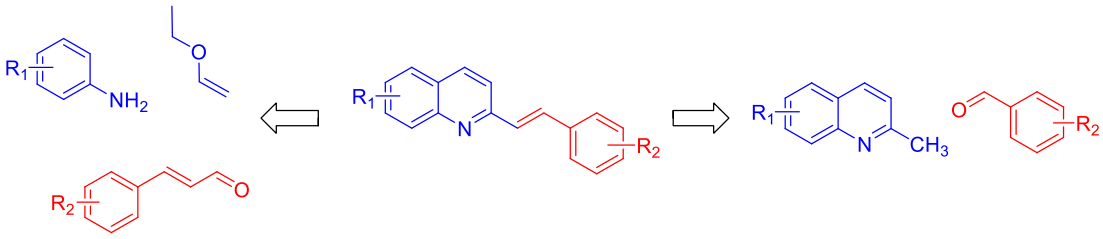

Scheme 2.3. Synthetic approach to substituted styrylquinolines

5. Several lines of evidence suggest that polyamines play a fundamental role in many biological processes. Indeed, they are involved in cell proliferation and have both pro- and antiapoptotic effects and in many signaling pathways through their effects on G proteins, protein kinases, nucleotide cyclases, and receptors.[87] Interestingly, in the context of central nervous system (CNS) diseases, it has been postulated that polyamines act as neuromodulators[88] and influence the properties of several neurotransmitter pathways, including catecholamines, γ-aminobutyric acid, nitric oxide, and glutamate.[89] Furthermore, polyamines that function as neuroprotectants,[90] and as antiprion chemotherapeutics[91] have been described.

With these concepts in mind, we planned to introduce diverse types of polyamino chains at C-4 position of the styrylquinoline moiety in order to provide novel molecules to treat PrDs and AD. The preparation of these 4-polyaminostyrylquinolines was planned via a seven-step synthetic route involving the amination of 4-chlorostyrylquinoline (Scheme 2.4).

87 Melchiorre, C.; Bolognesi, M. L.; Minarini, A.; Rosini, M.; Tumiatti, V. *J. Med. Chem.* **2010**, *53*, 5906.
88 Masuko, T.; Kusama-Eguchi, K.; Sakata, K. et al. *J. Neurochem*. **2003**, 84, 610.
89 Fiori, L. M.; Turecki, G. *J. Psychiatry Neurosci.* **2008**, *33*, 102.
90 Li, J.; Doyle, K. M.; Tatlisumak, T. *Curr. Med. Chem*. **2007**, *14*, 1807.
91 Supattapone, S.; Piro, J. R.; Rees, J. R. *CNS Neurol. Disord. Drug Targets* **2009**, *8*, 323.

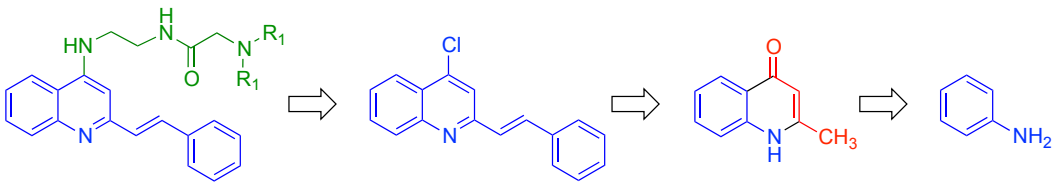

Scheme 2.4. Synthetic approach to 4-aminostyrylquinoline derivatives

6. Based on the concept of privileged structure and on the parallelism between neurodegenerative and protozoan diseases, we planned to screen our 4-aminostrylquinoline derivatives against trypanosomatid diseases. Thus, their anti-leishmanial and antitrypanosomal activities were preliminary evaluated *in vitro*, revealing good efficacies.

In the light of these results, we designed a further series of styrylquinolines introducing different polyamino chains at the quinoline C-8 position, in analogy to sitamaquine, a potent anti-leishmanial agent. The plan for the preparation of these 8-aminostyrylquinolines involved the alkylation of 8-aminostyrylquinoline, which in turn would be obtained from 8-nitroquinaldine (Scheme 2.5).

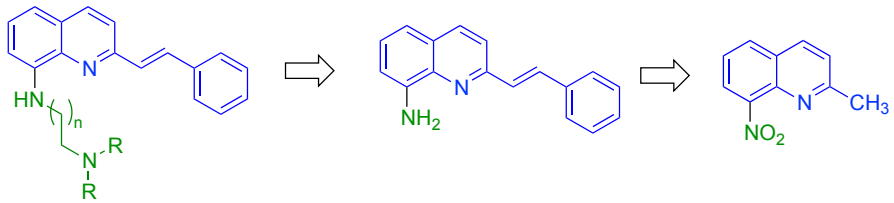

Scheme 2.5. Synthetic strategy for the preparation of 8-aminostyrylquinoline derivatives

7. In the course of the three-month stay abroad that is part of the requirements for the European Ph. D. Mention, we turned our attention to nanomedicine as another entry to the field of theranostics. The work developed at the University of East Anglia, UK, involved the functionalization of

superparamagnetic iron oxide nanoparticles (SPIONs), which are good candidates as theranostic agents. Due to their paramagnetic properties, these nanoparticles are particularly suitable for diagnostic techniques such as magnetic resonance imaging (MRI), acting as imaging tools complementary to optical probes, and at the same time they can transport a drug with the aid of a targeting moiety. This project involved an anticancer drug and the use of NDP-MSH, a peptide able to address the nanocarrier towards the melanocortin type-1 receptor (MC1R), which is overexpressed in many melanoma cells at high levels (Figure 2.2).

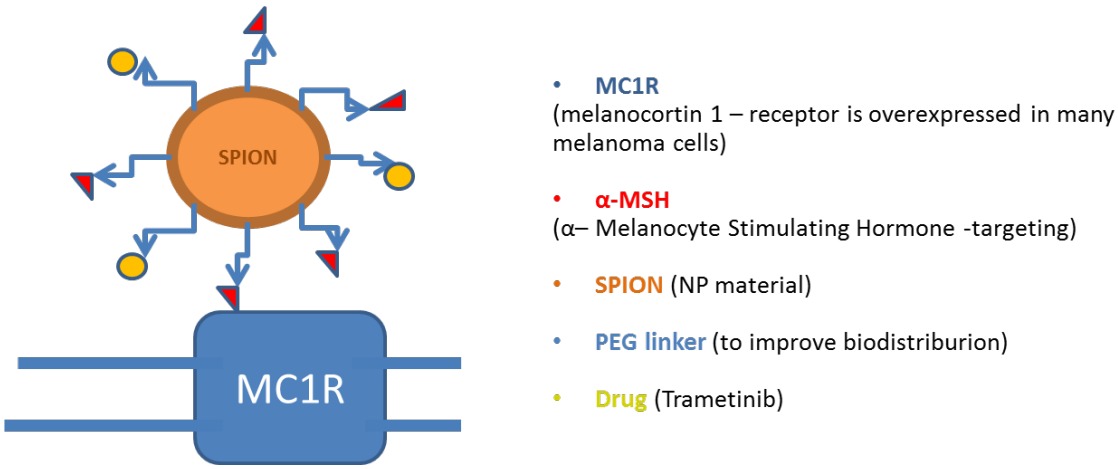

Figure 2.2. SPIONs can be functionalized with a targeting moiety (NDP-MSH), a drug and thanks to their intrinsic paramagnetic properties they can act as imaging tool

3. Development of general methods for the functionalization of π-defficient heterocyclic substrates of pharmacological interest

3.1. Introduction

Nitrogen heterocycles constitute the central core of many drugs and are crucial for the pharmaceutical and agrochemical industries.[25,92] Cross-coupling reactions able to generate carbon-carbon (C-C) and carbon-nitrogen (C-N) bonds on π-deficient heterocyclic substrates are of great importance in the synthesis of a large variety of bioactive agents[93] such as the antimalarials chloroquine, amodiaquine and quinacrine (see Chapter 1). Other examples include indolylquinolines, which are crucial in several biological processes and have shown to possess antileishmanial and antibacterial activities[94] and amino derivatives of the acridine and quinazoline nuclei with anticancer (amsacrine and gefitinib)[95,96] and anti-Alzheimer (bistacrine) activity.[97] Other related compounds of considerable biomedical interest are the amino derivatives of quinoxaline,[98] purine,[99] pyridine[100] and benzimidazole.[101] Some representative examples are shown in Figure 3.1.

92 Pozharskii, A. F.; Soldartenkov, A. T.; Katrizky, A. R. Heterocycles in Life and Society, 2nd Ed. *John Wiley & Sons*, Weinheim, Germany, **2011**; b) Pitt, W. R.; Parry, D. M.;Perry, B. G.;Groom, C. R. *J. Med. Chem*. **2009**, *52*, 2952.

93 Tracy, J. W.; Webster Jr., L. T. in *Goodman and Gilman'sThe Pharmacological Basis of Therapeutics* (Eds.: J. G. Hardman, L. E. Limbird), McGraw Hill, New York, **2001**, 1111.

94 a) Ray, S.; Sadhukhan, P.; Mandal, N.; Mahato, S.; Majumder, H. *Biochem. Biophys. Res. Commun*. **1997***, 230*, 171; b) Chakrabarti, G.; Basu, A.; Manna, P.; Mahato, S.; Mandal, N.; Bandyopadhyay, S. *J. Antimicrob. Chemother.* **1999**, *43*, 359.

95 a) Demeunynck, M.; Charmantray, F.; Martelli, A. *Curr. Pharm. Design* **2001**, *7*, 1703; b) Denny, W. A. *Curr. Med. Chem.* **2002**, *9*, 1655.

96 Marzaro, G.; Guiotto, A.; Chilin, A. *Expert Opin. Ther. Patents* **2012**, *22*, 223.

97 Tumiatti, V.; Minarini, A.; Bolognesi, M. L.; Milelli, A.; Rosini, M.; Melchiorre, C. *Curr. Med. Chem*. **2010**, *17*, 1825.

98 For a review, see: González, M.; Cerecetto, H. *Exp. Opin. Ther. Pat.* **2012**, *22*, 1289.

99 a) Laufer, S. A.; Domeyer, D. M.; Scior, T. R. F.; Albrecht, W.; Hauser, D. R. J. *J. Med. Chem.* **2005**, *48*, 710; b) Zatloukal, M.; Gemrotová, M.; Doležal, K.; Havlíček, L.; Spíchal, L.; Strnad, M. *Bioorg. Med. Chem.* **2008**, *16*, 9268.

100 Welsch, M. E.; Snyder, S. A.; Stockwell, B. R. *Curr. Opin. Chem. Biol.* **2010**, *14*, 347.

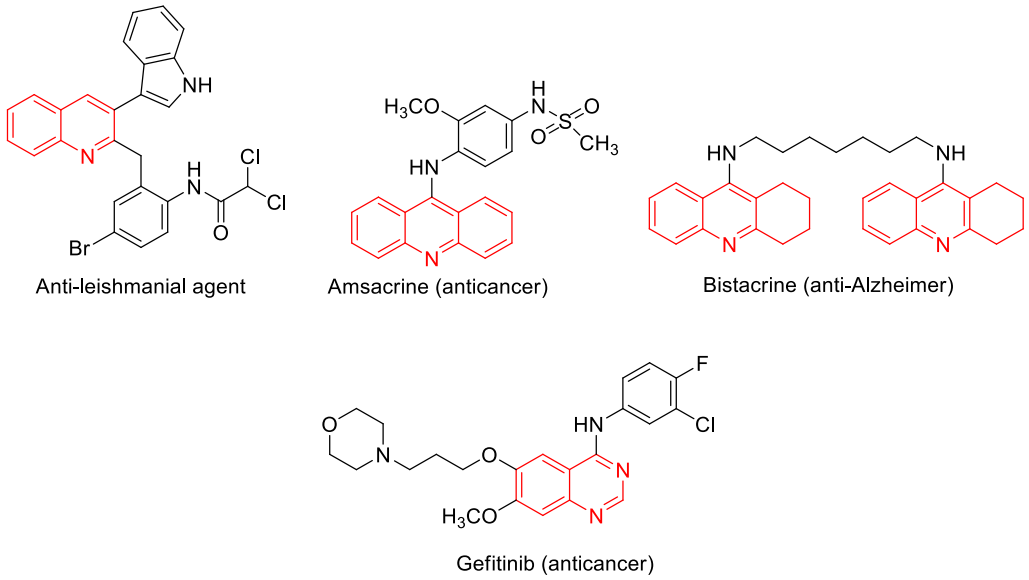

Figure 3.1. Examples of pharmacologically relevant compounds arising from the generation of C-C or C-N bonds on a π-deficient heterocyclic substrate

As highlighted in the Introduction, 6-chloro-2-methoxyacridine and 7-chloroquinoline are well-known prion recognition motifs as their derivatives have been shown to inhibit PrP^{Sc} formation in infected cells and to bind PrP.[25] Furthermore, the quinazoline fragment is also present in many compounds that have been evaluated against prion replication.[102] Therefore, we deemed reasonable that the functionalization of such nitrogen heterocycles could represent a valid strategy in our search for novel anti-prion agents.

Transition metal-catalyzed cross-coupling has been the most widely employed method for the generation of both C-N and C-C bonds on heterocyclic

101 a) Nofal, Z. M.; Fahmy, H. H.; Mohamed, H. S. *Arch. Pharm. Res*. **2002**, *25*, 250; b) Sørensen, U. S.; Strøbæk, D.; Christophersen, P.; Hougaard, C.; Jensen, M. L.; Nielsen, E. Ø.; Peters, D.; Teuber, L. *J. Med. Chem.* **2008**, *51,* 7625.

102 Cope, H.; Mutter, R.; Heal, W.; Pascoe, C.; Brown, P.; Pratt, S.; Chen, B. *Eur. J. Med. Chem.* **2006**, *41*, 1124.

substrates. However, Buchwald-Hartwig, Suzuki-Miyaura and related reactions require the use of expensive and cumbersome catalysts and phosphine ligands.[103] In the particular case of C-C bond formation, substantial efforts have been made to achieve the coupling between heteroarenes and aza-aromatic compounds, and several methods have been described that include: (1) the use of organolithium or organomagnesium reagents, which are problematic owing to their pyrophoric nature and the need for low temperatures in many cases;[104] (2) the multistep construction of the chemical moiety to be attached to the heterocycle;[105] (3) the use of more contrived protocols requiring specialized equipment such as photochemical[106] and electrochemical[107] reactions. Unfortunately, these methods are far from being general and are only appropriate for the preparation of specific compounds.

Another approach involves addition-elimination reactions between a halogenated nitrogen heterocycle and heteroarenes in the presence at least of one equivalent of the corrosive and irritating $AlCl_3$ in dichloroethane. Also in this case such protocol is not general because it works only if the carbon bearing the halogen is strongly activated by electron-withdrawing substituents, as in the case

103 a) Payack, J.; Vázquez, E.; Matty, L.; Kress, M.; McNamara, J. *J. Org. Chem.* **2005**, *70*, 175; b) Nishida, A.; Miyashita, N.; Fuwa, M.; Nakagawa, M. *Heterocycles*, **2003**, *59*, 473; c) Iglesias, M. J.; Prieto, A.; Nicasio, M. C. *Adv. Synth. Catal.* **2010**, *352*, 1949; d) Chen, L.; Yu, G. A.; Li, F.; Zhu, X.; Zhang, B.; Guo, R.; Li, X.; Yang, Q.; Jin, S.; Liu, C.; Liu, S. H. *J. Organomet. Chem.* **2010**, *695*, 1768; e) Seregin, V. I.; Gevorgyan, V. *Chem. Soc. Rev.* **2007**, *36*, 1173; f) Wagaw, S.; Buchwald, S. L. *J. Org. Chem.* **1996**, *61*, 7240.

104 a) Yamaguchi, M.; Kamei, K.; Koga, T.; Akima, M.; Maruyama, A.; Kuroki, T.; Ohi, N. *J. Med. Chem.* **1993**, *36*, 4052; b) Luth, A.; Lowe, W. *Eur. J. Med. Chem*. **2008**, *43*, 1478.

105 a) Kuethe, J.; Wong, A.; Davies, I. *Org. Lett.* **2003**, *5*, 3975; b) Zhu, S.; Ji, S.; Zhao, K.; Liu, Y. *Tetrahedron Lett.* **2008**, *49*, 2578; c) Lian, M.; Li, Q.; Zhu, Y.; Yin, G.; Wu, A. *Tetrahedron* **2012**, 68, 9598; d) Kamila, S.; Ankati, H.; Biehl, E. R. *Arkivoc*, **2011**, *9*, 94.

106 Ohkura, K.; Seki, K.; Terashima, M.; Kanaoka, Y. *Heterocycles* **1990**, *30*, 957.

107 Chahma, M.; Combellas, C.; Thiébault, A. *Synthesis* **1994**, 366.

of 1,4-dichlorophthalazine, 2,4-dichloroquinazoline and 3-nitro(cyano)-2-chloropyridine.[108]

The addition-elimination reaction between a halogenated heterocycle and an amine is the most common approach for the generation of the C-N bond. It requires very harsh and unsafe conditions, such as heating at high temperatures in sealed tubes[109] or using large amounts of phenol as the reaction medium.[110] Also importantly from the point of view of waste generation, the conventional conditions often involve the use of a large excess of toxic reagents, such as amines,[24] or necessitate the use of extraction and chromatographic purification steps that involve the generation of waste from organic solvents and chromatographic stationary phases.[111]

In an effort to develop a general and green protocol useful for both the amination and (hetero)arylation of nitrogen heterocycles, we explored the use of different catalysts, phenol and $InCl_3$, carrying out the reactions under focused microwave (MW) irradiation that is able to heat the reactants without the need to heat the entire furnace or oil bath, leading to decreased reaction times and energy savings.

108 a) Pal, M.; Batchu, V. R.; Parasuraman, K.; Yeleswarapu, K. R. *J. Org. Chem.* **1993**, *68*, 6806; b) Pal, M.; Batchu, V. R.; Dager, I.; Swamy, N. K.; Padakanti, S. *J. Org. Chem.* **1995**, *70*, 2376; c) Kumar, S.; Sahu, D. P. *J. Heterocyclic Chem.* **2009**, *46*, 748.

109 Cheng, K. M.; Lee, C.; Klutchko, S.; Winters, T.; Reynolds, E. E.; Welch, K. M.; Flynn, M. A.; Doherty, A. M. *Bioorg. Med. Chem. Lett.* **1996**, *6*, 2999.

110 Hu, M. K.; Lu, C. F. *Tetrahedron Lett.* **2000**, *41*, 1815.

111 Melato, S.; Coghi, P.; Basilico, N.; Prosperi, D.; Monti, D. *Eur. J. Org. Chem.* **2007**, 6118.

3.2 Amination of π-deficient nitrogen heterocycles under MW irradiation in the presence of phenol

As mentioned in the Introduction, the acridine moiety constitutes the central core of many antiprion and antiprotozoan compounds (see Chapter 1.2).[28,30] Thus, we started our study with the amination of acridine derivatives, and to this end we examined the reactions between a variety of amines and 6,9-dichloro-2-methoxyacridine. In an effort to find out a general and green method, we sought conditions that avoided the use of solvents and excess of amine and that led to crude materials that were sufficiently pure to allow isolation of the final products without the need for extraction or chromatography. With this in mind, after some experimentation we found that the desired amination could be achieved very efficiently by irradiating equimolecular amounts of 6,9-dichloro-2-methoxyacridine, the suitable amine in presence of 2 equiv. of phenol that acts as the reaction medium and acid catalyst. The reaction was carried out under focalized MW irradiation at 150 W and 120 °C for 30-45 min achieving compound **1-12** (Scheme 3.1 and Table 3.1).[112] A control experiment using ethylenediamine under conventional conditions[113] (large excess of phenol, reflux overnight) afforded only a small amount of the desired compound, the major product being an acridin-9-one arising from the hydrolysis of the starting acridine.

112 **Staderini, M.**; Cabezas, N.; Bolognesi M. L.; Menéndez J. C. *Tetrahedron* **2013**, *69*, 1024.

113 a) de Souza, M. V. N.; Pais, K. C.; Kaiser, C. R.; Peralta, M. A.; de L. Ferreira, M.; Lourenço, M. C. S. *Bioorg. Med. Chem.* **2009**, *17*, 1474; b) Ressurreição, A. S.; Gonçalves, D.; Sitoe, A. R.; Albuquerque, I. S.; Gut, J.; Góis, A.; Gonçalves, L. M.; Bronze, M. R.; Hanscheid, T.; Biagini, G. A.; Rosenthal, P. J.; Prudêncio, M.; O'Neill, P.; Mota, M. M.; Lopes, F.; Moreira, R. *J. Med. Chem.* **2013**, *56*, 7679.

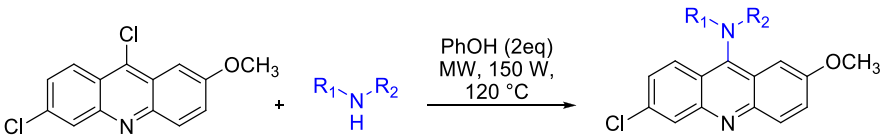

Scheme 3.1. General conditions for the amination of 6,9-dichloro-2-methoxyacridine

Phenol presumably acts by protonating the acridine nitrogen and thus increasing the electrophilicity of the halogenated C-9 position and promoting the attack from the nucleophile. The mechanism proposed for this transformation is represented in Scheme 3.2.

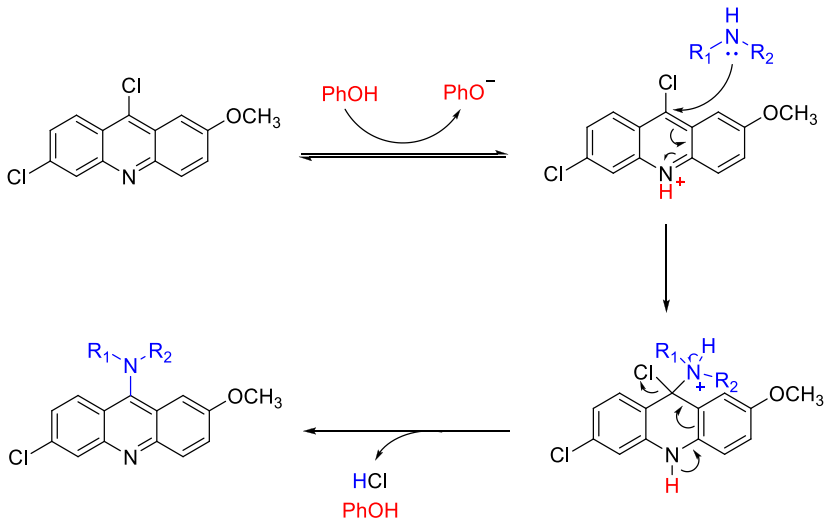

Scheme 3.2. Mechanism of action for the addition-elimination reaction in presence of phenol as acid catalyst.

This protocol worked equally well for aromatic (Table 3.1, entries 1-5), primary aliphatic (entries 6, 7), α-branched primary aliphatic (entry 8) and secondary aliphatic (entry 9) amines. A four-fold excess of ethylenediamine was needed in order to avoid products arising from double amination (entry 10), but it is noteworthy that similar reactions carried out under conventional conditions typically require an excess of up to 27 equiv. of the diamine.[24] In the case of less

reactive nitrogen nucleophiles, such as imidazole and benzimidazole, 2 equiv. of the nucleophile were needed (entries 11 and 12). Comparison of our results to those obtained using conventional conditions revealed consistent increases (7-53%) in the product yields together with dramatic shortening of reaction times in most cases. Most importantly, unlike the conventional method, compound

Table 3.1. Scope and yields of the synthesis of 9-aminoacridines

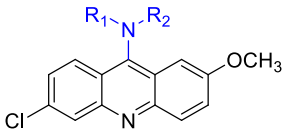

Entry	Cmpd.	R_1	R_2	MW-assisted conditions			Conventional conditions (reflux)			
				Eqs. of amine	Time min	Yield %	Eqs. of amine	Time	Yield %	Ref.
1	**1**	C_6H_5	H	1	30	95	1	90 min	88	102
2	**2**	4-MeO-C_6H_4	H	1	30	90	1	24 h	37	102
3	**3**	4-Me_2N-C_6H_4	H	1	45	94	2	24 h	70	28a
4	**4**	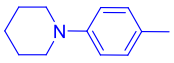	H	1	45	89	2	24 h	65	28a
5	**5**	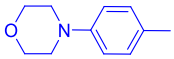	H	1	45	85	2	24 h	69	28a
6	**6**	*n*-Hex	H	1	30	88	40	4 h	61	114
7	**7**	C_6H_5-CH_2	H	1	30	98	--	--	--	--
8	**8**	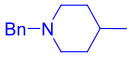	H	1	45	93	1.1	5 h	45	28
9	**9**			1	45	96	--	--	--	--
10	**10**	H_2N-CH_2-CH_2	H	4	30	82[a]	27	5 h	38	24
11	**11**			2	30	64	--	--	--	--
12	**12**			2	30	87	--	--	--	--

[a] Phenol was not necessary in this case.

114 Guetzoyan, L.; Yu, X. M.; Ramiandrasoa, F.; Pethe, S.; Rogier, C.; Pradines, B.; Cresteil, T.; Fauvet, M. P.; Mahy, J. P. *Bioorg. Med. Chem.* **2009**, *17*, 8032.

purification required simple washing of the crude with water followed by recrystallization, avoiding the use of volatile organic solvents.

As outlined in the Introduction, the bivalent strategy is a validated approach to design chemical entities to combat PrDs.[21] Since bivalent compounds could be accessible via the double amination of diamines, we also examined the possibility of achieving this transformation under our conditions. Indeed, as shown in Scheme 3.3, we found that treatment of a 1:2 mixture of piperazine and 6,9-dichloro-2-methoxyacridine under our usual conditions cleanly afforded compound **13** in 78% yield.

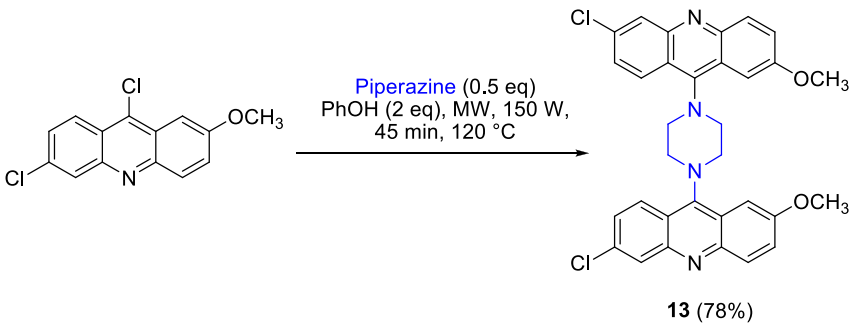

13 (78%)

Scheme 3.3. Double amination of a 9-chloroacridine

7-Chloroquinoline derivatives are also effective against prion replication and protozoan diseases.[33] Therefore, we studied the coupling of 4,7-dichloroquinoline and amines by applying our protocol. As in the case of the acridines, the reaction tolerated well the use of all structural types of amines affording compounds **14-21** (Scheme 3.4 and Table 3.2). Again, the use of diamines was possible (entries 4 and 5) affording compounds **17** and **18**, which have a functional group in their side chains that allows further structural manipulation. As shown in Table 3.2, our method required short reaction times and the yields were again excellent, generally speaking, and greatly improved the

results obtained under conventional conditions. Some of these reactions had been previously carried out under focused MW irradiation, albeit in different conditions involving the use of DMSO as solvent, and in slightly lower yields.[111]

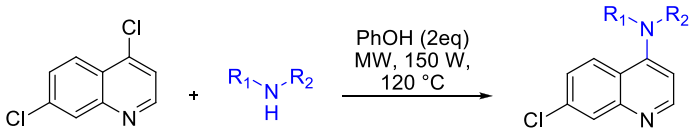

Scheme 3.4. Amination of 4-chloroquinolines

Table 3.2. Scope and yields in the synthesis of 4-aminoquinolines

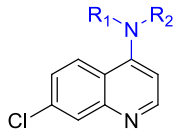

Entry	Cmpd.	R_1	R_2	MW-assisted conditions			Conventional conditions (reflux)			
				Eqs. of amine	Time min	Yield %	Eqs. of amine	Time	Yield, %	Ref.
1	**14**	4-MeO-C_6H_4	H	1	30	98	--	--	--	--
2	**15**	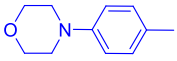	H	1	45	94[a]	--	--	--	--
3	**16**	C_6H_5-CH_2	H	1	30	91	2.1	10 h	80	115
4	**17**	H_2N-CH_2-CH_2	H	4	30	90[a]	5	7 h	75	115
5	**18**	H_3C-HN-CH_2-CH_2	CH_3	4	30	87	--	--	--	--
6	**19**	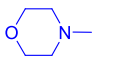		1	45	85[a]	--	--	--	--
7	**20**	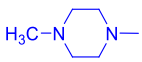		1	45	89	"excess"	4 h	80	116
8	**21**			2	30	85	--	--	--	--

[a]These compounds have also been prepared under microwave-assisted conditions, in DMSO solution, in yields of 85% (**15**), 94% (**17**), and 80% (**19**).[111]

115 Rojas Ruiz, F. A.; García-Sánchez, R. N.; Estupiñán, S. V.; Gómez-Barrio, A.; Torres Amado, D. F.; Pérez-Solórzano, B. M.; Nogal-Ruiz, J. J.; Martínez-Fernández, A. R.; Kouznetsov, V. V. *Bioorg. Med. Chem.* **2011**, *19*, 4562.

116 Warhurst, D. C.; Craig, J. C.; Adagu, I. S.; Guy, R. K.; Madrid, P. B.; Fivelman, Q. L. *Biochem. Pharmacol*. **2007**, *73*, 1910.

Because some 4-aminoquinazoline compounds have also been found active against prion amplification in a cell-based model,[102] we also examined briefly the amination reactions starting from 4-chloro-2-phenylquinazoline, which proceeded uneventfully under the previously established protocol to provide compounds **22-26** (Scheme 3.5 and Table 3.3). It is noteworthy that typical conventional conditions for similar transformations involve reflux in 1,4-dioxane for 24 h in the presence of 17 equiv. of amine.[117] Besides the drastically shorter reaction time, an improvement of up to 38% in the yields was again observed.

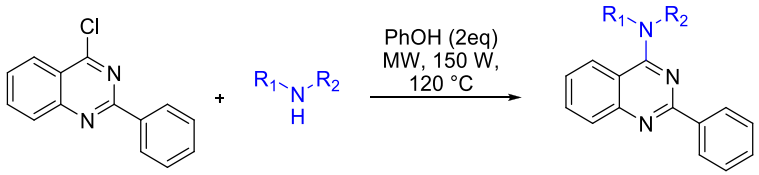

Scheme 3.5. Amination of 4-chloro-2-phenylquinazoline

Table 3.3. Scope and yields in the synthesis of4-chloro-2-phenylquinazoline

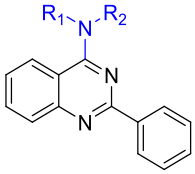

Entry	Cmpd.	R_1	R_2	MW-assisted conditions			Conventional conditions (reflux)			
				Eqs. of amine	Time min	Yield %	Eqs. of amine	Time	Yield %	Ref.
1	**22**	4-Cl-C_6H_4	H	1	30	98	2	18 h	50	117
2	**23**	C_6H_5-CH_2	H	1	30	94	17	24 h	84	117
3	**24**	$(H_3C)_2N$-CH_2-CH_2	H	1	30	91	2	18 h	83	102
4	**25**	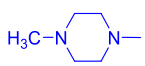		1	45	90	17	24 h	88	117
5	**26**			2	30	87	--	--	--	--

117 Nguyen, L. T.; Yang, S. H.; Khadka, D. B.; Van, H. T. M.; Cho, S. H.; Kwon, Y. J.; Lee, E. S.; Lee, K. T.; Cho, W. J. *Bioorg. Med. Chem.* **2011**, *19*, 4399.

In order to confirm the versatility of our protocol, we decided to study its application to the synthesis of two representative target molecules with well-established pharmacological activity. Thus, as shown in Scheme 3.6, the reaction between 9-chloroacridine and the commercially available *N*-(4-amino-3-methoxy)methanesulfonamide under our standard conditions afforded a 78% yield of the topoisomerase II inhibitor amsacrine (**27**), a currently marketed antileukemic drug.

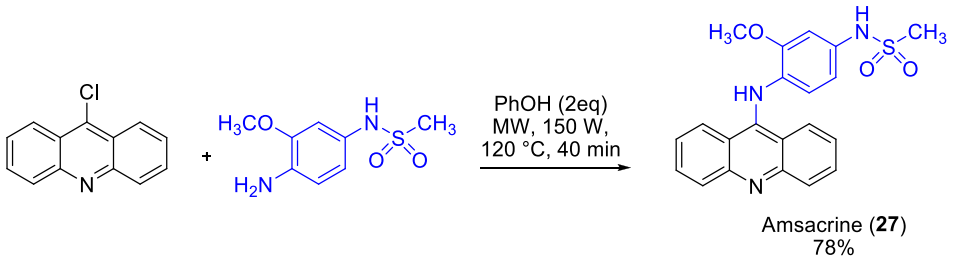

Scheme 3.6. Synthesis of amsacrine

The synthesis of bis(7)-tacrine using our methodology, providing a new example of a double amination *via* a pseudo-three-component reaction, is summarized in Scheme 3.7. The starting 9-chloro-1,2,3,4-tetrahydroacridine was prepared by a literature method,[118] refluxing anthranilic acid and cyclohexanone in a large excess of $POCl_3$. Afterwards, compound **28** was treated with half an equivalent of 1,7-heptanediamine under our microwave conditions to give bis(7)-tacrine (**29**) in 98% yield, which compares very favourably with the literature yield for this reaction under conventional heating conditions (47% yield after 2 h at 180 °C in a sealed tube containing phenol).[110]

118 Szymanski, P.; Karpiński, A.; Mikiciuk-Olasik, E. *Eur. J. Med. Chem.* **2011**, *46*, 3250.

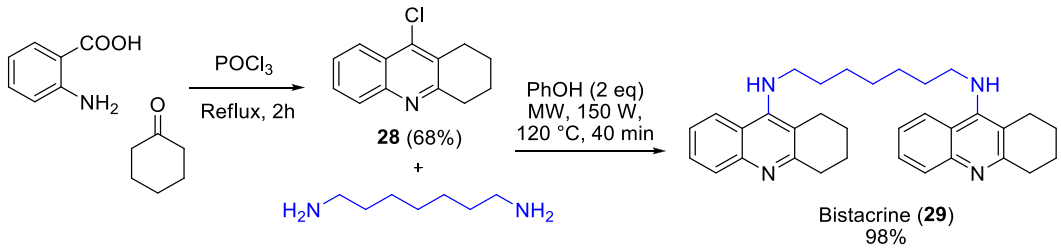

Scheme 3.7. Synthesis of bistacrine

Finally, we studied the application of our method to the generation of carbon-carbon bonds by treating 4,7-dichloroquinoline with indole. This heterocycle acted as enamine-like nucleophile and the reaction proceeded at the C-3 position to provide compound **30** together with a side product derived from 4-phenoxyquinoline in a 3:1 ratio. Unfortunately, in the case of a less reactive nucleophile such as ethyl 3-aminocrotonate, the phenoxy derivative was the main reaction product and the desired product **31** was obtained only in 29% yield (Scheme 3.8).

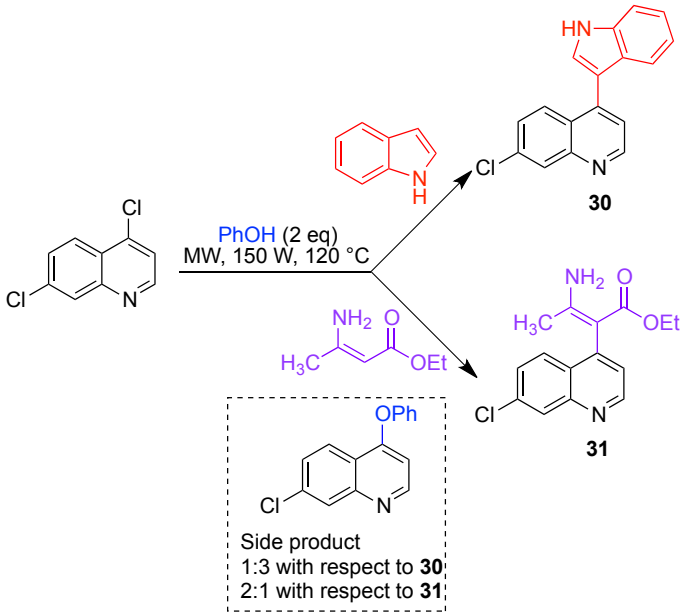

Scheme 3.8. Coupling reaction in the presence of phenol between 4,7-dichloroquinoline and indole and ethyl 3-aminocrotonate to afford **30** and **31**, respectively.

3.3. Lewis acid–catalyzed generation of C-C and C-N bonds on nitrogen heterocycles

In an effort to avoid the generation of the undesired phenoxy side product, we planned to replace phenol by a non-nucleophilic catalyst. Because of the near absence of precedent for the use of Lewis acids for this purpose, we were attracted to the study of this type of catalysts.

Due to the importance of the 7-chloroquinoline moiety as antiprion agent, we focused again on this fragment. In our first experiments, several Lewis acids, including CAN (cerium ammonium nitrate) and ytterbium (III) triflate, were assayed unsuccessfully. Subsequent work gave positive results with indium triflate, gallium trichloride, boron trifluoride etherate and indium chloride. After discarding the highly hygroscopic $In(OTf)_3$ and $GaCl_3$, we chose $InCl_3$ for further experiments because this catalyst is inexpensive, relatively stable and gave a slightly higher yield than $BF_3.Et_2O$ (Table 3.4). The best conditions were found to involve the reaction between equimolecular amounts of 4,7-dichloroquinoline and indole and 10% mol of $InCl_3$ in acetonitrile under focused MW irradiation at 150 W and 120 °C for 2 h to furnish **30** as the only product in 89% yield (Scheme 3.11 and Figure 3.2).[119] Since we did not employ rigorously dried solvents, it is likely that the catalyst experiences some hydrolysis under the reaction conditions. We therefore examined the catalytic effect of $In(OH)_3$ and In_2O_3, the likely hydrolysis products, but found them to be inactive (Table 3.4). This protocol worked equally well for other nucleophilic heterocycles such as pyrrole (**32**) and 4-hydroxycoumarin (**33**), for which only one hour was needed after increasing the temperature to 140 °C. In the case of 2-methylfuran (**34**), the reaction was carried during 3 h in dichloromethane (Figure 3.2).

119 **Staderini, M.**; Bolognesi, M. L.; Menéndez, J. C. *Adv. Synth. Cat.* **2015**, *357*, 185.

Table 3.4. Catalyst optimization[a]

Catalyst (10 mol%)	Yield, %
CAN	0
$Yb(OTf)_3$	0
$In(OTf)_3$	83
$GaCl_3$	84
$BF_3.Et_2O$	82
$InCl_3$	89
In_2O	0
$In(OH)_3$	0

[a]Reaction conditions: acetonitrile, MW, 150 W, 120 °C, 180 psi, 2 h

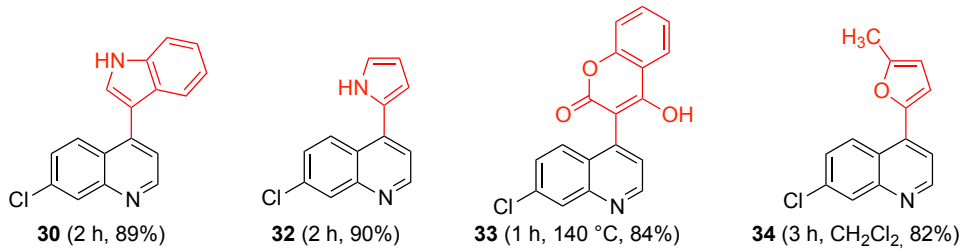

30 (2 h, 89%) **32** (2 h, 90%) **33** (1 h, 140 °C, 84%) **34** (3 h, CH_2Cl_2, 82%)

Figure 3.2. C-C bond forming reactions with heterocycles at the quinoline C-4 position

In view of the synthetic importance of β-enaminones and the poor results obtained in the preparation of compound **31** with the phenol-promoted method, we attempted the application of the new conditions to this case, achieving a good 75% yield. In order to examine the generality of this protocol, we prepared a series of β-enamino esters *via* the CAN-catalyzed reaction between the suitable primary amine and ethyl acetoacetate (Scheme 3.9 and Table 3.5),[120] whereas pyrrolidine, a secondary amine, was treated with ethyl acetoacetate in the absence of catalyst and solvent.[121] We noted that the primary amines lead to the formation of the desired product exclusively as *Z*-isomers, presumably because

120 Sridharan, V.; Avendaño, C.; Menéndez, J. C. *Synlett* **2007**, *6*, 881.
121 Vohra, R. K.; Renaud, J. L.; Bruneau, C. *Synthesis* **2007**, *5*, 731.

of the hydrogen bonding interaction between the amino and carbonyl groups, whereas in the case of a secondary amine only the *E*-isomer was isolated (compound **40**).

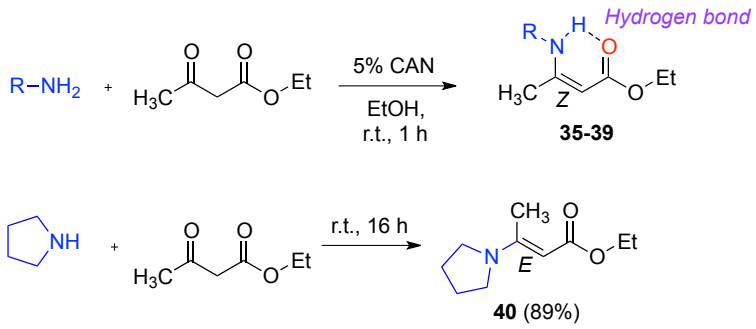

Scheme 3.9. General procedure for the synthesis of β-enamino esters

Table 3.5. Scope and yields of the synthesis of β-enamino esters from primary amines

Entry	Cmpd.	R	Yield, %
1	**35**	CH_3	71
2	**36**	*n*-But	77
3	**37**	*sec*-But	82
4	**38**	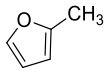	85
5	**39**	C_6H_5-CH_2	81

The *Z*-β-enaminones **35-39** reacted with quinoline to give the novel vinylation products **41-45** (Figure 3.3), which are of interest in view of the important role of β-enaminones as starting materials for synthesis.[122]

122 a) Govindh, B.; Diwakar, B. S.; Murthy, Y. L. N. *Org. Comm*. **2012**, *5*, 105; b) Suryavanshi, P. A.; Sridharan, V.; Menéndez, J. C. *Chem. Eur. J.* **2013**, *19*, 13207.

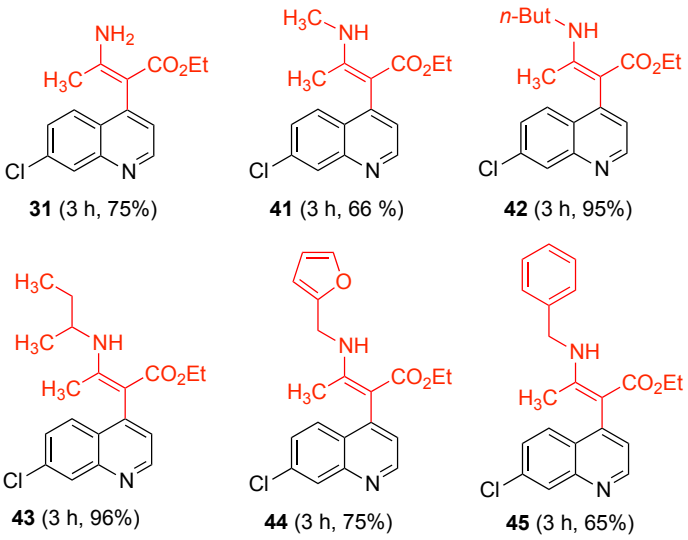

Figure 3.3. C-C bond forming reactions with β-enaminones at the quinoline C-4 position

To the contrary, the attempted reaction between 4,7-dichloroquinoline and compound **40** as *E*-isomer failed, probably due to the steric hindrance of the pyrrolidino group that hampers the nucleophilic attack to the heterocycle (Scheme 3.10).

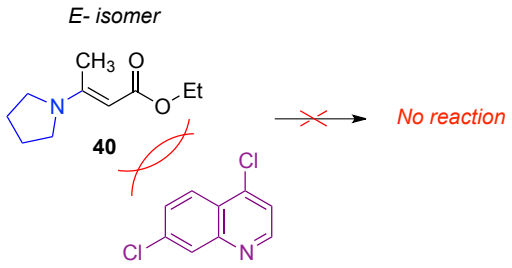

Scheme 3.10. An *E*-β-aminoester was not able to react with quinoline

Because the importance of β-amino acids and their related esters for their biological and pharmacological activities,[123] we studied the reduction of the C=C double bond in compounds **31** and **42**. Unfortunately, all our attempts using

123 Singh,G. S. *Mini-Rev. Med. Chem.***2004**, *4*, 96.

sodium triacetoxyborohydride,[124] generated *in situ* from sodium borohydride and acetic acid, $LiAlH_4$ and hydrogen in the presence of several catalysts were unsuccessful.

For comparison purposes, we carried out a few of our reactions under reflux conditions and also by heating in a sealed tube at 120 °C, which mimicked more closely the temperature conditions existing in the microwave experiments. We found dramatic differences in favor of the MW-assisted protocol in terms of both yields and decreased reaction times (Table 3.6).

Table 3.6. Comparison between reflux, heating in a sealed tube and microwave heating in the C-C coupling reactions of 4,7-dichloroquinoline

Cmpd.	Reflux	Sealed tube heating (120 °C)	MW
30	---	15 h, 69%	2 h, 89%
31	3 d, 45%	24 h, 25%	3 h, 82%
32	1 d, 50%	15 h, 72%	2 h, 90%
33	1 d, 62%	---	1 h, 84%[a]
44	1 d, 27%	15 h, 45%	3 h, 87%

[a] This experiment was performed at 140 °C

These encouraging results prompted us to extend the $InCl_3$–catalyzed method to other heterocyclic substrates, starting with 6,9-dichloro-2-methoxyacridine. These new reactions showed a similar scope to the ones starting from 4,7-dichloroquinoline, and afforded the target acridine derivatives **46-50** in excellent 84-93% isolated yields (Figure 3.4).

124 Sridharan, V.; Menéndez, J. C. *Org. Lett.* **2008**, *10*, 4303.

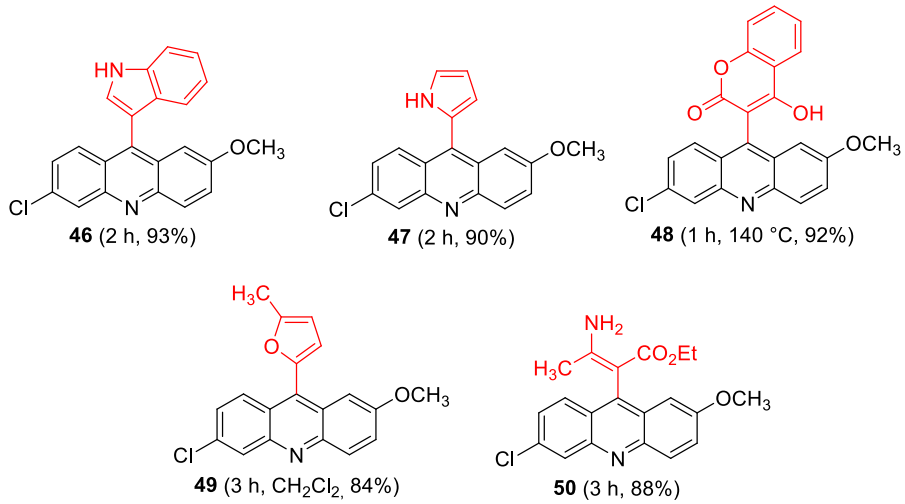

Figure 3.4. C-C bond forming reactions at the acridine C-9 position.

Finally, we also investigated the formation of C-C bonds at two other pharmaceutically relevant heterocyclic substrates, such as quinazoline and quinoxaline.[98] As shown in Figure 3.5, the results obtained were again satisfactory, and these reactions allowed the preparation of compounds **51-57**. 2-(3-Indolyl)quinoxaline **56** had been previously obtained in 47% overall yield *via* a multistep sequence based on the construction of the quinoxaline ring from an indole ketoaldehyde precursor,[105d] or in two steps and 58% overall yield from 3-acetylindole.[105c] Rather surprisingly, the reaction between 4-hydroxycoumarin and 2-chloroquinoxaline afforded the O-arylation product **58**, while its treatment with ethyl 3-aminocrotonate generated a C-C bond at the quinoxaline C-3 position to give **59**, as expected. Some of the reactions (*i.e.* those leading to **54**, **58** and **59**) gave comparatively low yields, which was due to the recovery of unreacted starting material. These results could not be improved by increasing the reaction times. The regioselective formation of compound **59** is noteworthy in that it must involve an addition to the position α to the halogen atom, followed by air oxidation of the initial adduct, instead of the usual addition to the

position *ipso* to the halogen followed by elimination of hydrogen halide. This behavior is relatively common in reactions involving hindered C-nucleophiles and ambivalent, monohalogenated electrophiles such as haloquinones,[125] and is probably due to steric effects.

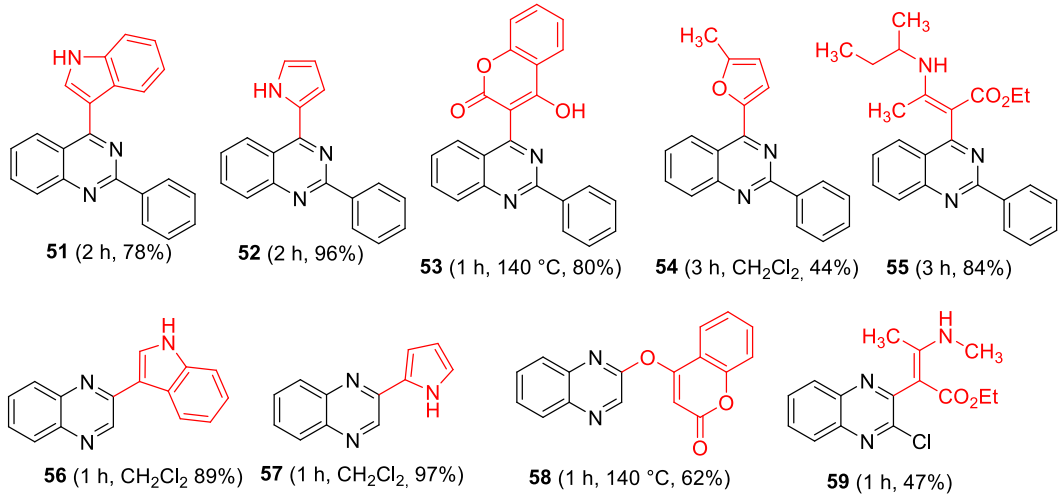

Figure 3.5. C-C bond forming reactions at the quinazoline C-4 and quinoxaline C-2 positions.

To summarize, our protocol allows the efficient CH functionalization of several heterocycles and Z-β-enaminones and their coupling to a variety of p-deficient heterocyclic substrates. The isolated yields obtained were in the 71–96% range, and the method was more general and efficient than the previously mentioned one based on the use of $AlCl_3$[108c] in that only catalytic amounts of $InCl_3$ were required and, furthermore, the activation of the substrate by the introduction of strong electron-withdrawing groups was not necessary (Scheme

125 For representative examples, see: a) Alonso, M. A.; López-Alvarado, P.; Avendaño, C.; Menéndez, J. C. *Tetrahedron* **2003**, *59*, 2821; b) Manzanaro, S.; Vicent, M. J.; Martín, M. J.; Salvador-Tormo, N.; Pérez, J. M.; Blanco, M. M.; Avendaño,C.; Menéndez, J. C.; de la Fuente, J. A. *Bioorg. Med. Chem*. **2004**, *12*, 6505.

3.11). Unfortunately, the coupling reaction with heteroarenes or β-enamino esters failed in the cases of purine, benzimidazole and pyridine substrates.

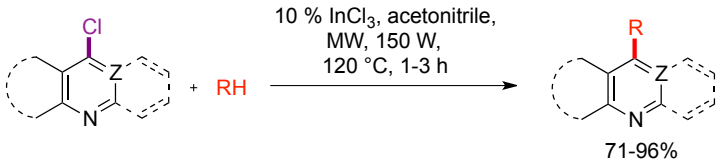

Scheme 3.11. General scheme illustrating the formation of C-C carbon bonds at π-deficient heterocyclic substrates

At this stage, we decided to study the extension of the new conditions to the S_NAr displacement of halogen atoms by amines in π-deficient heterocyclic substrates. While the previously developed phenol-catalyzed conditions overcame many drawbacks found using conventional procedures, only three heterocyclic nuclei were explored, namely acridine, quinoline and quinazoline. In addition, the toxicity and corrosive nature of phenol detracted from the user-friendliness and sustainability of the method. When tested on the 4,7-dichloroquinoline substrate, $InCl_3$ catalysis turned out to be extremely efficient for the reaction with aromatic, primary aliphatic and secondary aliphatic amines, and was also useful for the *N*-arylation of benzimidazole (Scheme 3.12 and Figure 3.6). Furthermore, compound isolation required simple filtration and no further purification was needed, and hence the use of volatile organic solvents in extraction and chromatographic purification steps was unnecessary.

MW irradiation was essential for success, as shown by the comparison of the conditions required and the yields obtained for the synthesis of **60** and **61** under reflux (Figure 3.7). This new method was also compared with our previous described protocol involving MW irradiation of the starting materials in the presence of two equivalents of phenol.[112] Reaction times and yields were similar but, since the new protocol avoided the use of the toxic and corrosive phenol, it

can be regarded as meeting more stringent green chemistry requirements. Furthermore, for the first time a Lewis acid was shown to be an effective catalyst for this type of amination reactions.

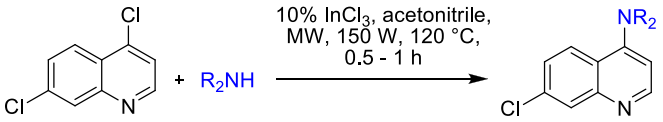

Scheme 3.12. C-N coupling reactions of 4,7-dichloroquinoline

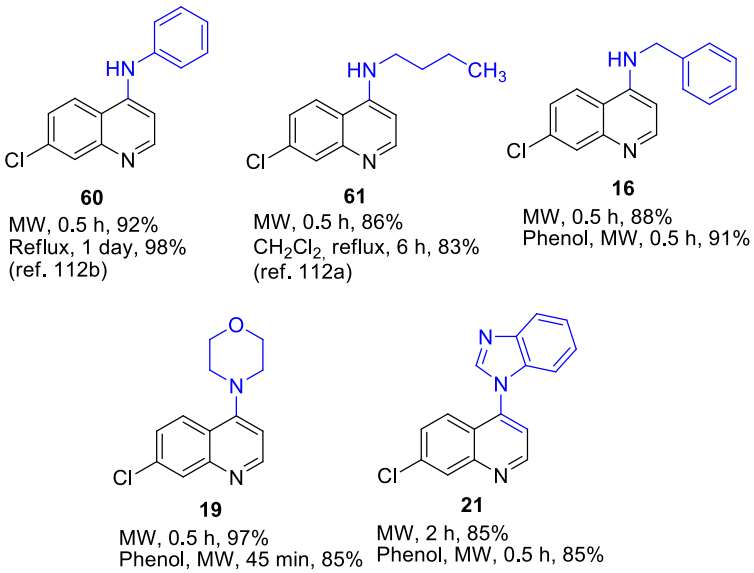

Figure 3.6. C-N bond forming reactions at the quinoline C-4 position

The coupling of 6,9-dichloro-2-methoxyacridine with representative amines was also carried out, affording compounds **5-7**, **9** and **11** in excellent yields as precipitates that, after filtration, did not require further purification (Figure 3.7). As in the case of quinoline, the reaction tolerated well the use of different structural types of amines. Similar results were obtained for quinazoline derivatives **23-25** and **62-63** (Figure 3.7). A comparison with the results obtained for these compounds employing our first-generation method revealed similar

yields, although the previously mentioned advantages associated to the avoidance of phenol are noteworthy. A considerable improvement of the yield of the imidazolyl derivative **11** was observed with regard to our previous method, and comparison with the literature revealed our protocol to give improved yields in the cases when a comparison was possible,[126] avoiding the use of phenol or bulky phosphonium ligands.[127]

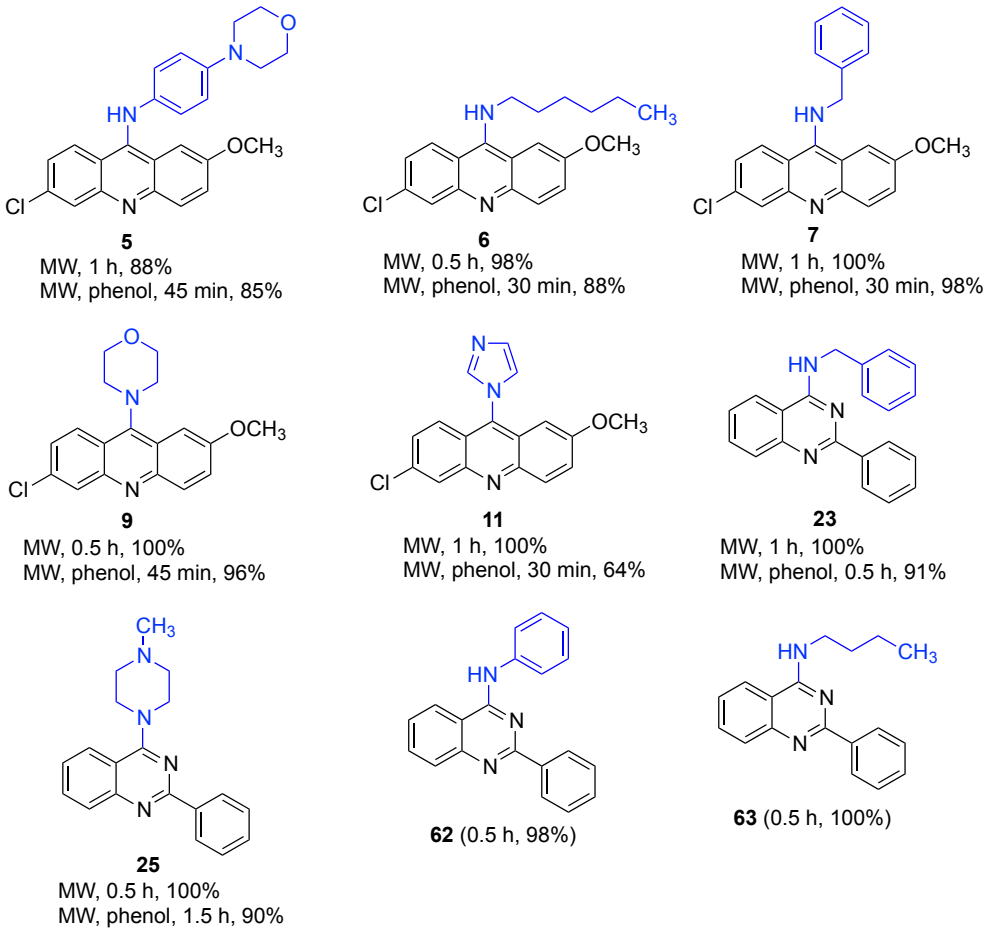

Figure 3.7. C-N bond forming reactions at the acridine and quinazoline C-9 and C-4 positions, respectively.

126 Xing, Z. Y.; Fu, Y.; Ye, F. *J. Heterocycl. Chem.* **2012**, *49*, 1210.

127 Wan, Z. K.; Wacharasindhu, S.; Levins, C. G.;Lin, M.;Tabei, K.; Mansour, T. S. *J. Org. Chem.* **2007**, *72*, 10194.

In order to confirm the generality of our new protocol, we examined the reactivity towards amines of several additional halogenated nitrogen heterocycles, namely 2-chloroquinoxaline,[128] 4-chloropurine,[129] 2-chloro-benzimidazole[101b,130] and 2-chloropyridine[131] and obtained excellent yields of compounds **64-78**, for which no general method of synthesis was available (Figure 3.8).

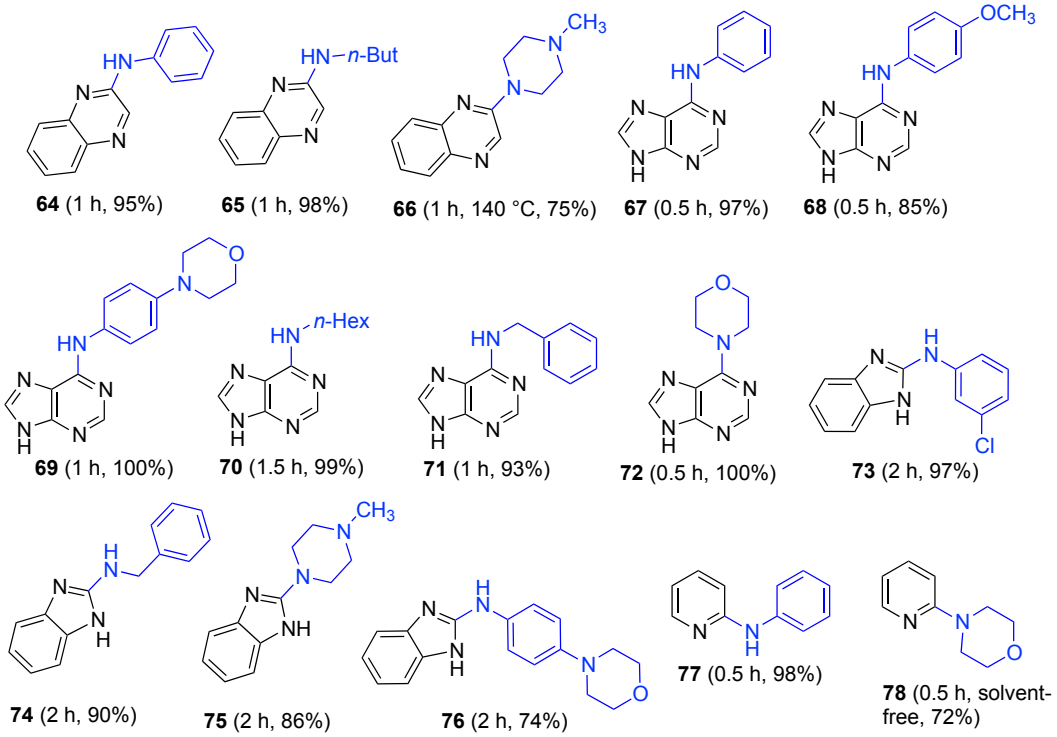

Figure 3.8. C-N bond forming reactions at the quinoxaline C-2, purine C-6, benzimidazole C-2 and pyridine C-2 positions.

128 a) Saari, R.; Törmä, J. C.; Nevalainen, T. *Bioorg. Med. Chem.* **2011**, 19, 939; b) Smits, R. A.; Lim, H. D.; Hanzer, A.; Zuiderveld, O. P.; Guaita, E.; Adami, M.; Coruzzi, G.; Leurs, R.; de Esch, I. J. *J. Med. Chem.* **2008**, *51*, 2457; c) Iijima, C.; Kyo, T. *Chem. Pharm. Bulletin* **1989**, *37*, 618.

129 a) Huang, L. K.; Cherng, Y. C.; Cheng, Y. R.; Jang, J. P.; Chao, Y. L.; Cherng, Y. J. *Tetrahedron*, **2007**, *63*, 5323; b) Qu, G.; Han, S.; Zhang, Z.; Geng, M.; Xue, F. *J. Braz. Chem. Soc.* **2006**, *17*, 915; c) Adamska, E.; Barciszewski, J.; Markiewicz, W. T. *Nucleosides, Nucleotides Nucleic Acids*, **2012**, *31*, 861.

130 a) Yella, R.; Patel, B. K. *J. Comb. Chem.* **2010**, *12*, 754; b) Verma, S. K.; Acharya, B. N.; Kaushik, M. P. *Org. Biomol. Chem.* **2011**, *9*, 1324.

131 Wagaw, S.; Buchwald, S. L. *J. Org. Chem.* **1996**, *61*, 7240.

As a final refinement, we applied our method to the synthesis of several representative drugs having both antimalarial and antiprion activities,[132] including amodiaquine, chloroquine and quinacrine. Thus, the reaction under our standard conditions between 4,7-dichloroquinoline and the commercially available 5-diethylaminopentan-2-amine afforded chloroquine (**79**), while the use of 4-amino-2-(diethylaminomethyl)-*o*-cresol furnished amodiaquine (**80**) in 73% and 71% yields, respectively (Scheme 3.13). Similarly, quinacrine (**81**) was prepared in good yield (75%) by reaction between 6,9-dichloro-2-methoxyacridine and 5-diethylaminopentan-2-amine (Scheme 3.14).

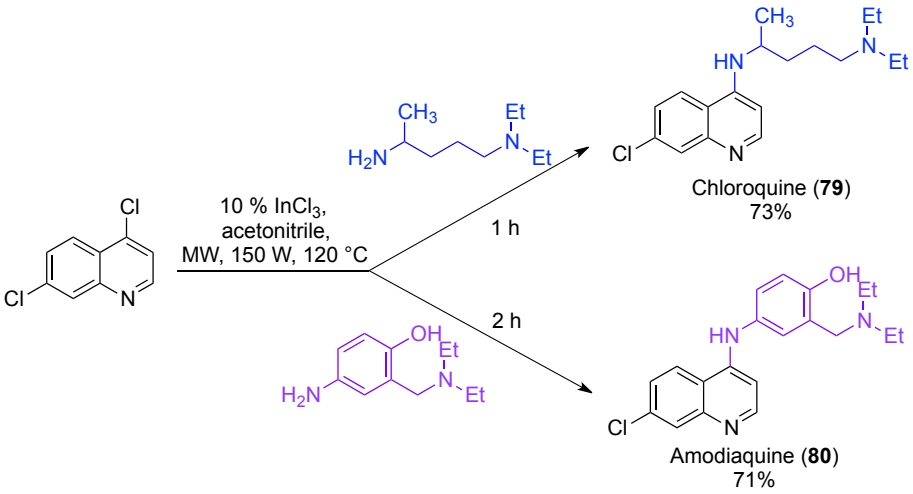

Scheme 3.13 Synthesis of chloroquine and amodiaquine.

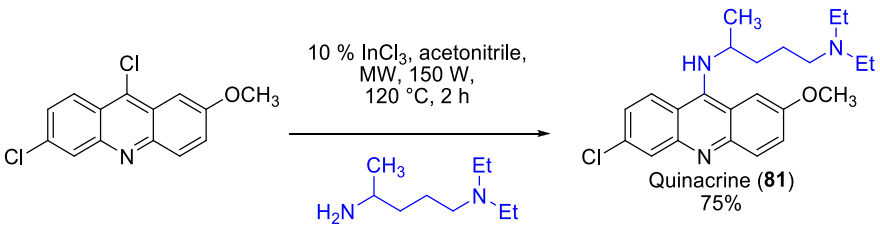

Scheme 3.14. Synthesis of quinacrine

132 Kaur, K.; Jain, M.; Reddy, R. P.; Jain, R. *Eur. J. Med. Chem.* **2010**, *45*, 3245.

The last proof of the versatility of our protocol came from an example of a double amination, in which we carried out again the synthesis of the anti-Alzheimer drug bis(7)-tacrine **29**. To this end, 9-chloro-1,2,3,4-tetrahydroacridine **28** was treated with half an equivalent of 1,7-heptanediamine in the presence of $InCl_3$ under our usual MW conditions to give the target compound in 88% yield (Scheme 3.15).

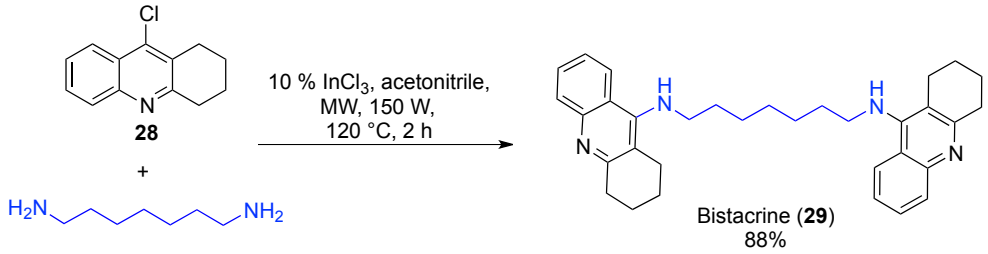

Scheme 3.15. Synthesis of the anti-Alzheimer drug bistacrine

Besides using this methodology for other parts of our work, the library of heterocycles described in this chapter is currently being studied by virtual screening methods at the group led by Dr. Sonsoles Marín-Santamaría, at CIB, Madrid.

4. Diketopiperazine based-ligands of prion protein

4.1. Design rationale

As outlined in the Introduction, most of the anti-prion compounds possess a symmetrical bifunctional structure, consisting of two moieties joined *via* an appropriate spacer. In general, for all these compounds the role of the spacer has been demonstrated to be critical in the molecular recognition process.[21] Therefore, in our search for novel bifunctional molecules, we initially focused on a nucleus that could provide the ideal features to interact with protein surfaces by behaving as a peptidomimetic. In this connection, the peptidic nature of diketopiperazines (DPKs) and their occurrence in biologically active natural products has inspired the use of DKP scaffolds as privileged structures. Furthermore, DKPs are able to modulate PPIs,[133] are synthetically readily accessible,[134] have neuroprotective activity,[135] can cross the blood brain barrier (BBB)[136] and have been extensively explored in medicinal chemistry.[137]

Therefore, it seemed conceivable that DKPs carrying (*Z*)-alkene units of general structure **I** (Figure 4.1) could serve as a template supporting a diverse array of pharmacophores towards the identification of novel bifunctional structures for prion diseases. Building on this concept, a compound library was generated by appending several aromatic and heteroaromatic rings at C-3 and C-6 of the 3,6-dimethylenepiperazine-2,5-dione scaffold (Figure 4.1).[138] The role of aromatic residues in molecular recognition and self-assembly processes leading

133 Niida, A.; Tanigaki, H.; Inokuchi, E.; Sasaki, Y.; Oishi, S.; Ohno, H.; Tamamura, H.; Wang, Z.; Peiper, S. C;. Kitaura, K.; Otaka, A.;Fujii, N. *J. Org. Chem.* **2006**, *71*, 3942.

134 Horton, D. A.; Bourne, G. T.;Smythe, M. L. *J. Comput. Aided Mol. Des.* **2002**, *16*, 415.

135 Faden, A.I.; Knoblach, S.M.; Movsesyan, V.A.; Cernak, I. *J. Alzheimers Dis.* **2004**, *6*, S93.

136 Teixido, M.; Zurita, E.; Malakoutikhah, M.; Tárrago, T.; Giralt, E. *J. Am. Chem. Soc.* **2007**, *129*, 11802.

137 O'Neill, J. C.;Blackwell, H. E. *Comb. Chem. High Throughput Screen* **2007**, *10*, 857.

138 Bolognesi, M. L.; Tran, H. N. A.; **Staderini, M.**; Monaco, A.; Lopez-Cobeñas, A.; Bongarzone, S.; Biarnes, X.; López-Alvarado, P.; Cabezas, N.; Caramelli, M.; Carloni, P.; Menéndez, J. C.; Legname, G. *ChemMedChem* **2010**, *5*, 1324.

to various fibrillar aggregates has been recognized as critical. Targeting these aromatic residues has been consequently proposed as an important strategy to inhibit amyloid formation.[139] The choice of pyridine[140] and quinoline[141,34] was dictated by the fact that these nuclei are quite frequent in antiprion compounds. Furan, thiophene and benzene derivatives were then also synthesized to enlarge the library chemical diversity. Heteroaromatic β-carboline derivatives were purposely designed with the aim to obtain potential fluorescent probes, owing to the excellent native fluorescence found in carboline systems[142] that has led to their use as probes for biomolecules.[143] To study the importance, if any, of an appropriate planar conformation, some monoreduced (structure **II**, Figure 4.1) and a saturated derivative (structure **III**, Figure 4.1) were also synthesized.

139 Frydman-Marom, A.; Rechter, M.; Shefler, I.; Bram, Y.; Shalev, D. E.; Gazit,E. *Angew. Chem. Int. Ed. Engl.* **2009**, *48*, 1981.

140 a) Perrier, V.; Wallace, A. C.; Kaneko, K.; Safar, J.; Prusiner, S. B.; Cohen, F. E. *Proc. Natl. Acad. Sci. U S A* **2000**, *97*, 6073; b) Reddy, T. R.; Mutter, R.; Heal, W.; Guo, K.; Gillet, V. J.; Pratt, S.; Chen, B. *J. Med. Chem.* **2006**, *49*, 607.

141 Klingenstein, R.; Melnyk, P.; Leliveld, S. R.; Ryckebusch, A.; Korth, C. *J. Med. Chem.* **2006**, *49*, 5300.

142 Martin, L.; Olives, A. I.; del Castillo, B.; Martin, M. A. *Luminescence* **2005**, *20*, 152.

143 Garcia-Zubiri, I. X.; Burrows, H. D.; Seixas de Melo, J. S.; Monteserin, M.; Arroyo, A.; Tapia, M. J. *J. Fluoresc.* **2008**, *18*, 961.

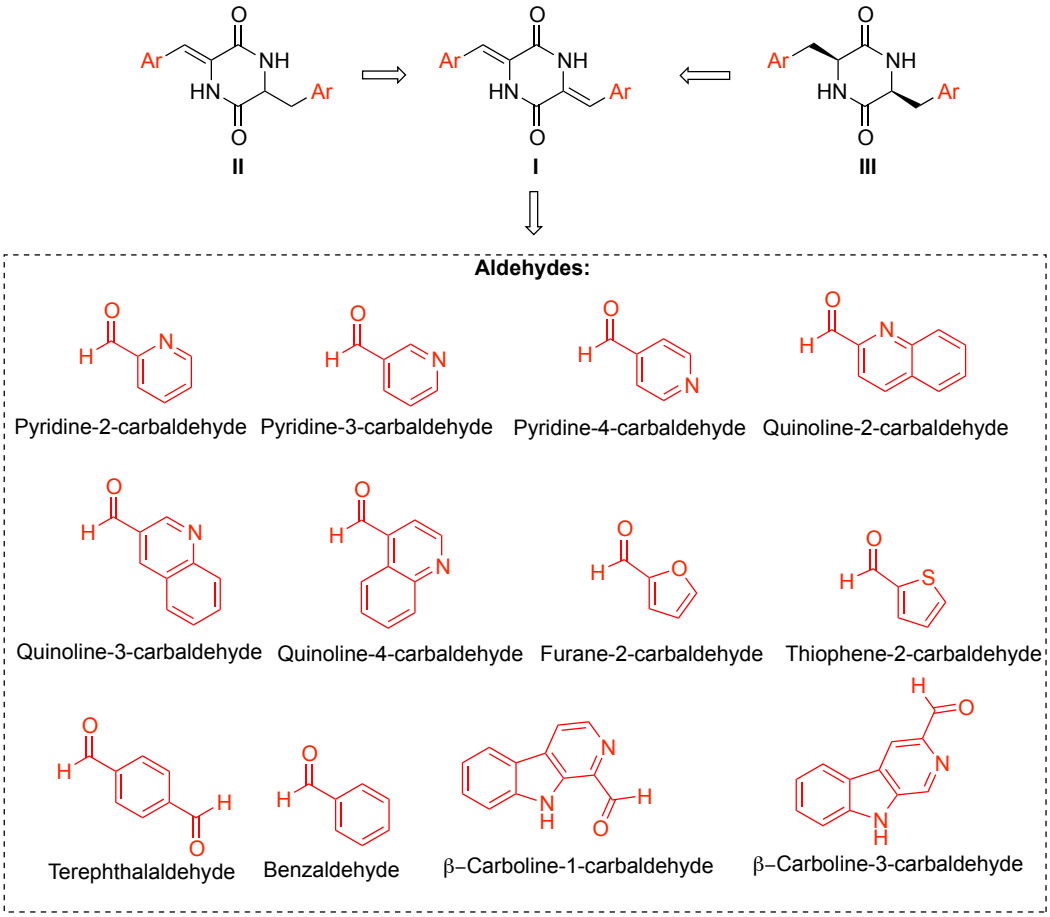

Figure 4.1. Chemical structure of the DKPs described in this chapter

4.2 Library synthesis

The preparation of 3,6-bis(arylmethylene)-2,5-piperazinedione compounds was achieved in a single step by using a pseudo-three-component reaction that involves a double condensation of 1,4-diacetylpiperazine-2,5-dione with two molecules of an aromatic aldehyde. Piperazine-2,5-dione is the result of a self-condensation of glycine and was available in the laboratory as glycine anhydride. The first step of our route consisted of the acetylation of the piperazine-2,5-dione nitrogen atoms in order to avoid the interference of their acidic protons. Furthermore, nitrogen acetylation promotes the subsequent condensation reaction by increasing the acidity of protons in α to carbonyl groups, due to the electron-withdrawing effect of the acetate group. For the preparation of the starting compound, the commercial glicyne anhydride was refluxed in acetic anhydride during three hours, affording compound **82** in 97% yield (scheme 4.1).

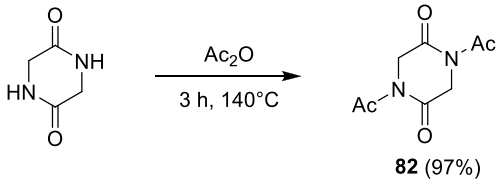

Scheme 4.1. Synthesis of 1,4-diacetylpiperazine-2,5-dione

For the double condensation reactions, we employed conditions based on those described by Katritzky,[144] which involve treatment of 1,4-diacetylpiperazine-2,5-dione (**82**) with two equivalents of the suitable aromatic aldehydes in dimethylformamide as solvent, using two equivalents of

144 Katritzky, A. R.; Fan, W. Q.; Szajda, M.; Li, Q. L.; Caster, K. C. *J. Heterocycl. Chem.* **1988**, *25*, 591.

triethylamine as base. In our initial experiments involving pyridine-2-carbaldehyde, pyridine-3-carbaldehyde and pyridine-4-carbaldehyde, the reactions were carried out at room temperature and afforded the double condensation products **83-85** in acceptable or good yields. Similar conditions were also applied to the case of quinoline-4-carbaldehyde, which furnished compound **86** in 84% yield. However, when the same room temperature conditions were applied to quinoline-2-carbaldehyde and quinoline-3-carbaldehyde, the only products that could be isolated, even after very long reaction times (4 days), were the monocondensation derivatives **87** and **88**. A similar result was obtained for benzaldehyde, studied as a model case, which gave compound **89**. The preparation of the double condensation products **90**, **91** and **92** required the use of harsher reaction conditions (refluxing DMF, larger excess of triethylamine, more concentrated solutions where Et_3N/DMF = 4:1 v/v). The lower reactivity generally observed for the quinoline aldehydes with regard to their pyridine counterparts can be attributed to delocalization of the electron-withdrawing effect of the nitrogen atom throughout the more extended aromatic system, while the different reactivity of the quinoline-2- and -3-carbaldehydes can be attributed to the steric effect of the nitrogen lone pair in the former case. These harsh conditions were also employed for the reactions involving other aromatic aldehydes such as terephtaldeyde, furan-2-carbaldehyde and thiophene-2-carbaldehyde, to furnish compounds **93**, **94** and **95** in good yields (Scheme 4.2).

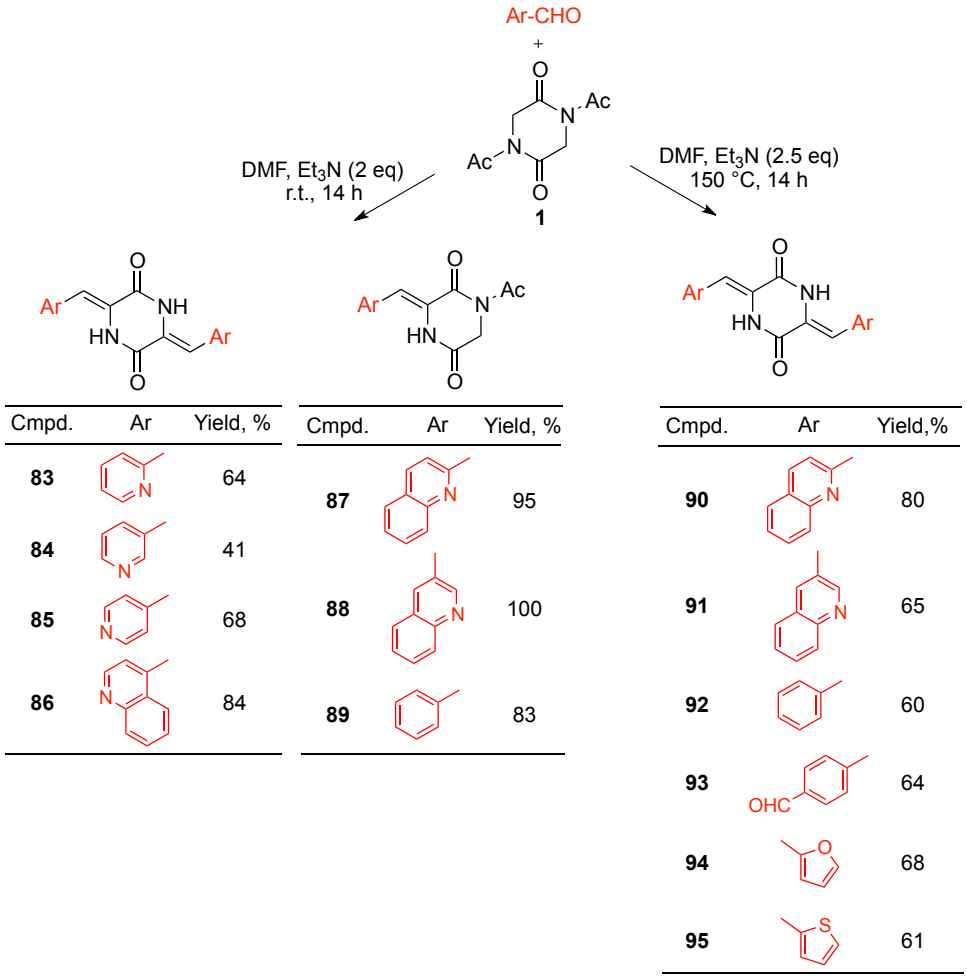

Cmpd.	Ar	Yield, %
83		64
84		41
85		68
86		84

Cmpd.	Ar	Yield, %
87		95
88		100
89		83

Cmpd.	Ar	Yield,%
90		80
91		65
92		60
93		64
94		68
95		61

Scheme 4.2. Scope and yields of the syntheses of mono and double condensation products

The reaction mechanism for the double condensation reaction is complex and involves anchimeric assistance from the *N*-acetyl substituents, which are lost in the course of the reaction.[145] Thus, the initial addition reaction involving the active methylene and the aldehyde molecule is followed by intramolecular transfer of the acyl group to the oxygen atom belonging initially to the aldehyde

145 (a) Gallina, C.; Liberatori, A. *Tetrahedron Lett*, **1973**, *14*, 1135. (b) Gallina, C.; Liberatori, A. *Tetrahedron*, **1974**, *30*, 667.

and a final elimination of acetate. These reactions lead exclusively to the *Z* isomer, probably because the *E* compound is de-stabilized by repulsive interactions between the aryl substituents and the carbonyl groups. The proposed mechanism is depicted in Scheme 4. 3.

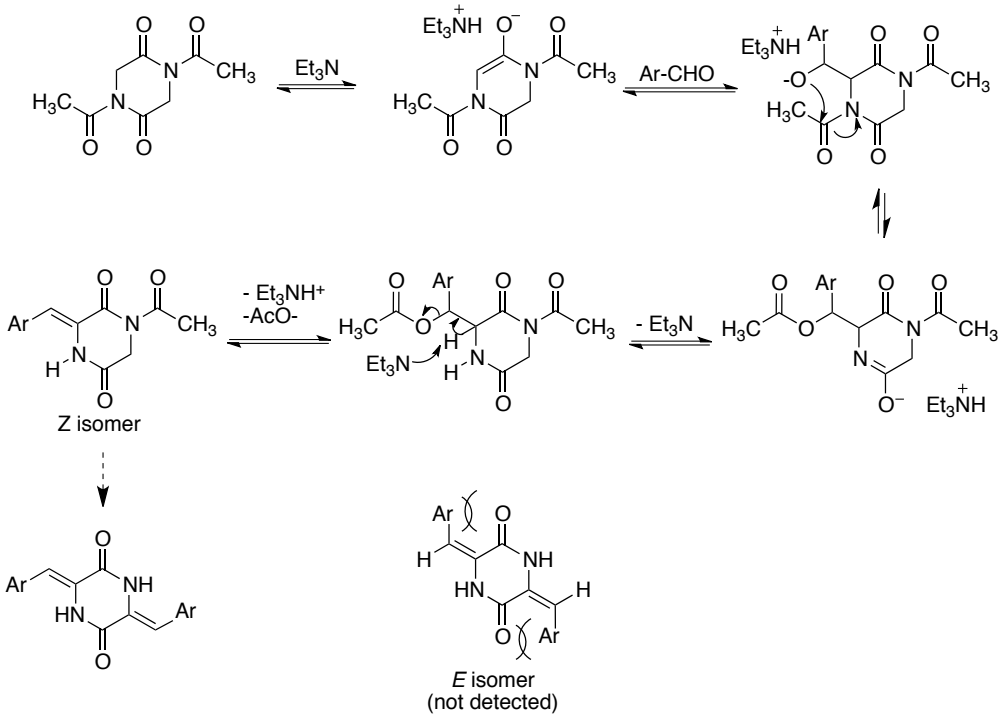

Scheme 4.3. The reaction mechanism for the double condensation reaction

All the aromatic aldehydes employed so far were commercially available. However, as previously mentioned, in order to obtain potential fluorescent probes we designed heteroaromatic β-carboline derivatives. The preparation of the corresponding β-carboline-derived aldehydes was accomplished via the Pictet-Spengler reaction,[146] utilizing the appropriate 3-(aminoethyl)indole and aldehyde derivatives. As shown in Scheme 4.4, we prepared β-carboline-1- and

146 Whaley, W. M.; Govindachari, T. R. *Org. React.* **1951**, *6*, 151.

3-carbaldehyde on the basis of the method described by Snyder et al.,[147] starting by the condensation between or tryptophan and formaldehyde or tryptamine and glyoxylic acid,[148] to give compounds **96** and **97**, respectively. These acid derivatives were subsequently transformed into the corresponding methyl esters **98** and **99** by heating in methanolic hydrogen chloride solution.

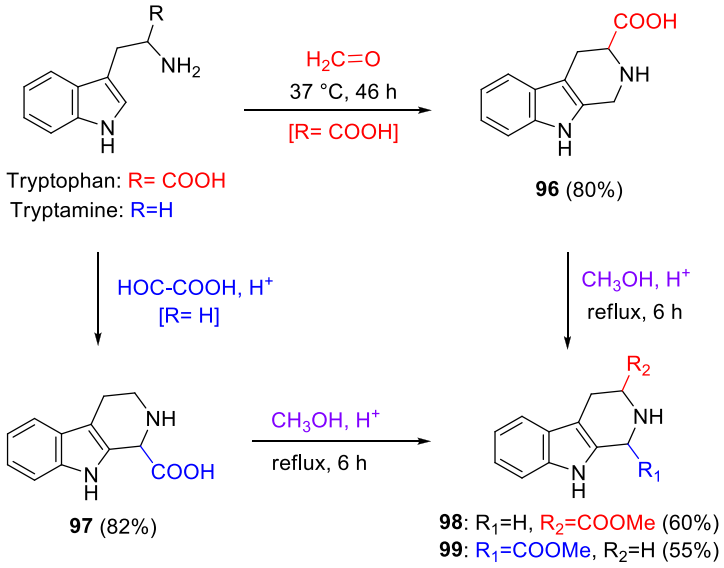

Scheme 4.4. Synthesis of the β-carboline-derived methyl esters

As summarized in Scheme 4.5, compound **99** was aromatized by exposure to 30% Pd/C in refluxing methanol for four days to afford **101**. In the case of compound **98**, these conditions failed and we needed to resort to the use of sulfur[149] to carry out its oxidation to **100**, suggesting that the different positions of ester group decreases the reactivity of the ring. Finally, the desired aldehydes

147 Snyder, H. R.; Walker, H. G.; Werber, F. X. *J. Am. Chem. Soc.* **1949**, *71*, 527.
148 Ho, B. T.; Walker, K. E. *Org. Synth.* **1988**, *6* ,965.
149 Cain, M.; Weber, R. W.; Guzman, F.; Cook, J. M.; Barker, S. A.; Rice, K. C.; Crawley, J. N.; Paul S. M.;Skolnick, P. *J. Med. Chem.***1983**, *25*, 1081.

were obtained by careful reduction of the ester groups of **100** and **101** with DIBALH to give **102** and **103**, respectively.[150] Condensation of these compounds with 1,4-diacetylpiperazine-2,5-dione required rather harsh conditions that involved heating of the starting materials with 2.5 equivalents of triethylamine in refluxing DMF and afforded compounds **104** and **105**, respectively.

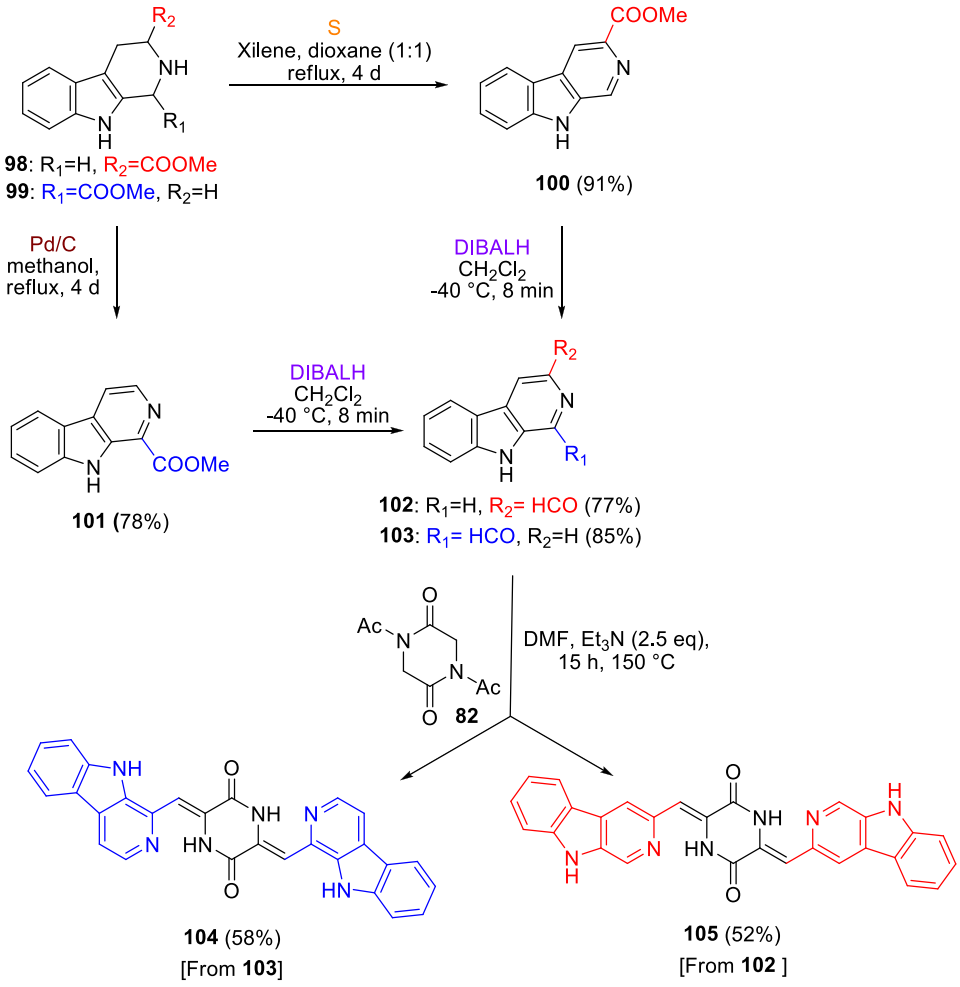

Scheme 4.5. Synthesis of the β-carboline-derived aldehydes and the corresponding double condensation products

150 Suzuky, H.; Adachi, M.; Ebihara, Y.; Gyoutoku, H.; Furuya, H.; Murakami, Y.;Okuno, H. *Synthesis* **2005**, *1*, 28.

In order to explore the importance of the planarity of our ligands, we planned the reduction of one or both double bonds of the condensation products. To this end, we treated compound **83** with Zn in refluxing acetic acid[151] for 1 hour and obtained the partially reduced compound **106** in 54% yield. Catalytic hydrogenation of **106** in the presence of 30% Pd-C at 30 psi afforded compound **107**, albeit in a moderate 34% yield. This compound could also be prepared in one step and in 58% yield by increasing the reaction time with the Zn/AcOH reagent to 24 h (Scheme 4.6). The conditions for the reduction of **83** to **106** were much milder than those found in the literature for a related case where Ar = Ph. This can be explained by taking into account that the mechanism of the reaction (Scheme 4.7) involves the generation of a carbanion in the benzylic position, which would be stabilized by the electron-withdrawing pyridine nitrogen.

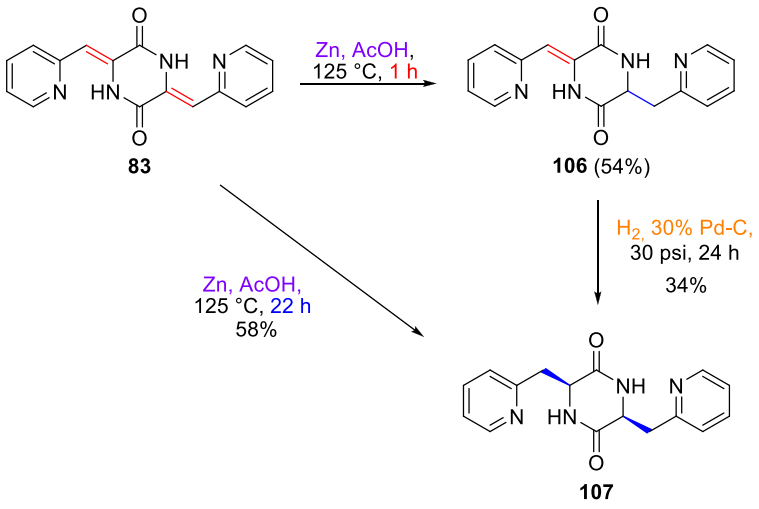

Scheme 4.6. Reduction methods of compound **83**

151 Marcuccio, S. M.; Elix, J. A. *Aust. J. Chem*. **1984**, *37*, 1791.

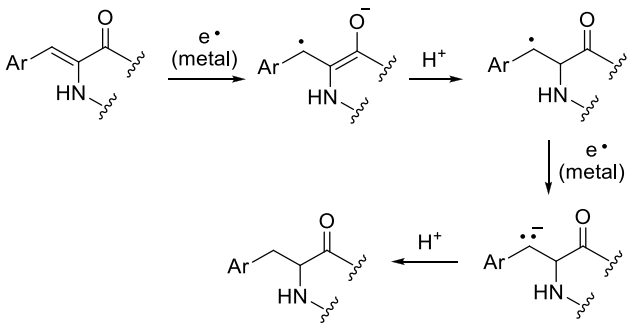

Scheme 4.7. Mechanism of the reaction of reduction in presence of Zn

With this precedent in hand, we also undertook the reduction of compound **93** in the presence of zinc in acetic acid. As shown in Scheme 4.9, this reaction afforded compound **108**, where one of the C=C double bonds and both aldehyde groups were reduced. Although the unoptimized yield for this reaction was modest, we consider this result to be of interest since compound **108** can be easily functionalized by exploiting the reactivity of its hydroxymethyl groups.

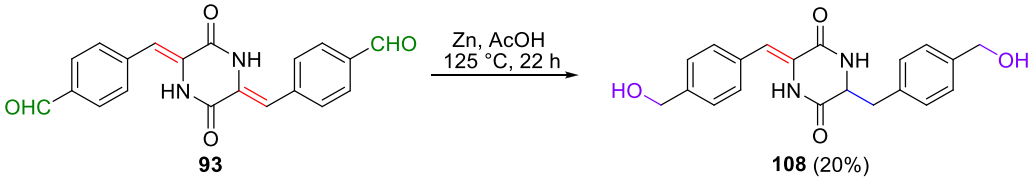

Scheme 4.9. Reduction of compound **93** to **108**.

4.3. Screening methodology

The biological study of our compound library was performed by H. N. Ai Tran under the supervision of Prof. G. Legname at the International School of Advanced Studies (SISSA), Trieste, Italy. A cell-screening assay was used to test antiprion activity across our library. The ability to reduce PrP^{Sc} concentrations in scrapie-infected mouse hypothalamus (ScGT1) cells was determined from Western blot densitometry of the proteinase K (PK)-resistant PrP^{Sc}. Compounds were initially screened at 10 µM and their effects in reducing PrP^{Sc} levels in comparison with the untreated control after 5-day exposure were considered. Prior, effects of library members on ScGT1 cells viability were determined (Tables 4.1 and 4.2). Compound toxicity is expressed as an average percent of viable cells when treated with a compound concentration of 10 µM, versus control cells treated with no compound. Anti-prion activity is expressed as the average percent of PK-resistant PrP reduction after incubation with compound at the given concentration, versus control cells incubated with no compound. For entries **83** and **105** the EC_{50} values, which represent the effective concentrations for half-maximal inhibition, were also calculated. Two well documented anti-prion agents, quinacrine and imipramine, were investigated as positive controls exhibiting an EC_{50} value of 6.2 ± 0.4 and 0.4 ± 0.1 µM, respectively.

4.4. Biological activity results and SAR

As a first step, the cytotoxic effects of all compounds were determined by calcein-AM assay in ScGT1 cell line. As summarized in Tables 4.1 and 4.2, treatment of ScGT1 (10 μM) did not lead to major modifications in cell viability for most compounds, with the exception of **104** where cell viability was lower than 50%. Therefore, the latter compound was not screened for prion replication, whereas the other library members were assayed at a concentration of 10 μM. From an analysis of the results, it is possible to conclude that at this concentration not all the tested DKPs displayed activity. In fact, among the selected aromatic rings, we observed null or very low activity for benzene (**92**), furan (**94**), thiophene (**95**) and quinoline (**86, 90** and **91**) derivatives. The most striking result of this investigation was the remarkable activity displayed by the 2-pyridyl derivative **83**, which at 10 μM is able to completely inhibit prion replication (100.8 ± 2.5 % of inhibition). Intriguingly, when the pyridine nitrogen was moved to positions 3 (**84**) and 4 (**85**), the activity decreased to percentages of 12.4 and 11.5, respectively. Similarly, the potent activity of **83** was reduced by fusing additional aromatic groups, as in the cases of the 2-quinolinyl (**86**) and β-carbolin-3-yl (**105**) compounds (Table 4.1).

Significant preliminary structure-activity relationships can be gathered from this first set of tested compounds. A DKP bearing a 2-pyridyl substituent was revealed as a strict requirement for potency in the cell line assay. The only exception to this trend was the 4-quinolyl derivative **86**, which was the only compound devoid of the apparently key molecular feature and displaying an activity higher than 20%.

Table 4.1. Screening results for the DKP double condensation products

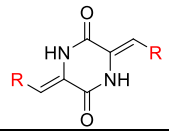

Cmpd.	R	% of viable cells at 10 µM	% PrP^{Sc} inhibition at 10 µM
83		50.9 ± 2.1	100.8 ± 2.5
84		102.7 ± 3.7	12.4 ± 0.5
85		108.5 ± 4.2	11.5 ± 0.5
90	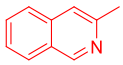	71.7 ± 3.1	5.1 ± 0.1
91	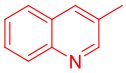	63.7 ± 2.8	3.5 ± 0.1
86		94.8 ± 4.1	20.6 ± 0.8
92		85.6 ± 3.1	0.11 ± 0.01
94		83.0 ± 2.9	0.14 ± 0.02
95		73.6 ± 3.5	1.8 ± 0.1
104	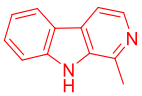	37.3 ± 2.6	ND[a]
105	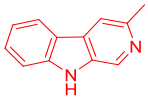	77.0 ± 3.2	10.4 ± 1.2

[a] Not determinated

The results obtained could imply that a planar conformation, as in **83**, is a basic requirement for activity. Starting from this assumption, we examined the effects of the reduction on the double bonds at the positions 3 and 6 of the DKP system. Thus, the partially saturated (**106** and **108**) and fully unsaturated (**107**) derivatives were also tested against prion replication in the same cell-based model (Table 4.2). Even in this series, the most active compound was again the 2-pyridyl derivative **106**. Again, this can be rationalized by the assumption that at least one half of the molecule is able to assume the planar conformation critical for activity. In line with this speculation, the doubly saturated compound **108** showed lower potency.

Table 4.2. Screening results for mono and fully reduced DKP products **106**-**108**

Cmpd.	% of viable cells at 10 μM	% PrP^{Sc} inhibition at 10 μM
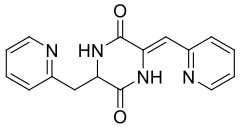 **106**	100.1 ± 4.4	18.1 ± 0.7
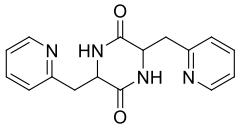 **107**	107.4 ± 4.6	12.2 ± 0.2
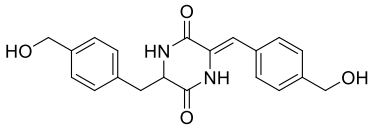 **108**	110.5 ± 5.3	13.8 ± 0.4

Given the high inhibitory activity of **83** and the possible use of **105** as a fluorescent probe, their antiprion potential was studied in more detail by calculating their EC_{50} values. For **83**, a remarkable single-digit micromolar EC_{50} value (4.1 ± 0.2 μm, Table 4.3) was observed, comparable to that of imipramine (6.2 ± 0.4 μm), a reference antiprion compound. Notably, **105** (EC_{50} = 15.8 ± 0.9

μm) was only fourfold less active than **83**, emerging as a promising fluorescent probe.

Table 4.3. EC_{50} was calculated for **83** and **105**[a]

Cmpd.	EC_{50} [μM][b]	Viable cells [%][c]	Westem Blot
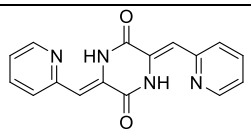 **83**	4.1 ± 0.2	75.2 ± 2.1	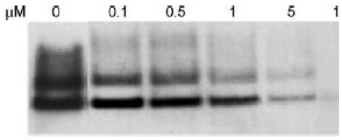
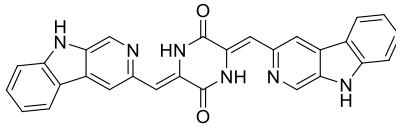 **105**	15.8 ± 0.9	60.4 ± 4.	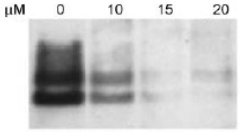

[a]Values given are the mean ± the standard deviation (SD) of three experiments. [b]The concentration of test compound required to reduce the PrP^{Sc} level in cells to 50% versus untreated cells (EC_{50}). [c]Cell viability at the EC_{50} concentration was determined by calcein-AM cytotoxicity assay and expressed as an average percentage of viable cells versus untreated control cells.

4.5. Modeling studies

To better elucidate the putative relationships between bioactivity and the planarity of tested compounds, their structural conformations were studied. To this end, three-dimensional low-energy geometries were computed by Salvatore Bongarzone at SISSA, Trieste. These studies showed that all doubly unsaturated DKP derivatives bearing an α heteroatom are fully planar, while the others display rotated aromatic rings (e.g. **92** is rotated by 33.6° with respect to the DKP plane, Figure 4.2). The difference between planar and non-planar molecules is due to the presence or absence of an intramolecular hydrogen bond between the aromatic substituents and the DKP ring.

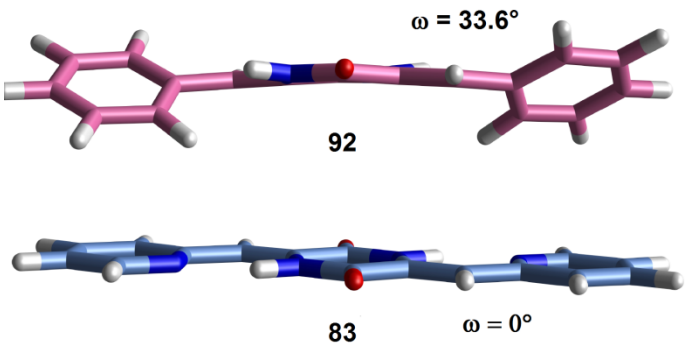

Figure 4.2. Three-dimensional structure of a planar (**83**) and a non-planar (**92**) DKP; the difference in geometry is due to the presence or absence of intramolecular hydrogen bonds

Molecular planarity may be a necessary, but not sufficient, condition for antiprion activity. In fact, modeling results predicted that compounds **90**, **94**, **95** and **105** are equally planar as **83**, but possessed lower activity (Table 4.1). To explain this result, the planarity strength, in terms of the barrier for the rotation of the arylmethylene side chains, was calculated (Table 4.4). The planar geometry of **83** was found to the most stable one, confirming that antiprion

activity of this subset of molecules is directly related to their capability to retain a planar conformation.

Table 4.4. Planarity degrees and planar stability of **83**, **90**, **92**, **94**, **95**, **105**

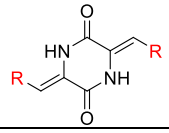

Cmpd.	R	Planarity degree (ω degrees)	Planar stability (ΔE Kcal/mol)
83		0.02	18.02
90	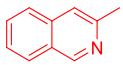	0.01	15.06
92		33.60	0.0
94		0.00	7.3
95		0.00	1.8
105	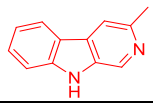	0.07	17.2

4.6. Mechanism of action

Based on the consideration that planar aromatic molecules are reported as good inhibitors of fibril formation in several neuronal amyloidosis, we decided to study the behavior of **83** by a known amyloid seeding assay (ASA).[26] N. H. Ai Tran performed this experiment using as templates recombinant (rec) mouse (recMo) full-length PrP(23–230) and truncated recMoPrP(89–230), which both form amyloid fibers. The antiaggregation potential of **83** (50 μm) was quantitatively detected by observing the decrease in the mean lag phase of the fibrillation reaction, compared with control samples. Compound **83** (50 mm) exhibited PrP amyloid fibril forming inhibitory activity, showing a much slower kinetics than the control, in which the lag phase was 57 h and 15 h for recMoPrP(23–230) and recMoPrP(89–230), respectively. In particular, **83** significantly extended the lag phase to 72 h in recMoPrP(23–230) and 48 h in recMoPrP(89–230) fibrillation assays. Given the potency of **83** at inhibiting recPrP fibril formation, we suggest that the compound might interact directly with recPrP to prevent its conversion to the pathogenic PrP^{Sc} like form.

5. Synthesis of GN8 fluorescent analogues and evaluation of their antiprion activity

5.1. Synthesis of GN8 and their fluorene and carbazole based analogues

The experimental work reported in this chapter was carried out with collaboration from three undergraduate students: Lucia Morelli, Alice D'Onofrio and Giulia Bianchini, who worked under my supervision. Our study started with the preparation of GN8 (**110**) in order to have a reference compound, using a variation of the published method.[37] To this end, we coupled the commercially available 4,4'-methylenedianiline with bromoacetic acid in the presence of Et_3N and 1-ethyl-3-(3-dimethylaminopropyl)carbodiimide hydrochloride (EDC·HCl), that was used to activate the carboxylic group. Afterwards, compound **109** was treated with pyrrolidine, carrying out the reaction in DMF at 80°C during 24 h, to afford GN8 **110** (Scheme 5.1).

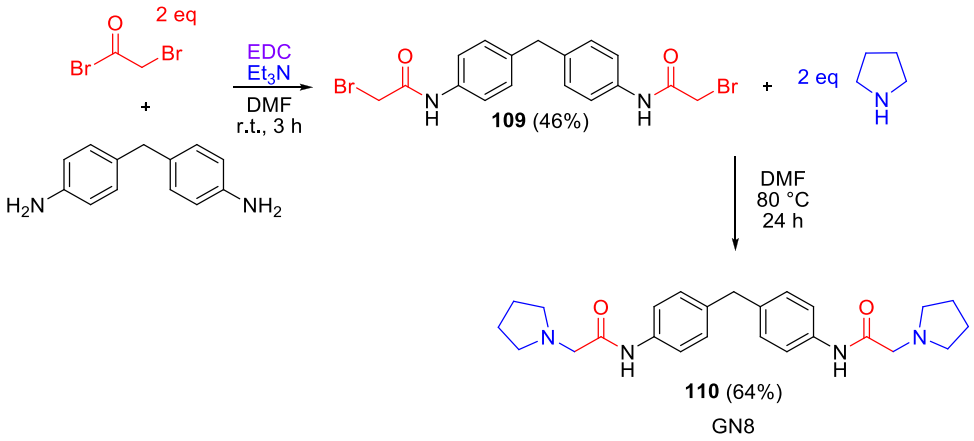

Scheme 5.1. Synthesis of GN8

Then, a series of fluorene based analogues was generated by transforming the commercially available 9*H*-fluorene-2,7-diamine into the bis-halide **111** *via* a coupling reaction with bromoacetylbromide in the presence of EDC. Because the product was obtained in very low yield (24%), we experimented with other catalysts, obtaining good results with 4-dimethylaminopyridine (DMAP) in THF

(Scheme 5.2). DMAP is often used as a catalyst for acyl transfer reactions and can be easily washed off with aqueous acid as a bromide salt. The mechanism of the activation of bromoacetyl bromide by DMAP is depicted in Scheme 5.3.

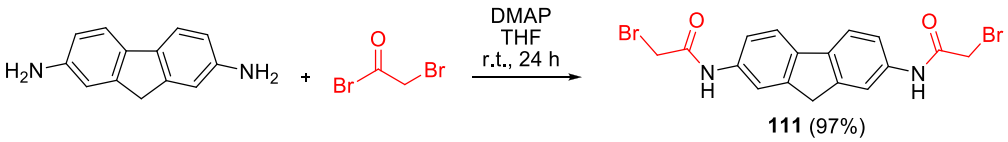

Scheme 5.2. Transformation of 9*H*-fluorene-2,7-diamine into the bis-halide **111**

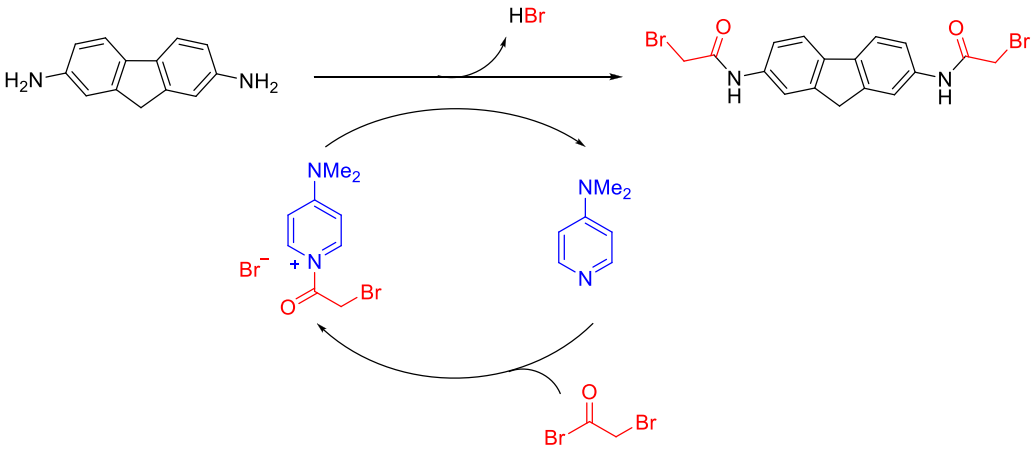

Scheme 5.3. Mechanism of the activation of bromoacetylbromide by DMAP.

Finally, intermediate **111** was treated with different amines to afford compounds **112-120** by double nucleophilic displacement of bromide anions by the *N*-nucleophiles (Table 5.1). These reactions were carried under the standard conditions previously developed for GN8 (Scheme 5.4).

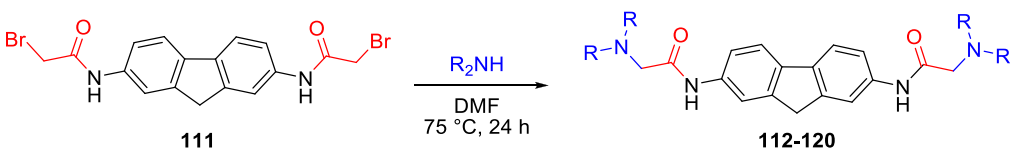

Scheme 5.4. Synthesis of the amino fluorene derivatives

Table 5.1. Scope and yield of the amino-fluorene derivatives

Entry	Cmpd.	NHR_2	Yield, %
1	**112**		90
2	**113**		34
3	**114**		64
4	**115**		80
5	**116**		57
6	**117**		73
7	**118**		64
8	**119**	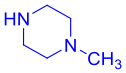	72
9	**120**	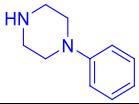	67

Another class of GN8-based ligands was generated by replacing the fluorene central core by carbazole, due to the intrinsic fluorescence of this ring system and its antioxidant properties. Our synthetic route started with the nitration of carbazole with a mixture of acetic and nitric acid (1:1) to give a mixture of 3,6-dinitrocarbazole **121** and 3-nitrocarbazole **122** in modest yields, using a published method.[152] (Scheme 5.5).

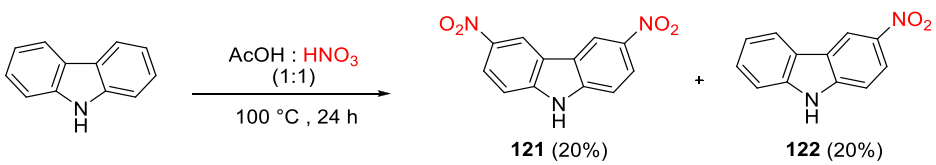

Scheme 5.5. Nitration of carbazole

152 Mudadu, M. S.; Singh, A. N.; Thummel, R. P. *J. Org. Chem.* **2008**, *73*, 6513.

The reduction of compound **121** also posed some problems, and several literature methods for nitro reduction[152,153] failed. Eventually, we found that **121** was reduced quantitatively to 3,6-diaminocarbazole **123** by using iron powder in a refluxing mixture of ethanol, water and acetic acid containing 37% aqueous hydrochloric acid (Scheme 5.6).[154]

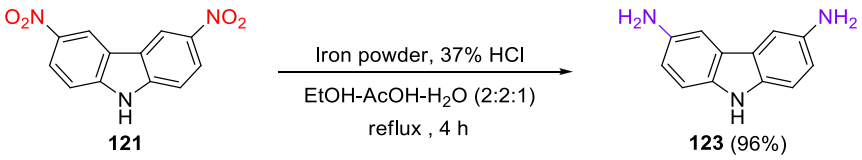

Scheme 5.6. Reduction of compound **121** to **123**

Then, compound **123** was transformed into bis-halide **124** by double acylation with bromoacetyl bromide by using DMPA under the same conditions applied in the case of fluorene (Scheme 5.7).

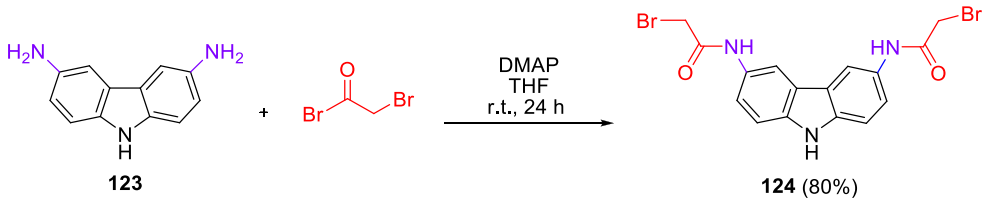

Scheme 5.7. Synthesis of the bis-halide derivative **124**

With compound **124** in hand, we carried out the coupling reaction with different amines in DMF, following the protocol established for the fluorene derivative, to afford compounds **125-133** (Scheme 5.8 and Table 5.2). In the case of the carbazole derivatives, the yields were generally only moderate, owing to

153 Barker, A.; Barker, C. C. *J. Chem. Soc.* **1954**, 870.

154 Aleksandrov, A. M.; Kashyap , R. P.; Pehk, T. J.; Petrenko, A. E.; Watson, W. H. *J. Org. Chem.* **1993**, *58*, 1831.

difficulties found in isolating the products from DMF and in their purification, which was hampered by their very low solubility in all media.

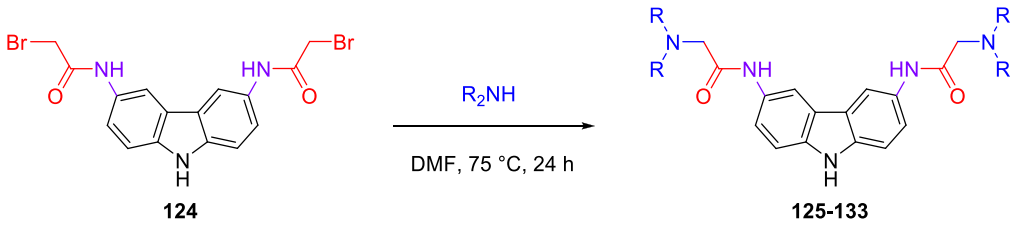

124 **125-133**

Scheme 5.8. General conditions to achieve carbazole products

Table 5.2. Scope and yield of the amino-carabazole derivatives

Entry	Cmpd.	NHR_2	Yield, %
1	**125**		58
2	**126**		60
3	**127**		47
4	**128**		40
5	**129**		38
6	**130**		55
7	**131**		48
8	**132**	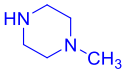	30
9	**133**	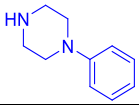	40

In order to verify the proposed relationship between molecular symmetry and anti-prion action, we also decided to synthesize a non-symmetric carbazole derivative. To this end, we treated 3-nitrocarbazole **122** with iron powder to obtain its reduced derivative **134** (Scheme 5.9). We then treated **134** with one

equivalent of bromoacetyl bromide to afford the halide **135**, which was subsequently treated with pyrrolidine to finally achieve compound **136**, containing a single side chain (Scheme 5.10).

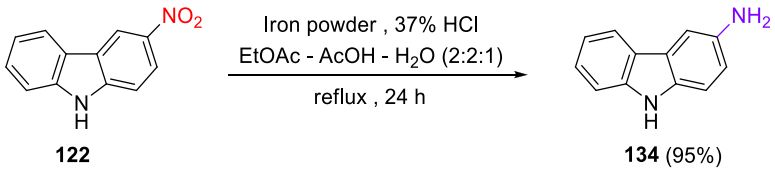

Scheme 5.9. Synthesis of compound **134**

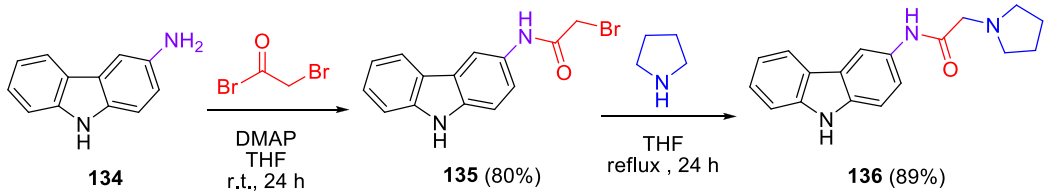

Scheme 5.10. Synthesis of the asymmetric carbazole derivative **136**

5.2. Fluorescence studies

As mentioned above, the fluorene and carbazole moieties were employed with the aim to obtain fluorescent probes potentially useful to trace PrP. Therefore, the native fluorescence of a series of selected compounds was studied by Dr. Víctor González-Ruiz under the supervision of Prof. Maria Antonia Martín at Sección Departamental de Química Analítica, Facultad de Farmacia, Universidad Complutense de Madrid.

Fluorescence emission can be affected by the polarity properties of the microenvironment. For this reason, the native fluorescence of some representative compounds, including the pyrrolidine derivatives **115** and **128**, closely related to GN8, and compounds **112** and **116** were investigated in different solvents: water, ethanol, cyclohexane and acetonitrile. Figures 5.1-5.5 show the fluorescence spectra obtained for these derivatives and fluorene, used as reference, and Table 5.3 summarizes the position of the corresponding maxima. As regards the fluorene derivatives, compounds **112**, **115** and **116** exhibited good fluorescent intensities although they are lower than those observed for fluorene in all solvents. In cyclohexane and ethanol, whose polarity mimics the protein environment, the fluorescence emission maxima were observed in the spectral range between 340 and 360 nm, far away from the NIR region, and was *ca.* 10 times higher than in water. This behavior led to the reasonable expectation that compounds **112**, **115** and **116** will probably show an increase in the fluorescence emission intensity upon binding to fibrils as a consequence of the resulting change in polarity associated to this microenvironment. With regard to the carbazole derivative **128**, interestingly, an emission maximum above 600 nm was observed, facilitating its use as a NIR tracer.

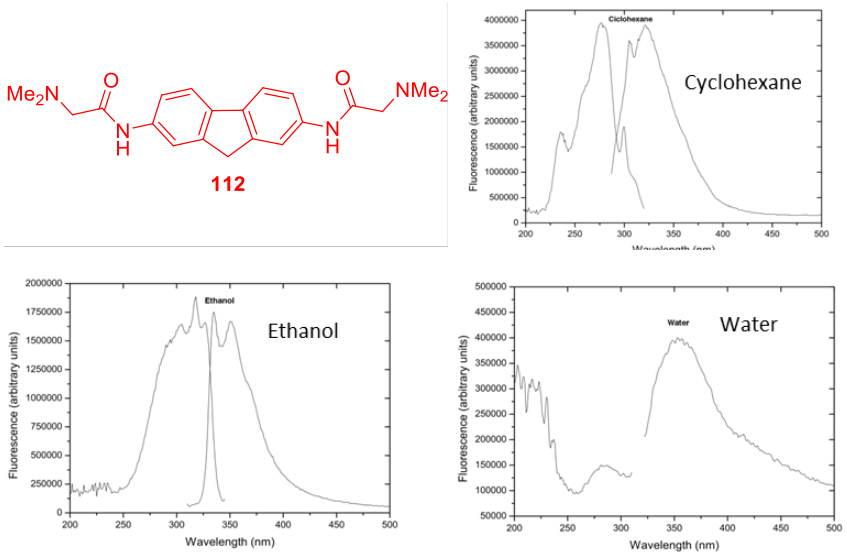

Figure 5.1. Corrected fluorescence excitation and emission spectra of compound **112** in different solvents at concentration 5.0 x 10^{-6} M

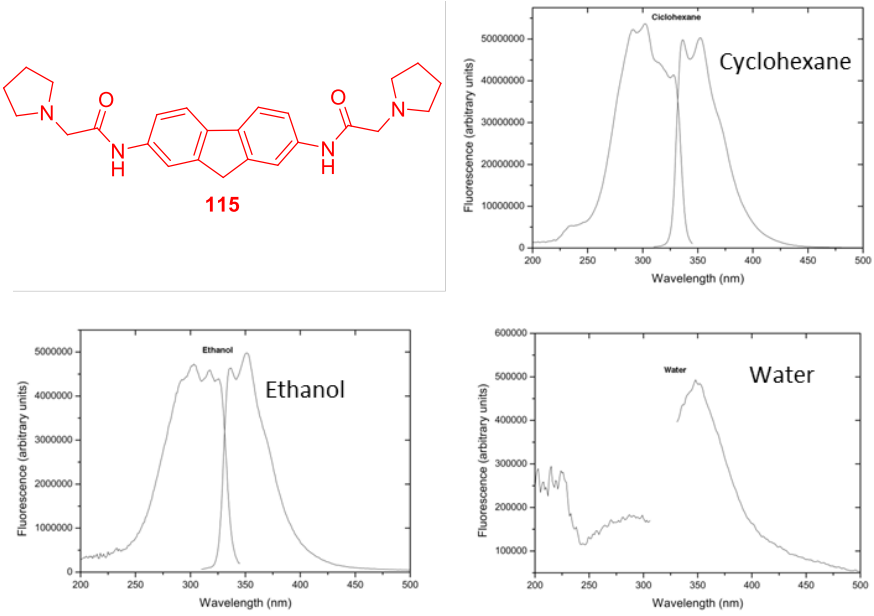

Figure 5.2. Corrected fluorescence excitation and emission spectra of compound **115** in different solvents at concentration 5.0 x 10^{-6} M

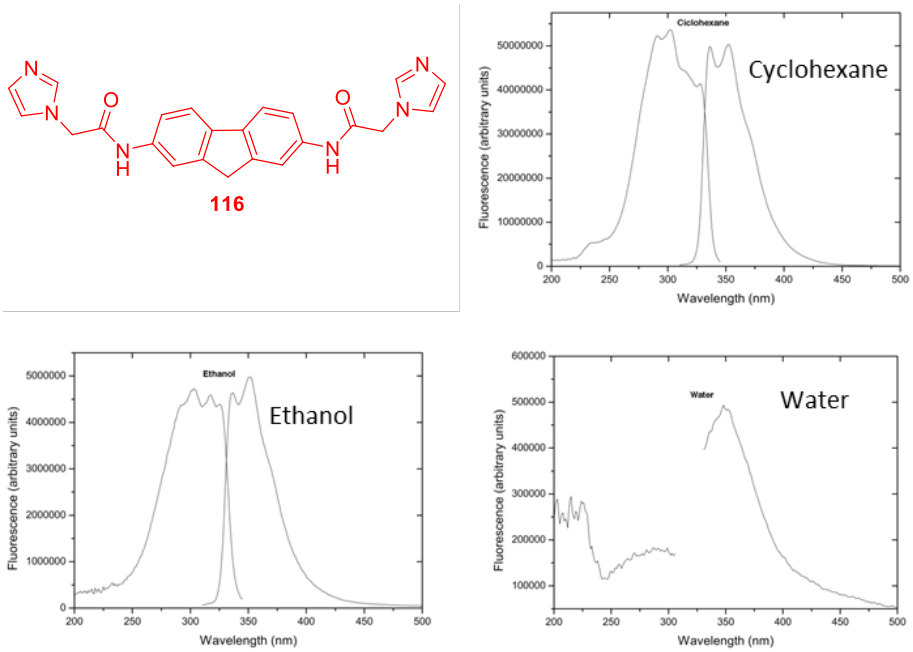

Figure 5.3. Corrected fluorescence excitation and emission spectra of compound **116** in different solvents at concentration 5.0 x 10^{-6} M

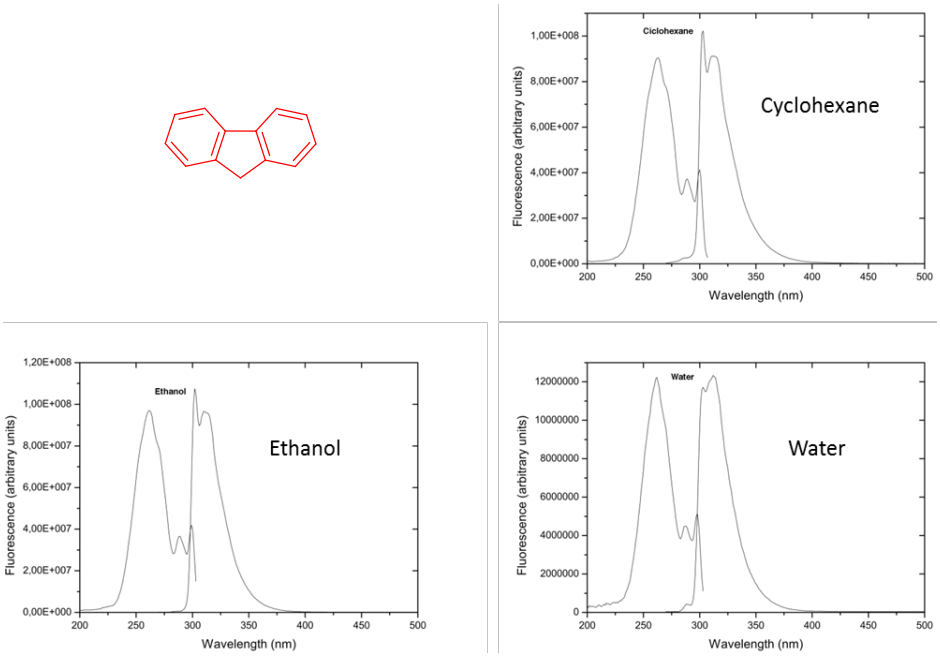

Figure 5.4. Corrected fluorescence excitation and emission spectra of fluorene in different solvents at concentration 5.0 x 10^{-6} M

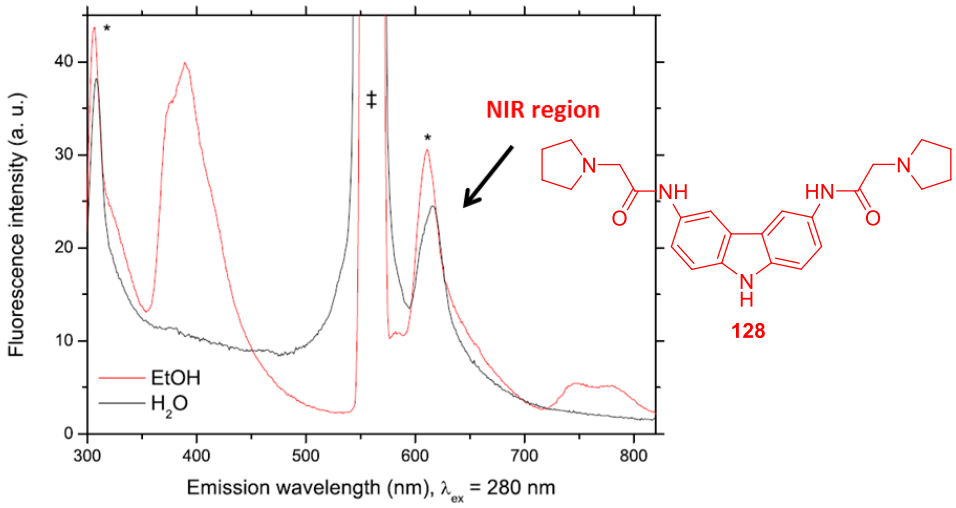

Figure 5.5. Fluorescence emission spectra of **128** in different solvents showing maxima above 600 nm, just in the NIR region

Table 5.3. Excitation and emission maxima of compounds **112**, **115**, **116**, **128** in different solvents

Cmpd.	EtOH		Cyclohexane		H_2O		Acetonitrile	
	λ_{ex} (nm)	λ_{em} (nm)	λ_{ex} (nm)	λ_{em} (nm)	λ_{ex} (nm)	λ_{em} (nm)	λ_{ex} (nm)	λ_{em} (nm)
112	303 317 326	337 351 368 (sh)	303 326	336 352 368 (sh)	285*	--	--	--
115	304 317 327	336 351 368 (sh)	236 280 300 340	328 343 360 (sh)	280 314	358 420	--	--
116	302 317 326	336 351 365 (sh)	303 327	336 352 365 (sh)	285*	--	--	--
128	269 538	315 387, 605 750, 784	265 534	308 604	265 540	309 385 610, 752	277 355 538	309 390 609, 753

*Slit 5

5.3. Antiprion activity evaluation in a cell-based model

The antiprion potential of of the synthetized compounds was assessed in ScGT1 infected cells by Dr. H. N. Ai Tran and Sivia Vanni under the supervision of Prof. Giuseppe Legname at SISSA, Trieste. A preliminary screening assay was used to test an initial selection of the fluorene derivatives **112**, **115**, **116**. Compound **116** was not assayed for prion replication since cell viability was lower than 50%. On the other hand, **112** and **115** showed activity at a concentration of in the low micromolar range against prion replication with EC_{50} values of 4.6 and 1.9 μM, which are similar to that of GN8 and, encouragingly, they displayed low toxicities (Table 5.4). Furthermore, they were found to delay fibril formation with efficacies similar to that of GN8, using the previously described amyloid seeding assay (ASA, Figure 5.6).

Table 5.4. EC_{50} and the cell viability at this concentration was calculated for compounds **112**, **115** and **116**

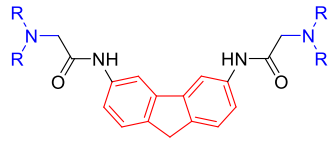

Cmpd.	NR_2	EC_{50} (μM)	% of viable cells at EC_{50}
GN8	-	1.5 ± 0.1	93.4 ± 7.3
112		4.6 ± 0.1	92.1 ± 5.7
115		1.9 ± 0.1	68.2 ± 3.8
116		--	--

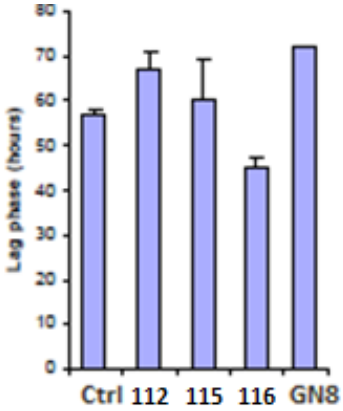

Figure 5.6. In vitro inhibitory activity of prion fibril formation for compounds **112**, **115-116** (50 μM) compared with GN8

As regards carbazole derivatives, the data concerning their toxicity and ability to inhibit the prion replication at different concentrations are summarized in Table 5.5. Most of the tested compounds (except **125** and **126**) showed some toxicity at 10 μM concentration, and compounds **125-128**, **132** and **136** were able to reduce the PrP^{Sc} levels and their efficacy was comparable with that of GN8. On the other hand, at 1 μM concentration compounds **125** and **126** exhibited a very low toxicity, with cell viability above 90%, and continued to be active against prion replication, even more that GN8, with a $\%PrP^{Sc}$ level of 44 and 33. Compounds **127** and **132** were able to inhibit scrapie propagation at 1 μM concentration, but unfortunately they were toxic. Importantly, at a 10 μM concentration still displayed very low toxicity.

Table 5.5. Screening results for GN8 and carbazole derivatives

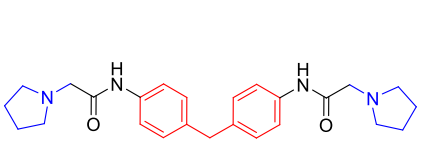

110, GN8

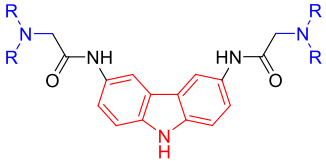

125-132

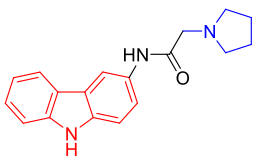

136

Cmpd.	NR_2	10 μM		1 μM		0.1 μM	
		% Cell viability	% PrP^{Sc} level	% Cell viability	% PrP^{Sc} level	% Cell viability	% PrP^{Sc} level
110, GN8		50	17	69	79	85	104
125		95	21	99	44	111	103
126		103	19	99	33	108	71
127		61	24	75	39	92	73
128		71	27	85	103	118	148
129		77	74	89	98	100	120
130		69	44	76	105	81	109
131		84	59	86	102	101	96
132	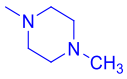	47	28	70	46	99	85
133	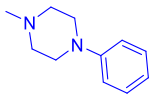	63	134	73	136	71	124
136	--	29	26	72	75	83	78

5.4. Fluorescent staining in ScN2A cells

In an effort to shed light on the molecular mechanism of action of our compounds, fluorescent staining with compound **128** was carried out using the ScN2A cell model, infected by scrapie. This experiment was performed by Suzana Aulić under the supervision of Prof. Giuseppe Legname at SISSA, Trieste. The choice of **128** was dictated by the fact that it emits fluorescence in the NIR region. It was found that a small amount of **128** was sufficient to observe many fluorescent spots in the treated cells examined by fluorescent microscopy, before and after denaturation with 6 M guanidinium chloride (GndHCl) (Figure 5.7A). The fact that fluorescent spots were still observed after the denaturation of the PrP^{C} means that **128** interacts only with PrP^{Sc} instead of PrP^{C} as GN8. Furthermore, the staining pattern was consistent with that observed with Thioflavin S (ThS), a common PrP^{Sc} dye (Figure 5.7B). In order to confirm the selective binding of **128** for the scrapie fibrils, the same experiment was carried in uninfected cells. As expected, no spots were observed confirming the selectivity of the biomarker for PrP^{Sc} (Figure 5.8).

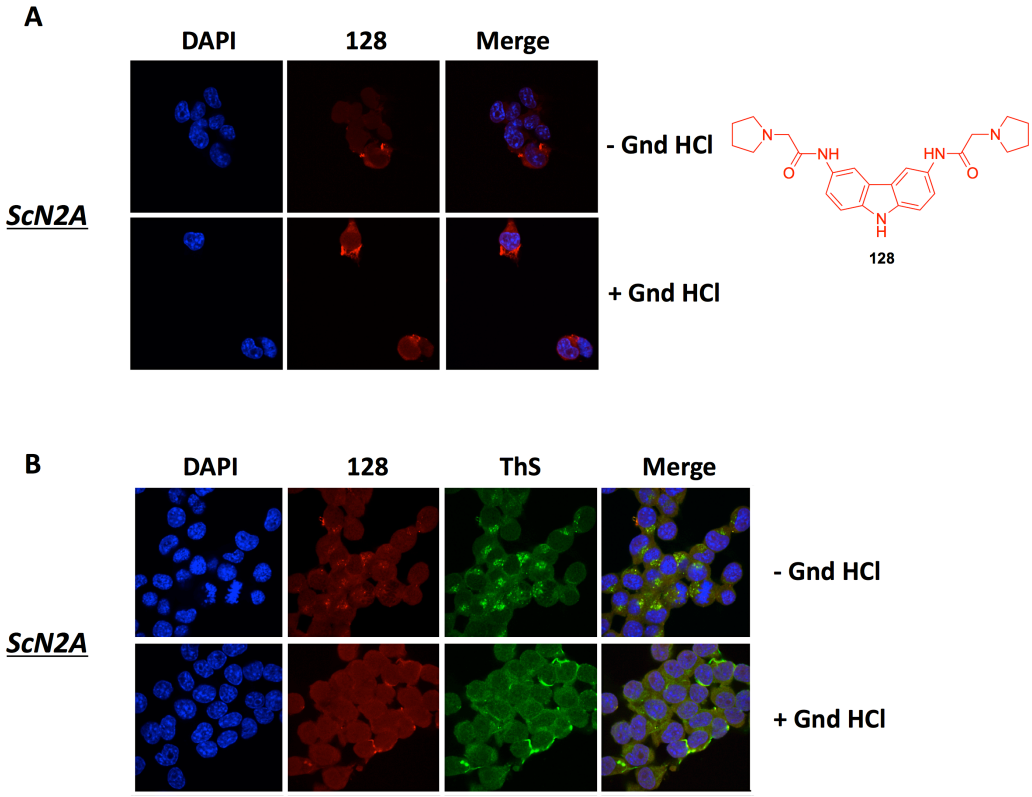

Figure 5.7. (A) Detection of PrP^{Sc} aggregates with **128** in ScN2A (scrapie prion-infected cells) by intensity fluorescence (IF) before and after denaturation with 6M GndHCl. (B) Comparison of the fluorescent staining with **128** (red) and Thioflavin-S (green), a dye that specifically binds to aggregates, in ScN2A cells before and after denaturation with 6M guanidinium hydrochloride (GndHCl).

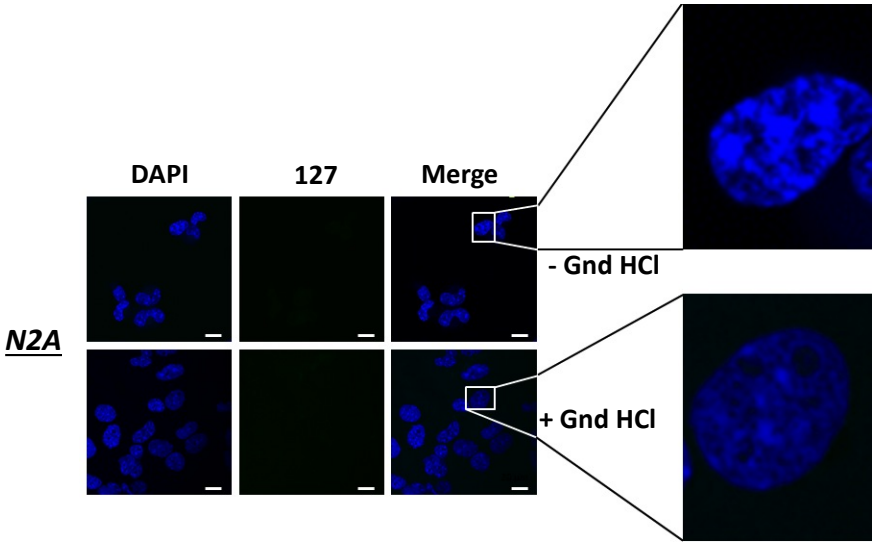

Figure 5.8. Uninfected N2A cells with or without denaturation step with 6 M GndHCl did not show staining in the presence of **128**

5.5. Proposed mechanism of action

In the light of these results, we propose for our compounds an antiprion mechanism of action alternative to that described for GN8. The previously summarized data demonstrate that compound **128** binds selectively prion fibrils, and therefore that its antiprion activity is due to the interaction with PrP^{Sc} instead of PrP^{C} as in the case of GN8. This would prevent prion propagation either by interfering with protein-protein interactions (PPIs) between PrP^{Sc} and PrP^{C} or by directly preventing fibril formation from PrP^{Sc}. On the other hand, Kuwata's group suggested that a restricted conformation of the GN8 molecule led to its antiprion activity by stabilizing PrP^{C} upon binding.[37] It emerges that modifying the structure of GN8 by generating a more planar and rigid molecule leads to a change in the biological target (Figure 5.9).

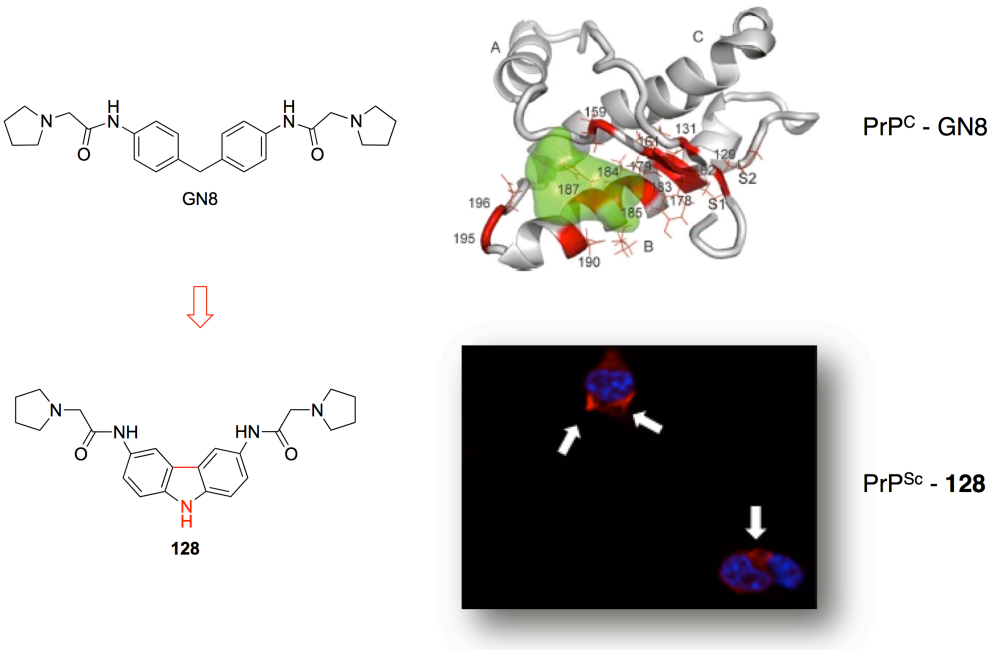

Figure 5.9. Rigidification of the structure of GN8 influenced the mechanism of action against the prion replication. Our data show that **128** exerts its antiprion activity by interacting with PrP^{Sc} instead of PrP^{C} as in the case of GN8

6. Fluorescent styrylquinolines as innovative therapeutic and diagnostic tools to combat protein misfolding diseases

6.1. Styryl compounds to detect and treat amyloid aggregates

As highlighted in the Introduction, one of the main goal of this thesis was the identification of novel fluorescent compounds capable of staining amyloid fibrils, and, ideally, of simultaneously blocking their aggregation.[46]

As a starting point, we noticed that several styryl derivatives, designed by Li et al. to improve the pharmacokinetic properties of CR and ThT, were employed as AD imaging agents *in vivo*.[155] Interestingly, some of them were also found to be active against prion replication in infected cells.[156] Furthermore, Ishikawa et al. reported that a styrylbenzene derivative (BSB) was useful to detect PrP^{Sc} aggregates *ex vivo* and showed effectiveness in cellular assays.[53] Therefore, we reasoned that the styryl moiety was important to the ability of small molecules to label and interfere with pathological fibrillar aggregates, both in PrD and AD.

We first reported a preliminary exploration of three styrylquinoline derivatives as $A\beta/PrP^{Sc}$ diagnostic and therapeutic small molecules. We focused on a quinoline moiety because it constitutes the core of many anti-prion compounds, while displaying good pharmacokinetic properties and a high degree of drug-likeness.[25] In one of the compounds, an amino group was purposely introduced (**139**) to have an electron-releasing substituent conjugated with the quinoline nitrogen to shift the fluorescence emission toward the NIR spectral region. In order to reinforce this effect by increasing the electron-withdrawing character of the quinoline nitrogen, the hydrochloride salt of **139** was also prepared.

155 Li, Q.; Min, J.; Ahn, Y. H.; Namm, J.; Kim, E. M.; Lui, R.; Kim, H. Y.; Ji, Y.; Wu, H.; Wisniewski, T.; Chang, Y. T. *ChemBioChem* **2007**, *8*, 1679.

156 Chung, E.; Prelli, F.; Dealler, S.; Lee, W. S.; Chang, Y. T.; Wisniewski, T. *PLoS ONE* **2011**, *6*, 24844.

In the light of the encouraging results obtained from these molecules, we developed a new series of styryquinolines. Accordingly, we designed a library of 54 compounds, which aims to explore structure activity relationships (SARs) around the 2-styrylquinoline scaffold and optimize its profile. Most of the compounds were purposely designed with the aim of pushing their emission wavelength into the ideal NIR region by introducing electron donor and electron-acceptor groups as terminal moieties in order to generate a "push-pull" molecule and at the same time improving the antiprion activity. Methoxy and chlorine substituents were introduced because they are present in many quinoline-derived antiprion compounds, while the dimethylamino group is well known as the best red-shift absorption-pushing group. In addition, we obtained some compounds in which the phenyl moiety was replaced by a pyridine or quinoline ring in order to have a further atom capable of hydrogen bonding interaction. Finally, methyl and fluorine substituents were also introduced to increase the library diversity (Figure 6.1).

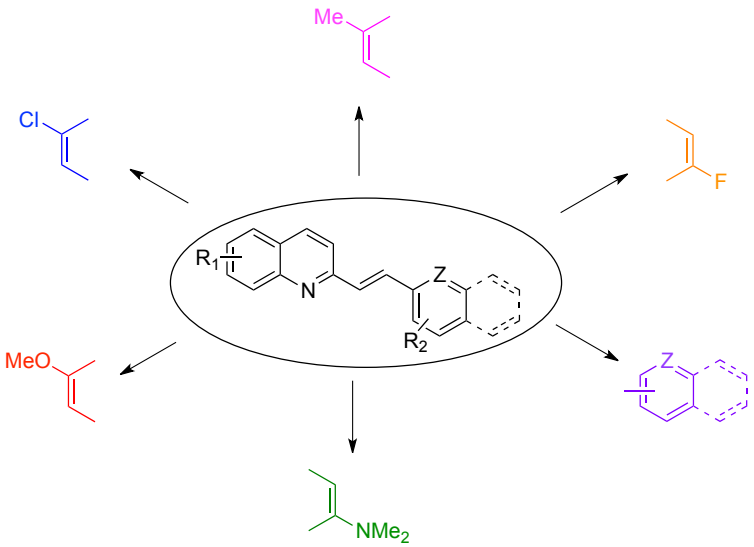

Figure 6.1. Chemical structure of styrylquinoline and its substituents

6.2. A fluorescent styrylquinoline with combined therapeutic and diagnostic activities against Alzheimer's and prion diseases

6.2.1. Synthesis of 2-styrylquinolines

Our investigation started with the synthesis of 2-functionalized tetrahydroquinolines followed by their aromatization to 2-styrylquinolines. This methodology has been well studied by our research group and it is based on a three-component reaction between arylamines, alkyl vinyl ether and cinnamaldehydes catalyzed by cerium(IV) ammonium nitrate (CAN) (Scheme 6.1).[157] Starting from the suitable anilines (toluidine and anisidine), we carried out the reaction in acetonitrile at r.t. during 2 h to obtain the corresponding 2-styryl-1,2,3,4-tetrahydroquinoline derivatives that were directly dehydrogenated in the presence of DDQ to give compounds **137** and **138** in good overall yields (Scheme 6.2).

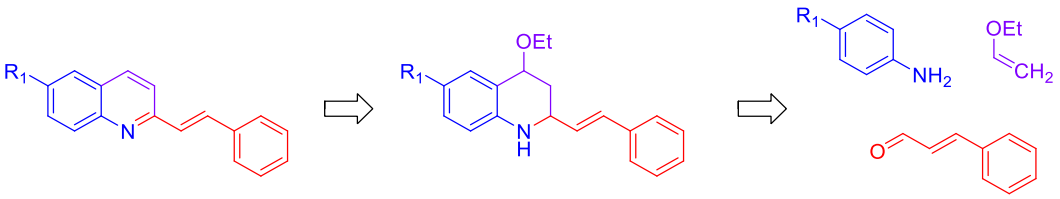

Scheme 6.1. Retrosynthesis of the styrylquinoline derivatives.

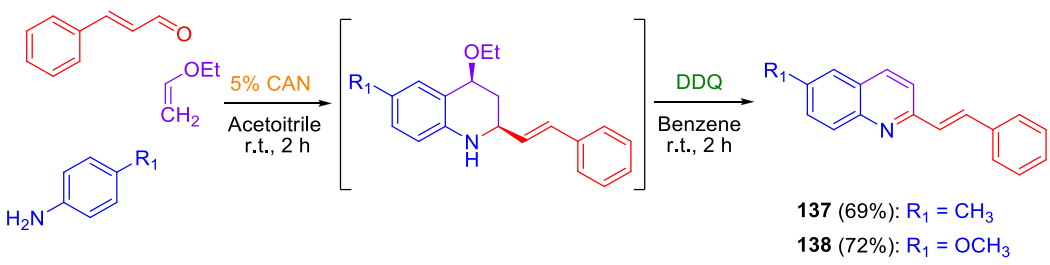

Scheme 6.2. Synthesis of 2-styrylquinolines

157 Sridharan, V.; Avendaño, C.; Menéndez J. C. *Tetrahedron* **2009**, *65*, 2087.

The mechanism that leads to the generation of 2-styryl-1,2,3,4-tetrahydroquinolines is depicted in Scheme 6.3. The first step consists of a type-II vinylogous Povarov reaction between an arylamine and cinnamaldehyde promoted by CAN, acting as a Lewis acid. This reaction involves the formation of an α,β-unsaturated derivative, as intermediate product, followed by a nucleophilic 1,2-additions from alkyl vinyl ether to afford the 2-styryl-1,2,3,4-tetrahidroquinoline compound. It is interesting to note that the reaction is fully diastereoselective and gives only 2-styryl-1,2,3,4-tetrahydroquinolines with a *cis* arrangement. This complete diastereoselectivity can be explained by assuming a stepwise mechanism for the vinylogous Povarov reaction, where a *cis* arrangement between the alkoxy and styryl groups leads to minimum interactions between these bulky substituents and the axial protons in the chair-like transition state of the cyclization step leading to the tetrahydroquinoline system.

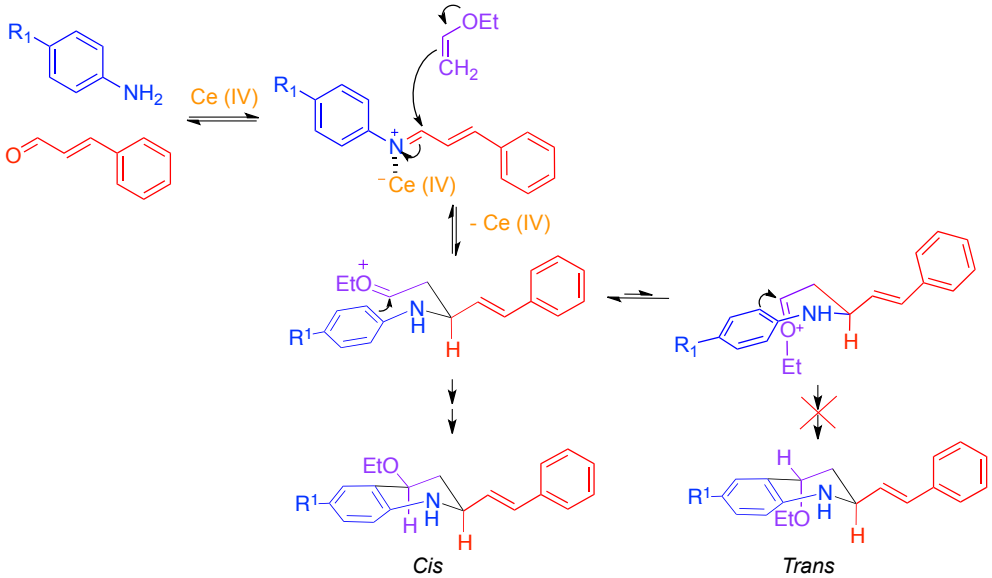

Scheme 6.3. Mechanism of the type-II vinylogous Povarov reaction

In order to improve the optical properties of our compounds, an amino group was purposely introduced on the styryl moiety of compound **137**. To this end, we treated this compound with a mixture of fuming and concentrated nitric acids, followed by reduction of the crude nitration product with iron powder and concentrated HCl.[154] This protocol afforded compound **139**, bearing the amino group at *para* position on the phenyl ring in 68% yield after chromatography together with a small amount of the corresponding *ortho* derivative, compound **140** (Scheme 6.4). Furthermore, in order to reinforce this effect by increasing the electron-withdrawing character of the quinoline nitrogen, the hydrochloride salt (compound **139·HCl**) was also prepared by treating compound **139** with a solution of methanol saturated with HCl. The protonation of the quinoline nitrogen was confirmed by ^{1}H-NMR studies of **139·HCl**, which showed

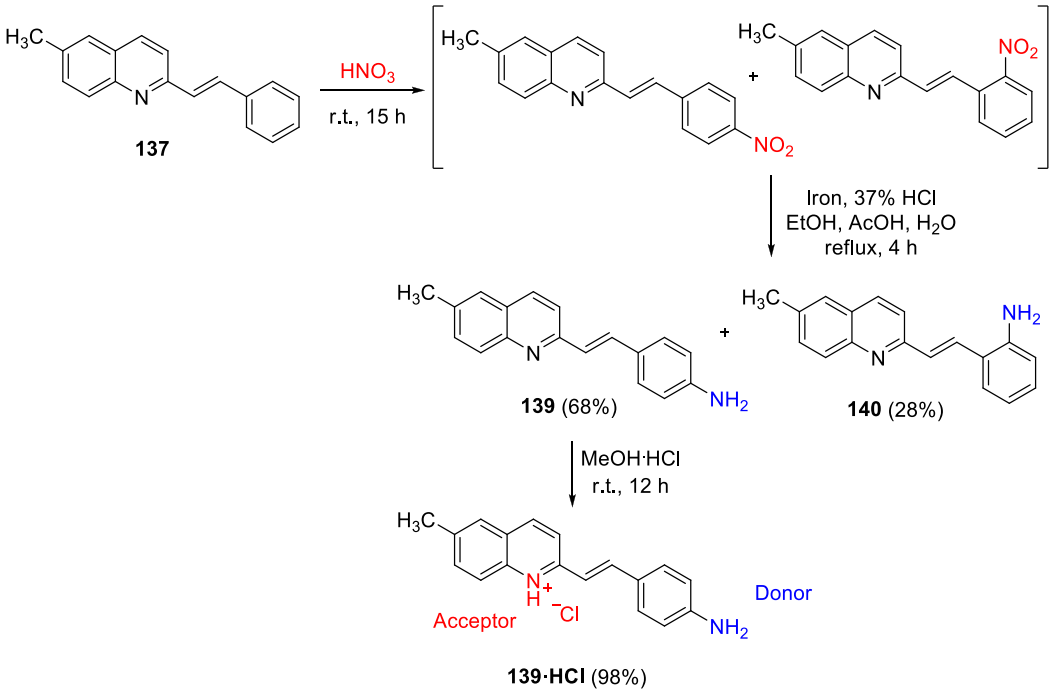

Scheme 6.4. Synthesis of compound **139** and its hydrochloride salt

significative displacements of the protons adjacent to the quinoline nitrogen, namely H-8 and the olefinic protons with regard to **139**, whereas the *o*-NH2 protons remained almost unaltered. Similar changes were observed in the ^{13}C-NMR spectra.

6.2.2. Native fluorescence study of styrylquinolines

The fluorescence study of our molecules was performed by Dr. Víctor González-Ruiz under the supervision of Prof. María Antonia Martín at Sección Departamental de Química Analítica, Facultad de Farmacia, Universidad Complutense de Madrid. Thus, the native fluorescence of styrylquinolines **137-139** and **139·HCl** was investigated in several solvents, including phosphate buffered saline (PBS) at physiological pH (Table 6.1). In the case of **139**, the fluorescence emission greatly depended on solvent polarity (Figure 6.2A,B and

Table 6.1. Excitation and emission maxima of compounds **137-139 and 139·HCl** in different solvents

Cmpd.	EtOH		Cyclohexane		H_2O		Acetonitrile		PBS	
	λ_{ex} (nm)	λ_{em} (nm)	λ_{ex} (nm)	λ_{em} (nm)	λ_{ex} (nm)	λ_{em} (nm)	λ_{ex} (nm)	λ_{em} (nm)	λ_{ex} (nm)	λ_{em} (nm)
137	285 324[a] 341	364[a] 380 401[a]	265	303 311[a]	278 322[a] 339	405	282 345 360[a]	391	--	--
138	284 347[a] 358	372[a] 390 407[a]	284 353	381 401 423[a]	283 352	412	284 354 366[a]	386 405	--	--
139	282 370	508	265 278 356	303 313 428, 560[a]	280 370 466	560 510	281 364	503	273 370	311 465 557
139·HCl	268 285 370 537[a]	309 520 604[a] 660[a]	--	--	268 284 369	310 462 557	--	--	273 282 368	310 465 554

[a]Shoulder

Table 1). It is interesting to note that the fluorescence emission of the protonated form of **139** (Figure 6.2B) in ethanol, whose polarity mimics the protein environment, was red-shifted with regard to the more polar water solvent. Since compound **139** would be adsorbed onto protein aggregates where its free movement would be restricted, the fluorescence emission spectrum of **139·HCl** in the solid state was also obtained (Figure 6.2C), showing an interesting emission maximum above 600 nm. On this basis, we consider **139** as a potential a NIR tracer.[158] An additional advantageous feature of **139** is its large Stokes shift

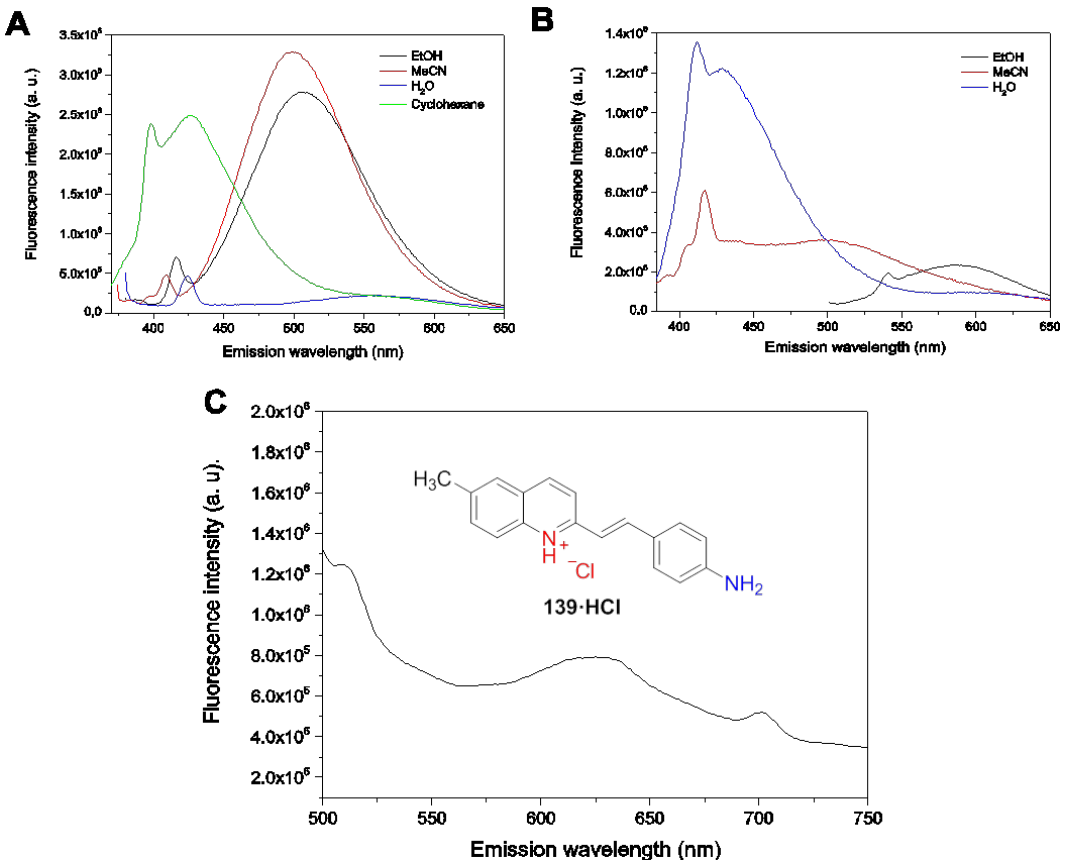

Figure. 6.2. Fluorescence spectra for **139** in its neutral (A) and protonated form (B) in solution, and for **139·HCl** in the solid state (C)

158 Raymons, S. B.; Kumar, A. T. N.; Boas, D. A.; Bacskai, B. J. *Phys. Med. Biol.* **2009**, *54*, 6201.

(> 150 nm), which minimizes interference from the exciting radiation. Furthermore, the structure of **139** allows its easy manipulation by increasing the electron-donating/accepting ability of the molecule to enhance the spectral bathochromic shift, facilitating its use as a lead in the generation of a second generation of improved fluorescent probes.

6.2.3. Prediction of brain penetration

To assess the potential value of our compounds as CNS directed ligands, the capability of **137-139** to cross the blood brain barrier (BBB) was studied by the parallel artificial membrane permeability assay (PAMPA).[159] The experiments were carried out by Dr. Daniel I. Pérez under the supervision of Prof. Ana Martínez at Instituto de Química Médica-CSIC, Madrid. The PAMPA test is a method that allows evaluating the permeability of a compound from a donor compartment, through a porcine brain lipid membrane, into an acceptor compartment. The donor plate is put on the acceptor plate to form a "sandwich", which is left undisturbed for a couple of hours. During this time a compound diffuses from the donor plate through the brain lipid membrane into the acceptor plate where its concentration is determined by an UV plate reader. The data obtained for our compounds are summarized in Table 6.2, and allowed

Table 6.2. BBB permeation prediction for **137-139**

Cmpd.	Pe (10^{-6} cm s^{-1})[a]	Prediction[b]
137	3.0 ± 0.6	CNS +/−
138	8.5 + 1.1	CNS +
139	23.1 ± 1.9	CNS +

[a]Mean ± standard deviation (SD) of two experiments. [b]CNS + means Pe > 3.74 × 10^{-6} cm s^{-1}, and CNS ± means Pe between 3.74 × 10^{-6} and 1.50 × 10^{-6} cm s^{-1}

159 Di, L.; Kerns, E. H.; Fan, K.; McConnell, O. J.; Carter, G. T. *Eur. J. Med. Chem.* **2003**, *38*, 223.

us to predict optimal BBB permeation for **138** and **139**, although the result was not so clear-cut in the case of **137**.

6.2.4. Antiaggregating potency towards Aβ

In vitro activities of compounds **137-139** on Aβ were investigated by Dr. Manuela Bartolini under the supervision of Prof. Vincenza Andrisano at the University of Bologna, Italy. The inhibitory potency of **137-139** as antiaggregating agents toward $A\beta_{42}$ was determined by a ThT based fluorometric assay.[160] When tested at a 1:1 ratio with $A\beta_{42}$, **137** and **138** did not significantly alter amyloid fibril formation, while **139** decreased the fluorescence signal by 42.4 ± 2.6%, thus behaving as an inhibitor of fibrilization and an amyloid binder. On the basis of data available in the literature, **139** can be ranked as a moderate inhibitor, with potency slightly lower than that of the well-known antiaggregating compound curcumin,[161] which, in the same assay conditions, was able to inhibit fibril formation by 73%. Furthermore, no negative or positive interference in the fluorescence signal of ThT was observed under the experimental conditions (Figure 6.3C). In the light of these findings, compound **139** was regarded as sufficiently interesting to warrant further study.

Due to its potential application as an amyloid sensor, the emission spectra of compound **139** in the absence and presence of aggregated $A\beta_{42}$ were recorded. While the excitation maxima for the bound and unbound forms of **139** did not significantly differ, a strong hypsochromic shift of the emission maximum (from 528 to 490 nm), concomitant with a hyperchromic effect upon binding, was observed (Figure 6.3A). In agreement with the previously mentioned studies in

160 Cavalli, A.; Bolognesi, M. L.; Capsoni, S.; Andrisano, V.; Bartolini, M.; Margotti, E.; Cattaneo, A.; Recanatini, M.; Melchiorre, C. *Angew. Chem. Int. Ed.* **2007**, *46*, 3689.

161 Yang, F.; Lim, G. P.; Begum, A. N.; Ubeda, O. J.; Simmons, M. R.; Ambegaokar, S. S.; Chen, P. P.; Kayed, R.; Glabe, C. G.; Frautschy, S. A.; Cole, G. M. *J. Biol. Chem.* **2005**, *280*, 5892.

solvents with decreasing polarity, this behavior seems related to a change in the environmental conditions, as the binding of **139** to the amyloid fibrils takes place in a lower dielectric constant environment. Indeed, adopting the β-sheet secondary structure in the $A\beta_{42}$ self-assembly process is likely to expose hydrophobic regions that are accessible to **139**. The spectral shift observed for **139** is similar to that reported for the $A\beta_{42}$ fluorescent sensor 1-anilinophthalene-8-sulfonic acid.[162] Furthermore, the fluorescence emission intensity at 450 nm linearly correlated with the concentration of preaggregated $A\beta_{42}$ (R^2 = 0.9992) (Figure 6.4).

Finally, to gain further insights into the binding mode of **139** to Aβ, displacement studies in the presence of aggregated $A\beta_{42}$ were carried out using a fixed concentration of $A\beta_{42}$ and ThT and an increasing concentration of **139**. Overlaid excitation spectra showed that **139** binds amyloid fibrils with a high affinity. At a low concentration (25 nM) and in the presence of $A\beta_{42}$, **139** showed a significant emission signal (Figure 6.3B) without affecting the ThT excitation and emission profile (Figure 6.3C). Conversely, at higher concentrations, **139** progressively displaced ThT from its binding site(s) (Figure 6.5).[163] This behavior led us to hypothesize that **139** may have a primary high affinity binding site distinct from ThT and a secondary low-affinity binding site in common with ThT.

162 Royer, C. A. *Chem. Rev.* **2006**, *106*, 1769.
163 Groenning, M. *J. Chem. Biol.* **2010**, *3*, 1.

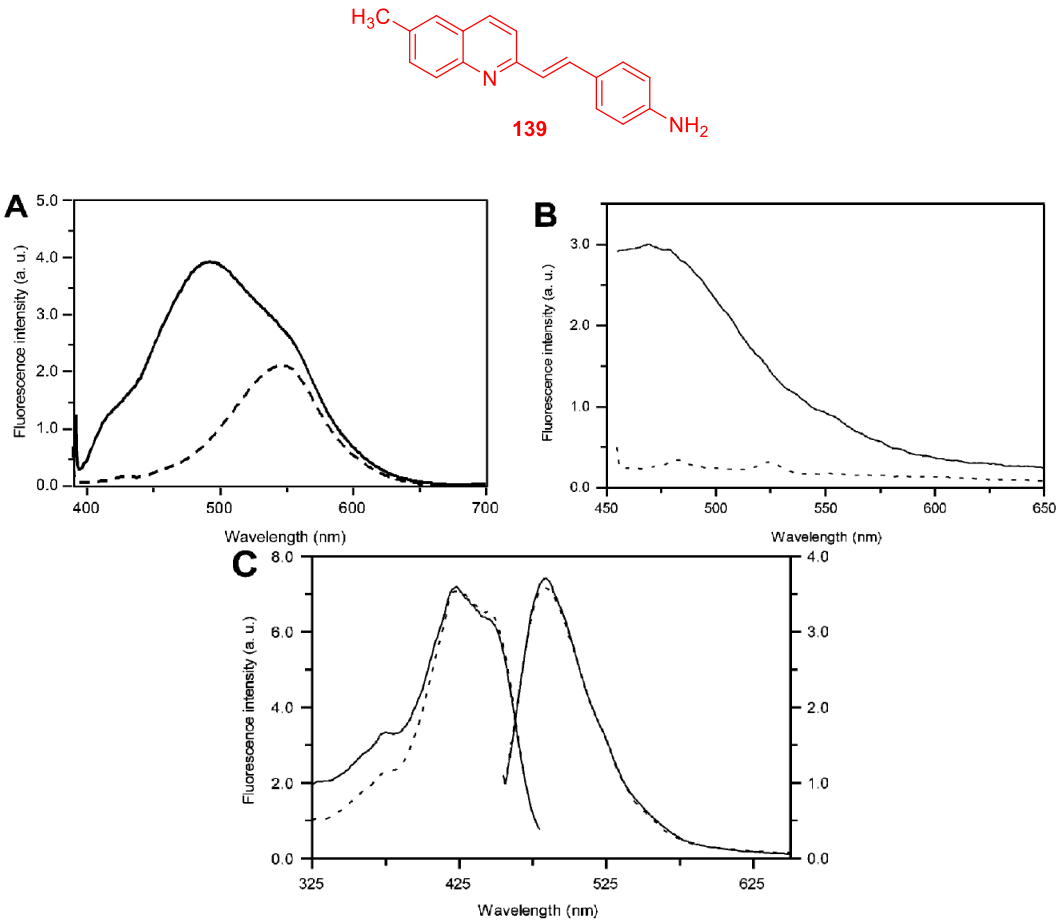

Figure.6.3. (**A**) Fluorescence emission spectra of **139** (5 μM) in aqueous phosphate buffer (10 mM, pH 7.4) in the absence (dotted line) and in the presence (solid line) of aggregated $A\beta_{42}$ (3 μM). (**B**) Fluorescence emission spectra of a solution containing aggregated $A\beta_{42}$ protein and **139** [25 nM] in glycine–NaOH buffer (50 mM, pH 8.5) recorded at the excitation maximum of ThT (λ_{ex} = 446 nm, dotted line) and at the excitation maximum of **139** (λ_{exc} = 375 nm, solid line).(**C**) Excitation (λ_{em} = 490 nm) and emission (λ_{exc} = 446 nm) spectra of a solution containing aggregated $A\beta_{42}$ protein in 1.5 μM ThT buffered solution (glycine-NaOH buffer, 50 mM pH 8.5) in the presence (dotted line) and absence (solid line) of **139** [25 nM]

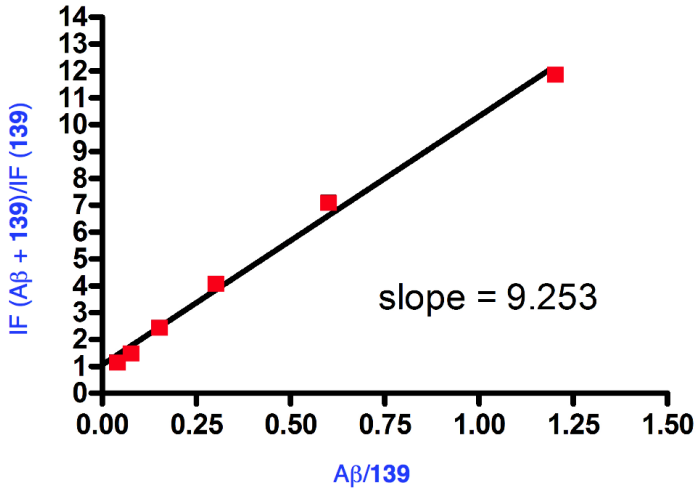

Figure 6.4. Linear dependence of the fluorescence emission intensity from the concentration of aggregated $A\beta_{42}$. λ_{exc} = 375 nm, λ_{em} = 450 nm. y = 7.861x + 0.1513; R^2 = 0.9992.

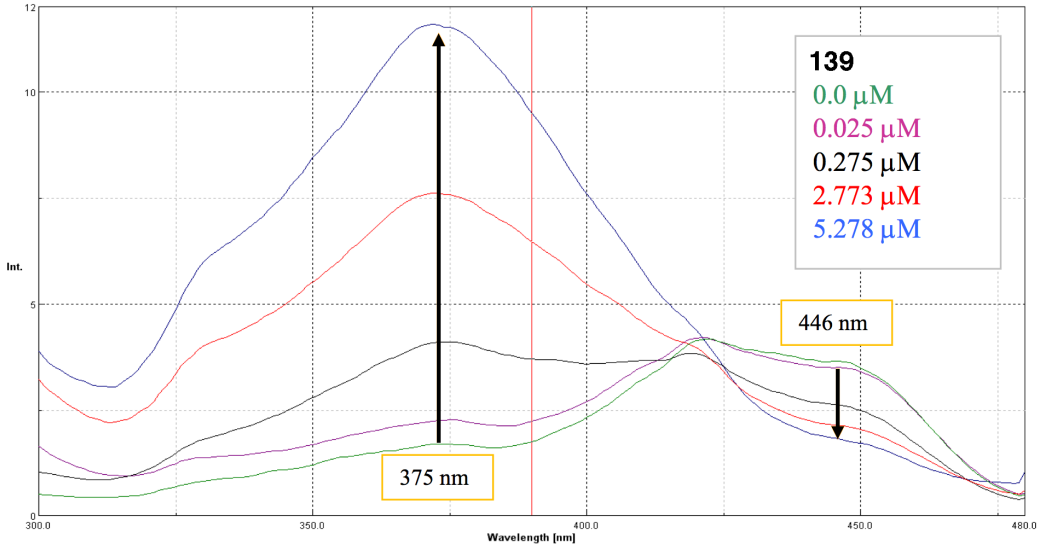

Figure 6.5. Overlaid excitation spectra of $A\beta_{42}$ protein diluted in 1.5 μM ThT buffered solution (glycine-NaOH buffer 50 mM, pH 8.5) in the presence of increasing concentrations of **139**; λ_{em} = 490 nm.

In order to discard the possible interference of human serum albumin (HSA) in future *in vivo* studies, a comparison between the changes in the fluorescence intensity in the presence of HSA and $A\beta_{42}$ was carried out. It evidenced a stronger fluorescence change for the latter, as deduced from the slopes of the titration plots (Figure 6.6).

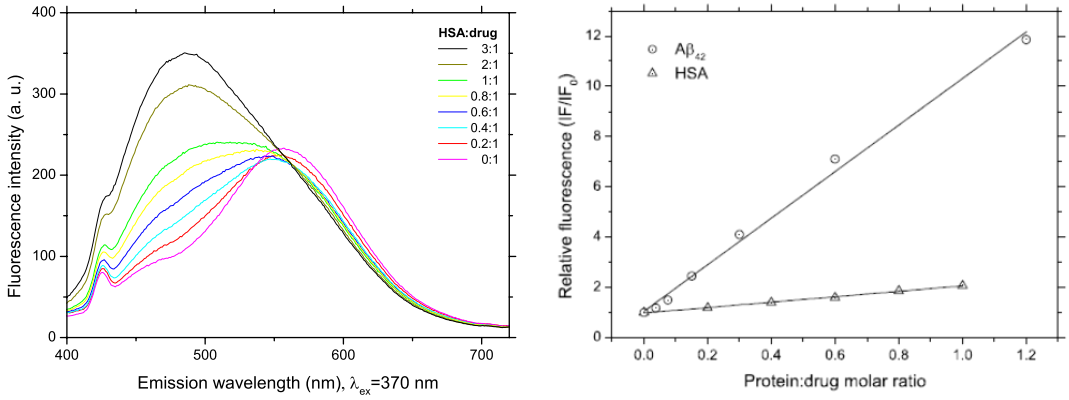

Figure 6.6. Left: Emission spectra of **139** in PBS in the presence of increasing amounts of human serum albumin (HSA). Right: Selective increase in the fluorescence of **139** in the presence of $A\beta_{42}$ protein with regard to HSA; $A\beta_{42}$: y = 9.27x + 1.04, R^2 = 0.9935; HSA: y = 1.08x + 0.97, R^2 = 0.9959.

6.2.5. Antiprion evaluation

The study on the antiprion activity of our molecules were conducted again by H. N. Ai Tran under the supervision of Prof. G. Legname at the Trieste International School of Advanced Studies (SISSA) employing the same protocol described above for diketopiperazines. First, the capability to inhibit prion fibril formation *in vitro* was studied, using the amyloid seeding assay (ASA). At a concentration of 50 µM, **137-139** delayed fibril formation, extending the lag phase to ≥70 h (control: 59 h) (Figure 6.7). A similar profile was found for GN8, the antiprion drug candidate that was described in the previous chapter. Taken together,

these results showed that compound **139** is indeed able to recognize and modulate $A\beta_{42}$ and PrP^{Sc} fibril aggregation *in vitro*.

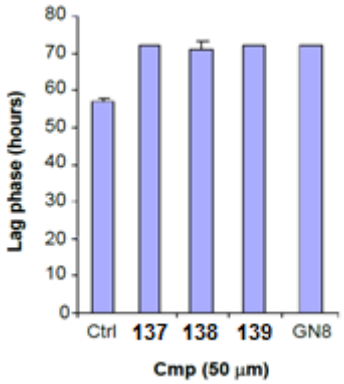

Figure 6.7. Prion fibril formation inhibitory activity *in vitro* for compounds **137-139** (50 μM) compared with GN8.

Next, the therapeutic antiprion potential (toxicity and activity) of **137-139** was preliminarily assessed in a cell-based model of PrD (ScGT1 cells). At a 1 μM concentration, **137** and **139** showed a very low toxicity, with cell viability above 90%, while **138** caused viability to decrease to 60%. Interestingly, at a 10 μM concentration **139** still showed a tolerable toxicity, with a residual 60% cell viability similar to that of drug candidate GN8 (Figure 6.8). The three compounds

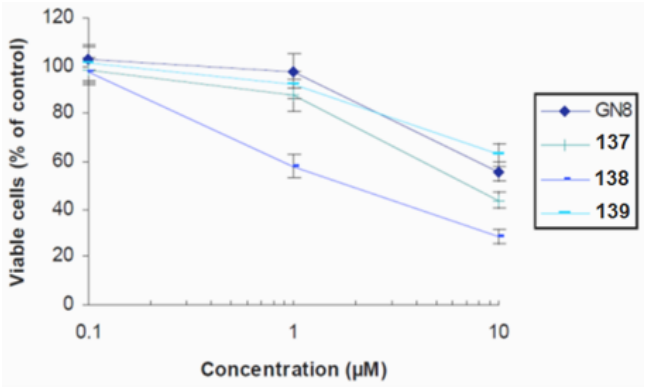

Figure 6.8. Cell viability profiles of **137-139** in comparison with GN8

were studied for their antiprion activity in a non-toxic range of concentrations (Table 6.3). They all showed remarkable activities (submicromolar EC_{50} values), which make them more potent than GN8 and equipotent to the gold standard quinacrine. Cell viability at the concentration corresponding to EC_{50} was particularly high for **139** (94.6%).

Table 6.3. Antiprion activity and cell viability of **137-139** on ScGT1 cells

Cmpd.	EC_{50} (mM)[a]	% of viable cells at EC_{50}[a]
Quinacrine	0.4 ± 0.1	100.0 ± 4.3
GN8	1.5 ± 0.1	93.4 ± 7.3
137	0.5 ± 0.1	90.5 ± 6.8
138	0.7 ± 0.1	74.9 ± 4.1
139	0.5 ± 0.1	94.6 ± 4.9

6.2.6. Fluorescent staining of PrP^{Sc} in ScGT1 cells

To confirm the labeling of PrP^{Sc} aggregates in living cells, fluorescent staining with **139·HCl** was carried out using the previously mentioned ScGT1 cell model by Suzana Aulić under the supervision of Prof. Giuseppe Legname at SISSA, Trieste. It was found that 0.025% of **139·HCl** (0.84 mM) was sufficient to observe many fluorescent spots in the treated cells before and after denaturation with 6M GndHCl examined by fluorescent microscopy (Figure 6.9A,B). The green colour of the spots is arbitrary and was manually selected; in other words, the fluorescent emission of our compound is not properly green. Importantly, no spots were observed in the uninfected cells (Figure 6.9D−F), confirming a specific binding for scrapie fibrils. Furthermore, **139·HCl** distinguished the abnormal, proteinase K (PK) aggregated and resistant PrP^{Sc} isoform from the normal, PK-sensitive PrP^{C} isoform. Thus, after eliminating PrP^{C} through a PK digestion step,

the previous fluorescence-staining pattern was observed (Figure 6.9C).). A further experiment proved that the staining pattern was consistent with that observed with 0.025% Thioflavin S (ThS), a common PrP^{Sc} dye (Figure 6.10).

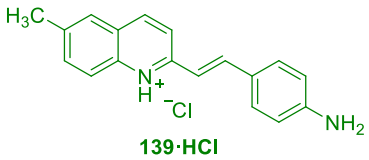

139·HCl

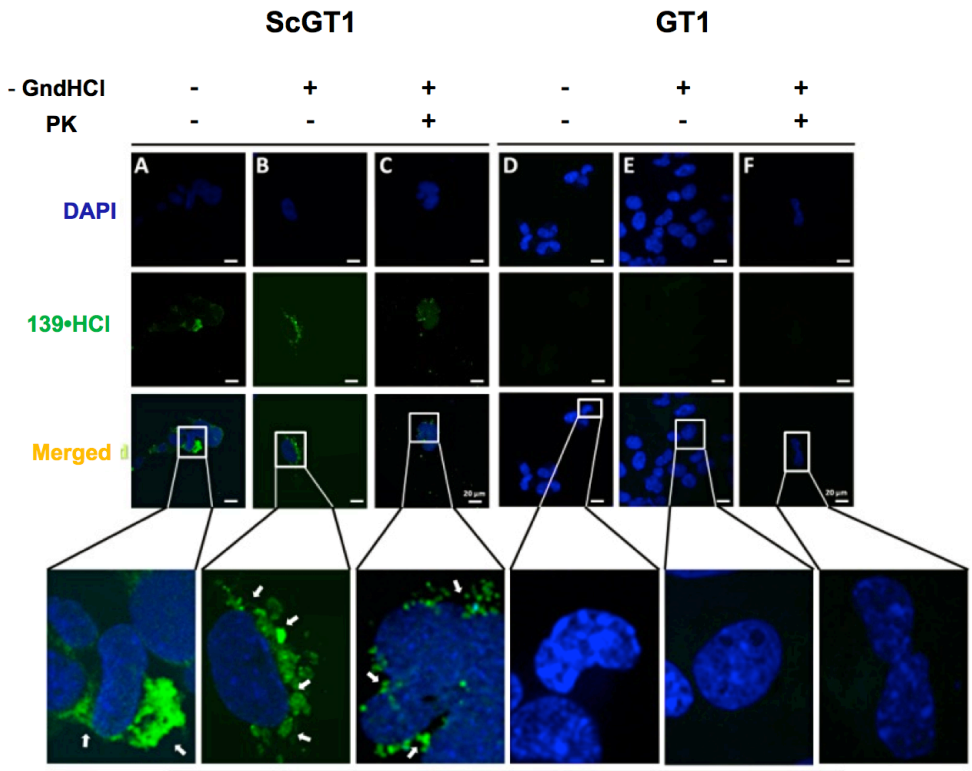

Figure 6.9. Detection of PrP^{Sc} aggregates with **139·HCl** in ScGT1 cells by IF before (**A**) and after (**B**) denaturation with 6M GndHCl. After PK digestion, PK resistant PrP (PrP^{Sc}) was observed with **139·HCl** (**C**). Uninfected GT1 cells with or without denaturation step with 6M GndHCl (**D**, **E**) and after PK digestion (**F**) did not show staining in the presence of 0.025% of **139·HCl**

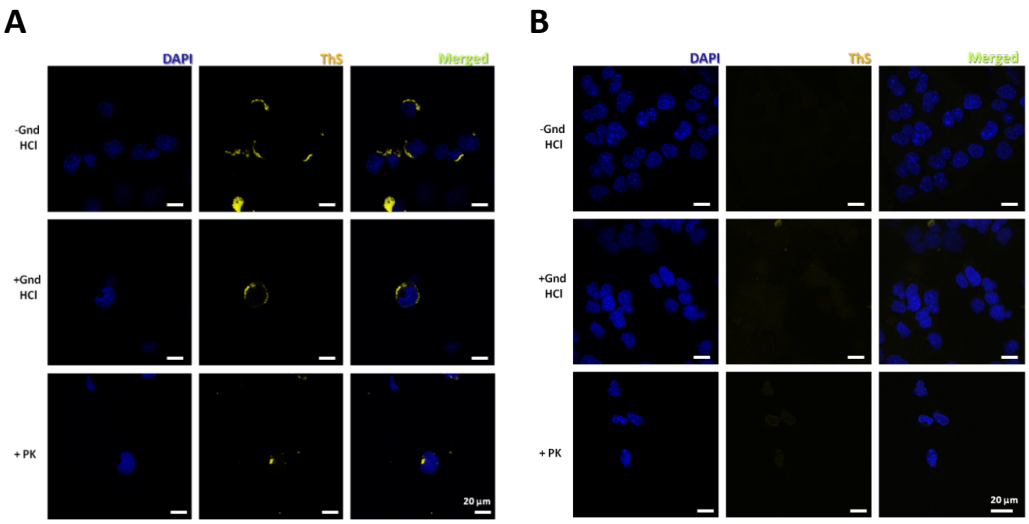

Figure. 6.10. Comparison of the methods used to visualize PrP^{Sc} in ScGT1 (scrapie prion-infected cells, panel A) and non-infected GT1 cells (panel B) before and after denaturation with 6M GndHCl, and after proteinase K digestion (PK) prior to staining with Thioflavin-S (yellow), a dye that specifically binds to aggregates, and counter staining with DAPI (blue). Scale bar 20µm

We primarily used the FITC filter set for these studies, but we confirmed the staining by employing the ThS one, which is within the NIR optical window (Figure 6.11).

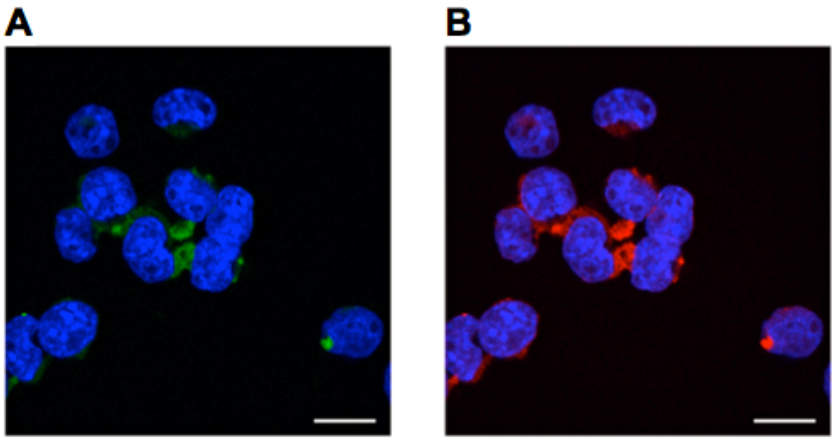

Figure 6.11. ScGT1 cell line treated with 6M GndHCl and stained with compound **139·HCl**. (A) FITC filter. (B) ThS filter. Nuclei stained with DAPI (blue). Scale bar 20µm

6.3. Second styrylquinoline library

6.3.1 Synthetic approaches

As anticipated, and in the light of the good results obtained for compound **139**, we decided to develop a larger, focused library of styrylquinoline derivatives. Our investigation started again with the application of the vinylogous variation of the Povarov reaction. In order to introduce varied substituents on the phenyl moiety, we needed suitable functionalized cinnamaldehydes, which we prepared using a literature method.[164] Thus, a Heck reaction between aryl iodides and acrolein diethyl acetal in the presence of $Pd(OAc)_2$, nBu_4NOAc, K_2CO_3, KCl, in DMF at 90 °C was followed by *in situ* hydrolytic deprotection to give the desired products **141-145** in high yields (Scheme 6.5).

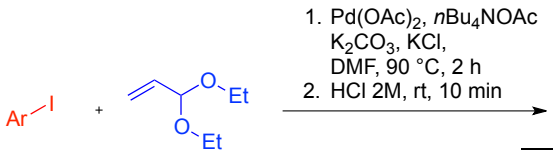

Comd.	Ar	Yield, %
141	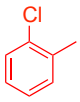	70
142	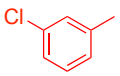	80
143	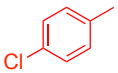	83
144	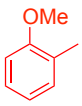	57
145	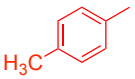	81

Scheme 6.5. Scope and yields of the synthesis of substituted cinnamaldehydes

164 Battistuzzi, G.; Cacchi, S.; Fabrizi, G. *Org. Lett.* **2003**, *5*, 777.

With these cinnamaldehydes in hand, we carried out the multicomponent reaction with arylamines and alkyl vinyl catalyzed by CAN under our standard conditions to obtain the corresponding 2-styryl-1,2,3,4-tetrahydroquinolines. This was followed by their dehydrogenation in the crude state in the presence of DDQ to give the 2-styryquinoline compounds **146-160** in moderate overall yields (Scheme 6.6 and Table 6.4).

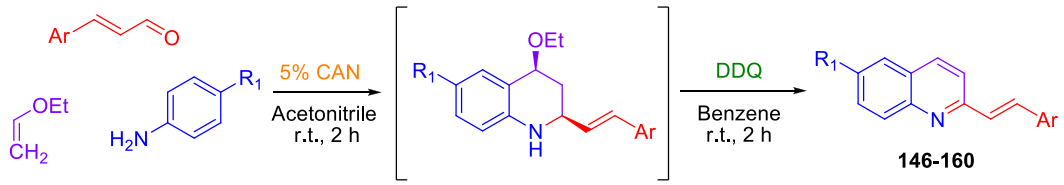

Scheme 6.6. Synthesis of 2-styrylquinolines

Table 6.4. Scope and yields of the synthesis of 2-styrlquinolines

Compd.	R_1	Ar	Overall yield, %
146	H		62
147	Cl		75
148	H		42
149	Me	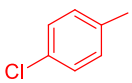	38
150	Cl		30
151	OMe		44
152	Me	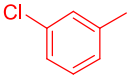	39
153	OMe		34
154	Me	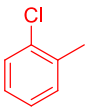	42
155	OMe		46
156	Me	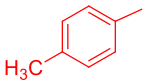	47
157	Cl		45
158	OMe		41
159	Me	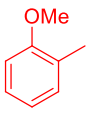	29
160	Cl		25

Unexpectedly, the reaction starting from cinnamaldehyde derivatives bearing a methoxy group at the *meta* and *para* positions failed or provided the

desired product only in trace amounts. Probably, this was due to the electron-releasing effect of the methoxy group, which reduces the electrophilicity of the aldehyde carbonyl group (Scheme 6.7). Steric hindrance to resonance was probably responsible for the isolation of compounds **159** and **160**, albeit in small yields, in the reactions starting from *o*-methoxycinnamaldehyde.

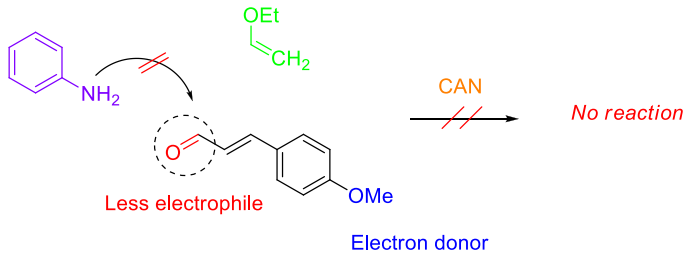

Scheme 6.7. Electron donor groups on the cinnamaldehyde moiety hamper the Povarov reaction

In an effort to overcome this problem, we sought another strategy for the synthesis of 2-styrylquinolines. It is well known that the most common method is based on acid- or base-catalyzed condensation of 2-methyquinolines (quinaldines) with aromatic aldehydes.[165]

As the first step, we prepared several substituted quinaldines exploiting again a CAN-catalyzed ABB' chemodifferentiating three-component reaction between anilines and vinyl ethers.[166] As shown in Scheme 6.8, the treatment of aniline derivatives with vinyl ethers in the presence of 5% CAN in acetonitrile at r.t. led to the corresponding 2-methyl-1,2,3,4-tetrahydroquinolines with about

165 a) Dabiri, M.; Salehi, P.; Baghbanzadeh, M.; Nikcheh, M. S. *Tetrahedron Lett.* **2008**, *49*, 5366; b) Leonard, J. T.; Roy, K. *Eur. J. Med. Chem.* **2008**, *43*, 81; c) Makhija, M. T. *Curr. Med. Chem.* **2006**, *13*, 2429; d) Normand-Bayle, M.; Bénard, C.; Zouhiri, F.; Mouscadet, J. F.; Leh, H.; Thomas, C. M.; Mbemba, G.; Desmaële, D.; d'Angelo, J. *Bioorg. Med. Chem. Lett.* **2005**, *15*, 4019; e) Yuan, H.; Parrill, A. L. *Bioorg. Med. Chem.* **2002**, *10*, 4169; f) Polanski, J.; Zouhiri, F.; Jeanson, L.; Desmaële, D.; d'Angelo, J.; Mouscadet, J. F.; Gieleciak, R.; Gasteiger, J.; Le Bret, M.*J. Med. Chem.* **2002**, *45*, 4647.

166 Sridharan, V.; Avendaño, C.; Menéndez J. C. *Tetrahedron*, **2007**, *63*, 673.

9:1 *cis*/*trans* diastereoselectivity. Since we were interested in their dehydrogenated derivatives, these two diastereoisomers were not separated by chromatography; instead, the crude products were directly dehydrogenated in the presence of palladium in refluxing toluene to give compounds **161-167** (Scheme 6.8 and Table 6.5). The yields were generally good, with the exception of the reactions starting from *m*-substituted anilines, which were complicated by the possibility to obtain two products, since the starting aniline is not symmetric.

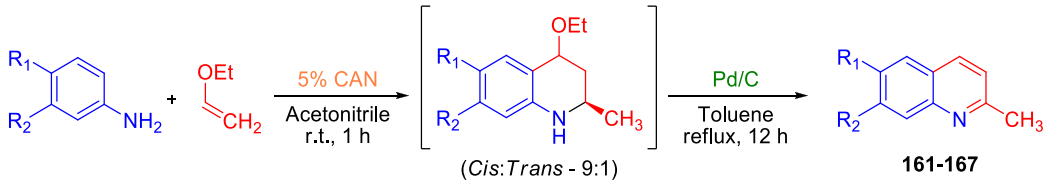

Scheme 6.8. Synthesis of 2-methylquinolines (quinaldines)

Table 6.5. Scope and yields of the synthesis of 2-methylquinolines

Entry	Cmpd.	R_1	R_2	Overall yield, %
1	**161**	H	H	78
2	**162**	CH_3	H	82
3	**163**	Cl	H	67
4	**164**	OMe	H	70
5	**165**	H	CH_3	40
6	**166**	H	Cl	45
7	**167**	H	OMe	Trace

The domino mechanism of the reaction that leads to the formation of 2-methyl-1,2,3,4-tetrahydroquinolines is summarized in Scheme 6.9 and involves five individual steps. First, a condensation reaction between aniline and one molecule of ethyl vinyl ether, which can be regarded as an enol ether derived

from acetaldehyde, takes place catalyzed by CAN that acts as Lewis acid to afford the imine intermediated product. Then, the latter compound undergoes a CAN-catalyzed imino Diels–Alder reaction (Povarov reaction) with a second molecule of ethyl vinyl ether, now acting as an electron-rich dienophile, to give the observed tetrahydroquinolines after the final cyclization step.

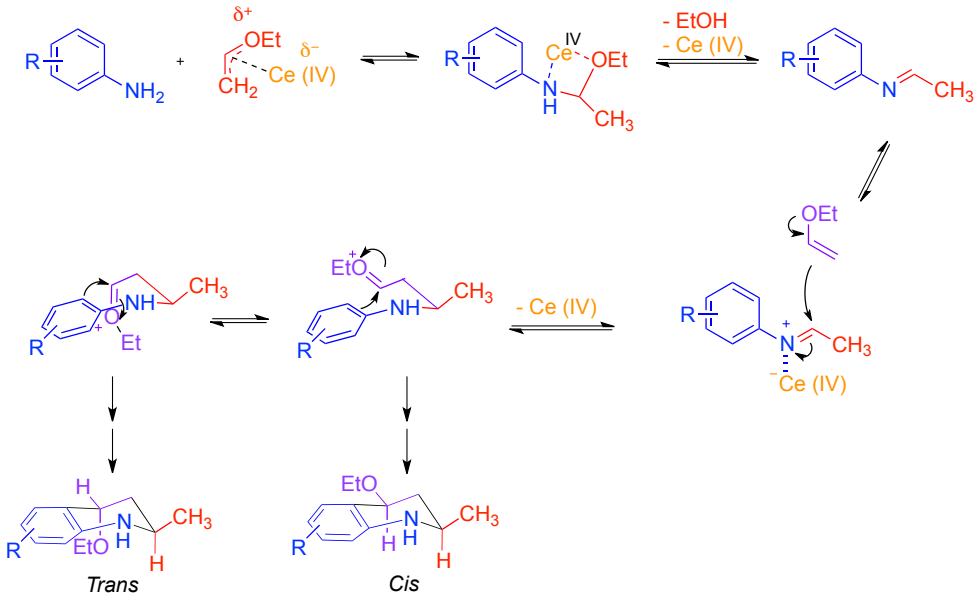

Scheme 6.9. Mechanism of the CAN-catalyzed three-component reaction between anilines and ethyl vinyl ether

Because this protocol turned out to be unsuitable for the synthesis of compound **167**, we looked for a more efficient method. Thus, we applied conditions found in literature based on the preparation of 7-hydroxyquinaldine followed by its transformation into the methoxy derivative (Scheme 6.10).[167] 7-hydroxyquinaldine (compound **168**) was obtained *via* the Skraup reaction by treating *m*-aminophenol with crotonaldehyde in the presence of concentrated

167 Chen, X. Y.; Shi, J.; Li, Y. M.; Wang, F. L.; Wu, X.; Guo, Q. X.; Liu, L. *Org. Lett.***2009**, *11*, 4426.

hydrochloric acid and tetrachloro-1,4-benzoquinone (*p*-chloranil), with 1-butanol as solvent.[168] Afterwards, the hydroxyl group was transformed into the desired methoxy by methylation in the presence of CH_3I and K_2CO_3 in DMF.

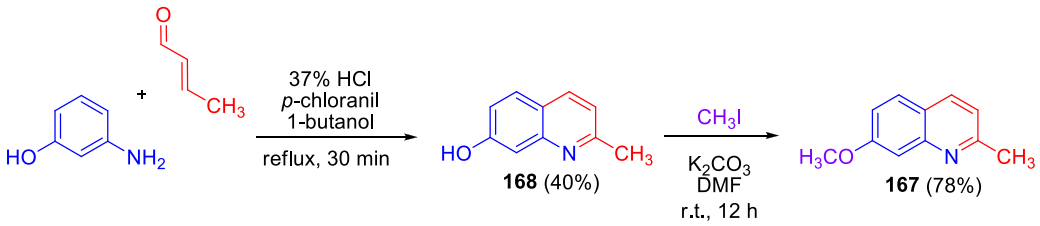

Scheme 6.10. Synthesis of compound **167** *via* Skraup reaction

With all the quinaldines in hand, we needed to study their reaction with aromatic aldehydes. Using common literature methods, this aldol-type condensation requires high temperatures and gives only moderate yields in many cases. An attempt to improve this reaction by applying MW irradiation is described in the literature,[169] but it involves the use of a domestic oven, which leads to well-known safety concerns and serious reproducibility issues related to the generation of an uneven pattern of hot and cold spots inside the oven cavity.[170] Even more importantly, the method was not general, allowing only the preparation of carboxyquinolines and little structural variation on the styryl chain.

With this precedent in mind, in an effort to circumvent these limitations, we investigated the condensation reaction under focused MW irradiation. After some experimentation, we found that microwave irradiation of a solvent-free mixture of quinaldine derivatives, aromatic aldehydes and acetic anhydride

168 Fedoryak, O. D.; Dore, T. M. *Org. Lett.* **2002**, *4*, 3419.
169 Musiol, R.; Podeszwa, B.; Finster, J.; Niedbala, H.; Polansli, J. *Monatsh. Chem.* **2006**, *137*, 1211.
170 Kappe, A. O. *Angew. Chem. Int. Ed.* **2004**, *43*, 6250.

afforded excellent yields of styrylquinolines in a single synthetic operation that leads to the generation of a carbon-carbon double bond in a very efficient diastereoselective fashion, with water and acetic acid as the only side products (Scheme 6.11).[171]

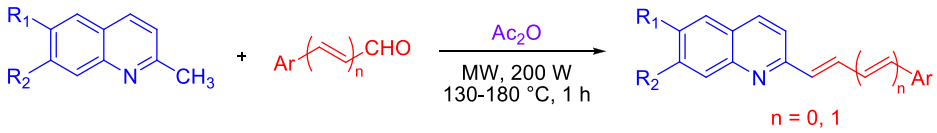

Scheme 6.11. General conditions for the synthesis of 2-styrylquinolines

This protocol was applied to different aromatic aldehydes such as pyridine-2-carbaldehyde, pyridine-3-carbaldehyde, pyridine-4-carbaldehyde, 3 and 4-methoxybenzaldehyde, 4-fluorobenzaldehyde, and substituted cinnamaldehydes including (*E*)-3-(4-chlorophenyl)acrylaldehyde and (*E*)-3-(2-nitrophenyl)-acrylaldehyde to obtain compounds **169-199** (Table 6.6).

171 **Staderini, M.**; Cabezas, N.; Bolognesi, M. L.; Menéndez, J. C. *Synlett* **2011**, *17*, 2577.

Table 6.6. Scope and yields of the synthesis of 2-styrylquinolines under focused MW irradiation

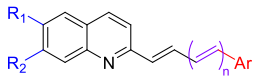

169-199

Cmpd.	R_1	R_2	Ar	n	T,°C	Yield, %
169	Me	H		0	130	87
170	Cl	H		0	130	91
171	OMe	H		0	130	75
172	Me	H		0	130	62
173	Cl	H		0	130	86
174	OMe	H		0	130	83
175	H	H		0	130	65
176	Me	H		0	130	76
177	Cl	H		0	130	80
178	OMe	H		0	130	85
179	H	Me		0	130	45
180	H	Cl		0	130	87
181	H	H		0	180	70
182	Me	H		0	180	93
183	Cl	H		0	180	80
184	OMe	H	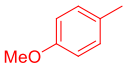	0	180	80
185	H	Me		0	180	77
186	H	Cl		0	180	84
187	H	OMe		0	180	81

Cmpd.	R_1	R_2	Ar	n	T,°C	Yield, %
188	Me	H	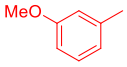	0	180	65
189	Cl	H		0	180	90
190	H	H		0	150	65
191	Me	H		0	150	84
192	Cl	H	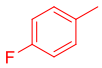	0	150	95
193	OMe	H		0	150	86
194	H	Me		0	150	64
195	H	OMe		0	150	61
196	H	OMe		0	150	78
197	Cl	H		1	150	93
198	Me	H	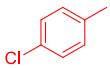	1	150	74
199	OMe	H		1	130	72

As summarized in Scheme 6.12, we propose this transformation to proceed through a domino sequence comprising an initial aldol addition, followed by intramolecular O-acetylation and elimination.

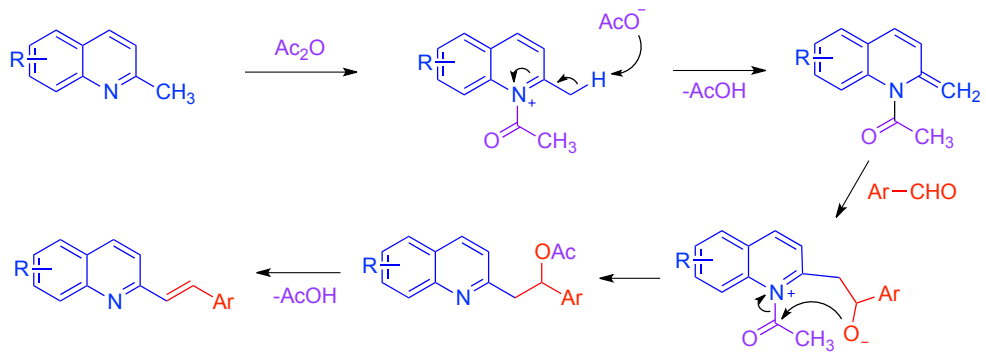

Scheme 6.12. Proposed mechanism for the Ac_2O-promoted aldol reaction

Unexpectedly, in the case of 4-(dimethylamino)benzaldehyde the microwave-enhanced aldol reaction failed. As an alternative, we resorted to a protocol that involved the use of potassium *t*-butoxide as base to catalyze the condensation reaction with quinladines.[172] The reaction was carried at r.t. during 24 h in DMF in the presence of LiH to ensure a dry non-protic reaction medium to give compounds **200-203** (Scheme 6.13 and Table 6.7). The same method was used for quinoline-2-carbaldehyde to obtain compound **204**.

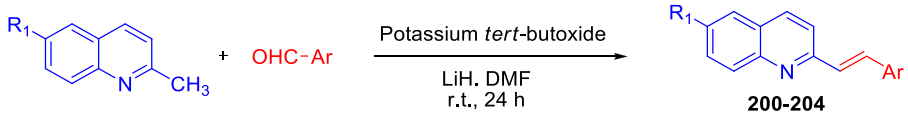

Scheme 6.13. Synthesis of compounds **200-204** in the presence of potassium *t*-butoxide

172 De, C.; Samuels, T. A.; Haywood, T. L.; Anderson, G. A.; Campbell, K.; Fletcher, K.; Murray, D. H.; S. O. Obare. *Tetrahedron Lett.* **2010**, *51*, 1754.

Table 6.7. Scope and yields of the synthesis of compounds **200-204**

Cmpd.	R_1	Ar	Yield, %
200	H	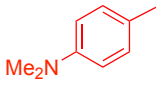	66
201	Me		81
202	Cl		90
203	OMe		63

Cmpd.	R_1	Ar	Yield, %
204	H	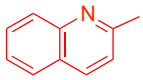	58

Since compound **139** had shown excellent optical and biological properties, we decided to explore the role of the amino moiety at different positions of the styrylquinoline fragment. We first decided to introduce an amino group at the quinoline C-4 position, and to this end we planned the use the Conrad-Limpach reaction to prepare the suitable quinolin-4-ones, which would then be submitted to aldol condensations and a hydroxy-amino exchange (Scheme 6.14).

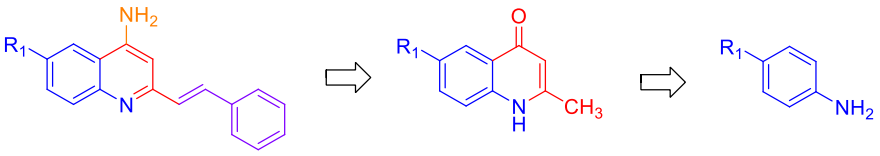

Scheme 6.14. Retrosynthetic scheme for the preparation of 4-aminostyrylquinolines.

We started with the reaction between the suitable aniline and ethyl acetoacetate to obtain the corresponding β-enaminones. This reaction is well described in the literature, and it is often carried out in the presence of a Lewis acid as catalyst.[120] In our case, we performed the reaction in the presence of the inexpensive and readily available $InCl_3$ in ethanol during 2 hours at room temperature to furnish compounds **205-208** in high yields (Scheme 6.15).

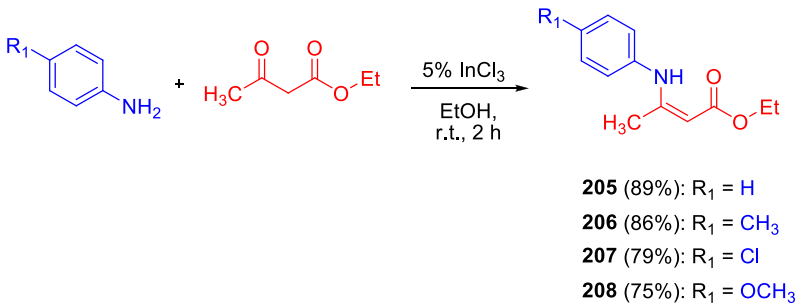

Scheme 6.15. Synthesis of compounds **205-208**

To obtain the 4-quinolone derivatives, we cyclized compounds **205**-**208** under thermal conditions with concomitant ethanol elimination.[173] We carried out the reaction in refluxing diphenyl ether connected to a Dean-Stark trap to recollect ethanol, thereby shifting the equilibrium towards the formation of the product. Once the reaction was completed, the flask was left to cool at r.t. and the precipitated product was recovered by filtration and washed with petroleum ether and acetone to give **209-212**. Importantly, the preparation of these compounds could be performed in multigram scale and did not require chromatographic purification (Scheme 6.16).

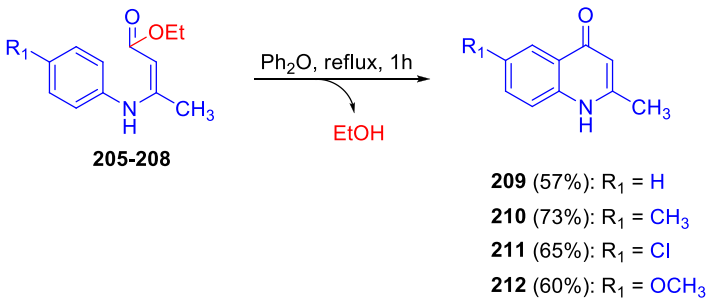

Scheme 6.16. Synthesis of compounds **209-212** *via* the Conrad-Limpach reaction

173 Curran, T. T. *Conrad-Limpach reaction*. In *Name Reactions in Heterocyclic Chemistry;* Li, J. J., Corey E. J., Eds.; Wiley & Sons: Hoboken, NJ, **2005**, pp 398.

Afterwards, we prepared 4-chloroquinaldine (**213**) by chlorinating compound **209** in the presence of a large excess of $POCl_3$. With this compound in hand, we attempted its condensation with benzaldehyde in the presence of Ac_2O under MW irradiation, but unexpectedly it did not work. Thus, we decided to use the previously mentioned alternative method with potassium *t*-butoxide, but also in this case we recovered only the starting materials (Scheme 6.17).

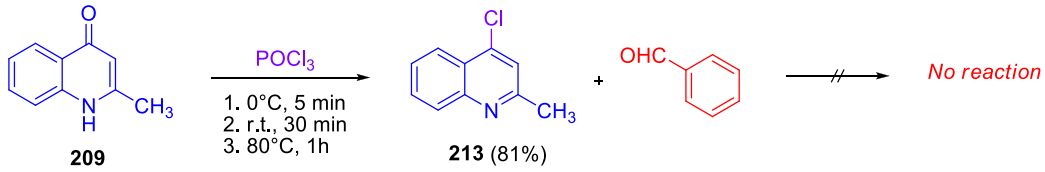

Scheme 6.17. Synthesis of compound **213** and its failed reaction with benzhadeyde

In view of this result, we changed the order of the steps by carrying out first the aldol condensation reaction between 2-methyl-4-quinolines and benzaldehyde under our standard conditions by using MW irradiation to afford compounds **214**-**217** in excellent yields.[171] In the cases of compounds **214** and **216**, the quinolone oxygen was acetylated during the reaction due to the presence of Ac_2O, but this was of no consequence to the overall route, since the desired 4-chloro-2-styrylquinolines were synthesized *via* treatment of compounds **214**-**217** with an excess of phosphorus oxychloride to give **218**-**221** (Scheme 6.18).[174]

174 Kakadiya, R.; Dong, H.; Kumar, A.; Narsinh, D.; Zhang, X.; Chou, T.C. *Bioorg. Med. Chem.* **2010**, *18*, 2285.

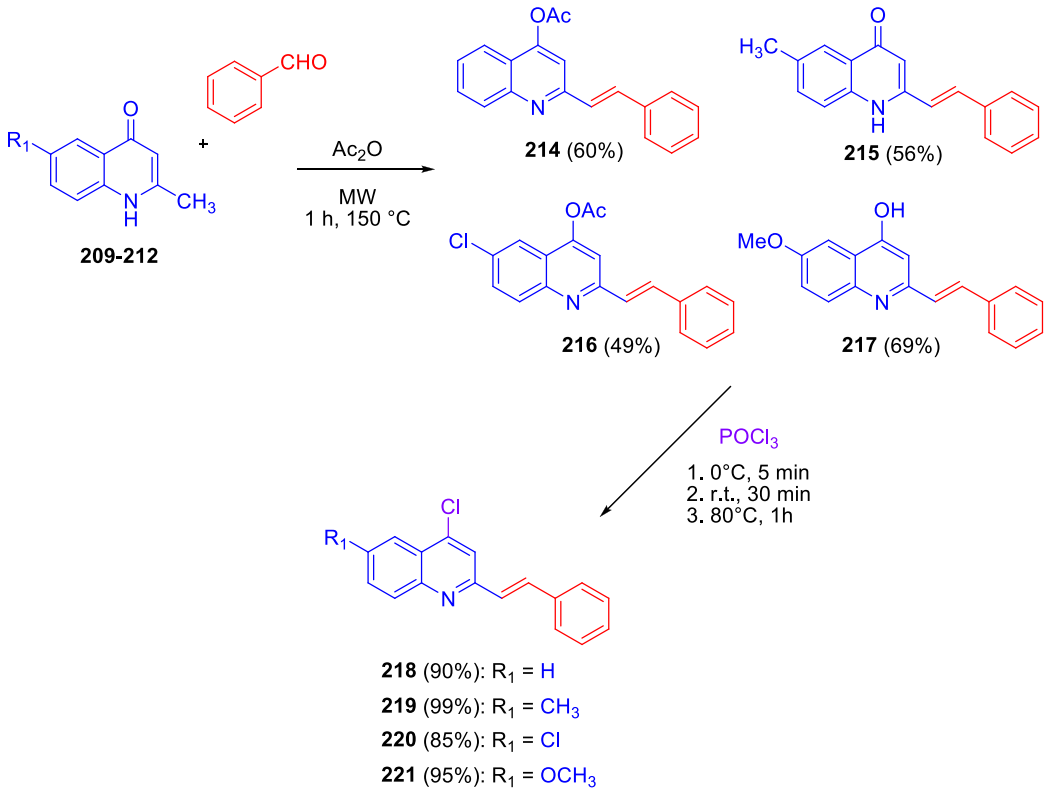

Scheme 6.18. Synthesis of the compounds **214-221**

As the final step, the 4-chlorostrylquinolines were treated a slow stream of ammonia in the presence of phenol, thereby replacing the chlorine atom with an amino group and achieving the preparation of compounds **222-225** in moderate yields (Scheme 6.19).[28b]

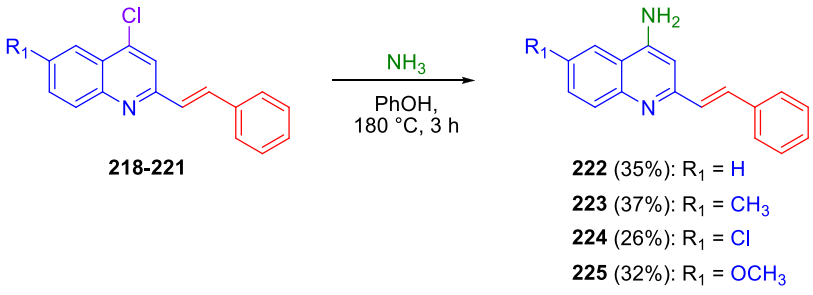

Scheme 6.19. Synthesis of compound **222-225** by using a slow stream of ammonia

6.3.2. Preliminary biological evaluation in ScN2a cells

In order to investigate the effects of the shifting of the amino group compared to compound **139**, compounds **222**, **223** and **225** were preliminary screened in mouse prion-infected ScN2a cells to test their antiprion activity. The experiments were carried out by Suzana Aulić under the supervision of Prof. Giuseppe Legname at SISSA, Trieste. Even though all the compounds were able to inhibit the prion replication in a low micromolar range and to delay the fibril formation (Figure 6.12), the displacement of the amino group to the quinoline ring led to a slight decrease in terms of activity and an increased toxicity in comparison with **139**. Thus, at 10 μM compound **139** showed a 60% cell viability, whereas for these new molecules the cell viability was almost 0 (Figure 6.12).

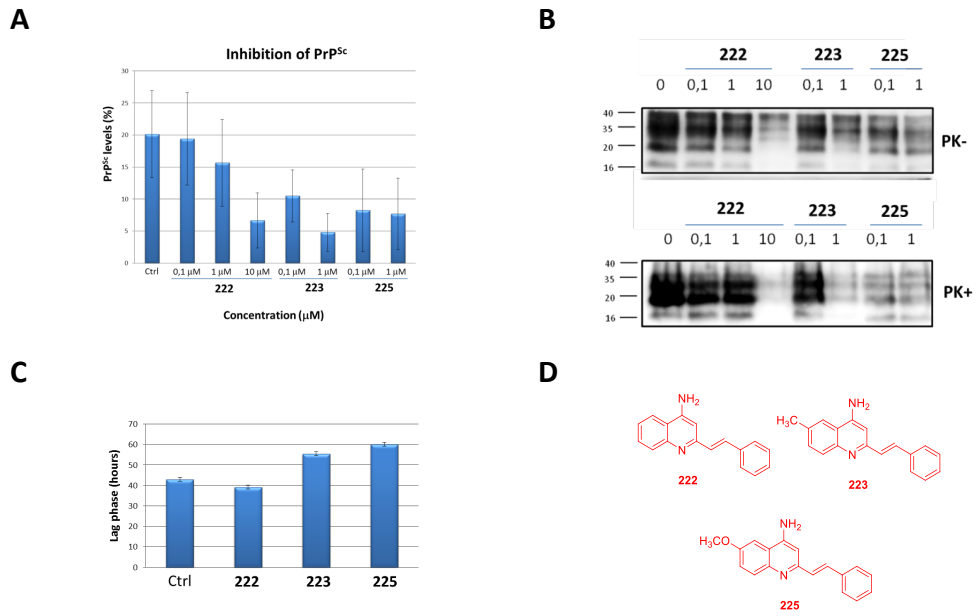

Figure 6.12. (**A**) Dose-dependent capacity of **222**, **223** and **225** to decrease PrP^{Sc} levels. (**B**) Western blotting of ScN2a cell lysates depicting the presence or absence of prions (PrP^{Sc}) following treatment with **222**, **223** and **225** before (top) or after (bottom) PK digestion. (**C**) Prion fibril formation inhibitory activity *in vitro* using ASA for compounds **222**, **223** and **225** (5μM). (**D**) Chemical structure of **222**, **223** and **225**

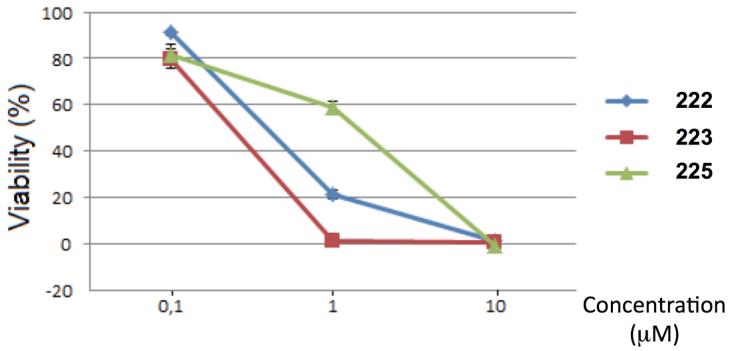

222	91.1%	21.4%	1.4%
223	79.9%	0.9%	0.6%
225	81.9%	58.7%	-0.6%

Figure 6.13. Cell viability profiles of **222**, **223** and **225**

6.3.3. Preliminary antiprion assessment *in vitro* by using PMCA

Furthermore, the anti-prion potential of selected compounds (**171-180**, **200-204**, Figure 6.14) was preliminary assessed *in vitro* by Dr. Natalia Fernández-Borges under the supervision of Prof. Joaquín Castílla at the Center for Cooperative Research in Biosciences, Bilbao. A model called protein-misfolding cyclic amplification (PMCA) was used instead of a cellular test.[175] PMCA reproduces the infectious process of the prion propagation involving cyclic amplification of protein misfolding that triggers a rapid conversion of a large amount of PrP^{C} into the PrP^{Sc} form in the presence of small quantities of PrP^{Sc}, acting as a template. Furthermore, PMCA yields a very efficient and sensitive amplification of scrapie-prion concentration by a factor up to 10^{9}, and this 9 log window is suitable to analyze the behavior of new compounds as inhibitors. An inhibition at 4-5 logs in this model can be considered as proof of very potent activity.

175 Saborio, G. P.; Permanne, B.; Soto, C. *Nature* **2001**, *411*, 810

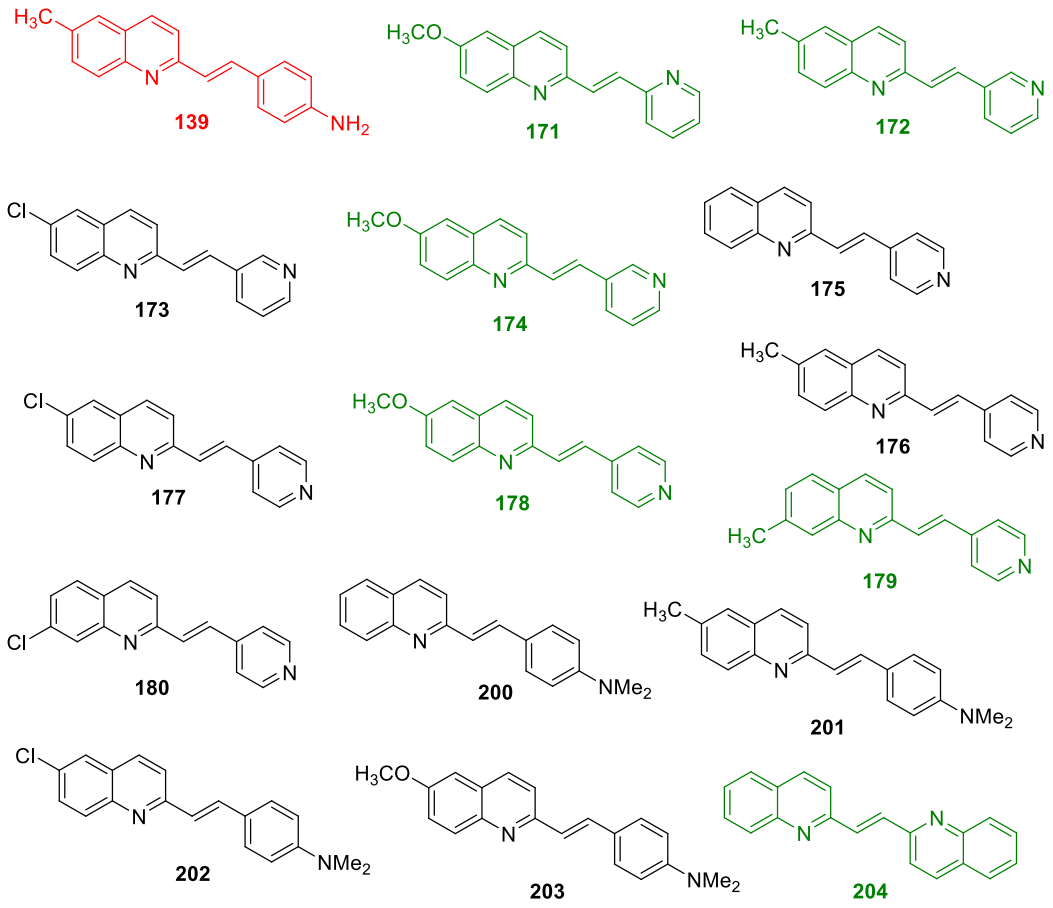

Figure 6.14. Chemical structures of the compounds that were tested *in vitro*, namely **139**, used as the reference compound, **171-180** and **200-204**

To perform the assay, PrP^{Sc} is incubated with Tg338 mice brain homogenates rich in PrP^{C} and the resulting aggregates are disrupted by sonication to generate multiple smaller units for the continued formation of new PrP^{Sc}. After cyclic amplification more than 97% of the protease-resistant PrP present in the sample corresponds to newly converted protein. When a compound is introduced in this model, its capability to inhibit the PrP^{Sc} formation is measured through densitometric analysis of immunoblots.

The histogram in Figure 6.15 summarizes the results obtained for our molecules, and shows that six of them (**171**, **172**, **174**, **178**, **179** and **204**) have a higher inhibitor potency against prion replication than **139**, our reference compound. Among them compound **204** is considered the best one, with a very strong inhibition effect (5 logs at 2 mM and 6,5 logs at 8 mM). Further studies on these compounds are in progress.

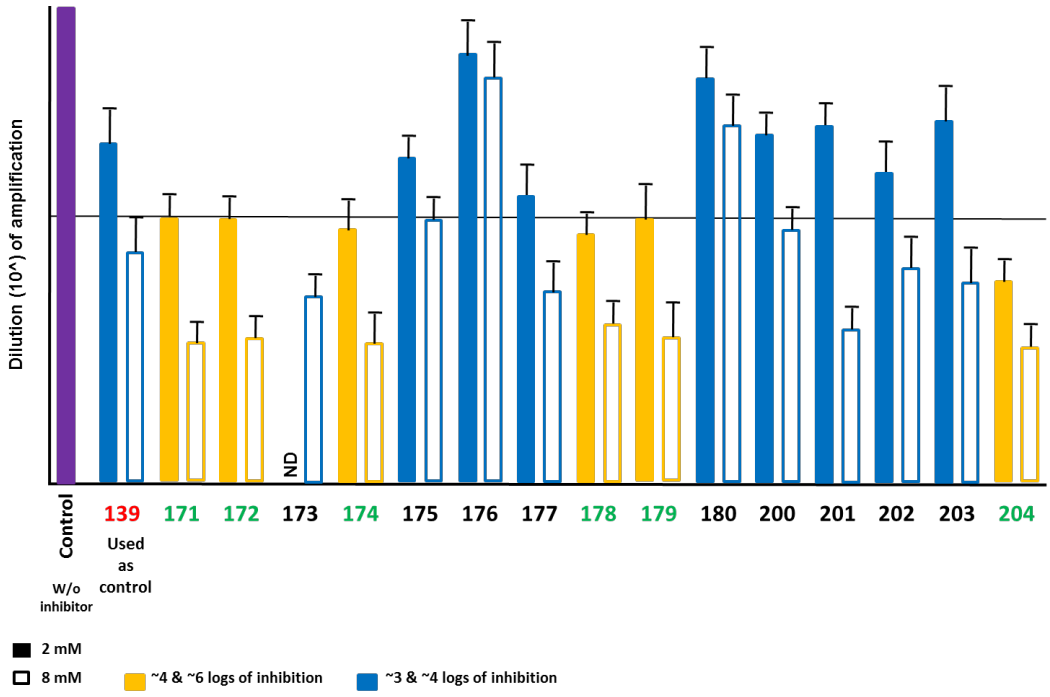

Figure 6.15. Inhibition of PrP^{Sc} propagation of compound **171-180** and **200-204** by using PMCA

7. Hybrid styrylquinoline-polyamines

7.1. Introduction

Several lines of evidence suggest that polyamines play a fundamental role in many biological processes. In the context of central nervous system (CNS) diseases, it has been postulated that polyamines act as neuromodulators[176] and influence the properties of several neurotransmitter pathways, including catecholamines, γ-aminobutyric acid, nitric oxide, and glutamate.[177] Furthermore, polyamines that function as neuroprotectants,[178] and as antiprion chemotherapeutics[179] have been described.

With these concepts in mind and building on our previous experience in the polyamine drug discovery field, we planned to introduce diverse types of polyamino chains at C-4 position of the styrylquinoline moiety in order to provide novel molecules to treat PrDs and AD. The biological study of these compounds in these neurodegenerative diseases is still in progress.

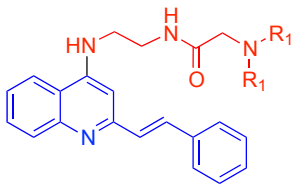

Based on the concept of privileged structure, the parallelism between neurodegenerative and protozoan diseases and the literature search summarized in Section 7.2, we decided to also screen our 4-aminostrylquinoline derivatives against trypanosomatid diseases (*Leishmania*, *Trypanosoma*).

176 Masuko, T.; Kusama-Eguchi, K.; Sakata, K. et al. *J. Neurochem*. **2003**, 84, 610.
177 Fiori, L. M.; Turecki, G. *J. Psychiatry Neurosci.* **2008**, *33*, 102.
178 Li, J.; Doyle, K. M.; Tatlisumak, T. *Curr. Med. Chem*. **2007**, *14*, 1807.
179 Supattapone, S.; Piro, J. R.; Rees, J. R. *CNS Neurol. Disord. Drug Targets* **2009**, *8*, 323.

7.2. Styrylquinolines and polyamines against leishmaniasis

Leishmaniasis is a complex of protozoan diseases due to the infection of mammals by different species of protozoans belonging to the genus *Leishmania*. Several species are responsible of multiple clinical forms ranging from the cutaneous form to the visceral, lethal if untreated. Such maladies belong to the family of the neglected tropical diseases that affect the less developed countries, for which no ideal therapeutic tools are available. A safe a reliable human vaccine is not yet available, and therefore treatment is exclusively based on chemotherapy. Indeed, classical therapies are expensive, toxic, and require parenteral administration.[180] In this scenario, we have embarked on a new drug discovery project devoted to the identification of novel small molecules for the treatment of leishmanial diseases, using compounds initially targeted at fibrillar proteins. With this in mind, we noticed that several 2-substituted quinoline exhibited *in vivo* activities against *Leishmania donovani* (see chemical structures in Figure 7.1). In particular, it seems that a double bond on the lateral chain is critical for antileishmanial activity.[181] Starting from this assumption, several substituted styrylquinoline derivatives were synthesized and tested across different cellular lines showing high *in vitro* antileishmanial activity and low toxicity (Figure 7.1).[182]

180 Mishra, B. B.; Singh, R. K.; Srivastava, A.; Tripathi, V. J.; Tiwari, V. K. *Mini Med. Chem.* **2009**, *9*, 107.

181 (a)Fakhfakh, M. A.; Fournet, A.; Prina, E.; Mouscadet, J. F.; Franck, X.; Hocquemiller, R.; Figadère, B. *Bioorg. Med. Chem.* **2003**, *17*, 5013; (b) Franck, X.; Fournet, A.; Prina, E.; Mahieux, R.; Hocquemiller, R.; Figadère, B. *Bioorg. Med. Chem. Lett.* **2004**, *14*, 3635; (c) Nakayama, H.; Desrivot, J.; Bories, C.; Franck, X.; Figadère, B.; Hocquemiller, R.; Fournet, A.; Loiseau, P. M. *Biomed. Pharmacother.* **2007**, *61*, 186.

182 Loiseau, P. M.; Gupta, S.; Verma, A.; Srivastava, S.; Puri, S. K.; Sliman, F.; Normand-Bayle, M.; Desmaele, D. *Antimicrob. Agents Chemother.* **2011**, *55*, 1777.

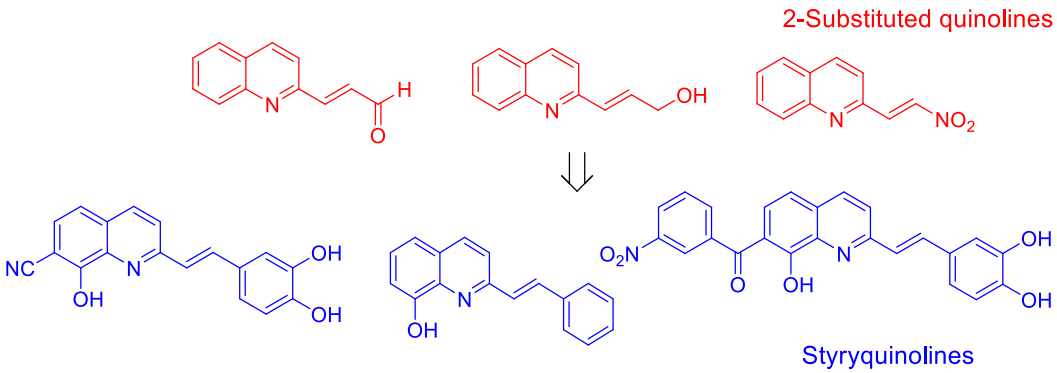

Figure. 7.1. Chemical structures of 2-substituted quinolines and styrylquinolines active against *Leishmania*

In this context, it is important to note that polyamines have been found to exhibit selective uptake by *Plasmodium* infected erythrocytes.[183] Generally speaking, polyamines play a vital role in all living systems, are found in large amounts in mammalian cells and are mainly responsible for maintaining cell viability. The presence of a polyamine tail is considered an attractive tool in antileishmanial drug discovery for the following reasons:

(i) Many polyamines and their conjugates have been shown to be active against trypanosomatid parasites.[184]

(ii) Enzymes involved in polyamine synthesis and metabolism are validated targets for antiparasitic drug development.[185]

(iii) The polyamine chain could exploit the parasite's polyamine transporters to improve the intracellular uptake of the conjugate.[186]

183 Stringer,T.; Taylor, D.; de Kock, C.; Guzgay, H. et al. *Europ. J. Med. Chem.* **2013**, *69*, 90.

184 Pinheiro, A. C.; Rocha, M. N.; Nogueira, P. M.; Nogueira, T. C.; Jasmim, L. F.; de Souza, M. V.; Soares, R. P. *Diagn. Microbiol. Infect. Dis.* **2011**, *71*, 273.

185 (a) Birkholtz, L. M.; Williams, M.; Niemand, J.; Louw, A. I.; Persson, L.; Heby, O. *Biochem. J.* **2011**, *438*, 229; (b) Willert, E.; Phillips, M. A. *Trends Parasitol.* **2012**, *28*, 66.

186 Reguera, R. M.; Tekwani, B. L.; Balana-Fouce, R. *Comp. Biochem. Physiol., Part C: Toxicol. Pharmacol.* **2005**, *140*, 151.

(iv) Polyamine conjugation, by increasing the cationic character of the molecule, may promote its accumulation directly into the mitochondrion.[187]

For instance, a fused benzoquinone compound conjugated with a polyamine (cadaverine) (see chemical structure in Figure 7.2) is an interesting hit compound toward *Trypanosoma brucei*. The antiparasitic activity shown by this molecule requires a fine-tuning between hydrophobicity and charge, as the first is required for passive translocation across membranes, whereas the second is responsible for the mitochondrial localization and the interactions with intracellular targets.[188]

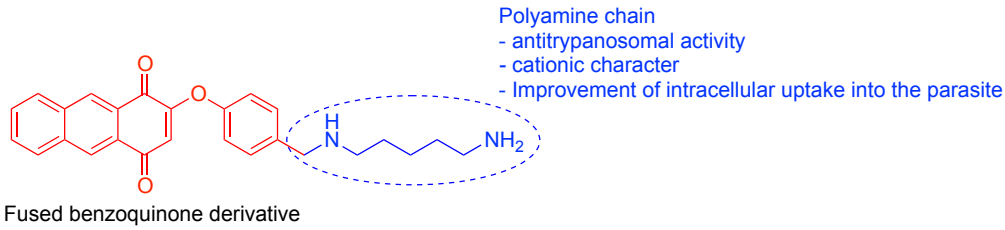

Figure 7.2. A fused benzoquinone derivative endowed with a polyamino chain that showed high antitrypanosomal activity.[188]

Also in the polyamine context, sitamaquine, a quinoline derivative featuring a polyamino chain at C-8 position, showed very high antileishmanial efficacy in preclinical models.[189] Its antileishmanial mechanism of action is still not clarified but it seems due to its ability to interfere with an intracellular redox cycle within the infected macrophages, thereby developing oxidative stress.[190] It has been hypothesized that sitamaquine crosses parasite membrane by passive diffusion

187 Simoni, E.; Bergamini, C.; Fato, R.; Tarozzi, A.; Bains, S.; Motterlini, R.; Cavalli, A.; Bolognesi, M. L.; Minarini, A.; Hrelia, P.; Lenaz, G.; Rosini, M.; Melchiorre, C. *J. Med. Chem.* **2010**, *53*, 7264.

188 Lizzi, F.; Veronesi, G.; Belluti, F.; Bergamini, C.; López-Sánchez, A.; Kaiser, M.; Brun, R.; Krauth-Siegel, R. L.; Hall, D. G.; Rivas, L.; Bolognesi, M. L. *J. Med. Chem*. **2012**, *55*, 10490.

189 Dietze, R.; Carvalho, S. F.; Valli, L. C.; Berman, J.; Brewer, T.; Milhous, W.; Sanchez, J.; Schuster, B.; Grogl, M. *Am. J. Trop. Med. Hyg*. **2001**, *65*, 685.

190 Yeates, C. *Curr. Opin. Investig. Drugs* **2002**, *3*, 1446.

thanks to favourable hydrophobic interactions between its aromatic ring and alkyl chains of membrane phospholipids, and between the positively charged amino chain and the negative polar headgroups of the membrane driving insertion of the drug (Figure 7.3).[191] This mode of interaction would also be possible for our compounds.

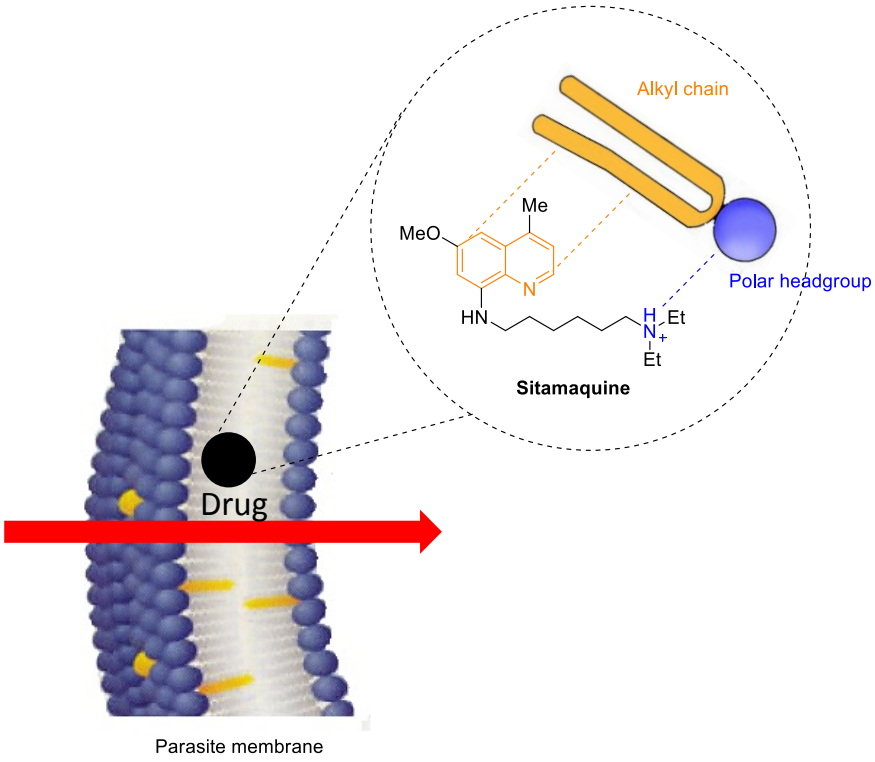

Figure 7.3. Sitamaquine is able to cross the parasite membrane.

In the light of these considerations, polyamine chains seem important for antileishmanial activity. Thus, viewing styrylquinoline as a privileged structure, we describe in this chapter novel compounds generated by introducing polyamino chains at the styrylquinoline framework to target trypanosomatid diseases, especially leishmaniasis.

191 Dueñas-Romero A. M.; Loiseau, P. M.; Saint-Pierre Chazalet, M. *Biochim. Biophys. Acta* **2007**, *1768*, 246.

7.3. Synthesis of 4-(polyamino)styrylquinoline compounds

This work was aided by experimental contributions from the undergraduate student Giulia Romanelli.

First, we generated the styrylquinoline nucleus followed by its functionalization with different polyamino chains. We started with the preparation of 4-chlorostyrylquinoline (**218**) following the experimental procedure described in the previous chapter. With compound **218** in hand, we carried out a nucleophilic aromatic substitution with ethylenediamine, which allowed the incorporation of a short amino chain at the C-4 position of the quinoline nucleus. As described in chapter 3.2, in order to avoid a competing double substitution involving two molecules of the haloquinoline and both amino groups of ethylenediamine, we treated compound **218** with a large excess (20 equivalents of ethylenediamine), under focused microwave irradiation at 120°C during 1 hour to afford compound **226** (Scheme 7.1).[112] Importantly, we avoided the use of chromatography for the isolation of the product, which required tedious evaporation of the excess diamine and recrystallization from methanol and hexane.

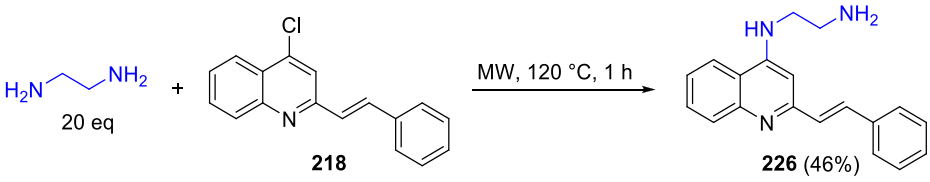

Scheme 7.1. Coupling reaction to obtain compound **226**

Compound **226** was transformed into the halide **227** by acylation with bromoacetyl bromide in the presence of pyridine (Scheme 7.2). In this case the work-up consisted only on washing the crude with slightly acidic water to afford

the final product in 46% yield. Pyridine was used to activate the acyl halide rather than the more commonly employed DMAP (see chapter 5.1), which did not give good results.

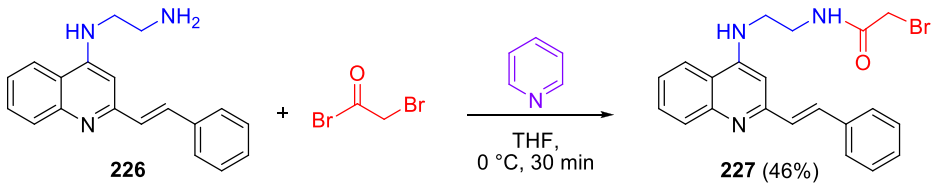

Scheme 7.2. Transformation of **226** into the halide derivative **227**

With compound **227** in hand, we undertook its reaction with a variety of amines, aiming at an initial exploration of structure-activity relationships. The required reaction is a simple nucleophilic substitution in which an incoming nucleophile replaces an outgoing leaving group, in this case represented by a bromide anion. We carried out the reaction between compound **227** and a variety of amines under MW irradiation in the presence of Ce_2CO_3 (Scheme 7.3 and Table 7.1). The final products were crystallized from MeOH-hexane mixtures or purified by chromatography using neutral alumina as stationary phase, since the standard silica gel retained the polyamine derivatives. The design of compound **238** (entry 13) was based on the introduction of the side chain of amodiaquine, which has μM activity against *L. donovani* amastigotes.[192]

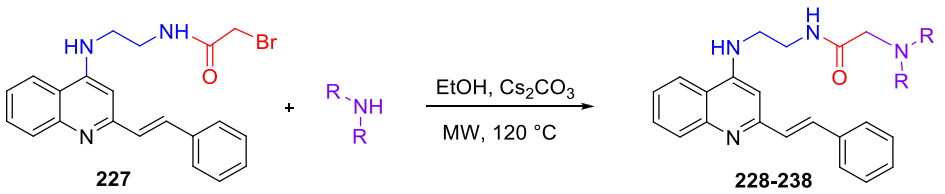

Scheme 7.3. Nucleophilic substitution reaction that affords compounds **228**-**238**

192 Guglielmo, S.; Bertinaria, M.; Rolando, B.; Crosetti, M.; Fruttero, R.; Yardley, V.; Croft, S. L.; Gasco, A. *Eur. J. Med. Chem.* **2009**, *44*, 5071.

Table 7.1. Scope and yields of the 4-aminostyrylquinoline derivatives

Entry	Cmpd.	NHR_2	Reaction time, h	Yield, %
1	**228**		0.5	72
2	**229**		0.5	71
4	**230**		0.5	69
6	**231**		0.5	70
7	**232**		0.5	59
8	**233**	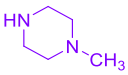	0.5	59
9	**234**	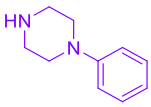	1	45
10	**235**	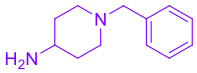	1	43
11	**236**		1	88
12	**237**	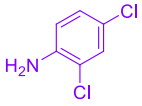	1	42
13	**238**	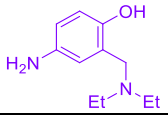	1	54

The 3-indolyl moiety is present in several compounds active against *Leishmania*, including indolylquinolines.[193] Thus, we planned to combine such motif with the styrylquinoline residue in order to obtain a potential new lead compound. To this end, according to our procedure described in chapter 3.3,[119] we treated 4-chlorostyrylquinoline **218** with indole in the presence of $InCl_3$, under MW irradiation, to afford compound **239** (Scheme 7.4).

193 Chakrabarti, G.; Basu, A.; Manna, P.; Mahato, S.; Mandal, N.; Bandyopadhyay, S. *J. Antimicrob. Agents Chemother.* **1999**, *43*, 359.

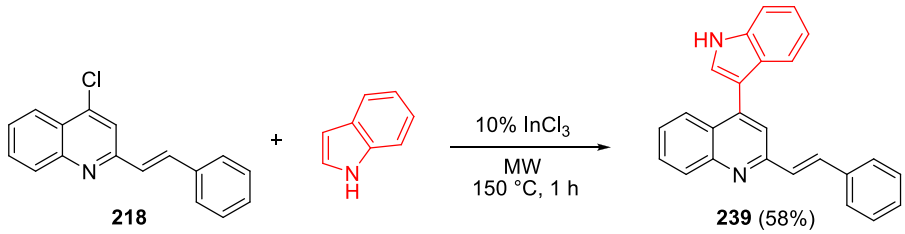

Scheme 7.4. Coupling reaction between **218** and indole that led to the formation of compound **239**

In an effort to enlarge the library, we planned to synthesize other stryrylquinoline derivatives introducing hydroxyl groups on the phenyl residue, since several potent antileishmanial compounds, including the styrylquinolines mentioned in section 7.2, feature such moieties[194] (Figure 7.4).

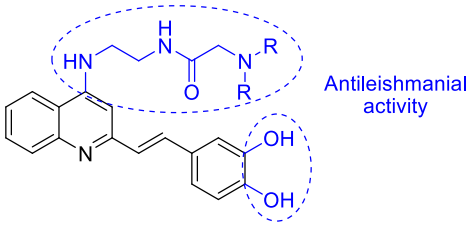

Figure. 7.4. The introduction of two hydroxyl groups could an improved anti-leishmanial activity.

To this end, we first reacted 2-methylquinolin-4-one, compound **209**, with 3,4-dihydroxybenzaldehyde in the presence of acetic anhydride under MW irradiation. As expected, we obtained compound **240** having both hydroxyl groups acetylated because of their reaction with acetic anhydride (Scheme 7.5).

194 Loiseau, P. M.; Gupta, S.; Verma, A.; Srivastava, S.; Puri, S. K.; Sliman, F.; Normand-Bayle, M.; Desmaele, D. *Antimicrob. Agents Chemother.* **2011**, *55*, 1777.

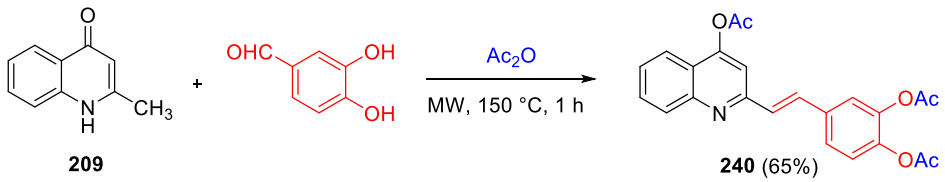

Scheme 7.5. Synthesis of compound **240**

The subsequent chlorination was carried out using the procedure previously described, to give the 4-chlorostyrylquinoline derivative **241** in good yield (Scheme 7.6).

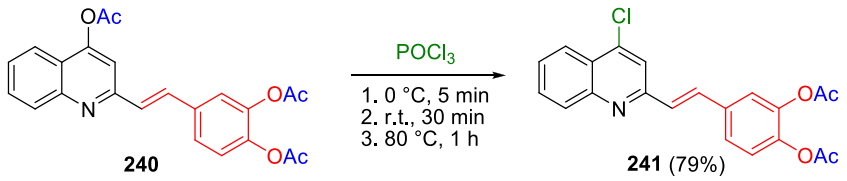

Scheme 7.6. Chlorination of **240** to afford **241**

Unfortunately, all attempts to treat compound **241** with a large excess of ethylenediamine gave only complex mixtures (Scheme 7.7). In order to account for this lack of success, we hypothesize that a reaction took place between the acetyl groups and the amine, interfering with the nucleophilic aromatic substitution.

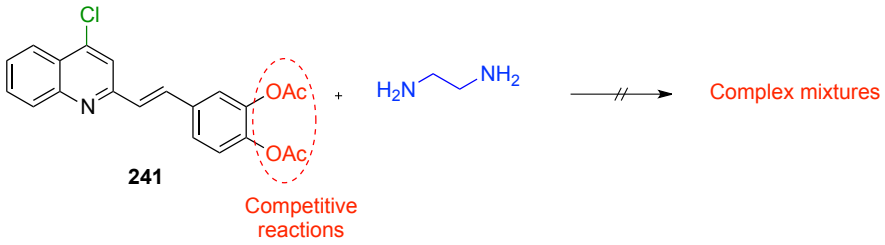

Scheme 7.7. The SnAr with ethylenediamine did not work because of the presence of the acetyl groups

In an effort to overcome this problem, we decided to protect the hydroxyl groups with chloromethyl methyl ether, usually abbreviated as MOM-Cl. The protocol that we finally implemented is based on a published method using NaH,[195] but unfortunately we isolated the product (**242**) only in low yield (Scheme 7.8). The optimization of these conditions will be tackled in the future by other members of the group.

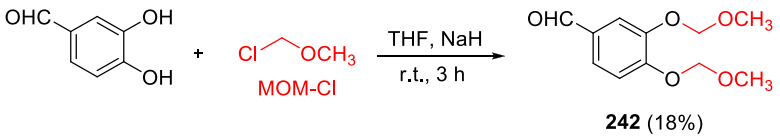

242 (18%)

Scheme 7.8. Preparation of compound **242**

195 Flaherty, D. P.; Kiyota, T.; Dong, Y.; Ikezu, T.; Vennerstrom, J. L. *J. Med. Chem.* **2010**, *53*, 7992.

7.4. Biological study

The biological studies were carried out by Drs. María Ángeles Abengózar and Luis Rivas, at the Centro de Investigaciones Biológicas, CSIC, Madrid. As a first step, the activity of compounds **228-239** was evaluated against *L. pifanoi* axenic amastigote (strain MHOM-ET-67/L82), and *L. donovani* promastigote (strain MHOM/SD/00/1S-2D) in a phenotypic screening. For *Leishmania* promastigotes, all compounds inhibited the proliferation of the parasite (Figure 7.5) showing IC_{50} values in the range between 1.3 μM and 9.6 μM (Table 7.2). It is interesting to note that the IC_{50} of all these compounds was lower than that of miltefosine (hexadecylphosphocholine, HePC), a reference antileishmanial drug.[196]

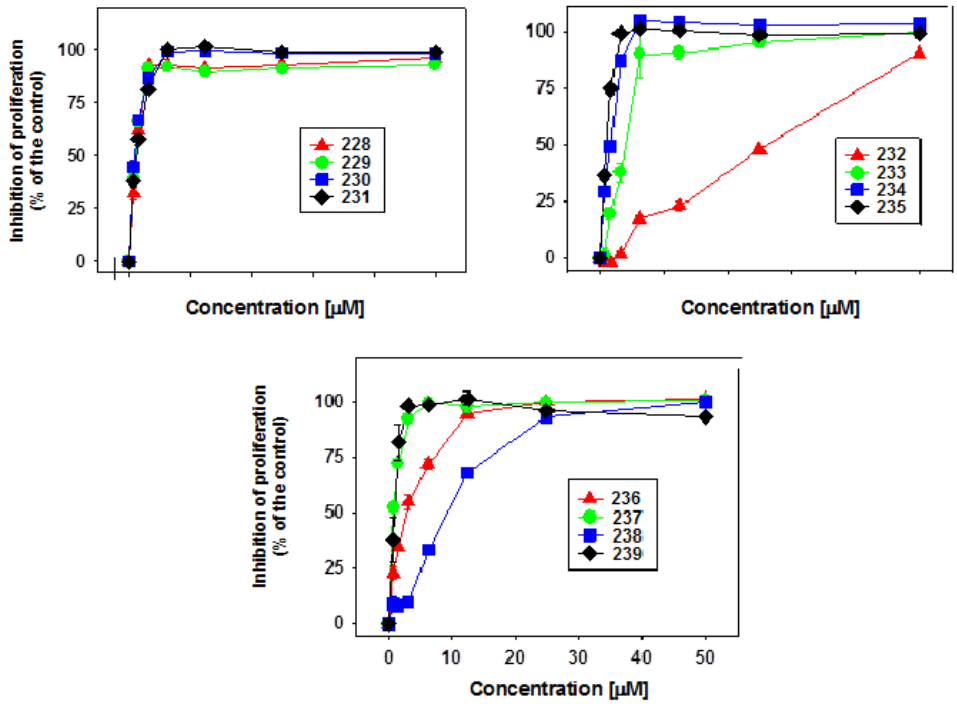

Figure 7.5. Inhibition of *L. donovani* promastigote proliferation by compounds **228-239**

196 Saugar, J. M.; Delgado, J.; Hornillos, V.; Luque-Ortega, J. R.; Amat-Guerri, F.; Acuna, A. U.; Rivas, R. *J. Med. Chem.* **2007**, *50*, 5994.

Table 7.2. *In vitro* activity of compounds **146** and **228-239**, expressed as IC_{50} (μM), against *Leishmania donovani* promastigotes[a]

Cmpd.	IC_{50}
146	>50
228	1.6 ± 0.0
229	1.6 ± 0.0
230	2.1 ± 0.2
231	2.1± 0.2
232	1.3 ± 0.1
233	3.5 ± 0.3
234	2.1 ± 0.1
235	1.5 ± 0.1
236	3.9 ± 0.5
237	5.1 ± 0.1
238	9.6 ± 0.4
239	1.5 ± 0.6
Mitefosine	12.5 ± 2.9[196]

[a]IC_{50}: drug concentration required to inhibit 50% parasite proliferation.

In order to elucidate the role of the polyamine chains, 2-styrylquinoline (**146**) was also tested and found to display a low activity (IC_{50} > 50 μM), confirming that the polyamine tail is critical for the activity. On the other hand, an analysis of the data reported in Figure 7.6 discloses a high inhibitory potency against *L.* amastigote cell proliferation for some of the compounds, namely **234-235**, **237-239**.

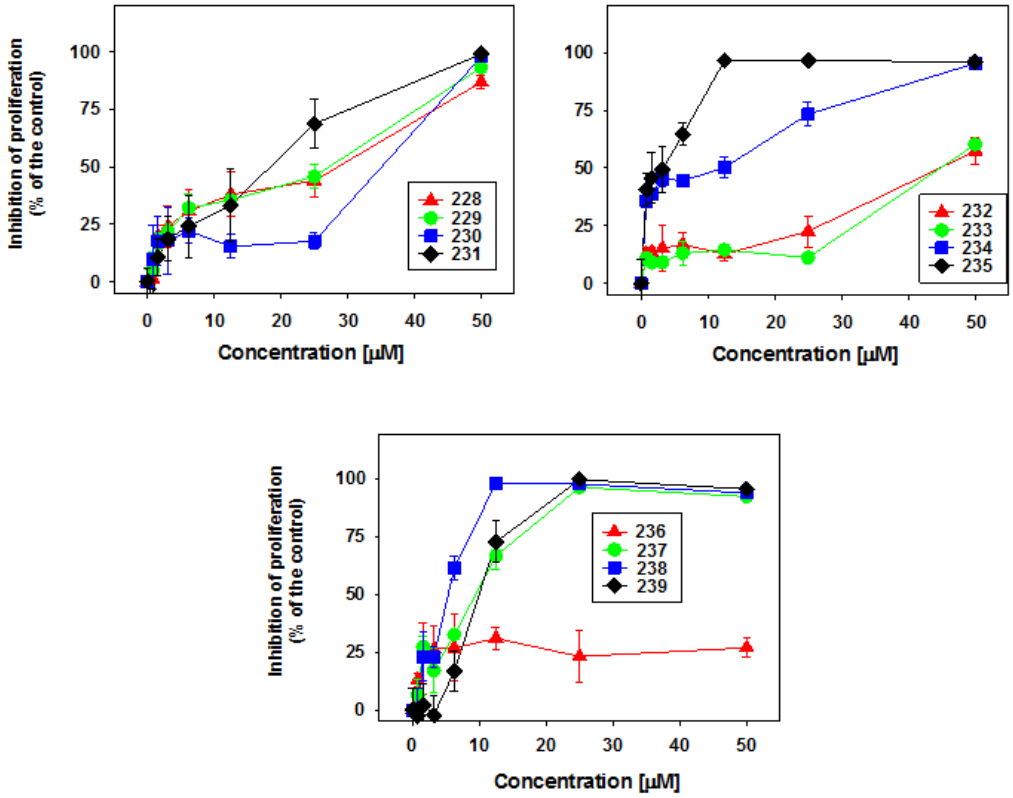

Figure 7.6. Inhibition of *L. pifanoi* amastigote proliferation by compounds **228-239**.

The anti-leishmanial efficacy of compound **237** was confirmed with an *in vitro* model of macrophage infection using peritoneal macrophages infected with *L. pifanoi* amastigotes previously labelled intracellularly with carboxyfluorescein succinimidyl ester (CFSE) to facilitate their visualization inside the macrophage. As expected, **237** reduced the infection index (number of parasites/macrophage), as assessed by counting intracellular parasites in a standard fluorescence microscope (Figure 7.7).

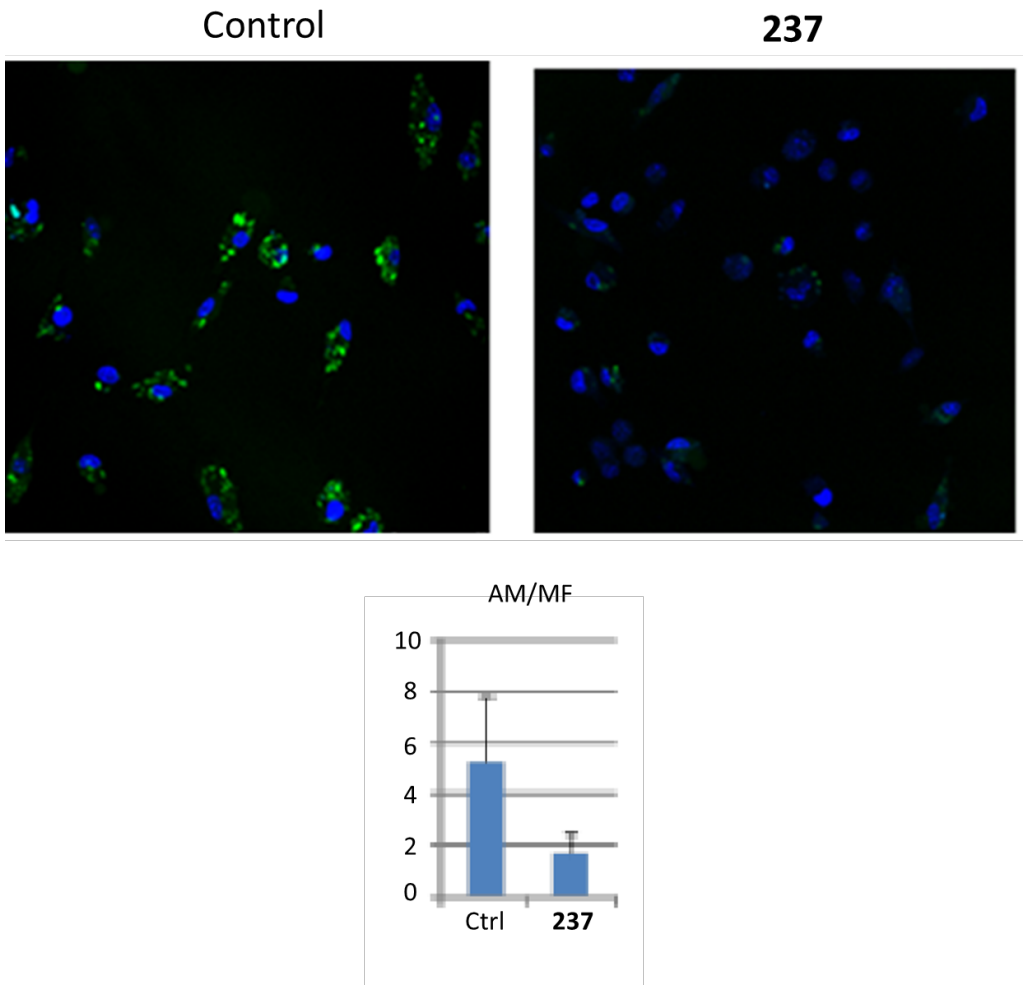

Figure 7.7. Peritoneal infected macrophages with *L. pifanoi* amastigotes, after 12h incubation with **237**, were observed under a confocal microscope. Amastigotes were preloaded with CFSE (carboxyfluorescein succinimidyl ester) (green) and the cell nuclei were stained with DAPI (blue). **237** reduced the infection index (number of parasites/ macrophage).

Furthermore, the toxicity of all the molecules was assessed on murine peritoneal macrophages, revealing a good biological profile for **232, 233, 236, 238** and **239** (Figure 7.8).

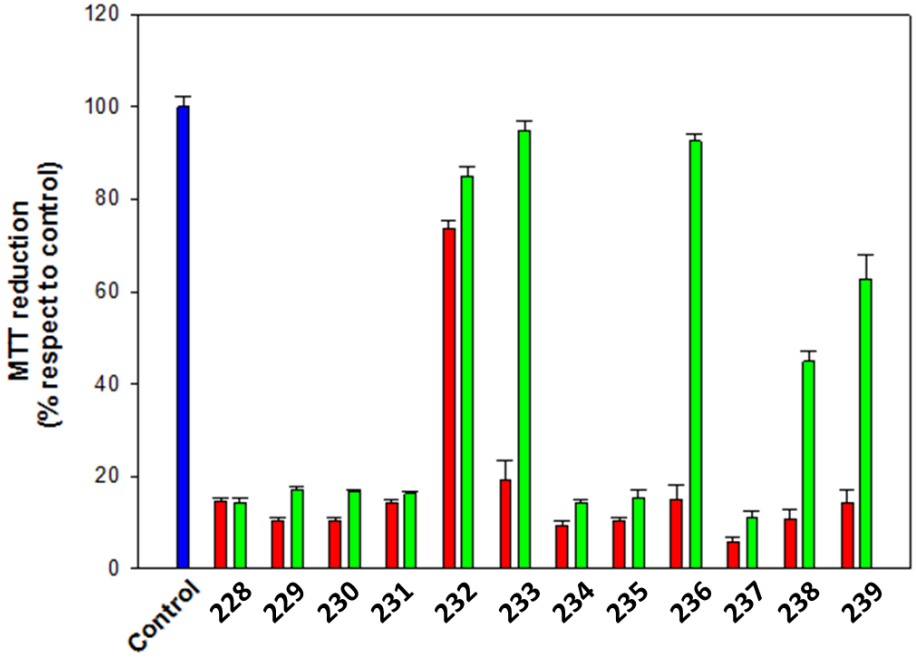

Figure 7.8. Toxicity of styrilquinolines (**228-239**, 25 and 50 μM) on peritoneal macrophages

In an effort to shed light on the molecular mechanism of action of the styrylquinoline compounds and locate their target, we decided to study their activity towards mitochondrial function, which is one of the mechanisms of action of polyamine compounds[188] and quinolines as Tafenoquine and sitamaquine.[197,198] It is worth noting that drugs acting at a mitochondrial level can be particularly effective against *Leishmania*, as for these parasites, with a single mitochondrion, oxidative phosphorylation is essential to fulfill their energetic requirements.[199]

197 Carvalho, L.; Luque-Ortega, J. R.; López-Martín, C.; Castanys, S.; Rivas, L.; Gamarro, F. *Antimicrob. Agents Chemother*. **2011**, *55*, 4204.

198 Carvalho, L.; Luque-Ortega, J. R.; Manzano, J. I.; Castanys, S.; Rivas, L.; Gamarro, F. *Antimicrob. Agents Chemother.* **2010**, *54*, 5344.

199 Fidalgo, L. M.; Gille, L. *Pharm. Res.* **2011**, *28*, 2758.

In order to study whether our compounds affected the bioenergetic metabolism of *Leishmania*, for which the mitochondrial synthesis of ATP accounts for nearly 70% of the total production, we used an engineered parasite strain (3-Luc promastigotes) that allows real-time monitoring of changes in the cytoplasmic free ATP pool in living parasites, as it expresses a cytoplasmic form of firefly luciferase.[200] Upon addition of a lipophilic luciferin ester that can cross the parasite's membrane, in vivo luminescence is generated, free cytoplasmic ATP being the limiting substrate for this reaction

The *in vivo* luminescence measurements showed that most of the compounds induced a fast and concentration-dependent drop in the free cytoplasmic ATP content after their addition. As an example, we show the behaviour of compound **237**, which, at the concentration of 25 μM, reached the end point 15−20 min after its addition (Figure 7.9).

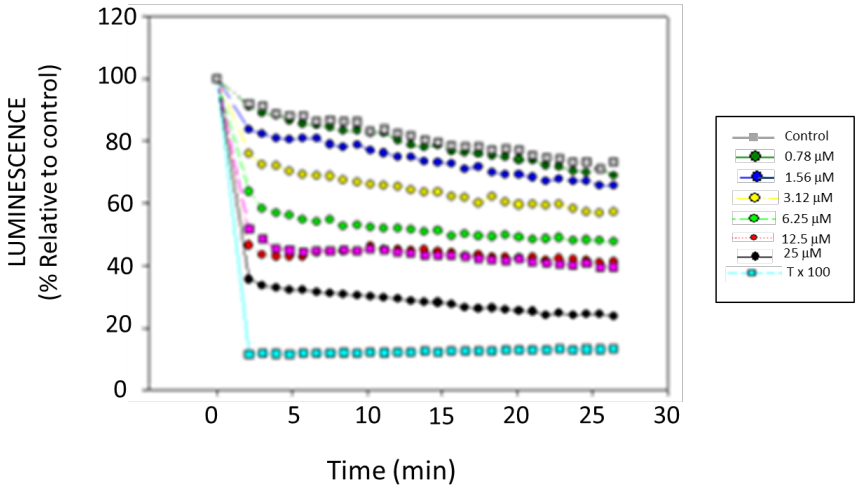

Figure 7.9. Decrease of luminescence caused by **137**. DMNEP-luciferin was added to *L. donovani* 3-Luc promastigote cell line, and when luminescence reached a steady state, drug was added (t = 0, 100% luminescence).

200 Luque-Ortega, J. R.; Rivero-Lezcano, O. M.; Croft, S. L.; Rivas, L. *Antimicrob. Agents Chemother.* **2001**, *45*, 1121.

This dramatic drop in ATP levels can be attributed to alterations in mitochondrial function, or to changes in cell membrane permeability. To discern which of the two possibilities was real, we determined whether our compounds affected the mitochondrial electrochemical potential ($\Delta\psi_m$), which is essential to drive ATP synthesis. We measured $\Delta\psi_m$ by using the fluorescent probe rhodamine 123, whose accumulation in mitochondria is driven by $\Delta\psi_m$, as analyzed by flow cytometry (Figure 7.10). Compounds **231**, **234**, **235** and **237** had the highest inhibitory potency at a concentration of 50 μM and were selected for further study to establish the dependence of inhibition with concentration. We observed that these molecules, at 25 μM, markedly decreased rhodamine fluorescence reaching values similar to those induced by KCN used as a control for fully

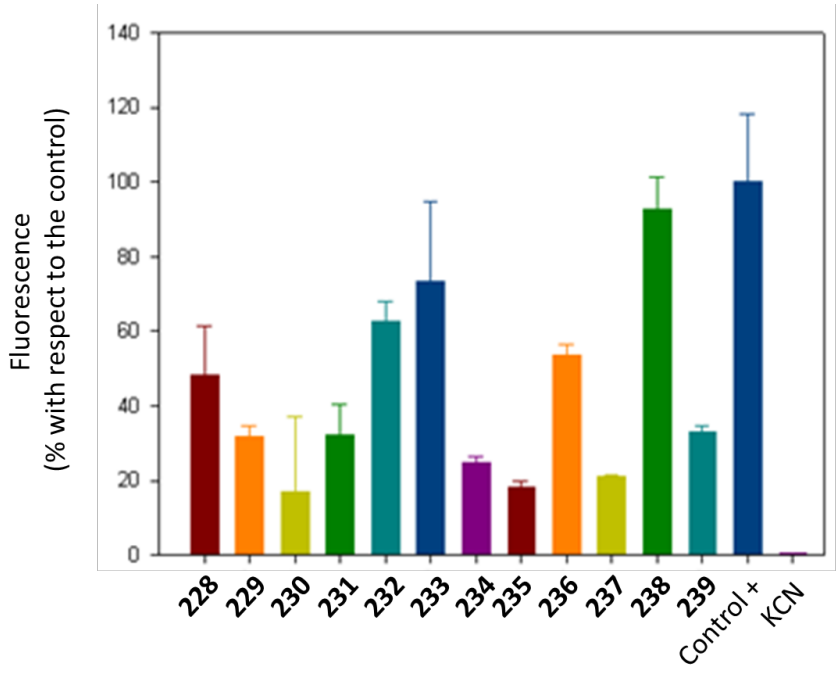

Figure 7.10. Variation of the mitochondrial electrochemical potential (Ψ_m) by styrylquinoline compounds on *L. donovani* promastigotes. Parasites were treated for 4 h with the compounds at a concentration of 50 μM, and Rhodamine 123 uptake was monitored by cytofluorometry

depolarized mitochondria. This behavior can be a consequence of mitochondrial damage, with dissipation of the electrochemical gradient across the inner mitochondrial membrane and lower rhodamine 123 accumulation.

In addition, we discarded the possibility that changes in cytoplasmic ATP concentration could be due to alterations in the permeability of the cell membrane by the experiment summarized in Figure 7.11. Promastigotes were incubated with SYTOX Green, and its increase in fluorescence (λ_{exc} = 504 nm and λ_{em} = 524 nm) due to its binding to intracellular nucleic acids was monitored. Results were expressed as percentage relative to fully permeabilized cells, achieved by addition of 0.1% Triton X-100, and show that none of our compounds alter membrane permeability.

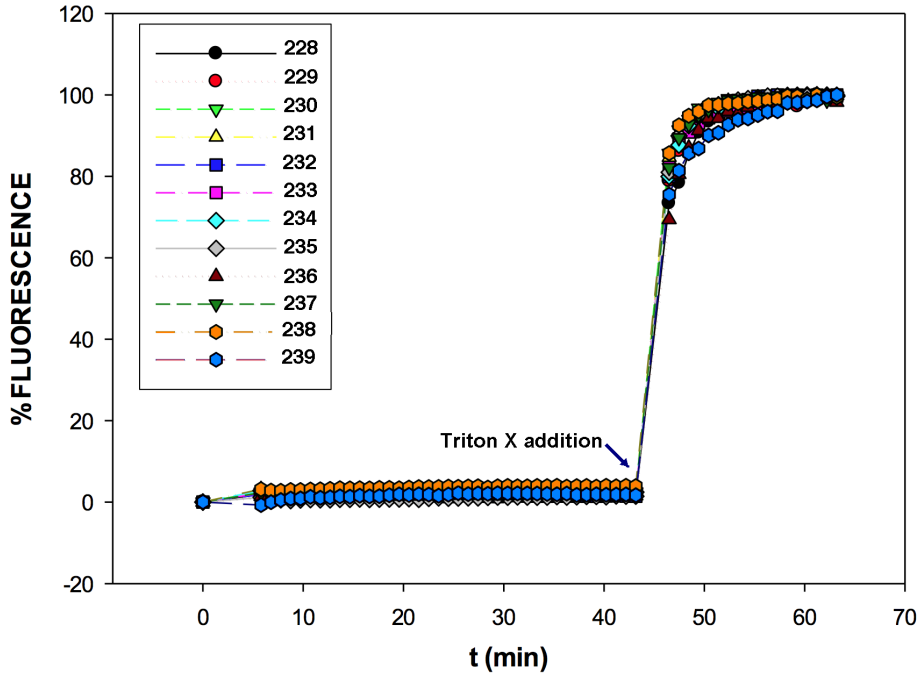

Figure 7.11. Membrane permeability assays

Owing to the key role of mitochondria in apoptosis,[201] we also investigated the possibility that the killing of *Leishmania* involved some kind of programmed death process, characterized by the appearance of the population sub-G1, with fragmented chromatin and lower binding of propidium iodide. The experiments summarized in Figure 7.12, using miltefosine (HePc) as a reference, discard this possibility.

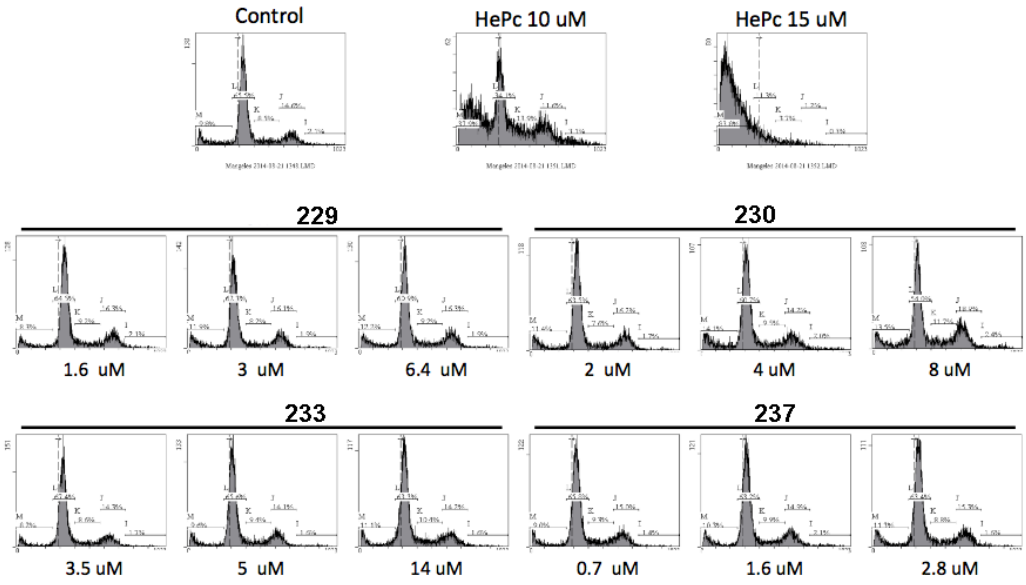

Figure 7.12. Absence of apoptosis induction from compounds **229**, **230**, **233** and **237**

In a further step, the morphological damage inflicted to the promastigote cells was visualized by transmission electron microscopy (Figure 7.13). In the case of **229**, we noted the enlargement of acidocalsisomes (black spots); for **230** and **237** multivesicular bodies were observed, whereas in the case of **234** an abnormal division of the flagella and morphological alterations of the mitochondrion were observed.

[201] Wang, C.; Youle, R. J. *Annu. Rev. Genet*. **2009**, *43*, 95.

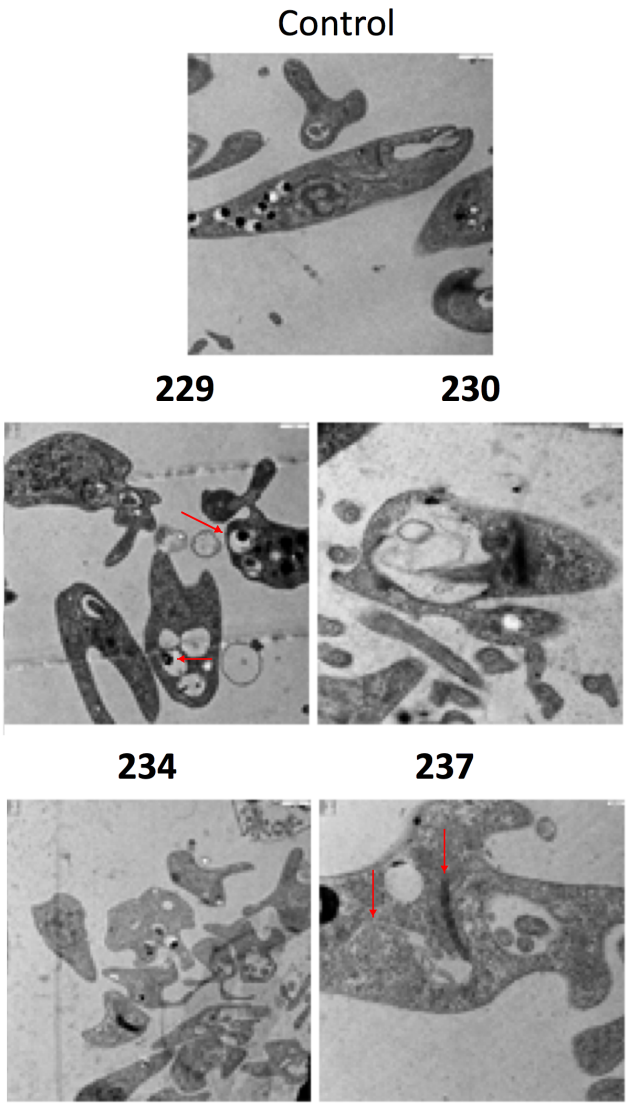

Figure 7.13. Electron microscopy images showing morphological changes in *L. donovani* promastigotes treated with compounds **229**, **230**, **234** and **237**

Taken together, the results shown above suggested that our styrylquinolines exert their leishmanicidial action by interfering with the mitochondrial activity on the parasite leading to the exhaustion of ATP with the concomitant bioenergetic collapse of the parasite. Some compounds, especially **237**, exhibit a promising antileishmania profile.

7.5. Synthesis of 8-aminostyrylquinolines

In the light of the good results obtained from the biological screening of the 4-aminostyrylquinoline derivatives, and also taking into account the structure of sitamaquine, we decided to investigate the shift of the amino chain to the C-8 position on the quinoline nucleus.

As starting point, we prepared 2-methylquinoline (compound **161**) according to the procedure described in chapter 6.3.1 involving a three-component reaction catalyzed by CAN.[166] Then, compound **161** was treated with a mixture of HNO_3 and H_2SO_4 (1:4) to afford a mixture of C-5, and C-8 mononitrated products **243** and **244** (35% and 41%, respectively), which required a careful separation by chromatography on silica gel (Scheme 7.9).[202]

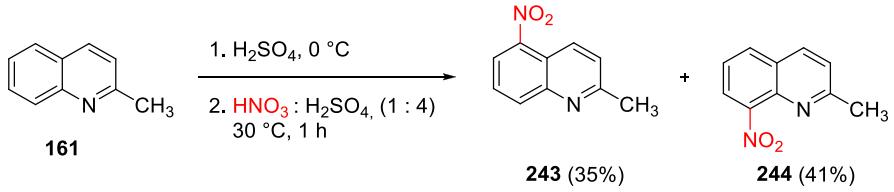

Scheme 7.9. Nitration of 2-methylquinaldine led to the formation of two mononitrated products

In order to obtain 8-nitro-2-styrylquinoline, we reacted compound **244** with benzaldehyde following our standard protocol in the presence of Ac_2O under focused MW irradiation.[171] Unexpectedly, the condensation reaction did not work. We supposed that it was due to the electron-withdrawing effect and steric hindrance of the nitro group at the C-8 position, which must hamper the initial acetylation of the quinoline nitrogen (Scheme 7.10). In an effort to overcome this problem, we decided to deprotonate the quinaldine methyl group using as the

202 Petit, M.; Tran, C.; Roger, T.; Gallavardin, T.; Dhimane, H.; Palma-Cerda, F.; Blanchard-Desce, M.; Acher, F. C.; Ogden, D.; Dalko, P. I. *Org. Lett.* **2012**, *14*, 6366.

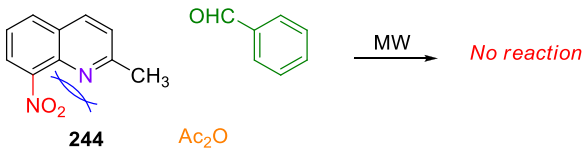

Scheme 7.10. Condensation reaction between **244** and benzaldehyde did not work

base potassium *t*-butoxide, which had been previously employed for the synthesis of some styrylquinoline derivatives (**200**-**204**) as reported in chapter 6.3.1. Unfortunately, these conditions failed in this case. After several unsuccessful additional attempts exploring bases such as LDA, NaH, n-BuLi, TEA and K_2CO_3, we changed our approach and decided to investigate the Wittig olefination reaction. To this end, we first transformed compound **244** into the corresponding aldehyde (**245**) carrying out the reaction with selenious acid (H_2SeO_3) in a refluxing mixture of dioxane and water (10:1) during 1 h (Scheme 7.11).[203] Afterwards, we prepared the phosphonium salt (**246**) by reacting benzylbromide with triphenylphosphine in toluene under focused MW irradiation for 10 min (Scheme 7.11). Finally, we carried out the Wittig reaction according to a method reported by Kimber et al that involved stirring compounds **245** and **246** in a biphasic system (dichloromethane and 50% NaOH aqueous solution) for 2 hours to afford the desired olefin as a mixture of the *cis* and *trans* isomers.[203] In order to isolate the *E* adduct as the only product, we treated the mixture with a catalytic amount of *p*-toluenesulfonic acid in refluxing ethanol, obtaining compound **247** in 80% yield (Scheme 7.11).

203 Kimber, M. C.; Mahadevan, I. B.; Lincoln, S. F.; Ward, A. D.; Tiekink, E. R. T. *J. Org. Chem.* **2000**, *65*, 8204.

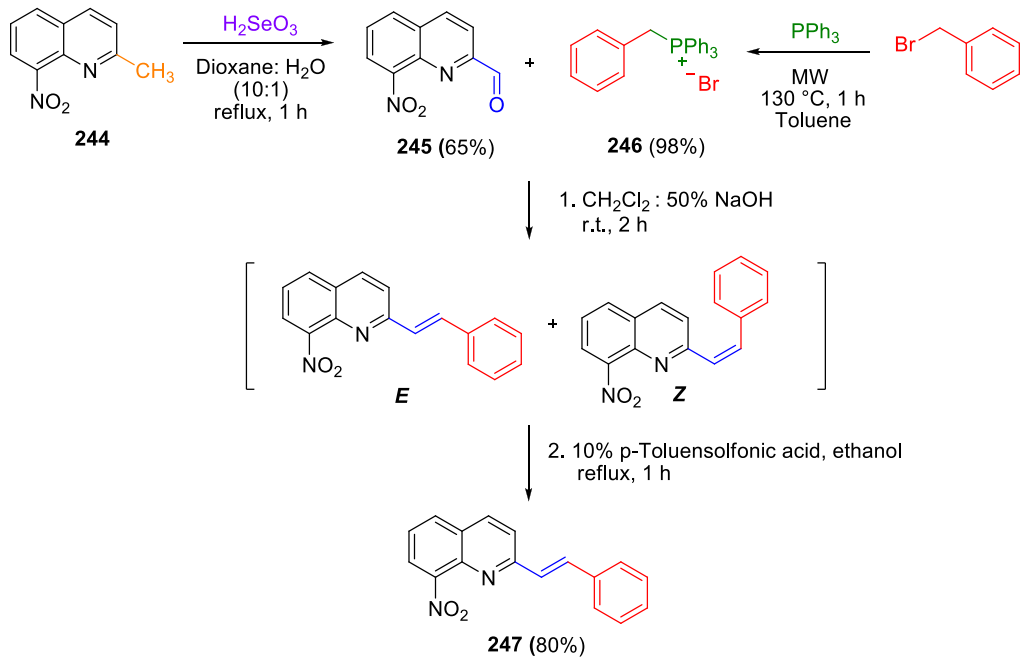

Scheme 7.11. Synthetic route to compound **247** *via* the Wittig reaction

The reduction of compound **247** was achieved following the protocol reported in the previous chapters (5.1 and 6.2.1), using iron powder in a refluxing mixture of ethanol, acetic acid, water and hydrochloride acid (Scheme 7.12).[154]

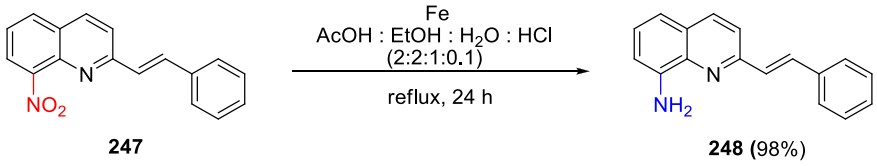

Scheme 7.12. Reduction of compound **247** to **248**

The transformation of **248** into the target polyamino derivatives is in progress.

8. Nanoparticles as promising tools for the development of theranostics

8.1. Introduction

In the course of the three-month stay abroad that is part of the requirements for the European Ph. D. Mention, I carried out the following experimental work under the supervision of Dr. Francesca Baldelli-Bombelli at School of Pharmacy, University of East Anglia, Norwich.

Malignant melanoma is considered one of the most lethal cancers. It represents a severe public health problem due its incidence that is rising quickly.[204] Melanoma progression is related to altered expression of cell surface proteins, including adhesion proteins and receptors. It is interesting to note that the melanocortin type-1 receptor (MC1R) is overexpressed in many melanoma cells at high levels. Thus, it seemed reasonable to consider MC1R as a validated target for imaging and therapeutic intervention.[205] The endogenous agonist for melanocortin receptors is the melanocyte stimulating hormone (MSH),[206] and a wide number of analogous ligands have been developed in order to find out a compound capable of targeting melanoma cells. Among them, a small-molecular-weight peptide, [Nle4, D-Phe7]-α-melanocyte-stimulating hormone (NDP-MSH), showed very high affinity for MCR1 (IC_{50} = 0.21 nmol/L), turning out to be an optimum targeting moiety.[207]

It must be borne that in cancer therapy most of the drawbacks are represented by drug toxicity, non-specificity and development of resistance to

204 Welch, H. G.; Woloshin, S.; Schwartz, L. M. *Br. Med. J.* **2005**, *331*, 481.

205 Siegrist, W.; Solca, F.; Stutz, S.; Giuffre, L.; Carrel, S.; Girard, J.; Eberle, A. N. *Cancer Res.* **1989**, *49*, 6352.

206 Corander, M. P.; Fenech, M.; Coll, A. P. *Circulation* **2010**, *120*, 2260.

207 a) Sawyer, T. K.; Sanfilippo, P. J.; Hruby, V. J.; Engel, M. H.; Heward, C. B.; Burnett, J. B.; Hadley, M. E. *Proc. Natl. Acad. Sci. U.S.A.* **1980**, *77*, 5754; b) Chen, J.; Giblin, M. F.; Wang, N.; Jurisson, S. S.; Quinn, T. P. *Nucl. Med. Biol.* **1999**, *26*, 687.

(MDR and other mechanisms). Moreover, in many cases the treatment is effective only at an early stage of the disease, thus there is an urgent need for new tools for an earlier diagnosis. In this regard, nanotechnology could improve the pharmacokinetic and pharmacodynamic properties of existing molecules combining them with nanomaterials. Indeed, theranostic targeted nanoparticles can be developed with the aim of obtaining a platform that joins diagnostic and therapeutic components in one unique particle.[208] Interestingly, nanosystems can target a specific site through the functionalization with a ligand able to bind specifically to a receptor particularly abundant in the site of interest with respect to other tissues or organs.

With this in mind, Lu et al. associated NDP-MSH to pegylated gold nanoparticles (Au NPs) which were tested on melanoma cells. These NPs showed a better biodistribution with respect to the pegylated ones and specific photothermal ablation of melanoma cells was possible.[209]

208 Desai N. *AAPS Journal* **2012**, *14*, 282.

209 Lu, W.; Xiong, C.; Zhang, G.; Huang, Q.; Zhang, R.; Zhang, J. Z.; Li, C. *Clin. Cancer. Res.* **2009**, *15*, 876.

8.2. SPION coating and purification

Magnetic iron oxide nanoparticles were prepared according to the protocol described by Sun et al., treating iron(III) acetylacetonate, $Fe(acac)_3$, with 1,2-hexadecanediol in the presence of oleic acid and oleylamine to afford monodispersed magnetite (Fe_3O_4) nanoparticles.[210] Such NPs are soluble in organic solvents and need to be transferred to aqueous solutions to be suitable for biological applications. With this purpose, we planned to functionalize the SPION surface with an amphiphilic polymer, and chose poly(maleic anhydride-alt-1-octadecene) (PMAO) for this purpose, following the approach reported by Pellegrino et *al*.[211] PMAO, thanks to its octadecyl chains, can intercalate with the oleate and dodecanethiol chains of SPIONs through hydrophobic interactions, and simultaneously expose the anhydride ring. The latter, after hydrolysis to

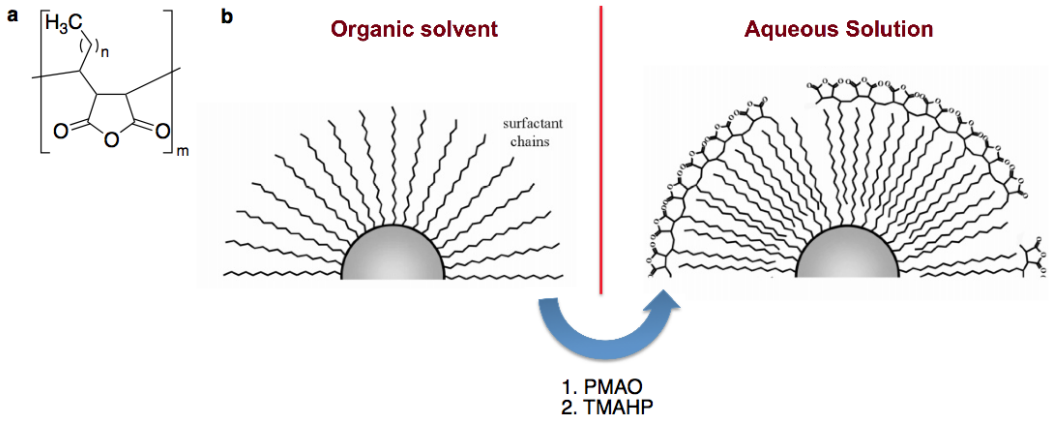

Figure 8.1. Transfer of SPIONs to the aqueous phase through intercalation of the hydrophobic tail of PMAO (**a**) with the first stabilizing ligand (oleic acid/ dodecanethiol) and exposure of hydrophilic head to water (**b**).

210 Sun, S.; Zeng, H.; Robinson, D. B.; Raoux, S.; Rice, P. M.; Wang, S. X.; Li, G. *J. Am. Chem. Soc.* **2004**, *126*, 273.

211 Pellegrino, T.; Manna, L.; Kudera, S. et al. *Nano Lett.* **2004**, *4*, 703.

carboxylic acid in the presence of a base such as TMAHP (tetramethylammonium hydroxide pentahydrate), provides water solubility through charged groups (COO^-) and also acts as an anchor for the attachment of biological molecules or other kinds of linkers (Figure 8.1).

Then, the SPION solution was dialyzed for three days against water (Figure 8.2), followed by ultracentrifugation through sucrose gradient to remove the excess polymer used. Subsequently, another dialysis in water was carried out for further three days in order to purify NPs from the residues of sucrose.

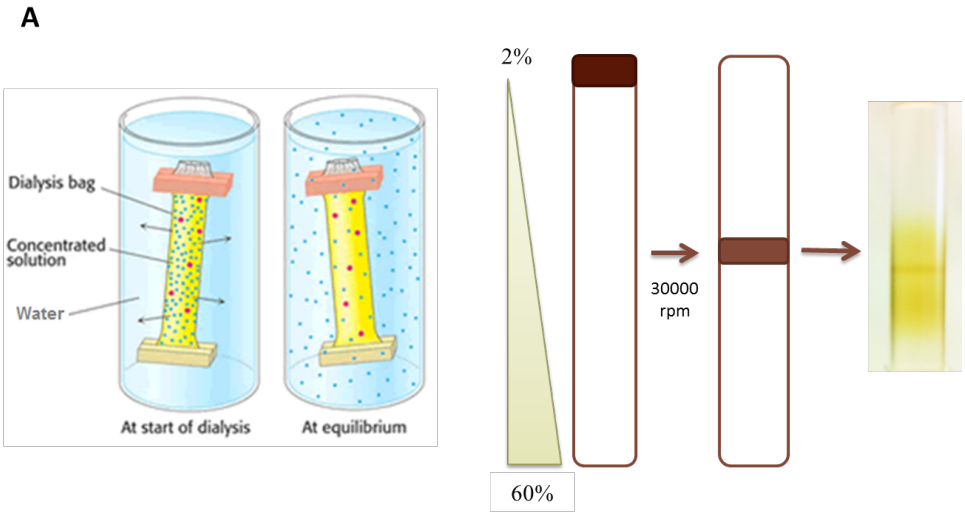

Figure 8.2. The purification of the SPIONs was carried out by a dialysis against water (**a**) followed by ultracentrifugation through sucrose gradient to remove the excess of the polymer (**b**)

The coated SPIONs were characterized by dynamic light scattering (DLS), which is one of the most used techniques to study particles in suspension and measure their size and surface charge, expressed by the zeta potential.[212] The prepared NPs turned out to be monodispersed, with a polydispersity index (PDI)

212 Berne, B.J.; Pecora, R. Dynamic light scattering: with applications to chemistry, biology, and physics; *Courier Dover Publications* **2000**.

of 0.192, and small in size (average diameter = 42.72 nm). The zeta potential was negative (-21.1 mV) due to the charge of carboxylic groups (Figure 8.3).

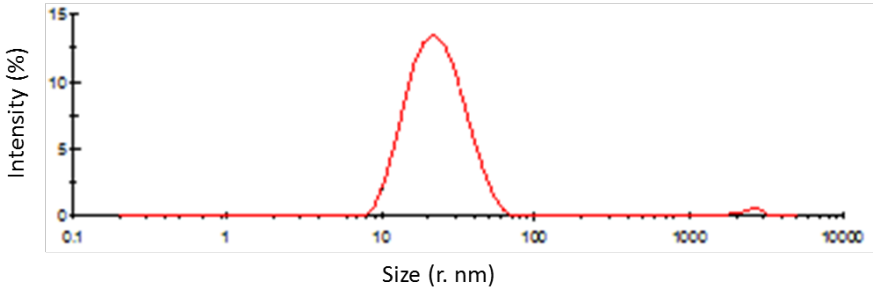

Figure 8.3. DLS size distribution of coated SPIONs

8.3. Functionalization of polystyrene NPs with PEG

As outlined above, we planned to functionalize SPION surfaces with a peg-peptide adduct through a coupling reaction between the carboxyl groups of the polymer wrapping SPIONs and the terminal amino group of polyethylene glycol. In an effort to tune this reaction, we decided to functionalize the surfaces of 20 nm polystyrene NPs and Jeffamine M-1000 polyetheramine, a low molecular weight amino-PEG derivative, both of which were commercially available. We carried out the coupling using an excess of PEG in the presence of 1-ethyl-3-(3-dimethylaminopropyl)carbodiimide (EDAC), as catalyst, in phosphate-buffered saline solution (PBS) at pH 7.4 (Scheme 8.1). After several attempts, we found

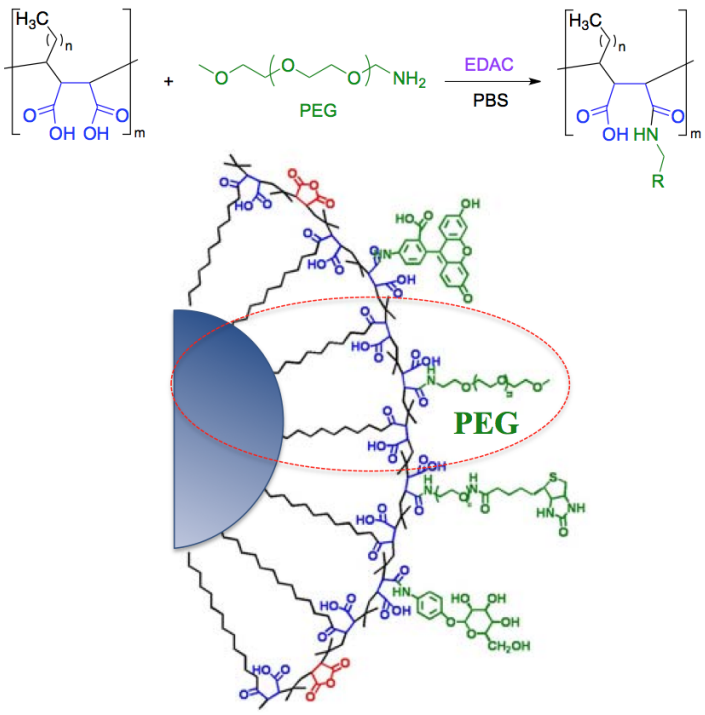

Scheme 8.1. Coupling reaction between the carboxyl groups of the polystyrene surface and PEG in the presence of EDAC

that the ideal experimental conditions to saturate the surface involved the use of 50 μl of polystyrene NPs solution (number of NPs = 4.5302 x 10^{13}) using 700 μl of PEG in PBS (M = 0.02) and 700 μl of EDAC in PBS (M = 0.15).

Considering that the surface of polystyrene has a negative charge, due to the presence of carboxylic groups, the fact that the zeta potential of the reaction mixture is around 0 means that each carboxylic groups have reacted. The functionalized NPs were dialyzed against PBS for three days to remove the excess of PEG, and were characterized by DLS showing good monodispersity (PDI = 0.139 ± 0.014) and an average diameter of 80.06 ± 0.075 (Figure 8.4).

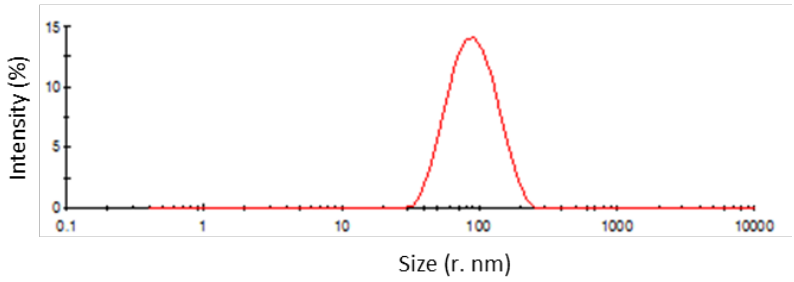

Figure 8.4. DLS size distribution of polystyrene NPs functionalized with PEG.

8.4. Synthesis of an analogue of the MSH peptide

The solid phase synthesis of the peptide (H-Ser-Tyr-Ser-Nle-Glu-His-d-Phe-Arg-Trp-Gly-Lys(Dde)-Pro-Val-NH_2) was carried out according to the Lu et al[209] procedure. The peptide was synthesized manually by the successive coupling of the required thirteen amino acids, with Fmoc protection, using diisopropylethylamine (DIPEA) as base, 20% piperazine in DMF as deprotecting agent and Rink amide resin (4-(2',4'-dimethoxyphenyl-Fmocaminomethyl) phenoxy resin (Scheme 8.2). When coupling was complete, the peptide was cleaved from the resin by a cocktail of trifluoroacetic acid (TFA), water and 1,2-ethanedithiol and was precipitated out by the addition of diethyl ether to give a white solid. The peptide structure was verified by mass spectroscopy, *m/z* = 1769, and analytical HPLC showing an intense peak with retention 18.97 min.

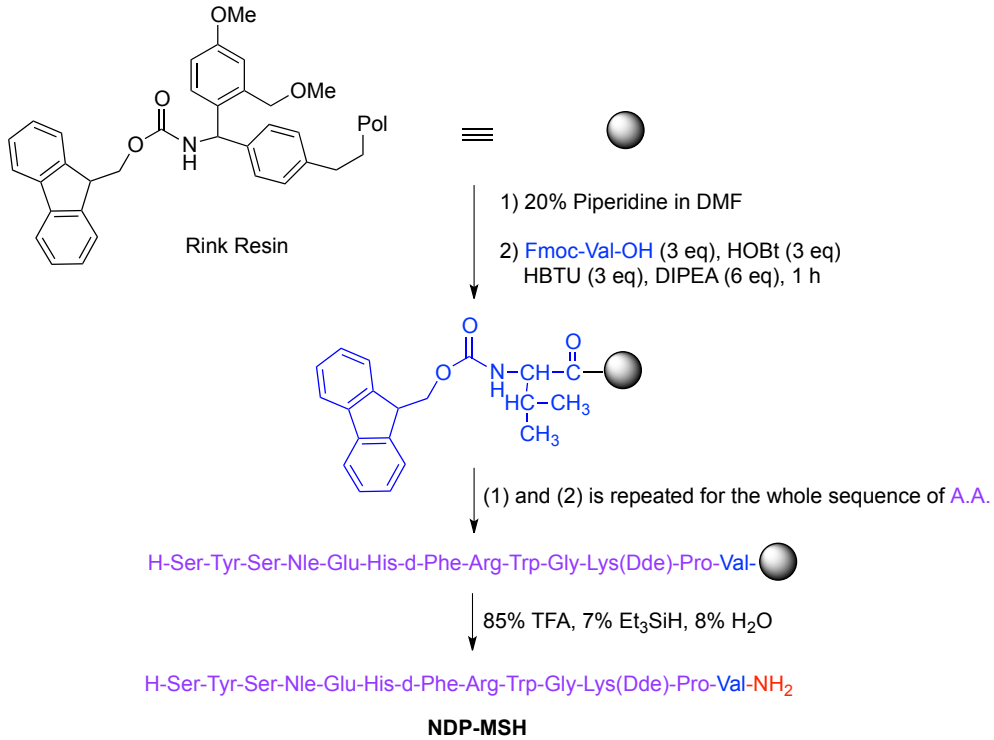

Scheme 8.2. Solid phase synthesis of NDP-MSH

8.5. Covalent coupling between the specific ligand (MSH) and PEG

The synthesis of the abduct between the MSH peptide and PEG was achieved following a procedure found in lecterature.[209] First, we reacted NHS-PEG 750 with the scramble version of MSH peptide to have a negative control. We carried out the coupling reaction using 5 mg of scramble peptide (0.003 mmol), 2.2 equivalents of NHS-PEG 750 in the presence of DIPEA, in DMF for 24 h at r.t. (Scheme 8.3). When the reaction was completed we tried to remove the excess of PEG by gel permeation chromatography unsuccessfully. We could isolate the product by using a semi-preparative HPLC and it was characterized by mass spectroscopy MALDI-TOF revealing a series of peaks around 3000, typical of polymers. Then, NSH-PEG 750 was finally reacted with NDP-MSH to give the NDP-MSH-PEG adduct in 94% yield. Both conjugated products are under biological evaluation to check if they are able to induce proliferation of melanoma cells.

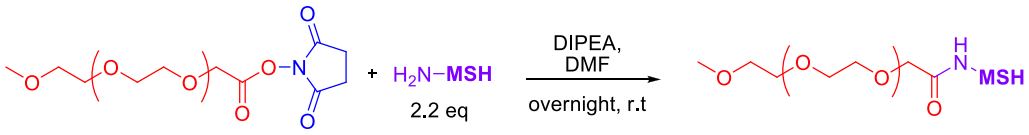

Scheme 8.3. Synthesis of the adduct PEG-MSH

When we applied this method for the reaction between a bi-dentate PEG, BOC-PEG-NHS, and NDP-MSH, unexpectedly, we could not separate the conjugation product from the excess of PEG by the semi-preparative HPLC (Scheme 8.4). Thus, we decided to purify the crude of the reaction through gel permeation chromatography in order to separate compounds with different molecular weight, followed by a dialysis against water. The whole purification

procedure allowed us to achieve the adduct NDP-MSH-PEG-BOC. The next step would have been the cleavage of BOC to make free the amino group of PEG as long as it could react with SPIONs.

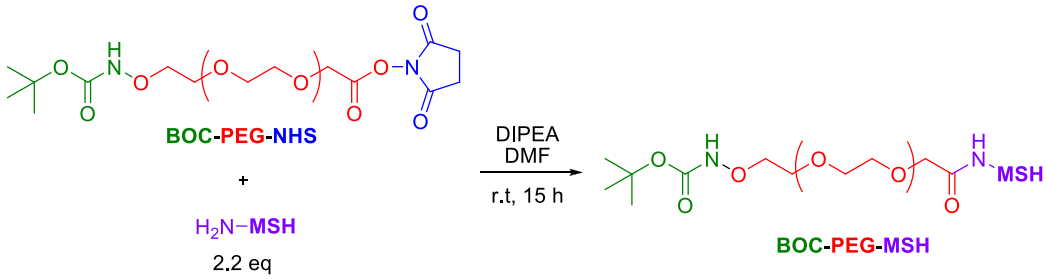

Scheme 8.4. Synthesis of the adduct BOC-PEG.MSH

9. Experimental section

9.1. General information

All air-and/or moisture sensitive reactions were carried out under an argon atmosphere in oven-dried glassware. Solvents and reagents were transferred by syringe or via cannula through rubber septa.

Reagents: All reagents employed for the reactions which are commercially available (Aldrich, Alfa-Aesar, Fluka, Merck, Panreac, Probus, Scharlau) were used directly without further purification. When required, solvents were dried using standard procedures.

Chromatography: Analytical thin layer chromatography (TLC) was carried out using commercially available aluminium-backed plate coated with silica gel (ScharlauCf530 or Macherey-Nagel AlugramSil G/UV254) or neutral aluminium oxide 60F254 (UV254), with fluorescent indicator and visualized under ultra-violet (UV) light lamp Camag UV-II (at 254 and 366 nm), staining with suitable stained solvents which were prepared by standard reported procedure followed by heating or with molecular iodine. Flash column chromatography was performed using silica gel SDS 60 ACC or Scharlau Ge 048 or neutral aluminium oxide Merck 90 standardized (0.063-0.200 mM, 70-230 mesh ASTM) and the eluent indicated in each case. Automated flash chromatography was performed in a Combiflash RF 200 system.

Melting Point: Melting points were determined by Stuart Scientific apparatus, SMP3 Modelora Kofler-type heating platinum microscope from Reicher, 723 Model.

IR Spectroscopy: Infrared spectra (IR) were taken using a Perkin-Elmer FTIR Paragon 1000 spectrometer. Samples were prepared on sodium chloride window in a film form or as disks (potassium bromide).

NMR Spectroscopy: NMR spectra were obtained on a Bruker Avance 250 spectrometer operating at 250 and 62.9 MHz for ^{1}H and ^{13}C NMR spectra, respectively (CAI de Resonancia Magnética Nuclear, Universidad Complutense) with the signal of the residual non-deuterated solvent as an internal standard. All the coupling constants are given in Hz and the multiplicities of ^{1}H signals indicated as s (singlet), d (doublet), t (triplet), q (quartet), m (multiplet), m complex (complex multiplet), br s (extend singlet).

Elemental Analysis: Quantitative combustion elemental analysis for carbon, hydrogen and nitrogen were determined by the CAI de Microanálisis Elemental, Universidad Complutense, using a Leco 932 CHNS microanalyzer.

9.2. Versatile and general methods for the functionalization of π-deficient heterocyclic substrates

9.2.1. General procedure for the free amination of π-deficient nitrogen heterocycles under MW using phenol as catalyst and reaction medium

The suitable starting heterocycle (1 mmol), the corresponding amine, 1 equivalent, except ethylene diamine (4 eq), imidazole and benzimidazole (2 eq), and 2 equivalents of phenol were charged in a pressure-tight microwave tube containing a stirring bar. The reaction mixture was submitted to microwave irradiation for 30-45 min. at 120 °C, with an irradiation power of 150 W, using a CEM Discover SP focused microwave reactor. The crude mixture was diluted with 5 ml of a 10% KOH aqueous solution and stirred until a precipitate was formed. Filtration afforded a solid that was dried overnight to give the final products.

9.2.1.1. Synthesis of 9-aminoacridine derivatives

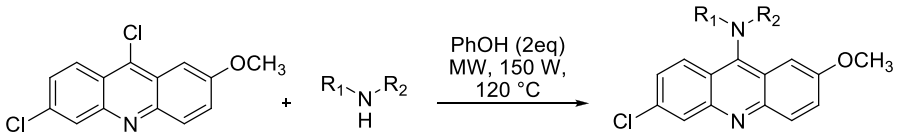

1-12

Cmpd.	R_1	R_2
1	C_6H_5	H
2	4-MeO-C_6H_4	H
3	4-Me_2N-C_6H_4	H
4	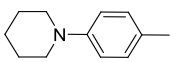	H
5	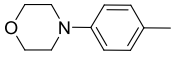	H
6	*n*-Hex	H

Cmpd.	R_1	R_2
7	C_6H_5-CH_2	H
8	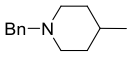	H
9		
10	H_2N-CH_2-CH_2	H
11		
12		

6-Chloro-2-methoxy-*N*-phenylacridin-9-amine (1):

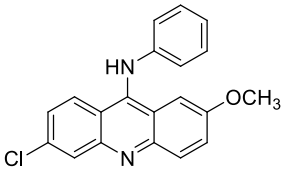

Prepared from 6,9-dichloro-2-methoxyacridine (280 mg, 1 mmol) and aniline (94 mg, 1 mmol); reaction time: 30 min; yield: 95%; yellow solid.

Elemental analysis (%) calcd for $C_{20}H_{15}ClN_2O$: C 71.75, H 4.52, N 8.37 ; found: C 71.43, H 4.24, N 7.91.

Mp:201 – 204 °C

IR (neat) ν: 2356, 1629, 1559, 1493, 1420, 1226, 828, 753 cm^{-1}.

^{1}H NMR (250 MHz, $CDCl_3$) δ 8.21 (d, *J* = 2.0 Hz, 1H), 8.11 (d, *J* = 9.4 Hz, 1H), 7.99 (d, *J* = 9.3 Hz, 1H), 7.48 (dd, *J* = 9.4, 2.7 Hz, 1H), 7.36 (dd, *J* = 9.3, 2.1 Hz, 1H), 7.30 – 7.24 (m, 2H), 7.12 (d, *J* = 2.7 Hz, 1H), 6.98 (t, *J* = 7.4 Hz, 1H), 6.84 (d, *J* = 7.6 Hz, 2H), 6.48 (br s, 1H), 3.79 (s, 3H) ppm.

^{13}C NMR (63 MHz, Acetone) δ 158.0, 149.6, 149.0, 146.8, 135.3, 133.0, 130.8, 130.4 (2C), 129.5, 127.3, 126.7, 126.5, 122.9, 122.0, 120.8, 118.4 (2C), 101.4, 56.2 ppm.

6-Chloro-2-methoxy-*N*-(4-methoxyphenyl)acridin-9-amine (2):

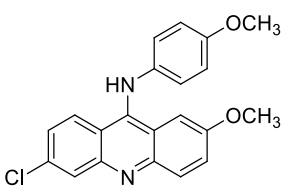

Prepared from 6,9-dichloro-2-methoxyacridine (280 mg, 1 mmol) and *p*-anisidine (123 mg, 1 mmol); reaction time: 30 min; yield: 90%; yellow solid.

Elemental analysis (%) calcd for $C_{21}H_{17}ClN_2O_2$: C 69.14, H 4.70, N 7.68; found: C 68.99, H 4.75, N 7.55.

Mp: 301 – 304 °C

IR (neat) ν: 3306, 1630, 1560, 1507, 1466, 1420, 1362, 1237, 1033 cm^{-1}.

^{1}H NMR (250 MHz, $CDCl_3$) δ 8.14 (s, 1H), 8.04 (d, *J* = 9.4 Hz, 1H), 7.93 (d, *J* = 9.3 Hz, 1H), 7.43 (dd, *J* = 9.4, 2.7 Hz, 1H), 7.29 (dd, *J* = 9.2, 2.0 Hz, 1H), 7.10 (d, *J* = 2.6 Hz, 1H), 6.92 – 6.83 (m, 4H), 3.82 (s, 3H), 3.76 (s, 3H) ppm.

^{13}C NMR (63 MHz, Acetone) δ 157.6, 156.4, 149.8, 148.9, 145.3, 140.0, 135.1, 132.9, 129.4, 127.3, 126.3, 125.7, 121.6 (2C), 121.4, 119.2, 115.7 (2C), 101.4, 56.2 (2C) ppm.

N^1-(6-chloro-2-methoxyacridin-9-yl)-N^4,N^4-dimethylbenzene-1,4-diamine (3):

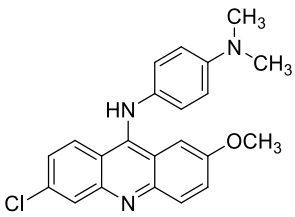

Prepared from 6,9-dichloro-2-methoxyacridine (280 mg, 1 mmol) and *N,N*-dimethyl-*p*-phenylenediamine (136 mg, 1 mmol); reaction time: 45 min; yield: 94%; deep red solid.

Elemental analysis (%) calcd for $C_{22}H_{20}ClN_3O$: C 69.93, H 5.33, N 11.12; found: C 69.78, H 5.65, N 10.74.

Mp: 197 – 200 °C

IR (neat) ν: 1629, 1559, 1515, 1474, 1420, 1349, 1260, 1225 cm^{-1}.

^{1}H NMR (250 MHz, $CDCl_3$) δ 8.12 (d, *J* = 1.5 Hz, 1H), 8.03 (d, *J* = 9.4 Hz, 1H), 7.92 (d, *J* = 9.3 Hz, 1H), 7.40 (dd, *J* = 9.1, 2.3 Hz, 1H), 7.25 (dd, *J* = 11.5, 1.9 Hz, 1H), 7.13 (d, *J* = 2.4 Hz, 1H), 6.96 (d, *J* = 8.7 Hz, 2H), 6.73 (d, *J* = 8.8 Hz, 2H), 3.75 (s, 3H), 2.95 (s, 6H) ppm.

6-Chloro-2-methoxy-*N*-(4-(piperidin-1-yl)phenyl)acridin-9-amine (4):

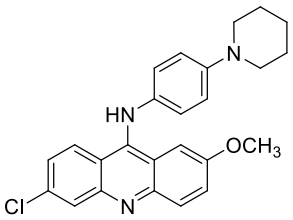

Prepared from 6,9-dichloro-2-methoxyacridine (280 mg, 1 mmol) and *N*-(4-aminophenyl)piperidine (177 mg, 1 mmol); reaction time: 45 min; yield: 89%; deep red solid.

Elemental analysis (%) calcd for $C_{25}H_{24}ClN_3O$: C 71.85, H 5.79, N 10.05; found: C 71.70, H 5.53, N 9.72.

Mp: 216 – 219 °C

IR (neat) ν: 1626, 1570, 1508, 1269, 1235, 1157, 1084, 752 cm^{-1}.

^{1}H NMR (250 MHz, $CDCl_3$) δ 8.14 (s, 1H), 8.04 (d, *J* = 9.4 Hz, 1H), 7.93 (d, *J* = 9.3 Hz, 1H), 7.39 – 7.32 (m, 2H); 7.25-7.21 (m, 2H), 7.15 (s, 1H), 7.04 – 6.87 (m, 4H), 3.76 (s, 3H), 3.13 (t, *J* = 5.4 Hz, 4H), 1.75 – 1.60 (m, 6H) ppm.

^{13}C NMR (63 MHz, $CDCl_3$) δ 156.2, 156.2, 154.7, 151.0, 139.8, 130.0 (2C), 128.0, 127.2, 125.0, 124.5, 122.4, 120.9, 119.8, 117.4, 116.5, 115.8 (2C), 103.0, 56.1, 50.8 (2C), 26.0 (2C), 24.6 ppm.

6-Chloro-2-methoxy-*N*-(4-morpholinophenyl)acridin-9-amine (5):

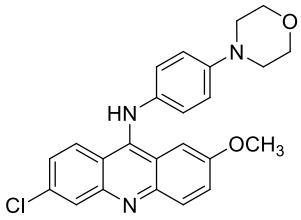

Prepared from 6,9-dichloro-2-methoxyacridine (280 mg, 1 mmol) and 4-morpholinoaniline (180 mg, 1 mmol); reaction time: 45 min; yield: 85%; brown solid.

Elemental analysis (%) calcd for $C_{24}H_{22}ClN_3O_2$: C 68.65, H 5.28, N 10.01; found: C 68.34, H 5.63, N 9.67.

Mp: 240 – 243 °C

IR (neat) ν: 1630, 1560, 1510, 1420, 1226, 1119, 928 cm^{-1}.

^{1}H NMR (250 MHz, $CDCl_3$) δ 8.14 (s, 1H), 8.05 (d, *J* = 9.2 Hz, 1H), 7.93 (d, *J* = 9.2 Hz, 1H), 7.42 (dd, *J* = 9.4, 2.6 Hz, 1H), 7.29 – 7.26 (m, 1H, overlapped with the residual $CHCl_3$ signal), 7.12 (d, *J* = 2.5 Hz, 1H), 6.93 – 6.85 (m, 4H), 3.91 – 3.90 (t, *J* = 4.7 Hz, 4H), 3.77 (s, 3H), 3.12 (t, *J* = 4.7, 4H) ppm.

^{13}C NMR (63 MHz, $CDCl_3$) δ 156.7, 148.2, 147.3, 143.7, 138.4, 135.5, 131.2, 128.0, 128.0, 125.8, 125.8, 125.3, 120.6, 120.3 (2C), 118.5, 117.6 (2C), 100.3, 67.3 (2C), 55.8, 50.5 (2C) ppm.

6-Chloro-*N*-hexyl-2-methoxyacridin-9-amine (6):

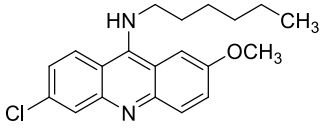

Prepared from 6,9-dichloro-2-methoxyacridine (280 mg, 1 mmol) and hexylamine (102 mg, 1 mmol); reaction time: 30 min; yield: 88%; yellow solid.

Elemental analysis (%) calcd for $C_{20}H_{23}ClN_2O$: C 70.06, H 6.76, N 8.17; found: C 70.39, H 6.80, N 8.51.

Mp: 102 – 105 °C

IR (neat) ν: 1665, 1606, 1561, 1518, 1465, 1433, 1356, 1235, 1112, 1032 cm^{-1}.

^{1}H NMR (250 MHz, $CDCl_3$) δ 8.10 (d, *J* = 2.0 Hz, 1H), 8.06 (d, *J* = 4.7 Hz, 1H), 8.02 (d, *J* = 4.9 Hz, 1H), 7.46 (dd, *J* = 9.4, 2.7 Hz, 1H), 7.34 (dd, *J* = 9.3, 2.1 Hz, 1H), 7.23 (d, *J* = 2.6 Hz, 1H), 4.72 (br s, 1H), 4.00 (s, 3H), 3.77 – 3.69 (m, 2H), 1.79 (dt, *J* = 14.8, 7.3 Hz, 2H), 1.53 – 1.41 (m, 2H), 1.36 – 1.30 (m, 4H), 0.90 (t, *J* = 7.2 Hz, 3H) ppm.

^{13}C NMR (63 MHz, DMSO) δ 155.4, 150.8, 148.6, 146.5, 133.7, 131.2, 127.6, 126.9, 124.6, 123.0, 117.4, 114.9, 100.9, 56.0, 49.8, 31.3, 30.8, 26.3, 22.4, 14.2 ppm.

***N*-Benzyl-6-chloro-2-methoxyacridin-9-amine (7):**

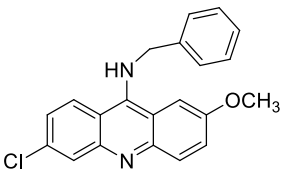

Prepared from 6,9-dichloro-2-methoxyacridine (280 mg, 1 mmol) and benzylamine (107 mg, 1 mmol); reaction time: 30 min; yield: 98%; yellow solid.

Elemental analysis (%) calcd for $C_{21}H_{17}ClN_2O$: C 72.31, H 4.91, N 8.03; found: C 72.29, H 4.86, N 7.73.

Mp: 174 – 177 °C

IR (neat) ν: 1630, 1557, 1432, 1345, 1228, 1069, 1028, 825 cm^{-1}.

^{1}H NMR (250 MHz, $CDCl_3$) δ 8.13 (d, *J* = 1.9 Hz, 1H), 8.02 (t, *J* = 9.7 Hz, 2H), 7.46 – 7.39 (m, 6H), 7.33 (dd, *J* = 9.3, 2.0 Hz, 1H), 7.17 (d, *J* = 2.5 Hz, 1H), 4.90 (s, 2H), 3.81 (s, 3H) ppm.

^{13}C NMR (63 MHz, $CDCl_3$) δ 156.6, 149.9, 148.6, 147.3, 139.7, 135.3, 131.9, 129.5 (2C), 128.7, 128.4, 127.8 (2C), 125.4, 125.32, 124.2, 118.6, 116.7, 99.6, 55.8, 55.1 ppm.

***N*-(1-Benzylpiperidin-4-yl)-6-chloro-2-methoxyacridin-9-amine (8):**

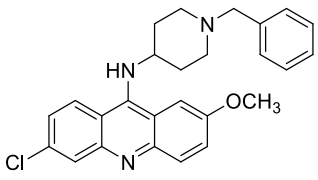

Prepared from 6,9-dichloro-2-methoxyacridine (280 mg, 1 mmol) and 4-amino-1-benzylpiperidine (190 mg, 1 mmol); reaction time: 45 min; yield: 93%; yellow solid.

Elemental analysis calcd (%) for $C_{26}H_{26}ClN_3O$: C 72.29, H 6.07, N 9.73; found: C 72.19, H 5.73, N 9.75.

Mp: 135 – 138 °C

IR (neat) ν: 1629, 1518, 1466, 1344, 1233, 923 cm^{-1}.

^{1}H NMR (250 MHz, $CDCl_3$) δ 8.12 (d, *J* = 1.8 Hz, 1H), 8.06 – 7.99 (m, 2H), 7.46 (dd, *J*= 9.4, 2.6 Hz, 1H), 7.40 – 7.31 (m, 6H), 7.21 (d, *J* = 2.5 Hz, 1H), 3.99 (s, 3H), 3.76 – 3.67 (m, 1H), 3.53 (s, 2H), 2.93 (d, *J* = 11.3 Hz, 2H), 2.07 (t, *J* = 10.5 Hz, 4H), 1.83 – 1.75 (m, 2H) ppm.

^{13}C NMR (63 MHz, $CDCl_3$) δ 156.8, 149.7, 148.3, 147.1, 137.8, 135.5, 131.5, 129.8 (2C), 128.7 (2C), 128.2, 127.8, 125.7, 125.5, 124.5, 120.2, 118.0, 99.4, 63.5, 57.8, 55.9, 52.9 (2C), 34.2 (2C) ppm.

4-(6-Chloro-2-methoxyacridin-9-yl)morpholine (9):

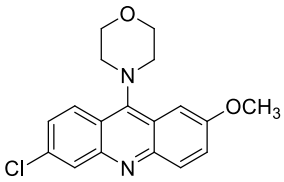

Prepared from 6,9-dichloro-2-methoxyacridine (280 mg, 1 mmol) and morpholine (90 mg, 1 mmol); reaction time: 45 min; yield: 96%; yellow solid.

Elemental analysis calcd (%) for $C_{18}H_{17}ClN_2O_2$: C 65.75, H 5.21, N 8.52; found: C 65.69, H 4.82, N 8.39.

Mp: 259 – 262 °C

IR (neat) ν: 1628, 1553, 1466, 1417, 1222, 1113, 1026, 928 cm^{-1}.

^{1}H NMR (250 MHz, $CDCl_3$) δ 8.37 (d, *J* = 9.3 Hz, 1H), 8.21 (d, *J* = 1.9 Hz, 1H), 8.12 (d, *J* = 9.4 Hz, 1H), 7.58 (d, *J* = 2.7 Hz, 1H), 7.52-7.44 (m, 2H), 4.08 (t, *J* = 4.4 Hz, 4H), 4.04 (s, 3H), 3.61 (t, *J* = 4.4 Hz, 4H) ppm.

^{13}C NMR (63 MHz, $CDCl_3$) δ 157.5, 152.1, 148.9, 148.2, 135.4, 131.7, 128.5, 127.0, 126.0, 126.0, 125.9, 123.7, 100.4, 68.6 (2C), 56.0, 52.4 (2C) ppm.

N^1-(6-Chloro-2-methoxyacridin-9-yl)ethane-1,2-diamine (10):

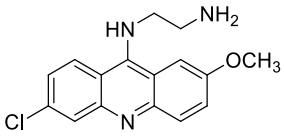

Prepared from 6,9-dichloro-2-methoxyacridine (280 mg, 1 mmol) and ethylenediamine (240 mg, 4 mmol); reaction time: 30 min; yield: 82%; yellow solid.

Elemental analysis calcd (%) for $C_{16}H_{23}ClN_3O$: C 63.68, H 5.34, N 13.92; found: C 63.34, H 5.23, N 13.88.

Mp: 127 – 130 °C

IR (neat) ν: 2922, 1630, 1560, 1518, 1466, 1432, 1234, 1073, 1031 cm^{-1}.

^{1}H NMR (250 MHz, $CDCl_3$) δ 8.18 (d, *J* = 9.3 Hz, 1H), 8.10 (d, *J* = 2.0 Hz, 1H), 8.03 (d, *J* = 9.2 Hz, 1H), 7.48 – 7.41 (m, 2H), 7.34 (dd, *J* = 9.3, 2.1 Hz, 1H), 4.00 (s, 3H), 3.78 – 3.73 (m, 2H), 3.04 (t, *J* = 5.6 Hz, 2H) ppm.

^{13}C NMR (63 MHz, $CDCl_3$) δ 156.4, 147.3, 146.3, 144.3, 135.2, 131.9, 128.7, 125.0, 124.9, 118.9, 116.8, 110.0, 104.3, 55.9, 52.1, 42.4 ppm.

6-Chloro-9-(1*H*-imidazol-1-yl)-2-methoxy acridine (11):

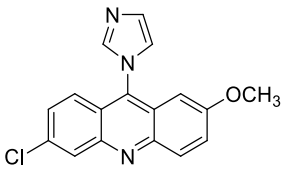

Prepared from 6,9-dichloro-2-methoxyacridine (280 mg, 1 mmol) and imidazole (140 mg, 2 mmol); reaction time: 30 min; yield: 64%; yellow solid.

Elemental analysis calcd (%) for $C_{17}H_{12}ClN_3O$: C 65.92, H 3.90, N 13.57; found: C 65.90, H 4.03, N 13.39.

Mp: 221 – 224 °C

IR (neat) ν: 3095, 1635, 1560, 1476, 1423, 1236, 831 cm^{-1}.

^{1}H NMR (250 MHz, $CDCl_3$) δ 8.32 (d, *J* = 1.2 Hz, 1H), 8.21 (d, *J* = 9.5 Hz, 1H), 7.87 (s, 1H), 7.56 (dd, *J* = 9.5, 2.8 Hz, 1H), 7.53 – 7.45 (m, 3H), 7.34 (t, *J* = 1.2 Hz, 1H), 6.63 (d, *J* = 2.7 Hz, 1H), 3.85 (s, 3H) ppm.

^{13}C NMR (63 MHz, $CDCl_3$) δ 159.5, 147.8, 147.7, 139.2, 136.7, 136.1, 131.90, 130.9, 129.6, 128.7, 127.3, 124.7, 123.9, 122.3, 122.2, 97.6, 56.1 ppm.

9-(1*H*-benzo[*d*]imidazol-1-yl)-6-chloro-2-methoxyacridine (12):

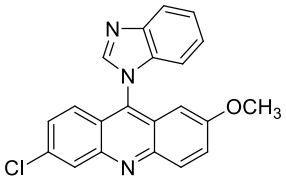

Prepared from 6,9-dichloro-2-methoxyacridine (280 mg, 1 mmol) and benzimidazole (240 mg, 2 mmol); reaction time: 30 min; yield: 87%; yellow solid.

Elemental analysis calcd (%) for $C_{21}H_{14}ClN_3O$: C 70.10, H 3.92, N 11.68; found: C.69.77, H 3.80, N 11.62.

Mp: 232 – 235 °C

IR (neat) ν: 1636, 1475, 1422, 1236, 828 cm^{-1}.

^{1}H NMR (250 MHz, $CDCl_3$) δ 8.40 (d, *J* = 1.6 Hz, 1H), 8.30 (d, *J* = 9.5 Hz, 1H), 8.25 (s, 1H), 8.08 (d, *J* = 8.1 Hz, 1H), 7.59 (dd, *J* = 9.5, 2.7 Hz, 1H), 7.51 – 7.48 (m, 1H), 7.45 (d, *J* = 2.0 Hz, 1H), 7.38 (s, 1H), 7.33 (d, *J* = 5.5 Hz, 1H), 6.95 (d, *J* = 8.1 Hz, 1H), 6.54 (d, *J* = 2.7 Hz, 1H), 3.70 (s, 3H) ppm.

^{13}C NMR (63 MHz, $CDCl_3$) δ 159.5, 148.1, 147.9, 144.0, 143.7, 136.2, 135.7, 135.2, 132.1, 129.6, 128.9, 127.5, 125.0, 124.8, 124.1, 123.9, 122.4, 121.3, 111.2, 97.9, 56.1 ppm.

9.2.1.2. 1,4-Bis(6-chloro-2-methoxyacridin-9-yl)piperazine (13):

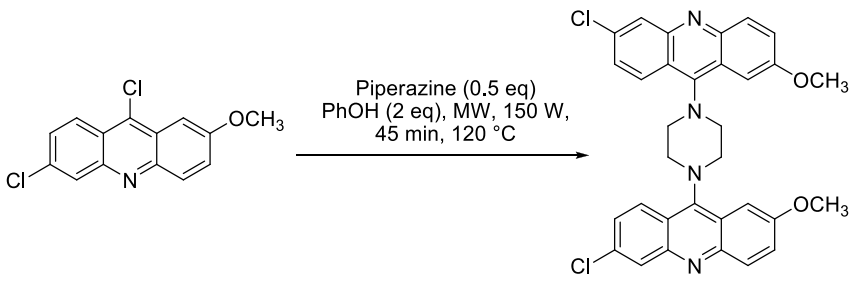

13

Prepared from 6,9-dichloro-2-methoxyacridine (280 mg, 1 mmol) and piperazine (43 mg, 0.5 mmol); reaction time: 45 min; yield: 78%; brown solid.

Elemental analysis calcd (%) for $C_{32}H_{26}Cl_2N_4O_2$: C 67.49, H 4.60, N 9.84; found: C 67.19, H 4.52, N 9.62.

Mp: 249 – 252 °C

IR (neat) ν: 1629, 1556, 1416, 1374, 1230, 1010, 927, 808, 752 cm^{-1}.

^{1}H NMR (250 MHz, $CDCl_3$) δ 8.55 (d, *J* = 9.3 Hz, 2H), 8.27 (d, *J* = 2.0 Hz, 2H), 8.18 (d, *J* = 9.5 Hz, 2H), 7.80 (d, *J* = 2.7 Hz, 2H), 7.59 – 7.54 (m, 4H), 4.11 (s, 6H), 3.97 (s, 8H) ppm.

^{13}C NMR (63 MHz, $CDCl_3$) δ 157.5 (2C), 152.2 (2C), 149.3 (2C), 142.6 (2C), 137.8 (2C), 135.2 (2C), 132.5 (2C), 132.4 (2C), 129.3 (2C), 127.0 (2C), 125.9 (2C), 125.5 (2C), 100.8 (2C), 55.9 (2C), 54.0 (4C) ppm.

9.2.1.3. Synthesis of 4-aminoquinoline derivatives

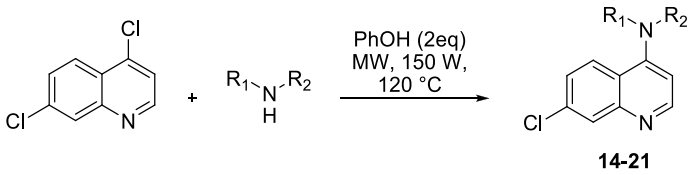

14-21

Cmpd.	R_1	R_2
14	4-MeO-C_6H_4	H
15	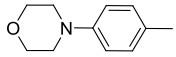	H
16	C_6H_5-CH_2-	H
17	H_2N-CH_2-CH_2	H
18	H_3C-HN-CH_2-CH_2	H
19		
20	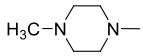	
21		

7-Chloro-*N*-(4-methoxyphenyl)quinolin-4-amine (14):

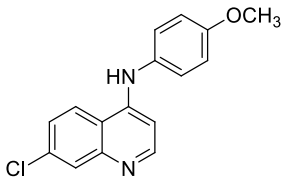

Prepared from 4,7-dichloroquinoline (200 mg, 1 mmol) and *p*-anisidine (123mg, 1 mmol); reaction time: 30 min; yield: 98%; pale brown solid.

Elemental analysis calcd (%) for $C_{16}H_{13}ClN_2O$: C 67.49, H 4.60, N 9.84; found: C 67.09, H 4.63, N 9.72.

Mp: 207 – 210 °C

IR (neat) ν: 2938, 1576, 1509, 1376, 1251, 772 cm^{-1}.

^{1}H NMR (250 MHz, $CDCl_3$) δ 8.51 (d, *J* = 5.4 Hz, 1H), 8.03 (d, *J* = 2.1 Hz, 1H), 7.89 (d, *J* = 9.0 Hz, 1H), 7.46 (dd, *J* = 8.9, 2.1 Hz, 1H), 7.26 (d, *J* = 8.9 Hz, 2H), 7.00 (d, *J* = 8.9 Hz, 2H), 6.70 (d, *J* = 5.4 Hz, 1H), 3.88 (s, 3H) ppm.

^{13}C NMR (63 MHz, $CDCl_3$) δ 158.1, 152.3, 149.9, 149.5, 135.6, 132.1, 129.3, 126.6 (2C), 126.3, 121.50, 117.9, 115.4 (2C), 101.8, 56.0 ppm.

7-Chloro-*N*-(4-morpholinophenyl)quinolin-4-amine (15):

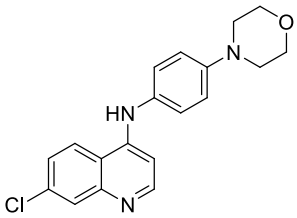

Prepared from 4,7-dichloroquinoline (200 mg, 1 mmol) and 4-morpholinoaniline (180 mg, 1 mmol); reaction time: 45 min; yield: 94%; grey solid.

Elemental analysis calcd (%) for $C_{19}H_{18}ClN_3O$: C 67.15, H 5.34, N 12.37; found: C 67.30, H 5.14, N 12.64.

Mp: 275 – 278 °C

IR (neat) ν: 2987, 2358, 1562, 1515, 1450, 1327, 1254 cm^{-1}.

^{1}H NMR (250 MHz, $CDCl_3$) δ 8.52 (d, *J* = 5.4 Hz, 1H), 8.04 (d, *J* = 2.1 Hz, 1H), 7.87 (d, *J* = 9.0 Hz, 1H), 7.47 (dd, *J* = 8.9, 2.2 Hz, 1H), 7.25 (d, *J* = 8.9 Hz, 2H), 7.01 (d, *J* = 8.9 Hz, 2H), 6.73 (d, *J* = 5.4 Hz, 1H), 6.57 (br s, 1H), 3.93 (t, *J* = 4.8 Hz, 4H), 3.22 (t, *J* = 4.8 Hz, 4H) ppm.

^{13}C NMR (63 MHz, DMSO) δ 152.3, 149.9, 149.6, 148.8, 134.1, 131.6, 128.0, 125.6 (2C), 124.9, 124.7, 118.2, 116.3 (2C), 100.9, 66.5 (2C), 49.0 (2C) ppm.

***N*-Benzyl-7-chloroquinolin-4-amine (16):**

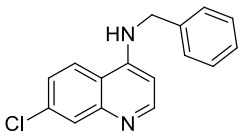

Prepared from 4,7-dichloroquinoline (200 mg, 1 mmol) and benzylamine (107 mg, 1 mmol); reaction time: 30 min; yield: 91%; white solid.

Elemental analysis calcd (%) for $C_{16}H_{13}ClN_2$: C 71.51, H 4.88, N 10.42; found: C 71.49, H 4.64, N 10.35.

Mp: 167 – 170 °C

IR (neat) ν: 1576, 1492, 1430, 1366, 1281, 1228, 1132, 894 cm^{-1}.

^{1}H NMR (250 MHz, $CDCl_3$) δ 8.57 (d, *J* = 5.3 Hz, 1H), 8.01 (d, *J* = 2.1 Hz, 1H), 7.72 (d, *J* = 9.0 Hz, 1H), 7.51 – 7.31 (m, 6H), 6.49 (d, *J* = 5.3 Hz, 1H), 5.34 (br s, 1H), 4.56 (d, *J* = 5.2 Hz, 2H) ppm.

^{13}C NMR (63 MHz, $CDCl_3$) δ 152.7, 149.9, 149.5, 137.6, 135.4, 129.4, 129.3, 128.4, 128.0, 125.9, 121.55, 117.7, 100.1, 48.0 ppm.

***N*^{1}-(7-Chloroquinolin-4-yl)ethane-1,2-diamine (17):**

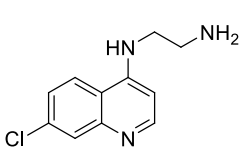

Prepared from 4,7-dichloroquinoline (200 mg, 1 mmol) and ethylenediamine (240 mg, 4 mmol); reaction time: 30 min; yield: 90%; white solid.

Elemental analysis calcd (%) for $C_{11}H_{12}ClN_3$: C 59.60, H 5.46, N 18.95; found: C 59.46, H 5.11, N 18.82.

Mp: 169 – 172 °C

IR (neat) ν: 1582, 1532, 1480, 1451, 1368, 1165, 1133 cm^{-1}.

^{1}H NMR (250 MHz, $CDCl_3$) δ 8.55 (d, *J* = 5.4 Hz, 1H), 7.98 (d, *J* = 2.1 Hz, 1H), 7.78 (d, *J* = 8.9 Hz, 1H), 7.39 (dd, *J* = 8.9, 2.2 Hz, 1H), 6.44 (d, *J* = 5.4 Hz, 1H), 3.37 (t, *J* = 5.7 Hz, 2H), 3.14 (t, *J* = 5.7 Hz, 2H) ppm.

^{13}C NMR (63 MHz, DMSO) δ 152.3, 150.6, 149.5, 133.7, 127.8, 124.6, 124.4, 117.9, 99.1, 45.8, 40.1 ppm.

N^1-(7-Chloroquinolin-4-yl)-*N*^{1},*N*^{2}-dimethylethane-1,2-diamine (18):

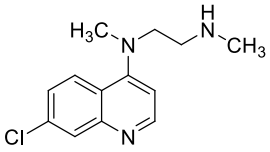

Prepared from 4,7-dichloroquinoline (200 mg, 1 mmol) and *N*^{1},*N*^{2}-dimethylethane-1,2-diamine (350 mg, 4 mmol); reaction time: 30 min; yield: 87%; yellow oil.

Elemental analysis calcd (%) for $C_{13}H_{10}ClN_3$: C 62.52, H 6.46, N 16.83; found: C 62.34, H 6.16, N 16.55.

IR (neat) ν: 3029, 2932, 2842, 1605, 1569, 1498, 1432, 1418, 908, 876 cm^{-1}.

^{1}H NMR (250 MHz, $CDCl_3$) δ 8.68 (d, *J* = 5.1 Hz, 1H), 8.13 (d, *J* = 9.0 Hz, 1H), 8.03 (d, *J* = 2.1 Hz, 1H), 7.43 (dd, *J* = 9.0, 2.2 Hz, 1H), 6.85 (d, *J* = 5.2 Hz, 1H), 3.42 (t, *J* = 6.4 Hz, 2H), 3.01 (s, 3H), 2.94 (t, *J* = 6.4 Hz, 2H), 2.48 (s, 3H) ppm.

^{13}C NMR (63 MHz, $CDCl_3$) δ 157.8, 151.9, 150.8, 135.1, 129.1, 126.2, 126.1, 122.3, 109.2, 56.0, 49.5, 41.3, 37.1 ppm.

4-(7-Chloroquinolin-4-yl)morpholine (19):

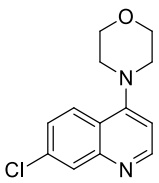

Prepared from 4,7-dichloroquinoline (200 mg, 1 mmol) and morpholine (90 mg, 1 mmol); reaction time: 45 min; yield: 85%; white solid.

Elemental analysis calcd (%) for $C_{13}H_{13}ClN_2$: C 62.78, H 5.27, N 11.26; found: C 62.56, H 5.17, N 10.94.

Mp: 134 – 137 °C

IR (neat) ν: 2888, 1606, 1575, 1498, 1423, 1259, 922 cm^{-1}.

^{1}H NMR (250 MHz, $CDCl_3$) δ 8.77 (d, *J* = 5.0 Hz, 1H), 8.08 (d, *J* = 2.1 Hz, 1H), 7.98 (d, *J* = 9.0 Hz, 1H), 7.47 (dd, *J* = 9.0, 2.1 Hz, 1H), 6.89 (d, *J* = 5.0 Hz, 1H), 4.02 (t, *J* = 4.6 Hz, 4H), 3.25 (t, *J* = 4.6 Hz, 4H) ppm.

^{13}C NMR (63 MHz, $CDCl_3$) δ 157.2, 152.4, 150.6, 135.4, 129.4, 126.8, 125.4, 122.2, 109.4, 67.2 (2C), 53.0 (2C) ppm.

7-Chloro-4-(4-methylpiperazin-1-yl)quinoline (20):

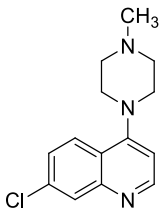

Prepared from 4,7-dichloroquinoline (200 mg, 1 mmol) and 1-methylpiperazine (100 mg, 1 mmol); reaction time: 45 min; yield: 89%; pale brown solid.

Elemental analysis calcd (%) for $C_{14}H_{16}ClN_3$: C 64.24, H 6.16, N 16.05; found: C 63.99, H 6.23, N 15.74.

Mp: 79 – 82 °C

IR (neat) ν: 2936, 2840, 2793, 1607, 1573, 1497, 1455, 1421, 784 cm^{-1}.

^{1}H NMR (250 MHz, $CDCl_3$) δ 8.74 (d, *J* = 5.0 Hz, 1H), 8.06 (d, *J* = 1.9 Hz, 1H), 7.97 (d, *J* = 9.0 Hz, 1H), 7.45 (dd, *J* = 9.0, 1.9 Hz, 1H), 6.87 (d, *J* = 5.0 Hz, 1H), 3.28 (t, *J* = 4.3 Hz, 4H), 2.74 (t, *J* = 4.3 Hz, 4H), 2.45 (s, 3H) ppm.

^{13}C NMR (63 MHz, $CDCl_3$) δ 157.4, 152.3, 150.5, 135.3, 129.2, 126.6, 125.6, 122.3, 109.5, 55.4 (2C), 52.5 (2C), 46.5 ppm.

4-(1*H*-Benzo[*d*]imidazol-1-yl)-7-chloroquinoline (21):

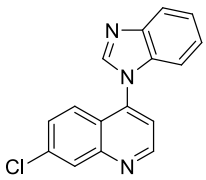

Prepared from 4,7-dichloroquinoline (200 mg, 1 mmol) and benzimidazole (240 mg, 2 mmol); reaction time: 30 min; yield: 85%; white solid.

Elemental analysis calcd (%) for $C_{16}H_{10}ClN_3$: C 68.70, H 3.60, N 15.02; found: C 68.35, H 3.39, N 15.15.

Mp: 149 – 152 °C

IR (neat) ν: 1592, 1560, 1490, 1456, 1426, 1236, 1209, 948, 745 cm^{-1}.

^{1}H NMR (250 MHz, $CDCl_3$) δ 9.14 (d, *J* = 4.6 Hz, 1H), 8.32 (d, *J* = 1.9 Hz, 1H), 8.21 (s, 1H), 8.00 (d, *J* = 8.1 Hz, 1H), 7.66 (d, *J* = 9.0 Hz, 1H), 7.59 – 7.53 (m, 2H), 7.48 – 7.42 (m, 1H), 7.40 – 7.34 (m, 1H), 7.23 (d, *J* = 7.7 Hz, 1H) ppm.

^{13}C NMR (63 MHz, $CDCl_3$) δ 152.3, 150.7, 144.1, 143.1, 141.3, 137.3, 134.9, 129.7, 129.5, 124.8, 124.7, 124.0, 122.9, 121.4, 118.6, 111.0 ppm.

9.2.1.4. Synthesis of 4-amino-2-phenylquinazoline

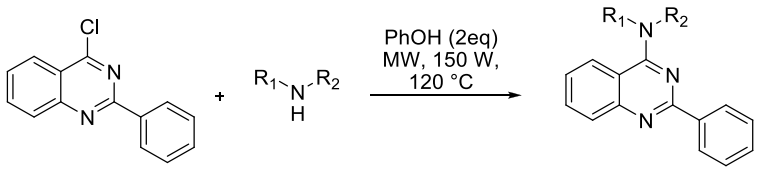

22-26

Cmpd.	R_1	R_2
22	4-Cl-C_6H_4	H
23	C_6H_5-CH_2-	H
24	$(H_3C)_2N$-CH_2-CH_2	H
25	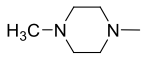	
26		

***N*-(4-Chlorophenyl)-2-phenylquinazolin-4-amine (22):**

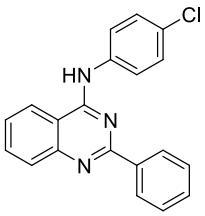

Prepared from 4-chloro-2-phenylquinazoline (241 mg, 1 mmol) and 4-chloroaniline (130 mg, 1 mmol); reaction time: 30 min; yield: 98%; grey solid.

Elemental analysis calcd (%) for $C_{20}H_{14}ClN_3$: C 72.40, H 4.25, N 12.66; found: C 72.43, H 4.27, N 12.31.

Mp: 183 – 186 °C

IR (neat) ν: 1620, 1598, 1558, 1520, 1485, 1441, 1357, 1327, 757 cm^{-1}.

^{1}H NMR (250 MHz, $CDCl_3$) δ 8.57 – 8.54 (m, 2H), 8.05 (d, *J* = 8.4 Hz, 1H), 7.92 – 7.85 (m, 4H), 7.61 – 7.45 (m, 7H) ppm.

^{13}C NMR (63 MHz, $CDCl_3$) δ 160.7, 157.5, 151.5, 138.9, 137.6, 133.5, 130.8, 129.8, 129.4 (2C), 129.4, 128.9 (2C), 128.9 (2C), 126.7, 122.9 (2C), 120.5, 114.1 ppm.

***N*-Benzyl-2-phenylquinazolin-4-amine (23):**

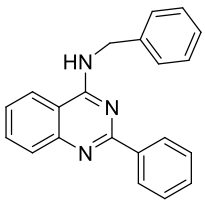

Prepared from 4-chloro-2-phenylquinazoline (241 mg, 1 mmol) and benzylamine (107 mg, 1 mmol); reaction time: 30 min; yield: 94%; grey solid.

Elemental analysis calcd (%) for $C_{21}H_{17}N_3$: C 81.00, H 5.50, N 13.49; found: C 81.14, H 5.57, N 13.17.

Mp: 121 – 124 °C

IR (neat) ν: 1586, 1571, 1529, 1494, 1455, 1438, 1407, 678 cm^{-1}.

^{1}H NMR (250 MHz, $CDCl_3$) δ 8.61 (dd, *J* = 7.3, 2.4 Hz, 2H), 7.99 (d, *J* = 8.4 Hz, 1H), 7.75 (dd, *J* = 13.4, 7.3 Hz, 2H), 7.53 – 7.36 (m, 9H), 6.03 (br s, 1H), 5.06 (d, *J* = 5.2 Hz, 2H) ppm.

^{13}C NMR (63 MHz, $CDCl_3$) δ 161.0, 159.8, 151.1, 139.3, 139.1, 133.0, 130.6, 129.3, 129.2 (2C), 128.9 (2C), 128.7 (2C), 128.6 (2C), 128.1, 125.9, 120.9, 114.0, 45.7 ppm.

N^1,*N*^{1}-Dimethyl-*N*^{3}-(2-phenylquinazolin-4-yl)propane-1,3-diamine (24):

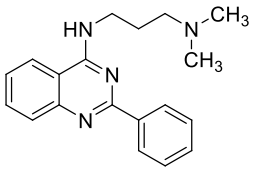

Prepared from 4-chloro-2-phenylquinazoline (241 mg, 1 mmol) and *N*^{1},*N*^{1}-dimethylpropane-1,3-diamine (105 mg, 1 mmol); reaction time: 30 min; yield: 91%; grey solid.

Elemental analysis calcd (%) for $C_{19}H_{22}N_4$: C 74.48, H 7.24, N 18.29; found: C 74.19, H 6.84, N 18.09.

Mp: 69 – 72 °C

IR (neat) ν: 3243, 2942, 2821, 1616, 1574, 1534, 1489, 1457, 692, 675 cm^{-1}.

^{1}H NMR (250 MHz, $CDCl_3$) δ 8.62 – 8.58 (m, 2H), 7.93 (d, *J* = 8.0 Hz, 1H), 7.75 – 7.69 (m, 1H), 7.64 (d, *J* = 8.1 Hz, 1H), 7.56 – 7.47 (m, 3H), 7.44 – 7.38 (m, 1H), 3.91 (q *J* = 5.8 Hz, 2H), 2.61 (t, *J* = 5.8 Hz, 2H), 2.39 (s, 6H), 1.97 – 1.88 (m, 2H) ppm.

^{13}C NMR (63 MHz, $CDCl_3$) δ 161.3, 160.3, 150.8, 139.7, 132.6, 130.3, 129.0, 128.8 (2C), 128.6 (2C), 125.6, 121.4, 114.69, 60.2, 46.0 (2C), 42.7, 25.2 ppm.

4-(4-Methylpiperazin-1-yl)-2-phenylquinazoline (25):

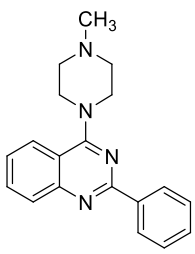

Prepared from 4-chloro-2-phenylquinazoline (241 mg, 1 mmol) and 1-methylpiperazine (100 mg, 1 mmol); reaction time: 45 min; yield: 90%; white solid.

Elemental analysis calcd (%) for $C_{19}H_{20}N_4$: C 74.97, H 6.62, N

18.41; found: C 74.75, H 6.61, N 18.07.

Mp: 92 – 95 °C

IR (neat) ν: 2935, 2843, 2793, 1612, 1563, 1536, 1502, 1435, 1351 cm^{-1}.

^{1}H NMR (250 MHz, $CDCl_3$) δ 8.58 (dd, *J* = 7.4, 2.2 Hz, 2H), 8.00 (d, *J* = 8.5 Hz, 1H), 7.93 (d, *J* = 8.2 Hz, 1H), 7.76 (t, *J* = 7.1 Hz, 1H), 7.53 – 7.42 (m, 4H), 2.95 (t, *J* = 4.5 Hz, 2H), 2.72 (t, *J* = 4.5 Hz, 2H), 2.45 (s, 3H) ppm.

^{13}C NMR (63 MHz, $CDCl_3$) δ 165.2, 159.8, 153.3, 139.1, 132.8, 130.6, 129.4, 128.8 (2C), 128.8 (2C), 125.3, 125.3, 115.8, 55.4 (2C), 50.1 (2C), 46.6 ppm.

4-(1*H*-Imidazol-1-yl)-2-phenylquinazoline (26):

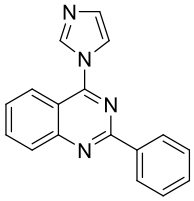

Prepared from 4-chloro-2-phenylquinazoline (241 mg, 1 mmol) and imidazole (140 mg, 2 mmol); reaction time: 30 min; yield: 87%; white solid.

Elemental analysis calcd (%) for $C_{17}H_{12}N_4$: C 74.98, H 4.44, N 20.58; found: C 74.70, H 4.62, N 20.86.

Mp: 154 – 157 °C

IR (neat) ν: 1570, 1551, 1472, 1420, 1382, 1354, 1325, 1255, 654, 706 cm^{-1}.

^{1}H NMR (250 MHz, $CDCl_3$) δ 8.68 – 8.64 (m, 2H), 8.44 (s, 1H), 8.22 (t, *J* = 8.9 Hz, 2H), 8.02 (ddd, *J* = 8.4, 7.0, 1.4 Hz, 1H), 7.83 (s, 1H), 7.72 (ddd, *J* = 8.2, 7.0, 1.2 Hz, 1H), 7.60 – 7.55 (m, 3H), 7.41 (s, 1H) ppm.

^{13}C NMR (63 MHz, $CDCl_3$) δ 160.6, 155.6, 154.3, 138.2, 137.2, 135.1, 131.7, 131.1, 129.9, 129.1 (2C), 129.0 (2C), 128.7, 124.4, 120.1, 116.6 ppm.

9.2.1.5. Amsacrine (27):

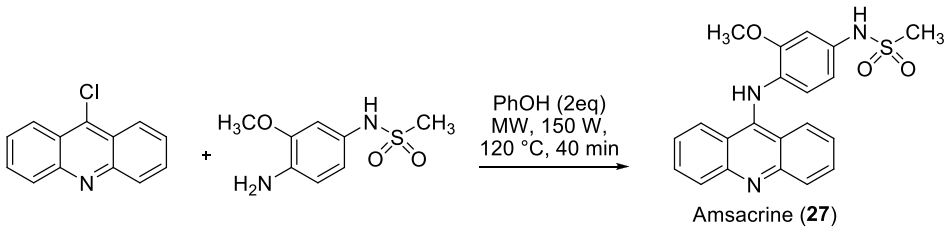

Prepared from 9-chloroacridine (215 mg, 1 mmol) and *N*-(4-amino-3-methoxy)methanesulfonamide (220 mg, 1 mmol) according to our method under MW irradiation; reaction time: 40 min; yield: 78%; orange solid.

Elemental analysis calcd (%) for $C_{21}H_{19}N_3O_3S$: C 64.10, H 4.87, N 10.68, S 8.15; found: C 64.39, H 4.98, N 10.85, S 8.29.

Mp: 233 – 236 °C

IR (neat) ν: 3347, 1560, 1512, 1474, 1321, 1149, 730, 667 cm^{-1}.

^{1}H NMR (250 MHz, Acetone) δ 8.36 (br s, 1H), 8.04 (s, 2H), 7.55 – 7.49 (m, 4H), 7.09 – 7.03 (m, 3H), 6.92 (dd, *J* = 8.3, 2.2 Hz, 1H), 6.70 (d, *J* = 8.3 Hz, 1H), 3.70 (s, 3H), 3.01 (s, 3H) ppm.

^{13}C NMR (63 MHz, Acetone) δ 150.3 (2 C), 143.2 (broad signal, 2 C), 134.0, 132.2 (4 C) , 128.2 (2 C), 121.8, 121.8 (broad signal, 2 C), 119.9, 115.8 (2 C), 107.9 (2 C), 56.4, 39.1 ppm.

9.2.1.6. Synthesis of bistacrine

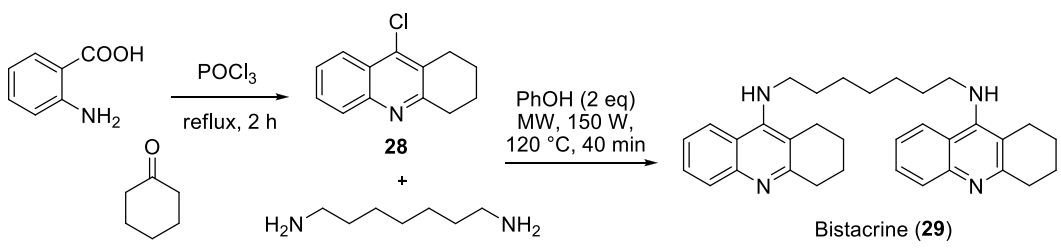

9-chloro-1,2,3,4-tetrahydroacridine (28):

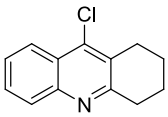

To a mixture of anthranilic acid (500 mg, 3.64 mmol) and cyclohexanone (357.8 mg, 3.64 mmol) was carefully added 5 ml of $POCl_3$ in an ice bath. The mixture was refluxed for 2 h, then cooled at room temperature, and concentrated under reduced pressure. The residue was diluted with ethyl acetate (10 ml), neutralized with aqueous K_2CO_3 (5 ml), and washed with brine. The organic layer was dried over anhydrous Na_2SO_4 and concentrated under reduced pressure to give a yellow solid in 68% yield.

^{1}H NMR (250 MHz, $CDCl_3$) δ 8.19 (dd, *J* = 8.4, 1.0 Hz, 1H), 8.00 (d, *J* = 8.0 Hz, 1H), 7.69 (ddd, *J* = 8.4, 6.9, 1.4 Hz, 1H), 7.56 (ddd, *J* = 8.2, 6.9, 1.2 Hz, 1H), 3.15 (t, *J* = 5.4 Hz, 2H), 3.04 (t, *J* = 5.6 Hz, 2H), 1.97 (dt, *J* = 6.7, 3.3 Hz, 4H) ppm.

^{13}C NMR (63 MHz, $CDCl_3$) δ 159.7, 147.0, 141.7, 129.5, 129.1, 129.0, 126.7, 125.6, 123.9, 34.5, 27.8, 23.0, 22.9 ppm.

Bistacrine (29):

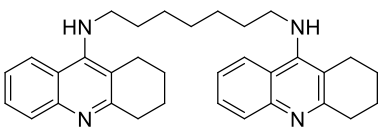

Prepared from 9-chloro-1,2,3,4-tetrahydroacridine (220 mg, 1 mmol) and 1,7-heptanediamine (65 mg, 0.5 mmol) according to our method under MW irradiation; reaction time: 40 min; yield: 98%; yellow solid.

Elemental analysis calcd (%) for $C_{33}H_{40}N_4$: C 80.45, H 8.18, N 11.37; found: C 80.07, H 8.03, N 11.52.

Mp: 65 – 68 °C

IR (neat) ν: 1614, 1580, 1561, 1498, 1420, 1358, 1296, 1272, 678 cm^{-1}.

^{1}H NMR (250 MHz, $CDCl_3$) δ 7.95 (t, *J* = 9.3 Hz, 4H), 7.58 (t, *J* = 7.6 Hz, 2H), 7.37 (t, *J* = 7.6 Hz, 2H), 3.96 (br s, 2H), 3.51 – 3.46 (m, 4H), 3.09 (s, 4H), 2.73 (s, 4H), 1.94 (s, 8H), 1.69 – 1.65 (m, 4H), 1.40 (s, 6H) ppm.

^{13}C NMR (63 MHz, $CDCl_3$) δ 158.9 (2C), 151.1 (2C), 148.0 (2C), 129.3 (2C), 128.6 (2C), 124.0 (2C), 123.2 (2C), 120.7 (2C), 116.4 (2C), 49.8 (2C), 34.6 (2C), 32.1 (2C), 29.5, 27.3 (2C), 25.2 (2C), 23.5 (2C), 23.2 (2C) ppm.

9.2.2. General procedure for the preparation of β-enamino esters

To a stirred solution of 3 mmol of amine and 3 mmol of ethyl acetoacetate in 3 ml of EtOH was added 5 mol% of CAN (82 mg). The mixture was stirred at r.t. for 1 h. After completion of the reaction the mixture was dissolved in CH_2Cl_2, washed with H_2O, dried, and evaporated. No further purification was needed.

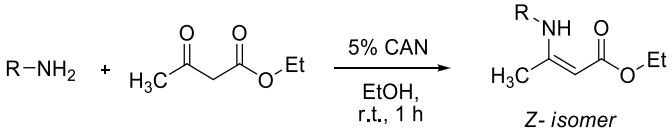

Cmpd.	R
35	CH_3
36	*n*-But
37	*sec*-But
38	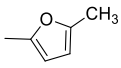
39	C_6H_5-CH_2

(*Z*)-ethyl 3-(methylamino)but-2-enoate (35):

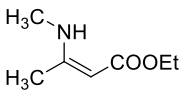

Prepared from methylamine (93.2 mg, 3 mmol) and ethyl acetoacetate (390.4 mg, 3 mmol); yield: 71%; orange oil.

^{1}H NMR (250 MHz, $CDCl_3$) δ 8.50 (br s, 1H), 4.48 (s, 1H), 4.10 (q, *J* = 7.1 Hz, 2H), 2.93 (d, *J* = 5.2 Hz, 3H), 1.94 (s, 3H), 1.26 (t, *J* = 7.1 Hz, 3H) ppm.

(*Z*)-ethyl 3-(butylamino)but-2-enoate (36):

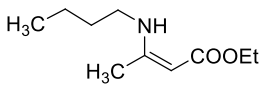

Prepared from *n*-butylamine (220 mg, 3 mmol) and ethyl acetoacetate (390.4 mg, 3 mmol); yield: 77%; yellow oil.

^{1}H NMR (250 MHz, $CDCl_3$) δ 8.56 (br s, 1H), 4.43 (s, 1H), 4.08 (q, *J* = 7.1 Hz, 2H), 3.20 (q, *J* = 7.0 Hz, 2H), 1.92 (s, 3H), 1.61 – 1.47 (m, 2H), 1.44 – 1.36 (m, 2H), 1.25 (t, *J* = 7.1 Hz, 3H), 0.94 (t, *J* = 7.2 Hz, 3H) ppm.

(*Z*)-ethyl 3-(sec-butylamino)but-2-enoate (37):

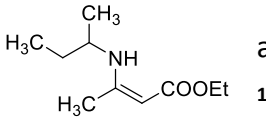

Prepared from *sec*-butylamine (220 mg, 3 mmol) and ethyl acetoacetate (390.4 mg, 3 mmol); yield:82%; yellow oil.

^{1}H NMR (250 MHz, $CDCl_3$) δ 8.54 (br s, 1H), 4.41 (s, 1H), 4.10 (q, *J* = 7.1 Hz, 2H), 3.51 – 3.40 (m, 1H), 1.94 (s, 3H), 1.59 – 1.48 (m, 2H), 1.27 (t, *J* = 7.1 Hz, 3H), 1.19 (d, *J* = 6.5 Hz, 3H), 0.95 (t, *J* = 7.4 Hz, 3H) ppm.

(*Z*)-ethyl 3-(furan-2-ylmethylamino)but-2-enoate (38):

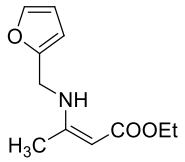

Prepared from furfurylamine (292 mg, 3 mmol) and ethyl acetoacetate (390.4 mg, 3 mmol); yield:85%; orange oil.

^{1}H NMR (250 MHz, $CDCl_3$) δ 8.83 (br s, 1H), 7.38 – 7.37 (m, 1H), 6.33 (dd, *J* = 3.2, 1.9 Hz, 1H), 6.22 (dd, *J* = 3.2, 0.7 Hz, 1H), 4.55 (s, 1H), 4.40 (d, *J* = 6.3 Hz, 2H), 4.11 (q, *J* = 7.1 Hz, 2H), 2.02 (s, 3H), 1.27 (t, *J* = 7.1 Hz, 3H) ppm.

(*Z*)-ethyl 3-(benzylamino)but-2-enoate (39):

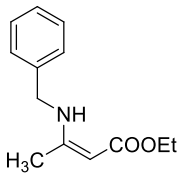

Prepared from benzylamine (322 mg, 3 mmol) and ethyl acetoacetate(390.4 mg, 3 mmol); yield: 81%; yellow oil.

^{1}H NMR (250 MHz, $CDCl_3$) δ 8.98 (br s, 1H), 7.41 – 7.26 (m, 5H), 4.56 (s, 1H), 4.46 (d, *J* = 6.4 Hz, 2H), 4.13 (q, *J* = 7.1 Hz, 2H), 1.94 (s, 3H), 1.28 (t, *J* = 7.2 Hz, 3H) ppm.

9.2.2.1. (*E*)-ethyl 3-(pyrrolidin-1-yl)but-2-enoate (40):

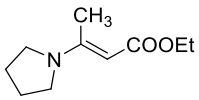

A mixture of pyrrolidine (320 mg, 4.5 mmol) and ethyl acetoacetate (390.4 mg, 3 mmol) was stirred at r.t. for 16 h until completion of the reaction. The crude mixture was dissolved in CH_2Cl_2 and was purified over alumina by chromatography to obtain a pale yellow oil in 89% yield.

^{1}H NMR (250 MHz, $CDCl_3$) δ 4.45 (s, 1H), 4.08 (q, *J* = 7.1 Hz, 2H), 3.30 (br s, 3H), 2.46 (s, 3H), 1.95 1.90 (m, 4H), 1.25 (t, *J* = 7.1 Hz, 3H) ppm.

9.2.3. General procedure for the $InCl_3$ catalyzed generation of C-C and C-N bond on nitrogen heterocycles

The suitable starting heterocycle (0.5 mmol), the corresponding nucleophile (1 equiv) and 10 mol% of $InCl_3$ (11 mg) were charged in a pressure-tight microwave tube containing 2 ml of acetonitrile (except 2-methylfuran CH_2Cl_2) and a stirring bar. The reaction mixture was submitted to microwave irradiation for 30 min – 3 h at 120 °C (except 4-hydroxycumarine 140 °C), with an irradiation power of 150 W, using a CEM Discover SP focused microwave reactor. If a precipitate was

formed, simple filtration gave the final products otherwise the mixture was dissolved in CH_2Cl_2, washed with H_2O, dried, and evaporated. In the latter case, analytically pure compounds were obtained by flash chromatography on silica gel.

9.2.3.1. C-C coupling reactions of 4,7-dichloroquinoline

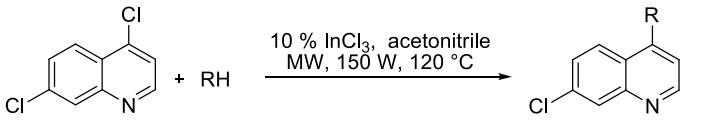

30-34, 41-45

Cmpd.	RH	Cmpd.	RH
30	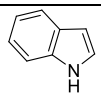	**41**	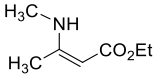
31	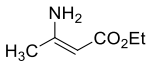	**42**	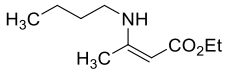
32		**43**	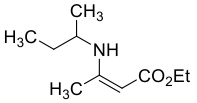
33	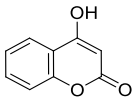	**44**	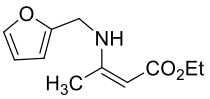
34		**45**	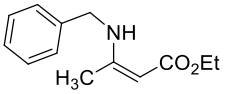

7-Chloro-4-(1*H*-indol-3-yl)quinolinium chloride (30):

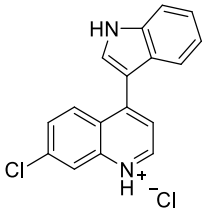

Prepared from 4,7-dichloroquinoline (100 mg, 0.5 mmol) and indole (60 mg, 0.05 mmol); reaction time:2 h; precipitate formation to give the product as a yellow solid in 89%.

Elemental analysis calcd (%) for $C_{17}H_{12}Cl_2N_2$: C 64.78, H 3.84, N 8.89; found: C 64.61, H 3.64, N 8.85.

Mp: 259 262 °C

IR (neat) ν: 3291, 3088, 1626, 1591, 1517, 1421, 1234, 830, 739 cm^{-1}.

^{1}H NMR (250 MHz, DMSO) δ 12.56 (br s, 1H), 9.26 (d, *J* = 5.7 Hz, 1H), 8.64 (d, *J* = 9.2 Hz, 1H), 8.55 (d, *J* = 1.8 Hz, 1H), 8.31 (d, *J* = 2.7 Hz, 1H), 8.18 (d, *J* = 5.7 Hz, 1H), 8.02 (dd, *J* = 9.1, 1.9 Hz, 1H), 7.88 (d, *J* = 7.7 Hz, 1H), 7.75 (d, *J* = 7.9 Hz, 1H), 7.47 – 7.33 (m, 2H) ppm.

^{13}C NMR (63 MHz, MeOD) δ 152.7, 147.4, 144.1, 140.6, 139.3, 131.3 (2C), 130.6, 127.5, 126.9, 124.9, 123.8, 123.1, 122.0, 120.5, 114.0, 113.2 ppm.

(*Z*)-Ethyl 3-amino-2-(7-chloroquinolin-4-yl)but-2-enoate (31):

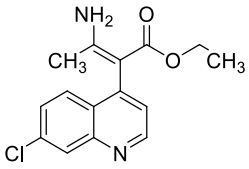

Prepared from 4,7-dichloroquinoline (100 mg, 0.5 mmol) and ethyl 3-aminocrotonate (65 mg, 0.05 mmol); reaction time 3 h; purification by chromatography to give the product as a white solid in 75% yield.

Elemental analysis calcd (%) for $C_{15}H_{15}ClN_2O_2$: C 61.97, H 5.20, N 9.64; found: C 61.32, H 5.32, N 9.15.

Mp: 156 159 °C

IR (neat) ν: 3416, 3312, 2979, 2925, 1664, 1614, 1251, 1101 cm^{-1}.

^{1}H NMR (250 MHz, $CDCl_3$): δ 8.89 (d, *J* = 4.5, 1H), 8.15 (d, *J* = 2.0, 1H), 7.83 (d, *J* = 8.9, 1H), 7.47 (dd, *J* = 9.0, 2.1 Hz, 1H), 7.25 (d, *J* = 4.5, 1H), 4.08 – 3.95 (m, 2H), 1.66 (s, 3H), 0.99 (t, *J* = 7.1 Hz, 3H) ppm.

^{13}C NMR (63 MHz, $CDCl_3$): δ 169.2, 159.3, 151.5, 149.3, 146.2, 135.3, 128.8, 128.4, 127.8, 127.6, 125.1, 93.3, 59.7, 21.8, 14.7 ppm.

7-Chloro-4-(1*H*-pyrrol-2-yl)quinolinium chloride (32):

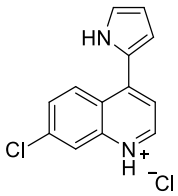

Prepared from 4,7-dichloroquinoline (100 mg, 0.5 mmol) and pyrrole (35 mg, 0.05 mmol); reaction time: 2 h; precipitate formation to give the product as a yellow solid in 90% yield.

Elemental analysis calcd (%) for $C_{13}H_{10}Cl_2N_2$: C 58.89, H 3.80, N 10.57; found: C 58.49, H 4.10, N 10.48.

Mp: 178 181 °C

IR (neat) ν: 1583, 1498, 1431, 1370, 1257, 1136, 1041, 916 cm^{-1}.

^{1}H NMR (250 MHz, $CDCl_3$) δ 9.01 (br s, 1H), 8.83 (d, *J* = 4.6 Hz, 1H), 8.35 (d, *J* = 9.1 Hz, 1H), 8.11 (d, *J* = 2.1 Hz, 1H), 7.51 (dd, *J* = 9.1, 2.2 Hz, 1H), 7.35 (d, *J* = 4.6 Hz, 1H), 7.14 – 7.11 (m, 1H), 6.75 – 6.72 (m, 1H), 6.51 – 6.48 (m, 1H) ppm.

^{13}C NMR (63 MHz, $CDCl_3$) δ 151.2, 149.7, 139.9, 135.9, 129.0, 128.1, 127.9, 127.7, 124.5, 121.5, 119.2, 112.8, 111.1 ppm.

7-Chloro-4-(4-hydroxy-2-oxo-2*H*-chromen-3-yl)quinolinium chloride (33):

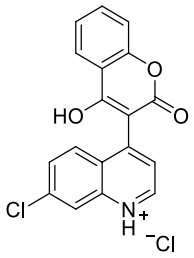

Prepared from 4,7-dichloroquinoline (100 mg, 0.5 mmol) and 4-hydroxycumarine (82 mg, 0.05 mmol); reaction time: 1 h; temperature: 140 °C; precipitate formation to give the product as a yellow solid in 84% yield.

Elemental analysis calcd (%) for $C_{18}H_{11}Cl_2NO_3$: C 60.02, H 3.08, N 3.89; found: C 59.49, H 3.11, N 4.00.

Mp: 257 260 °C

IR (neat) ν: 2581, 1732, 1598, 1494, 1381, 1199, 1848, 961 cm^{-1}.

^{1}H NMR (250 MHz, DMSO) δ 9.20 (d, *J* = 5.1 Hz, 1H), 8.34 (s, 1H), 8.08 (d, *J* = 8.7 Hz, 2H), 7.92 (d, *J* = 5.1 Hz, 1H), 7.78 – 7.71 (m, 2H), 7.50 – 7.40 (m, 2H) ppm.

^{13}C NMR (63 MHz, DMSO) δ 164.5, 161.4, 153.6, 149.2, 147.0, 141.4, 137.8, 133.6, 129.8, 129.5, 127.3, 125.8, 124.9, 124.5, 122.4, 117.2, 116.9, 100.4 ppm.

7-Chloro-4-(5-methylfuran-2-yl)quinoline (34):

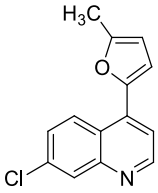

Prepared from 4,7-dichloroquinoline (100 mg, 0.5 mmol) and 2-methyfurano (42 mg, 0.05 mmol) in dichloromethane; reaction time: 3 h; purification by chromatography to give the product as a red solid in 82% yield.

Elemental analysis calcd (%) for $C_{14}H_{10}ClNO$: C 69.00, H 4.14, N 5.75; found: C 68.82, H 4.05, N 5.52.

Mp: 69 72 °C

IR (neat) ν: 3066, 1619, 1506, 1207, 1089 cm^{-1}.

^{1}H NMR (250 MHz, MeOD) δ 8.77 (d, *J* = 5.0 Hz, 1H), 8.67 (d, *J* = 9.2 Hz, 1H), 7.96 (s, 1H), 7.81 (d, *J* = 5.1 Hz, 1H), 7.64 (dd, *J* = 9.0, 1.0 Hz, 1H), 7.30 (d, *J* = 3.3 Hz, 1H), 6.34 (d, *J* = 2.8 Hz, 1H), 2.49 (d, *J* = 37.6 Hz, 3H) ppm.

^{13}C NMR (63 MHz, MeOD) δ 159.4, 150.0, 149.6, 146.9, 141.2, 139.2, 130.5, 130.0, 126.0, 123.9, 119.7, 118.8, 111.4, 14.3 ppm.

(*Z*)-Ethyl 2-(7-chloroquinolin-4-yl)-3-(methylamino)but-2-enoate (41):

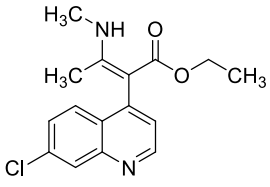

Prepared from 4,7-dichloroquinoline (100 mg, 0.5 mmol) and (*Z*)-ethyl 3-(methylamino)but-2-enoate (**35**) (72 mg, 0.05 mmol); reaction time: 3 h; purification by chromatography to give the product as a pale brown solid in 66% yield.

Elemental analysis calcd (%) for $C_{16}H_{17}ClN_2O_2$: C 63.05, H 5.62, N 9.19; found: C 62.95, H 5.44, N 9.03.

Mp: 98 101 °C

IR (neat) ν: 3263, 2974, 2930, 1647, 1597, 1265, 1231, 1061 cm^{-1}.

^{1}H NMR (250 MHz, $CDCl_3$) δ 9.60 (br s, 1H), 8.78 (d, *J* = 4.4 Hz, 1H), 8.03 (d, *J* = 2.1 Hz, 1H), 7.73 (d, *J* = 8.9 Hz, 1H), 7.35 (dd, *J* = 9.0, 2.1 Hz, 1H), 7.11 (d, *J* = 4.4 Hz, 1H), 3.95 – 3.81 (m, 2H), 2.94 (d, *J* = 5.2 Hz, 3H), 1.56 (s, 3H), 0.88 (t, *J* = 7.1 Hz, 3H) ppm.

^{13}C NMR (63 MHz, $CDCl_3$) δ 169.7, 162.5, 151.7, 149.4, 146.7, 135.1, 128.9, 128.8, 127.9, 127.4, 125.5, 91.1, 59.4, 30.5, 17.0, 14.8 ppm.

(*Z*)-Ethyl 3-(butylamino)-2-(7-chloroquinolin-4-yl)but-2-enoate (42):

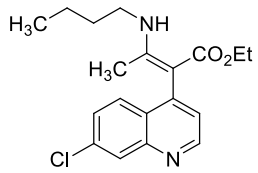

Prepared from 4,7-dichloroquinoline (100 mg, 0.5 mmol) and (*Z*)-ethyl 3-(butylamino)but-2-enoate (**36**) (92 mg, 0.05 mmol); reaction time: 3 h; purification by chromatography to give the product as a pale brown solid in 95% yield.

Elemental analysis calcd (%) for $C_{19}H_{23}ClN_2O_2$: C 65.79, H 6.68, N 8.08; found: C 65.29, H 6.55, N 8.12.

Mp: 101 – 104 °C

IR (neat) ν: 3251, 2970, 2932, 1645, 1594, 1264, 1228, 877 cm^{-1}.

^{1}H NMR (250 MHz, $CDCl_3$) δ 9.75 (br t, *J* = 5.0 Hz, 1H), 8.88 (d, *J* = 4.4 Hz, 1H), 8.12 (d, *J* = 2.1 Hz, 1H), 7.83 (d, *J* = 8.9 Hz, 1H), 7.44 (dd, *J* = 8.9, 2.1 Hz, 1H), 7.21 (d, *J* = 4.4 Hz, 1H), 4.07 – 3.89 (m, 2H), 3.37 – 3.29 (m, 2H), 1.78 – 1.66 (m, 2H), 1.65 (s, 3H), 1.58 – 1.43 (m, 2H), 1.04 – 0.94 (m, 6H) ppm.

^{13}C NMR (63 MHz, $CDCl_3$) δ 169.6, 161.6, 151.7, 149.5, 146.8, 135.1, 128.9, 128.8, 128.0, 127.4, 125.5, 90.8, 59.3, 43.7, 32.6, 20.6, 17.2, 14.8, 14.3 ppm.

(*Z*)-Ethyl 3-(sec-butylamino)-2-(7-chloroquinolin-4-yl)but-2-enoate (43):

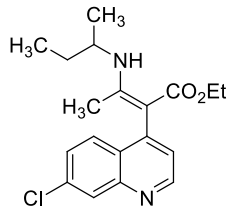

Prepared from 4,7-dichloroquinoline (100 mg, 0.5 mmol) and (*Z*)-ethyl 3-(*sec*-butylamino)but-2-enoate (**37**) (92 mg, 0.05 mmol); reaction time: 3 h; purification by chromatography to obtain the product as a white solid in 96% yield.

Elemental analysis calcd (%) for $C_{19}H_{23}ClN_2O_2$: C 65.79, H 6.68, N 8.08; found: C 65.73, H 6.58, N 8.13.

Mp: 115 118 °C

IR (neat) ν: 3250, 2971, 2927, 1645, 1594, 1561, 1536, 1335, 1241, 710 cm^{-1}.

^{1}H NMR (250 MHz, $CDCl_3$) δ 9.66 (br d, *J* = 8.9 Hz, 1H), 8.78 (d, *J* = 4.4 Hz, 1H), 8.02 (d, *J* = 2.1 Hz, 1H), 7.73 (dd, *J* = 8.9, 4.9 Hz, 1H), 7.35 (dd, *J* = 8.9, 2.1 Hz, 1H), 7.13 (dd, *J* = 4.4, 1.5 Hz, 1H), 3.95 – 3.81 (m, 2H), 3.55 – 3.39 (m, 1H), 1.59 – 1.52 (m, 2H), 1.56 (s, 3H), 1.20 (dd, *J* = 6.4, 2.0 Hz, 3H), 0.98 – 0.84 (m, 6H) ppm.

^{13}C NMR (63 MHz, $CDCl_3$) δ 169.6, 160.8, 151.8, 149.5, 146.9, 135.1, 128.9, 128.0, 127.9, 127.4, 125.6, 90.5, 59.3, 50.9, 31.4, 22.2, 17.2, 14.8, 11.0 ppm.

(*Z*)-Ethyl 2-(7-chloroquinolin-4-yl)-3-(furan-2-ylmethyl-amino)but-2-enoate (44):

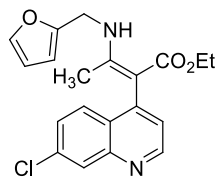

Prepared from 4,7-dichloroquinoline (100 mg, 0.5 mmol) and(*Z*)-ethyl 3-(furan-2-ylmethylamino)but-2-enoate (**38**) (104 mg, 0.05 mmol); reaction time 3 h; purification by

chromatography to obtain the product as a yellow oil in 75% yield.

Elemental analysis calcd (%) for $C_{20}H_{19}ClN_2O_3$: C 64.78, H 5.16, N 7.55; found: C 64.55, H 4.99, N 7.23.

IR (neat) ν: 3255, 2980, 2930, 1651, 1583, 1444, 1262, 1231, 1095, 1071, 1016 cm^{-1}.

^{1}H NMR (250 MHz, $CDCl_3$) δ 10.03 (br t, *J* = 5.6 Hz, 1H), 8.89 (d, *J* = 4.6 Hz, 1H), 8.23 (d, *J* = 2.0 Hz, 1H), 7.85 (d, *J* = 9.0 Hz, 1H), 7.49 (dd, *J* = 9.0, 2.1 Hz, 1H), 7.44 (dd, *J* = 1.8, 0.8 Hz, 1H), 7.28 (d, *J* =4.6 Hz, 1H), 6.40 (dd, *J* = 3.2, 1.9 Hz, 1H), 6.31 (dd, *J* = 3.2, 0.8 Hz, 1H), 4.52 (d, *J* = 5.9 Hz, 2H), 4.04 – 3.94 (m, 2H), 1.75 (s, 3H), 0.97 (t, *J* = 7.1 Hz, 3H) ppm.

^{13}C NMR (63 MHz, $CDCl_3$) δ 167.9, 159.6, 150.1, 149.2, 146.8, 146.4, 141.6, 134.5, 127.3, 126.6, 126.5 (2C), 123.9, 109.5, 106.4, 91.0, 58.2, 39.5, 15.8, 13.3 ppm.

(*Z*)-Ethyl 3-(benzylamino)-2-(7-chloroquinolin-4-yl)but-2-enoate (45):

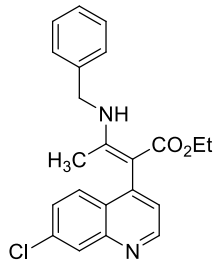

Prepared from 4,7-dichloroquinoline (100 mg, 0.5 mmol) and (*Z*)-ethyl 3-(benzylamino)but-2-enoate (**39**) (110 mg, 0.05 mmol); reaction time 3 h; purification by chromatography to obtain the product as a yellow oil in 65% yield.

Elemental analysis calcd (%) for $C_{22}H_{21}ClN_2O_2$: C 69.38, H 5.56, N 7.36; found: C 69.01, H 5.34, N 7.24.

IR (neat) ν: 3237, 2977, 2923, 1651, 1607, 1260, 1230 cm^{-1}.

^{1}H NMR (250 MHz,$CDCl_3$) δ10.13 (br t, *J* = 5.9 Hz, 1H), 8.88 (d, *J* = 4.4 Hz, 1H), 8.13 (d, *J* = 2.1 Hz, 1H), 7.84 (d, *J* = 8.9 Hz, 1H), 7.48 – 7.34 (m, 6H), 7.23 (d, *J* = 4.4 Hz, 1H), 4.56 (d, *J* = 6.1 Hz, 2H), 4.07 – 3.93 (m, 2H), 1.66 (s, 3H), 0.98 (t, *J* = 7.1 Hz, 3H) ppm.

^{13}C NMR (63 MHz, $CDCl_3$) δ 169.7, 161.5, 151.7, 149.4, 146.5, 138.6, 135.2, 129.4 (2C), 128.9, 128.7, 128.0, 127.8, 127.5, 127.3 (2C), 125.4, 92.2, 59.5, 47.7, 17.3, 14.7 ppm.

9.2.3.2. C-C coupling reaction of 6,9-dichloro-2-methoxyacridine

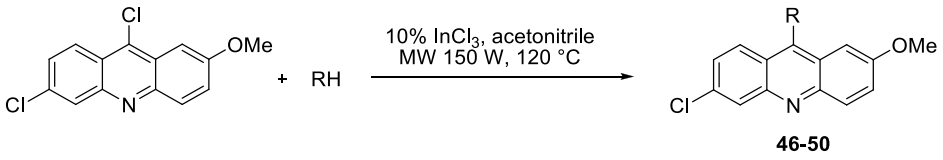

46-50

Cmpd.	RH
46	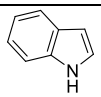
47	
48	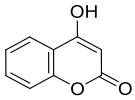
49	
50	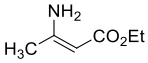

6-Chloro-9-(1*H*-indol-3-yl)-2-methoxyacridinium chloride (46):

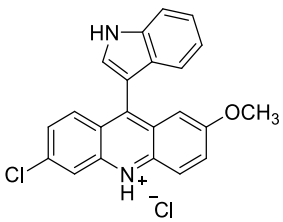

Prepared from 6,9-dichloro-2-methoxyacridine (139 mg, 0.5 mmol) and indole (60 mg, 0.05 mmol); reaction time: 2 h; precipitate formation to give the product as a yellow solid in 93% yield.

Elemental analysis calcd (%) for $C_{22}H_{16}Cl_2N_2O$: C, 66.85; H, 4.08; N, 7.09; found: C

66.72, H 4.15, N 7.24.

Mp: 221 224 °C

IR (neat) ν: 1628, 1563, 1535, 1466, 1419, 1209, 701 cm^{-1}.

^{1}H NMR (250 MHz, $CDCl_3$) δ 8.79 (br s, 1H), 8.28 (d, *J* = 1.8 Hz, 1H), 8.19 (d, *J* = 9.4 Hz, 1H), 7.89 (d, *J* = 9.3 Hz, 1H), 7.63 (d, *J* = 8.2 Hz, 1H), 7.51 (dd, *J* = 7.7, 2.4 Hz, 2H), 7.39 – 7.31 (m, 2H), 7.23 – 7.12 (m, 3H), 3.69 (s, 3H) ppm.

^{13}C NMR (63 MHz, $CDCl_3$) δ 157.5, 147.6, 146.9, 139.5, 136.5, 135.3, 131.3, 128.9, 128.2, 128.2, 127.6, 127.1, 126.1, 125.7, 125.3, 123.4, 121.1, 120.7, 112.0, 111.4, 103.2, 55.8 ppm.

6-Chloro-2-methoxy-9-(1*H*-pyrrol-2-yl)acridinium chloride (47):

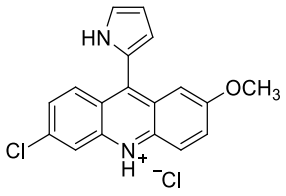

Prepared from 6,9-dichloro-2-methoxyacridine (139 mg, 0.5 mmol) and pyrrole (35 mg, 0.05 mmol); reaction time: 2 h; precipitate formation to give the product as a yellow solid in 90%.

Elemental analysis calcd (%) for $C_{18}H_{14}Cl_2N_2O$: C 62.62, H 4.09, N 8.11; found: C 62.23, H 4.25, N 8.21.

Mp: 236 239 °C

IR (neat) ν: 1630, 1473, 1232, 807 cm^{-1}.

^{1}H NMR (250 MHz, $CDCl_3$) δ 9.40 (br s, 1H), 8.06 (d, *J* = 2.0 Hz, 1H), 7.94 (d, *J* = 9.4 Hz, 1H), 7.82 (d, *J* = 9.4 Hz, 1H), 7.35 – 7.27 (m, 3H), 7.05 (d, *J* = 2.1 Hz, 1H), 6.60 – 6.57 (m, 2H), 3.84 (s, 3H) ppm.

^{13}C NMR (63 MHz, acetone-d_6) δ 158.7, 148.6, 148.1, 138.7, 135.3, 132.6, 130.1, 129.1, 127.9, 127.8, 126.7, 125.6, 121.6, 121.4, 113.5, 110.3, 103.8, 56.2 ppm.

6-Chloro-9-(4-hydroxy-2-oxo-2*H*-chromen-3-yl)-2-methoxyacridinium chloride (48):

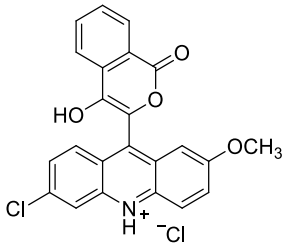

Prepared from 6,9-dichloro-2-methoxyacridine (139 mg, 0.5 mmol) and 4-hydroxycumarine (82 mg, 0.05 mmol); reaction time: 1 h; temperature: 140°C; precipitate formation to give the product as an orange solid in 92% yield.

Elemental analysis calcd (%) for $C_{23}H_{15}Cl_2NO_4$: C 62.74, H 3.43, N 3.18; found: C 62.31, H 3.39, N 3.45.

Mp> 300 °C

IR (neat) ν: 1696, 1606, 1228, 1043, 951, 761 cm^{-1}.

^{1}H NMR (250 MHz, DMSO) δ 8.43 (d, *J* = 2.0 Hz, 1H), 8.34 (d, *J* = 9.4 Hz, 1H), 8.14 (d, *J* = 9.3 Hz, 1H), 8.08 (dd, *J* = 7.9, 1.4 Hz, 1H), 7.85 – 7.76 (m, 2H), 7.67 (dd, *J* = 9.3, 2.1 Hz, 1H), 7.58 (dd, *J* = 8.3, 0.7 Hz, 1H), 7.51 – 7.44 (m, 1H), 7.28 (d, *J* = 2.6 Hz, 1H), 3.85 (s, 3H) ppm.

^{13}C NMR (63 MHz, DMSO) δ 164.2, 161.2, 158.2, 154.0, 139.4, 137.0, 133.5, 129.3, 129.1, 129.0, 128.3, 128.1, 127.3, 127.3, 125.2, 124.6, 124.5, 123.9, 117.0, 116.9, 103.0, 98.5, 56.4 ppm.

6-Chloro-2-methoxy-9-(5-methylfuran-2-yl)acridinium chloride (49):

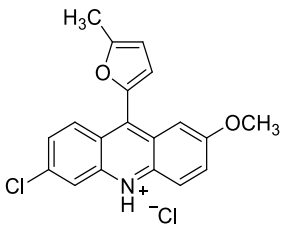

Prepared from 6,9-dichloro-2-methoxyacridine (139 mg, 0.5 mmol) and 2-methyfurano (42 mg, 0.05 mmol) in dichloromethane; reaction time: 3 h; precipitate formation to give the product as a brown solid in 84% yield.

Elemental analysis calcd (%) for $C_{19}H_{15}Cl_2NO_2$: C 63.35, H 4.20, N 3.89; found: C 63,01, H 3.97, N 3,63.

Mp: 170 173 °C

IR (neat) ν: 3120, 1626, 1526, 1453, 1240 cm^{-1}.

^{1}H NMR (250 MHz, MeOD) δ 8.64 (d, *J* = 9.5 Hz, 1H), 8.26 – 8.21 (m, 2H), 7.99 – 7.84 (m, 3H), 7.47 (s, 1H), 6.72 (s, 1H), 4.05 (s, 3H), 2.66 (s, 3H) ppm.

^{13}C NMR (63 MHz, MeOD) δ 159.6, 145.0, 143.4, 142.0, 139.8, 131.8, 130.3, 129.4, 125.6, 125.1, 123.1, 123.1, 122.6, 121.7, 118.8, 110.4, 104.4, 55.6, 13.0 ppm.

(*Z*)-9-(3-Amino-1-ethoxy-1-oxobut-2-en-2-yl)-6-chloro-2-methoxyacridinium (50):

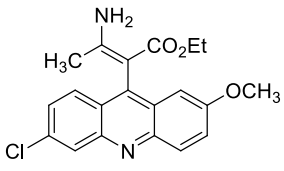

Prepared from 6,9-dichloro-2-methoxyacridine (139 mg, 0.5 mmol) and ethyl 3-aminocrotonate (65 mg, 0.05 mmol); reaction time: 3 h; purification by chromatography to obtain the product as an orange solid in 88% yield.

Elemental analysis calcd (%) for $C_{20}H_{19}ClN_2O_3$: C 58.98, H 4.95, N 6.88; found: C 58.78, H 4.96, N 7.06.

Mp: 245 246 °C

IR (neat) ν: 3348, 3240, 3164, 1660, 1628, 1426, 1239, 1017 cm^{-1}.

^{1}H NMR (250 MHz, MeOD) δ 8.34 – 8.24 (m, 3H), 7.96 (dd, *J* = 9.5, 2.6 Hz, 1H), 7.83 (d, *J* = 9.5 Hz, 1H), 7.47 (d, *J* = 2.5 Hz, 1H), 4.02 (s, 3H), 4.04 – 3.94 (m, 2H), 1.58 (s, 3H), 0.88 (t, *J* = 7.1 Hz, 3H) ppm.

^{13}C NMR (63 MHz, DMSO) δ 167.8, 161.9, 157.5, 156.4, 135.8, 135.4, 135.1, 132.8, 128.9, 128.4, 127.5, 127.5, 127.4, 125.9, 102.3, 86.5, 58.4, 55.9, 20.4, 14.7 ppm.

9.2.3.3. C-C coupling reaction of 4-chloro-2-phenylquinazoline

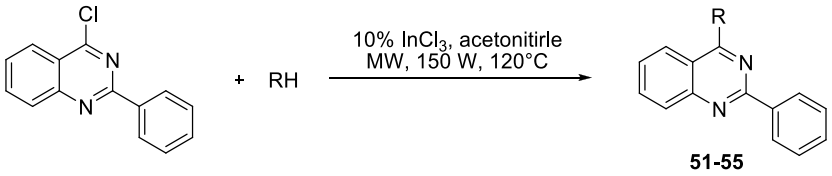

Cmpd.	RH
51	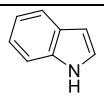
52	
53	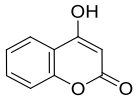
54	
55	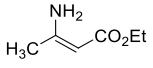

4-(1*H*-Indol-3-yl)-2-phenylquinazolin-1-ium chloride (51):

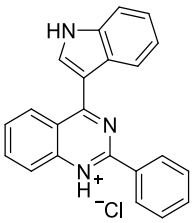

Prepared from 4-dichloro-2-phenylquinazoline (120 mg, 0.5 mmol) and indole (60 mg, 0.05 mmol); reaction time: 2 h; precipitate formation to give the product as a pale yellow solid in 78% yield.

Elemental analysis calcd (%) for $C_{22}H_{16}ClN_3$: C 73.84, H 4.51, N 11.74; found: C 73.97, H 4.76, N 11.71.

Mp: 244 247 °C

IR (neat) ν: 1524, 1483, 1456, 1438, 1341, 1240, 745, 706 cm^{-1}.

^{1}H NMR (250 MHz, $CDCl_3$) δ 8.77 (dd, *J* = 8.0, 1.7 Hz, 2H), 8.42 (d, *J* = 6.9 Hz, 2H), 8.19 (d, *J* = 8.4 Hz, 1H), 7.95 – 7.88 (m, 2H), 7.63 – 7.54 (m, 5H), 7.41 – 7.37 (m, 2H) ppm.

^{13}C NMR (63 MHz, $CDCl_3$) δ 164.0, 160.8, 152.3, 139.0, 137.1, 136.9, 133.7, 130.8, 129.3, 129.0 (2C), 129.0 (2C), 127.3, 127.1, 127.0, 123.7, 122.3, 122.1, 121.9, 114.8, 111.9 ppm.

2-Phenyl-4-(1*H*-pyrrol-2-yl)quinazolin-1-ium chloride (52):

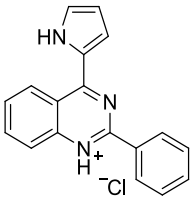

Prepared from 4-dichloro-2-phenylquinazoline (120 mg, 0.5 mmol) and pyrrole (35 mg, 0.05 mmol); reaction time: 2 h; precipitate formation to give the product as a brown solid in 96% yield.

Elemental analysis calcd (%) for $C_{18}H_{14}ClN_3$: C 70.24, H 4.58, N 13.65; found: C 70.63, H 4.88; N 13.62.

Mp: 196 199 °C

IR (neat) ν: 3440, 2923, 1561,1488, 1431, 1338, 760 cm^{-1}.

^{1}H NMR (250 MHz, MeOD) δ 8.54 – 8.46 (m, 3H), 7.90 – 7.79 (m, 2H), 7.61 – 7.55 (m, 1H), 7.48 – 7.44 (m, 3H), 7.28 (d, *J* = 3.9 Hz, 1H), 7.20 – 7.19 (m, 1H), 6.39 (dd, *J* = 3.6, 2.5 Hz, 1H) ppm.

^{13}C NMR (63 MHz, MeOD) δ 160.4, 160.2, 150.1, 137.6, 136.2, 133.1, 130.4 (2C), 130.3 (2C), 130.2, 129.6, 128.3, 127.1, 124.4, 120.8, 120.4, 113.9 ppm.

4-Hydroxy-3-(2-phenylquinazolin-4-yl)-1*H*-isochromen-1-one (53):

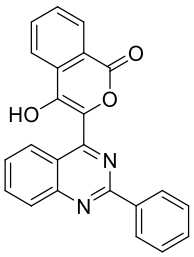

Prepared from 4-dichloro-2-phenylquinazoline (120 mg, 0.5 mmol) and 4-hydroxycumarine (82 mg, 0.05 mmol); reaction time: 1 h; temperature: 140 °C; precipitate formation to give the product as a yellow solid in 80% yield.

Elemental analysis calcd (%) for $C_{23}H_{14}N_2O_3$: C 75.40, H 3.85, N 7.65; found: C 75.28, H 3.79, N 7.78.

Mp: 276 279 °C

IR (neat) ν: 1704, 1609, 1558, 1470, 1381, 1356, 756 cm^{-1}.

^{1}H NMR (250 MHz, DMSO) δ 8.57 – 8.53 (m, 2H), 8.17 – 8.02 (m, 4H), 7.82 – 7.76 (m, 1H), 7.70 – 7.45 (m, 6H) ppm.

^{13}C NMR (63 MHz, MeOD) δ 164.6, 162.9, 161.2, 158.7, 153.3, 150.7, 137.0, 134.9, 133.5, 131.0, 128.9 (2C), 128.4, 128.2 (2C), 127.7, 127.2, 124.4 (2C), 123.2, 116.6, 116.6, 101.5 ppm.

4-(5-Methylfuran-2-yl)-2-phenylquinazoline (54):

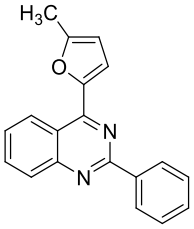

Prepared from 4-dichloro-2-phenylquinazoline (120 mg, 0.5 mmol) and 2-methyfurano (42 mg, 0.05 mmol) in dichloromethane; reaction time: 3 h; purification by chromatography to obtain the product as a yellow solid in 44% yield.

Elemental analysis calcd (%) for $C_{19}H_{14}N_2O$: C 79.70, H 4.93, N 9.78; found: C 79.76, H 4.54, N 9.42.

Mp: 99 102 °C

IR (neat) ν: 3060, 1563, 1545, 1515, 1334, 764, 706 cm^{-1}.

^{1}H NMR (250 MHz, $CDCl_3$) δ 8.95 (d, *J* = 8.5 Hz, 1H), 8.69 (dd, *J* = 7.6, 1.8 Hz, 2H), 8.10 (d, *J* = 8.6 Hz, 1H), 7.92 – 7.86 (m, 1H), 7.68 – 7.55 (m, 5H), 6.35 (d, *J* = 2.6 Hz, 1H), 2.59 (s, 3H). ppm.

^{13}C NMR (63 MHz, $CDCl_3$) δ 160.5, 157.0, 155.6, 153.1, 152.9, 138.7, 133.8, 130.8, 129.5, 128.9 (2C), 128.9 (2C), 127.5, 127.2, 119.9, 118.0, 109.5, 14.8 ppm.

(*Z*)-Ethyl 3-(sec-butylamino)-2-(2-phenylquinazolin-4-yl)but-2-enoate (55):

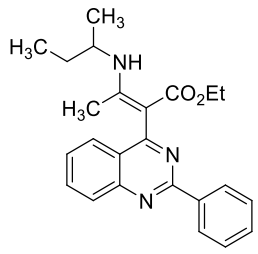

Prepared from 4-dichloro-2-phenylquinazoline (120 mg, 0.5 mmol) and (*Z*)-ethyl 3-(*sec*-butylamino)but-2-enoate (**37**) (92 mg, 0.5 mmol); reaction time: 3 h; purification by chromatography to obtain the product as a pale yellow solid in 84% yield.

Elemental analysis calcd (%) for $C_{24}H_{27}N_3O_2$: C 74.01, H 6.99, N 10.79; found: C 73.77, H 6.86, N 10.65.

Mp: 123 126 °C

IR (neat) ν: 3246, 3147, 3064, 2974, 2923, 1646, 1596, 1254, 710 cm^{-1}.

^{1}H NMR (250 MHz, $CDCl_3$) δ 9.93 (br d, *J* = 8.6 Hz, 1H), 8.65 – 8.61 (m, 2H), 8.09 (d, *J* = 8.4 Hz, 1H), 7.97 (d, *J* = 7.7 Hz, 1H), 7.87 – 7.81 (m, 1H), 7.59 – 7.47 (m, 4H), 4.05 – 3.94 (m, 2H), 3.73 – 3.57 (m, 1H), 1.94 (s, 3H), 1.74 – 1.63 (m, 2H), 1.33 (d, *J* = 6.4 Hz, 3H), 1.06 (t, *J* = 7.4 Hz, 3H), 0.92 (t, *J* = 7.1 Hz, 3H) ppm.

^{13}C NMR (63 MHz, $CDCl_3$) δ 169.8, 169.2, 162.6, 160.9, 151.6, 139.1, 133.6, 130.6, 129.1, 129.0 (2C), 128.9 (2C), 127.8, 126.6, 125.7, 92.8, 59.2, 51.0, 31.2, 22.1, 17.1, 14.7, 10.9 ppm.

9.2.3.4. C-C coupling reaction of2-chloroquinaxoline

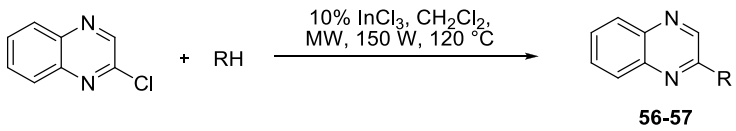

56-57

Cmpd.	RH
56	
57	

2-(1*H*-Indol-3-yl)quinoxalin-1-ium chloride (56):

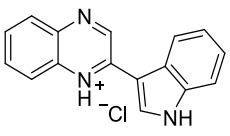

Prepared from 2-chloroquinaxoline (83 mg, 0.5 mmol) and pyrrole (35 mg, 0.05 mmol) in dichloromethane; reaction time: 1 h; precipitate formation to give the product as an orange solid in 89% yield.

Elemental analysis calcd (%) for $C_{16}H_{12}ClN_3$: C 68.21, H 4.29, N 14.91; found: C 67.96, H 4.03, N 14.42.

Mp: 205 208 °C

IR (neat) ν: 3255, 1553, 1446, 1170, 1133 cm^{-1}.

^{1}H NMR (250 MHz, MeOD) δ 9.33 (s, 1H), 8.79 – 8.75 (m, 1H), 8.31 (s, 1H), 8.11 (d, *J* = 7.7 Hz, 1H), 8.01 (d, *J* = 8.4 Hz, 1H), 7.83 – 7.77 (m, 1H), 7.72 – 7.67 (m, 1H), 7.53 – 7.49 (m, 1H), 7.29 – 7.26 (m, 2H) ppm.

^{13}C NMR (63 MHz, DMSO) δ 151.2, 144.8, 142.1, 139.5, 137.5, 130.5, 129.6, 128.9, 128.7, 128.2, 125.8, 123.1, 122.7, 121.3, 113.1, 112.5 ppm.

2-(1*H*-Pyrrol-2-yl)quinoxalin-1-ium chloride (57):

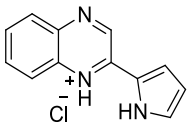

Prepared from 2-chloroquinaxoline (83 mg, 0.5 mmol) and indole (60 mg, 0.05 mmol) in dichloromethane; reaction time: 1 h; precipitate formation to give the product as a yellow solid in 97% yield.

Elemental analysis calcd (%) for: $C_{12}H_{10}ClN_3$: C 62.21, H 4.35, N 18.14; found: C 62.45, H 4.52, N 18.34.

Mp: 149 152 °C

IR (neat) ν: 3189, 1568, 1430, 1128, 1115, 753, 717 cm^{-1}.

^{1}H NMR (250 MHz, $CDCl_3$) δ 9.80 (br s, 1H), 9.16 (s, 1H), 8.07 – 7.96 (m, 2H), 7.77 – 7.63 (m, 2H), 7.10 – 7.06 (m, 2H), 6.44 – 6.425 (m, 1H) ppm.

^{13}C NMR (63 MHz, $CDCl_3$) δ 145.4, 143.1, 142.4, 141.2, 130.7, 129.9, 129.6, 128.8, 128.6, 122.7, 111.5, 110.9 ppm.

9.2.3.5. 4-(Quinoxalin-2-yloxy)-2*H*-chromen-2-one (58):

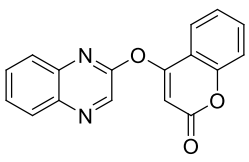

Prepared from 2-chloroquinaxoline (83 mg, 0.5 mmol) and 4-hydroxycumarine (82 mg, 0.05 mmol); purification by chromatography to obtain the product as a yellow solid in 62% yield.

Elemental analysis calcd (%) for $C_{17}H_{10}N_2O_3$: C 70.34, H 3.47, N 9.65; found: C, 70.11, H 3.22, N 9.45.

Mp: 124 127 °C

IR (neat) ν: 2923, 1724, 1384, 1301, 1216, 1178, 762 cm^{-1}.

^{1}H NMR (250 MHz, $CDCl_3$) δ 8.89 (s, 1H), 8.23 – 8.19 (m, 1H), 8.01 – 7.98 (m, 2H), 7.89 – 7.79 (m, 2H), 7.70 – 7.65 (m, 1H), 7.48 – 7.37 (m, 2H), 6.72 (s, 1H) ppm.

^{13}C NMR (63 MHz, $CDCl_3$) δ 162.5, 161.6, 154.4, 154.1, 141.2, 139.9, 139.2, 133.4,

131.9, 129.9, 129.7, 128.6, 124.8, 123.5, 117.5, 115.9, 100.8 ppm.

9.2.3.6. (*Z*)-Ethyl 2-(3-chloroquinoxalin-2-yl)-3-(methylamino)but-2-enoate (59):

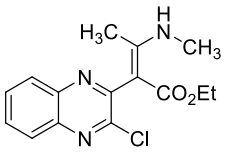

Prepared from 2-chloroquinaxoline (83 mg, 0.5 mmol) and(*Z*)-ethyl 3-(methylamino)but-2-enoate (**35**) (72 mg, 0.05 mmol); purification by chromatography to obtain the product as a yellow solid in 47% yield.

Elemental analysis calcd (%) for $C_{15}H_{16}ClN_3O_2$: C 58.92, H 5.27, N 13.74; found: C 59.31, H 5.74, N 13.72.

Mp: 114 117 °C

IR (neat) ν: 3384, 2920, 1693, 1431, 1209, 1105, 760 cm^{-1}.

^{1}H NMR (250 MHz, $CDCl_3$) δ 8.38 – 8.34 (m, 1H), 8.14 – 8.10 (m, 1H), 7.74 – 7.70 (m, 2H), 4.55 (q, *J* = 7.1 Hz, 2H), 3.96 (s, 3H), 3.00 (s, 3H), 1.53 (t, *J* = 7.1 Hz, 3H) ppm.

^{13}C NMR (63 MHz, $CDCl_3$) δ 164.6, 156.9, 142.1, 142.0, 141.1, 139.1, 130.3, 128.4, 128.4, 127.5, 102.9, 60.8, 28.6, 15.0, 13.7 ppm.

9.2.3.5. C-N coupling reaction of 4,7-dichloroquinoline

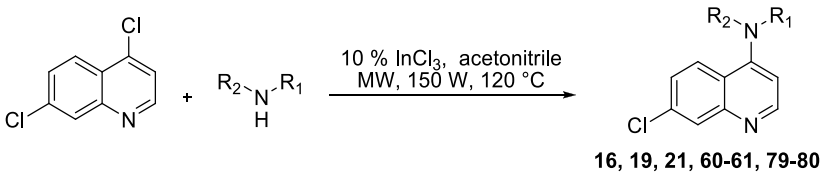

16, 19, 21, 60-61, 79-80

Cmpd.	R_1	R_2
16	C_6H_5-CH_2-	H
19		
16		
60	C_6H_5	H
61	*n*-But	H
79	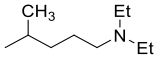	H
80	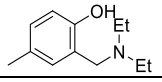	H

Data for compounds **16**, **19** and **21** have been provided above (section 9.2.1.3). By using this method in the presence of $InCl_3$, these compounds have been obtained in 88%, 97%, 85% yield, respectively.

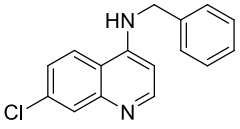

16 (0.5 h, 88%)

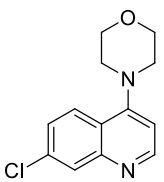

19 (0.5 h, 97%)

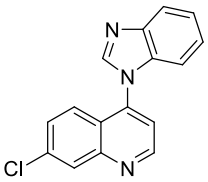

21 (2 h, 85%)

7-Chloro-4-(phenylamino)quinolinium chloride (60):

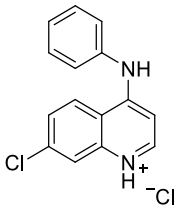

Prepared from 4,7-dichloroquinoline (100 mg, 0.5 mmol) and aniline (47 mg, 0.5 mmol); reaction time: 30 min; precipitate formation to give the product as a yellow solid in 92% yield.

Elemental analysis calcd (%) for $C_{15}H_{12}N_2$: C 61.87, H 4.15, N 9.62; found: C 61.17, H 4.14, N 9.57.

Mp: 240 243 °C

IR (neat) ν: 3416, 2922, 2644, 1611, 1540, 1454, 1365, 1212, 1093, 898, 743 cm^{-1}.

^{1}H NMR (250 MHz, DMSO) δ 11.32 (br s, 1H), 8.96 (d, *J* = 9.1 Hz, 1H), 8.52 (d, *J* = 7.0 Hz, 1H), 8.22 (d, *J* = 2.1 Hz, 1H), 7.87 (dd, *J* = 9.1, 2.1 Hz, 1H), 7.63 – 7.41 (m, 5H), 6.78 (d, *J* = 7.0 Hz, 1H) ppm.

^{13}C NMR (63 MHz, DMSO) δ 155.3, 143.7, 139.5, 138.7, 137.3, 130.3 (2C), 128.0, 127.7, 126.6, 125.8 (2C), 119.5, 116.3, 100.6 ppm.

***N*-Butylquinolin-4-amine (61):**

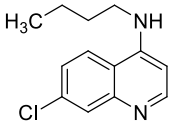

Prepared from 4,7-dichloroquinoline (100 mg, 0.5 mmol) and *n*-butylamine (37 mg, 0.5 mmol); reaction time: 30 min; precipitate formation to give the product as a pale yellow solid in 92% yield.

Elemental analysis calcd (%) for $C_{13}H_{15}N_2$: C 66.52, H 6.44, N 11.93; found: C 66.21, H 6.13, N 11.64.

Mp: 127 130 °C

IR (neat) ν: 3266, 2958, 2932, 2872, 1612, 1581, 1542, 1454, 1367, 1222, 1142, 899, 806 cm^{-1}.

^{1}H NMR (250 MHz, $CDCl_3$) δ 8.28 (d, *J* = 5.9 Hz, 1H), 8.07 (d, *J* = 9.0 Hz, 1H), 7.83 (d, *J* = 2.1 Hz, 1H), 7.21 (dd, *J* = 9.0, 2.1 Hz, 1H), 6.82 (brs, 1H), 6.30 (d, *J* = 6.0 Hz,

1H), 3.29– 3.28 (m2H), 1.73 – 1.61 (m, 2H), 1.45 – 1.28 (m, 2H), 0.88 (t, *J* = 7.3 Hz, 3H).ppm.

^{13}C NMR (63 MHz, $CDCl_3$) δ 152.2, 148.9, 146.1, 136.6, 126.1, 125.8, 123.5, 117.1, 98.8, 43.5, 31.0, 20.7, 14.2 ppm.

Chloroquine (79):

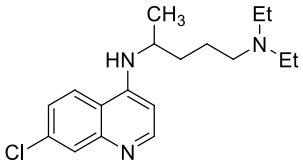

Prepared from 4,7-dichloroquinoline (100 mg, 0.5 mmol) and 2-amino-5-diethylaminopentane (79 mg, 0.5 mmol); reaction time: 1 h; purification by chromatography to obtain the product as a pale yellow solid in 73% yield.

Elemental analysis calcd (%) for $C_{18}H_{26}ClN_3$: C 67.59, H 8.19, N 13.14; found: C 67.24, H 8.01, N 13.10.

Mp: 89 92 °C

IR (neat) ν: 3230, 2917, 2848, 1571, 1450, 1077, 800 cm^{-1}.

^{1}H NMR (250 MHz, MeOD) δ 8.36 (d, *J* = 5.7 Hz, 1H), 8.22 (d, *J* = 9.1 Hz, 1H), 7.79 (d, *J* = 2.1 Hz, 1H), 7.43 (dd, *J* = 9.0, 2.2 Hz, 1H), 6.60 (d, *J* = 6.1 Hz, 1H), 3.91 – 3.84 (m, 1H), 2.71 – 2.60 (m, 6H), 1.73 – 1.66 (m, 4H), 1.36 (d, *J* = 6.4 Hz, 3H), 1.08 (t, *J* = 7.2 Hz, 6H) ppm.

^{13}C NMR (63 MHz, MeOD) δ 152.8, 152.6, 150.2, 136.8, 127.9, 126.3, 124.9, 119.2, 100.3, 53.8, 48.2, 35.3, 31.2, 24.1, 20.8, 11.2 ppm.

Amodiaquine hydrochloride (80):

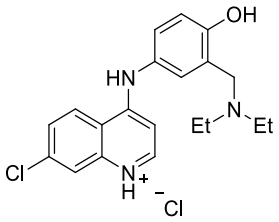

Prepared from 4,7-dichloroquinoline (100 mg, 0.5 mmol) and 4-amino-alpha-diethylamino-*o*-cresol (97 mg, 0.5

mmol); reaction time: 2 h; precipitate formation to give the product as a yellow solid in 71% yield.

Elemental analysis calcd (%) for $C_{20}H_{23}Cl_2N_3O$: C 61.23, H 5.91, N 10.71; found: C 61.31, H 6.11, N 10.89.

Mp: 207 210 °C

IR (neat) ν: 1565, 1535, 1255, 869, 847, 815 cm^{-1}.

^{1}H NMR (250 MHz, MeOD) δ 8.58 (d, *J* = 9.0 Hz, 1H), 8.41 (dd, *J* = 6.9, 1.0 Hz, 1H), 7.97 (s, 1H), 7.79 (dd, *J* = 9.1, 1.9 Hz, 1H), 7.56 (d, *J* = 1.5 Hz, 1H), 7.46 (dd, *J* = 8.7, 1.6 Hz, 1H), 7.15 (dd, *J* = 8.7, 0.8 Hz, 1H), 6.84 (dd, *J* = 6.9, 1.0 Hz, 1H), 4.41 (s, 2H), 3.37 – 3.25 (m, 4H), 1.42 (t, *J* = 7.2 Hz, 6H) ppm.

^{13}C NMR (63 MHz, MeOD) δ 158.1, 157.4, 145.6, 142.1, 141.3, 131.6, 130.8, 130.6, 129.3, 126.6, 121.7, 119.8, 118.4, 117.8, 102.1, 52.8, 49.2 (2C), 9.6 (2C) ppm.

9.2.3.6. C-N coupling reaction of 6,9-dichloro-2-methoxyacridine

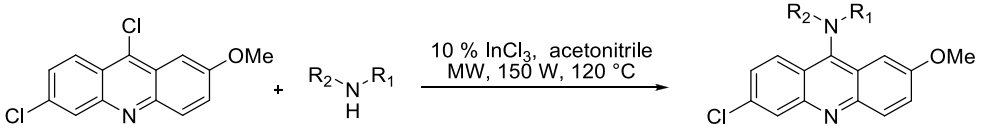

5-7, 9, 11, 81

Cmpd.	R_1	R_2	Reaction time, h	Yield, %.
5	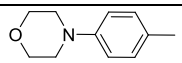	H	1	88
6	*n*-Hex	H	0.5	98
7	C_6H_5-CH_2	H	1	100
9			0.5	100
11			1	100
81	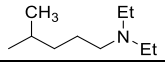	H	2	75

Data of compound **5-7**, **9** and **11** have been provided above (section 9.2.1.1).

Quinacrine (81):

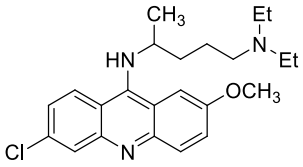

Prepared from 6,9-dichloro-2-methoxyacridine (140 mg, 1 mmol) and 2-amino-5-diethylaminopentane (79 mg, 0.5 mmol); purification by chromatography to obtain the product as a yellow solid.

Elemental analysis calcd (%) for $C_{23}H_{30}ClN_3O$: C 69.07, H 7.56, N 10.51; found: C 69.34, H 7.21, N 10.38.

Mp: 247 250 °C

IR (neat) ν: 3260, 2921, 1628, 1558, 1462, 1434, 1226, 1067, 1028 cm^{-1}.

^{1}H NMR (250 MHz, $CDCl_3$) δ 8.12 (d, *J* = 2.1 Hz, 1H), 8.04 (d, *J* = 9.4 Hz, 2H), 7.46 (dd, *J* = 9.4, 2.7 Hz, 1H), 7.37 (dd, *J* = 9.3, 2.1 Hz, 1H), 7.26 (d, *J* = 2.6 Hz, 1H), 4.49 (br d, *J* = 10.7 Hz, 1H), 4.11 – 4.00 (m, 1H), 4.01 (s, 3H), 2.55 – 2.40 (m, 6H), 1.74 – 1.62 (m, 4H), 1.30 (d, *J* = 6.4 Hz, 3H), 1.00 (t, *J* = 7.2 Hz, 6H) ppm.

^{13}C NMR (63 MHz, $CDCl_3$) δ 156.6, 149.7, 148.6, 147.4, 135.2, 132.0, 128.8, 125.4, 125.1, 124.3, 119.8, 117.8, 99.7, 56.4, 56.0, 53.1, 47.2 (2C), 37.3, 24.3, 22.7, 11.8 (2C) ppm.

9.2.3.7. C-N coupling reaction of 4-chloro-2-phenylquinazoline

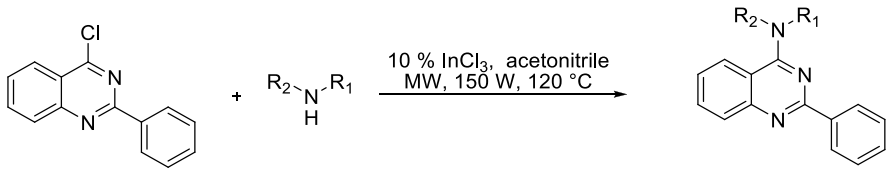

23, 25, 62, 63

Cmpd.	R_1	R_2
23	C_6H_5-CH_2	H
25	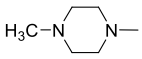	
62	C_6H_5	H
63	*n*-But	H

Data of compound **23** and **25** have been provided above (section 9.2.1.4).

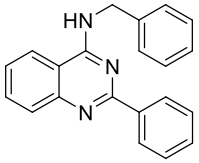

23 (1 h, 100%)

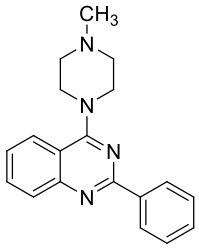

25 (0.5 h, 100%)

2-Phenyl-4-(phenylamino)quinazolin-1-ium chloride (62):

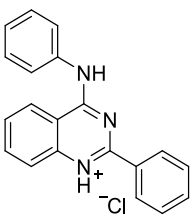

Prepared from 4-dichloro-2-phenylquinazoline (120 mg, 0.5 mmol) and aniline (47 mg, 0.5 mmol); reaction time: 30 min; precipitate formation to give the product as a yellow solid in 98% yield.

Elemental analysis calcd (%) for $C_{20}H_{16}N_3$: C 71.96, H 4.83, N 12.59; found: C 71.25, H 4.78, N 12.66.

Mp: 162 165 °C

IR (neat) ν: 3211, 1628, 1608, 1549, 1457, 1421, 754, 698 cm^{-1}.

^{1}H NMR (250 MHz, MeOD) δ 8.67 (d, *J* = 8.3 Hz, 1H), 8.30 – 8.26 (m, 2H), 8.19 – 8.07 (m, 2H), 7.93 – 7.73 (m, 4H), 7.70 – 7.55 (m, 4H), 7.47 – 7.40 (m, 1H) ppm.

^{13}C NMR (63 MHz, MeOD) δ 161.7, 159.9, 141.4, 138.3, 138.1, 135.4, 132.8, 130.8 (2C), 130.6 (2C), 130.5 (2C), 130.5, 128.8, 126.4 (2C), 125.6, 121.1, 114.4 ppm.

***N*-Butyl-2-phenylquinazolin-4-amine (63):**

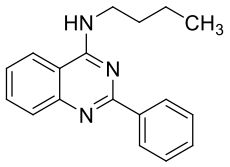

Prepared from 4-dichloro-2-phenylquinazoline (120 mg, 0.5 mmol) and *n*-butylamine (37 mg, 0.5 mmol); reaction time: 30 min; precipitate formation to give the product as a white solid in 100% yield.

Elemental analysis calcd (%) for $C_{18}H_{19}N_3$: C 77.95, H 6.90, N 15.15; found: C 77.52, H 6.47, N 14.79.

Mp: 103 106 °C

IR (neat) ν: 3237, 3138, 2953, 2956, 1631, 1563, 1458, 1375, 716 cm^{-1}.

^{1}H NMR (250 MHz, MeOD) δ 8.41 – 8.35 (m, 3H), 8.10 – 7.98 (m, 2H), 7.82 – 7.67 (m, 4H), 3.97 (t, *J* = 7.2 Hz, 2H), 1.93 – 1.81 (m, 2H), 1.63 – 1.47 (m, 2H), 1.06 (t, *J* = 7.3 Hz, 3H) ppm.

^{13}C NMR (63 MHz, MeOD) δ 162.5, 159.9, 140.9, 137.5, 135.2, 133.3, 130.8 (2C), 130.4 (2C), 130.0, 125.2, 121.2, 114.0, 43.7, 32.4, 21.7, 14.6 ppm.

9.2.3.8. C-N coupling reaction of 2-chloroquinaxoline

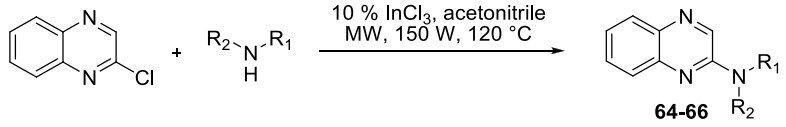

Cmpd.	R_1	R_2
64	C_6H_5	H
65	*n*-But	H
66	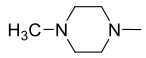	

2-(phenylamino)quinoxalin-1-ium chloride (64):

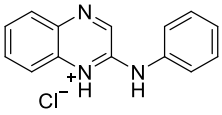

Prepared from 2-chloroquinaxoline (83 mg, 0.5 mmol) and aniline (47 mg, 0.5 mmol); reaction time: 1 h; precipitate formation to give the product as an orange solid in 95% yield.

Elemental analysis calcd (%) for $C_{14}H_{12}N_3$: C 65.25, H 4.69, N 16.30; found: C 65.41, H 4.57, N 16.27.

Mp: 211 214°C

IR (neat) ν: 3278, 3189, 1644, 1553, 1501, 760 cm^{-1}.

^{1}H NMR (250 MHz, MeOD) δ 8.75 (s, 1H), 8.06 (d, *J* = 8.1 Hz, 1H), 7.80 – 7.79 (m, 2H), 7.69 – 7.59 (m, 5H), 7.52 – 7.46 (m, 1H) ppm.

^{13}C NMR (63 MHz, MeOD) δ 148.0, 145.1, 143.8, 137.5, 136.6, 134.1, 131.9 (2C), 130.9, 129.7, 128.7, 125.4 (2C), 121.1 ppm.

_N_-butylquinoxalin-2-amine (65):

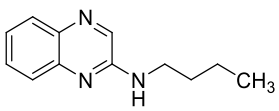

Prepared from 2-chloroquinaxoline (83 mg, 0.5 mmol) and *n*-butylamine (37 mg, 0.5 mmol); reaction time: 1 h; precipitate formation to give the product as a yellow solid in 98% yield.

Elemental analysis calcd (%) for $C_{12}H_{15}N_3$: C 71.61, H 7.51, N 20.88; found: C 71.14, H 7.45, N 20.75.

Mp: 59 62 °C

IR (neat) ν: 3421, 3278, 2958, 2930, 2801, 1588, 1547, 759 cm^{-1}.

^{1}H NMR (250 MHz, $CDCl_3$) δ 8.21 (s, 1H), 7.88 (dd, *J* = 8.1, 1.2 Hz, 1H), 7.71 (dd, *J* = 8.3, 1.4 Hz, 1H), 7.62 – 7.55 (m, 1H), 7.42 – 7.35 (m, 1H), 4.92 (brs, 1H), 3.61 – 3.53 (m, 2H),1.77 – 1.65 (m, 2H), 7.57 – 7.42 (m, 2H), 1.01 (t, *J* = 7.2 Hz, 3H) ppm.

^{13}C NMR (63 MHz, $CDCl_3$) δ 152.4, 142.3, 138.8, 137.5, 130.4, 129.2, 126.6, 124.6, 41.4, 32.0, 20.6, 14.3 ppm.

2-(4-methylpiperazin-1-yl)quinoxaline (66):

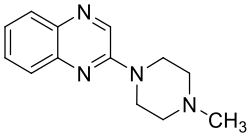

Prepared from 2-chloroquinaxoline (83 mg, 0.5 mmol) and 1-methylpiperazine (50 mg, 0.5 mmol); reaction time: 1 h; precipitate formation to give the product as a yellow solid in 75% yield.

Elemental analysis calcd (%) for $C_{13}H_{16}N_4$: C 68.39, H 7.06, N 24.54; found: C 68.11, H 6.83, N 24.17.

Mp: 108 112 °C

IR (neat) ν: 2942, 2844, 2803, 1553, 1439, 1298, 1268, 760 cm^{-1}.

^{1}H NMR (250 MHz, $CDCl_3$) δ 8.62 (s, 1H), 7.95 – 7.91 (m, 1H), 7.73 (dd, *J* = 8.3, 1.0 Hz, 1H), 7.66 – 7.60 (m, 1H), 7.50 – 7.43 (m, 1H), 4.04– 4.03 (m, 4H), 2.86 (s, 4H), 2.57 (s, 3H) ppm.

^{13}C NMR (63 MHz, $CDCl_3$) δ 152.4, 141.7, 137.0, 135.8, 130.3, 128.8, 126.6, 125.0, 54.8 (2C), 46.2, 44.7 (2C) ppm.

9.2.3.9. C-N coupling reaction of 6-chloropurine

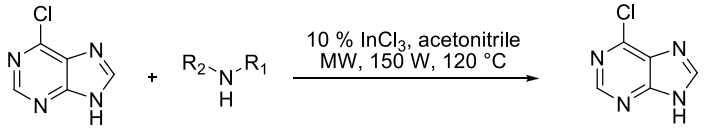

67-72

Cmpd.	R_1	R_2
67	C_6H_5	H
68	4-MeO-C_6H_4	H
69	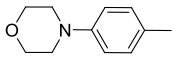	H
70	*n*-Hex	H
71	C_6H_5-CH_2	H
72		

6-(Phenylamino)-9*H*-purin-3-ium chloride (67):

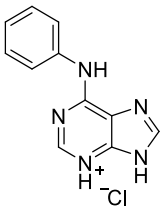

Prepared from 6-chloropurine (77 mg, 0.5 mmol) and aniline (47 mg, 0.5 mmol); reaction time: 30 min; precipitate formation to give the product as a pale yellow solid in 97% yield.

Elemental analysis calcd (%) for $C_{11}H_{10}N_5$: C 53.34, H 4.07, N 28.28; found: C 53.79, H 3.89, N 28.23.

Mp: 281 284 °C

IR (neat) ν: 3321, 3100, 1655, 1595, 1501, 1449, 1388, 754 cm^{-1}.

^{1}H NMR (250 MHz, MeOD) δ 8.55 (s, 1H), 8.49 (s, 1H), 7.75 (d, *J* = 7.8 Hz, 2H), 7.56 – 7.49 (m, 2H), 7.36 (t, *J* = 7.4 Hz, 1H) ppm.

^{13}C NMR (63 MHz, MeOD) δ 151.7, 150.7, 148.3, 145.2, 138.1, 131.2, 131.1 (2C), 128.2, 124.7 (2C) ppm.

6-(4-Methoxyphenylamino)-9*H*-purin-3-ium chloride (68):

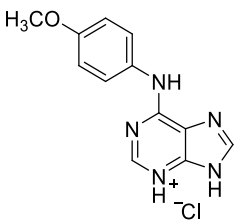

Prepared from 6-chloropurine (77 mg, 0.5 mmol) and *p*-anisidine (62 mg, 0.5 mmol); reaction time: 30 min; precipitate formation to give the product as a yellow solid in 85% yield.

Elemental analysis calcd (%) for $C_{12}H_{12}N_5$: C 51.90, H 4.36, N 25.22; found: C 51.63, H 4.12, N 24.81.

Mp: 279 282 °C

IR (neat) ν: 3321, 1652, 1617, 1512, 1444, 1205, 1026, 835 cm^{-1}.

^{1}H NMR (250 MHz, DMSO) δ 11.51 (br s, 1H), 8.72 (s, 1H), 8.68 (s, 1H), 7.76 (d, *J* = 8.9 Hz, 2H), 7.03 (d, *J* = 8.9 Hz, 2H), 3.79 (s, 3H) ppm.

^{13}C NMR (63 MHz, DMSO) δ 157.1, 149.9, 148.5, 148.3, 143.6, 130.6, 123.8 (2C), 123.7, 114.6 (2C), 55.7 ppm.

6-(4-Morpholinophenylamino)-9*H*-purin-3-ium chloride (69):

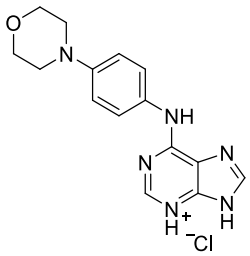

Prepared from 6-chloropurine (77 mg, 0.5 mmol) and 4-morpholinoaniline (90 mg, 0.5 mmol); reaction time: 1 h; precipitate formation to give the product as a pale brown solid in 100% yield.

Elemental analysis calcd (%) for $C_{15}H_{17}N_6$: C 54.14, H 5.15, N 25.25; found: C 54.60, H 5.27, N 25.72.

Mp: 238 241 °C

IR (neat) ν: 3315, 3237, 1656, 1585, 1512, 1238, 1120, 636 cm^{-1}.

^{1}H NMR (250 MHz, DMSO) δ 11.27 (br s, 1H), 8.65 (s, 1H), 8.63 (s, 1H), 7.73 (d, *J* = 8.5 Hz, 2H), 7.12 (d, *J* = 8.7 Hz, 2H), 3.80 (br s, 4H), 3.18 (br s, 4H) ppm.

^{13}C NMR (63 MHz, DMSO) δ 153.3, 149.9, 148.8, 148.5, 143.4, 130.6, 123.1 (2C), 116.4 (2C), 114.0, 66.2 (2C), 49.5 (2C) ppm.

***N*-hexyl-9*H*-purin-6-amine (70):**

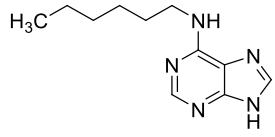

Prepared from 6-chloropurine (77 mg, 0.5 mmol) and hexylamine (51 mg, 0.5 mmol); reaction time: 1.5 h; precipitate formation to give the product as a white solid in 99% yield.

Elemental analysis calcd (%) for $C_{11}H_{17}N_5$: C 60.25, H 7.81, N 31.94; found: C, 60.49, H 7.87, N 31.60.

Mp: 158 161 °C

IR (neat) ν: 3474, 3025, 2930, 1633, 1565, 1330, 1142, 928 cm^{-1}.

^{1}H NMR (250 MHz, MeOD) δ 8.24 (s, 1H), 8.09 (s, 1H), 3.61 (t, *J* = 6.1 Hz, 2H), 1.78 – 1.67 (m, 2H), 1.47 – 1.38 (m, 6H), 0.94 (t, *J* = 6.7 Hz, 3H) ppm.

^{13}C NMR (63 MHz, MeOD) δ 156.1, 156.1, 154.2, 141.0, 119.4, 42.2, 33.2, 31.0, 28.1, 24.1, 14.8 ppm.

_N_-benzyl-9_H_-purin-6-amine (71):

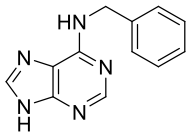

Prepared from 6-chloropurine (77 mg, 0.5 mmol) and benzylamine (54 mg, 0.5 mmol); reaction time: 1 h; precipitate formation to give the product as a white solid in 93% yield.

Elemental analysis calcd (%) $C_{12}H_{11}N_5$: C 63.99, H 4.92, N 31.09; found: C 63.70, H 4.81, N 31.12.

Mp: 235 238 °C

IR (neat) ν: 3474, 3281, 1652, 1453, 1120, 891, 698 cm^{-1}.

^{1}H NMR (250 MHz, MeOD) δ 8.37 (s, 1H), 8.22 (s, 1H), 7.42 – 7.30 (m, 5H), 4.89 (s, 2H) ppm.

^{13}C NMR (63 MHz, MeOD) δ 154.8, 152.0, 150.8, 142.9, 139.7, 130.1 (2C), 129.3, 129.2 (2C), 129.0, 46.2 ppm.

4-(9_H_-purin-6-yl)morpholine (72):

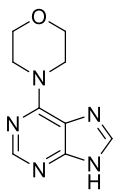

Prepared from 6-chloropurine (77 mg, 0.5 mmol) and morpholine (44 mg, 0.5 mmol); reaction time: 30 min; precipitate formation to give the product as a pale yellow solid in 100% yield.

Elemental analysis calcd (%) for: $C_9H_{11}N_5$: C 52.67, H 5.40, N 34.13; found: C 53.00, H 5.31, N 34.01.

Mp: 299 302 °C

IR (neat) ν: 3423, 3091, 2965, 2932, 2857, 1600, 1299, 1258, 1114, 647 cm^{-1}.

^{1}H NMR (250 MHz, MeOD) δ 8.06 (s, 1H), 7.82 (s, 1H), 4.09 (t, *J* = 4.7 Hz, 4H), 3.71 (t, *J* = 5.0 Hz, 4H) ppm.

^{13}C NMR (63 MHz, MeOD) δ 160.1, 155.5, 154.5, 151.7, 119.6, 68.5 (2C), 47.6 (2C) ppm.

9.2.3.10. C-N coupling reaction of 2-chlorobenzimidazole

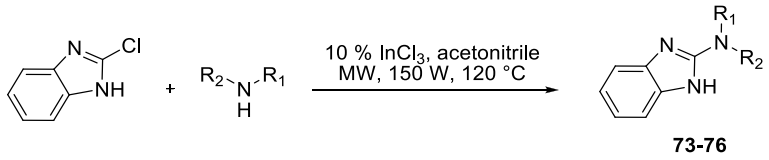

73-76

Cmpd.	R_1	R_2
73	3-Cl-C_6H_4	H
74	C_6H_5-CH_2	H
75	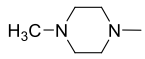	
76	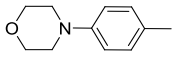	H

2-(3-chlorophenylamino)-1*H*-benzo[*d*]imidazol-3-ium chloride (73):

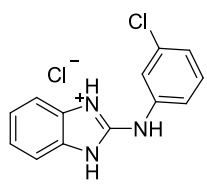

Prepared from 2-chlorobenzimidazole (76 mg, 0.5 mmol) and 3-chloroaniline (64 mg, 0.5 mmol); reaction time: 2 h; precipitate formation to give the product as a white solid in 97% yield.

Elemental analysis calcd (%) for $C_{13}H_{11}N_3$: C 55.73, H 3.96, N 15.00; found: C 55.85, H 3.83, N 14.67.

Mp: 182 185 °C

IR (neat) ν: 3396, 3054, 2922, 1591, 1557, 1462, 1350, 1264, 1242, 1053, 922, 747 cm^{-1}.

^{1}H NMR (250 MHz, MeOD) δ 7.60 – 7.53 (m, 2H), 7.50 – 7.41 (m, 4H), 7.40 – 7.36 (m, 2H) ppm.

^{13}C NMR (63 MHz, MeOD) δ 150.0, 139.0, 137.1, 133.1, 131.4 (2C), 128.7, 125.9 (2C), 125.0, 123.3, 113.3 (2C) ppm.

***N*-benzyl-1*H*-benzo[*d*]imidazol-2-amine (74):**

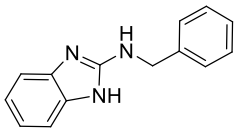

Prepared from 2-chlorobenzimidazole (76 mg, 0.5 mmol) and benzylamine (54 mg, 0.5 mmol); reaction time: 2 h; precipitate formation to give the product as a white solid in 90% yield.

Elemental analysis calcd (%) for $C_{14}H_{13}N_3$: C 75.31, H 5.87, N 18.82; found: C 75.04, H 5.93, N 18.76.

Mp: 164 167 °C

IR (neat) ν: 3395, 1632, 1580, 1464, 1268, 738 cm^{-1}.

^{1}H NMR (250 MHz, MeOD) δ 7.43 – 7.26 (m, 5H), 7.23 – 7.19 (m, 2H), 7.00 – 6.97 (m, 2H), 4.60 (s, 2H) ppm.

^{13}C NMR (63 MHz, MeOD) δ 157.3, 141.1 (2C), 139.6, 129.9 (2C), 128.7 (2C), 128.6, 121.7 (2C), 113.2 (2C), 47.8 ppm.

2-(4-methylpiperazin-1-yl)-1*H*-benzo[*d*]imidazole (75):

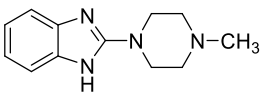

Prepared from 2-chlorobenzimidazole (76 mg, 0.5 mmol) and 1-methylpiperazine (50 mg, 0.5 mmol); reaction time: 2 h; precipitate formation to give the product as a white solid in 86% yield.

Elemental analysis calcd (%) for $C_{12}H_{16}N_4$: C 66.64, H 7.46, N 25.90; found: C 66.68, H 7.38, N 25.68.

Mp: 91 93 °C

IR (neat) ν: 3395, 2936, 2844, 2797, 1626, 1558, 1463, 1000 cm^{-1}.

^{1}H NMR (250 MHz, MeOD) δ7.34 – 7.29 (m, 2H), 7.14 – 7.09 (m, 2H),3.67 – 3.65 (m, 4H), 2.82 – 2.80 (m, 4H), 2.52 (s, 3H) ppm.

^{13}C NMR (63 MHz, MeOD) δ 156.1, 137.5 (2C), 123.2 (2C), 113.6 (2C), 55.0 (2C), 47.0 (2C), 45.9 ppm.

2-(4-Morpholinophenylamino)-1*H*-benzo[*d*]imidazol-3-ium chloride (76):

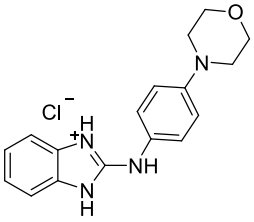

Prepared from 2-chlorobenzimidazole (76 mg, 0.5 mmol) and 4-morpholinoaniline (90 mg, 0.5 mmol); reaction time: 2 h; precipitate formation to give the product as a grey solid in 74% yield.

Elemental analysis calcd (%) for $C_{17}H_{19}N_4$: C 61.72, H 5.79, N 16.94; found: C 61.62, H 5.63, N 16.88.

Mp: 257 260 °C

IR (neat) ν: 3213, 1666, 1515, 1238, 1115, 922, 765 cm^{-1}.

^{1}H NMR (250 MHz, MeOD) δ 7.43 – 7.30 (m, 6H), 7.15 (d, *J* = 9.0 Hz, 2H), 3.88 (t, *J* = 4.8 Hz, 4H), 3.23 (t, *J* = 4.9 Hz, 4H) ppm.

^{13}C NMR (63 MHz, MeOD) δ 152.9, 151.4, 131.6 (2C), 128.7, 127.4 (2C), 125.5 (2C), 118.4 (2C), 113.0 (2C), 68.3 (2C), 50.7 (2C) ppm.

9.2.3.11. C-N coupling reaction of 2-chloropyridine

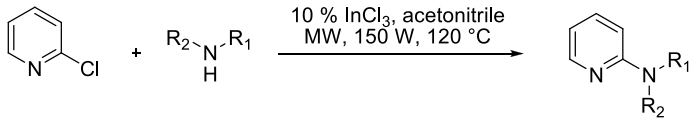

Cmpd.	R_1	R_2
77	C_6H_5	H
78		

***N*-phenylpyridin-2-amine (77):**

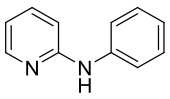

Prepared from 2-chloropyridine (76 mg, 0.5 mmol) and aniline (47 mg, 0.5 mmol); reaction time: 30 min; precipitate formation to give the product as a pale brown solid in 97% yield.

Elemental analysis calcd (%) for $C_{11}H_{10}N_2$: C 77.62, H 5.92, N 16.46; found: C 77.27, H 5.88, N 16.47.

Mp: 106 109 °C

IR (neat) ν: 3225, 3178, 3009, 1592, 1444, 1328, 769 cm^{-1}.

^{1}H NMR (250 MHz, $CDCl_3$) δ 8.24 (dd, *J* = 5.0, 1.0 Hz, 1H), 7.56 – 7.49 (m, 1H), 7.36 (d, *J* = 4.4 Hz, 4H), 7.14 – 7.02 (m, 1H), 6.91 (d, *J* = 8.4 Hz, 1H), 6.79 – 6.74 (m, 1H), 6.64 (br s, 1H) ppm.

^{13}C NMR (63 MHz, $CDCl_3$) δ 156.6, 148.8, 141.0, 138.2, 129.7 (2C), 123.2, 120.8 (2C), 115.4, 108.6 ppm.

4-(pyridin-2-yl)morpholine(78):

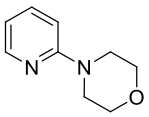

Prepared from 2-chloropyridine (76 mg, 0.5 mmol) and morpholine (44 mg, 0.5 mmol); reaction time: 30 min; purification by chromatography to obtain the product as a yellow oil in 72% yield.

Elemental analysis calcd (%) for $C_9H_{12}N_2$: C 65.83, H 7.37, N 17.06; found: C 65.52, H 7.28, N 16.95.

IR (neat) ν: 2961, 2852, 1591, 1481, 1437 cm^{-1}.

^{1}H NMR (250 MHz, $CDCl_3$) δ 8.25 – 8.22 (m, 1H), 7.56 – 7.49 (m, 1H), 6.71 – 6.65 (m, 2H), 3.85 (t, *J* = 4,7 Hz, 4H), 3.52 (t, *J* = 5,0 Hz, 4H) ppm.

^{13}C NMR (63 MHz, $CDCl_3$) δ 160.0, 148.4, 138.0, 114.3, 107.4, 67.2 (2C), 46.0 (2C) ppm. **9.2.3.13.**

9.2.3.12. Bistacrine (29):

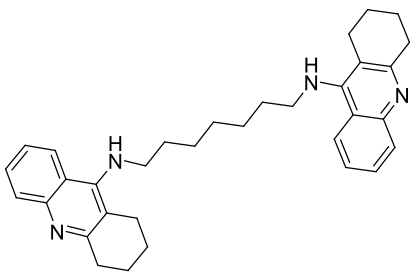

Prepared from compound **28** (220 mg, 1 mmol) and 1,7-heptanediamine (65 mg, 0.5 mmol); reaction time 2 h; purification by chromatography to give the product as a yellow solid in 88% yield.

Data of **29** have been provided above (section 9.1.2.6).

9.3. Synthesis of DKPs

9.3.1. Synthesis of starting materials

9.3.1.1 *N,N*-Diacetylation of 2,5 piperazine dione (82):

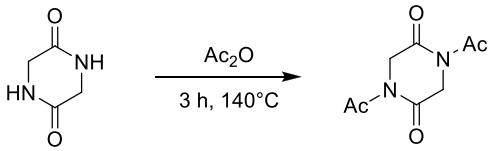

82

4.0 g (35.06 mmol) of 2,5-piperazinedione were placed in a flask with 30 ml of acetic anhydride. The flask was connected to a condenser with a calcium chloride guard tube and heated at 150°C. The solution was stirred for 3 hours at this temperature and then evaporated under vacuum. To the dark residue was added hexane (5 ml), which was evaporated obtaining a pale brown solid. After recrystallization in ethanol, compound 82 was obatained in 97% yield (6.692 g).

IR (KBr disk): 2945.6, 1708.2, 1706.0, 1432.4, 1363.6 cm^{-1}.

^{1}H-NMR (250 MHz, $CDCl_3$) δ 4.60 (s, 4H), 2.58 (s, 6H) ppm.

^{13}C-NMR (63 MHz, DMSO) δ 172.3 (2C), 170.5 (2C), 47.8 (2C), 27.2 (2C) ppm.

9.3.1.2. Preparation of β-carboline-1 and 3-carboxaldehyde

9.3.1.2.1. 1,2,3,4-Tetrahydro-β-carboline-3-carboxylic acid (96):

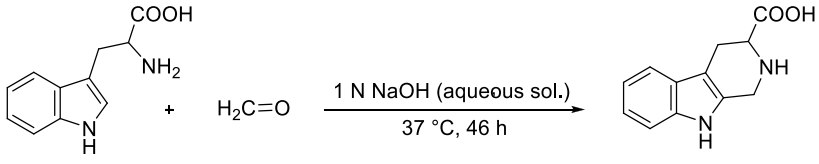

96

Ten grams (0.049 mol) of *dl*-tryptophan was dissolved in 500 ml of 0.1 N sodium hydroxide containing 5,6 ml (0.07 mol) of aqueous formalin (40%). The solution was incubated at 37 °C for 46 hours. It was neutralized with 4 ml of glacial acetic acid, and the resulting precipitate was filtered and washed with water to obtain **96** in 80% yield as yellow powder.

^{1}H-NMR (250 MHz, DMSO) δ 11.02 (br s, 1H), 7.44 (d, *J* = 7.5 Hz, 1H), 7.34 (d, *J* = 7.9 Hz, 1H), 7.11 – 6.97 (m, 2H), 4.30 –4.24 (m, 1H), 3.2 (d, 1H, *J* = 4.5 Hz), 3.13 (d, 1H, *J* = 4.7 Hz), 2.93 –2.77 (m, 2H) ppm.

9.3.1.2.2. 1,2,3,4-Tetrahydro- β -carboline-1-carboxylic acid (97):

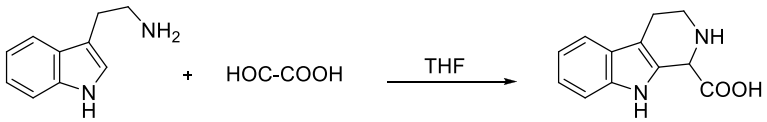

97

9 grams (0.049 mol) of tryptamine were dissolved in 100 ml of THF and 10 ml of 37% HCl aqueous solution were added. The resulting precipitate was filtered to obtain tryptamine hydrochloride. This compound was dissolved in 200 ml of water by stirring and warming on a steam bath to approximately 45 °C. After cooling to r.t., a solution of 4.6 g (0.05 mol) of glyoxylic acid monohydrate in 12 ml of water was added followed by the slow addition (about 3 minutes) of a cooled solution of 2.3 g (0.04 mol) of NaOH in 12 ml of water. Precipitation of tetrahydro-β-carboline-1-carboxylic acid took place during the addition of the potassium hydroxide solution. After stirring at r.t. for 1 hour, the solid was filtered and washed with 20 ml of water to give **97** in 82% yield as grey powder.

^{1}H-NMR (250 MHz, DMSO) δ 10.72 (br s, 1H), 7.47 (d, *J* = 8.3 Hz, 1H), 7.40 (d, *J* = 7.7 Hz, 1H), 7.08 – 6.94 (m, 2H), 4.70 (1H), 3.48 – 3.25 (m, 2H, overlapped with the residual DMSO signal), 2.99 –2.80 (m, 2H) ppm.

9.3.1.2.3. General procedure to convert the acid derivatives to the methy esters

The acid derivatives **96** and **97** (0.028 mol) was dissolved in saturated methanolic HCl solution (150 ml), and the mixture was held at refluxed under argon for 6 h. The solvent was removed under reduced pressure, and a saturated Na_2CO_3 solution was added to the residue. The aqueous alkaline suspension was extracted with $CHCl_3$ (2 x 50 ml) and EtOAc (3 x 50 ml), and the combined extracts were dried (anhydrous Na_2SO_4) and evaporated *in vacuo* to give compounds **98** and **99**.

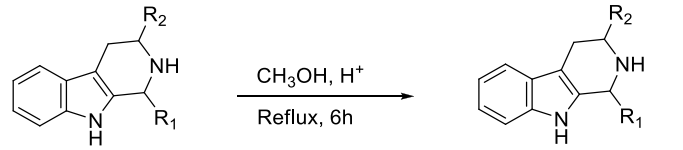

96: R_1=H, R_2=COOH
97: R_1=COOH, R_2=H

98: R_1=H, R_2=COOMe
99: R_1=COOMe, R_2=H

3-Carbomethoxy-1,2,3,4-tetrahydro-β-carboline (98):

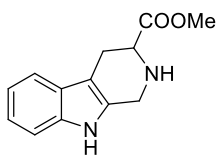

Prepared from compound **96** (6 g, 0.028 mol); yield 60%; yellow-off oil.

^{1}H-RMN (250 MHz, $CDCl_3$) δ 8.10 (br s, 1H), 7.50 (d, *J* = 7.2, 1H), 7.32 (d, *J* = 7.6,1H), 7.21 – 7.10 (m, 2H), 4.19 – 4.08 (m, 2H), 3.85–3.78 (m, 4H), 3.21 – 3.13 (m, 1H), 2.98 – 2.88 (m, 1H), 2.50 (br s, 1H) ppm.

1-Carbomethoxy-1,2,3,4-tetrahydro- β-carboline (99):

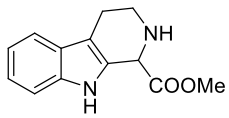

Prepared from compound **97** (6 g, 0.028 mol); yield 55%; red powder.

^{1}H-RMN (250 MHz, DMSO) δ: 10.73 (br s, 1H), 7.42 – 7.34 (m, 2H), 7.10 – 6.94 (m, 2H), 4.74 (s, 1H), 3.73 (s, 3H), 3.18 – 3.01 (m, 2H), 2.64 – 2.60 (m, 2H) ppm.

9.3.1.2.4. 3-Carbomethoxy-β-carboline (100):

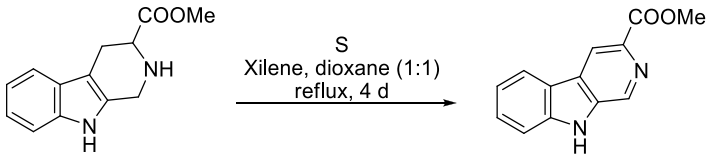

98 **100**

A solution of **98** (2.66 g, 0.012 mol) in dioxane (125 ml) and xilene (125 ml) was treated with sulfur (3,3 g), and the mixture was held at reflux for 4 days. The mixture was then refluxed for an additional 2 days with sulfur (1.4 g) added at the beginning of each day. The solvent was removed under reduced pressure to provide a brown residue. A fine suspension of this residue was made in HCl (1N, 75 ml). The suspension was filtered and the precipitate was washed with H_2O (50 ml). The combined aqueous fractions were extracted with benzene (3 x 13 ml) and then basified with concentrated aqueous solution of NH_3 (40 ml) to yield a thick, cream-colored precipitate, which was filtered and dried for 12 h under vacuum at 40 °C. The crude mixture was purified through silica column chromatography using petroleum ether-ethyl acetate mixture as eluent (7:1) to afford the pure product **100** as a yellow solid in 91%.

^{1}H-RMN (250 MHz, $CDCl_3$) δ 10.00 (br s, 1H), 9.25 (s, 1H), 8.87 (s, 1H), 8.20 (d, *J* =

7.9 Hz, 1H), 7.69 – 7.60 (m, 2H), 7.42 – 7.36 (m, 1H), 3.82 (s, 3H) ppm.

9.3.1.2.5. 1-Carbomethoxy-β-carboline (101):

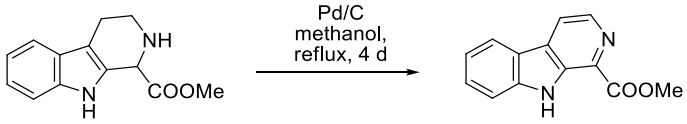

99 **101**

A solution of **99** (3.3 g, 0.014 mol) in methanol (250 ml) was refluxed with 30% Pd/C (1.1 g) for 4 days. After completation of the reaction, as indicated by TLC, the mixture was filtered through celite and the filtrate was evaporated under reduced pressure. The crude mixture was purified through silica column chromatography using petroleum ether/ethyl acetate mixture as eluent (7/1) to afford the pure product **101** as a white solid in 78% yield.

^{1}H-RMN (250 MHz, $CDCl_3$) δ: 9.96 (br s, 1H), 8.61 (d, *J* = 5 Hz, 1H), 8.20 – 8.17 (m, 2H), 7.68 – 7.60 (m, 2H), 7.39 – 7.33 (m, 1H), 4.15 (s, 3H) ppm.

9.3.1.2.6. General procedure for the ester group reduction to aldehyde with DIBALH

To a stirred solution of carbomethoxy-β-carboline (**100-101**) (100 mg, 0.39 mmol) in CH_2Cl_2 (5 ml), was added 2.3 ml of DIBAL solution (1.0 M, in CH_2Cl_2) at -40°C under an argon atmosphere. The mixture was stirred at –40°C for 8 min and then quenched by the sequential addition of MeOH (0.5 ml) and 10 % NaOH (0.5 ml). The mixture was stirred at r.t. for an additional 0.5 h. The reaction mixture was diluted with 10 ml of $CHCl_3$, dried over anhydrous Na_2SO_4, and then evaporated in *vacuo.* The residue was subjected to column chromatography

using petroleum ether-ethyl acetate mixture as eluent (1:1) to give the pure product as crystal.

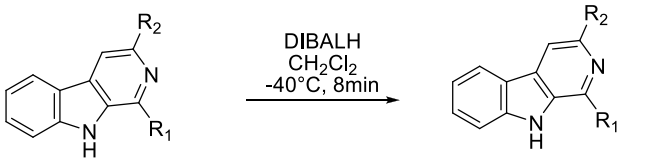

100: R_1=H, R_2=COOMe
101: R_1=COOMe, R_2=H

102: R_1=H, R_2= HCO
103: R_1= HCO, R_2=H

β-Carboline-3-carbaldehyde: (102):

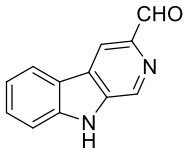

Prepared from compound **100** (100 mg, 0.39 mmol); yield: 77%; white crystal.

^{1}H-RMN (250 MHz, $CDCl_3$) δ 10.23 (s, 1H), 9.89 (br s, 1H), 9.34 (s, 1H), 8.81 (s, 1H), 8.28 (d, *J* = 8.1 Hz, 1H), 7.73 – 7.71 (m, 2H), 7.50 – 7.44 (m, 1H) ppm.

β-Carboline-1-carbaldehyde (103):

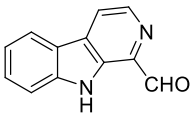

Prepared from compound **101** (100 mg, 0.39 mmol); yield: 85%; white-off crystal.

^{1}H-RMN (250 MHz, $CDCl_3$) δ 10.39 (s, 1H), 10.10 (br s, 1H),8.68 (d, *J* = 5 Hz, 1H), 8.23–8.20(m, 2H), 7.71 –7.62 (m, 2H),7.44 –7.37 (m, 1H) ppm.

9.3.2. General procedure for the double aldol condensation at r.t.

A solution of 1,4-diacetylpiperazine-2,5-dione **82** (1.0 g, 5.05 mmol) , the suitable aromatic aldehyde (10 mmol) and triethylamine (2 ml, 1.45 g, 14.3 mmol) in dimethylformamide (10 ml) was stirred at 25 °C for 14 h, in a system protected

with a $CaCl_2$ tube. The resulting precipitate was filtered, washed with ethyl acetate and then with refluxing ethanol or methanol for 1 h to give compounds **83-86** as powders.

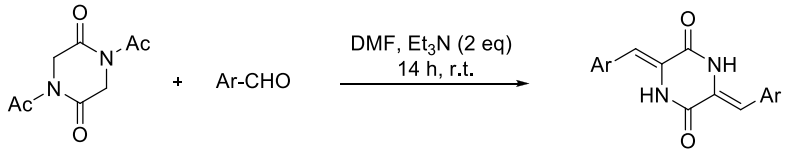

Cmpd.	Ar
83	
84	
85	
86	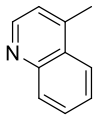

3,6-Bis(2-pyridylmethylidene)piperazine-2,5-dione (83):

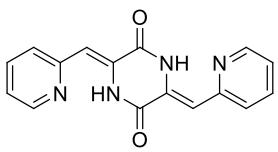

Prepared from **82** (1.0 g, 5.05 mmol) and 2-pyridinecarbaldehyde (1.07 g, 10 mmol); yield: 64%; light yellow solid.

Elemental analysis (%) calcd for $C_{16}H_{12}N_4O_2$: C, 71.40; H, 7.67; N, 13.32; O, 7.61; found: C 64.87, H 4.34, N 18.89.

Mp > 300 °C

IR (KBr disk) ν: 3421.8, 3120.5, 1694.8, 1647.7, 1581.8, 1450.0, 1412.3, 1346.4 cm^{-1}.

^{1}H-NMR (250 MHz, DMSO) δ 12.73 (br s, 2H), 8.77 (dd, *J* = 7.4, 0.9 Hz, 2H), 7.95 (td, *J* = 7.7, 1.7 Hz, 2H), 7.74 (d, *J* = 7.9 Hz, 2H), 7.42 (ddd, *J* = 7.5, 7.4, 0.9 Hz, 2H), 6.81 (s, 2H)ppm.

^{13}C-NMR (63 MHz, CF_3CO_2D) δ 157.9 (2C), 148.3 (2C), 144.9 (2C), 142.7 (2C), 131.7 (2C), 128.7 (2C), 127.0 (2C), 107.9 (2C) ppm.

3,6-Bis(3-pyridylmethylidene)piperazine-2,5-dione (84):

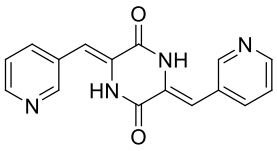

Prepared from **82** (1.0 g, 5.05 mmol) and 3-pyridinecarbaldehyde (1.07 g, 10 mmol); yield: 41%; yellow powder.

Elemental analysis (%) calcd for $C_{16}H_{12}N_4O_2$: C 65.75, H 4.14, N 19.17; found C 64.79; H 4.43; N 18.83.

Mp > 300 °C

IR (KBr disk) ν: 3440, 3194, 3031, 1666, 1639, 1411, 699 cm^{-1}.

^{1}H-NMR (250 MHz, DMSO) δ 10.79 (br s, 2H), 8.72 (s, 2 H), 8.50 (d, *J* = 3.7 Hz, 2H), 7.95 (d, *J* = 8 Hz, 2H), 7.45 (dd, *J* = 7.88, 3.7 Hz, 2H), 6.79 (s, 2H) ppm.

^{13}C-NMR (63 MHz, CF_3CO_2D) δ 158.9 (2C), 146.1 (2C), 141.7(2C), 141.0 (2C), 133.4 (2C), 129.4 (2C), 126.6 (2C), 112.3 (2C) ppm.

3,6-Bis(4-pyridylmethylidene)piperazine-2,5-dione (85):

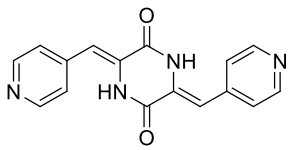

Prepared from **82** (1.0 g, 5.05 mmol) and 4-pyridinecarbaldehyde (1.07 g, 10 mmol); yield: 68%; yellow powder.

Elemental analysis (%) calcd for $C_{16}H_{12}N_4O_2$: C 65.75, H 4.14, N 19.17; found: C 59.75, H 4.19, N 19.19.

Mp > 300 °C

IR (KBr disk) ν: 3428, 3213, 1684, 1632, 1396, 808 cm^{-1}.

^{1}H-NMR (250 MHz, DMSO) δ 10.87 (br s, 2H), 8.64 (d, *J* = 5.9 Hz, 4H), 7.60 (d, *J* = 5.9 Hz, 4H), 6.77 (s, 2H) ppm.

^{13}C-NMR (63 MHz, DMSO) δ 157.9 (2C), 150.1 (4C), 141.0 (2C), 129.7 (2C), 124.0 (4C), 112.5 (2C) ppm.

3,6-Bis(4-quinolylmethylidene)piperazine-2,5-dione (86):

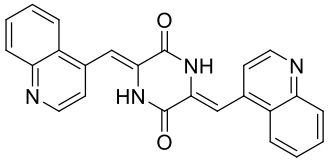

Prepared from **82** (1.0 g, 5.05 mmol) and quinoline-4-carbaldehyde (1.6 g, 10 mmol); yield: 84%; yellow solid.

Elemental analysis (%) calcd for $C_{24}H_{16}N_4O_2$: C 73.46, H 4.11, N 14.28; found: C 71.96, H 4.41, N 13.82.

Mp > 300 °C

IR (KBr disk) ν: 3433, 3046, 1686, 1633, 1506, 756 cm^{-1}.

^{1}H-NMR (250 MHz, DMSO) δ 10.71 (br s, 2H), 8.95 (d, *J* = 4.5 Hz, 2H), 8.10 (d, *J* = 7.5 Hz, 2H), 8.01 (d, *J* = 7.5 Hz, 2H), 7.86 –7.80 (m, 2H), 7.70 – 7.64 (m, 2H), 7.60 (d, *J* = 4.5 Hz, 2H)), 7.18 (s, 2H) ppm.

^{13}C-NMR (63 MHz, CF_3CO_2D) δ 160.8 (2C), 153.7 (2C), 146.0 (2C), 140.4 (2C), 139.3 (2C), 134.4 (2C), 132.9 (2C), 130.6 (2C), 128.3 (2C), 124.5 (2C), 123.5 (2C), 115.7 (2C) ppm.

9.3.2.1. Mono condensation products

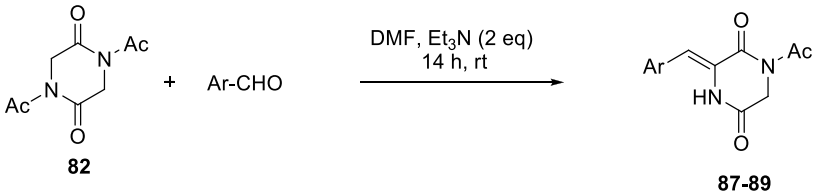

82 **87-89**

Cmpd.	Ar
87	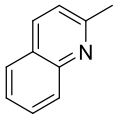
88	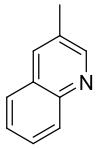
89	

1-Acetyl-3-(2-quinolylmethylidene)piperazine-2,5-dione (87):

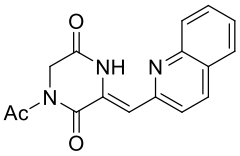

Prepared from **82** (1.0 g, 5.05 mmol) and quinoline-2-carbaldehyde (1.6 g, 10 mmol); yield: 95%; orange solid.

Mp > 300 °C

^{1}H-NMR (250 MHz, DMSO) δ 13.09 (br s, 1H), 8.50 (d, *J* = 8.8 Hz, 1H), 8.06 – 8.01 (m, 2H), 7.97 – 7.96 (m, 1H), 7.90 – 7.83 (m, 1H), 7.71 – 7.65 (m, 1H), 7.05 (s, 1H), 4.42 (s, 2H), 2.57 (s, 3H) ppm.

1-Acetyl-3-(3-quinolylmethylidene)piperazine-2,5-dione (88):

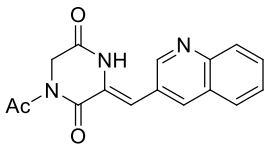

Prepared from **82** (1.0 g, 5.05 mmol) and quinoline-3-carbaldehyde (1.6 g, 10 mmol); yield: 100%; yellow solid.

Mp > 300 °C

^{1}H-NMR (250 MHz, DMSO) δ 10.83 (br s, 1H), 9.04 (d, *J* = 2.1 Hz, 1H), 8.56 (d, *J* = 1.9 Hz, 1H), 8.06 – 8.01 (m, 2H), 7.84 – 7.77 (m, 1H), 7.66 (t, *J* = 7.5 Hz, 1H), 7.14 (s, 1H), 4.42 (s, 2H), 2.55 (s, 3H) ppm.

1-Acetyl-3-benzylidenepiperazine-2,5-dione (89):

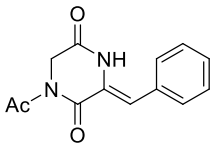

Prepared from **82** (1.0 g, 5.05 mmol) and benzaldehyde (1.02 g, 10.8 mmol); yield: 83%; white solid.

Mp > 300 °C

^{1}H-NMR (250 MHz, DMSO) δ 10.40 (br s, 1H), 7.63 – 7.60 (m, 2H), 7.48 –7.37 (m, 3H), 6.98 (s, 1H), 4.39 (s, 2H), 2.51 (s, 3H overlapped with the residual DMSO signal) ppm.

9.3.3. General procedure for the double aldol condensation at reflux

A solution of 1,4-diacetylpiperazine-2,5-dione **82** (0.5 g, 2.52 mmol), the suitable aromatic aldehyde (5.05 mmol), triethylamine (3 ml, 21.51 mmol) in dimethylformamide (2 ml) was refluxed at 150 °C in a system protected with a $CaCl_2$ tube for 16 h. Partial evaporation of the solvent was compensated by the addition of a 5:1 mixture of triethylamine and dimethylformamide (2 ml). The reaction mixture was cooled and the resulting precipitate was filtered and washed with 5 ml of ethyl acetate and 1 ml of water. The resulting solid was washed with refluxing methanol for 1 hour to complete its purification, leading to compounds **90-95**, **104** and **105**.

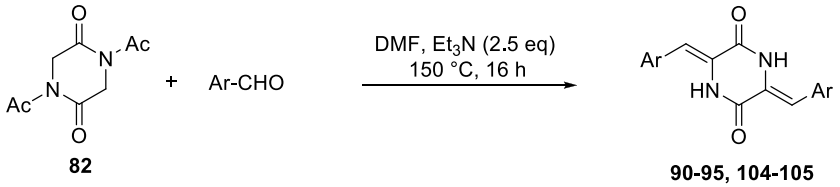

Cmpd.	Ar	Cmpd.	Ar
90	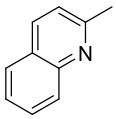	**94**	
91	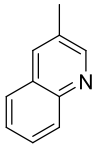	**95**	
92		**104**	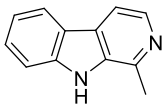
93	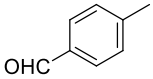	**105**	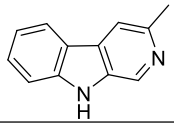

3,6-Bis(2-quinolylmethylidene)piperazine-2,5-dione (90):

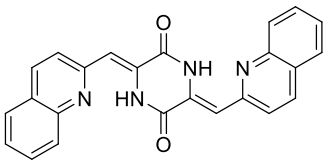

Prepared from **82** (0.5 g, 2.52 mmol) and quinoline-2-carbaldehyde (0.93 g, 5.05 mmol); yield: 80%; green solid.

Elemental analysis (%) calcd for $C_{24}H_{16}N_4O_2$: C 73.46, H 4.11, N 14.28; found: C 72.85, H 4.27, N 14.06.

Mp > 300 °C

IR (KBr disk) ν: 3426, 3134, 1680, 1637, 1418, 835 cm^{-1}.

^{1}H-NMR (250 MHz, CF_3CO_2D) δ 8.94 (d, *J* = 7.2 Hz, 2H), 8.13 – 8.02 (m, 8H), 7.89 – 7.85 (m, 2H), 7.36 (s, 2H) ppm.

^{13}C-NMR (63 MHz, CF_3CO_2D) δ 160.3 (2C), 150.9 (2C), 149.2 (2C), 141.2 (2C), 139.5 (2C), 134.8 (2C), 133.8 (2C), 131.5 (2C), 131.4 (2C), 124.5 (2C), 122.4 (2C), 111.1 (2C) ppm.

3,6-Bis(3-quinolylmethylidene)piperazine-2,5-dione (91):

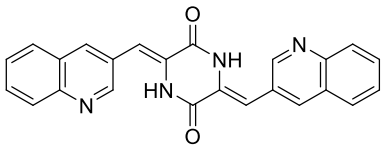

Prepared from **82** (0.5 g, 2.52 mmol) and quinoline-3-carbaldehyde (0.93 g, 5.05 mmol); yield: 65%; yellow solid.

Elemental analysis (%) calcd for $C_{24}H_{16}N_4O_2$: C 73.46, H 4.11, N 14.28; found: C 72.21, H 4.16, N 13.95.

Mp > 300 °C

IR (KBr disk) ν: 3446, 3186, 1680, 1627, 1399, 758 cm^{-1}.

^{1}H-NMR (250 MHz, DMSO) δ 11.00 (br s, 2H), 9.00 (d, *J* = 2.2 Hz, 2H), 8.57 (d, *J* = 1.6 Hz, 2H), 8.04 – 7.94 (m, 4H), 7.78– 7.72 (m, 2H), 7.66 – 7.61 (m, 2H), 6.95 (s, 2H) ppm.

^{13}C-NMR (63 MHz, CF_3CO_2D) δ 159.0 (2C), 147.6 (2C), 144.0 (2C), 137.3 (2C), 137.0 (2C), 131.7 (2C), 129.8 (2C), 129.6 (2C), 128.9 (2C), 126.3 (2C), 119.8 (2C), 113.0 (2C) ppm.

3,6-Dibenzylidenepiperazine-2,5-dione (92):

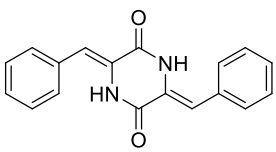

Prepared from **82** (0.5 g, 2.52 mmol) and benzaldheyde (0.55 g, 5.05 mmol); yield: 60%; white solid.

Elemental analysis (%) calcd for $C_{18}H_{14}N_2O_2$: C 74.47, H 4.86, N 9.65, found: C 73.81, H 4.84, N 9.67.

Mp > 300 °C

IR (KBr disk) ν: 3191.5, 3079.4, 1679.2, 1629.4, 1390.0, 1000.2, 926.4 cm^{-1}.

^{1}H-NMR (250 MHz, CF_3CO_2D) δ 7.38 – 7.33 (m, 10H), 7.27 (s, 2H) ppm.

^{13}C-NMR (63 MHz, CF_3CO_2D) δ 162.8 (2C), 133.4 (2C), 132.7 (2C), 131.9 (4C), 130.9 (4C), 126.3 (2C), 125.6 (2C) ppm.

3,6-Bis(4-formylphenylmethylidene)piperazine-2,5-dione (93):

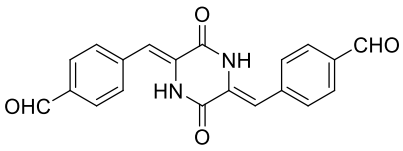

Prepared from **82** (0.5 g, 2.52 mmol) and terephthaldicarbaldehyde (0.68 g, 5.05 mmol); yield: 64%; yellow solid.

Elemental analysis (%) calcd for$C_{20}H_{14}N_2O_4$: C 69.36, H 4.07, N 8.09; found: C 68.36, H 4.28, N 8.47.

Mp > 300 °C

IR (KBr disk): 3448, 3239, 2852, 1683, 1564, 820 cm^{-1}.

^{1}H-NMR (250 MHz, CF_3CO_2D) δ 9.90 (s, 2H), 8.08 (d, *J* = 6.2 Hz, 4H), 7.65 (d, *J* = 6.3 Hz, 4H), 7.36 (s, 2H) ppm.

^{13}C-NMR (63 MHz, CF_3CO_2D) δ 199.1 (2C), 161.8 (2C), 141.5 (2C), 137.7 (2C), 133.9 (4C), 131.7 (4C), 127.8 (2C), 123.0 (2C) ppm.

3,6-Bis(2-furylmethylene)piperazine-2,5-dione (94):

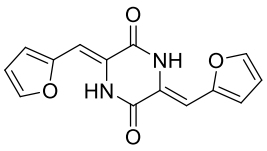

Prepared from **82** (0.5 g, 2.52 mmol) and furane-2-carbaldehyde (0.5 g, 5.05 mmol); yield: 68%; yellowish green solid.

Elemental analysis (%) calcd for $C_{14}H_{10}N_2O_4$: C 62.22, H 3.73, N 10.37; found: C 62.47, H 3.34, N 10.89.

Mp > 300 °C

IR (NaCl) ν: 3277, 1688, 1631, 1482, 1340, 944 cm^{-1}.

^{1}H-NMR (250 MHz, $CDCl_3$) δ 9.31 (br s, 2H), 7.62 (d, *J* = 1.3, 2H), 6.79 (s, 2H), 6.62 (d, *J* = 3.5, 2H), 6.57 – 6.55 (m, 2H) ppm.

^{13}C-NMR (63 MHz, $CDCl_3$) δ 157.1, 151.1, 144.6, 123.8, 115.2, 112.9, 103.3 ppm.

3,6-Bis(2-thienylmethylene)piperazine-2,5-dione (95):

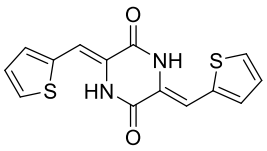

Prepared from **82** (0.5 g, 2.52 mmol) and thiophene-2-carbaldehyde (0.57 g, 5.05 mmol); yield: 61%; yellow solid.

Elemental analysis (%) calcd for $C_{14}H_{10}N_2O_2S_2$: C 55.61, H 3.33, N 9.26, S 21.21; found: C 55.87, H 3.34, N 8.89, S 21.41.

Mp > 300 °C

IR (KBr disk) ν: 3218, 3102, 1678, 1613, 1416, 816 cm^{-1}.

^{1}H-NMR (250 MHz, CF_3CO_2D) δ 7.53 (d, *J* = 5.05, 2H), 7.40 (s, 2H), 7.36 (d, *J* = 3.08, 2H), 7.12 – 7.09 (m, 2H) ppm.

^{13}C-NMR (63 MHz, CF_3CO_2D) δ 162.1 (2C), 135.8 (2C), 134.8 (2C), 132.3 (2C), 130.6 (2C), 122.4 (2C), 118.1 (2C) ppm.

3,6-Bis(1-β-carbolinylmethylene)piperazine-2,5-dione (104):

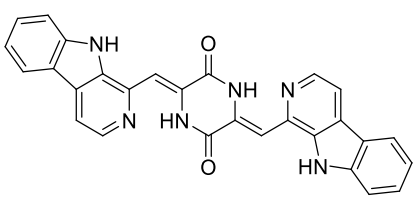

Prepared from **82** (0.5 g, 2.52 mmol) and β-carboline-1-carbaldehyde **103** (1 g, 5.05 mmol); yield: 58%; yellowish green solid.

Elemental analysis (%) calcd for $C_{28}H_{18}N_6O_2$: C 71.48, H 3.86, N 17.86; found: C 71.61, H 3.74, N 17.87.

Mp > 300 °C

IR (KBr disk) ν: 3385, 3058, 1676, 1561, 1457, 1322, 1275, 824 cm^{-1}.

^{1}H-NMR (250 MHz, CF_3CO_2D) δ 8.62 (d, *J* = 6.3, 2H), 8.53 (d, *J* = 6.3, 2H), 8.42 (d, *J* = 8.2, 2H), 7.96 – 7.90 (m, 2H), 7,80 (d, *J* = 8.4, 2H), 7.69 (s, 2H), 7.64 – 7.59 (m, 2H) ppm.

^{13}C-NMR (63 MHz, CF_3CO_2D) δ 163.2 (2C), 136.6 (2C), 134.0 (2C), 132.5 (2C), 129.7 (2C), 125.9 (2C), 125.3 (2C), 122.5 (2C), 119.9 (2C), 118.2 (2C), 115.4 (2C), 115.1 (2C), 113.7 (2C), 108.8 (2C) ppm.

3,6-Bis(3- β-carbolinylmethylene)piperazine-2,5-dione (105):

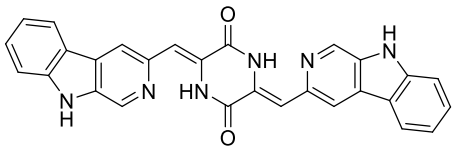

Prepared from **82** (0.5 g, 2.52 mmol) and β-carboline-3-carbaldehyde **102** (1 g, 5.05 mmol); yield: 52%; green-off solid.

Elemental analysis (%) calcd for $C_{28}H_{18}N_6O_2$: C 71.48, H 3.86, N 17.86; found: C 71.81, H 3.86, N 17.67.

Mp > 300 °C

IR (KBr disk) ν: 3424, 3161, 1673, 1644, 1472, 742 cm^{-1}.

^{1}H-NMR (250 MHz, CF_3CO_2D) δ 9.01 (s, 2H), 8.72 (s, 2H), 8.36 (d, *J*=8.0, 2H), 7.87 – 7.81(m, 2H), 7,71 (d, *J*=8.0, 2H), 7.54 – 7.48 (m, 2H), 7.50 (s, 2H) ppm.

^{13}C-NMR (63 MHz, CF_3CO_2D) δ 156.7 (2C), 141.1 (2C), 140.3 (2C), 134.8 (2C), 134.5 (2C), 128.7 (2C), 127.4 (2C), 126.9 (2C), 122.7 (2C), 120.1 (2C), 119.6 (2C), 115.3 (2C), 111.7 (2C), 109.2 (2C) ppm.

9.3.4. General Procedure for the monoreduction of double condensation compounds

A mixture of **83** or **93** and an excess of zinc in 10 ml glacial acetic acid was refluxed at 125 °C for 1-16 h, as specified in each case. Thereafter the reaction mixture was filtered to remove zinc and zinc diacetate, as a white salt. The filtrate was concentrated and the residue was solubilized in CH_2Cl_2 and washed with a 1 M $NaHCO_3$ aqueous solution. This solution was extracted with four 3 ml portions of CH_2Cl_2, and the combined extracts were dried (anhydrous Na_2SO_4) and evaporated *in vacuo* to give **106** and **108** as coloured powder.

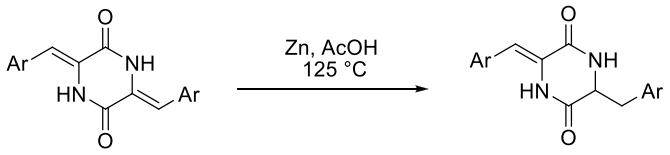

83, 93 **106, 108**

Cmpd.	Ar
106	
108	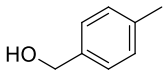

3-(2'-Pyridylmethyl)-6-(2"-pyridylmethylene)piperazine-2,5-dione (106):

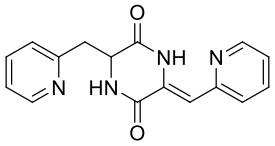

Prepared from **83** (0.200 g, 0.68 mmol) and zinc (0.500 g 7.54 mmol); reaction time: 1 h; yield: 55%; white powder.

Elemental analysis (%) calcd for $C_{16}H_{14}N_4O_2$: C 65.30, H 4.79, N 19.04; found: C 64.60, H 5.20, N 18.66.

Mp: 215 °C

IR (NaCl) ν: 3266.6, 1685.3, 1643.5, 1588.4, 1379.7 cm^{-1}.

^{1}H-NMR (250 MHz, $CDCl_3$) δ 12.75 (br s, 1H), 8.65 (d, *J* = 4.7 Hz, 1H), 8.57 (d, *J* = 4.6 Hz, 1H), 7.93 (br s, 1H), 7.79 – 7.67 (m, 2H), 7.38 – 7.21 (m, 4H), 6.78 (s, 1H), 4.85 – 4.79 (m, 1H), 3.76 (dd, *J* = 15.8, 2.5 Hz, 1H), 3.34 – 3.24 (dd, *J* = 16.0, 10.6 Hz, 1H) ppm.

^{13}C-NMR (63 MHz, $CDCl_3$) δ 166.0, 158.9, 157.5, 155.4, 149.4, 148.8, 137.5, 137.5, 130.9, 126.3, 124.4, 122.6, 122.4, 109.1, 55.1, 40.9 ppm.

3-[4-(Hydroxymethyl)benzyl]-6-[4(hydroxymethyl)benzylidene]-piperazine-2,5-dione (108):

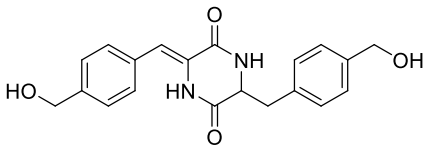

Prepared from **93** (0.200 g, 0.57 mmol) and zinc (0.47 g, 6.31 mmol); reaction time: 16 h; yield: 20%; yellow powder.

Elemental analysis (%) calcd for $C_{20}H_{20}N_2O_4$: C 68.17, H 5.72, N 7.95; found: C 68.26, H 5.99, N 7.57.

Mp: 170 °C

IR (NaCl) ν: 3198, 3058, 1737, 1671, 1629, 1024 cm^{-1}.

^{1}H-NMR (250 MHz, $CDCl_3$) δ 7.82 (br s, 1H), 7.45 – 7.13 (m, 8H), 6.84 (s, 1H), 6.33 (br s, 1H), 5.13 (s, 2H), 5.08 (s, 2H), 4.47 – 4.43 (m, 1H), 3.43 (dd, *J* = 13.6, 3.8 Hz, 1H), 3.12 (dd, *J* = 13.8, 8.1 Hz, 1H) ppm.

^{13}C-NMR (63 MHz, $CDCl_3$) δ: 165.2, 159.9, 137.1, 136.0, 135.0, 133.0, 130.4 (2C), 129.6 (2C), 129.5 (2C), 128.9 (2C), 125.7, 116.1, 66.2, 66.1, 57.4, 41.1 ppm.

9.3.5. 3,6-Bis(pyridin-2-ylmethyl)piperazine-2,5-dione (107):

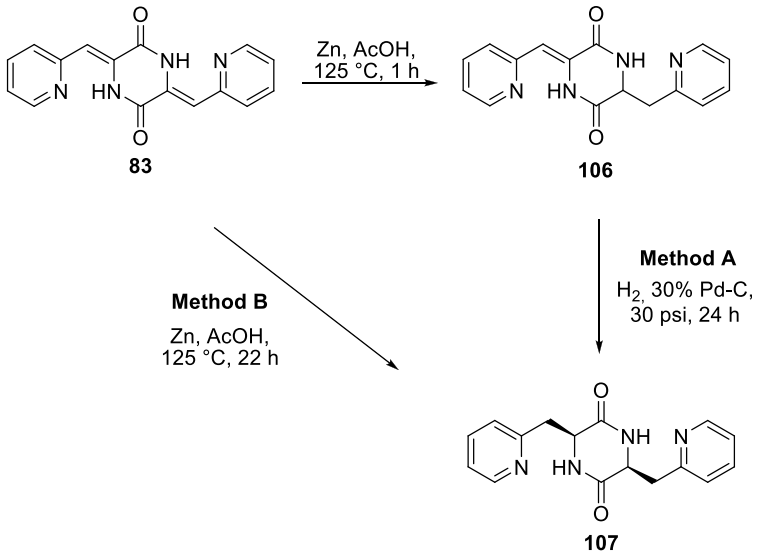

Method A. To a solution of 0.11 g (0.37 mmol) of **106** in 15 ml of methanol was added 0.03 g of 30% palladium on charcoal, and the mixture was shaken in a Parr hydrogenator at 30 psi for 24 h. Thereafter, the Pd/C was removed by suction filtration through a funnel with celite and the filtrate was evaporated *in vacuo* to give compound **107** as a white powder in 34% yield.

Method B.A mixture of 0.20 g (0.68 mmol) of **83** and 0.50 g (7.54 mmol) of zinc in 10 ml of glacial

acetic acid was refluxed at 125 °C for 22 h. Thereafter, the reaction mixture was filtered to remove zinc and zinc diacetate as a white salt. The filtrate was concentrated and the residue was solubilized in 10 ml of CH_2Cl_2 and washed with a 1 M aqueous $NaHCO_3$ solution. The aqueous solution was extracted with four 3 ml portions of CH_2Cl_2, and the combined extracts were dried (anhydrous Na_2SO_4) and evaporated *in vacuo* to give **107** as a white powder in 58% yield.

Elemental analysis (%) calcd for $C_{16}H_{16}N_4O_2$: C 64.85, H 5.44, N 18.91; found: C 64.55, H 5.69, N 19.17.

Mp: 180 °C

IR (NaCl) ν: 3228, 1676, 1592, 1438, 1329 cm^{-1}.

^{1}H-NMR (250 MHz, $CDCl_3$) δ: 8.56 – 8.54 (m, 2H), 7. 90 (br s, 2H), 7.72 – 7.64 (m, 2H), 7.26 – 7.20 (m, 4H), 4.54 (dd, *J* = 10.6, 1.2 Hz, 2H), 3.76 – 3.60 (m, 2H), 3.26 – 3.05 (m, 2H) ppm.

^{13}C-NMR (63 MHz, $CDCl_3$) δ: 39.3, 40.0, 53.9, 54.0, 122.0, 122.1, 124.1, 136.9, 136.9, 149.0, 157.2, 157.4, 167.2, 167.2 ppm.

9.4. Synthesis of GN8 analogues

9.4.1. Synthesis of GN8

9.4.1.1. *N,N'*-[4,4'-methylenebis(4,1-phenylene)]bis(2-bromoacetamide) (109):

A solution of 4,4'-methylenedibenzenamine (0.202 g, 1.02 mmol), 2-bromoacetic acid (0.284 g, 2.06 mmol), EDC (0.382 g, 2.00 mmol) and triethylamine (2.00 mmol), in dry DMF (5 ml) was stirred under argon for 2 hours. After dilution with EtOAc (15 ml), the organic layer was separated, washed with 1 N aqueous HCl (2 x 5 ml), 5% aqueous $NaHCO_3$ (2 x 5 ml) and dried over anhydrous Na_2SO_4. Evaporation afforded compound **109** as a pale brown solid in 46% yield.

^{1}H-NMR (250 MHz, DMSO) δ 10.34 (br s, 2H), 7.50 (d, *J* = 8.5 Hz, 4H), 7,17 (d, *J* = 8.5 Hz, 4H), 4.02 (s, 4H), 3.86 (s, 2H) ppm.

^{13}C-NMR (63 MHz, DMSO,) δ 165.5 (2C), 137.7 (2C), 137.5 (2C), 129.9 (4C), 120.2 (4C), 41.0, 31.3 (2C) ppm.

9.4.1.2. GN8 (110):

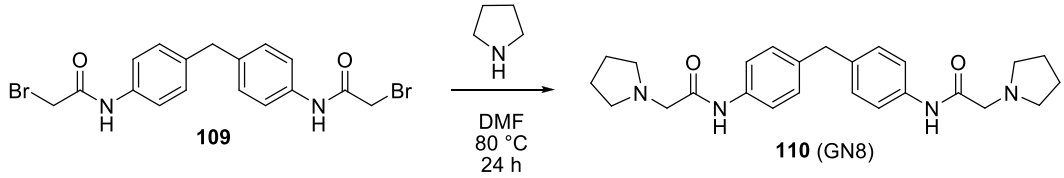

Compound **109** (0.100 g, 0.227 mmol) and 2 equivalents of pyrrolidine (32 mg, 0.454 mmol), were stirred for 24 h at 75 °C. The mixture was cooled, and then

diluted with EtOAc (5 ml), washed with H_2O (3 x 1 ml), dried over anhydrous Na_2SO_4 and concentrated to give compound **110** as a pale brown solid in 64% yield.

Elemental analysis (%) calcd for $C_{25}H_{32}N_4O_2$: C 71.40, H 7.67, N 13.32; found: C 71.16, H 7.72, N 13.35.

Mp: 144 – 147 °C

IR (NaCl) ν: 3257, 2954, 2799, 1681, 1664, 1513814 cm^{-1}.

^{1}H-NMR (250 MHz, DMSO) δ 9.70 (br s, 2H), 7.54 (d, *J* = 8.4 Hz, 4H), 7.13 (d, *J* = 8.4 Hz, 4H), 3.84 (s, 2H), 3.30 (s, 4H), 2.64 (br s, 8H), 1.76 (br s, 8H) ppm.

^{13}C-NMR (63 MHz, DMSO,) δ 169.0 (2C), 137.5 (2C), 137.3 (2C), 129.6 (4C), 120.4 (4C), 60.1 (2C), 54.6 (4C), 41.0, 24.2 (4C) ppm.

9.4.2. Preparation of the fluorene derivatives

9.4.2.1. *N,N'*-(9H-fluorene-2,7-diyl)bis(2-bromoacetamide) (111):

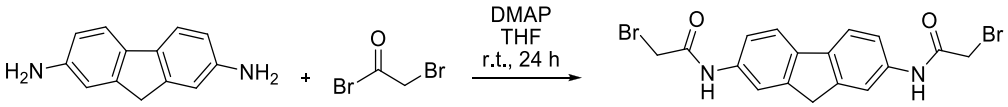

111

To a stirred mixture of 9*H*-fluorene-2,7-diamine (0.3 g, 1.53 mmol) and DMAP (0.46 g, 3.8 mmol) in 15 mL of THF under inert atmosphere, bromoacetyl bromide (0.33 ml, 3.8 mmol) was added dropwise. The resulting mixture was stirred at r.t. for 24 h, then 15 mL of 0.1N HCl were added to remove the DMAP excess and the solution was left stirring for 30 minutes. Then the mixture was filtered under vacuum, the solid washed with water until acid-free and dried to give compound **111** as a pale brown solid in 97% yield.

IR (KBr disk) ν: 3257, 1683 cm^{-1}.

^{1}H-NMR (250 MHz, DMSO) δ 10.49 (br s, 2H), 7.91 (s, 2H), 7.80 (d, *J* = 8.2 Hz, 2H), 7.55 (dd, *J* = 8.2, 2.5 Hz, 2H), 4,08 (s, 4H, H2), 3,94 (s, 2H) ppm.

^{13}C-NMR (63 MHz, DMSO) δ 165.5 (2C), 144.6 (2C), 138.1 (2C), 137.6 (2C), 120.7 (2C), 118.9 (2C), 116.9 (2C), 37.5, 31.4 (2C) ppm.

9.4.2.2. Amino-fuorene derivatives:

To a stirred mixture of compound **111** (0.2 g, 0.45 mmol) in 2 ml of dry DMF at 75 °C was added two equivalents of the suitable amine. The reaction was stirred for 24 hours, cooled to r.t. and then 5 mL of EtOAc were added. The resulting precipitate was filtered under vacuum, washed with ice-cooled water (3 x 1 ml) and dried to give compounds **112-120**.

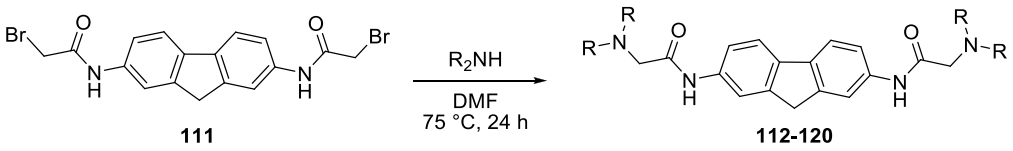

111 **112-120**

Cmpd.	R_2NH
112	
113	
114	
115	
116	

Cmpd.	R_2NH
117	
118	
119	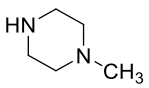
120	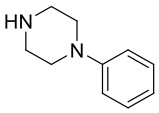

2-(Dimethylamino)-*N*-(7-[2-(dimethylamino)acetylamino]-9*H*-fluoren-2-yl)acetamide (112):

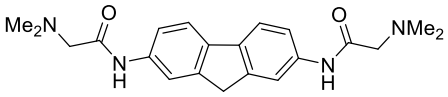

Prepared from **111** (0.2 g, 0.45 mmol) and dimethylamine (0.045 ml, 0.9 mmol); yield: 90%; pale brown solid.

Elemental analysis (%) calcd for $C_{21}H_{26}N_4O_2$: C 68.83, H 7.15, N 15.29; found: C 68.69, H 6.98, N 15.18.

Mp: 204 – 207°C

IR (KBr disk) ν: 3258, 1682, 1518 cm^{-1}.

^{1}H-NMR (250 MHz, DMSO) δ 9.78 (br s, 2H), 7.96 (s, 2H), 7.74 (d, *J* = 8.2 Hz, 2H), 7.61 (d, *J* = 8.2, 2H), 3.88 (s, 2H), 3.10 (s, 4H), 2.50 (s, 6H) ppm.

^{13}C-NMR (63 MHz, DMSO) δ 168.8 (2C), 143.8 (2C), 137.5 (2C), 136.7 (2C), 119.8 (2C), 118.6 (2C), 116.6 (2C), 63.7 (2C), 45.7 (4C), 37.0 ppm.

***N,N*′-(9H-fluorene-2,7-diyl)bis(2-(diethylamino)acetamide) (113):**

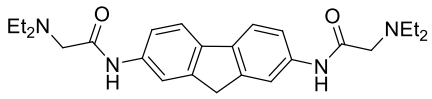

Prepared from **111** (0.2 g, 0.45 mmol) and diethylamine (0.09 ml, 0.9 mmol); yield: 34%; pale brown solid.

Elemental analysis (%) calcd for $C_{25}H_{34}N_4O_2$: C 71.06, H 8.11, N 13.26; found: C 70.89, H 7.98, N 13.18.

Mp: 210 213 °C

IR (KBr disk) ν: 3260, 1672, 1434 cm^{-1}.

^{1}H-NMR (250 MHz, DMSO) δ 10.41 (br s, 2H), 7.92 (s, 2H), 7.80 (d, *J* = 8.2 Hz, 2H), 7.60 (d, *J* = 8.2, 2H), 3.94 (s, 2H), 3.82 (s, 4H), 3.03 (br s, 8H), 1.18 (t, *J* = 7.5, 12H) ppm.

^{13}C-NMR (63 MHz, DMSO) δ 171.3 (2C), 149.3 (2C), 142.4 (2C), 142.3 (2C), 125.4 (2C), 123.8 (2C), 121.8 (2C), 60.5 (2C), 53.9 (4C), 42.3, 15.7 (4C) ppm.

***N,N'*-(9H-fluorene-2,7-diyl)bis(2-(diisopropylamino)acetamide) (114):**

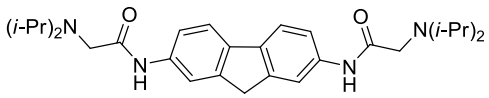

Prepared from **111** (0.2 g, 0.45 mmol) and diisopropylamine (0.13 ml, 0.9 mmol); yield: 64%; pale brown solid.

Elemental analysis (%) calcd for $C_{29}H_{42}N_4O_2$: C 72.77, H 8.84, N 11.70; found: C 72.89, H 8.98, N 11.48.

Mp: 215 218 °C

IR (KBr disk) ν: 3206, 1655, 1493 cm^{-1}.

^{1}H-NMR (250 MHz, DMSO) δ 9.40 (br s, 2H), 7.66 (br s, 2H), 7.51 (br s, 2H), 7.19 (br s, 2H), 3.66 (s, 2H), 2.88 (s, 4H), 2.27 (br s, 4H), 0.80 (br s, 24H) ppm.

^{13}C-NMR (63 MHz, DMSO) δ 171.5 (2C), 144.1 (2C), 136.9 (2C), 120.1 (2C), 118.7 (2C), 118.2 (2C), 116.2 (2C), 50.2 (4C), 50.1 (2C), 36.9, 20.6 (8C)ppm.

***N,N'*-(9H-fluorene-2,7-diyl)bis(2-(pyrrolidin-1-yl)acetamide (115):**

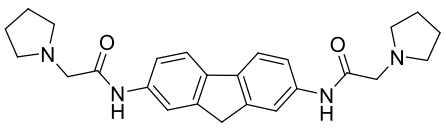

Prepared from **111** (0.2 g, 0.45 mmol) and pyrrolidine (0.076 ml, 0.9 mmol); yield: 80%; yellow solid.

Elemental analysis (%) calcd for $C_{25}H_{30}N_4O_2$: C 71.74, H 7.22, N 13.39; found: C 71.51, H 7.15, N 13.23.

Mp: 174 – 177 °C

IR (KBr disk) ν: 3324, 1689, 1475 cm^{-1}.

^{1}H-NMR (250 MHz, DMSO) δ 9.77 (s, 2H), 7.94 (s, 2H), 7.74 (d, *J* = 8.2 Hz, 2H), 7.59 (d, *J* = 8.2, 2H), 3.86 (s, 2H), 3.26 (s, 4H), 2.63 – 2.59 (m, 8H), 1.80 – 1.78 (m, 8H) ppm.

^{13}C-NMR (63 MHz, DMSO) δ 168.9 (2C), 143.8 (2C), 137.5 (2C), 136.7 (2C), 119.8 (2C), 118.6 (2C), 116.6 (2C), 59.9 (2C), 54.1 (4C), 36.9, 23.8 (4C) ppm.

2-(1*H*-Imidazol-1-yl)-*N*-(7-[2-(1*H*-imidazol-1-yl)acetyl] amino-9*H*-fluoren-2-yl)acetamide (116):

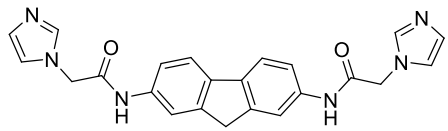

Prepared from **111** (0.2 g, 0.45 mmol) and imadazole (61 mg, 0.9 mmol); yield 57%; pale brown solid.

Elemental analysis (%) calcd for $C_{23}H_{20}N_6O_2$: C 66.98, H 4.89, N 20.38; found: C 66.85, H 4.82, N 20.28.

Mp: 236 239 °C

IR (KBr disk) ν: 3268, 2932, 1685, 1666, 1470, 1299, 1083, 820 cm^{-1}.

^{1}H-NMR (250 MHz, DMSO) δ 10.43 (s, 2H), 7.87 (s, 2H), 7.75 (d, *J* = 8.5 Hz, 2H), 7.65 (s, 2H), 7.53 (d, *J* = 8.5 Hz, 2H), 7.18 (s, 2H), 6.90 (s, 2H), 4.93 (s, 4H), 3.89 (s, 2H) ppm.

^{13}C-NMR (63 MHz, DMSO) δ 166.0 (2C), 144.0 (2C), 138.7 (2C), 137.6 (2C), 136.8 (2C), 128.3 (2C), 121.0 (2C), 120.1 (2C), 118.3 (2C), 116.3 (2C), 49.6 (2C), 37.0 ppm.

***N,N'*-(9*H*-fluorene-2,7-diyl)bis(2-(piperidin-1-yl)acetamide) (117):**

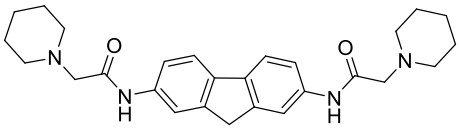

Prepared from **111** (0.2 g, 0.45 mmol) and piperidine (0.09 ml, 0.9 mmol); yield: 73%; orange solid.

Elemental analysis (%) calcd for $C_{27}H_{34}N_4O_2$: C 72.62, H 7.67, N 12.55; found: C 72.16, H 7.67, N 12.28.

Mp: 179 – 182 °C

IR (KBr disk) ν: 3298, 1613 cm^{-1}.

^{1}H-NMR (250 MHz, DMSO) δ 9.73 (s, 2H), 7.92 (s, 2H), 7.75 (d, *J* = 8.9 Hz, 2H), 7.59 (d, *J* = 8.9, 2H), 3.89 (s, 2H), 3.09 (s, 4H), 2.49 – 2.47 (m, 8H), 1.59 – 1.55 (m, 8H), 1.43 – 1.41 (m, 4H) ppm.

^{13}C-NMR (63 MHz, DMSO) δ 168.8 (2C), 143.9 (2C), 137.4 (2C), 136.8 (2C), 119.9 (2C), 118.5 (2C), 116.5 (2C), 63.1 (2C), 54.5 (4C), 36.9, 25.9 (4C), 23.9 (2C) ppm.

***N,N'*-(9*H*-fluorene-2,7-diyl)bis(2-morpholinoacetamide) (118):**

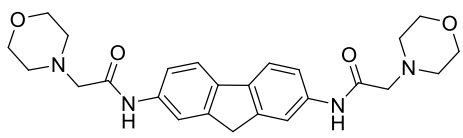

Prepared from **111** (0.2 g, 0.45 mmol) and morpholine (0.08 ml, 0.9 mmol); yield: 64%; yellow solid.

Elemental analysis (%) calcd for $C_{25}H_{30}N_4O_4$: C 66.65, H 6.71, N 12.44; found: C 66.77, H 6.32, N 12.17.

Mp: 204 – 207 °C

IR (KBr disk) ν: 3124, 1689, 1175 cm^{-1}.

^{1}H-NMR (250 MHz, DMSO) δ 9.81 (s, 2H), 7.93 (s, 2H), 7.74 (d, *J* = 8.9 Hz, 2H), 7.58 (d, *J* = 8.9, 2H), 3.89 (s, 2H), 3.66 (t, 8H) 3.15 (s, 4H), 2.54 – 2.51 (m, 8H) ppm.

^{13}C-NMR (63 MHz, DMSO) δ 168.4 (2C), 143.9 (2C), 137.4 (2C), 136.9 (2C), 119.9 (2C), 118.6 (2C), 116.7 (2C), 66.3 (4C), 62.3 (2C), 53.6 (4C), 37.0 ppm.

***N,N'*-(9*H*-fluorene-2,7-diyl)bis(2-(4-methylpiperazin-1-yl)acetamide) (119):**

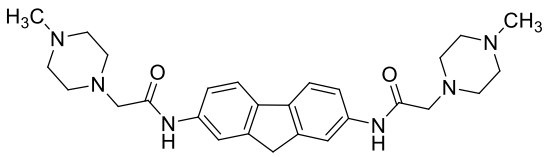

Prepared from **111** (0.2 g, 0.45 mmol) and 4-methylpiperazine (0.09 ml, 0.9 mmol); yield: 72%; yellow solid.

Elemental analysis (%) calcd for $C_{27}H_{36}N_6O2$: C 68.04, H 7.61, N 17.63; found: C 67.92, H 7.26, N 17.45.

Mp: 139 – 142 °C

IR (KBr disk) ν: 3278, 1683, 1472 cm^{-1}.

^{1}H-NMR (250 MHz, DMSO) δ 9.77 (s, 2H), 7.93 (s, 2H), 7.75 (d, *J* = 8.1 Hz, 2H), 7.59 (d, *J* = 8.1, 2H), 3.90 (s, 2H), 3.14 (s, 4H), 2.41 – 2.32 (m, 16H), 2.20 (s, 6H) ppm.

^{13}C-NMR (63 MHz, $CDCl_3$) δ 168.7 (2C), 144.7 (2C), 138.0 (2C), 136.5 (2C), 120.2 (2C), 118.6 (2C), 116.7 (2C) 62.3 (2C), 55.7 (4C), 53.9 (4C), 46.4 (2C), 37.5 ppm.

***N,N'*-(9*H*-fluorene-2,7-diyl)bis(2-(4-phenylpiperazin-1-yl)acetamide) (120):**

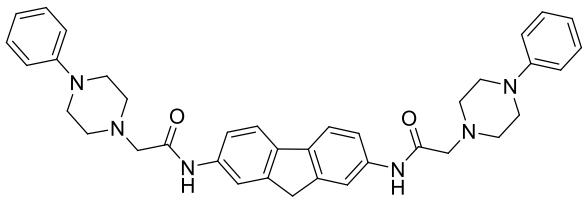

Prepared from **111** (0.2 g, 0.45 mmol) and 1-phenylpiperazine (0.14 ml, 0.9 mmol); yield: 67%; yellow solid.

Elemental analysis (%) calcd for $C_{37}H_{40}N_6O_2$: C 73.97, H 6.71, N 13.99; found: C 73.59, H 6.66, N 13.82.

Mp: 224 – 227°C

IR (KBr disk) ν: 3291, 2825, 1681 cm^{-1}.

^{1}H-NMR (250 MHz, CDCl3) δ 9.27 (s, 2H), 7.93 (s, 2H), 7.70 (d, *J* = 8.2 Hz, 2H), 7.48 (d, *J* = 8.25, 2H), 7.36 – 7.29 (m, 4H), 7.01 – 6.90 (m, 6H), 3.93 (s, 2H), 3.34 – 3.31 (m, 8H), 3.27 (s, 4H), 2.87 – 2.85 (m, 8H) ppm.

^{13}C-NMR (63 MHz, $CDCl_3$) δ 168.4 (2C), 151.4 (2C), 144.7 (2C), 138.1 (2C), 136.5 (2C), 129.7 (4C), 120.6 (2C), 120.2 (2C), 118.6 (2C), 116.8 (2C), 116.7 (4C), 62.4 (2C), 54.0 (4C), 49.9 (4C), 37.6 ppm.

9.4.3. Preparation of the carbazole derivatives

9.4.3.1. Nitration of carbazole

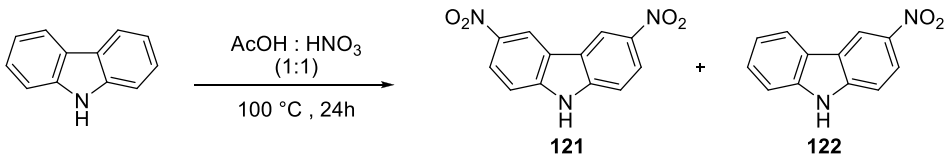

Carbazole (10.03 g, 60.0 mmol) was dissolved in glacial AcOH (80 ml). The mixture was stirred for 1.5 h at 40 °C. Then, a mixture of 30% HNO_3-AcOH (1:1, 16.4 ml) was added dropwise and the solution was stirred for 16 h at 90-100 °C. The brown precipitate was filtered and washed with cold AcOH (50 ml) and then with water. The solid was warmed in KOH/EtOH (200 ml, 60 g/l) at 50°C for 30 min and filtered. Water was added and the yellow precipitate was filtered. The insoluble solid was digested in 10% HCl at 100 °C for 2 h. The insoluble yellow solid was filtered, washed with water, and dried overnight in the presence of P_2O_5. Chromatography on neutral alumina, eluting with EtOAc:petroleum ether

(50:50), followed by EtOAc and then EtOAc:MeOH (145:5), provided compound **121** and **122**.

3,6-dinitro-9*H*-carbazole and 3-nitro-9*H*- carbazole (121):

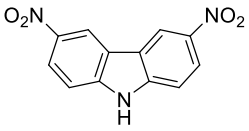

Yield: 20%; orange solid.

Mp > 300 °C

IR (KBr disk): 3379, 1611, 1584, 1510, 1335, 1306 cm^{-1}.

^{1}H-NMR (250 MHz, DMSO) δ 12.72 (br s, 1H), 9.50 (d, *J* = 2.2, 2H), 8.40 (dd, *J* = 9.0, 2.2 Hz, 2H), 7.77 (d, *J* = 9.0 Hz, 2H) ppm.

3-nitro-9*H*-carbazole (122):

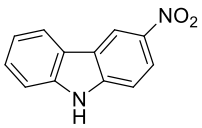

Yield: 20%; red solid.

^{1}H-NMR (250 MHz, DMSO) δ 12.10 (brs, 1H), 9.19 (s, 1H), 8.39 (d, *J* = 7.5 Hz, 1H), 8.31 (d, *J* = 10 Hz, 1H), 7.66 – 7.60 (m, 2H), 7.53 (t, *J* =7.6 Hz, 1H), 7.30 (t, *J* = 7.3 Hz, 1H) ppm.

9.4.3.2. 9*H*-carbazole-3,6-diamine (123):

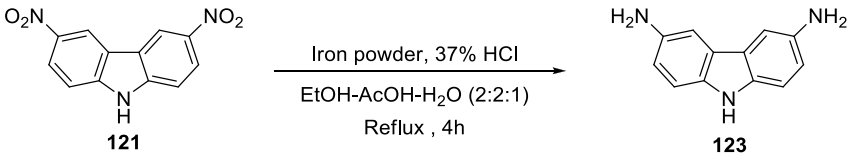

A mixture of **121** (0.500 g, 1.944 mmol), iron powder (2.50 g) and 37% HCl aqueous solution (3.8 ml) in 40 ml of a mixture of EtOH, AcOH and H2O (2:2:1) was refluxed for 4h with magnetic stirring. The solution was filtered on celite,

diluted with water (50 ml) and extracted with EtOAc (3 x 100 ml). The combined organic layers were washed with saturated $NaHCO_3$ aqueous solution (200 ml) and H_2O (2 x 200 ml) and dried over anhydrous Na_2SO_4. Evaporation of the solvent afforded compound **123** as a greyish yellow solid in 96% yield.

IR (KBr disk): 3428, 2364, 2344, 1735, 1636, 1097 cm^{-1}.

^{1}H-NMR (250 MHz, DMSO) δ 10.13 (s, 1H), 7.09 – 7.05 (m, 4H), 6.67 (d, *J* = 8.8 Hz, 2H), 4.60 (br s, 4H) ppm.

^{13}C-NMR (63 MHz, DMSO) δ 140.7 (2C), 133.9 (2C), 123.3 (2C), 115.1 (2C), 111.3 (2C), 104.1 (2C) ppm.

9.4.3.3. *N,N'*-(9*H*-carbazole-3,6-diyl)bis(2-bromoacetamide) (124):

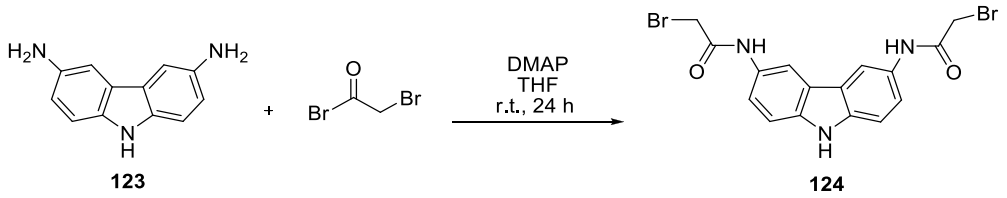

A solution of 9*H*-carbazole-3,6-diamine **123** (0.200 g, 1.014 mmol), bromoacetyl bromide (0.511 g, 2.535 mmol) and DMAP (0.309 g, 2.535 mmol) in dry THF (10 mL) was stirred under argon for 24 h. When the reaction was finished, THF was removed and an aqueous solution of 2N HCl (7 mL) was added and stirred for 1 h. The solid was filtered and washed with water. The product, after dried overnight under reduced pressure in the presence of P_2O_5, was identified as compound **124** and appeared as a grey brown solid in 80% yield.

^{1}H-NMR (250 MHz, DMSO) δ 11.22 (s, 1H), 10.41 (s, 2H), 8.39 (s, 2H), 7.48 – 7.56 (m, 4H), 4.09 (s, 4H) ppm.

^{13}C NMR (63 MHz, DMSO) δ 165.5 (2C), 134.6 (2C), 131.1 (2C), 122.6 (2C), 118.9 (2C), 116.9 (2C), 113.7 (2C), 31.4 (2C) ppm.

9.4.3.4. Amino-carbazole derivatives

To a stirred mixture of compound **124** (0.200 g, 0.445 mmol) in 2 ml of dry DMF was added two equivalents of the suitable amine. The reaction mixture was stirred while heated at 75 °C for 24 h. The mixture was cooled, and then diluted with EtOAc (5 ml), washed with H_2O (3 x 2 ml), dried over anhydrous Na_2SO_4 and concentrated under reduced pressure to give compounds **125-133**.

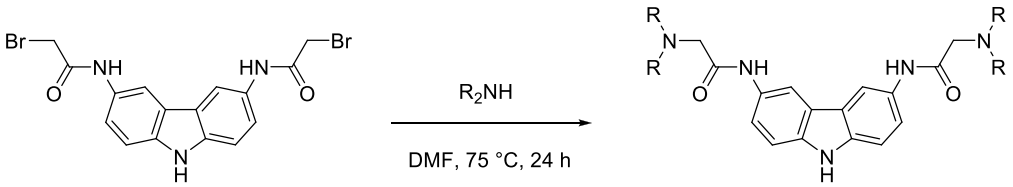

124 **125-133**

Cmpd.	R_2NH
125	
126	
127	
128	
129	

Cmpd.	R_2NH
130	
131	
132	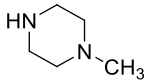
133	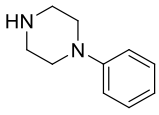

***N,N'*-(9*H*-carbazole-3,6-diyl)bis(2-(dimethylamino)acetamide) (125):**

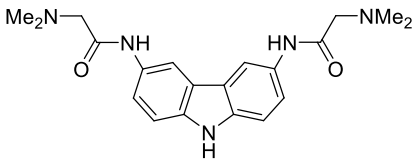

Prepared from **123** (0.200 g, 0.445 mmol) and dimethylamine (0.046 ml, 0.91 mmol); yield: 58%; reddish solid.

Elemental analysis (%) calcd for $C_{20}H_{25}N_5O_2$: C 65.37, H 6.66, N 19.06; found: C 65.09, H 6.31,N 19.35.

Mp: 131 – 134 °C

IR (KBr disk): 3279, 1667, 1586, 868 cm^{-1}.

^{1}H-NMR (250 MHz, DMSO) δ 9.71 (br s, 2H), 8.41 (s, 2H), 7.57 – 7.54 (m, 2H), 7.41 – 7.38 (m, 2H), 3.11 (s, 4H), 2.33 (s, 12H) ppm.

^{13}C-NMR (63 MHz, DMSO) δ 168.5 (2C), 137.3 (2C), 130,7 (2C), 122.4 (2C), 119.5 (2C), 111.4 (2C), 111.2 (2C), 63.7 (2C), 45.8 (4C) ppm.

***N,N'*-(9*H*-carbazole-3,6-diyl)bis(2-(diethylamino)acetamide) (126):**

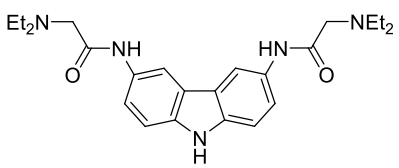

Prepared from **123** (0.200 g, 0.445 mmol) and diethylamine (0.094 ml, 0.91 mmol); yield: 60%; brown solid.

Elemental analysis (%) calcd for $C_{24}H_{29}N_5O_2$: C 68.06, H 7.85, N 16.53; found: C 67.8, H 7.55, N 16.44.

Mp: 134 – 137 °C

IR (KBr disk): 3269, 2968, 1870, 1584, 1297, 808 cm^{-1}.

^{1}H-NMR (250 MHz, DMSO) δ 9.65 (br s, 2H), 8.39 (d, *J* = 1.6 Hz), 7.58 (dd, *J* = 8.7, 1.9 Hz, 2H), 7.40 (d, *J* = 8.6 Hz, 2H), 3.18 (s, 4H), 2.65 (q, *J* = 7.1 Hz, 8H), 1.07 (t, *J* = 7.1 Hz, 12H) ppm.

^{13}C-NMR (63 MHz, DMSO) δ 169.6 (2C), 137.3 (2C), 130.5 (2C), 122.5 (2C), 119.3 (2C), 111.3 (2C), 111.2 (2C), 57.9 (2C), 48.3 (4C), 12.4 (4C') ppm.

***N,N'*-(9*H*-carbazole-3,6-diyl)bis(2-(diisopropylamino)acetamide) (127):**

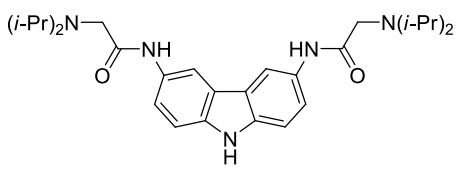

Prepared from **123** (0.200 g, 0.445 mmol) and diisopropilamine (0.13 ml, 0.91 mmol); yield: 47%; brown solid.

Elemental analysis (%) calcd for $C_{28}H_{41}N_5O_2$: C 70.11, H 8.62, N 14.60; found: C 69.90, H 8.37, N 14.34.

mp: 138 – 141 °C

IR (KBr disk): 3279, 2945, 1667, 1586, 1538, 868 cm^{-1}.

^{1}H-NMR (250 MHz, DMSO) δ 11.14 (br s, 1H), 9.60 (br s, 2H), 8.36 (s, 2H), 7.62 (d, *J* = 8.1 Hz), 7.42 (d, *J* = 8.1 Hz, 2H), 3.13 (s, 8H), 1.08 (d, *J* = 5.5 Hz, 24H) ppm.

^{13}C-NMR (63 MHz, DMSO) δ 171.09 (2C), 137.40 (2C), 130.30 (2C), 122.52 (2C), 119.14 (2C), 111.28 (2C), 111.23 (2C), 50.22 (2C), 50.09 (4C), 20.64 (8C) ppm.

***N,N'*-(9*H*-carbazole-3,6-diyl)bis(2-(pyrrolidin-1-yl)acetamide)(128):**

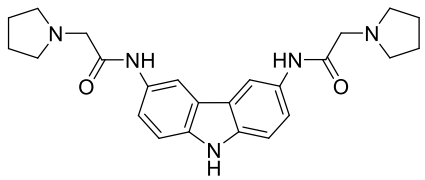

Prepared from **123** (0.200 g, 0.445 mmol) and pyrrolidine (0.076 ml, 0.91 mmol); yield: 40%; reddish solid.

Elemental analysis (%) calcd for $C_{24}H_{29}N_5O_2$: C 68.71, H 6.97, N 16.69; found: C 68.32, H 6.59, N 16.33.

Mp: 169 – 172 °C

IR (KBr disk): 3399, 1654, 1560, 1492, 1228, 814 cm^{-1}.

^{1}H-NMR (250 MHz, DMSO) δ 11.12 (br s, 1H), 9.78 (br s, 2H), 8.39 (s, 2H), 7.54 (d, *J* = 7.5 Hz, 2H), 7.42 (s, 2H), 3.38 (s, 4H, overlapped with the residual DMSO signal), 2.72 (s, 8H), 1.81 (s, 8H) ppm.

^{13}C-NMR (63 MHz, DMSO) δ 168.0 (2C), 137.3 (2C), 130.7 (2C), 122.4 (2C), 119.5 (2C), 111.3 (2C), 108.9 (2C), 59.5 (2C), 54.2 (4C), 23.8 (4C) ppm.

***N,N'*-(9*H*-carbazole-3,6-diyl)bis(2-(1*H*-imidazol-1-yl)acetamide)(129):**

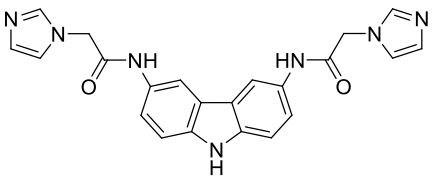

Prepared from **123** (0.200 g, 0.445 mmol) and imidazole (0.077 g, 0.91 mmol); yield: 38%; black solid.

Elemental analysis (%) calcd for $C_{22}H_{19}N_7O_2$: C 63.91, H 4.63, N 23.72; found: C 63.53, H 4.48, N 23.34.

Mp: 193 – 196 °C

IR (KBr disk): 3854, 1654, 1493, 1400, 1297, 814 cm^{-1}.

^{1}H-NMR (250 MHz, DMSO) δ 10.38 (br s, 1H), 8.32 (s, 2H), 7.69 (s, 2H), 7.50 – 7.45 (m, 4H), 7.22 (s, 2H), 6.93 (s, 2H), 3.20 (s, 4H) ppm.

^{13}C-NMR (63 MHz, DMSO) δ 166.0 (2C), 139.1 (2C), 137.8 (2C), 128.8 (2C), 122.9 (2C), 121.5 (2C), 119.7 (2C), 112.1 (2C), 112.0 (2C), 111.5 (2C), 50.1 (2C) ppm.

***N,N'*-(9*H*-carbazole-3,6-diyl)bis(2-(piperidin-1-yl)acetamide)(130):**

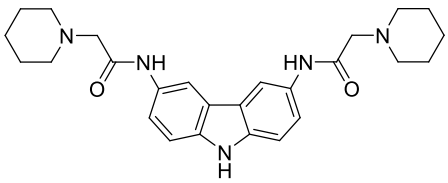

Prepared from **123** (0.200 g, 0.445 mmol) and piperidine (0.089 ml, 0.91 mmol); yield: 55%; brown solid.

Elemental analysis (%) calcd for $C_{26}H_{33}N_5O_2$: C 69.77, H 7.43, N 15.65; found: C 69.39, H 7.05, N 15.97.

Mp: 161 – 164°C

IR (KBr disk): 3278.0, 2933.1, 2811.4, 1664.6, 1584.6, 1533.4, 1492, 745.7, 642.7 cm^{-1}.

^{1}H-NMR (250 MHz, DMSO) δ 10.74 (br s, 1H), 9.27 (br s, 2H), 8.01 (s, 2H), 7.16 (s, 2H), 7.04 (s, 2H), 3.00 (s, 4H), 2.13 (s, 8H), 1.22 – 0.84 (m, 12H) ppm.

^{13}C-NMR (63 MHz, DMSO) δ 168.4 (2C), 137.3 (2C), 130.6 (2C), 122.5 (2C), 119.5 (2C), 111.4 (2C), 111.2 (2C), 63.1 (2C), 54.6 (4C), 25.9 (4C), 24.0 (2C) ppm.

***N,N'*-(9*H*-carbazole-3,6-diyl)bis(2-morpholinoacetamide) (131):**

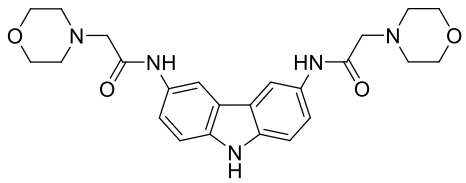

Prepared from **123** (0.200 g, 0.445 mmol) and morpholine (0.082 ml, 0.91 mmol); yield: 48%; brown solid.

Elemental analysis (%) calcd for $C_{24}H_{29}N_5O_4$: C 63.84, H 6.47, N 15.51; found: C 63.67, H 6.17, N 15.55.

Mp: 171 – 174 °C

IR (KBr disk): 3288, 1668, 1494, 1297, 911 cm $^{-1}$.

^{1}H-NMR (250 MHz, DMSO) δ 11.08 (br s, 1H), 9.69 (br s, 2H), 8.34 (s, 2H), 7.50 (d, *J* = 8.1 Hz, 2H), 7.36 (d, *J* = 8.5 Hz, 2H), 3.33 (s, 8H), 3.12 (s, 4H), 2.47 (s, 8H) ppm.

^{13}C-NMR (63 MHz, DMSO) δ 167.92 (2C), 137.3 (2C), 130.6 (2C), 122.4 (2C), 119.6 (2C), 111.6 (2C), 111.2 (2C), 66.5 (4C), 62.5 (2C), 53.7 (4C) ppm.

***N,N'*-(9*H*-carbazole-3,6-diyl)bis(2-(4-methylpiperazin-1-yl)acetamide)(132):**

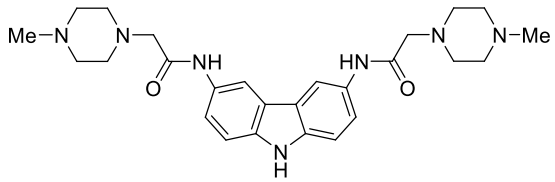

Prepared from **123** (0.200 g, 0.445 mmol) and 1-methyl-piperazine (0.10 ml, 0.91 mmol); yield: 30%; reddish solid.

Elemental analysis (%) calcd for $C_{26}H_{35}N_7O_2$: C 65.38, H 7.39, N 20.53; found: C 65.03, H 7.05, N 20.78.

Mp: 185 – 188 °C

IR (KBr disk): 3409, 2948, 1654, 1542, 1492, 1459 cm $^{-1}$.

^{1}H-NMR (250 MHz, DMSO) δ 11.20 (br s, 1H), 9.89 (br s, 2H), 8.43 (s, 2H), 7.55 (d, *J* = 8.2 Hz, 2H), 7.43 (d, *J* = 8.7Hz, 2H), 3.55 – 3.11 (m, 10H), 2.79 (s, 6H) ppm.

^{13}C-NMR (63 MHz, DMSO) δ 164.7 (2C), 137.4 (2C), 130.6 (2C), 122.4 (2C), 120.8 (2C), 111.4 (2C), 111.3 (2C), 65.3 (2C), 53.1 (4C), 49.9 (2C), 42.8 (4C) ppm.

***N,N'*-(9*H*-carbazole-3,6-diyl)bis(2-(4-phenylpiperazin-1-yl)acetamide)(133):**

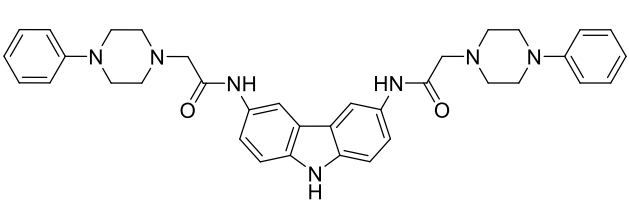

Prepared from **123** (0.200 g, 0.445 mmol) and 1-phenylpiperazine (0.14 ml, 0.91 mmol); yield: 40%; brown solid.

Elemental analysis (%) calcd for $C_{36}H_{39}N_7O_2$: C 71.86, H 6.53, N 16.29; found: C 71.48, H 6.29, N 15.97.

Mp: 176 – 179 °C

^{1}H-NMR (250 MHz, DMSO) δ 11.16 (br s, 1H), 9.87 (br s, 2H), 8.42 (s, 2H), 7.57 (d, *J* = 8.3 Hz, 2H), 7.42 (d, *J* = 8.4 Hz, 2H), 7.27 – 7.21 (m, 4H), 6.83 – 6.77 (m, 4H), 6.81 (d, *J* = 7.0 Hz, 2H), 3.28 (s, 12H), 2.81 (s, 8H) ppm.

^{13}C-NMR (63 MHz, DMSO) δ 151.2 (2C), 137.4 (2C), 130.6 (2C), 129.3 (4C), 122.4 (2C), 119.9 (2C), 119.6 (2C), 119.3 (2C), 115.8 (4C), 111.6 (2C), 111.3 (2C), 53.0 (6C), 48.2 (4C) ppm.

9.4.4. Non-symmetric carbazole derivative

9.4.4.1. 9*H*-carbazol-3-amine (134):

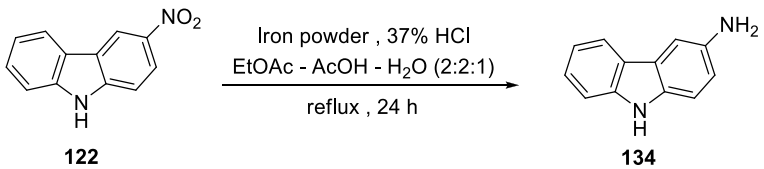

122 **134**

A mixture of **122** (0.100 g, 0.472 mmol), iron powder (2.50 g) and 37% HCl aqueous solution (3.8 ml) in 40 ml of a mixture of EtOH, AcOH and H_2O (2:2:1) was refluxed for 4 h with magnetic stirring. The solution was filtered on celite,

diluted with water (50 ml) and extracted with EtOAc (3 x 100 mL). The combined organic layers were washed with saturated aqueous $NaHCO_3$ (200 ml) and H_2O (2 x 200 ml) and dried over anhydrous Na_2SO_4. Evaporation of the solvent afforded compound **134** as a yellow solid in 95% yield.

^{1}H-NMR (250 MHz, d6-acetone,) δ 10.29 (s, 1H), 8.08 (d, *J* = 7.5 Hz, 1H), 7.52 – 7.35 (m, 4H), 7.19 – 7.13 (m, 1H), 6.81 (dd, *J* = 8.5, 2.0 Hz, 1H), 3.06 (br s, 2H) ppm.

9.4.4.2. 2-bromo-*N*-(9*H*-carbazol-3-yl)acetamide (135):

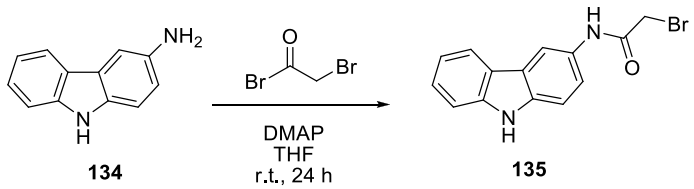

A solution of **134** (0.100 g, 0.507 mmol), bromoacetyl bromide (0.102 g, 0.507 mmol), DMAP (0.062 g, 0.507 mmol) in dry THF (10 ml) was stirred under argon for 24 hours. When the reaction was finished, an aqueous solution of 2N HCl (7 mL) was added and the solution was stirred for 1h. An extraction with EtOAc (3 x 15 ml) afforded the organic layer, that was washed with water (3 x 15 mL) and then was dried over anhydrous Na_2SO_4. Evaporation afforded compound **135** as a yellow-grey solid in 80% yield.

^{1}H-NMR (250 MHz, DMSO) δ 11.28 (s, 1H), 10.45 (s, 1H), 8.44 (s, 1H), 8.08 (d, *J* = 7.7 Hz, 1H), 7.58 – 7.44 (m, 3H), 7.41 (t, *J* = 7.6 Hz, 1H), 7.17 (t, *J* = 7.4 Hz, 1H), 4.13 (s, 2H) ppm.

^{13}C-NMR (63 MHz, DMSO) δ 165.2, 141.2, 137.5, 131.2, 126.6, 123.2, 123.0, 121.0, 119.7, 119.4, 112.1, 112.0, 111.9, 31.6 ppm.

9.4.4.3. *N*-(9*H*-carbazol-3-yl)-2-(pyrrolidin-1-yl)acetamide (136):

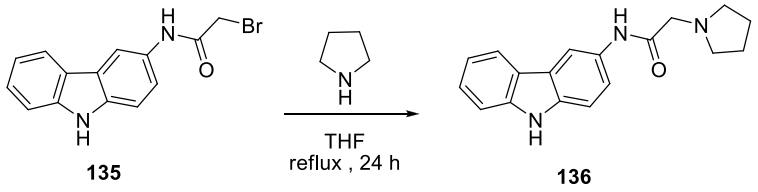

Compound **135** (0.050 g, 0.114 mmol) and pyrrolidine (0.21 ml, 0.25 mmol) were refluxed in THF (8 ml) for 24 h. THF was removed to give an yellow oil that was purified by chromatography on neutral alumina, eluting with EtOAc:Petroleum ether (50:50), to isolate compound **136** as a yellow-grey solid in 89% yield.

Elemental analysis (%) calcd for $C_{18}H_{19}N_3O$: C 73.69, H 6.53, N 14.32; found: C 73.32, H 6.57, N 13.95.

Mp: 146 – 149 °C

IR (KBr disk): 3406, 3328, 2962, 1676, 1560, 817 cm^{-1}.

^{1}H-NMR (250 MHz, d_6-acetone) δ 9.23 (br s, 1H), 8.62 (br s, 1H), 8.35 (d, *J* = 1.8 Hz, 1H), 8.07 (d, *J* = 7.8 Hz, 1H), 7.54 (dd, *J* = 8.6, 2.0 Hz, 1H), 7.41 (d, *J* = 3.8 Hz, 2H), 7.36 – 7.29 (m, 1H), 7.26 – 7.19 (m, 1H), 3.38 (s, 2H), 2.76 – 2.74 (m, 4H), 1.94 – 1.88 (m, 4H) ppm.

^{13}C-NMR (63 MHz, d_6-acetone,) δ 169.64, 140.7, 137.2, 130.4, 126.4, 123.9, 123.6, 121.0, 119.6 (2C), 112.5, 111.2, 111.2, 60.2, 55.1 (2C), 24.5 (2C) ppm.

9.5. Synthesis of styrylquinolines

9.5.1. Preparation of styrylquinoline compounds by using the Povarov reaction

9.5.1.1. Synthesis of cinnamaldheyde compounds

To a stirred solution of the suitable aryl iodides (0.5 mmol) in 2 ml of DMF were added acrolein diethyl acetal (1.5 mmol) Bu_4NOAc (1.0 mmol), K_2CO_3 (0.75 mmol), KCl (0.5 mmol) and $Pd(OAc)_2$ (0.015 mmol). The mixture was stirred for 2 h at 90 °C. After cooling, 2N HCl was slowly added and the solution was stirred for 10 min. Then, it was diluted with ether and washed with water. The organic layer was dried with anhydrous Na_2SO_4 and concentrated under reduced pressure. The residue was purified by chromatography to give **141-145**.

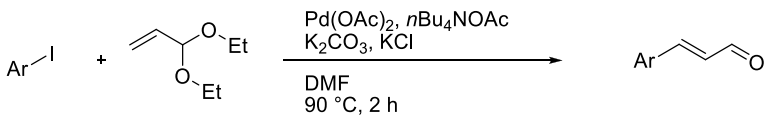

Comd.	Ar	Comd.	Ar
141	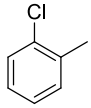	**144**	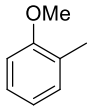
142	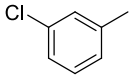	**145**	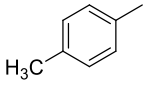
143	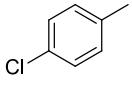		

(*E*)-2-chlorocinnamaldehyde (141):

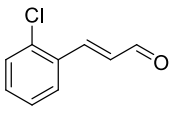

Prepared from 1-chloro-2-iodobenzene (0.119 g, 0.5 mmol) and acrolein diethyl acetal (0.195 g, 1.5 mmol); yield 70%; yellow

solid.

^{1}H NMR (250 MHz, $CDCl_3$) δ 9.79 (d, *J* = 7.7 Hz, 1H), 7.97 (d, *J* = 16.0 Hz, 1H), 7.70 (dd, *J* = 7.2, 2.0 Hz, 1H), 7.51 – 7.33 (m, 3H), 6.74 (dd, *J* = 16.0, 7.7 Hz, 1H) ppm.

^{13}C NMR (63 MHz, DMSO) δ 195.0, 167.5, 147.7, 139.1, 133.9, 130.3, 128.6, 128.1, 122.6 ppm.

(*E*)-3-chlorocinnamaldehyde(142):

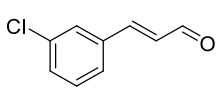

Prepared from 1-chloro-3-iodobenzene (0.119 g, 0.5 mmol) and acrolein diethylacetal (0.195 g, 1.5 mmol); yield 80%; yellow solid.

^{1}H NMR (250 MHz, $CDCl_3$) δ 9.71 (d, *J* = 7.6 Hz, 1H), 7.54 – 7.53 (m, 1H), 7.47 – 7.37 (m, 4H), 6.70 (dd, *J* = 16.0, 7.6 Hz, 1H) ppm.

^{13}C NMR (63 MHz, $CDCl_3$) δ 193.9, 151.4, 131.5, 130.8, 130.6, 130.0, 128.7, 128.5, 126.9 ppm.

(*E*)-4-chlorocinnamaldehyde (143):

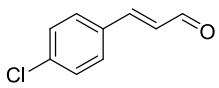

Prepared from 1-chloro-4-iodobenzene (0.119 g, 0.5 mmol) and acrolein diethyl acetal (0.195 g, 1.5 mmol); yield 83%; yellow solid.

^{1}H NMR (250 MHz, $CDCl_3$) δ 9.73 (d, *J* = 7.6 Hz, 1H), 7.55 – 7.42 (m, 5H), 6.72 (dd, *J* = 16.0, 7.6 Hz, 1H) ppm.

(*E*)-2-methoxycinnamaldehyde (144):

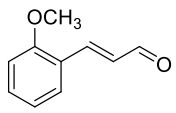

Prepared from1-iodo-2-methoxybenzene(0.117 g, 0.5 mmol) and acrolein diethyl acetal (0.195 g, 1.5 mmol); yield:57%; yellow solid.

^{1}H NMR (250 MHz, $CDCl_3$) δ 9.72 (d, *J* = 7.9 Hz, 1H), 7.88 (d, *J* = 16.1 Hz, 1H), 7.58 (dd, *J* = 7.7, 1.7 Hz, 1H), 7.45 (ddd, *J* = 8.4, 7.5, 1.7 Hz, 1H), 7.13 – 6.91 (m, 2H), 6.82 (dd, *J* = 16.1, 7.9 Hz, 1H), 3.95 (s, 3H) ppm.

^{13}C NMR (63 MHz, $CDCl_3$) δ 195.0, 158.7, 148.7, 133.2, 129.4, 129.3, 123.3, 121.3, 111.7, 56.0 ppm.

(*E*)-4-methylcinnamaldehyde (145):

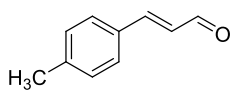

Prepared from1-iodo-4-methylbenzene (0.109 g, 0.5 mmol) and acrolein diethyl acetal (0.195 g, 1.5 mmol); yield: 81%; white solid.

^{1}H NMR (250 MHz, $CDCl_3$) δ 9.70 (d, *J* = 7.7 Hz, 1H), 7.50 – 7.44 (m, 3H), 7.26 (d, *J* = 8.0 Hz, 2H), 6.70 (dd, *J* = 15.9, 7.7 Hz, 1H), 2.42 (s, 3H) ppm.

9.5.1.2. Synthesis of 2-styrlquinolines

An equimolar (3 mmol) mixture of the suitable arylamine and cinnamaldehyde was dissolved in acetonitrile (20 ml) at r.t. Ethyl vinyl ether (0.320 g, 4.5 mmol) and 15 mol% of cerium ammonium nitrate (CAN), 0.247 g, were added to the stirred solution, and stirring was continued for 5 h. Upon completion of the reaction, as indicated by TLC, the mixture was extracted with dichloromethane (2 x 20 ml), dried (anhydrous Na_2SO_4) and evaporated. The resulting crude product

was dissolved in 20 ml of benzene and 2,3-dichloro-5,6-dicyano-1,4-benzoquinone (DDQ) (0.454 g, 2 mmol) was added slowly. The black suspension was stirred for 3 h at r.t. Upon completion of the reaction, CH_2Cl_2 (30 ml) and water (10 ml) were added, and the mixture was thoroughly shaken with saturated aqueous $NaHCO_3$ solution (5 ml) to get clear layer separation. The organic layer was separated and the aqueous layer was again extracted with CH_2Cl_2 (30 ml). The combined organic layers were dried (anhydrous Na_2SO_4) and evaporated. The crude product was purified through silica gel column using a petroleum ether/ethyl acetate mixture (95:05, v/v) to afford compounds **137-138** and **146-160**.

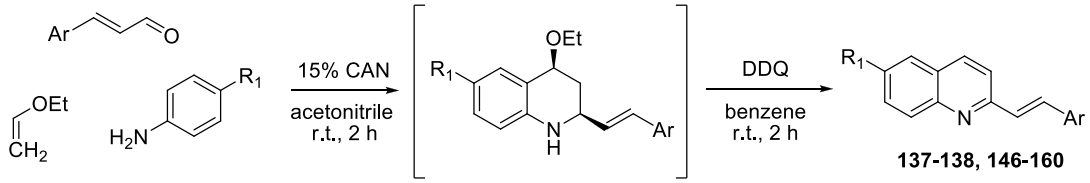

Compd.	R_1	Ar
137	CH_3	
138	OMe	
146	H	
147	Cl	
148	H	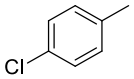
149	Me	
150	Cl	
151	OMe	

Compd.	R_1	Ar
152	Me	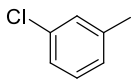
153	OMe	
154	Me	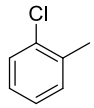
155	OMe	
156	Me	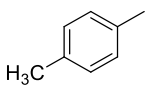
157	Cl	
158	OMe	
159	Me	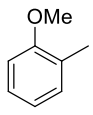
160	Cl	

(*E*)-6-methyl-2-styrylquinoline (137):

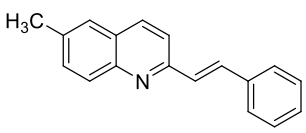

Prepared from *p*-toluidine (0.321 g, 3 mmol) and cinnamaldehyde (0.396 g, 3 mmol); overall yield: 69%; white solid.

Elemental analysis (%) calcd for $C_{18}H_{15}N$: C 88.13, H 6.16, N 5.71; found: C 87.96, H 6.08, N 5.60.

Mp: 129 – 132 °C

IR (neat) ν: 3028, 2909, 1634, 1590, 1496, 1445, 1371, 1122 cm^{-1}.

^{1}H NMR (250 MHz, $CDCl_3$) δ 8.06 (d, *J* = 8.7 Hz, 1H), 8.01 (d, *J* = 9.2 Hz, 1H), 7.71 – 7.65 (m, 4H), 7.58 – 7.55 (m, 2H), 7.46 – 7.35 (m, 4H), 2.56 (s, 3H). ppm.

^{13}C NMR (63 MHz, $CDCl_3$) δ 155.5, 147.2, 137.0, 136.5, 136.2, 134.3, 132.5, 129.5, 129.2, 129.2 (2C), 128.9, 127.8, 127.6 (2C), 126.9, 119.7, 22.0 ppm.

(*E*)-6-methoxy-2-styrylquinoline (138):

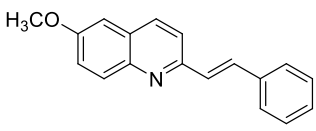

Prepared from *p*-anisidine (0.370 g, 3 mmol) and cinnamaldehyde (0.396 g, 3 mmol); overall yield: 72%; yellow solid.

Elemental analysis (%) calcd for $C_{18}H_{15}NO$: C 82.73, H 5.79, N 5.36. found: C 82.52, H 5.65, N 5.17.

Mp: 133 – 136

IR (neat) ν: 3028, 2935, 1618, 1597, 1557, 1500, 1478, 1336, 1162, 1113 cm^{-1}.

^{1}H NMR (250 MHz, $CDCl_3$) δ 8.05 (d, *J* = 6.7 Hz, 1H), 8.01 (d, *J* = 7.2 Hz, 1H), 7.68 – 7.62 (m, 4H), 7.46 – 7.34 (m, 5H), 7.08 (d, *J* = 2.7 Hz, 1H), 3.96 (s, 3H). ppm.

^{13}C NMR (63 MHz, $CDCl_3$) δ 158.1, 154.1, 144.6, 137.1, 135.6, 133.7, 131.0, 129.4, 129.2 (2C), 128.8, 128.7, 127.6 (2C), 122.8, 120.0, 105.6, 56.0.ppm.

(*E*)-2-styrylquinoline (146):

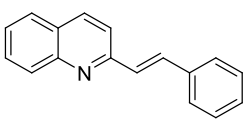

Prepared from aniline (0.279 g, 3 mmol) and cinnamaldehyde (0.396 g, 3 mmol); overall yield: 62%; white solid.

Elemental analysis (%) calcd for $C_{17}H_{13}N$: C 88.28, H 5.67, N 6.06; found: C 87.97, H 5.53, N 6.01.

Mp: 97 100 °C

IR (neat) ν: 3056, 3031, 1612, 1596, 1504, 1446, 1316, 1204, 1118 cm^{-1}.

^{1}H NMR (250 MHz, $CDCl_3$) δ 8.13 (d, *J* = 8.5 Hz, 2H), 7.81 – 7.66 (m, 6H), 7.55 – 7.36 (m, 5H) ppm.

^{13}C NMR (63 MHz, $CDCl_3$) δ 156.4, 148.7, 136.9, 136.8, 134.9, 130.2, 129.6, 129.4, 129.2 (2C), 129.1, 127.9, 127.8, 127.7 (2C), 126.6, 119.7 ppm.

(*E*)-6-chloro-2-styrylquinoline (147):

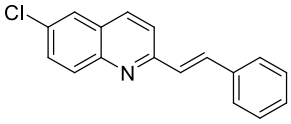

Prepared from 4-chloroaniline (0.383 g, 3 mmol) and cinnamaldehyde (0.396 g, 3 mmol); overall yield: 75%; white solid.

Elemental analysis (%) calcd for $C_{17}H_{12}ClN$: C 76.84, H 4.55, N 5.27; found: C 76.55, H 4.40, N 5.21.

Mp: 138 – 141 °C

IR (neat) ν: 3042, 2999, 1631, 1593, 1492, 1447, 1390, 1328, 1186, 1074 cm^{-1}.

^{1}H NMR (250 MHz, $CDCl_3$) δ 8.06 (d, *J* = 8.6 Hz, 1H), 8.04 (d, *J* = 8.9 Hz, 1H), 7.79 – 7.64 (m, 6H), 7.48 – 7.37 (m, 4H) ppm.

^{13}C NMR (63 MHz, $CDCl_3$) δ 156.6, 147.1, 136.7, 135.8, 135.3, 131.2, 131.1, 129.3 (2C), 129.2, 128.9, 128.6, 128.3 (2C), 127.7, 126.6, 120.6 ppm.

(*E*)-2-(4-chlorostyryl)quinoline (148):

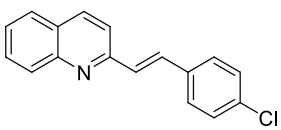

Prepared from aniline (0.279 g, 3 mmol) and **143** (0.500 g, 3 mmol); overall yield: 42%; white solid.

Elemental analysis (%) calcd for $C_{17}H_{12}ClN$: C 76.84, H 4.55, N 5.27; found: C 76.54, H 4.61, N 5.26.

Mp: 124 126 °C

IR (neat) ν: 1593, 1504, 1405, 968, 824 cm^{-1}.

^{1}H NMR ($CDCl_3$, 250 MHz) δ 7.44 – 7.37 (m, 3H), 7.84 7.51 (m, 7H), 8.10 (d, *J* = 8.3 Hz, 1H), 8.20 (d, *J* = 8.6 Hz, 1H) ppm.

^{13}C NMR ($CDCl_3$, 63 MHz) δ 156.0, 148.6, 136.9, 135.4, 134.7, 133.5, 130.3, 129.9, 129.6, 129.4 (2C), 128.8 (2C), 127.9, 127.8, 126.7, 119.7 ppm.

(*E*)-2-(4-chlorostyryl)-6-methylquinoline (149):

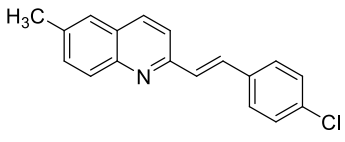

Prepared from *p*-toluidine (0.321 g, 3 mmol) and **143** (0.500 g, 3 mmol); overall yield: 38%; white solid.

Elemental analysis (%) calcd for $C_{18}H_{14}ClN$: C 77.28, H 5.04, N 5.01; found: C 77.56, H 4.79, N 5.38.

Mp: 122 – 125 °C

IR (neat) ν: 1587, 1555, 1490, 1085, 1006, 964, 826 cm^{-1}.

^{1}H NMR (250 MHz, $CDCl_3$) δ 8.08 (d, *J* = 8.5 Hz, 1H), 8.00 (d, *J* = 9.2 Hz, 1H), 7.68 – 7.57 (m, 6H), 7.41 – 7.29 (m, 3H), 2.57 (s, 3H) ppm.

^{13}C NMR (63 MHz, $CDCl_3$) δ 155.2, 147.2, 136.7, 136.2, 135.6, 134.6, 132.9, 132.6, 130.0, 129.4 (2C), 129.3, 128.7 (2C), 127.8, 126.9, 119.8, 22.0 ppm.

(*E*)-6-chloro-2-(4-chlorostyryl)quinoline (150):

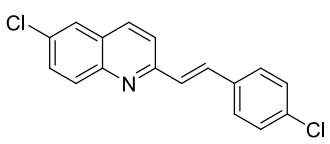

Prepared from 4-chloroaniline (0.383 g, 3 mmol) and **143** (0.500 g, 3 mmol); overall yield: 30%; pale yellow solid.

Elemental analysis (%) calcd for $C_{17}H_{11}Cl_2N$: C 68.02, H 3.69, N 4.67; found: C 67.97, H 3.84, N 5.07.

Mp: 158 – 161 °C

IR (neat) ν: 1584, 1488, 1388, 1186, 1087, 1070, 966, 818 cm^{-1}.

^{1}H NMR (250 MHz, $CDCl_3$) δ 8.08 (d, *J* = 8.7 Hz, 1H), 8.03 (d, *J* = 9.1 Hz, 1H), 7.80 (d, *J* = 2.3 Hz, 1H), 7.72 – 7.65 (m, 3H), 7.61 – 7.58 (m, 2H), 7.43 – 7.25 (m, 3H) ppm.

^{13}C NMR (63 MHz, $CDCl_3$) δ 156.3, 147.0, 135.9, 135.3, 134.9, 134.5, 133.9, 132.4, 131.2, 129.5 (2C), 129.4, 128.9 (2C), 128.3, 126.7, 120.8 ppm.

(*E*)-2-(4-chlorostyryl)-6-methoxyquinoline (151):

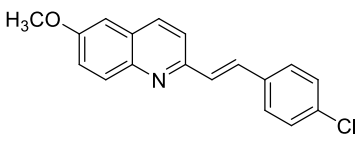

Prepared from *p*-anisidine (0.370 g, 3 mmol) and **143** (0.500 g, 3 mmol); overall yield: 44%; yellow solid.

Elemental analysis (%) calcd for $C_{18}H_{14}ClNO$: C 73.10, H 4.77, N 4.74; found: C 72.74, H 4.68, N 4.98.

Mp: 137 – 140 °C

IR (neat) ν: 1621, 1597, 1491, 1377, 1226, 1159, 1028, 831 cm^{-1}.

^{1}H NMR (250 MHz, $CDCl_3$) δ 8.05 (d, *J* = 8.6 Hz, 1H), 8.00 (d, *J* = 9.3 Hz, 1H), 7.64 – 7.56 (m, 4H), 7.42 – 7.32 (m, 4H), 7.09 (d, *J* = 2.8 Hz, 1H), 3.96 (s, 3H) ppm.

^{13}C NMR (63 MHz, $CDCl_3$) δ 158.2, 153.7, 144.7, 135.7, 135.6, 134.4, 132.2, 131.1, 130.0, 129.4 (2C), 128.8, 128.7 (2C), 122.9, 120.1, 105.6, 56.0 ppm.

(*E*)-2-(3-chlorostyryl)-6-methylquinoline (152):

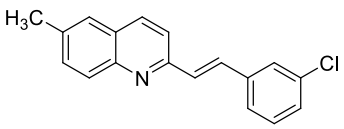

Prepared from *p*-toluidine (0.321 g, 3 mmol) and **142** (0.500 g, 3 mmol); overall yield: 39%; pale yellow solid.

Elemental analysis (%) calcd for $C_{18}H_{14}ClN$: C 77.28, H 5.04, N 5.01; found: C 77.01, H 4.81, N 4.78.

Mp: 115 – 118 °C

IR (neat) ν: 1737, 1591, 1560, 1494, 1200, 1095, 961, 824 cm^{-1}.

^{1}H NMR (250 MHz, $CDCl_3$) δ 8.12 (d, *J* = 8.2 Hz, 1H), 8.05 (d, *J* = 9.0 Hz, 1H), 7.69 – 7.53 (m, 6H), 7.42 – 7.29 (m, 3H), 2.58 (s, 3H) ppm

^{13}C NMR (63 MHz, $CDCl_3$) δ 154.6, 146.3, 138.7, 137.2, 137.0, 135.2, 133.0, 130.5, 130.0, 129.2, 129.0, 128.7, 127.9, 127.6, 126.9, 125.9, 119.7, 22.3 ppm.

(*E*)-2-(3-chlorostyryl)-6-methoxyquinoline (153):

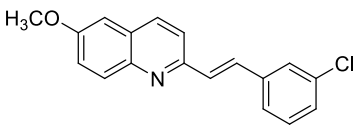

Prepared from *p*-anisidine (0.370 g, 3 mmol) and **142** (0.500 g, 3 mmol); overall yield: 34%; yellow solid.

Elemental analysis (%) calcd for $C_{18}H_{14}ClNO$: C 73.10, H 4.77, N 4.74; found: C 72.66, H 4.80, N 4.98.

Mp: 98 – 101 °C

IR (neat) ν: 1617, 1592, 1560, 1497, 1475, 1223, 1028, 831 cm^{-1}.

^{1}H NMR (250 MHz, $CDCl_3$) δ 8.07 (d, *J* = 8.6 Hz, 1H), 8.01 (d, *J* = 9.2 Hz, 1H), 7.65 – 7.51 (m, 4H), 7.42 – 7.32 (m, 4H), 7.10 (d, *J* = 2.7 Hz, 1H), 3.97 (s, 3H) ppm.

^{13}C NMR (63 MHz, $CDCl_3$) δ 158.2, 153.5, 144.7, 139.1, 135.6, 135.1, 132.0, 131.2, 130.8, 130.4, 128.9, 128.6, 127.4, 125.7, 122.9, 120.2, 105.6, 56.0 ppm.

(E)-2-(2-chlorostyryl)-6-methylquinoline (154):

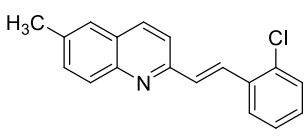

Prepared from *p*-toluidine (0.321 g, 3 mmol) and **141** (0.500 g, 3 mmol); overall yield: 42%; white solid.

Elemental analysis (%) calcd for $C_{18}H_{14}ClN$: C 77.28, H 5.04, N 5.01; found: C 76.95, H 4.63, N 4.69.

Mp: 73 – 76 °C

IR (neat) ν: 1738, 1591, 1436, 1371, 1216, 957, 823, 745 cm^{-1}.

^{1}H NMR (250 MHz, $CDCl_3$) δ 8.01 – 7.89 (m, 3H), 7.75 (dd, *J* = 7.5, 1.9 Hz, 1H), 7.67 (d, *J* = 8.6 Hz, 1H), 7.50 – 7.46 (m, 2H), 7.38 – 7.14 (m, 4H), 2.47 (s, 3H) ppm.

^{13}C NMR (63 MHz, $CDCl_3$) δ 155.4, 147.2, 136.8, 136.2, 135.1, 134.4, 132.5, 132.3, 130.4, 130.1, 129.8, 129.4, 127.9, 127.5, 127.3, 126.9, 119.4, 22.4 ppm.

(*E*)-2-(2-chlorostyryl)-6-methoxyquinoline (155):

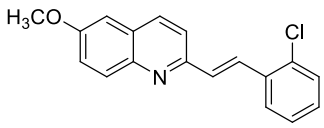

Prepared from *p*-anisidine (0.370 g, 3 mmol) and **141** (0.500 g, 3 mmol); overall yield: 46%; white solid.

Elemental analysis (%) calcd for $C_{18}H_{14}ClNO$: C 73.10, H 4.77, N 4.74; found: C 72.68, H 4.63, N 4.69.

Mp: 88 – 91 °C

IR (neat) ν: 1613, 1594, 1498, 1465, 1374, 1244, 1223, 746 cm^{-1}.

^{1}H NMR (250 MHz, $CDCl_3$) δ 8.04 – 7.95 (m, 3H), 7.81 (dd, *J* = 7.5, 1.7 Hz, 1H), 7.72 (d, *J* = 8.6 Hz, 1H), 7.45 – 7.21 (m, 5H), 7.06 (d, *J* = 2.7 Hz, 1H), 3.93 (s, 3H) ppm.

^{13}C NMR (63 MHz, $CDCl_3$) δ 158.2, 153.9, 144.6, 135.6, 135.2, 134.3, 132.2, 131.2, 130.3, 129.7, 129.4, 128.9, 127.5, 127.2, 122.8, 119.7, 105.6, 55.9. ppm.

(*E*)-6-methyl-2-(4-methylstyryl)quinoline (156):

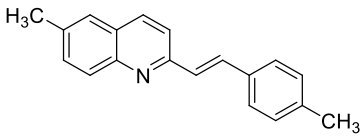

Prepared from *p*-toluidine (0.321 g, 3 mmol) and **145** (0.439 g, 3 mmol); overall yield: 47%; yellow solid.

Elemental analysis (%) calcd for $C_{19}H_{17}N$: C 87.99, H 6.61, N 5.40; found: C 87.72, H 6.62, N 5.49.

Mp: 160 – 163 °C

IR (neat) ν: 1588, 1548, 1510, 1490, 1177, 1118, 980, 830 cm^{-1}.

^{1}H NMR (250 MHz, $CDCl_3$) δ 8.06 (d, *J* = 8.6 Hz, 1H), 7.99 (d, *J* = 9.2 Hz, 1H), 7.68 – 7.55 (m, 6H), 7.38 (d, *J* = 16.3 Hz, 1H), 7.24 (d, *J* = 7.9 Hz, 2H), 2.56 (s, 3H), 2.41 (s, 3H) ppm.

^{13}C NMR (63 MHz, $CDCl_3$) δ 155.8, 147.2, 139.0, 136.4, 136.0, 134.3, 132.4, 129.9 (2C), 129.2, 128.6, 127.7, 127.6 (2C), 126.9, 119.6, 31.3, 22.0, 21.8 ppm.

(*E*)-6-chloro-2-(4-methylstyryl)quinoline (157):

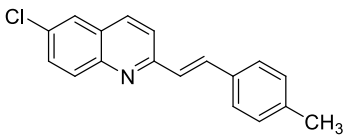

Prepared from 4-chloroaniline (0.383 g, 3 mmol) and **145** (0.439 g, 3 mmol); overall yield: 45%; yellow solid.

Elemental analysis (%) calcd for $C_{18}H_{14}ClN$: C 77.28, H 5.04, N 5.01; found: C 76.82, H 5.02, N 5.29.

Mp: 179 – 181 °C

IR (neat) ν: 1590, 1487, 1186, 1114, 1072, 973, 828, 816 cm^{-1}.

^{1}H NMR (250 MHz, $CDCl_3$) δ 8.04 (t, *J* = 8.5 Hz, 2H), 7.79 (d, *J* = 2.2 Hz, 1H), 7.74 – 7.64 (m, 3H), 7.57 (d, *J* = 8.1 Hz, 2H), 7.36 (d, *J* = 16.3 Hz, 1H), 7.25 (d, *J* = 8.0 Hz, 2H), 2.42 (s, 3H) ppm.

^{13}C NMR (63 MHz, $CDCl_3$) δ 156.9, 147.1, 139.4, 135.7, 135.3, 134.0, 132.1, 131.1, 131.0, 130.0 (2C), 128.2, 128.0, 127.7 (2C), 126.6, 120.6, 21.8 ppm.

(*E*)-6-methoxy-2-(4-methylstyryl)quinoline (158):

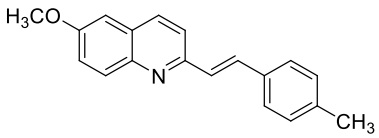

Prepared from *p*-anisidine (0.370 g, 3 mmol) and **145** (0.439 g, 3 mmol); overall yield: 41%; yellow solid.

Elemental analysis (%) calcd for $C_{19}H_{17}NO$: C 82.88, H 6.22, N 5.09; found: C 82.53, H 6.34, N 5.28.

Mp: 158 – 161 °C

IR (neat) ν: 1619, 1586, 1481, 1375, 1331, 1226, 989, 834 cm^{-1}.

^{1}H NMR (250 MHz, $CDCl_3$) δ 8.06 – 7.98 (m, 2H), 7.68 – 7.54 (m, 4H), 7.40 – 7.22 (m, 5H), 3.97 (s, 3H), 2.41 (s, 3H) ppm.

^{13}C NMR (63 MHz, $CDCl_3$) δ 158.0, 154.4, 144.7, 138.9, 135.5, 134.3, 133.7, 131.0, 129.9, 128.6, 128.5, 127.5, 122.7, 119.9, 105.7, 56.0, 21.8 ppm.

(*E*)-2-(2-methoxystyryl)-6-methylquinoline (159):

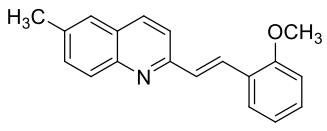

Prepared from *p*-toluidine (0.321 g, 3 mmol) and **144** (0.486 g, 3 mmol); overall yield: 29%; yellow solid.

Elemental analysis (%) calcd for $C_{19}H_{17}NO$: C 82.88, H 6.22, N 5.09; found: C 83.04, H 6.46, N 4.98.

Mp: 100 – 103 °C

IR (neat) ν: 1587, 1490, 1460, 1239, 1024, 965, 828, 755 cm^{-1}.

^{1}H NMR (250 MHz, $CDCl_3$) δ 8.08 – 7.98 (m, 3H), 7.78 – 7.73 (m, 2H), 7.57 – 7.44 (m, 3H), 7.37 – 7.30 (m, 1H), 7.06 – 6.95 (m, 2H), 3.96 (s, 3H), 2.56 (s, 3H) ppm.

^{13}C NMR (63 MHz, $CDCl_3$) δ 157.8, 156.3, 147.1, 136.4, 136.0, 132.3, 130.1, 129.2, 127.7, 127.6, 126.8, 126.0, 121.2, 119.4, 111.4, 55.9, 22.0 ppm.

(*E*)-6-chloro-2-(2-methoxystyryl)quinoline (160):

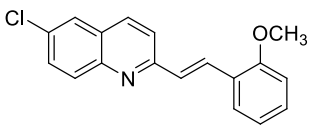

Prepared from 4-chloroaniline (0.383 g, 3 mmol) and **144** (0.486 g, 3 mmol); overall yield: 25%; yellow solid.

Elemental analysis (%) calcd for $C_{18}H_{14}ClNO$: C 73.10, H 4.77, N 4.74; found: C 72.91, H 4.46, N 5.02.

Mp: 99 – 102 °C

IR (neat) ν: 1590, 1488, 1455, 1240, 1020, 827, 754 cm^{-1}.

^{1}H NMR (250 MHz, $CDCl_3$) δ 8.10 – 8.03 (m, 3H), 7.81 – 7.64 (m, 4H), 7.49 – 7.32 (m, 2H), 7.07 – 6.96 (m, 2H), 3.97 (s, 3H) ppm.

^{13}C NMR (63 MHz, $CDCl_3$) δ 157.9, 156.3, 146.9, 135.7, 132.0, 131.1, 130.9, 130.4, 130.3, 129.4, 128.2, 127.7, 126.6, 125.7, 121.3, 120.4, 111.4, 56.0 ppm.

9.5.1.3. Introduction of an amino group on 137

6-Methyl-2-styrylquinoline (**137**) (0.25 g, 1.019 mmol) was added over 10 minutes to a stirred mixture of acid nitric 65% (8 ml) and fuming nitric acid (2 ml) at 0-5°C. The mixture was stirred at room temperature overnight. The solution was poured into ice water, and the solid was filtered, washed with water until acid-free, and dried to give an orange solid corresponding to the mixture of two nitro derivatives. This solid (0.670 g, 2.3 mmol), iron powder (1.05 g) and 37% aqueous HCl (0.1 ml) were refluxed for 4 h in 21.6 ml of a mixture of EtOH, AcOH

and H_2O (8.7:8.7:4.2) with magnetic stirring. The solution was filtered on celite, diluted with water (20 ml) and extracted with EtOAc (3 x 50 ml). The combined organic layers were washed with saturated aqueous $NaHCO_3$ and H_2O (2 x 100 ml), dried over anhydrous Na_2SO_4 and evaporated of the solvent to achieve a mixture of the two amino derivatives, **139** and **140**, which were separated through silica gel column using petroleum ether/ethyl acetate mixture (60:40, v/v).

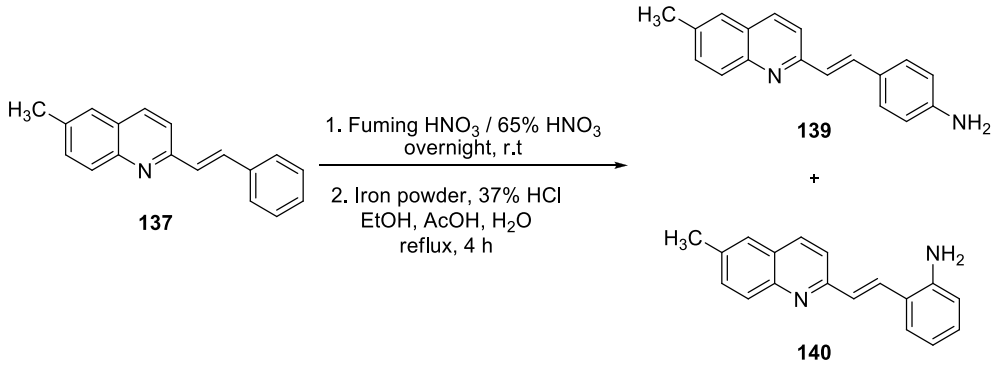

(*E*)-6-Methyl-4'-amino-2-styrylquinoline (139):

Overall yield: 68%; orange solid.

Elemental analysis (%) calcd for $C_{18}H_{16}N_2$: C 83.04, H 6.19, N 10.76; found: C 78.53, H 5.95, N 10.26.

Mp: 164 167 °C

IR (neat) ν: 3416, 3319, 3212, 3030, 2918, 1593, 1517, 1497, 1394, 1318, 1123 cm^{-1}.

^{1}H NMR (250 MHz, $CDCl_3$) δ 8.06 – 7.98 (m, 2H), 7.66 – 7.47 (m, 7H), 6.73 (d, *J* = 8.5 Hz, 2H), 3.87 (br s, 2H), 2.55 (s, 3H) ppm.

^{13}C NMR (63 MHz, $CDCl_3$) δ 156.3, 147.5, 147.1, 136.1, 136.0, 134.6, 132.3, 131.0, 129.1 (2C), 129.0, 127.5, 126.9, 125.7, 119.4, 115.5 (2C), 22.0.ppm.

MS (electrospray): 261 (M^+ + 1).

(*E*)-6-Methyl-2'-amino-2-styrylquinoline (140):

Yield: 28%; yellow solid.

Elemental analysis (%) calcd for $C_{18}H_{16}N_2$: C 83.04, H 6.19, N 10.76; found: C 82.24, H 6.20, N 10.82.

Mp: 167 – 170 °C

IR (neat) ν: 3363, 3212, 1637, 1596, 1456, 1319, 963 cm^{-1}.

^{1}H NMR (250 MHz, $CDCl_3$) δ 8.07 (d, *J* = 8.6 Hz, 1H), 8.01 (d, *J* = 9.2 Hz, 1H), 7.85 (d, *J* = 16.2 Hz, 1H), 7.62 (d, *J* = 8.6 Hz, 1H), 7.58 7.55 (m, 3H), 7.30 (d, *J* = 16.0 Hz, 1H), 7.18 (td, *J* = 7.9, 1.5 Hz, 1H), 6.85 (t, *J* = 7.5 Hz, 1H), 6.77 (dd, *J* = 8.0, 0.9 Hz, 1H), 4.02 (br s, 2H), 2.57 (s, 3H) ppm.

^{13}C NMR (63 MHz, $CDCl_3$) δ 155.6, 147.0, 145.1, 136.5, 136.3, 132.5, 130.0, 129.9, 129.9, 129.1, 127.9, 127.7, 126.9, 123.1, 120.1, 119.5, 116.9, 22.0 ppm.

MS (electrospray): 261 (M^+ + 1).

9.5.1.4. 6-Methyl-4'-amino-2-styrylquinolinium hydrochloride (139·HCl):

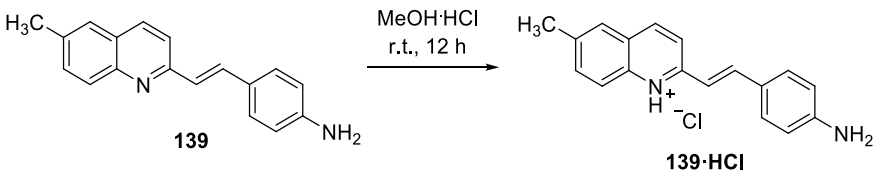

The hydrochloride salt was prepared by adding compound **139** (0.5 g, 1.9 mmol) to a solution of methanol saturated with HCl (3 ml). The resulting suspension was

stirred overnight, the precipitate was filtered and dried to obtain **139·HCl** in 98% yield as a red solid.

Elemental analysis (%) calcd for $C_{18}H_{17}ClN_2$: C 72.84, H 5.77, N 9.44; found: C 72.98, H 5.81, N 9.40.

^{1}H NMR (250 MHz, D_2O) δ 8.31 (d, *J* = 8.9 Hz, 1H), 7.70 (d, *J* = 9.0 Hz, 1H), 7.45 – 7.41 (m, 3H), 7.33 (d, *J* = 16.3 Hz, 1H), 7.21 (d, *J* = 8.3 Hz, 2H), 6.85 (d, *J* = 8.5 Hz, 2H), 6.56 (d, *J* = 16.2 Hz, 1H), 2.14 (s, 3H) ppm.

^{13}C NMR (63 MHz, D_2O) δ 150.5, 144.5, 142.8, 140.7, 138.0, 137.0, 135.1, 131.1, 130.3 (2C), 127.7, 127.0, 121.2 (2C), 118.9, 117.7, 116.2, 20.8 ppm.

9.5.2. Preparation of styrylquinoline compounds under focused MW irradiation

9.5.2.1. Synthesis of quinaldines

An equimolar (3 mmol) mixture of the suitable arylamine and ethyl vinyl ether (0.541 g, 7.5 mmol) was dissolved in acetonitrile (20 ml). 15 mol% of CAN (0.247 g) was added to the stirred solution, and stirring was continued for 1 h. Upon completion of the reaction, as indicated by TLC, the mixture was extracted with dichloromethane (2 x 20 ml), dried (anhydrous Na_2SO_4) and evaporated. The resulting crude product was dissolved in 20 ml of toluene and refluxed for two hours in presence of 200 mg of 10% Pd on activated carbon (Pd–C). Upon completion of the reaction, the mixture was filtered through Celite and the solvent was evaporated under reduced pressure. The crude product was purified through silica gel column using a petroleum ether/ethyl acetate mixture (95:05, v/v) as mobile phase.

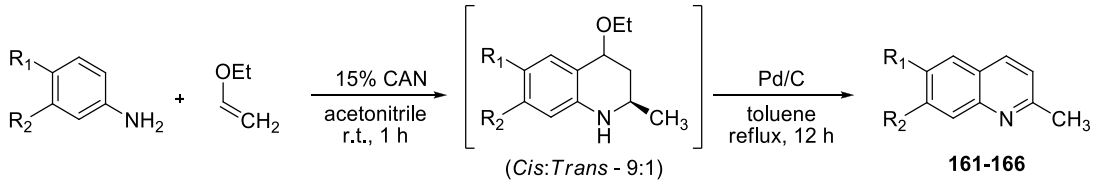

Cmpd.	R_1	R_2
161	H	H
162	CH_3	H
163	Cl	H
164	OMe	H
165	H	CH_3
166	H	Cl

2-methylquinoline (161):

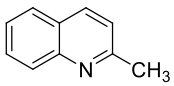

Prepared from aniline (0.279 g, 3 mmol); overall yield: 78 %; pale yellow oil.

^{1}H NMR (250 MHz, $CDCl_3$) δ 8.08 (d, *J* = 8.2 Hz, 1H), 8.06 (d, *J* = 8.2 Hz, 1H), 7.81 (dd, *J* = 8.1, 1.2 Hz, 1H), 7.75 – 7.68 (m, 1H), 7.52 (ddd, *J* = 8.1, 7.0, 1.2 Hz, 1H), 7.32 (d, *J* = 8.4 Hz, 1H), 2.79 (s, 3H) ppm.

2,6-dimethylquinoline (162):

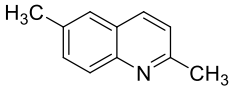

Prepared from *p*-toluidine (0.321 g, 3 mmol); overall yield: 82 %; yellow oil.

^{1}H NMR (250 MHz, $CDCl_3$) δ 7.83 (d, *J* = 8.7 Hz, 2H), 7.43 – 7.37 (m, 2H), 7.12 (d, *J* = 8.3 Hz, 1H), 2.62 (s, 3H), 2.40 (s, 3H) ppm.

^{13}C NMR (63 MHz, $CDCl_3$) δ 158.4, 146.7, 136.1, 135.8, 132.1, 128.6, 126.9, 126.8, 122.4, 25.6, 21.9 ppm.

6-chloro-2-methylquinoline (163):

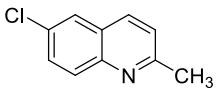

Prepared from 4-chloroaniline (0.383 g, 3 mmol); overall yield: 67 %; yellow oil.

^{1}H NMR (250 MHz, $CDCl_3$) δ 7.95 (d, *J* = 5.2 Hz, 1H), 7.91 (d, *J* = 4.6 Hz, 1H), 7.72 (d, *J* = 2.3 Hz, 1H), 7.60 (dd, *J* = 9.0, 2.3 Hz, 1H), 7.28 (d, *J* = 8.5 Hz, 1H), 2.73 (s, 4H) ppm.

^{13}C NMR (63 MHz, $CDCl_3$) δ 159.7, 146.6, 135.6, 131.7, 130.6 (2C), 127.4, 126.6, 123.3, 25.7 ppm.

6-methoxy-2-methylquinoline (164):

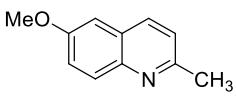

Prepared from *p*-anisidine (0.370 g, 3 mmol); overall yield: 70 %; orange oil.

^{1}H NMR (250 MHz, $CDCl_3$) δ 7.92 (d, *J* = 9.7 Hz, 2H), 7.36 – 7.31 (m, 1H), 7.22 (dd, *J* = 8.4, 1.3 Hz, 1H), 7.02 (d, *J* = 2.6 Hz, 1H), 3.89 (s, 3H), 2.70 (s, 3H) ppm.

^{13}C NMR (63 MHz, $CDCl_3$) δ 157.5, 156.7, 144.3, 135.5, 130.4, 127.7, 122.6, 122.3, 105.6, 55.9, 25.4 ppm.

2,7-dimethylquinoline (165):

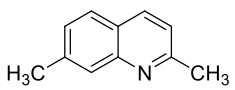

Prepared from *m*-toluidine (0.321 g, 3 mmol); overall yield: 40 %; white solid.

^{1}H NMR (250 MHz, $CDCl_3$) δ 8.17 (d, *J* = 8.6 Hz, 1H), 7.97 – 7.81 (m, 1H), 7.65 – 7.53 (m, 1H), 7.30 – 7.17 (m, 2H), 2.72 (s, 3H), 2.64 (s, 3H) ppm.

7-chloro-2-methylquinoline(166):

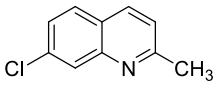

Prepared from 3-chloroaniline (0.383 g, 3 mmol); overall yield: 45 %; grey solid.

^{1}H NMR (250 MHz, $CDCl_3$) δ 8.09 – 8.02 (m, 2H), 7.74 (d, *J* = 8.7 Hz, 1H), 7.47 (dd, *J* = 8.7, 2.0 Hz, 1H), 7.32 (d, *J* = 8.5 Hz, 1H), 2.77 (s, 2H) ppm.

2-methylquinolin-7-ol (168):

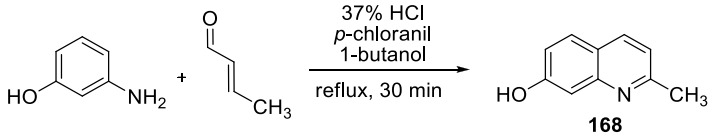

168

m-Aminophenol (775 mg, 7.1 mmol) was dissolved in 2 ml of concentrated hydrochloric acid (12N), and then *p*-chloranil (1.75 g, 7.1 mmol) and 1-butanol (2.5 ml) were added. The mixture was stirred and heated to reflux (105°C) at which point a solution of crotonaldehyde (0.8 ml, 9.23 mmol) in 1-butanol (0.2 ml) was added to the refluxing solution dropwise over 20 min. After the addition was complete, the mixture was allowed to reflux for another 30 minutes. The 1-butanol was removed by reduced pressure, and the residue was dissolved in water and washed with ether. The aqueous layer was neutralized with 10% NaOH and extracted with EtOAc. The EtOAc layer was dried over Na_2SO_4 and evaporated. The crude material was purified through column on silica using EtOAc/hexane (6:4) as mobile phase to yield **168** in 40% yield as a white solid.

^{1}H NMR (250 MHz, $CDCl_3$) δ 7.87 (d, *J* = 8.9 Hz, 1H), 7.35 – 7.30 (m, 1H), 7.21 (s, 1H), 7.04 (d, *J* = 8.3 Hz, 1H), 6.77 (dd, *J* = 8.8, 2.1 Hz, 1H), 2.66 (s, 3H) ppm.

7-methoxy-2-methylquinoline (167):

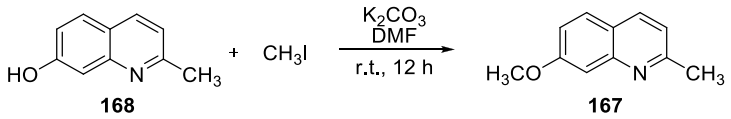

7-Hydroxyquinaldine **168** (3.18 g, 20 mmol) and K_2CO_3 (5.52 g, 40 mmol) were dissolved in 18 ml of DMF. The CH_3I was added to the mixture, and the reaction was stirred overnight at r.t. When the reaction was finished, the CH_3I was removed by evaporation. The residue was diluted with 150 ml of water and extracted with EtOAc. The organic layer was dried over anhydrous Na_2SO_4 and evaporated under reduced pressure. The crude material was purified through column on silica using EtOAc/petroleum ether (1:1) as mobile phase to afford **167** in 78% yield as brown solid.

^{1}H NMR (250 MHz, $CDCl_3$) δ 7.99 (d, *J* = 8.3 Hz, 1H), 7.68 (d, *J* = 8.9 Hz, 1H), 7.40 (d, *J* = 2.4 Hz, 1H), 7.21 – 7.15 (m, 2H), 3.98 (s, 3H), 2.77 (s, 3H) ppm.

9.5.2.2. Preparation of 2-styrylquinolines by aldol condensation

The suitable quinaldine derivative (1 mmol) and the corresponding aromatic aldehyde (1 equiv) were suspended in acetic anhydride (0.5 ml) in a pressure-tight microwave tube containing a stirring bar. The reaction mixture was heated under microwave irradiation for 1 h at 130-180 °C, with an irradiation power of 200 W. The solvent was removed under reduced pressure to give a black residue which was purified by chromatography through a silica column using petroleum ether/ethyl acetate (90:10, v/v) as the mobile phase to give compounds **169-199.**

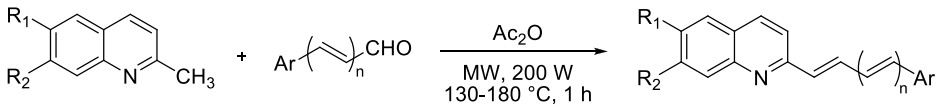

169-199

n = 0, 1

Cmpd.	R_1	R_2	Ar	n
169	Me	H		0
170	Cl	H		0
171	OMe	H		0
172	Me	H		0
173	Cl	H		0
174	OMe	H		0
175	H	H		0
176	Me	H		0
177	Cl	H		0
178	OMe	H		0
179	H	Me		0
180	H	Cl		0
181	H	H		0
182	Me	H		0
183	Cl	H		0
184	OMe	H	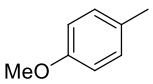	0
185	H	Me		0
186	H	Cl		0
187	H	OMe		0

Cmpd.	R_1	R_2	Ar	n
188	Me	H	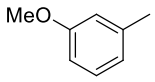	0
189	Cl	H		0
190	H	H		0
191	Me	H		0
192	Cl	H	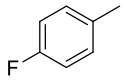	0
193	OMe	H		0
194	H	Me		0
195	H	OMe		0
196	H	OMe		0
197	Cl	H		1
198	Me	H	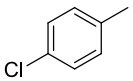	1
199	OMe	H	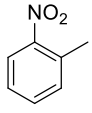	1

(*E*)-6-methyl-2-(2-(pyridin-2-yl)vinyl)quinoline (169):

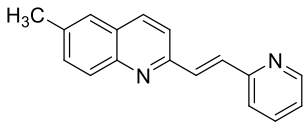

Prepared from **162** (0.157 g, 1 mmol) and pirydine-2-carbaldehyde (0.107 g, 1 mmol); temperature of reaction: 130 °C; yield: 87 %; brown solid.

Elemental analysis (%) calcd for $C_{17}H_{14}N_2$: C 82.90, H 5.73, N 11.37; found: C 83.19, H 5.59, N 11.33.

Mp: 120 – 123 °C

IR (neat) ν: 2918, 1585, 1558, 1495, 1468, 1429, 975, 825 cm^{-1}.

^{1}H NMR (250 MHz, $CDCl_3$) δ 8.57 (ddd, *J* = 4.8, 1.6, 0.8 Hz, 1H), 7.98 (d, *J* = 8.6 Hz, 1H), 7.92 (d, *J* = 9.3 Hz, 1H), 7.73 (d, *J* = 4.2 Hz, 2H), 7.63 (ddd, *J* = 7.6, 3.3, 1.8 Hz, 1H), 7.57 (d, *J* = 8.5 Hz, 1H), 7.51 – 7.44 (m, 3H), 7.12 (ddd, *J* = 7.4, 4.8, 1.2 Hz, 1H), 2.46 (s, 3H) ppm.

^{13}C NMR (63 MHz, $CDCl_3$) δ 155.6, 154.9, 150.2, 147.3, 137.1, 136.8, 136.3, 133.6, 133.1, 132.5, 129.5, 128.1, 126.9, 123.1, 123.1, 120.8, 22.0 ppm.

(*E*)-6-methyl-2-(2-(pyridin-2-yl)vinyl)quinoline (170):

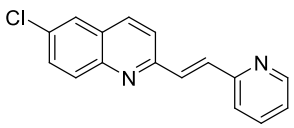

Prepared from **163** (0.178 g, 1 mmol) and pirydine-2-carbaldehyde (0.107 g, 1 mmol); temperature of reaction: 130 °C; yield: 91 %; pale brown solid.

Elemental analysis (%) calcd for $C_{16}H_{11}ClN_2$: C 72.05, H 4.16, N 10.50; found: C 72.27, H 4.16, N 10.59.

Mp: 138 – 141 °C

IR (neat) ν: 1590, 1581, 1562, 1488, 1426, 1069, 983, 822 cm^{-1}.

^{1}H NMR (250 MHz, $CDCl_3$) δ 8.69 – 8.67 (m, 1H), 8.09 – 8.03 (m, 2H), 7.84 (s, 2H), 7.79 (d, *J* = 2.3 Hz, 1H), 7.77 – 7.64 (m, 3H), 7.59 – 7.55 (m, 1H), 7.24 (ddd, *J* = 7.5, 4.8, 1.1 Hz, 1H) ppm.

^{13}C NMR (63 MHz, $CDCl_3$) δ 156.0, 155.3, 150.3, 147.1, 137.1, 136.0, 134.5, 132.5, 132.5, 131.4, 131.1, 128.5, 126.7, 123.4 (2C), 121.7 ppm.

(*E*)-6-methoxy-2-(2-(pyridin-2-yl)vinyl)quinoline (171):

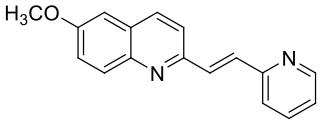

Prepared from **164** (0.173 g, 1 mmol) and pirydine-2-carbaldehyde (0.107 g, 1 mmol); temperature of reaction: 130 °C; yield: 75%; pale brown solid.

Elemental analysis (%) calcd for $C_{17}H_{14}N_2O$: C 77.84, H 5.38, N 10.68; found: C 77.15, H 5.32, N 10.50.

Mp: 107 – 110 °C

IR (neat) ν: 1613, 1590, 1558, 1499, 1463, 1427, 1218, 1023, 975, 848 cm^{-1}.

^{1}H NMR (250 MHz, $CDCl_3$) δ 8.67 (ddd, *J* = 4.8, 1.7, 0.8 Hz, 1H), 8.04 (t, *J* = 9.4 Hz, 2H), 7.88 – 7.56 (m, 5H), 7.39 (dd, *J* = 9.2, 2.8 Hz, 1H), 7.22 (ddd, *J* = 7.4, 4.8, 1.2 Hz, 1H), 7.08 (d, *J* = 2.8 Hz, 1H), 3.96 (s, 3H) ppm.

^{13}C NMR (63 MHz, $CDCl_3$) δ 158.2, 155.7, 153.4, 150.2, 144.8, 137.0, 135.6, 133.1, 132.9, 131.3, 129.0, 123.1, 123.0, 122.9, 121.1, 105.5, 56.0 ppm.

(E)-6-methyl-2-(2-(pyridin-3-yl)vinyl)quinoline (172):

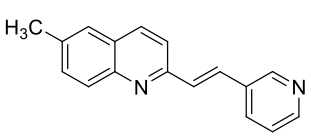

Prepared from **162** (0.157 g, 1 mmol) and pirydine-3-carbaldehyde (0.107 g, 1 mmol); temperature of reaction: 130 °C; yield: 62%; pale yellow solid.

Elemental analysis (%) calcd for $C_{17}H_{14}N_2$: C 82.90, H 5.73, N 11.37; found: C 82.03, H 5.64, N 11.38.

Mp: 105 – 108 °C

IR (neat) ν: 3025, 1589, 1555, 1493, 1412, 1215, 963, 827 cm^{-1}.

^{1}H NMR (250 MHz, $CDCl_3$) δ 8.86 (d, *J* = 2.0 Hz, 1H), 8.57 (dd, *J* = 4.8, 1.4 Hz, 1H), 8.10 (d, *J* = 8.6 Hz, 1H), 8.03 – 7.96 (m, 2H), 7.69 (d, *J* = 9.8 Hz, 1H), 7.64 (d, *J* = 1.9 Hz, 1H), 7.60 – 7.56 (m, 2H), 7.46 (d, *J* = 16.4 Hz, 1H), 7.36 (dd, *J* = 7.9, 4.8 Hz, 1H), 2.57 (s, 3H) ppm.

^{13}C NMR (63 MHz, $CDCl_3$) δ 154.7, 149.8, 149.6, 147.2, 136.9, 136.3, 133.6, 132.8, 132.7, 131.5, 130.4, 129.4, 128.0, 126.9, 124.1, 119.8, 22.0 ppm.

(*E*)-6-chloro-2-(2-(pyridin-3-yl)vinyl)quinoline (173):

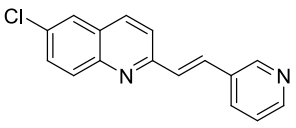

Prepared from **163** (0.178 g, 1 mmol) and pirydine-3-carbaldehyde (0.107 g, 1 mmol); temperature of reaction: 130 °C; yield: 86%; yellow solid.

Elemental analysis (%) calcd for $C_{16}H_{11}ClN_2$: C 72.05, H 4.16, N 10.50; found: C 72.22, H 4.16, N 10.67.

Mp: 130 – 133 °C

IR (neat) ν: 3030, 1595, 1547, 1491, 1189, 1072, 962, 880, 817 cm^{-1}.

^{1}H NMR (250 MHz, $CDCl_3$) δ 8.87 (d, *J* = 2.1 Hz, 1H), 8.59 (dd, *J* = 4.8, 1.6 Hz, 1H), 8.10 (d, *J* = 8.6 Hz, 1H), 8.05 (d, *J* = 9.0 Hz, 1H), 7.99 (dt, *J* = 8.0, 1.8 Hz, 1H), 7.81 (d, *J* = 2.3 Hz, 1H), 7.74 (d, *J* = 13.1 Hz, 1H), 7.71 – 7.66 (m, 2H), 7.45 (d, *J* = 16.4 Hz, 1H), 7.37 (dd, *J* = 8.0, 4.8 Hz, 1H) ppm.

^{13}C NMR (63 MHz, $CDCl_3$) δ 155.8, 150.0, 149.7, 147.0, 136.1, 133.8, 132.6, 132.5, 131.4, 131.3 (2C), 130.9, 128.4, 126.7, 124.1, 120.8 ppm.

(*E*)-6-methoxy-2-(2-(pyridin-3-yl)vinyl)quinoline (174):

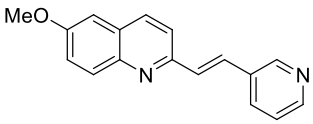

Prepared from **164** (0.173 g, 1 mmol) and pirydine-3-carbaldehyde (0.107 g, 1 mmol); temperature of reaction: 130 °C; yield: 83%; yellow solid.

Elemental analysis (%) calcd for $C_{17}H_{14}N_2O$: C 77.84, H 5.38, N 10.68; found: C 76.89, H 5.41, N 10.53.

Mp: 118 – 121 °C

IR (neat) ν: 1613, 1594, 1496, 1375, 1222, 1021, 964, 821 cm^{-1}.

^{1}H NMR (250 MHz, $CDCl_3$) δ 8.84 (d, *J* = 2.0 Hz, 1H), 8.56 (dd, *J* = 4.8, 1.5 Hz, 1H), 8.08 – 7.94 (m, 3H), 7.67 – 7.60 (m, 2H), 7.47 – 7.31 (m, 3H), 7.09 (d, *J* = 2.8 Hz, 1H), 3.96 (s, 3H) ppm.

^{13}C NMR (63 MHz, $CDCl_3$) δ 158.3, 153.3, 149.6, 149.5, 144.7, 135.7, 133.6, 132.8, 131.4, 131.1, 129.7, 128.9, 124.1, 123.0, 120.1, 105.6, 56.0 ppm.

(*E*)-2-(2-(pyridin-4-yl)vinyl)quinoline (175):

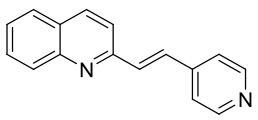

Prepared from **161** (0.143 g, 1 mmol) and pirydine-4-carbaldehyde (0.107 g, 1 mmol); temperature of reaction: 130 °C; yield: 65%; yellow solid.

Elemental analysis (%) calcd for $C_{16}H_{12}N_2$: C 82.73, H 5.21, N 12.06; found: C 82.56, H 5.25, N 12.07.

Mp: 120 123 °C

IR (neat) ν: 1673, 1596, 1522, 1474, 1413, 1139, 827 cm^{-1}.

^{1}H NMR ($CDCl_3$, 250 MHz) δ 7.87 − 7.51 (m, 8H), 8.13 (d, *J* = 8.5, 1H), 8.22 (d, *J* = 8.6, 1H), 8.69 8.67 (m, 2H) ppm.

^{13}C NMR ($CDCl_3$, 63 MHz) δ 155.1, 150.8 (2C), 148.6, 144.2, 137.1, 133.6, 131.9, 130.4, 129.8, 128.1, 127.9, 127.2, 121.8 (2C), 120.0 ppm.

(*E*)-6-methyl-2-(2-(pyridin-4-yl)vinyl)quinoline (176):

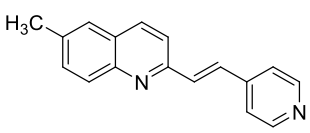

Prepared from **162** (0.157 g, 1 mmol) and pirydine-4-carbaldehyde (0.107 g, 1 mmol); temperature of reaction: 130 °C; yield: 76%; yellow solid.

Elemental analysis (%) calcd for $C_{17}H_{14}N_2$: C 82.90, H 5.73, N 11.37; found: C 82.36, H 5.64, N 11.16.

Mp: 131 – 134 °C

IR (neat) ν: 3028, 1670, 1593, 1579, 1408, 1373, 955, 832 cm^{-1}.

^{1}H NMR (250 MHz, $CDCl_3$) δ 8.66 – 8.64 (m, 2H), 8.10 (d, *J* = 8.5 Hz, 1H), 8.01 (d, *J* = 9.2 Hz, 1H), 7.65 (d, *J* = 8.6 Hz, 1H), 7.59 – 7.57 (m, 4H), 7.49 (dd, *J* = 4.6, 1.5 Hz, 2H), 2.57 (s, 3H) ppm.

^{13}C NMR (63 MHz, $CDCl_3$) δ 154.3, 150.8 (2C), 147.2, 144.3, 137.2, 136.4, 133.8, 132.8, 131.3, 129.5, 128.1, 126.9, 121.7 (2C), 120.0, 22.1 ppm.

(*E*)-6-chloro-2-(2-(pyridin-4-yl)vinyl)quinoline (177):

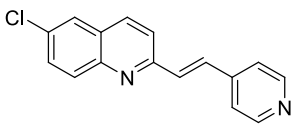

Prepared from **163** (0.178 g, 1 mmol) and pirydine-4-carbaldehyde (0.107 g, 1 mmol); temperature of reaction: 130 °C; yield: 80%; yellow solid.

Elemental analysis (%) calcd for $C_{16}H_{11}ClN_2$: C 72.05, H 4.16, N 10.50; found: C 71.67, H 4.23, N 9.95.

Mp: 138 – 141 °C

IR (neat) ν: 3019, 1667, 1592, 1581, 1407, 1372, 1072, 955, 826 cm^{-1}.

^{1}H NMR (250 MHz, $CDCl_3$) δ 8.69 (d, *J* = 5.7 Hz, 2H), 8.12 (d, *J* = 8.6 Hz, 1H), 8.06 (d, *J* = 9.0 Hz, 1H), 7.83 (d, *J* = 2.1 Hz, 1H), 7.72 – 7.68 (m, 2H), 7.62 (d, *J* = 14.2 Hz, 2H), 7.53 – 7.51 (m, 2H) ppm.

^{13}C NMR (63 MHz, $CDCl_3$) δ 155.3, 150.7 (2C), 147.0, 144.2, 136.2, 133.3, 132.9, 132.3, 131.4 (2C), 128.6, 126.7, 121.8 (2C), 121.0 ppm.

(*E*)-6-methoxy-2-(2-(pyridin-4-yl)vinyl)quinoline (178):

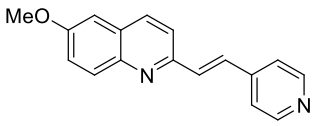

Prepared from **164** (0.173 g, 1 mmol) and pirydine-4-carbaldehyde (0.107 g, 1 mmol); temperature of reaction: 130 °C; yield: 85%; yellow solid.

Elemental analysis (%) calcd for $C_{17}H_{14}N_2O$: C 77.84, H 5.38, N 10.68; found: C 78.12, H 5.23, N 10.40.

Mp: 127 – 130 °C

IR (neat) ν: 1617, 1593, 1500, 1479, 1409, 1378, 1225, 1026, 834 cm^{-1}.

^{1}H NMR (250 MHz, $CDCl_3$) δ 8.67 – 8.65 (m, 2H), 8.09 (d, *J* = 8.5 Hz, 1H), 8.02 (d, *J* = 9.3 Hz, 1H), 7.66 (d, *J* = 8.6 Hz, 1H), 7.58 (s, 2H), 7.50 (dd, *J* = 4.6, 1.6 Hz, 2H), 7.42 (dd, *J* = 9.2, 2.8 Hz, 1H), 7.10 (d, *J* = 2.8 Hz, 1H), 3.97 (s, 3H) ppm.

^{13}C NMR (63 MHz, $CDCl_3$) δ 158.5, 152.7, 150.5 (2C), 144.7, 144.6, 135.8, 133.8, 131.3, 130.6, 129.2, 123.2, 121.7 (2C), 120.4, 105.5, 56.0 ppm.

(*E*)-7-methyl-2-(2-(pyridin-4-yl)vinyl)quinoline (179):

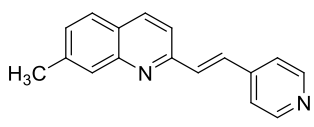

Prepared from **165** (0.157 g, 1 mmol) and pirydine-4-carbaldehyde (0.107 g, 1 mmol); temperature of reaction: 130 °C; yield: 45%; yellow solid.

Elemental analysis (%) calcd for $C_{17}H_{14}N_2$: C 82.90, H 5.73, N 11.37; found: C 82.75, H 5.44, N 11.01.

Mp: 136 – 139 °C

IR (neat) ν: 1671, 1620, 1592, 1414, 1301, 984, 835, 812 cm^{-1}.

^{1}H NMR (250 MHz, $CDCl_3$) δ 8.66 – 8.64 (m, 2H), 8.35 (dd, *J* = 8.7, 0.6 Hz, 1H), 7.97 (d, *J* = 8.5 Hz, 1H), 7.69 (d, *J* = 8.8 Hz, 1H), 7.64 – 7.58 (m, 3H), 7.49 (dd, *J* = 4.6, 1.6 Hz, 2H), 7.37 – 7.36 (m, 1H), 2.71 (s, 3H) ppm.

^{13}C NMR (63 MHz, $CDCl_3$) δ 154.6, 150.8 (2C), 148.9, 144.3, 134.9, 133.6, 133.6, 131.7, 130.2, 128.1, 127.7, 127.4, 121.8 (2C), 119.6, 19.1 ppm.

(*E*)-7-chloro-2-(2-(pyridin-4-yl)vinyl)quinoline (180):

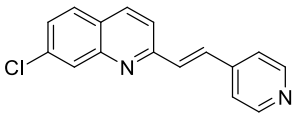

Prepared from **166** (0.178 g, 1 mmol) and pirydine-4-carbaldehyde (0.107 g, 1 mmol); temperature of reaction: 130 °C; yield: 87%; orange solid.

Elemental analysis (%) calcd for $C_{16}H_{11}ClN_2$: C 72.05, H 4.16, N 10.50; found: C 72.45, H 4.34, N 10.81.

Mp: 149 – 152 °C

IR (neat) ν: 3339, 1591, 1495, 1409, 1216, 1143, 1065, 980, 836 cm^{-1}.

^{1}H NMR (250 MHz, $CDCl_3$) δ 8.70 – 8.67 (m, 2H), 8.19 (d, *J* = 8.6 Hz, 1H), 8.13 (d, *J* = 2.0 Hz, 1H), 7.77 (d, *J* = 16.5 Hz, 1H), 7.73 (d, *J* = 17.8 Hz, 1H), 7.67 (d, *J* = 2.3 Hz, 1H), 7.57 (d, *J* = 11.0 Hz, 1H), 7.54 – 7.50 (m, 3H) ppm.

^{13}C NMR (63 MHz, $CDCl_3$) δ 156.0, 150.8 (2C), 149.1, 144.0, 136.9, 136.3, 133.1, 132.7, 129.2, 128.8, 128.1, 126.4, 121.8 (2C), 120.4 ppm.

(*E*)-2-(4-methoxystyryl)quinoline (181):

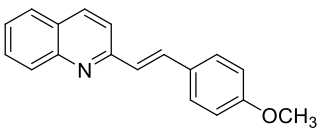

Prepared from **161** (0.143 g, 1 mmol) and 4-methoxybenzaldehyde (0.136 g, 1 mmol); temperature of reaction: 180 °C; yield: 70%; white solid.

Elemental analysis (%) calcd for $C_{18}H_{15}NO$: C 82.73, H 5.79, N 5.36; found: C 82.35, H 6.91, N 5.01.

Mp: 128 – 131 °C

IR (neat) ν: 1615, 1534, 1425, 982, 836 cm^{-1}.

^{1}H NMR (250 MHz, $CDCl_3$) δ 8.15 (d, *J* = 8.6 Hz, 1H), 8.10 (d, *J* = 8.4 Hz, 1H), 7.82 (d, *J* = 8.4 Hz, 1H), 7.77 – 7.61 (m, 5H), 7.55 – 7.49 (m, 1H), 7.32 (d, *J* = 16.2 Hz, 1H), 6.98 (d, *J* = 8.7 Hz, 2H), 3.89 (s, 3H) ppm.

^{13}C NMR (63 MHz, $CDCl_3$) δ 163.9, 160.4, 155.9, 136.2, 136.0, 134.1, 131.0, 129.8, 129.1, 128.9 (2C), 127.6, 126.8, 119.5 (2C), 114.6, 114.0, 55.7 ppm.

(*E*)-2-(4-methoxystyryl)-6-methylquinoline (182):

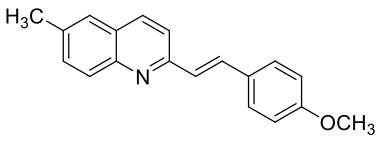

Prepared from **162** (0.157 g, 1 mmol) and 4-methoxybenzaldehyde (0.136 g, 1 mmol); temperature of reaction: 180 °C; yield: 93%; yellow solid.

Elemental analysis (%) calcd for $C_{19}H_{17}NO$: C 82.88, H 6.22, N 5.09; found: C 82.49, H 5.98, N 5.23.

Mp: 155 – 158 °C

IR (neat) ν: 1651, 1482, 1333, 1215, 981, 816 cm^{-1}.

^{1}H NMR (250 MHz, $CDCl_3$) δ 8.06 (d, *J* = 8.6 Hz, 1H), 7.99 (d, *J* = 9.3 Hz, 1H), 7.67 – 7.55 (m, 6H), 7.30 (d, *J* = 16.3 Hz, 1H), 6.97 (d, *J* = 8.8 Hz, 2H), 3.89 (s, 3H), 2.57 (s, 3H) ppm.

^{13}C NMR (63 MHz, $CDCl_3$) δ 163.9, 160.4, 155.9, 136.3, 136.1, 134.2, 132.4, 132.1, 131.0, 129.8, 129.2, 129.0 (2C), 126.9, 119.5, 114.7 (2C), 55.8, 22.0 ppm.

(*E*)-6-chloro-2-(4-methoxystyryl)quinoline (183):

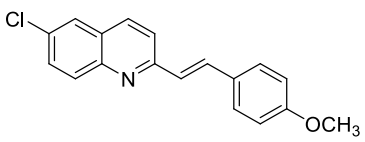

Prepared from **163** (0.178 g, 1 mmol) and 4-methoxybenzaldehyde (0.136 g, 1 mmol); temperature of reaction: 180 °C; yield: 80%; pale yellow solid.

Elemental analysis (%) calcd for $C_{18}H_{14}ClNO$: C 73.10, H 4.77, N 4.74; found: C 73.30, H 5.09, N 4.76.

Mp: 154 157 °C

IR (neat) ν: 1592, 1510, 1487, 1290, 1255, 1179, 1026, 968, 824 cm^{-1}.

^{1}H NMR (250 MHz, $CDCl_3$) δ 8.05 (d, *J* = 8.5 Hz, 1H), 8.02 (d, *J* = 8.6 Hz, 1H), 7.78 (d, *J* = 2.2 Hz, 1H), 7.71 (d, *J* = 3.8 Hz, 1H), 7.68 – 7.60 (m, 4H), 7.28 (d, *J* = 16.3 Hz, 1H), 6.97 (d, *J* = 8.7 Hz, 2H), 3.89 (s, 3H) ppm.

^{13}C NMR (63 MHz, $CDCl_3$) δ 160.7, 157.0, 147.1, 135.7, 135.0, 131.9, 131.0, 131.0, 129.5, 129.1 (2C), 128.1, 126.8, 126.6, 120.5, 114.7 (2C), 55.8 ppm.

(*E*)-6-methoxy-2-(4-methoxystyryl)quinoline (184):

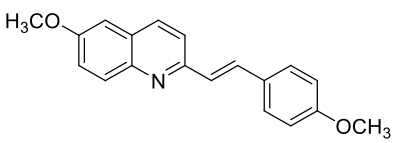

Prepared from **164** (0.173 g, 1 mmol) and 4-methoxybenzaldehyde (0.136 g, 1 mmol); temperature of reaction: 180 °C; yield: 80%; yellow solid.

Elemental analysis (%) calcd for $C_{19}H_{17}NO_2$: C 78.33, H 5.88, N 4.81; found: C 77.46, H 5.87, N 4.93.

Mp: 155 – 158 °C

IR (neat) ν: 1591, 1508, 1479, 1248, 1222, 1173, 1025, 829 cm^{-1}.

^{1}H NMR (250 MHz, $CDCl_3$) δ 8.03 (d, *J* = 9.0 Hz, 1H), 7.99 (d, *J* = 9.5 Hz, 1H), 7.66 – 7.57 (m, 4H), 7.38 (dd, *J* = 9.2, 2.8 Hz, 1H), 7.27 (d, *J* = 16.4 Hz, 1H), 7.08 (d, *J* = 2.7 Hz, 1H), 6.96 (d, *J* = 8.8 Hz, 2H), 3.96 (s, 3H), 3.88 (s, 3H) ppm.

^{13}C NMR (63 MHz, $CDCl_3$) δ 160.3, 157.9, 154.5, 144.7, 135.5, 133.3, 130.9, 129.9, 128.9 (2C), 128.5, 127.3, 122.6, 119.9, 114.6 (2C), 105.7, 56.0, 55.8 ppm.

(*E*)-2-(4-methoxystyryl)-7-methylquinoline (185):

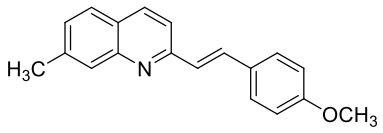

Prepared from **165** (0.157 g, 1 mmol) and 4-methoxybenzaldehyde (0.136 g, 1 mmol); temperature of reaction: 180 °C; yield: 77%; white solid.

Elemental analysis (%) calcd for $C_{19}H_{17}NO$: C 82.88, H 6.22, N 5.09; found: C 82.57, H 6.18, N 5.32.

Mp: 133 135 °C

IR (neat) ν: 1594, 1513, 1252, 1178, 1030, 814 cm^{-1}.

^{1}H NMR (250 MHz, $CDCl_3$) δ 8.31 (d, *J* = 8.8 Hz, 1H), 7.95 (d, *J* = 8.5 Hz, 1H), 7.72 – 7.58 (m, 5H), 7.35 – 7.29 (m, 2H), 6.97 (d, *J* = 8.7 Hz, 2H), 3.88 (s, 3H), 2.71 (s, 3H) ppm.

^{13}C NMR (63 MHz, $CDCl_3$) δ 160.5, 156.2, 148.9, 134.8, 134.3, 133.1, 129.9, 129.8, 129.0 (2C), 127.8, 127.3, 126.9, 126.9, 119.1, 114.7 (2C), 55.8, 19.1, ppm.

(*E*)-7-chloro-2-(4-methoxystyryl)quinoline (186):

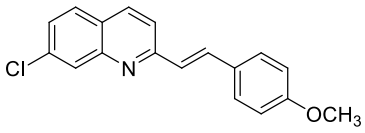

Prepared from **166** (0.178 g, 1 mmol) and 4-methoxybenzaldehyde (0.136 g, 1 mmol);

temperature of reaction: 180 °C; yield: 84%; white solid.

Elemental analysis (%) calcd for $C_{18}H_{14}ClNO$: C 73.10, H 4.77, N 4.74; found: C 73.19, H 4.81, N 4.86.

Mp: 149 151 °C

IR (neat) ν:1604, 1511, 1408, 1251, 1178, 1033, 970, 832 cm^{-1}.

^{1}H NMR (250 MHz, $CDCl_3$) δ 8.13 – 8.09 (m, 2H), 7.75 – 7.61 (m, 5H), 7.46 (dd, *J* = 8.6, 2.1 Hz, 1H), 7.23 (d, *J* = 16.1 Hz, 1H), 6.98 (d, *J* = 8.7 Hz, 2H), 3.89 (s, 3H) ppm.

^{13}C NMR (63 MHz, $CDCl_3$) δ 160.7, 157.7, 149.1, 136.4, 135.9, 135.2, 129.5, 129.2 (2C), 129.1, 128.5, 127.3, 126.7, 125.9, 120.0, 114.7 (2C), 55.8 ppm.

(*E*)-7-methoxy-2-(4-methoxystyryl)quinoline (187):

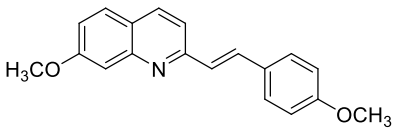

Prepared from **167** (0.173 g, 1 mmol) and 4-methoxybenzaldehyde (0.136 g, 1 mmol); temperature of reaction: 180 °C; yield: 81%; yellow solid.

Elemental analysis (%) calcd for $C_{19}H_{17}NO_2$: C 78.33, H 5.88, N 4.81; found: C 77.99, H 5.79, N 4.93.

Mp: 167 – 170 °C

IR (neat) ν: 1613, 1593, 1509, 1453, 1253, 1208, 1171, 1026, 837 cm^{-1}.

^{1}H NMR (250 MHz, $CDCl_3$) δ 8.06 (d, *J* = 8.5 Hz, 1H), 7.71 – 7.53 (m, 5H), 7.43 (d, *J* = 2.4 Hz, 1H), 7.28 (d, *J* = 16.1 Hz, 1H), 7.17 (dd, *J* = 7.3, 2.5 Hz, 1H), 6.97 (d, *J* = 8.8, 2H), 4.00 (s, 3H), 3.89 (s, 3H) ppm.

^{1}C NMR (63 MHz, $CDCl_3$) δ 161.3, 160.5, 156.9, 150.4, 136.3, 134.1, 129.8, 129.0 (2C), 128.9, 127.3, 122.8, 119.5, 117.6, 114.7 (2C), 107.05, 55.9, 55.8 ppm.

(*E*)-2-(3-methoxystyryl)-6-methylquinoline (188):

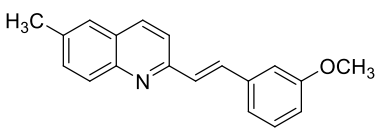

Prepared from **162** (0.157 g, 1 mmol) and 3-methoxybenzaldehyde (0.136 g, 1 mmol); temperature of reaction: 180 °C; yield: 65%; white solid.

Elemental analysis (%) calcd for $C_{19}H_{17}NO$: C 82.88, H 6.22, N 5.09; found: C 83.00, H 6.12, N 4.71.

Mp: 71 – 74 C°

IR (neat) ν: 2829, 1576, 1486, 1431, 1255, 1151, 1046, 823 cm^{-1}.

^{1}H NMR (250 MHz, $CDCl_3$) δ 8.08 (d, *J* = 8.6 Hz, 1H), 8.01 (d, *J* = 9.2 Hz, 1H), 7.69 (d, *J* = 3.9 Hz, 1H), 7.64 (d, *J* = 11.7 Hz, 1H), 7.59 – 7.56 (m, 2H), 7.42 (d, *J* = 16.4 Hz, 1H), 7.38 – 7.22 (m, 3H), 6.94 – 6.90 (m, 1H), 3.90 (s, 3H), 2.57 (s, 3H) ppm.

^{13}C NMR (63 MHz, $CDCl_3$) δ 160.3, 155.5, 147.2, 138.4, 136.6, 136.1, 134.2, 132.5, 130.2, 129.8, 129.3, 127.8, 126.9, 120.5, 119.6, 115.1, 112.2, 55.7, 22.0 ppm.

(*E*)-6-chloro-2-(3-methoxystyryl)quinoline (189):

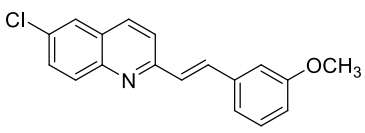

Prepared from **163** (0.178 g, 1 mmol) and 3-methoxybenzaldehyde (0.136 g, 1 mmol); temperature of reaction: 180 °C; yield: 90%; white solid.

Elemental analysis (%) calcd for $C_{18}H_{14}ClNO$: C 73.10, H 4.77, N 4.74; found: C 73.04, H 4.80, N 4.82.

Mp: 108 111 °C

IR (neat) ν: 1580, 1428, 1393, 1272, 969, 884 cm^{-1}.

^{1}H NMR (250 MHz, $CDCl_3$) δ 8.06 (*J* = 7.9 Hz, 1H), 8.03 (d, *J* = 8.1 Hz, 1H), 7.79 (d, *J* = 2.3 Hz, 1H), 7.72 – 7.65 (m, 3H), 7.39 (d, *J* = 16.6, 1H), 7.38 – 7.21 (m, 3H), 6.92 (ddd, *J* = 8.0, 2.5, 2.4 Hz, 1H), 3.89 (s, 3H) ppm.

^{13}C NMR (63 MHz, $CDCl_3$) δ 55.7, 112.4, 115.3, 120.5, 120.6, 126.7, 128.2, 129.2, 130.2, 131.0, 131.1, 132.2, 135.2, 135.8, 138.1, 147.0, 156.6, 160.3 ppm.

(*E*)-2-(4-fluorostyryl)quinoline (190):

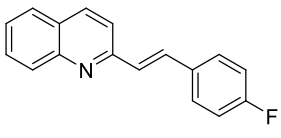

Prepared from **161** (0.143 g, 1 mmol) and 4-fluorobenzaldehyde (0.124 g, 1 mmol); temperature of reaction: 150 °C; yield: 65%; white solid.

Elemental analysis (%) calcd for $C_{17}H_{12}FN$: C 81.91, H 4.85, N 5.62; found: C 82.06, H 4.71, N 5.29.

Mp: 114 – 117 °C

IR (neat) ν: 1593, 1552, 1505, 1216, 826, 751 cm^{-1}.

^{1}H NMR (250 MHz, $CDCl_3$) δ 8.16 (d, *J* = 8.8 Hz, 1H), 8.11 (d, *J* = 8.5 Hz, 1H), 7.83 – 7.80 (m, 1H), 7.78 – 7.62 (m, 5H), 7.53 (ddd, *J* = 8.1, 7.0, 1.1 Hz, 1H), 7.35 (d, *J* = 16.3 Hz, 1H), 7.12 (dd, *J* = 9.6, 7.7 Hz, 2H) ppm.

^{13}C NMR (63 MHz, $CDCl_3$) δ 163.4 (d, *J* = 248.7 Hz), 156.2, 148.7, 136.8, 133.6, 133.1 (d, *J* = 3.4 Hz), 130.2, 129.6, 129.3 (d, *J* = 8.2 Hz, 2C), 129.1, 127.9, 127.8, 126.6, 119.7, 116.3 (d, *J* = 21.8 Hz, 2C). ppm.

(*E*)-2-(4-fluorostyryl)-6-methylquinoline (191):

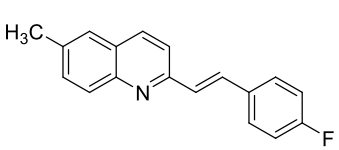

Prepared from **162** (0.157 g, 1 mmol) and 4-fluorobenzaldehyde (0.124 g, 1 mmol); temperature

of reaction: 150 °C; yield: 84%; white solid.

Elemental analysis (%) calcd for $C_{18}H_{14}FN$: C 82.11, H 5.36, N 5.32; found: C 81.73, H 5.27, N 4.95.

Mp: 145 – 148 °C

IR (neat) ν: 3031, 1740, 1591, 1507, 1373, 1215, 966, 830 cm^{-1}.

^{1}H NMR (250 MHz, $CDCl_3$) δ 8.07 (d, *J* = 8.6 Hz, 1H), 8.00 (d, *J* = 9.2 Hz, 1H), 7.69 – 7.56 (m, 6H), 7.33 (d, *J* = 16.6 Hz, 1H), 7.16 7.09 (m, 2H), 2.57 (s, 3H) ppm.

^{13}C NMR (63 MHz, $CDCl_3$) δ 167.21 (d, *J* = 245.8 Hz), 161.3, 155.4, 147.2, 136.6, 136.2, 133.3 (d, *J* = 3.4 Hz), 133.0, 132.5, 129.3 (2C), 129.1, 127.8, 126.9, 119.7, 116.2 (d, *J* = 21.7 Hz, 2C), 22.0 ppm.

(*E*)-6-chloro-2-(4-fluorostyryl)quinoline (192):

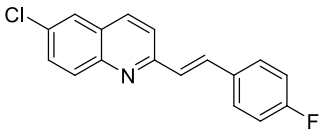

Prepared from **163** (0.178 g, 1 mmol) and 4-fluorobenzaldehyde (0.124 g, 1 mmol); temperature of reaction: 150 °C; yield: 95%; pale yellow solid.

Elemental analysis (%) calcd for $C_{17}H_{11}ClFN$: C 71.96, H 3.91, N 4.94; found: C 72.18, H 4.05, N 5.16.

Mp: 140 143 °C

IR (neat) ν: 1593, 1512, 1222, 968, 887, 830 cm^{-1}.

^{1}H NMR (250 MHz, $CDCl_3$) δ 8.06 8.04 (m, 2H), 7.80 (d, *J* = 2.2 Hz, 1H), , 7.73 7.61 (m, 5H), 7.30 (d, *J* = 16.3 Hz, 1H), 7.16 7.10 (m, 2H) ppm.

^{13}C NMR (63 MHz, $CDCl_3$) δ 163.4 (d, *J* = 249.2 Hz), 156.4, 147.0, 134.0, 135.9, 133.0, 132.3, 131.2, 131.1, 129.4 (d, *J* = 8.2 Hz, 2C), 128.6, 128,3, 126.6, 120.7, 116.3 (d, *J* = 21.8 Hz, 2C), ppm.

(*E*)-2-(4-fluorostyryl)-6-methoxyquinoline (193):

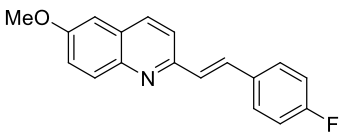

Prepared from **164** (0.173 g, 1 mmol) and 4-fluorobenzaldehyde (0.124 g, 1 mmol); temperature of reaction: 150 °C; yield: 86%; pale yellow solid.

Elemental analysis (%) calcd for $C_{18}H_{14}FNO$: C 77.40, H 5.05, N 5.01; found: C 77.15, H 5.01, N 4.77.

Mp: 138 141°C

IR (neat) ν: 1592, 1510, 1232, 1164, 1031, 965, 856, 837 cm^{-1}.

^{1}H NMR (250 MHz, $CDCl_3$) δ 8.05 (d, *J* = 8.4 Hz, 1H), 8.02 (d, *J* = 8.9 Hz, 1H), 7.65 7.58 (m, 4H), 7.39 (dd, *J* = 9.3, 2.8 Hz, 1H), 7.33 (d, *J* = 16.6 Hz, 1H), 7.14 7.08 (m, 3H), 3.96 (s, 3H), ppm.

^{13}C NMR (63 MHz, $CDCl_3$) δ163.2 (d, *J* = 248.4 Hz), 158.1, 153.9, 144.6, 135.7, 133.3, 133.2, 132.5, 130.9, 129 (d, *J* = 8.1 Hz, 2C), 128.7, 122.9, 119.2, 116.2 (d, *J* = 21.7 Hz, 2C), 105.6, 56.0 ppm.

(*E*)-2-(4-fluorostyryl)-7-methylquinoline (194):

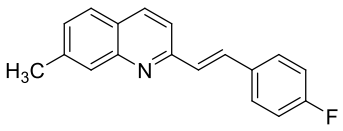

Prepared from **165** (0.157 g, 1 mmol) and 4-fluorobenzaldehyde (0.124 g, 1 mmol); temperature of reaction: 150 °C; yield: 64%; white solid.

Elemental analysis (%) calcd for $C_{18}H_{14}FN$: C 82.11, H 5.36, N 5.32; found: C 81.83, H 5.30, N 5.44.

Mp: 105 – 108 °C

IR (neat) ν: 1590, 1505, 1226, 1160, 984, 833 cm^{-1}.

^{1}H NMR (250 MHz, $CDCl_3$) δ 8.31 (d, *J* = 8.8 Hz, 1H), 7.96 (d, *J* = 8.5 Hz, 1H), 7.69 – 7.60 (m, 5H), 7.37 7.31 (m, 2H), 7.15 7.08 (m, *2*H), 2.71 (s,3H) ppm.

^{13}C NMR (63 MHz, $CDCl_3$) δ 163.3 (d, *J* = 248.6 Hz), 155.7, 148.9, 134.9, 133.4, 133.3, 133.2 (d, *J* = 3.4 Hz), 129.9, 129.3 (d, *J* = 8.1 Hz, 2C), 129.1, 127.9, 127.2, 127.1, 119.3, 116.2 (d, *J* = 21.8 Hz, 2C), 19.1 ppm.

(*E*)-2-(4-fluorostyryl)-7-methoxyquinoline (195):

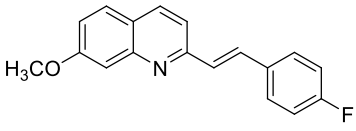

Prepared from **167** (0.173 g, 1 mmol) and 4-fluorobenzaldehyde (0.124 g, 1 mmol); temperature of reaction: 150 °C; yield: 61%; white solid.

Elemental analysis (%) calcd for $C_{18}H_{14}FNO$: C 77.40, H 5.05, N 5.01; found: C 77.04, H 5.01, N 5.11.

Mp: 123 – 126 °C

IR (neat) ν: 1618, 1593, 1458, 1381, 1217, 1024, 831 cm^{-1}.

^{1}H NMR (250 MHz, $CDCl_3$) δ 8.08 (d, *J* = 8.4 Hz, 1H), 7.71 – 7.60 (m, 4H), 7.53 (d, *J* = 8.5 Hz, 1H), 7.44 (d, *J* = 2.4 Hz, 1H), 7.31 (d, *J* = 16.3 Hz, 1H), 7.19 (dd, *J* = 8.9, 2.5 Hz, 1H), 7.16 7.09 (m, *J* = 2H), 4.00 (s, 3H) ppm.

^{13}C NMR (63 MHz, $CDCl_3$) δ 163.1 (d, *J* = 273.3 Hz), 161.4, 156.3, 150.3, 136.5, 133.3, 133.2, 129.2 (d, *J* = 8.2 Hz, 2C), 129.1, 128.9, 123.0, 119.8, 117.7, 116.2 (d, *J* = 21.8 Hz, 2C), 107.5, 56.0 ppm

(*E*)-7-methoxy-2-styrylquinoline (196):

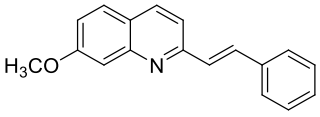

Prepared from **167** (0.173 g, 1 mmol) andbenzaldehyde (0.106 g, 1 mmol); temperature of reaction: 150 °C; yield: 78%; white solid.

Elemental analysis (%) calcd for $C_{18}H_{15}NO$: C 82.73, H 5.79, N 5.36; found: C 82.55, H 5.82, N 5.57.

Mp: 86 89 °C

IR (neat) ν: 1619, 1596, 1510, 1458, 1383, 1262, 1218, 1028, 922, 835 cm^{-1}.

^{1}H NMR (250 MHz, $CDCl_3$) δ 8.09 (d, *J* = 8.4Hz,1H), 7.75 7.66 (m, 4H), 7.56 (d, *J* = 8.4 Hz, 1H), 7.47 7.35 (m, 5H), 7.18 (dd, *J* = 8.9, 2.5 Hz, 1H), 4.00 (s, 3H) ppm.

^{13}C NMR (63 MHz, $CDCl_3$) δ 161.4, 156.5, 150.4, 137.0, 136.4, 134.5, 129.4, 129.2 (2C), 128.9, 128.9, 127.6 (2C), 123.0, 119.7, 117.7, 107.5, 55.9 ppm.

6-chloro-2-((1*E*,3*E*)-4-phenylbuta-1,3-dienyl)quinoline (197):

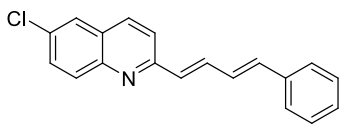

Prepared from **163** (0.178 g, 1 mmol) and cinnamaldehyde (0.132 g, 1 mmol); temperature of reaction: 150 °C; yield: 93%; yellow solid.

Elemental analysis (%) calcd for $C_{19}H_{14}ClN$: C 78.21, H 4.84, N 4.80; found: C 78.45, H 5.01, N 5.03.

Mp: 105 108 °C

IR (neat) ν:1590, 1486, 1070, 1002, 892, 826, 752 cm^{-1}.

^{1}H NMR (250 MHz, $CDCl_3$) δ 8.04 (d, *J* = 8.5 Hz, 1H), 8.01 (d, *J* = 8.9 Hz, 1H), 7.78 (d, *J* = 2.3 Hz, 1H), 7.65 (dd, *J* = 9.0, 2.3 Hz, 1H), 7.62 7.52 (m, 4H), 7.43 7.31 (m, 3H), 7.15 6.87 (m, 3H), ppm.

^{13}C NMR (63 MHz, $CDCl_3$) δ 156.6, 147.1, 137.3, 136.8, 135.8, 135.7, 132.7, 132.1, 131.1, 131.0, 129.2 (2C), 128.8, 128.7, 128.2, 127.2 (2C), 126.6, 120.8 ppm.

2-((1*E*,3*E*)-4-(4-chlorophenyl)buta-1,3-dienyl)-6-methylquinoline (198):

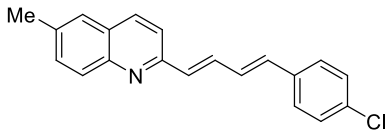

Prepared from **165** (0.157 g, 1 mmol) and **143** (0.167 g, 1 mmol); temperature of reaction: 150 °C; yield: 74%; yellow solid.

Elemental analysis (%) calcd for $C_{20}H_{16}ClN$: C 78.55, H 5.27, N 4.58; found: C 78.26, H 5.05, N 4.26.

Mp: 210 213°C

IR (neat) ν: 1589, 1489, 1087, 986, 820 cm^{-1}.

^{1}H NMR (250 MHz, $CDCl_3$) δ 8.07 7.98 (m, 2H) 7.60 7.33 (m, 8H), 7.11 6.97 (m, 2H), 6.82 (d, *J* = 15.6 Hz, 1H), 2.56 (s, 3H) ppm.

^{13}C NMR (63 MHz, $CDCl_3$) δ 155.3, 147.2, 136.6, 136.1, 135.9, 134.6, 134.4, 134.0, 133.8, 132.5, 129.6, 129.3 (2C), 129.2, 128.3 (2C), 127.7, 126.8, 119.8, 22.0 ppm.

6-methoxy-2-((1*E*,3*E*)-4-(2-nitrophenyl)buta-1,3-dienyl)quinoline (199):

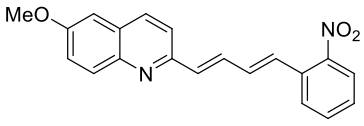

Prepared from **164** (0.173 g, 1 mmol) and trans-2-nitrocinnamaldehyde (0.177 g, 1 mmol); temperature of reaction: 130 °C; yield: 72%; yellow solid.

Elemental analysis (%) calcd for $C_{20}H_{16}N_2O_3$: C 72.28, H 4.85, N 8.43; found: C 72.01, H 5.01, N 8.21.

Mp: 181 – 183 °C

IR (neat) ν: 1647, 1629, 1517, 1345, 1282, 986 cm^{-1}.

^{1}H NMR (250 MHz, $CDCl_3$) δ 8.07 – 7.95 (m, 3H), 7.78 (d, *J* = 7.5 Hz, 1H), 7.65 – 7.32 (m, 6H), 7.12 7.02 (m, 3H), 3.96 (s, 3H) ppm.

^{13}C NMR (63 MHz, $CDCl_3$) δ 158.4, 153.3, 148.3, 144.3, 135.8, 135.5, 134.0, 133.7, 133.4, 132.8, 130.9, 129.8, 128.9, 128.6, 128.3, 125.3, 123.1, 119.9, 105.6, 56.0 ppm.

9.5.3. Synthesis of 2-styryquinolines by base-catalyzed aldol condensation

Equivalent moles of the suitable quinaldine (1.5 mmol) and the corresponding aldehyde (1.5 mmol) were dissolved in 3 ml of dry DMF. The solution was stirred in a round bottom flask attached to a drying tube. Lithium hydride (30 mg, 3.75 mmol) and potassium *t*-butoxide (0.213 g, 1.9 mmol) were added to solution one after another and the reaction mixture was stirred for 24 h. Then, it was poured into the beaker containing ice and saturated ammonium chloride (NH_4Cl) and the mixture was stirred for about 15 minutes until the formation of a precipitate. The resulting solid was filtered and washed with cold water, collected and dried overnight in the presence of P_2O_5.

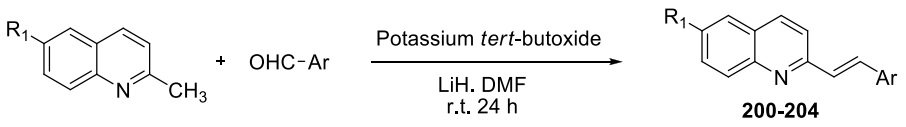

200-204

Cmpd.	R_1	Ar
200	H	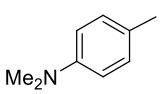
201	Me	
202	Cl	
203	OMe	

Cmpd.	R_1	Ar
204	H	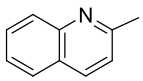

(*E*)-*N,N*-dimethyl-4-(2-(quinolin-2-yl)vinyl)aniline (200):

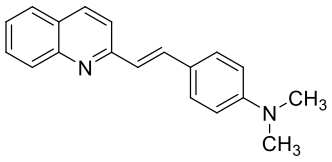

Prepared from **161** (0.215 g, 1.5 mmol) and 4-(dimethylamino)benzaldehyde (0.223 g, 1.5 mmol); yield: 66%; red solid.

Elemental analysis (%) calcd for $C_{19}H_{18}N_2$: C 83.18, H 6.61, N 10.21; found: C 83.46, H 6.66, N 10.43.

Mp: 129 132 °C

IR (neat) ν: 3023, 2804, 1594, 1524, 1363, 1187, 965, 823 cm^{-1}.

^{1}H NMR (250 MHz, $CDCl_3$) δ 8.11 (d, *J* = 8.6 Hz, 2H), 7.80 7.74 (m, 1H), 7.71 – 7.68 (m, 2H), 7.62 – 7.51 (m, 3H), 7.52 7.46 (m, 1H), 7.28 (d, *J* = 16.3 Hz, 1H), 6.76 (d, *J* = 8.8 Hz, 2H), 3.05 (s, 6H) ppm.

^{13}C NMR (63 MHz, $CDCl_3$) δ 157.2, 151.2, 136.7, 130.3, 130.1, 129.2, 129.1 (2C), 127.9, 127.4, 126.1, 124.9, 124.4, 123.7, 119.4, 112.6 (2C), 40.7 (2C) ppm.

(*E*)-*N,N*-dimethyl-4-(2-(6-methylquinolin-2-yl)vinyl)aniline (201):

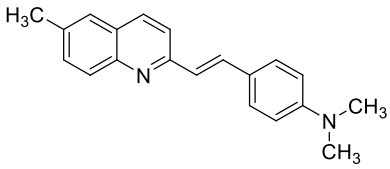

Prepared from **162** (0.236 g, 1.5 mmol) and 4-(dimethylamino)benzaldehyde (0.223 g, 1.5 mmol); yield: 81%; orange solid.

Elemental analysis (%) calcd for $C_{20}H_{20}N_2$: C 83.30, H 6.99, N 9.71; found: C 83.64, H 7.00, N 10.03.

Mp: 146 – 149 °C

IR (neat) ν: 3147, 3029, 2910, 1606, 1587, 1523, 1364, 1181, 1164, 827 cm^{-1}.

^{1}H NMR (250 MHz, $CDCl_3$) δ 8.02 (d, *J* = 8.5 Hz, 1H), 7.99 (d, *J* = 8.7 Hz, 1H), 7.67 7.52 (m, 6H), 7.26 (d, *J* = 16.9 Hz, 1H), 6.76 (d, *J* = 8.8 Hz, 2H), 3.04 (s, 6H), 2.55 (s, 3H) ppm.

^{13}C NMR (63 MHz, $CDCl_3$) δ 156.4, 151.1, 138.8, 136.0, 135.9, 135.0, 132.3, 129.0 (2C), 128.8, 127.4, 126.9, 125.1, 124.6, 119.3, 112.6 (2C), 40.8 (2C), 22.0 ppm.

(*E*)-4-(2-(6-chloroquinolin-2-yl)vinyl)-*N,N*-dimethylaniline (202):

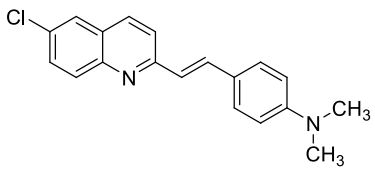

Prepared from **163** (0.266 g, 1.5 mmol) and 4-(dimethylamino)benzaldehyde (0.223 g, 1.5 mmol); yield: 90%; red solid.

Elemental analysis (%) calcd for $C_{19}H_{17}ClN_2$: C 73.90, H 5.55, N 9.07; found: C 73.67, H 5.39, N 9.19.

Mp:155 – 158 °C

IR (neat) ν: 3025, 2801, 1591, 1521, 1357, 1065, 971, 822 cm^{-1}.

^{1}H NMR (250 MHz, $CDCl_3$) δ 7.99 (d, *J* = 8.8 Hz, 2H), 7.75 – 7.54 (m, 6H), 7.20 (d, *J* = 16.3 Hz, 1H), 6.75 (d, *J* = 8.3 Hz, 2H), 3.04 (s, 6H) ppm.

^{13}C NMR (63 MHz, $CDCl_3$) δ 157.6, 151.3, 147.1, 135.8, 135.5, 131.5, 130.8, 129.3, 129.1 (2C), 127.9, 126.6, 124.8, 124.2, 120.4, 112.6 (2C), 40.7 (2C) ppm.

(*E*)-4-(2-(6-methoxyquinolin-2-yl)vinyl)-*N,N*-dimethylaniline (203):

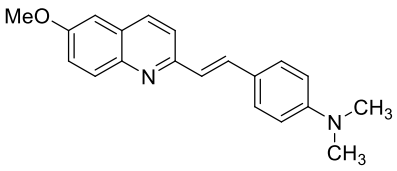

Prepared from **164** (0.260 g, 1.5 mmol) and 4-(dimethylamino)benzaldehyde (0.223 g, 1.5 mmol); yield: 63%; red solid.

Elemental analysis (%) calcd for $C_{20}H_{20}N_2O$: C 78.92, H 6.62, N 9.20; found: C 77.82, H 6.51, N 9.97.

Mp: 160 – 163 °C

IR (neat) ν: 3130, 3033, 2890, 1607, 1591, 1226, 1163, 831 cm^{-1}.

^{1}H NMR (250 MHz, $CDCl_3$) δ 7.99 (d, *J* = 8.9 Hz, 2H), 7.65 – 7.53 (m, 4H), 7.36 (dd, *J* = 9.2, 2.7 Hz, 1H), 7.22 (d, *J* = 16.3 Hz, 1H), 7.06 (d, *J* = 2.7 Hz, 1H), 6.75 (d, *J* = 8.8 Hz, 2H), 3.94 (s, 3H), 3.03 (s, 6H) ppm.

^{13}C NMR (63 MHz, $CDCl_3$) δ 157.7, 155.0, 151.1, 144.4, 135.4, 134.3, 130.6, 128.9 (2C), 128.3, 125.2, 124.7, 122.5, 119.7, 112.6 (2C), 105.8, 55.9, 40.8 (2C) ppm.

(*E*)-1,2-di(quinolin-2-yl)ethene (204):

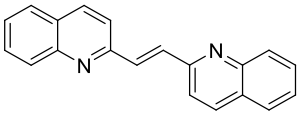

Prepared from **161** (0.215 g, 1.5 mmol) and quinoline-2-carbaldehyde (0.236 g, 1.5 mmol); yield: 58%; yellow solid.

Elemental analysis (%) calcd for $C_{20}H_{14}N_2$: C 85.08, H 5.00, N 9.92; found: C 84.81, H 5.23, N 10.01.

Mp: 115 – 118 °C

IR (neat) ν: 1622, 1407, 1328, 1213, 1140, 828, 745 cm^{-1}.

^{1}H NMR (250 MHz, $CDCl_3$) δ 8.34 (s, 2H), 8.24 (d, *J* = 8.5 Hz, 1H), 7.90 (dd, *J* = 8.1, 0.9 Hz, 1H), 7.82 – 7.76 (m, 2H), 7.65 – 7.56 (m, 4H), 7.37 – 7.29 (m, 2H), 7.11 – 7.01 (m, 2H) ppm.

^{13}C NMR (63 MHz, $CDCl_3$) δ 182.7, 156.6, 155.0, 147.8, 138.1, 137.3, 137.0, 131.6, 130.6, 130.0, 129.2, 128.1, 128.0, 127.6, 124.5, 124.0, 123.3, 118.9, 118.6, 90.6 ppm.

9.5.4. Synthesis of 4-amino-2-styrylquinolines

9.5.4.1. Preparation of β-enaminones

To a stirred solution of 3 mmol of the suitable amine and 3 mmol of ethyl acetoacetate in 3 ml of EtOH was added 5% mol of CAN (0.247 g). The mixture was stirred at r.t. for 2 hours. After completion of the reaction the mixture was dissolved in CH_2Cl_2, washed with H_2O, dried, and evaporated. No further purification was needed.

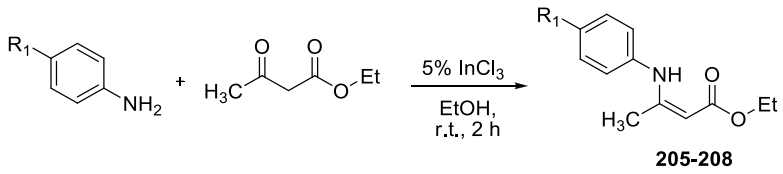

205-208

Cmpd.	R_1
205	H
206	CH_3
207	Cl
208	OCH_3

(*Z*)-ethyl 3-(phenylamino)but-2-enoate (205):

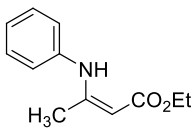

Prepared from aniline (0.280 g, 3 mmol) and ethyl acetoacetate (0.390 g, 3 mmol); yield: 89%; black oil.

^{1}H NMR (250 MHz, $CDCl_3$) δ 10.42 (br s, 1H), 7.35 (dd, *J* = 10.6, 5.1 Hz, 2H), 7.22 – 7.09 (m, 3H), 4.72 (s, 1H), 4.18 (q, *J* = 7.1 Hz, 2H), 2.02 (s, 3H), 1.31 (t, *J* = 7.1 Hz, 3H) ppm.

^{13}C NMR (63 MHz, $CDCl_3$) δ 170.8, 159.3, 139.8, 129.5 (2C), 125.3, 124.7(2C), 86.5, 59.1, 20.7, 15.0 ppm.

(*Z*)-ethyl 3-(p-tolylamino)but-2-enoate (206):

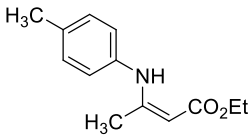

Prepared from *p*-toluidine (0.321 g, 3 mmol) and ethyl acetoacetate (0.390 g, 3 mmol); yield: 86%; black oil.

^{1}H NMR (250 MHz, $CDCl_3$) δ 10.31 (br s, 1H), 7.15 (d, *J* = 8.1 Hz, 2H), 7.00 (d, *J*= 8.3 Hz, 2H), 4.69 (s, 1H), 4.17 (q, *J* = 7.1 Hz, 2H), 2.36 (s, 3H), 1.98 (s, 3H), 1.31 (t, *J* = 7.1 Hz, 3H) ppm.

(*Z*)-ethyl 3-(4-chlorophenylamino)but-2-enoate (207):

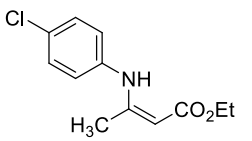

Prepared from 4-chloroaniline (0.383 g, 3 mmol) and ethyl acetoacetate (0.390 g, 3 mmol); yield: 79%; black oil.

^{1}H NMR (250 MHz, $CDCl_3$) δ 10.37 (br s, 1H), 7.31 (d, *J* = 8.9 Hz, 2H), 7.03 (d, *J* = 8.7 Hz, 2H), 4.74 (s, 1H), 4.17 (q, *J* = 7.2 Hz, 2H), 2.00 (s, 3H), 1.31 (t, *J* = 7.1 Hz, 3H) ppm.

(*Z*)-ethyl 3-(4-methoxyphenylamino)but-2-enoate (208):

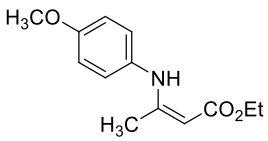

Prepared from *p*-anisidine (0.370 g, 3 mmol) and ethyl acetoacetate (0.390 g, 3 mmol); yield: 75%; black oil.

^{1}H NMR (250 MHz, $CDCl_3$) δ 10.17 (br s, 1H), 7.04 (d, *J* = 8.8 Hz, 2H), 6.87 (d, *J* = 8.8 Hz, 2H), 4.67 (s, 1H), 4.16 (q, *J* = 7.1 Hz, 2H), 3.82 (s, 3H), 1.90 (s, 3H), 1.30 (t, *J* = 7.1 Hz, 3H) ppm.

9.5.4.2. General procedure for preparing quinolone compounds

Diphenyl ether (30 ml) was stirred and heated at reflux while a β-enaminone compound (**209-210**) was added rapidly. Stirring and refluxing continued for 10-15 until no more ethanol is separated by using the Dean-Stark trap. The mixture was allowed to cool down to r.t. while precipitation arises. The solid was filtered off and washed with hexane and acetone. No further purification was needed.

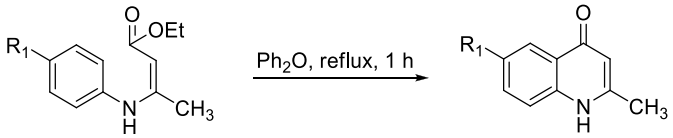

205-208 **209-212**

Cmpd.	R_1
209	H
210	CH_3
211	Cl
212	OCH_3

2-methylquinolin-4(1*H*)-one (209):

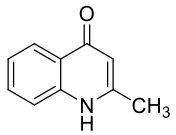

Prepared from **205** (4.00 g, 19.5 mmol); yield: 57%; grey powder. **^{1}H NMR** (300 MHz, DMSO) δ 11.71 (br s, 1H), 8.19 (d, *J* = 7.1 Hz, 1H), 7.80 – 7.74 (m, 1H), 7.65 (d, *J* = 8.2 Hz, 1H), 7.46 – 7.40 (m, 1H), 6.07 (s, 1H), 2.50 (s, 3H) ppm.

^{13}C NMR (63 MHz, DMSO) δ 177.1, 150.0, 140.5, 131.80, 125.2, 124.9, 123.1, 118.1, 108.8, 19.8 ppm.

2,6-dimethylquinolin-4(1*H*)-one (210):

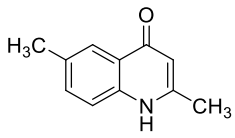

Prepared from **206** (4.275 g, 19.5 mmol); yield: 73%; pale brown solid.

^{1}H NMR (250 MHz, DMSO) δ 11.64 (br s, 1H), 7.95 (s, 1H), 7.58 – 7.49 (m, 2H), 5.99 (s, 1H), 2.50 (s, 3H), 2.44 (s, 3H) ppm.

6-chloro-2-methylquinolin-4(1*H*)-one (211):

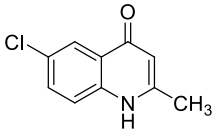

Prepared from **207** (4.674 g, 19.5 mmol); yield: 65%; grey solid.

^{1}H NMR (250 MHz, DMSO) δ 11.87 (br s, 1H), 8.08 (d, *J* = 2.5 Hz, 1H), 7.78 (dd, *J* = 8.8, 2.5 Hz, 1H), 7.65 (d, *J* = 8.8 Hz, 1H), 6.08 (s, 1H), 2.47 (s, 3H) ppm.

6-methoxy-2-methylquinolin-4(1*H*)-one (212):

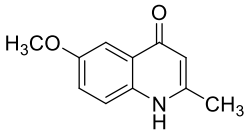

Prepared from **208** (4.590 g, 19.5 mmol); yield: 60%; brown solid.

^{1}H NMR (250 MHz, DMSO) δ 11.57 (br s, 1H), 7.48 – 7.45 (m, 2H), 7.26 (dd, *J* = 9.0, 2.8 Hz, 1H), 5.88 (s, 1H), 3.82 (s, 3H), 2.33 (s, 3H) ppm.

9.5.4.3. 4-chloro-2-methylquinoline (213):

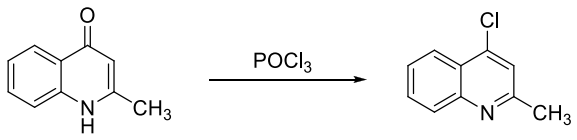

209 **213**

2-methylquinolinone **209** (0.300 g, 1.88 mmol) was added portionwise to a solution of an excess of phosphorus oxychloride (30 ml) at 0 ^{o}C. After being stirred for 30 min at r.t., the reaction mixture was heated at 80 °C for 30 min to 1 h. The excess of phosphorus oxychloride was removed by vacuum distillation. The residue was poured slowly onto a mixture of crushed ice and saturated $NaHCO_3$ solution with vigorous stirring. The pH of the solution was adjusted to about 9.0 by addition of ammonium hydroxide. The formed precipitate was collected by filtration to afford compound **213** in 81% yield as a white solid.

^{1}H NMR (250 MHz, $CDCl_3$) δ 8.20 (dd, *J* = 8.3, 1.0 Hz, 1H), 8.06 (d, *J* = 8.4 Hz, 1H), 7.76 (ddd, *J* = 8.4, 7.0, 1.4 Hz, 1H), 7.65 – 7.54 (m, 1H), 7.42 (s, 1H), 2.75 (s, 3H) ppm.

^{13}C NMR (63 MHz, $CDCl_3$) δ 159.3, 149.1, 143.0, 130.8, 129.3, 127.1, 124.3, 122.4, 122.4, 25.6 ppm.

9.5.4.4. General procedure for the condensation between methylquinolinones and benzaldehyde

The suitable 2-methyquinolinone compound (1 mmol) (**209-212**) and benzaldehyde (1 mmol) were suspended in Ac_2O (0.5 ml) in a pressure-tight microwave tube containing a stirring bar. The mixture was heated under microwave irradiation for 1 h at 150 °C, with an irradiation power of 200 W,

using a CEM Discover SP microwave reactor. The solvent was removed under reduced pressure to give a black residue that was purified by chromatography through a silica column using PE-EtOAc (90:10, v/v) as mobile phase to obtain compounds **214-217**.

209-212 **214-217**

Cmpd.	R_1
214	H
215	CH_3
216	Cl
217	OCH_3

(*E*)-2-styrylquinolin-4-yl acetate (214):

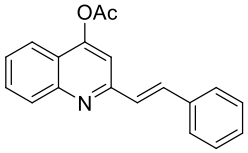

Prepared from **209** (0.160 g, 1 mmol) and benzaldehyde (0.106 g, 1 mmol); yield: 60%; yellow solid.

^{1}H NMR (250 MHz, DMSO) δ 8.08 (d, *J* = 8.4 Hz, 1H), 8.01 (d, *J* = 7.7 Hz, 1H), 7.89 – 7.76 (m, 5H), 7.66 – 7.61 (m, 1H), 7.54 – 7.39 (m, 4H), 2.55 (s, 3H) ppm.

^{13}C NMR (75 MHz, DMSO) δ 168.7, 156.7, 154.3, 149.2, 136.0, 134.8, 130.5, 129.0, 128.9 (2C), 128.8, 128.3, 127.3 (2C), 126.7, 121.5, 121.3, 112.0, 20.8 ppm.

(*E*)-6-methyl-2-styrylquinolin-4(1H)-one (215):

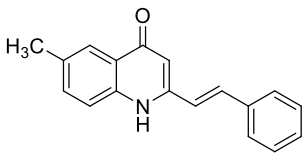

Prepared from **210** (0.173 g, 1 mmol) and benzaldehyde (0.106 g, 1 mmol); yield: 56%; yellow solid.

^{1}H NMR (250 MHz, DMSO) δ 11.51 (br s, 1H), 7.86 (s, 1H), 7.69 – 7.57 (m, 4H), 7.52 – 7.40 (m, 4H), 7.13 (d, *J* = 16.6 Hz, 1H), 6.33 (s, 1H), 2.41 (s, 3H) ppm.

^{13}C NMR (63 MHz, DMSO) δ 177.7, 147.4, 139.2, 136.4, 135.4, 134.1, 133.1, 130.1 (2C), 129.9 (2C), 128.1, 126.0, 124.9, 123.2, 119.0, 108.2, 21.6 ppm.

(*E*)-6-chloro-2-styrylquinolin-4-yl acetate (216):

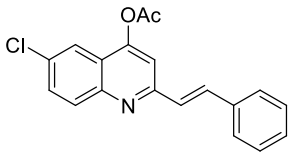

Prepared from **211** (0.194 g, 1 mmol) and benzaldehyde (0.106 g, 1 mmol); yield: 49%; pale yellow solid.

^{1}H NMR (250 MHz, $CDCl_3$) δ 8.09 (d, *J* = 9.1 Hz, 1H), 7.90 (d, *J* = 2.2 Hz, 1H), 7.71 (d, *J* = 2.4 Hz, 1H), 7.68 – 7.64 (m, 4H), 7.47 – 7.37 (m, 4H), 2.55 (s, 3H) ppm.

^{13}C NMR (63 MHz, $CDCl_3$) δ 168.4, 157.5, 153.9, 148.2, 136.4, 136.3, 132.9, 131.9, 130.9, 129.5, 129.3 (2C), 128.2, 127.9 (2C), 122.4, 120.69, 111.9, 21.7 ppm.

(E)-6-methoxy-2-styrylquinolin-4-ol (217):

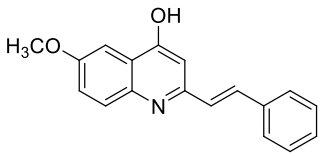

Prepared from **212** (0.190 g, 1 mmol) and benzaldehyde (0.106 g, 1 mmol); yield: 69%; yellow solid.

^{1}H NMR (250 MHz, DMSO) δ 7.74 – 7.66 (m, 3H), 7.50 – 7.35 (m, 6H), 7.18 (d, *J* = 16.6 Hz, 1H), 6.49 (s, 1H), 3.86 (s, 3H) ppm.

^{13}C NMR (63 MHz, DMSO) δ 168.7, 156.2, 147.0, 135.8, 135.5, 135.3, 129.7, 129.4 (2C), 127.7 (2C), 125.9, 123.1, 122.4, 120.7, 106.2, 104.2, 55.8 ppm.

9.5.4.5. General procedure for preparing 4-chlorostyrylquinolines

The suitable styrylquinoline compound (3.5 mmol) (**214-217**) was added portion-wise to a solution of excess phosphorus oxychloride at 0 ^{o}C. After being stirred for 30 min at room temperature, the reaction mixture was heated at 80 °C for 30 min to 1h. The excess phosphorus oxychloride was removed by vacuum distillation. The residue was poured slowly onto a mixture of crushed ice and saturated $NaHCO_3$ solution with vigorous stirring. The pH of the solution was adjusted to about 9.0 by addition of ammonium hydroxide. The solid product separated out was collected by filtration, dried and used for the next reaction without further purification.

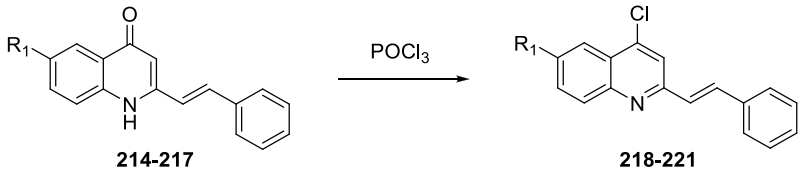

214-217 **218-221**

Cmpd.	R_1
218	H
219	CH_3
220	Cl
221	OCH_3

(*E*)-4-chloro-2-styrylquinoline (218):

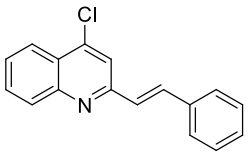

Prepared from **214** (1.01 g, 3.5 mmol); yield: 90%; yellow solid.

^{1}H NMR (250 MHz, $CDCl_3$) δ 8.21 (dd, *J* = 8.4, 1.1 Hz, 1H), 8.12 (d, *J* = 8.2 Hz, 1H), 7.82 – 7.75 (m, 2H), 7.74 – 7.58 (m, 4H), 7.48 – 7.33 (m, 4H) ppm.

^{13}C NMR (63 MHz, $CDCl_3$) δ 156.3, 149.4, 143.2, 136.6, 135.8, 131.1, 129.9, 129.4, 129.3 (2C), 128.3, 127.8 (2C), 127.5, 125.9, 124.4, 119.7.

(*E*)-4-chloro-6-methyl-2-styrylquinoline (219):

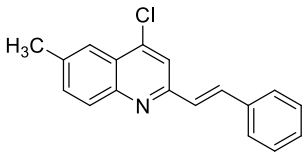

Prepared from **215** (0.915 g, 3.5 mmol); yield: 99%; yellow solid.

^{1}H NMR (250 MHz, $CDCl_3$) δ 8.16 (d, *J* = 8.6 Hz, 1H), 7.99 (s, 1H), 7.82 (s, 1H), 7.75 – 7.64 (m, 4H), 7.52 – 7.38 (m, 4H), 2.62 (s, 3H) ppm.

^{13}C NMR (63 MHz, $CDCl_3$) δ 154.7, 149.1, 146.1, 143.8, 138.5, 136.9, 136.2, 134.1, 129.8, 129.3 (2C), 128.3, 128.0 (2C), 125.7, 123.5, 119.4, 22.3 ppm.

(*E*)-4,6-dichloro-2-styrylquinoline (220):

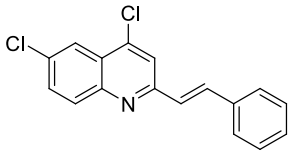

Prepared from **216** (1.133 g, 3.5 mmol); yield: 85%; yellow solid.

^{1}H NMR (250 MHz, $CDCl_3$) δ 8.20 (d, *J* = 2.3 Hz, 1H), 8.04 (d, *J* = 9.0 Hz, 1H), 7.79 (s, 1H), 7.76 – 7.65 (m, 4H), 7.48 – 7.36 (m, 4H) ppm.

^{13}C NMR (63 MHz, $CDCl_3$) δ 156.6, 147.8, 142.1, 136.4, 136.2, 133.5, 132.0, 131.5, 129.5, 129.3 (2C), 127.9, 127.8 (2C), 126.5, 123.5, 120.6 ppm.

(*E*)-4-chloro-6-methoxy-2-styrylquinoline (221):

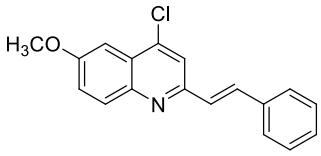

Prepared from **217** (0.970 g, 3.5 mmol); yield: 95%; yellow solid.

^{1}H NMR (250 MHz, $CDCl_3$) δ 8.34 (d, *J* = 8.8 Hz, 1H), 7.93 (s, 1H), 7.79 – 7.63 (m, 4H), 7.55 – 7.38 (m, 5H), 4.03 (s, 3H) ppm.

^{13}C NMR (63 MHz, MeOD) δ 162.5, 152.0, 150.3, 145.2, 136.3, 132.8, 130.7 (2C), 130.6, 130.6, 130.0 (2C), 128.9, 125.1, 121.2, 120.0, 104.9, 57.5 ppm.

9.5.4.6. General procedure for preparing 4-aminostyrylquinolines

A mixture of the suitable 4-chloro-styrylquinoline (**218-221**) and excess phenol (200 mg) was heated at 180 °C for 1 h. A slow stream of ammonia was passed through the reaction mixture at 180 °C for 2 h. After cooling to room temperature, the mixture was poured into 10% KOH aqueous solution. The solid separated was collected by filtration, washed with water and dried to give the products (**222-225**), which were purified through column on silica gel.

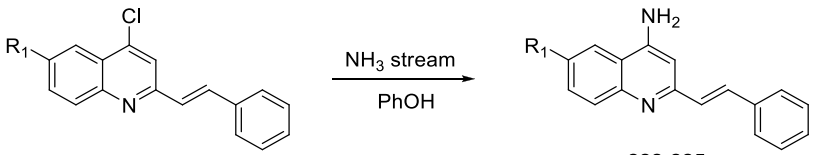

218-221 **222-225**

Cmpd.	R_1
222	H
223	CH_3
224	Cl
225	OCH_3

(*E*)-2-styrylquinolin-4-amine (222):

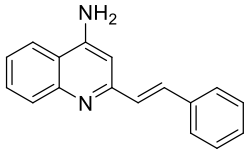

Prepared from **218** (100 mg, 0.38 mmol); yield: 35%; brown solid.

Elemental analysis calcd (%) for $C_{17}H_{14}N_2$: C 82.90, H 5.73, N 11.37; found: C 82.50, H 5.45, N 11.02.

Mp: 103 106 °C

IR (neat) ν: 3350, 3167, 1615, 1516, 1439, 1209, 756 cm^{-1}.

^{1}H NMR (250 MHz, $CDCl_3$) δ 8.04 (d, *J* = 8.4 Hz, 1H), 7.77 (d, *J* = 8.4 Hz, 1H), 7.70 – 7.59 (m, 4H), 7.46 – 7.25 (m, 5H), 6.91 (s, 1H), 4.96 (br s, 2H) ppm.

^{13}C NMR (63 MHz, MeOD) δ 157.4, 155.1, 149.1, 138.3, 136.0, 131.7, 130.3 (2C), 130.2, 129.2, 128.6 (2C), 128.2, 125.8, 123.3, 119.7, 100.9 ppm.

(*E*)-6-methyl-2-styrylquinolin-4-amine (223):

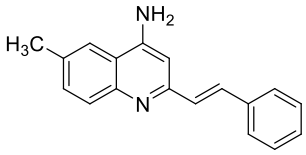

Prepared from **219** (100 mg, 0.36 mmol); yield: 37%; pale brown solid.

Elemental analysis calcd (%) for $C_{18}H_{16}N_2$: C 83.04, H 6.19, N 10.76; found: C 83.39, H 6.50, N 10.51.

Mp: 138 141 °C

IR (neat) ν: 3325, 3143, 2918, 1634, 1594, 1491, 821 cm^{-1}.

^{1}H NMR (250 MHz, MeOD) δ 8.04 (s, 1H), 7.81 – 7.69 (m, 5H), 7.48 – 7.45 (m, 3H), 7.22 (d, *J* = 16.4 Hz, 1H), 7.02 (s, 1H), 2.57 (s, 3H) ppm.

^{13}C NMR (63 MHz, MeOD) δ 158.7, 152.2, 140.0, 138.2, 137.1, 136.7, 131.5, 130.6 (2C), 130.2, 129.2 (2C), 123.4, 122.7, 122.5, 118.1, 100.6, 21.9 ppm.

(*E*)-6-chloro-2-styrylquinolin-4-amine (224):

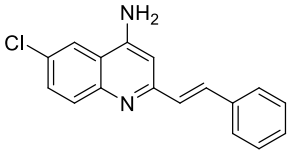

Prepared from **220** (100 mg, 0.33 mmol); yield: 26%; grey solid.

Elemental analysis calcd (%) for $C_{17}H_{13}ClN_2$: C 72.73, H 4.67, N 9.98; found: C 72.39, H 4.80, N 9.61.

Mp: 142 145 °C

IR (neat) ν: 3342, 3195, 2925, 1636, 1584, 753 cm^{-1}.

^{1}H NMR (250 MHz, MeOD) δ 7.87 (s, 1H), 7.75 (d, *J* = 8.6 Hz, 1H), 7.66 – 7.53 (m, 4H), 7.45 – 7.35 (m, 3H), 7.21 (d, *J* = 16.4 Hz, 1H), 6.98 (s, 1H) ppm.

^{13}C NMR (63 MHz, MeOD) δ 155.7, 155.3, 146.2, 138.1, 136.4, 136.3, 134.2, 130.4 (broad signal, 3C), 128.7 (2C), 128.0, 127.0, 122.6, 119.4, 100.8 ppm.

(*E*)-6-methoxy-2-styrylquinolin-4-amine (225):

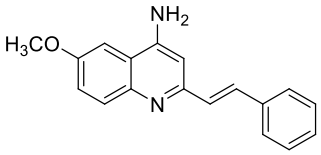

Prepared from **221** (100 mg, 0.34 mmol); yield: 32%; dark solid.

Elemental analysis calcd (%) for $C_{18}H_{16}N_2$: C 78.24, H 5.84, N 10.14; found: C 78.39, H 5.80, N 10.51.

Mp: 222 225 °C

IR (neat) ν: 3309, 3197, 2924, 1586, 1513, 1232,1030, 831 cm^{-1}.

^{1}H NMR (250 MHz, $CDCl_3$) δ 7.97 (d, *J* = 9.3 Hz, 1H), 7.64 – 7.54 (m, 3H), 7.44 – 7.25 (m, 5H), 7.00 – 6.93 (m, 2H), 4.64 (br s, 1H), 3.97 (s, 3H) ppm.

^{13}C NMR (63 MHz, MeOD) δ 158.5, 155.9, 153.6, 145.6, 138.6, 134.4, 132.1, 130.5, 130.3 (2C), 129.8, 128.4 (2C), 123.3, 120.6, 101.9, 101.1, 56.5 ppm.

9.6. Synthesis of 4-aminostyrylquinolines against leishmaniasis

9.6.1. (*E*)-N^1-(2-styrylquinolin-4-yl)ethane-1,2-diamine (226):

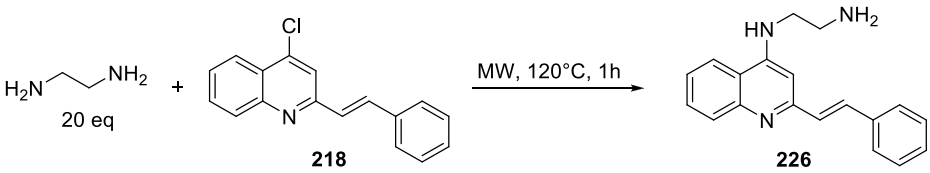

Ethylenediamine (1.130 g, 18.8 mmol) was added to 4-chloro-2-styrylquinoline **218** (0.250 g, 0.94 mmol) in a pressure-tight microwave tube containing a stirring bar. The mixture was heated under microwave irradiation for 1 h at 120 °C, with an irradiation power of 200 W, using a CEM Discover SP microwave reactor. Thereafter, the reaction mixture was treated with aqueous solution of KOH 10%, extracted with CH_2Cl_2, dried with anhydrous Na_2SO_4 and evaporated *in vacuo.* The excess of ethylenediamine was removed by distillation in EtOH. The resulting residue was subsequently crystallized in MeOH and hexane to give compound **226** as a yellow solid in 40% yield.

^{1}H NMR (250 MHz, MeOD) δ 8.11 (d, *J* = 8.3 Hz, 1H), 7.87 (d, *J* = 8.4 Hz, 1H), 7.70 – 7.64 (m, 4H), 7.47 – 7.29 (m, 5H), 6.94 (s, 1H), 3.58 (t, *J* = 6.3 Hz, 2H), 3.06 (t, *J* = 6.4 Hz, 2H) ppm.

^{13}C NMR (63 MHz, DMSO) δ 155.9, 151.0, 148.7, 137.0, 132.5, 130.5, 129.4, 129.2, 129.2 (2C), 128.6, 127.4 (2C), 123.8, 122.0, 118.7, 97.4, 46.5, 40.6 ppm.

9.6.2. (*E*)-2-bromo-N-(2-(2-styrylquinolin-4-ylamino)ethyl)acetamide (227):

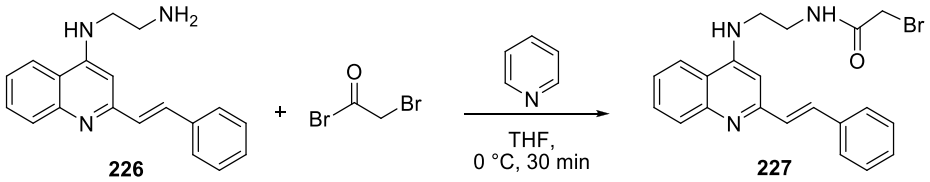

A solution of **227** (0.250 g, 0.864 mmol), bromoacetyl bromide (0.209 g, 1.037 mmol) and pyridine (0.079 g, 2.59 mmol) in dry THF (10 ml) was stirred under argon for 30 minutes at 0 °C. When the reaction was finished, the solvent was removed under vacuum, and the resulting residue was dissolved in CH_2Cl_2 and washed with acidic water (2N HCl) to remove the excess of pyridine. Compound **227** was purified through silica gel column and was isolated as a red solid in 46% yield.

^{1}H NMR (250 MHz, MeOD) δ 8.27 (d, *J* = 8.4 Hz, 1H), 8.11 (d, *J* = 16.5 Hz, 1H), 7.92 – 7.91 (m, 2H), 7.79 – 7.64 (m, 3H), 7.49 – 7.47 (m, 3H), 7.34 – 7.27 (m, 2H), 4.12 (s, 1H), 3.91 (s, 1H), 3.83 – 3.80 (m, 2H), 3.67 – 3.65 (m, 2H) ppm.

^{13}C NMR (63 MHz, MeOD) δ 171.0, 157.6, 152.3, 142.7, 139.8, 136.7, 135.2, 132.1, 130.6 (2C), 129.6 (2C), 128.3, 124.1, 121.2, 120.6, 118.3, 97.0, 44.4, 43.6, 29.3 ppm.

9.6.3. General procedure for the synthesis of 4-aminostyrylquinolines

227 (80 mg, 0.195 mmol), the suitable amine (1 equiv) and Cs_2CO_3 (0.127 g, 0.39 mmol, 2 equiv) were suspended in EtOH (1 ml) in a pressure-tight microwave tube containing a stirring bar. The mixture was heated under microwave irradiation for 30 minutes at 120 °C, with an irradiation power of 200 W, using a CEM Discover SP microwave reactor. Thereafter, the reaction mixture was

dissolved in CH_2Cl_2 and washed with water. The combined organic layers were dried with anhydrous Na_2SO_4 and evaporated *in vacuo.* The compounds obtained were subsequently crystallized from MeOH-hexane mixtures or purified through neutral alumina column.

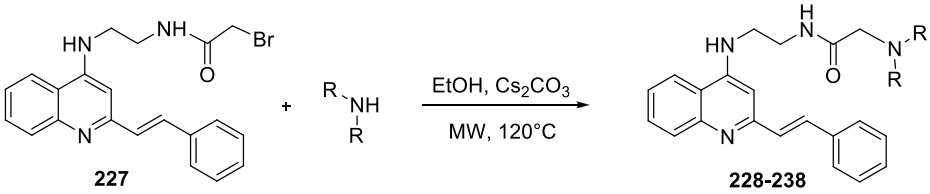

Cmpd.	R_2NH
228	
229	
230	
231	
232	
233	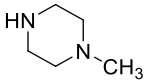

Cmpd.	R_2NH
234	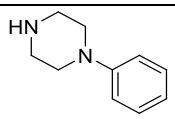
235	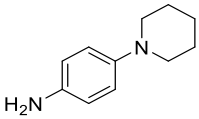
236	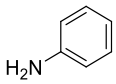
237	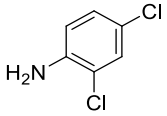
238	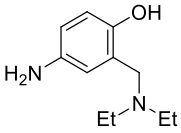

(*E*)-2-(Dimethylamino)-N-[2-(2-styrylquinolin-4-ylamino)ethyl]acetamide (228):

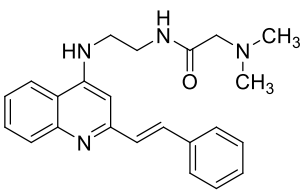

Prepared from **227** (80 mg, 0.195 mmol) and dimethylamine (0.02 ml, 0.195 mmol); the compound

was crystallized from MeOH-hexane mixture to give **228** in 72% yield as an orange powder.

Elemental analysis (%) calcd for $C_{23}H_{26}N_4O$: C 73.77, H 7.00, N 14.96; found: C 73.61, H 7.16, N 14.40.

Mp 57 60 °C

IR (neat) ν: 3346, 2923, 2850, 2780, 1660, 1588, 1365, 1044cm^{-1}.

^{1}H NMR (250 MHz, $CDCl_3$) δ 7.99 (d, *J* = 8.4 Hz, 1H), 7.85 (d, *J* = 8.3 Hz, 1H), 7.76 (d, *J* = 6.7 Hz, 1H), 7.71 – 7.60 (m, 4H), 7.47-7.32 (m, 4H), 6.62 (s, 1H), 6.55 (br s, 1H), 3.86-3.75 (m, 2H), 3.60 – 3.47 (m, 2H), 3.03 (s, 2H), 2.30 (s, 6H) ppm.

^{13}C NMR (63 MHz, $CDCl_3$) δ 174.0, 156.7, 150.7, 137.3, 133.7, 133.5, 130.5, 129.8 (2C), 129.1 (2C), 128.7, 127.6 (2C), 125.0, 120.6, 118.7, 96.3, 63.3, 46.5 (2C), 46.2, 38.9 ppm.

(*E*)-2-(Diethylamino)-N-[2-(2-styrylquinolin-4-ylamino)ethyl]acetamide (229):

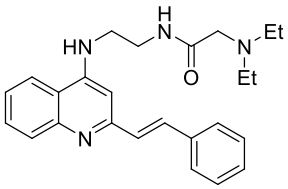

Prepared from **227** (80 mg, 0.195 mmol) and diethylamine (14 mg, 0.195 mmol); the compound was crystallized from MeOH-hexane mixture to give **229** in 71% yield as an orange powder.

Elemental analysis (%) calcd for $C_{25}H_{30}N_4O$: C 74.59, H 7.51, N 13.92; found: C 74.52, H 7.10, N 13.50.

Mp: 54 57 °C

IR (neat) ν: 3341, 2959, 2905, 2850, 1658, 1588, 1430, 1367, 756 cm^{-1}.

^{1}H NMR (250 MHz, $CDCl_3$) δ 7.99 (d, *J* = 8.4 Hz, 1H), 7.86 (d, *J* = 7.6 Hz, 1H), 7.71-7.59 (m, 4H), 7.49 – 7.30 (m, 5H), 6.62 (s, 1H), 3.85 – 375 (m, 2H), 3.60 – 3.46 (m, 2H), 3.12 (s, 2H), 2.56 (q, *J* = 7.1 Hz, 4H), 1.04 – 0.93 (m, 6H) ppm.

^{13}C NMR (63 MHz, $CDCl_3$) δ 175.6, 156.6, 150.8, 137.2, 133.6, 130.3, 130.3, 129.8, 129.6, 129.1 (2C), 128.7, 127.6 (2C), 125.1, 120.6, 118.7, 96.2, 57.8, 49.2 (2C), 46.2, 38.9, 12.7 (2C) ppm.

(*E*)-2-(pyrrolidin-1-yl)-*N*-(2-(2-styrylquinolin-4-ylamino)ethyl)acetamide (230):

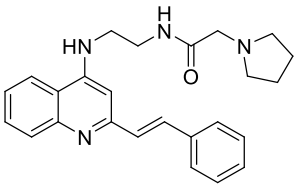

Prepared from **227** (80 mg, 0.195 mmol) and pyrrolidine (14 mg, 0.195 mmol); the compound was crystallized from MeOH-hexane mixture to give **230** in 69% yield as a red solid.

Elemental analysis (%) calcd for $C_{25}H_{28}N_4O$: C 74.97, H 7.05, N 13.99; found: C 74.04, H 6.98, N 13.83.

Mp: 68 71 ^{o}C

IR (neat) ν: 3346, 2918, 2848, 2809, 1655, 1588, 1539, 1365 cm^{-1}.

^{1}H NMR (250 MHz, $CDCl_3$) δ 7.98 (d, *J* = 7.7 Hz, 1H), 7.85 (d, *J* = 8.1 Hz, 1H), 7.70 – 7.60 (m, 4H), 7.48-7.32 (m, 5H), 6.62 (s, 1H), 6.59 (br s, 1H), 3.85-3-78 (m, 2H), 3.60 – 3.46 (m, 2H), 3.26 (s, 2H), 2.67-2.53 (m, 4H),1.85-1.75 (m, 4H) ppm.

^{13}C NMR (63 MHz, $CDCl_3$) δ 174.4, 156.7, 150.7, 148.9, 137.3, 133.5, 130.5, 129.8 (2C), 129.1 (2C), 128.7, 127.6 (2C), 125.0, 120.6, 118.7, 96.3, 59.4, 55.1 (2C), 46.2, 38.9, 24.4 (2C) ppm.

(*E*)-2-(piperidin-1-yl)-*N*-(2-(2-styrylquinolin-4-ylamino)ethyl)acetamide (231):

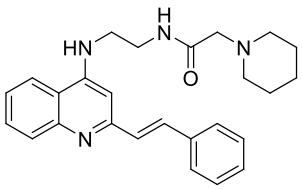

Prepared from **227** (80 mg, 0.195 mmol) and piperidine (17 mg, 0.195 mmol); the compound was crystallized from MeOH-hexane mixture to give **231** in 70% yield as

a yellow solid.

Elemental analysis (%) calcd for $C_{26}H_{30}N_4O$: C 75.33, H 7.29, N 13.52; found: C 75.66, H 7.05, N 13.70.

Mp: 71 74 °C

IR (neat) ν: 3348, 2936, 2851, 1659, 1563, 1538, 1366, 1129 cm^{-1}.

^{1}H NMR (250 MHz, $CDCl_3$) δ 8.10 (d, *J* = 8.3 Hz, 1H), 7.97 (d, *J* = 8.1 Hz, 1H), 7.8-7.72 (m, 4H), 7.6-7.4 (m, 5H), 6.74 (s, 1H), 3.99 – 3.84 (m, 2H), 3.72-3.58 (m, 2H), 3.14 (s, 2H), 2.62-2.48 (m, 4H), 1.70 – 1.67 (m, 4H), 1.57 – 1.55 (m, 2H) ppm.

^{13}C NMR (63 MHz, $CDCl_3$) δ 174.2, 156.6, 150.8, 137.2, 133.6, 130.3, 130.3, 129.8, 129.7, 129.1 (2C), 128.7, 127.6 (2C), 125.1, 120.6, 118.7, 96.2, 62.6, 55.4 (2C), 46.2, 38.9, 26.6 (2C), 24.0 ppm.

(*E*)-2-Morpholino-*N*-[2-(2-styrylquinolin-4-ylamino)ethyl]acetamide (232):

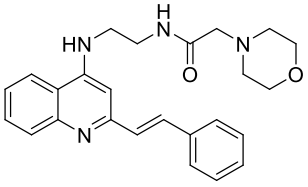

Prepared from **227** (80 mg, 0.195 mmol) and morpholine (17 mg, 0.195 mmol); the compound was crystallized from MeOH-hexane mixture to give **232** in 59% yield as an orange powder.

Elemental analysis (%) calcd for $C_{25}H_{28}N_4O_2$: C 72.09, H 6.78, N 13.45; found: C 71.73, H 6.81, N 13.24.

Mp: 67 70 °C

IR (neat) ν: 3297, 2918, 2850, 1656, 1599, 1560, 1538, 1464 cm^{-1}.

^{1}H NMR (250 MHz, $CDCl_3$) δ 8.03 (d, *J* = 8.0 Hz, 1H), 7.88 (d, *J* = 8.5 Hz, 1H), 7.79 (s, 1H), 7.72 (s, 1H), 7.68 – 7.57 (m, 3H), 7.48 – 7.31 (m, 4H), 6.59 (s, 1H), 3.88 3.77 (m, 2H), 3.77 – 3.65 (m, 4H), 3.62 3.45 (m, 2H), 3.10 (s, 2H), 2.60 – 2.49 (m, 4H) ppm.

^{13}C NMR (63 MHz, $CDCl_3$) δ 173.2, 153.1, 151.5, 147.6, 136.8, 131.4, 130.4, 129.6, 129.2 (2C), 129.1, 128,4, 127.8 (2C), 125.4, 120.9, 118.3, 95.8, 67.3 (2C), 62.2, 54.3 (2C), 45.9, 38.8 ppm.

(*E*)-2-(4-Methylpiperazin-1-yl)-*N*-[2-(2-styrylquinolin-4-ylamino]ethyl)acetamide (233):

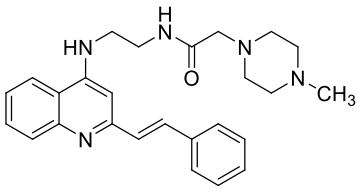

Prepared from **227** (80 mg, 0.195 mmol) and 1-methylpiperazine (20 mg, 0.195 mmol); the compound was crystallized from MeOH-hexane mixture to give **233** in 59% yield as an orange powder.

Elemental analysis (%) calcd for $C_{26}H_{31}N_5O$: C 72.70, H 7.27, N 16.30; found: C 71.87, H 7.86, N 15.39.

Mp: 64 67 °C

IR (neat) ν: 3348, 2923, 2850, 1666, 1588, 1537, 1373, 756 cm^{-1}.

^{1}H NMR (250 MHz, $CDCl_3$) δ 7.99 (d, *J* = 8.5 Hz, 1H), 7.83 (d, *J* = 8.1 Hz, 1H), 7.61-7.50 (m, 4H), 7.38 – 7.20 (m, 5H), 6.52 (s, 1H), 6.05 (br s, 1H), 3.75 – 3.64 (m, 2H), 3.48 – 3.38 (m, 2H), 3.11 (s, 2H), 2.52-2.41 (m, 4H), 2.37-2.25 (m, 4H), 2.28 (s, 3H) ppm.

^{13}C NMR (63 MHz, $CDCl_3$) δ 173.5, 156.7, 150.7, 148.9, 137.2, 133.5, 130.4, 129.8 (2C), 129.3 (2C), 128.7, 127.6 (2C), 125.1, 120.5, 118.7, 96.3, 61.6, 55.5 (2C), 53.9 (2C), 46.4, 46.0, 38.9 ppm.

(*E*)-2-(4-Phenylpiperazin-1-yl)-N-[2-(2-styrylquinolin-4-ylamino)ethyl]acetamide (234):

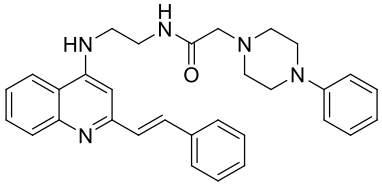

Prepared from **227** (80 mg, 0.195 mmol) and 1-phenylpiperazine (32 mg, 0.195 mmol); the compound was purified by chromatography through a neutral alumina column using DCM-MeOH (95:5, v/v) as mobile phase to give **234** in 45% yield as an orange solid.

Elemental analysis (%) calcd for $C_{31}H_{33}N_5O$: C 75.73, H 6.77, N 14.25; found: C 75.01, H 6.44, N 13.92.

Mp: 92 95 ^{o}C

IR (neat) ν: 3352, 2940, 2825, 1661, 1588, 1538, 1435, 969, 757 cm^{-1}.

^{1}H NMR (250 MHz, MeOD) δ 8.04 (dd, *J* = 8.4, 0.9 Hz, 1H), 7.88 (dd, *J* = 8.5, 0.7 Hz, 1H), 7.76 – 7.61 (m, 4H), 7.47 – 7.31 (m, 5H), 7.23 7.15 (m, 2H), 7.03 (s, 1H), 6.86 – 6.78 (m, 3H), 3.35 3.31 (m, 8H), 3.05 (s, 2H), 3.03 – 2.97 (m, 2H), 2.59 – 2.52 (m, 2H) ppm.

^{13}C NMR (63 MHz, MeOD) δ 174.2, 158.3, 153.2, 153.0, 149.6, 138.5, 135.9, 131.3, 130.4 (2C), 130.3 (2C), 130.2, 130.1, 129.2, 128.7 (2C), 126.0, 122.4, 121.5, 120.1, 117.9 (2C), 96.8, 62.7, 54.8 (2C), 50.9 (2C), 43.9, 39.7 ppm.

(*E*)-2-[4-(piperidin-1-yl)phenylamino]-*N*-[2-(2-styrylquinolin-4-ylamino)ethyl]acetamide (235):

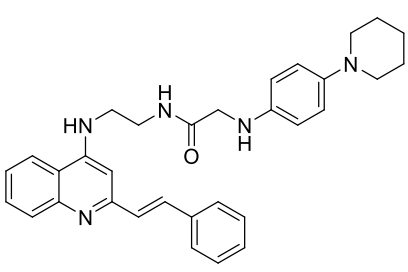

Prepared from **227** (80 mg, 0.195 mmol) and *N*-(4-aminophenyl)piperidine (34 mg, 0.195 mmol); the compound was purified by chromatography through a neutral alumina

column using DCM-MeOH (95:5, v/v) as mobile phase to give **235** in 43% yield as an orange solid.

Elemental analysis (%) calcd for $C_{32}H_{35}N_5O$: C 76.01, H 6.98, N 13.85; found: C 75.68, H 6.84, N 13.81.

Mp: 69 72 °C

IR (neat) ν: 3330, 2918, 2838, 1585, 1555, 1228, 1118, 756 cm^{-1}.

^{1}H NMR (250 MHz, $CDCl_3$) δ 7.99 (d, *J* = 7.6 Hz, 1H), 7.83 (d, *J* = 7.9 Hz, 1H), 7.71-7.60 (m, 4H), 7.48 – 7.30 (m, 5H), 7.16 (s, 1H), 6.97 (d, *J* = 4.6 Hz, 1H), 6.89 – 6.81 (m, 1H), 6.71 – 6.60 (m, 2H), 6.49 (br s, 1H), 4.04 (s, 2H), 3.88 3.76 (m, 2H), 3.66 3.48 (m, 2H), 3.26 – 3.11 (m, 2H), 3.04 – 2.96 (m, 2H), 1.78 1.69 (m, 4H), 1.59 1.53 (m, 2H) ppm.

^{13}C NMR (63 MHz, $CDCl_3$) δ 173.0, 156.7, 150.6, 148.9, 146.2, 140.2, 137.3, 133.5, 130.4, 129.8 (2C), 129.1 (2C), 128.7, 127.6 (2C), 125.0, 120.5, 119.6 (2C), 118.7, 116.6 (2C), 96.4, 53.0 (2C), 46.0, 38.8, 26.6 (2C), 24.6, 15.5 ppm.

(*E*)-2-(Phenylamino)-*N*-[2-(2-styrylquinolin-4-ylamino)ethyl]acetamide (236):

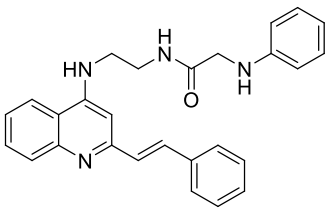

Prepared from **227** (80 mg, 0.195 mmol) and aniline (18 mg, 0.195 mmol); the compound was purified by chromatography through a neutral alumina column using DCM-MeOH (95:5, v/v) as mobile phase to give **236** in 88% yield as a yellow solid.

Elemental analysis (%) calcd for $C_{27}H_{26}N_4O$: C 76.75, H 6.20, N 13.26; found: C 76.45, H 6.17, N 12.88.

Mp: 71 74 °C

IR (neat) ν: 3350, 1655, 1585, 1560, 1535, 1434, 1118, 756 cm^{-1}.

^{1}H NMR (250 MHz, MeOD) δ 8.03 (d, *J* = 8.3 Hz, 1H), 7.87 (d, *J* = 8.5 Hz, 1H), 7.77 – 7.60 (m, 4H), 7.49 – 7.24 (m, 6H), 7.15 – 6.99 (m, 3H), 6.76 – 6.66 (m, 2H), 3.75 (s, 2H), 3.75 –3.42 (m, 4H) ppm.

^{13}C NMR (63 MHz, $CDCl_3$) δ 172.1, 159.4, 154.0, 150.6, 139.5, 136.7, 132.1, 131.4 (2C), 131.3 (2C), 131.0 (2C), 130.1, 129.6 (2C), 126.9, 123.4 (2C), 121.1, 120.7, 118.0, 97.7, 45.1, 42.0, 40.4 ppm.

(*E*)-2-(2,4-Dichlorophenylamino)-*N*-[2-(2-styrylquinolin-4-ylamino)ethyl]acetamide (237):

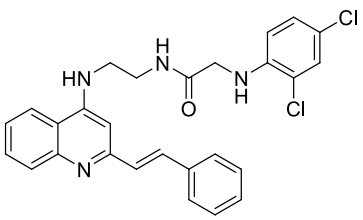

Prepared from **227** (80 mg, 0.195 mmol) and 2,4-dichloroaniline (32 mg, 0.195 mmol); the compound was purified by chromatography through a neutral alumina column using DCM-MeOH (95:5, v/v) as mobile phase to give **237** in 42% yield as a yellow solid.

Elemental analysis (%) calcd for $C_{27}H_{24}Cl_2N_4O$: C 65.99, H 4.92, N 11.40; found: C 65.58, H 4.89, N 11.31.

Mp: 59 62 ^{o}C

IR (neat) ν: 3326, 2918, 1660, 1585, 1536, 1435, 1112, 754 cm^{-1}.

^{1}H NMR (250 MHz, $CDCl_3$) δ 7.99 (d, *J* = 7.6 Hz, 1H), 7.83 (d, *J* = 7.6 Hz, 1H), 7.65 (m, 4H), 7.40 (m, 6H), 7.16 (t, *J* = 6.3 Hz, 1H), 6.63 (s, 1H), 6.49 (s, 1H), 4.04 (s, 2H), 3.86 3.79 (m, 2H), 3.58 – 3.52 (m, 2H) ppm.

^{13}C NMR (63 MHz, $CDCl_3$) δ 173.0, 156.7, 150.6, 148.9, 137.3, 133.5, 130.4, 129.8, 129.7, 129.2, 129.1 (2C), 129.1, 128.7, 128.7, 128.6, 128.2, 127.9, 127.6 (2C), 125.0, 120.5, 118.7, 96.4, 70.1, 67.6, 46.0 ppm.

(*E*)-2-((diethylamino)methyl)-4-(2-styrylquinolin-4-ylamino)phenol (238):

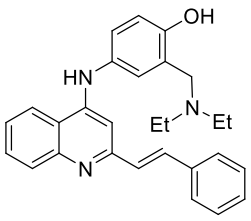

Prepared from **227** (80 mg, 0.195 mmol) and 4-amino-alpha-diethylamino-*o*-cresol (38 mg, 0.195 mmol); the compound was purified by chromatography through a neutral alumina column using DCM-MeOH (95:5, v/v) as mobile phase to give **238** in 54% yield as a green solid.

Elemental analysis (%) calcd for $C_{28}H_{29}N_3O$: C 79.40, H 6.90, N 9.92; found: C 78.91, H 6.50, N 9.39.

Mp: 127 130 °C

IR (neat) ν: 3176, 3050, 3026, 1586, 1552, 1492, 1439, 1257, 752 cm^{-1}.

^{1}H NMR (250 MHz, MeOD) δ 8.38 (d, *J* = 8.4 Hz, 1H), 7.96 (d, *J* = 8.3 Hz, 1H), 7.86 (t, *J* = 7.7 Hz, 1H), 7.66 7.54 (m, 3H), 7.43 7.35 (m, 3H), 7.27 7.14 (m, 2H), 7.04 (d, *J* = 9.3 Hz, 1H), 6.97 (s, 1H), 6.78 (d, *J* = 8.4 Hz, 2H), 4.17 (s, 2H), 3.03 (q, *J* = 7.1 Hz, 4H), 1.30 (t, *J* = 7.1 Hz, 6H) ppm.

^{13}C NMR (63 MHz, MeOD) δ 158.1, 155.0, 145.2, 138.8, 137.4, 133.7, 131.7, 131.1, 130.5 (2C), 129.3, 129.1 (2C), 128.9, 127.5, 125.5, 125.2, 123.5, 122.6, 120.9, 119.5, 118.4, 99.4, 55.3, 48.6 (2C), 10.8 (2C) ppm.

9.6.4. (*E*)-4-(1*H*-Indol-3-yl)-2-styrylquinoline (239):

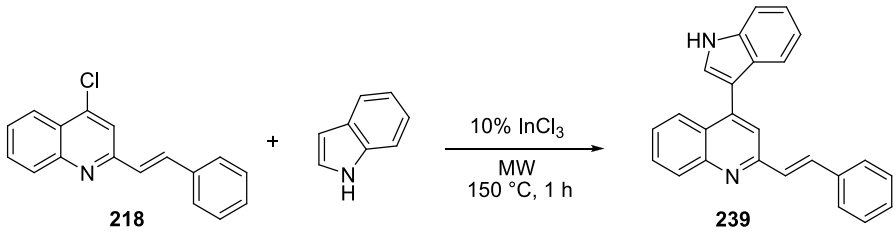

4-Chlorostyrylquinoline **218** (0.100 g, 0.34 mmol), indole (44 mg, 0.34 mmol) and 10% mol of $InCl_3$ (8 mg) were charged in a pressure-tight microwave tube containing 2 ml of acetonitrile and a stirring bar. The reaction mixture was submitted to microwave irradiation for 1 h at 150 C°, with an irradiation power of 150 W, using a CEM Discover SP focused microwave reactor. The crude mixture was dissolved in CH_2Cl_2, washed with H_2O, dried, and evaporated. The pure compound was obtained by flash chromatography on silica gel as a pale yellow solid in 58% yield.

Elemental analysis (%) calcd for C 86.68; H 5.24; N 8.09; found: C 86.53, H 5.44, N 7.76.

Mp: 94 97 °C

IR(neat) ν: 3408, 3054, 3028, 1586, 1500, 1243, 962, 742 cm^{-1}.

^{1}H NMR (250 MHz, $CDCl_3$) δ 8.79 (br s, 1H), 8.22 (d, *J* = 8.4 Hz, 1H), 8.14 (d, *J* = 8.4 Hz, 1H), 7.82 (d, *J* = 19.5 Hz, 1H), 7.78 – 7.66 (m, 4H), 7.59 – 7.54 (m, 3H), 7.48 – 7.33 (m, 6H), 7.28 – 7.22 (m, 1H) ppm.

^{13}C NMR (63 MHz, $CDCl_3$) δ 156.1, 149.3, 142.8, 137.0, 136.7, 134.8, 130.1, 129.8, 129.5, 129.2 (2C), 129.0, 127.7 (2C), 127.3, 127.2, 126.7, 126.4, 125.0, 123.4, 121.1, 120.5, 120.2, 114.6, 112.1 ppm.

9.6.5. (*E*)-4-[2-(4-Acetoxyquinolin-2-yl)vinyl]-1,2-phenylene diacetate (240):

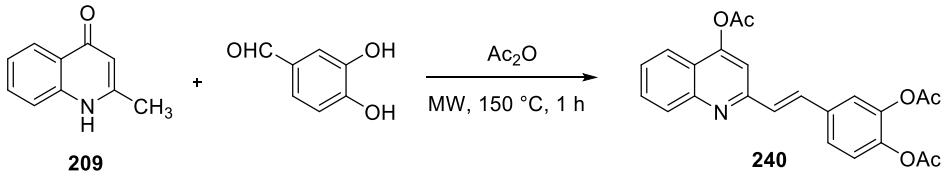

Compound **209** (0.100 g, 0.628 mmol) and 3,4-dihydroxybenzaldehyde (0.104 g, 0.754 mmol) were suspended in Ac_2O (1 ml) in a pressure-tight microwave tube containing a stirring bar. The mixture was heated under microwave irradiation for 1 h at 150 °C, with an irradiation power of 200 W, using a CEM Discover SP microwave reactor. The solvent was removed under reduced pressure to give a black residue that was purified by chromatography through a silica column using PE-EtOAc (90:10, v/v) as the mobile phase. The product **240** was isolated as a pale yellow solid in 65% yield.

^{1}H NMR (250 MHz, $CDCl_3$) δ 8.04 (d, *J* = 8.4 Hz, 1H), 7.82 (d, *J* = 8.3 Hz, 1H), 7.70 – 7.63 (m, 1H), 7.54 (d, *J* = 16.3 Hz, 1H), 7.49 – 7.38 (m, 4H), 7.19 – 7.14 (m, 2H), 2.44 (s, 3H), 2.26 (s, 3H), 2.24 (s, 3H) ppm.

^{13}C NMR (63 MHz, $CDCl_3$) δ 167.2 (3C), 155.3, 153.3, 148.8, 141.3, 141.2, 134.3, 132.1, 129.4, 128.6, 128.3, 125.6, 124.5, 122.7, 120.9, 120.4, 120.1, 110.0, 20.2, 19.7, 19.6 ppm.

9.6.6. (*E*)-4-[2-(4-Chloroquinolin-2-yl)vinyl]-1,2-phenylene diacetate (241):

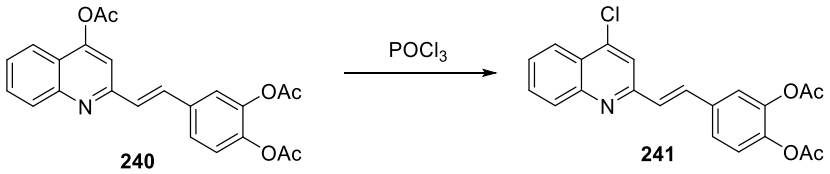

Compound **240** (0.100 g, 0.25 mmol) was added portionwise to a solution of excess phosphorus oxychloride (15 ml) at 0 ^{o}C. After being stirred for 30 min at room temperature, the reaction mixture was heated at 80 °C for 30 min to 1h. The excess phosphorus oxychloride was removed by vacuum distillation. The residue was poured slowly onto a mixture of crushed ice and saturated $NaHCO_3$ solution with vigorous stirring. The pH of the solution was adjusted to about 9.0 by addition of ammonium hydroxide. The solid product that separated out was collected by filtration, dried and used for the next reaction without further purification. The product was isolated in 79% yield as a grey solid.

^{1}H NMR (250 MHz, $CDCl_3$) δ 8.24 (d, *J* = 8.2 Hz, 2H), 7.87 – 7.64 (m, 4H), 7.58 – 7.52 (m, 2H), 7.40 (d, *J* = 16.0 Hz, 1H), 7.27 (d, *J* = 7.2 Hz, 1H), 2.36 (s, 3H), 2.34 (s, 3H) ppm.

^{13}C NMR (63 MHz, $CDCl_3$) δ 168.6 (2C), 155.1, 147.5, 144.8, 143.2, 142.9, 135.6, 135.1, 132.0, 128.6, 128.2, 127.4, 126.4, 125.9, 124.6, 124.3, 122.7, 119.7, 21.1 (2C) ppm.

9.6.7. 3,4-Di(methoxymethoxy)benzaldehyde (242):

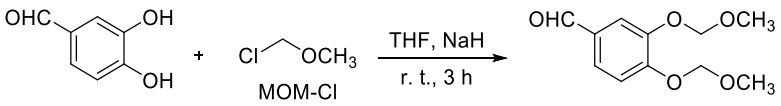

242

Washed NaH (60% w/w 1.104 g, 46 mmol) in THF (10 ml) was added to a solution of 3,4-dihydroxybenzaldehyde (2.05 g, 14.9 mmol) in THF (5 ml). The mixture was stirred for 1 h at r.t. Then, chloromethyl methyl ether (3.38 g, 46 mmol) was added dropwise and after 2 h the reaction was quenched with H_2O (20 ml) and extracted with ether (50 ml). The mixture was washed with H_2O (2 x 50 ml), 5% NaOH solution (2 x 50 ml), and brine (2 x 50 ml). The organic layers were collected and dried with anhydrous Na_2SO_4, and the solvent removed *in vacuo* to achieve **242** as a white oil in 18 % yield.

^{1}H NMR (250 MHz, $CDCl_3$) δ 9.89 (s, 1H), 7.71 (d, *J* = 1.9 Hz, 1H), 7.54 (dd, *J* = 8.4, 1.9 Hz, 1H), 7.31 (d, *J* = 8.6, 1H), 5.35 (s, 2H), 5.33 (s, 2H), 3.55 (s, 6H) ppm.

9.7. Synthesis of 8-aminostyrylquinolines against Leishmaniasis

9.7.1. General procedure for nitration of 2-methylquinoline

2-Methylquinoline **161** (2 g, 13.96 mmol) was dissolved in cold H_2SO_4 (7 ml) at 0 °C, then a cold mixture of H_2SO_4/HNO_3 (7 ml/3.5 ml) was added, and the mixture was stirred for 30 min at 0 °C, then heated for 30 min at 50 °C. The solution was neutralized by slow addition of a concentrated solution of NaOH, the resulted precipitate was filtered and washed with water. The solid was dried overnight in the presence of P_2O_5. The roughly 1/1 mixture of 8-nitro (41%) and 5-nitro (35%) quinaldine isomers was separated by column on silica gel (petroleum ether/ ethyl acetate - 93/7).

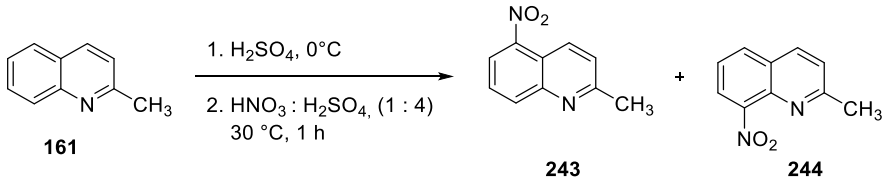

2-methyl-5-nitroquinoline (243):

Yield: 35%; white solid.

^{1}H NMR (250 MHz, $CDCl_3$) δ 8.91 (d, *J* = 9.0 Hz, 1H), 8.38 – 8.30 (m, 2H), 7.79 (t, *J* = 8.1 Hz, 1H), 7.55 (d, *J* = 9.0 Hz, 1H), 2.82 (s, 3H) ppm.

^{13}C NMR (63 MHz, $CDCl_3$) δ 161.1, 148.5, 145.9, 136.2, 132.3, 127.9, 125.5, 124.2, 119.9, 25.7 ppm.

2-Methyl-8-nitroquinoline (244):

Yield: 41%; white solid.

^{1}H NMR (250 MHz, $CDCl_3$) δ 8.15 (d, *J* = 8.5 Hz, 1H), 8.02 – 7.98 (m, 2H), 7.58 (d, *J* = 7.9 Hz, 1H), 7.45 (d, *J* = 8.5 Hz, 1H), 2.81 (s, 3H) ppm.

^{13}C NMR (63 MHz, $CDCl_3$) δ 162.60, 139.55, 136.28, 131.90, 127.82, 127.79, 124.68, 124.23, 123.73, 26.26 ppm.

9.7.2. 8-Nitroquinoline-2-carbaldehyde (245):

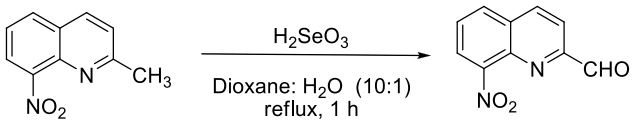

244 **245**

To a solution of selenious acid (0.05 g, 0.38 mmol) in dioxane (1 ml) and water (0.1 ml) was added 8-nitro-quinaldine **244** (0.05 g, 0.26 mmol) in dioxane (1 ml) and the reaction refluxed for 1 h. The hot solution was then filtered from the selenium metal and cooled and the solvent removed under reduced pressure. The residue oil was basified with saturated $NaHCO_3$ and the precipitate collected. Purification of the crude solid by flash chromatography (petroleum ether/ ethyl acetate, 90/10) yielded the aldehyde **265** as a white solid in 65%.

^{1}H NMR (250 MHz, $CDCl_3$) δ 10.23 (d, *J* = 0.9 Hz, 1H), 8.48 (dd, *J* = 8.5, 0.7 Hz, 1H), 8.22 – 8.15 (m, 3H), 7.81 (dd, *J* = 8.2, 7.6 Hz, 1H) ppm.

^{13}C NMR (63 MHz, $CDCl_3$) δ 193.37, 154.24, 139.60, 138.23, 138.14, 132.26, 130.88, 128.32, 124.92, 119.42 ppm.

9.7.3. Benzyltriphenylphosphonium bromide (246):

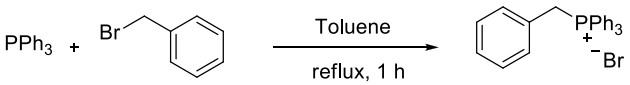

246

The benzylbromide (0.250 g, 1.46 mmol) and triphenylphosphine (0.380 g, 1.46 mmol) was refluxed in 10 ml of toluene for 1 h. The formed precipitate was filtered to obtain the product as a white solid in 98% yield. No further purification was needed.

^{1}H NMR (250 MHz, $CDCl_3$) δ 7.82 – 7.61 (m, 15H), 7.27 – 7.12 (m, 5H), 5.43 (d, *J* = 14.4 Hz, 2H) ppm.

^{13}C NMR (63 MHz, $CDCl_3$) δ 135.42 (d, *J* = 3.0 Hz, 3C), 134.80 (d, *J* = 9.8 Hz, 6C), 131.92 (d, *J* = 5.6 Hz, 3C), 130.57 (d, *J* = 12.5 Hz, 3C), 129.24 (d, *J* = 3.3 Hz, 3C), 128.81 (d, *J* = 3.9 Hz, 2C), 127.48 (d, *J* = 8.6 Hz, 1C), 118.16 (d, *J* = 85.7 Hz, 3C), 31.22 (d, *J* = 47.0 Hz, 1C) ppm.

9.7.4. (*E*)-8-nitro-2-styrylquinoline (247):

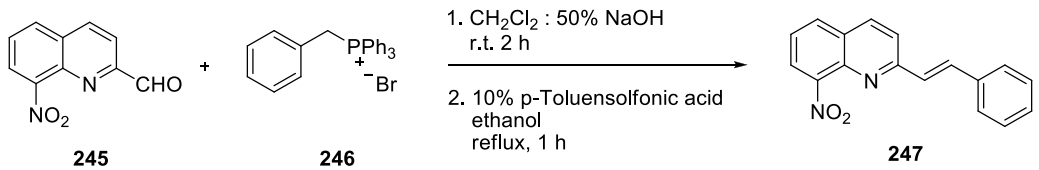

245 **246** **247**

Compound **245** (0.200 g, 0.989 mmol) and 1 equiv of benzyltriphenylphosphonium bromide **246** (0.428 g, 0.989 mmol) were stirred in a biphasic solvent system consisting of 3 ml of CH_2Cl_2 and 3 ml of sodium hydroxide (50%) for 2 h. The aqueous layer was then extracted with CH_2Cl_2, the resultant organic extract dried and filtered, and the solvent removed under

reduced pressure. TLC indicated two products, presumably the cis and trans adducts, which upon reflux for 1 h in ethanol and catalytic p-toluenesulfonic acid monohydrate (50 mg, 10%) were converted to one product. Removal of ethanol under reduced pressure followed by purification using flash chromatography (8:2, hexane/ethyl acetate) yielded the required compound **247** in 80% yield as yellow solid.

^{1}H NMR (250 MHz, $CDCl_3$) δ 8.22 (d, *J* = 8.7 Hz, 1H), 8.04 – 7.97 (m, 2H), 7.85 (d, *J* = 16.2 Hz, 1H), 7.75 (d, *J* = 8.7 Hz, 1H), 7.67 (dd, *J* = 8.0, 1.2 Hz, 2H), 7.58 – 7.52 (m, 1H), 7.48 – 7.38 (m, 4H) ppm.

^{13}C NMR (63 MHz, $CDCl_3$) δ 158.46, 148.45, 140.03, 137.15, 136.66, 136.45, 131.94, 129.57, 129.25 (2C), 128.50, 128.21, 128.04 (2C), 124.85, 124.30, 121.94 ppm.

9.7.5. (*E*)-2-styrylquinolin-8-amine (248):

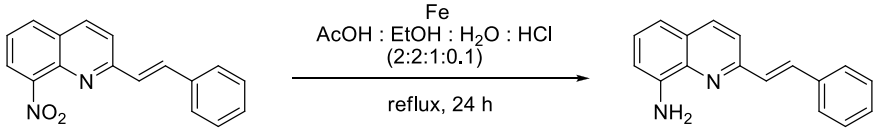

247 **248**

Compound **247** (0.06 g, 0.216 mmol), iron powder (100 mg, 0.324 mmol), glacial acetic acid, ethanol, water (0.4 ml/0.4 ml/0.2 ml) and 2 drops of aqueous HCl were refluxed for 24 h. Water was added and the mixture extracted with chloroform. The organic layer was washed with saturated $NaHCO_3$ solution, dried and the solvent removed under reduced pressure. The compound was purified by chromatography that yielded **248** in 98 % yield as a yellow solid.

^{1}H NMR (250 MHz, $CDCl_3$) δ 8.07 (d, *J* = 8.6 Hz, 1H), 7.75 – 7.62 (m, 4H), 7.47 – 7.32 (m, 5H), 7.16 (d, *J* = 7.5 Hz, 1H), 6.96 (d, *J* = 7.5 Hz, 1H), 5.10 (br s, 2H) ppm. **^{13}C NMR** (63 MHz, $CDCl_3$) δ 153.43, 144.29, 138.53, 137.13, 136.71, 133.63, 129.54, 129.20 (2C), 128.83, 128.23, 127.56 (2C), 127.48, 120.14, 116.29, 110.74 ppm.

9.8. Functionalization of nanoparticles

9.8.1. Spion coating

SPION nanoparticles dissolved in toluene were precipitated with ethanol and separated by centrifugation (765 rcf, 20min). The pellet was dried and resolubilized in chloroform. Poly(maleic anhydride-alt-1-octadecene) in excess was dissolved stirring for 1 hour in chloroform. The solutions were mixed and the chloroform slowly evaporated under pressure control lowering it starting from 210 mbar to 70 mbar step by step. To completely eliminate the solvent, the obtained sample was put under gentle stream of nitrogen for 1 hour. An alkaline solution of water and TMAH and 0.1M NaOH were used to solubilize the dried film and sonicated for 15 min and left overnight. The solution was filtered by 0.22μm pores syringe filter and concentrated by ultracentrifugation with Amicon filter units 50kDa at 405 rcf49.

9.8.2. Functionalization of polystyrene NPs with PEG

Stock solution of Jeffamine PEG (M = 0.02) and EDAC (M = 0.15) in PBS were prepared. 50 μl of 20 nm polystyrene NPs (M = 0.02) were placed in a 15 ml falcon tube with 700 μl of PEG solution and 700 μl of EDAC. The solution was stirred overnight and then dialysed against PBS at pH 7.4 (10 mM NaCl) to eliminate the excess of PEG by using a dialysis tube of Mw 100kDa cut-off for three days changing the solvent twice a day. The NPs were characterized by DLS (Zeta potential = -1.17 ± 1.75, average diameter = 80.06 ± 0.075, PDI = 0.139 ± 0.14), FTRI-ATR (Figure 9.1) and TGA (Figure 9.2) spectra.

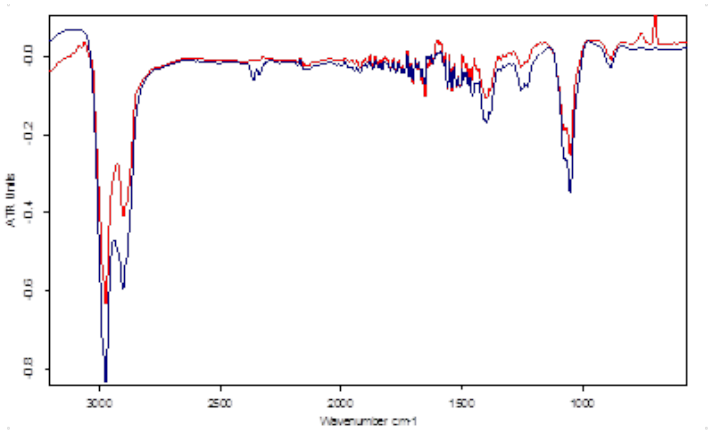

Fig. 9.1 FTRI spectra of polystyrene NPs (red line) and NPs-PEG (blue line).

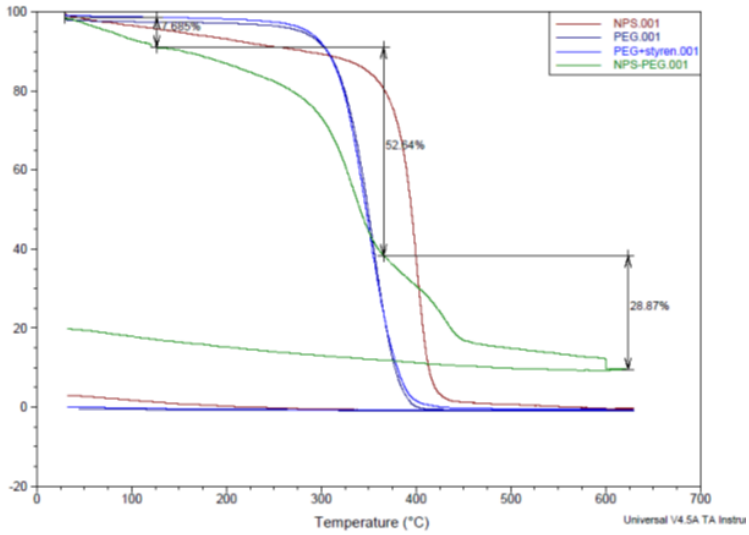

Fig. 9.2. TGA spectra of Polystyrene NPs (brown line), Jeffamine PEG M1000 (purple line), mixture of NPs and PEG (blue line) and functionalized NPs with PEG (green line). We can observe how the slope of the curve related to the functionalized NPs change compared with the starting materials.

9.8.3. Synthesis of an analog of the MSH peptide

The partially protected NDP-MSH peptide, H-Ser-Tyr-Ser-Nle-Glu-His-d-Phe-Arg-Trp-Gly-Lys(Dde)-Pro-Val-NH_2, was synthesized manually using *N*α-Fmoc chemistry. Briefly, Rink amide resin (4-(2',4'-dimethoxyphenyl-Fmocaminomethyl) phenoxy resin, substitution 0.6 mmol/g) was swollen in dichloromethane:DMF (1:1) for three hours. The resin was washed with DMF (3 × 10 ml), and the *N*α-Fmoc protecting group was removed by 25% piperidine in DMF (1 × 5 min and 1 × 20 min). The resin was washed with DMF (3 × 5 ml), and the first *N*α-Fmoc amino acid was coupled adding preactivated ester (3 equiv of *N*α-Fmoc amino acid, 3 equiv of HOBt, and 3 equiv of HBTU) in DMF solution and 6 equiv of DIEA. The mixture was incubated for 40 min. At the end of the coupling, the resin was washed with DMF (3 × 10 ml) and a Kaiser ninhydrin test was done to check the extent of coupling. If coupling was complete, the resin was once again washed with DMF, and the same procedure was repeated to couple the remaining amino acids.

The cleavage cocktail consisting of tifluoroacetic acid (TFA, 7.8 ml), triethylsilane (0.7 ml), 1,2-ethanedithiol (0.7 ml) water (0.8 ml) was chilled on ice. The cold solution was then added to the resin-bound protected peptide and the reaction mixture incubated for 2.5 h at room temperature. The crude peptide was precipitated out by pouring the mixture into a round bottom flask filled with diethyl ether (40 ml) to give a white solid. The organic layer was decanted off after centrifugation of the peptide for 5 min at 12,000 rpm. The precipitate was washed with diethyl ether (3 × 40 ml) and dried in vacuum overnight. The crude peptide did not need further purification.

9.8.4. Covalent coupling between the peptidic ligand and PEG

To a solution of 5 mg of peptide (scramble or MSH, 0.003 mmol) and 0.0066 mmol of NHS-PEG 750 dissolved in DMF were added 30 μl of DIPEA and the reaction mixture was stirrer for 24 h at room temperature. The reaction was monitored by the ninhydrin Kaiser test. When it resulted negative the DMF was evaporated under vacuum. The white solid residue was dissolved in the 0.5 ml of water and purified through semi-prep HPLC. The sample was eluted with water containing 0.1% TFA and acetonitrile containing 0.1% TFA varying from 0% to 90% over 25 min at a flow rate of 1 ml/min. The conjugated products were characterized by mass spectra (Figure 9.3).

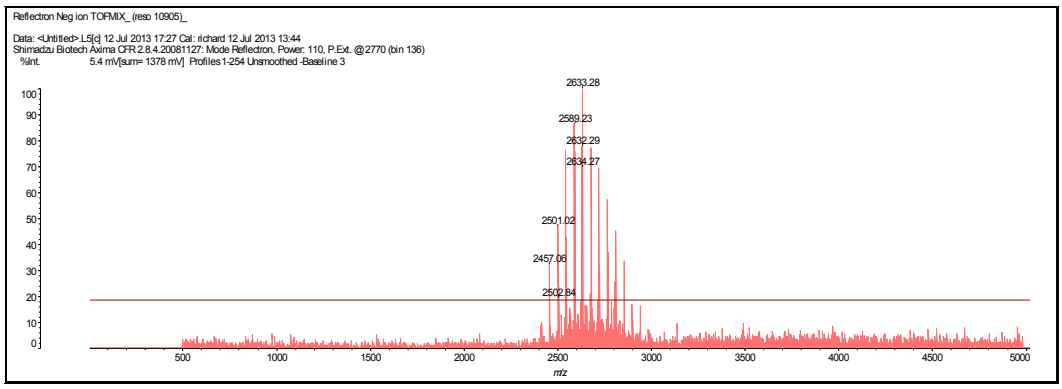

Fig. 9.3. MALDI-TOF spectra of the conjugated product between MSH peptide and PEG 750

In the case of the bi-dentate PEG, 10 mg of MSH peptide and 25 mg of NSH-PEG-BOC were dissolved in 1 ml of DMF. To the mixture, 45 μl of DIPEA were added and was stirred for 3 days at r.t. After removal of solvent, the residue was dissolved in 1 ml of water and purified through a Sephadex G-25 (GE Healthcare) gel permeation chromatography column using water as the eluting solvent. The eluted PEG fractions (1.5 ml each) containing peptide (UV absorption at 280 nm)

were collected, and the product was dialyzed against water for three days to eliminate residues of PEG by using a dialysis tube of Mw 100kDa cut-off for three days changing the solvent each two hours.

10. Conclusions

1. Focused MW irradiation of equimolecular mixtures of 9-chloroacridines, 4-chloroquinolines and 4- chloroquinazolines with amines in the presence of 2 equiv of phenol led to a general, fast and high-yielding synthesis of aminated heterocycles, with a very broad scope in terms of the types of amine that can be employed. Furthermore, workup consisted of a simple washing with water and purification could be achieved by crystallization of the crude product, avoiding the use of organic solvents in extraction and chromatographic purification steps. These features lead us to the conclusion that our protocol, besides constituting a green approach, solves a long-standing synthetic problem and will facilitate the generation of libraries of a class of compounds of great significance in medicinal chemistry and drug discovery.

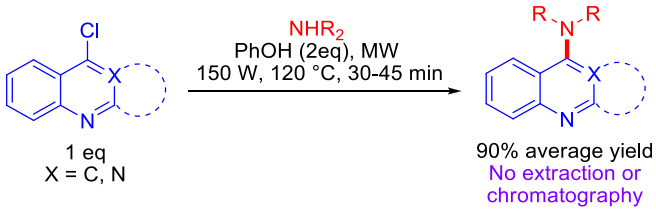

2. We have developed a simple, general, one-pot coupling reaction that allows the rapid and fully regioselective generation of both aromatic C-C and C-N bonds on a variety of nitrogen heterocycles, focusing on quinoline and acridine moiety due to their relevance in neurodegenerative and protozoan diseases. The process is highly affordable, as it requires only an equimolecular mixture of simple starting materials and a catalytic amount of the relatively inexpensive Lewis acid $InCl_3$. Furthermore, in most cases workup required only a simple filtration and hence no organic solvents were needed for extraction and chromatographic purification steps. Some noteworthy features of the method include: (a) the high yields and relatively short reaction times compared with those needed under conventional conditions; (b) the first use of a Lewis acid as a

catalyst in heteroarylation, vinylation and amination reactions on π-deficient heterocyclic substrates; (c) the confirmation of the generality of the method by its application to target-oriented synthesis.

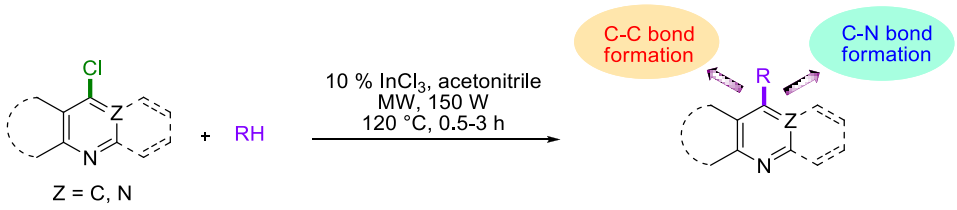

3. We have identified DKP as a novel scaffold in antiprion drug design. Compound **83**, thanks to its planar conformation, is able to perturb PrP amyloid fibril formation by preventing the process *in vitro*. Moreover, it has been shown to inhibit prion replication in the low micromolar range in a cellular context. For these reasons, **83** is a lead candidate for further optimization studies. Even if preliminary, these results represent a first step toward the discovery of novel DKPs with potential towards PrDs. A second major outcome of this work was the identification of the β-carboline derivative **104**. Fluorescent probes that specifically target amyloid aggregates are of great relevance to advance our understanding of the molecular pathogenesis underlying cerebral amyloidosis.

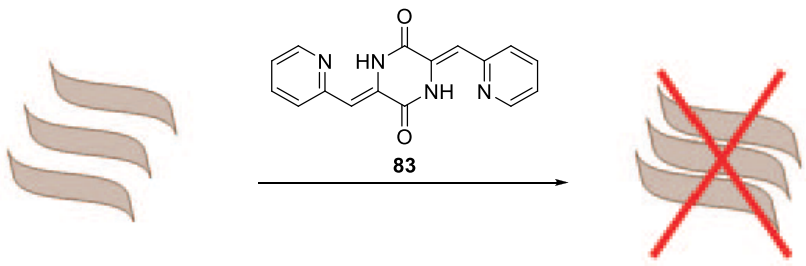

4. We reported the synthesis of two small libraries of fluorene and carbazole-based analogues of GN8, the study of their native fluorescence, the evaluation of their antiprion activity in infected cells, and the staining of fibrillar

plaques. Preliminary results showed that some compounds (**124** and **125**) turned out to be more active and less toxic that GN8. Furthermore, compound **128** has been shown to be able to interact selectivity with PrP^{Sc} preventing partially prion replication and, due to its fluorescence, can be regarded as potential diagnostic tool for prion diseases. More importantly, we have demonstrated how modifying the structure of GN8 generating a more planar and rigid molecule the biological target changes.

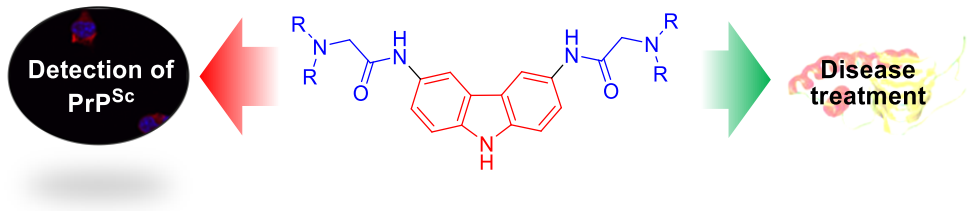

5. We preliminary explored styrylquinolines **137-138** as $A\beta/PrP^{Sc}$ diagnostic and therapeutic small molecules. Among them, **139** is potentially useful to diagnose, treat and monitor response to therapy in PMD. Indeed, from a medicinal chemistry perspective **139** offers peculiar advantages: (1) a low molecular weight, (2) a small-molecule scaffold that is easily amenable to further manipulation to improve fluorescence response and amyloid-binding properties. Most importantly, with respect to the previously reported NIR amyloid tracers, it offers the additional advantage of a concomitant promising anti-fibrillar profile (*in vitro* and in a cellular context), together with a low toxicity. If these peculiar properties are confirmed *in vivo*, **139** is likely to become the first purposely-designed therapeutic and diagnostic tool (theranostic) for PrD and AD.

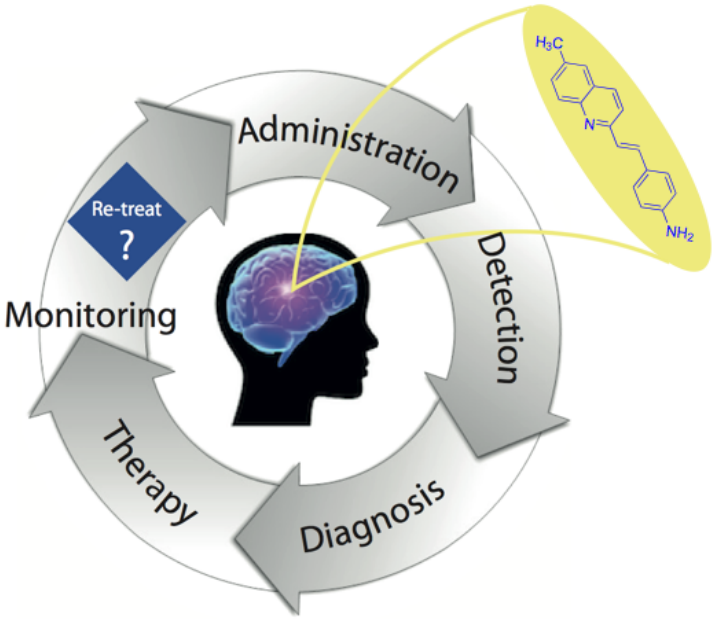

6. Starting from compound **139**, which is endowed with therapeutic and diagnostic features, we designed and generated a new series of styrylquinoline derivatives with the purpose of improving such characteristics. The synthesis was achieved via a vinylogous variation of the Povarov reaction to afford 2-styryl-1,2,3,4-tetrahydroquinolines followed by their dehydrogenation or, alternatively, by microwave-assisted aldol condensation between substituted quinaldines and aromatic aldehydes. As regard the the biological data, our preliminary results showed that 7 molecules have higher antiprion activity that that of **139** and further studies are being performed to explore the possibility of using these compounds for treatment and diagnosis of PMD *in vivo*.

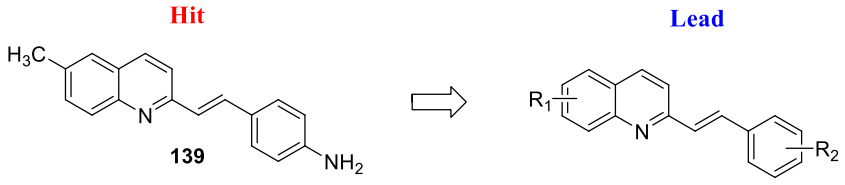

7. Considering the styrylquinoline fragment as a privileged structure, we generated a small library of 4-aminostyryquinoline derivatives. The anti-leishmanial activity was preliminary evaluated *in vitro* in promastigote and amastigote forms across all the library of synthesized compounds revealing a very high efficacy. In addition, further experiments showed that the polyamine chain is critical for the activity and the styrylquinolines could exert their leishmanicidial action by interfering with the parasite mitochondrial functionality.

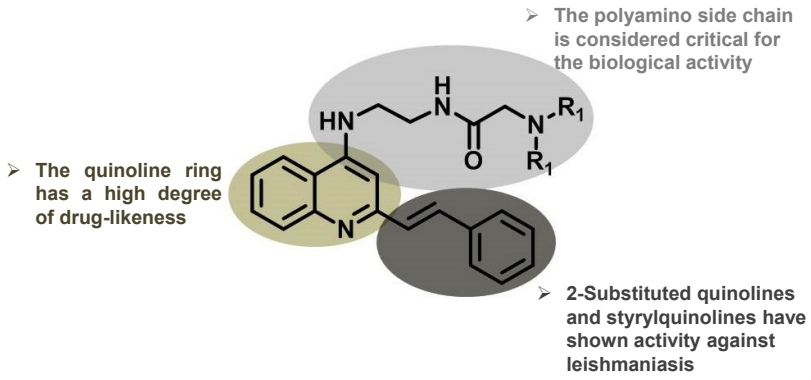

8. Based on the good results obtained from the 4-aminostyrylquinoline derivatives, we planned to develop a new series of styrylquinolines endowed with different polyanimo chains at the quinoline C-8 position that will be tested against Leishmanasis at Luis Rivas's lab at CIB.

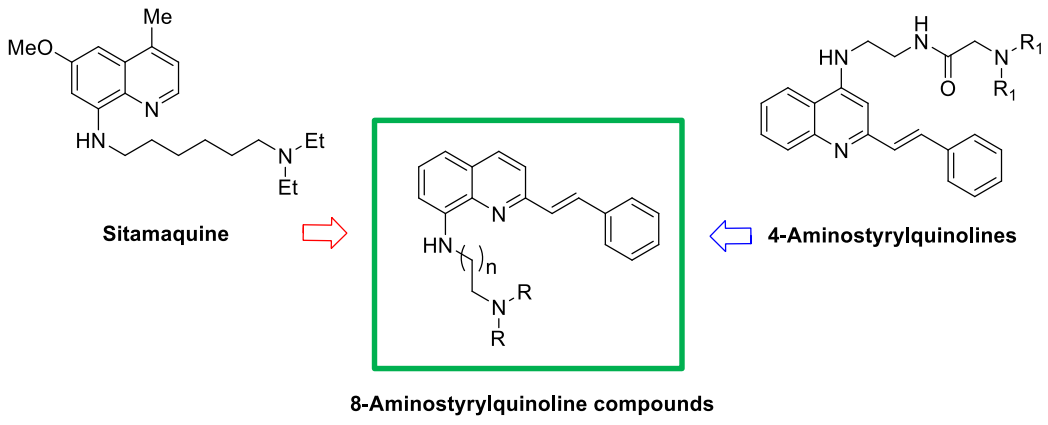

9. In order to explore nanomedicine as another facet of the theranostic field, we investigated nanoparticle chemistry. We developed an efficient protocol to synthetize conjugated product between NDP-MSH peptide and its scramble version with NHS-PEG. Furthermore, we found a general method to functionalize 20 nm NPs with PEG. With the preparation of coated SPIONs, we paved the way to the final step of the synthesis combining them with the targeting ligand to obtain new innovative tools against metastatic melanoma.

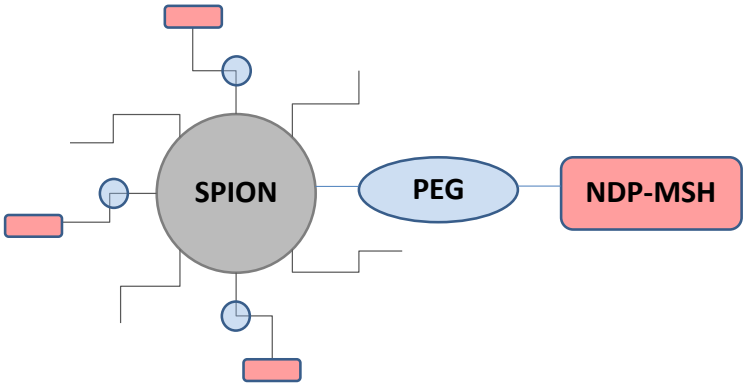

Appendix. Representative spectra

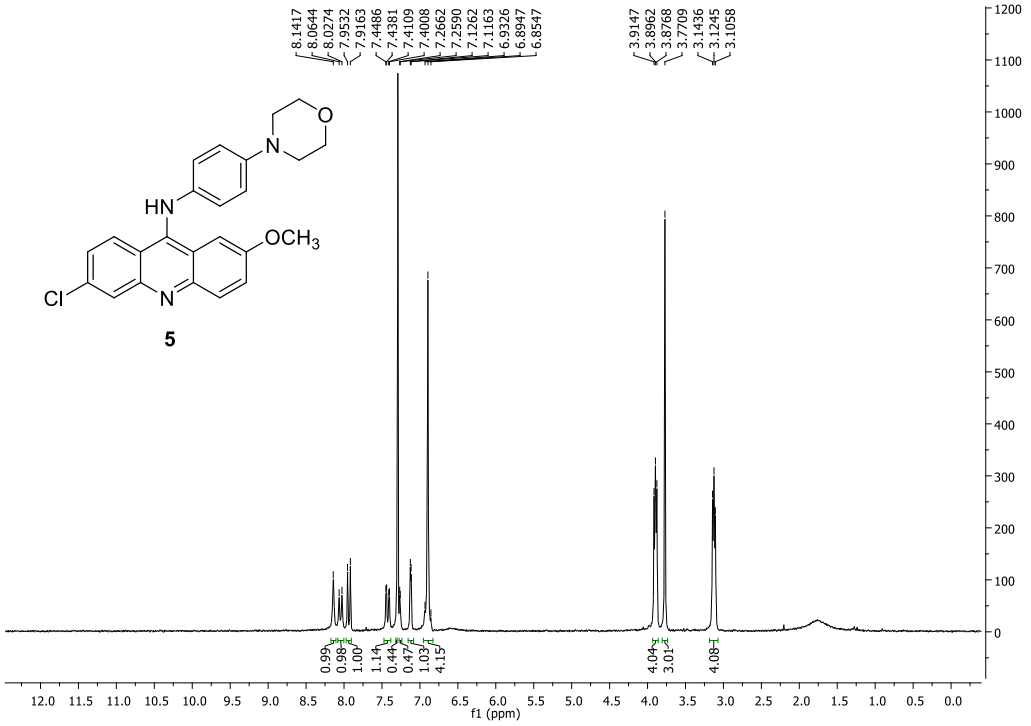
8.1417
8.0644
8.0274
7.9532
7.9163
7.4486
7.4381
7.4109
7.4008
7.2662
7.2590
7.1262
7.1163
6.9326
6.8947
6.8547
3.9147
3.8962
3.8768
3.7709
3.1436
3.1245
3.1058
HN
O
N
OCH3
Cl
N
5
f1 (ppm)

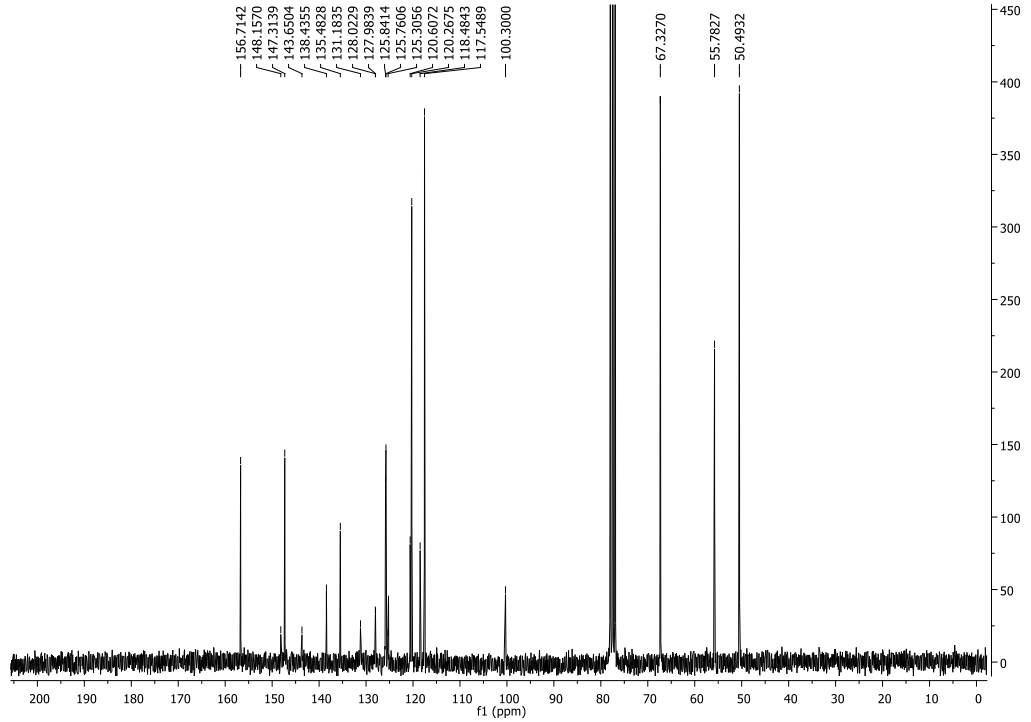
156.7142
148.1570
147.3139
143.6504
138.4355
135.4828
131.1835
128.0229
127.9839
125.8414
125.7606
125.3056
120.6072
120.2675
118.4843
117.5489
100.3000
67.3270
55.7827
50.4932
f1 (ppm)

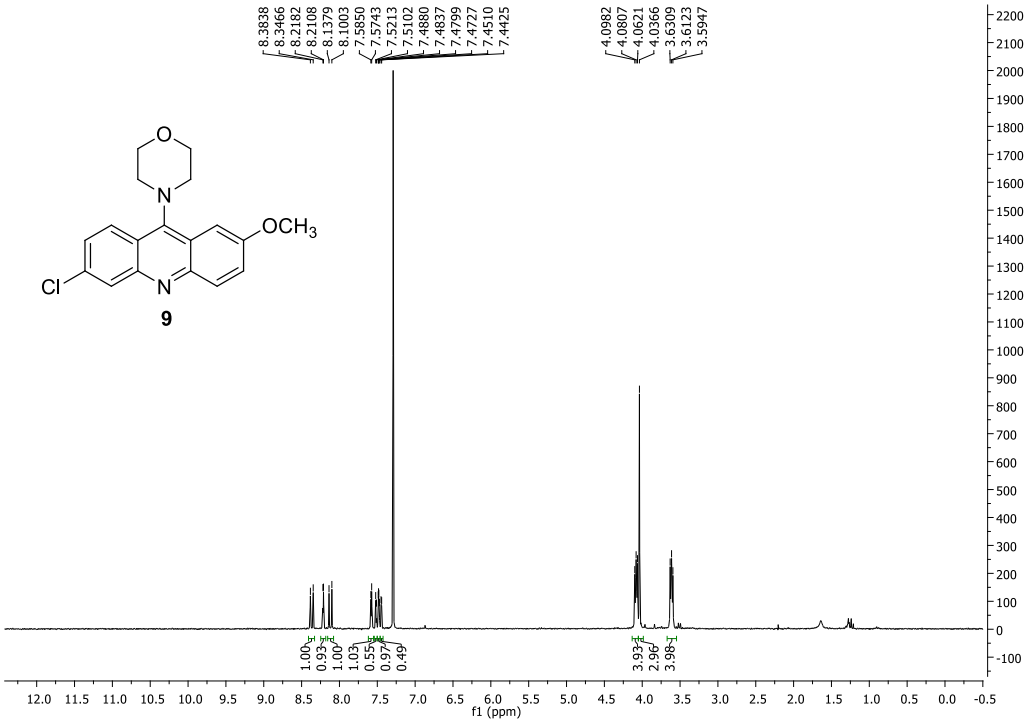
8.3838
8.3466
8.2182
8.2108
8.1379
8.1003
7.5850
7.5743
7.5213
7.5102
7.4880
7.4837
7.4799
7.4727
7.4510
7.4425
4.0982
4.0807
4.0621
4.0366
3.6309
3.6123
3.5947
1.00
0.93
1.00
1.03
0.55
0.97
0.49
3.93
2.96
3.98
f1 (ppm)

9

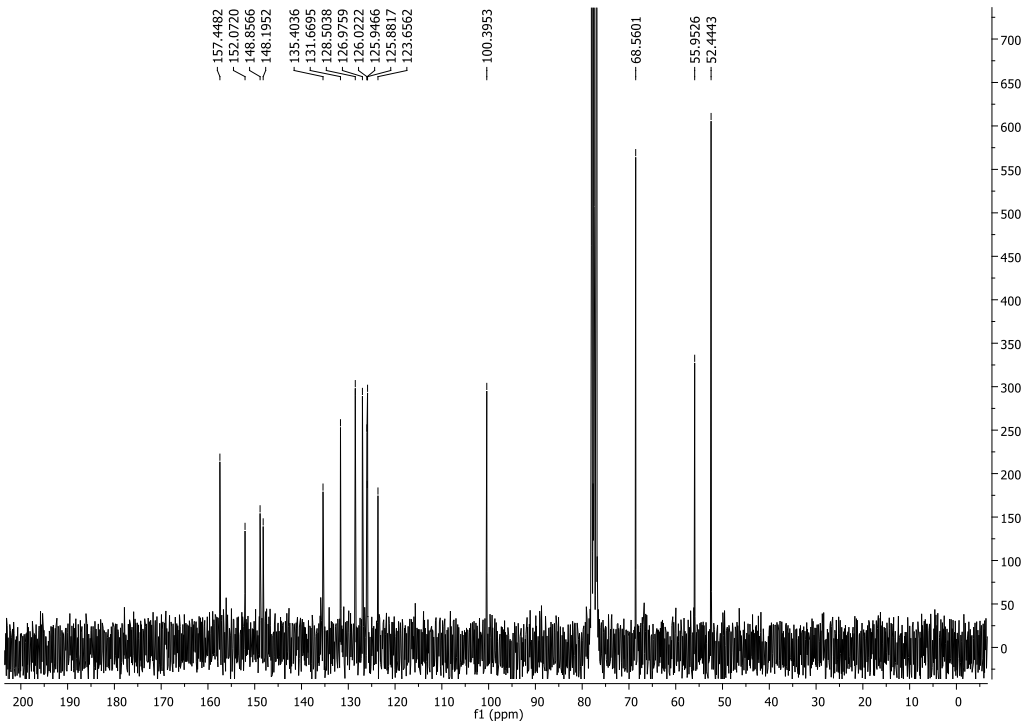
157.4482
152.0720
148.8566
148.1952
135.4036
131.6695
128.5038
126.9759
126.0222
125.9466
125.8817
123.6562
100.3953
68.5601
55.9526
52.4443
f1 (ppm)

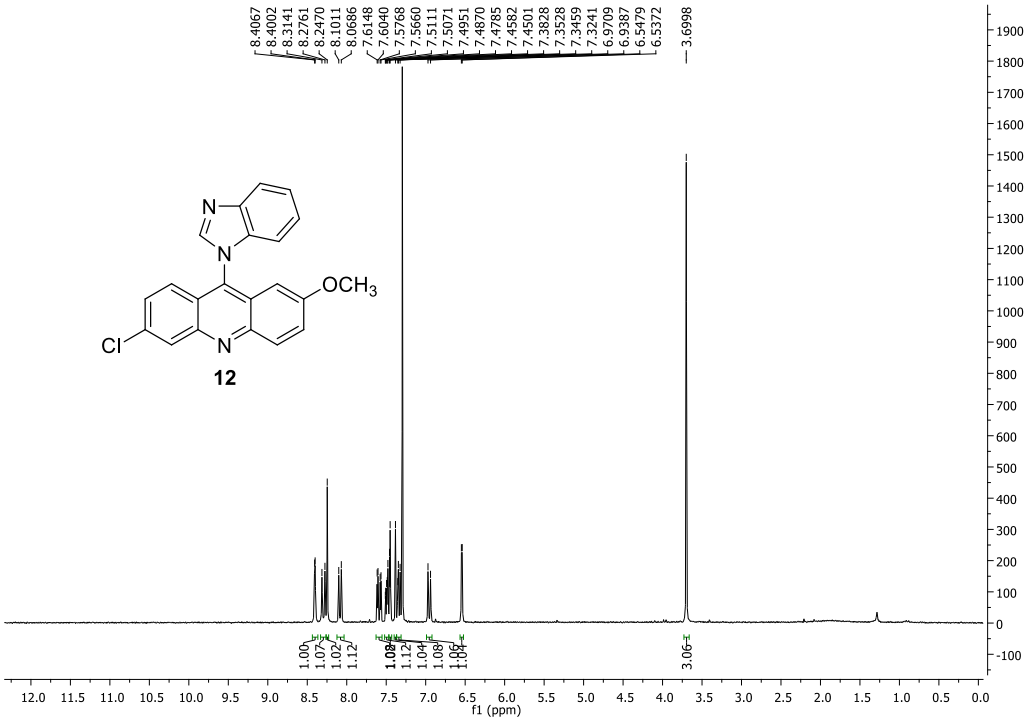
8.4067
8.4002
8.3141
8.2761
8.2470
8.1011
8.0686
7.6148
7.6040
7.5768
7.5660
7.5111
7.5071
7.4951
7.4870
7.4785
7.4582
7.4501
7.3828
7.3528
7.3459
7.3241
6.9709
6.9387
6.5479
6.5372
3.6998
N
N
OCH3
Cl
N
12
1.00
1.07
1.02
1.12
1.08
1.12
1.04
1.08
1.06
1.04
3.06
f1 (ppm)

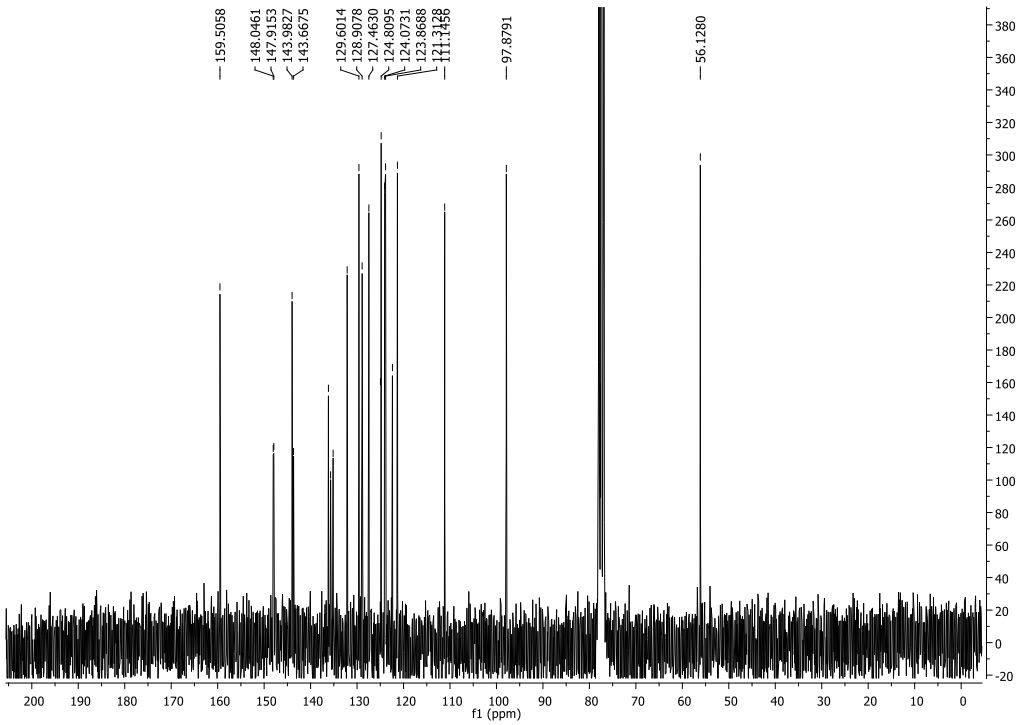
159.5058
148.0461
147.9153
143.9827
143.6675
129.6014
128.9078
127.4630
124.8095
124.0731
123.8688
121.3128
111.1456
97.8791
56.1280
f1 (ppm)

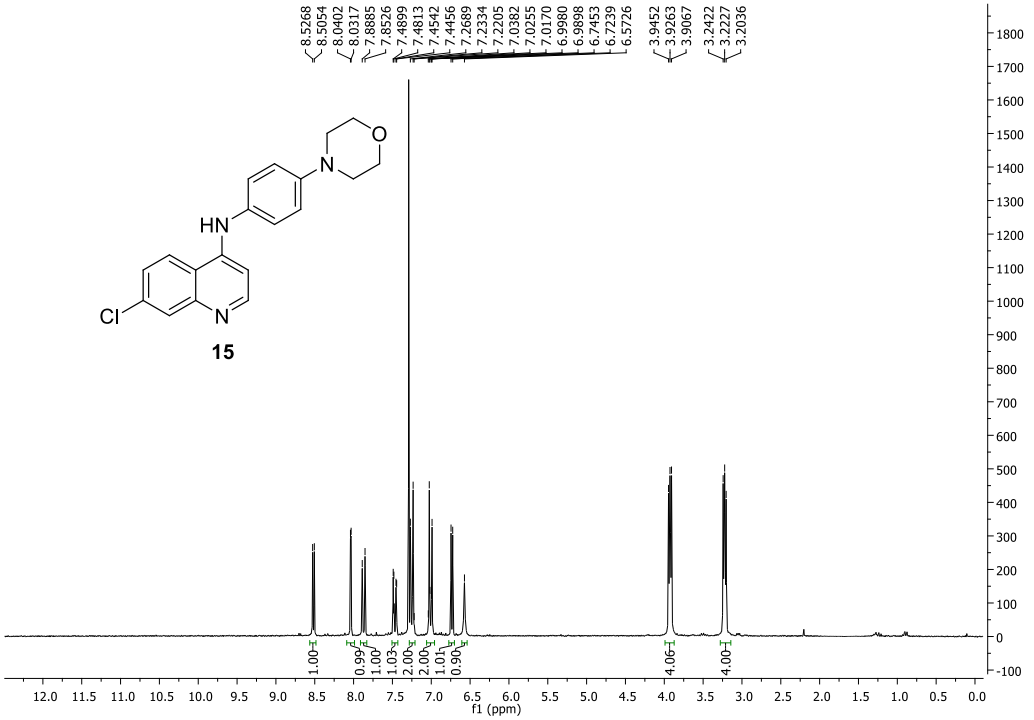
8.5268
8.5054
8.0402
8.0317
7.8885
7.8526
7.4899
7.4813
7.4542
7.4456
7.2689
7.2334
7.2205
7.0382
7.0255
7.0170
6.9980
6.9898
6.7453
6.7239
6.5726
3.9452
3.9263
3.9067
3.2422
3.2227
3.2036
O
N
HN
Cl
N
15
1.00
0.99
1.00
1.03
2.00
2.00
1.01
0.90
4.06
4.00
f1 (ppm)

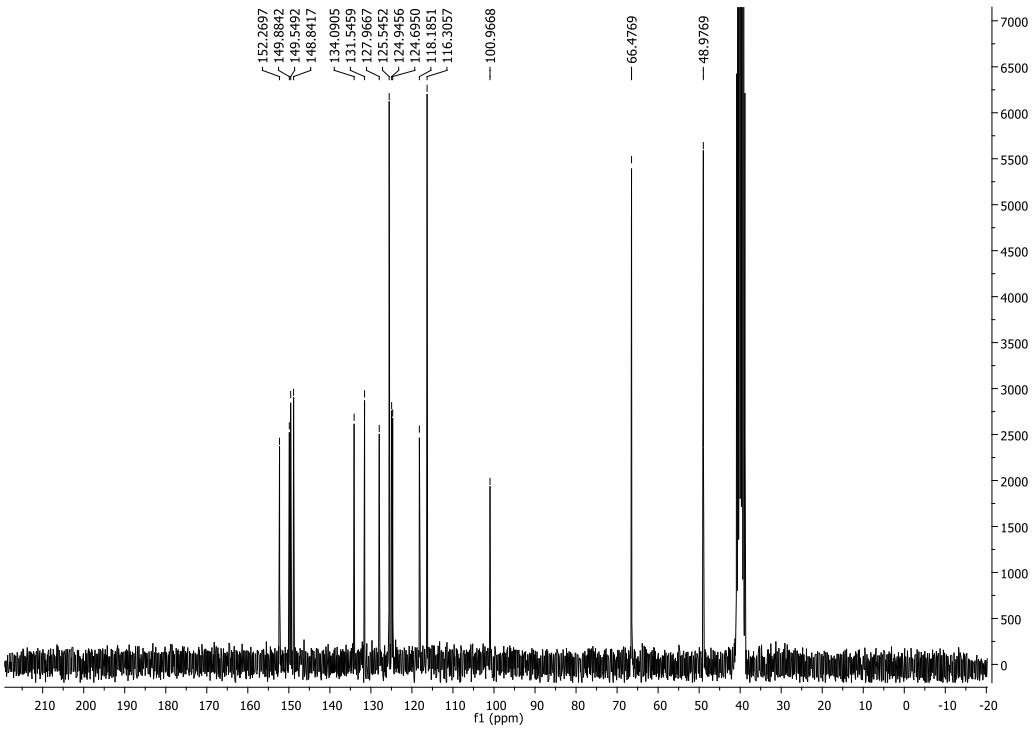
152.2697
149.8842
149.5492
148.8417
134.0905
131.5459
127.9667
125.5452
124.9456
124.6950
118.1851
116.3057
100.9668
66.4769
48.9769
f1 (ppm)

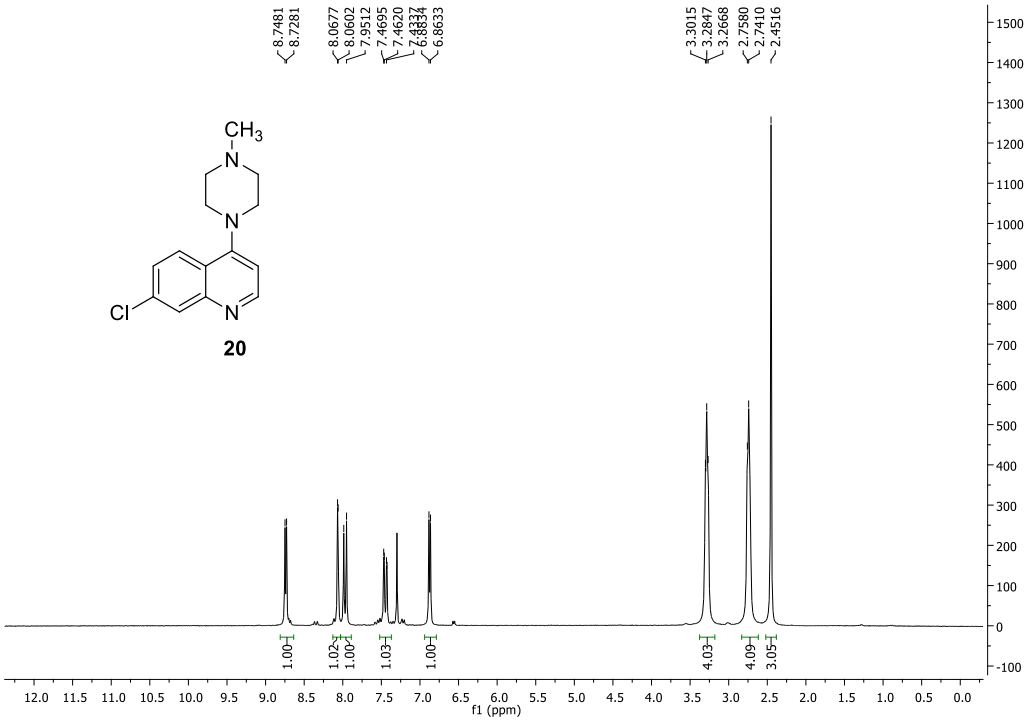
8.7481
8.7281
8.0677
8.0602
7.9512
7.4695
7.4620
6.8633
3.3015
3.2847
3.2668
2.7580
2.7410
2.4516
1.00
1.02
1.00
1.03
1.00
4.03
4.09
3.05
f1 (ppm)

20

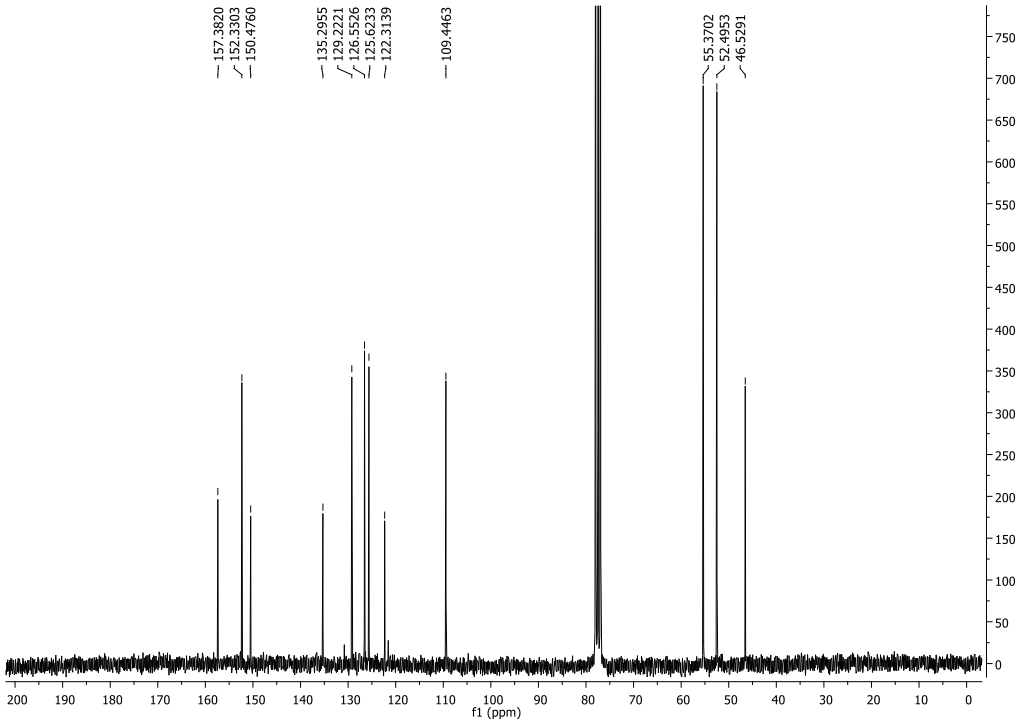
157.3820
152.3303
150.4760
135.2955
129.2221
126.5526
125.6233
122.3139
109.4463
55.3702
52.4953
46.5291
f1 (ppm)

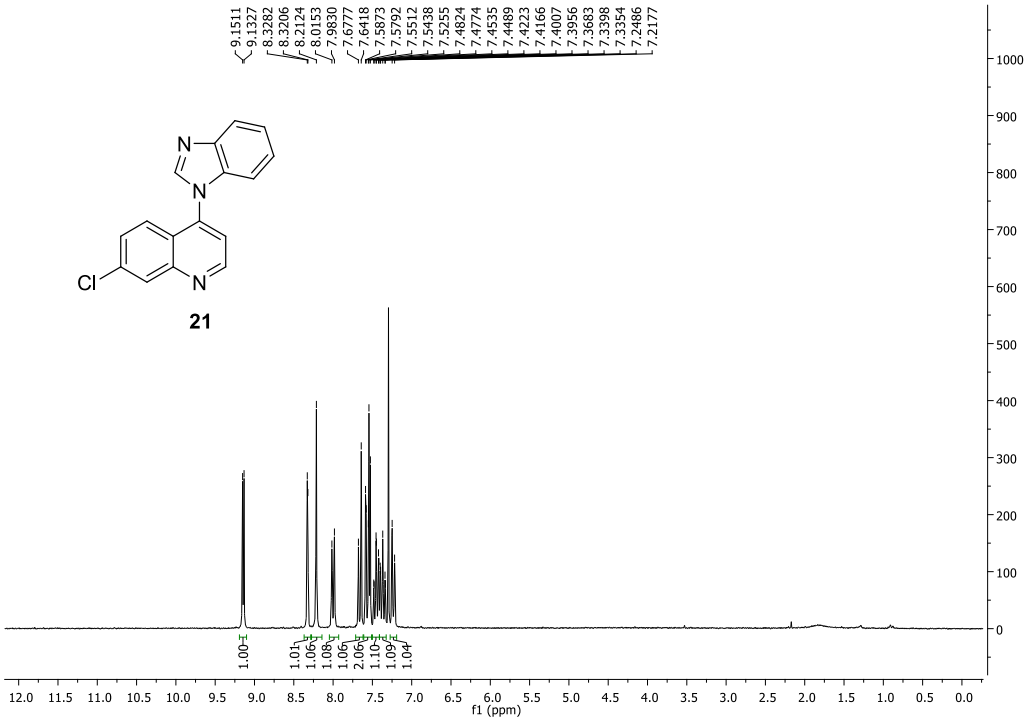
9.1511
9.1327
8.3282
8.3206
8.2124
8.0153
7.9830
7.6777
7.6418
7.5873
7.5792
7.5512
7.5438
7.5255
7.4824
7.4774
7.4535
7.4489
7.4223
7.4166
7.4007
7.3956
7.3683
7.3398
7.3354
7.2486
7.2177
N
N
Cl
N
21
1.00
1.01
1.06
1.08
1.06
2.06
1.10
1.09
1.04
f1 (ppm)

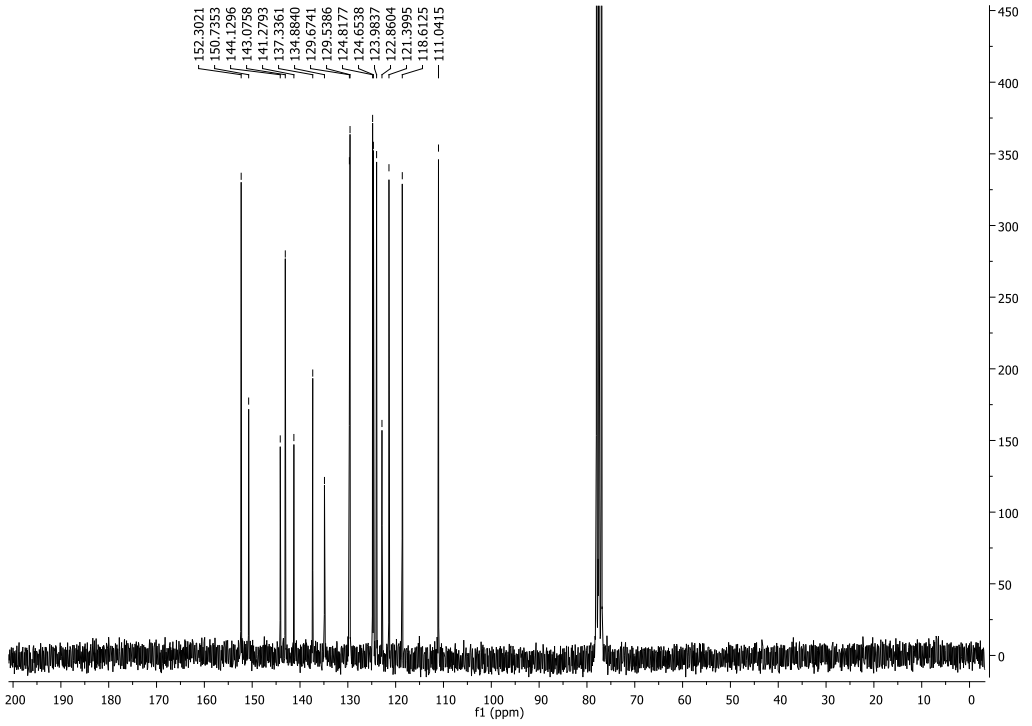
152.3021
150.7353
144.1296
143.0758
141.2793
137.3361
134.8840
129.6741
129.5386
124.8177
124.6538
123.9837
122.8604
121.3995
118.6125
111.0415
f1 (ppm)

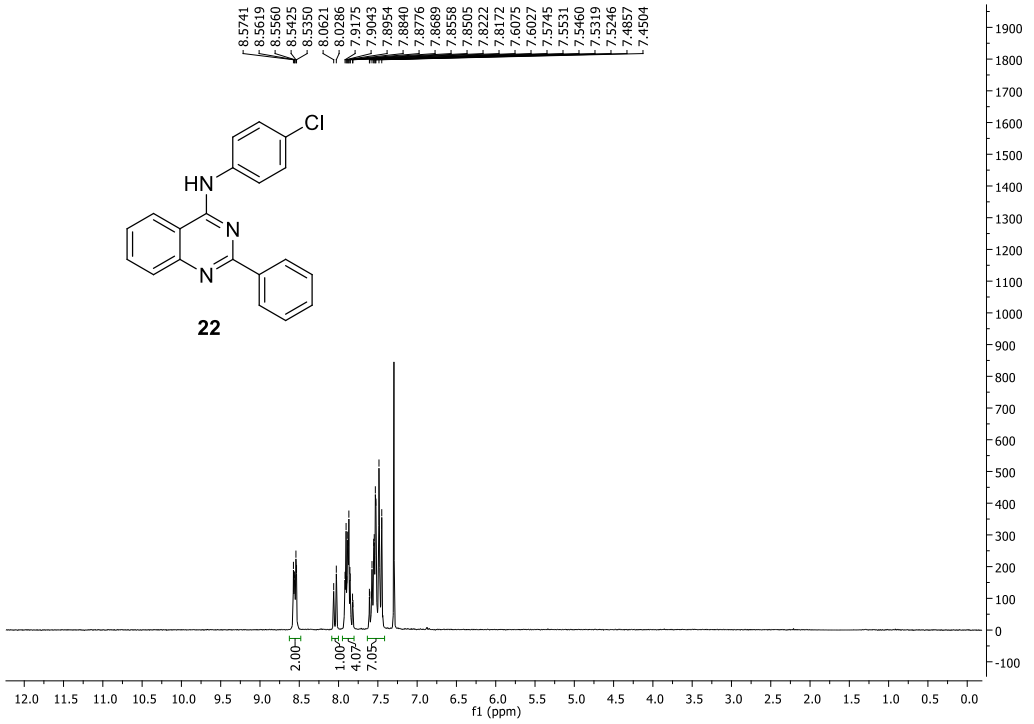
8.5741
8.5619
8.5560
8.5425
8.5350
8.0621
8.0286
7.9175
7.9043
7.8954
7.8840
7.8776
7.8689
7.8558
7.8505
7.8222
7.8172
7.6075
7.6027
7.5745
7.5531
7.5460
7.5319
7.5246
7.4857
7.4504
Cl
HN
N
N
22
2.00
1.00
4.07
7.05
f1 (ppm)

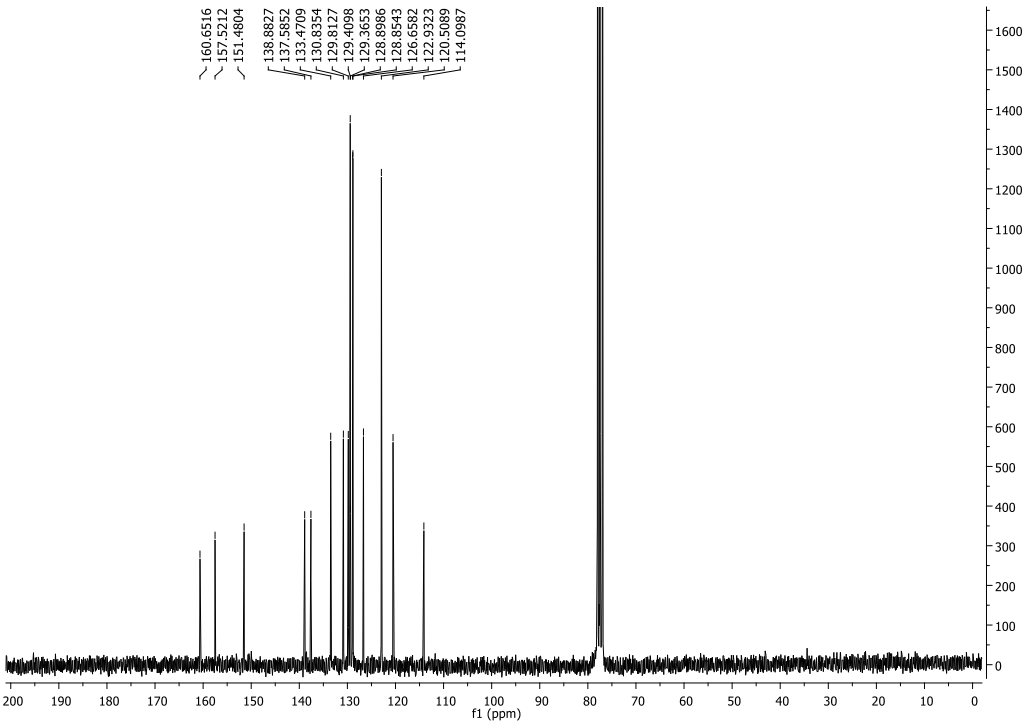
160.6516
157.5212
151.4804
138.8827
137.5852
133.4709
130.8354
129.8127
129.4098
129.3653
128.8986
128.8543
126.6582
122.9323
120.5089
114.0987
f1 (ppm)

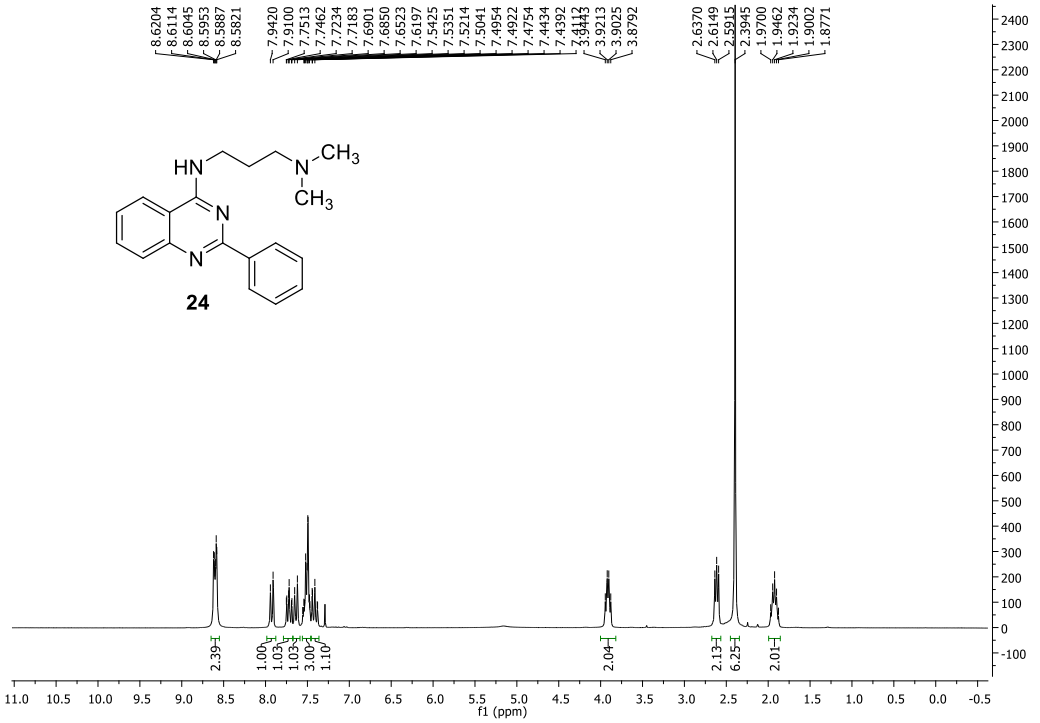
8.6204
8.6114
8.6045
8.5953
8.5887
8.5821
7.9420
7.9100
7.7513
7.7462
7.7234
7.7183
7.6901
7.6850
7.6523
7.6197
7.5425
7.5351
7.5214
7.5041
7.4954
7.4922
7.4754
7.4434
7.4392
3.9213
3.9025
3.8792
2.6370
2.6149
2.5915
2.3945
1.9700
1.9462
1.9234
1.9002
1.8771
HN
N
CH3
CH3
N
N
24
2.39
1.00
1.05
1.05
3.00
1.10
2.04
2.13
6.25
2.01
f1 (ppm)

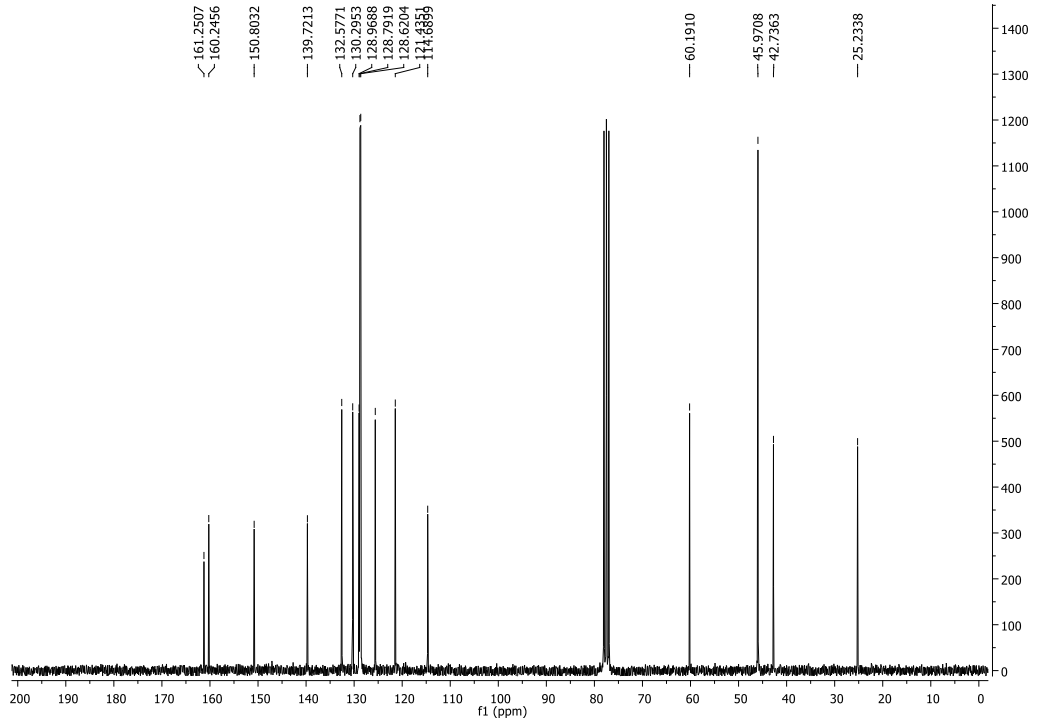
161.2507
160.2456
150.8032
139.7213
132.5771
130.2953
128.9688
128.7919
128.6204
60.1910
45.9708
42.7363
25.2338
f1 (ppm)

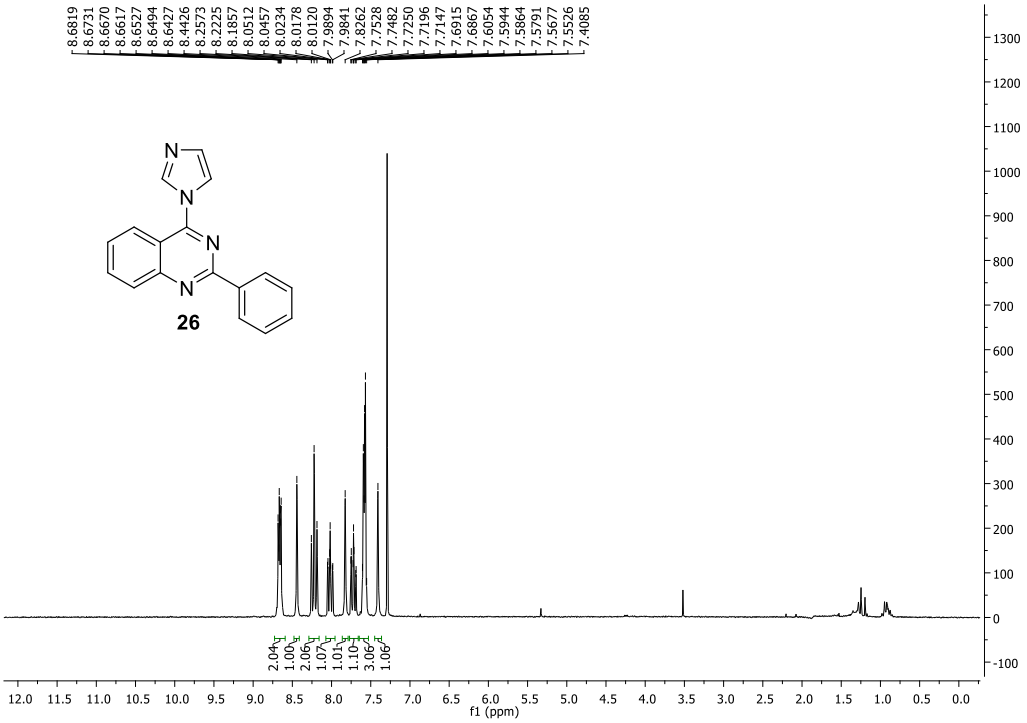
8.6819
8.6731
8.6670
8.6617
8.6527
8.6494
8.6427
8.4426
8.2573
8.2225
8.1857
8.0512
8.0457
8.0234
8.0178
8.0120
7.9894
7.9841
7.8262
7.7528
7.7482
7.7250
7.7196
7.7147
7.6915
7.6867
7.6054
7.5944
7.5864
7.5791
7.5677
7.5526
7.4085
N
N
N
N
26
2.04
1.00
2.06
1.07
1.01
1.10
3.06
1.06
f1 (ppm)

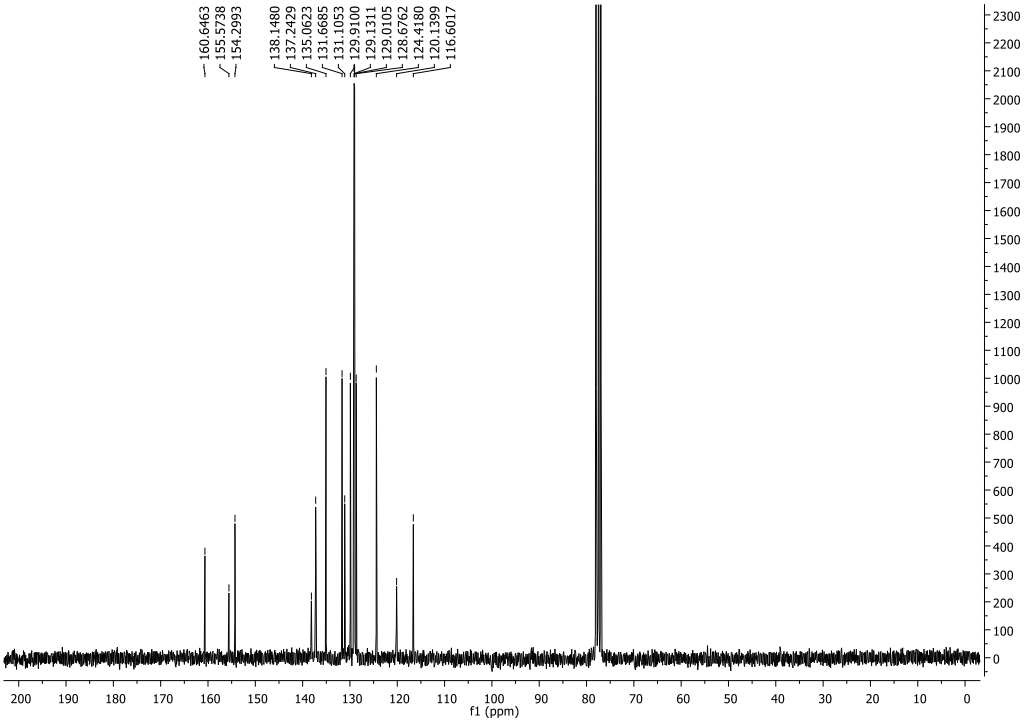
160.6463
155.5738
154.2993
138.1480
137.2429
135.0623
131.6685
131.1053
129.9100
129.1311
129.0105
128.6762
124.4180
120.1399
116.6017
f1 (ppm)

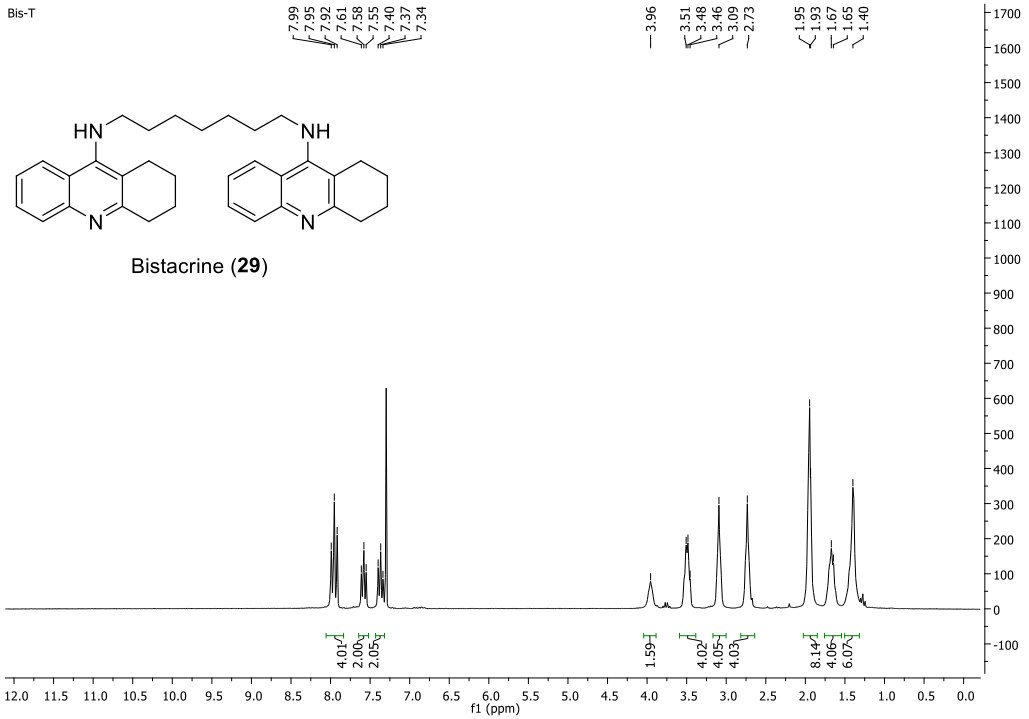

Bistacrine (**29**)

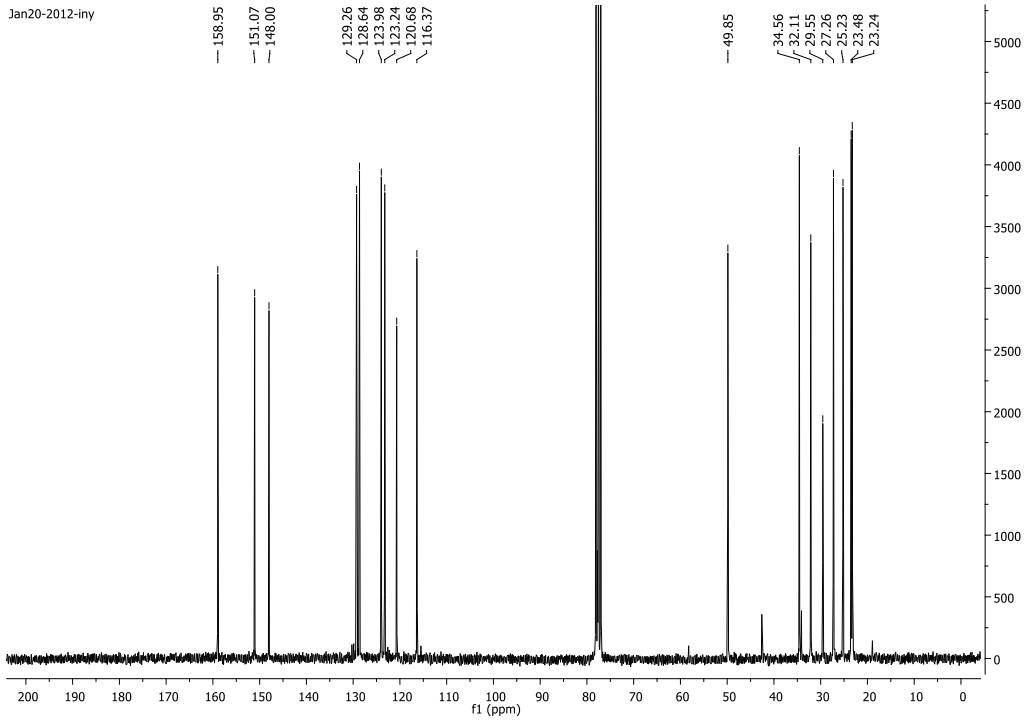

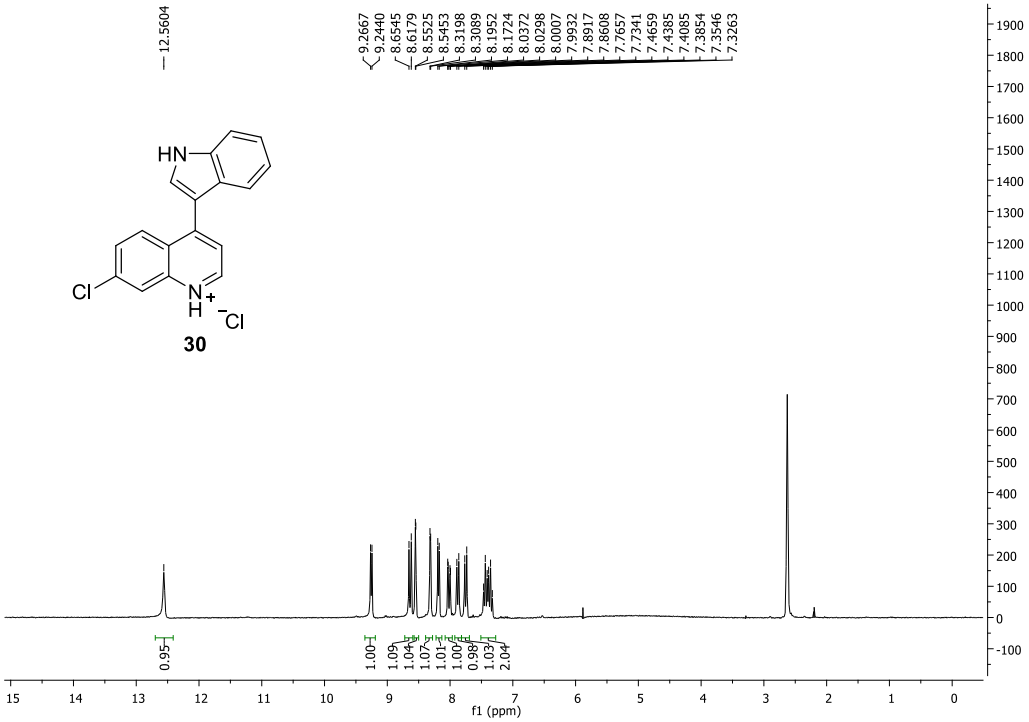
12.5604
9.2667
9.2440
8.6545
8.6179
8.5525
8.5453
8.3198
8.3089
8.1952
8.1724
8.0372
8.0298
8.0007
7.9932
7.8917
7.8608
7.7657
7.7341
7.4659
7.4385
7.4085
7.3854
7.3546
7.3263
HN
Cl
N+
H
Cl
30
0.95
1.00
1.09
1.04
1.07
1.01
1.00
0.98
1.03
2.04
f1 (ppm)

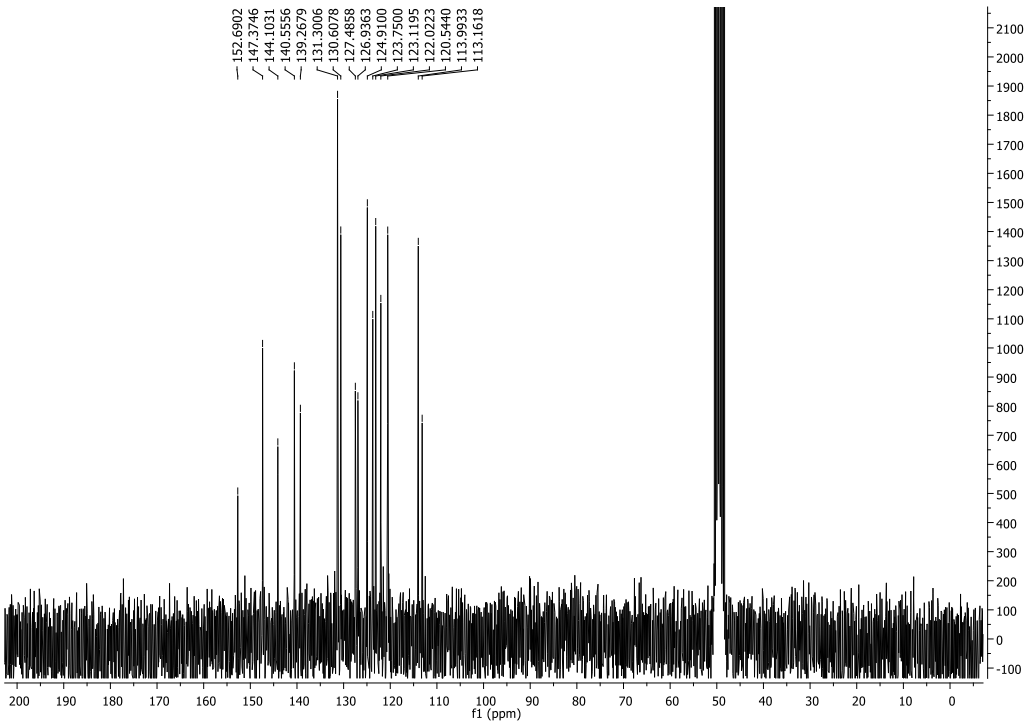
152.6902
147.3746
144.1031
140.5556
139.2679
131.3006
130.6078
127.4858
126.9363
124.9100
123.7500
123.1195
122.0223
120.5440
113.9933
113.1618
f1 (ppm)

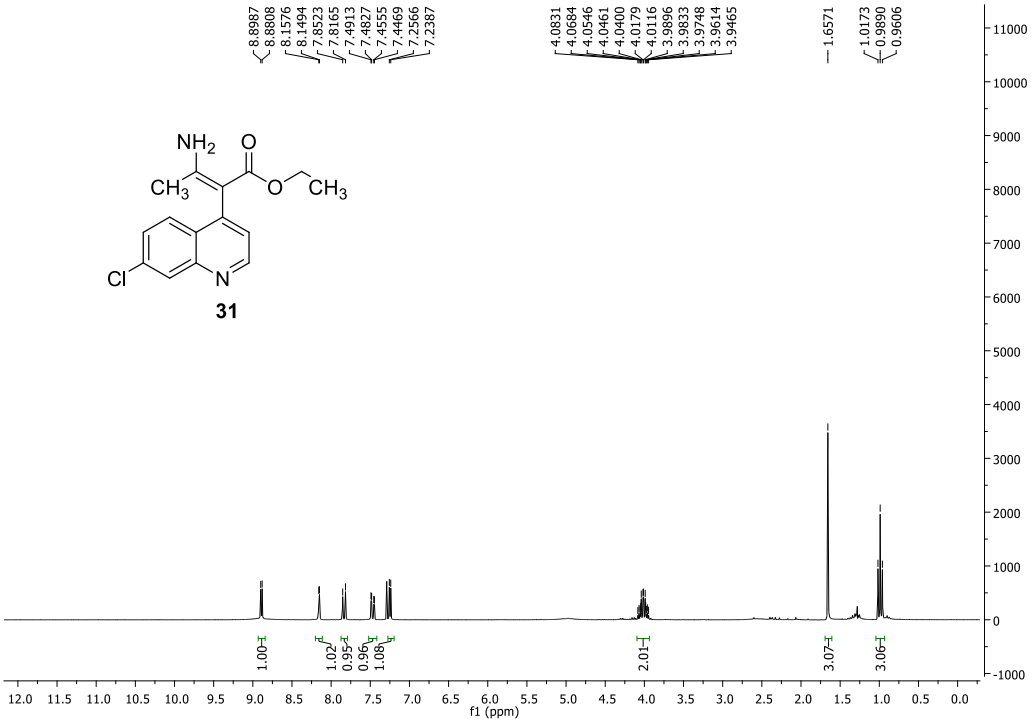
8.8987
8.8808
8.1576
8.1494
7.8523
7.8165
7.4913
7.4827
7.4555
7.4469
7.2566
7.2387
4.0831
4.0684
4.0546
4.0461
4.0400
4.0179
4.0116
3.9896
3.9833
3.9748
3.9614
3.9465
1.6571
1.0173
0.9890
0.9606
NH2
O
CH3
O
CH3
Cl
N
31
1.00
1.02
0.95
0.96
1.08
2.01
3.07
3.06
f1 (ppm)

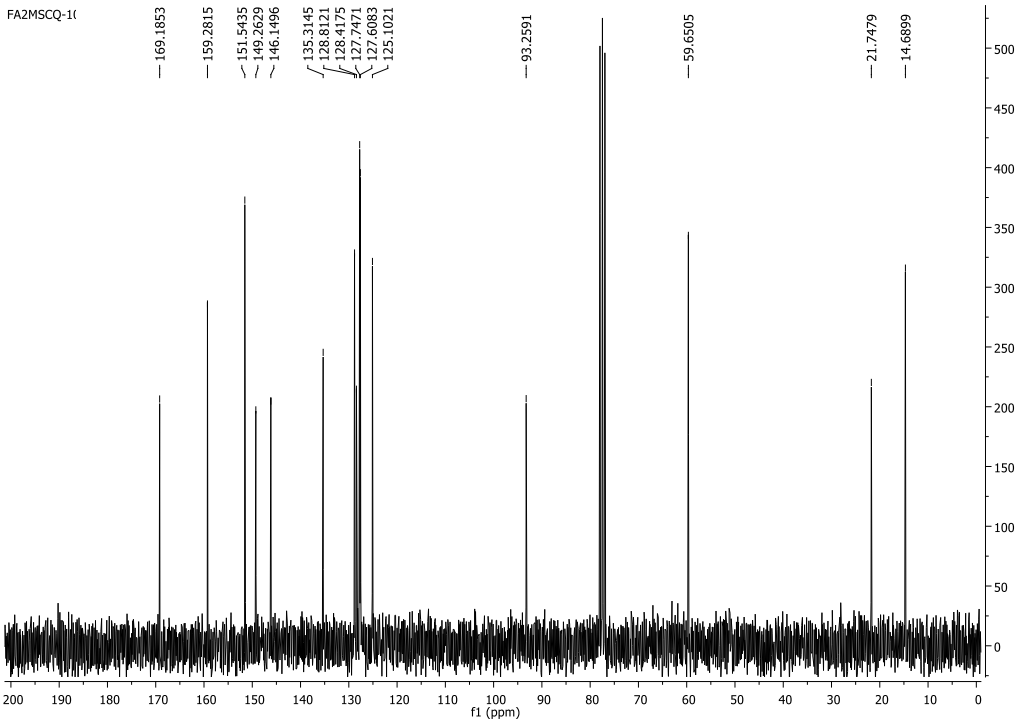
FA2MSCQ-1(
169.1853
159.2815
151.5435
149.2629
146.1496
135.3145
128.8121
128.4175
127.7471
127.6083
125.1021
93.2591
59.6505
21.7479
14.6899
f1 (ppm)

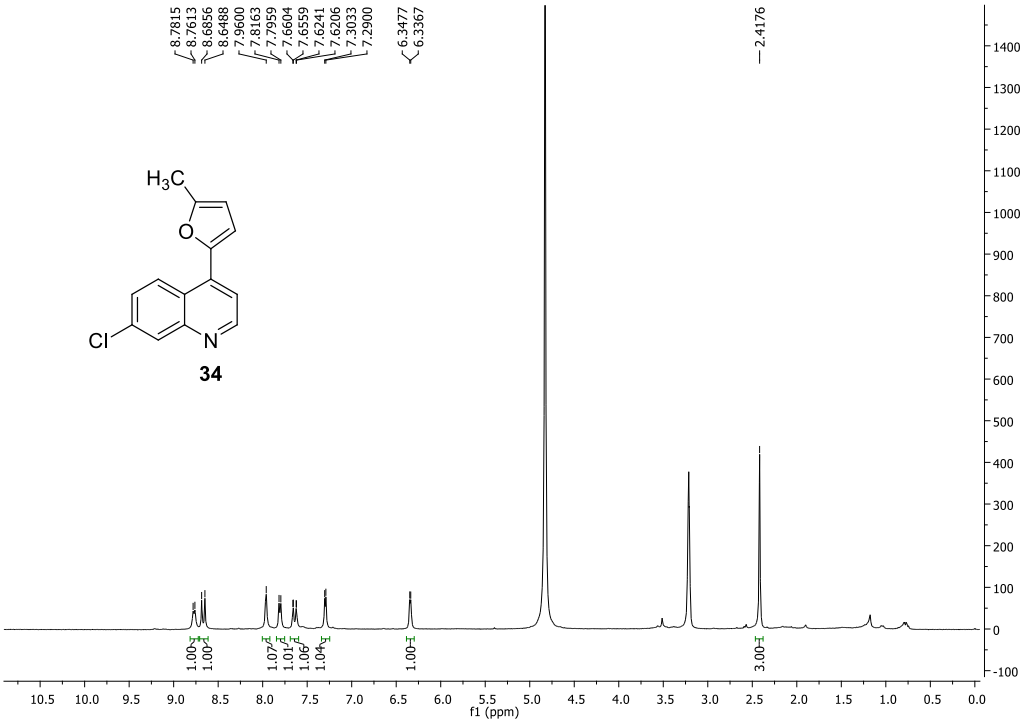
8.7815
8.7613
8.6856
8.6488
7.9600
7.8163
7.7959
7.6604
7.6559
7.6241
7.6206
7.3033
7.2900
6.3477
6.3367
2.4176
1.00
1.00
1.07
1.01
1.06
1.04
1.00
3.00
f1 (ppm)

H3C
O
Cl
N

34

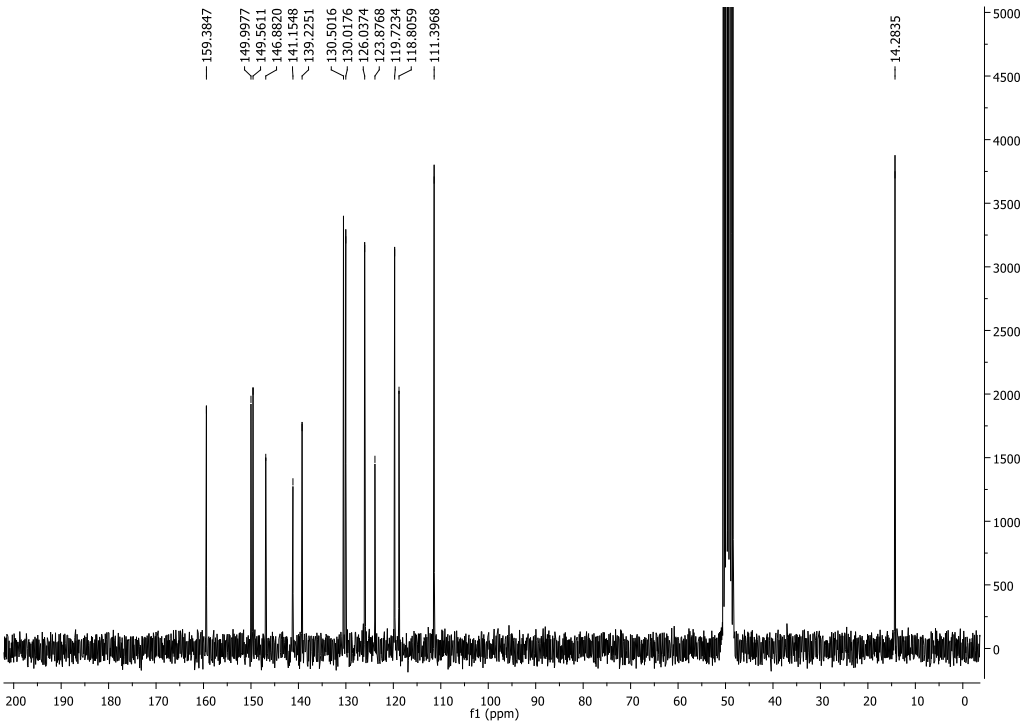
159.3847
149.9977
149.5611
146.8820
141.1548
139.2251
130.5016
130.0176
126.0374
123.8768
119.7234
118.8059
111.3968
14.2835
f1 (ppm)

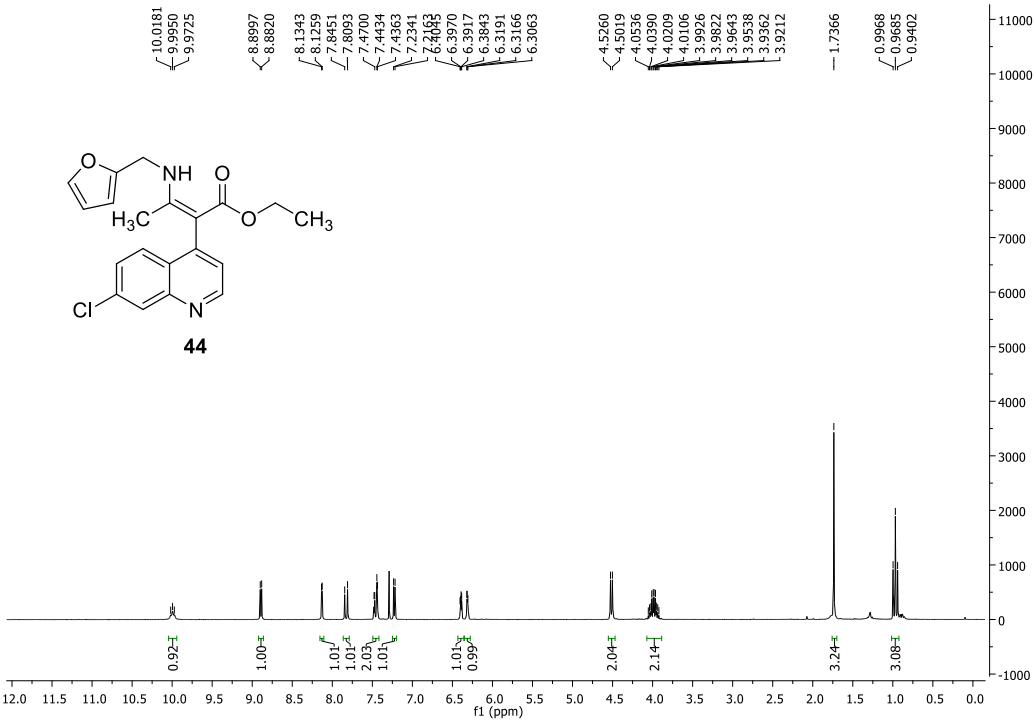
10.0181
9.9950
9.9725
8.8997
8.8820
8.1343
8.1259
7.8451
7.8093
7.4700
7.4434
7.4363
7.2341
6.4043
6.3970
6.3917
6.3843
6.3191
6.3166
6.3063
4.5260
4.5019
4.0536
4.0390
4.0209
4.0106
3.9926
3.9822
3.9643
3.9538
3.9362
3.9212
1.7366
0.9968
0.9685
0.9402
O
NH
O
H3C
O
CH3
Cl
N
44
f1 (ppm)

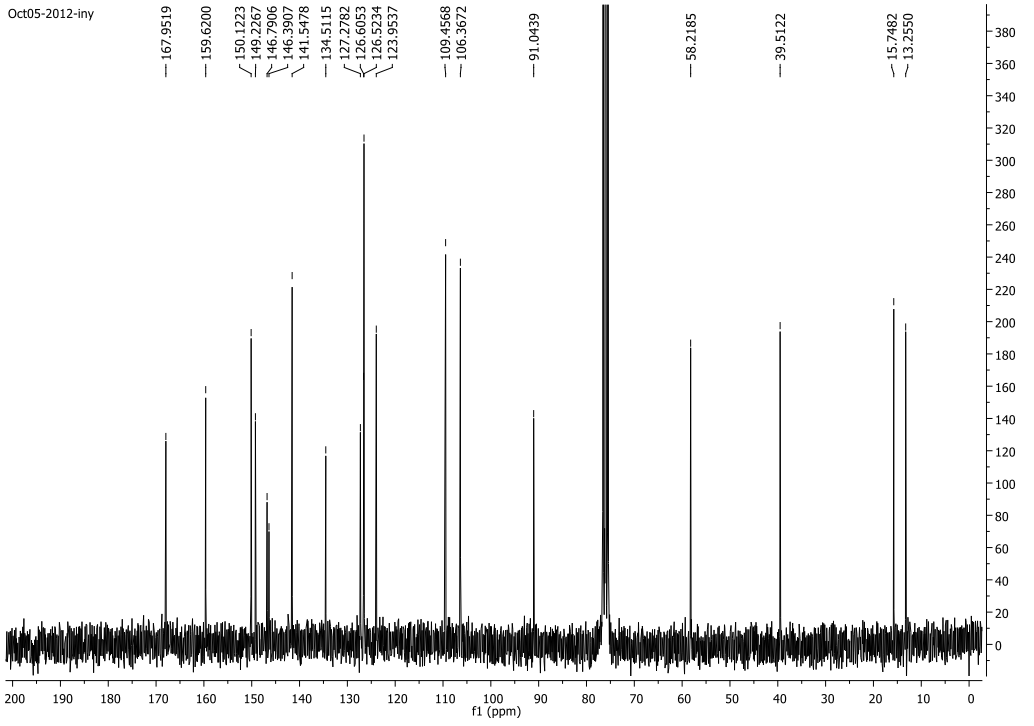
Oct05-2012-iny
167.9519
159.6200
150.1223
149.2267
146.7906
146.3907
141.5478
134.5115
127.2782
126.6053
126.5234
123.9537
109.4568
106.3672
91.0439
58.2185
39.5122
15.7482
13.2550
f1 (ppm)

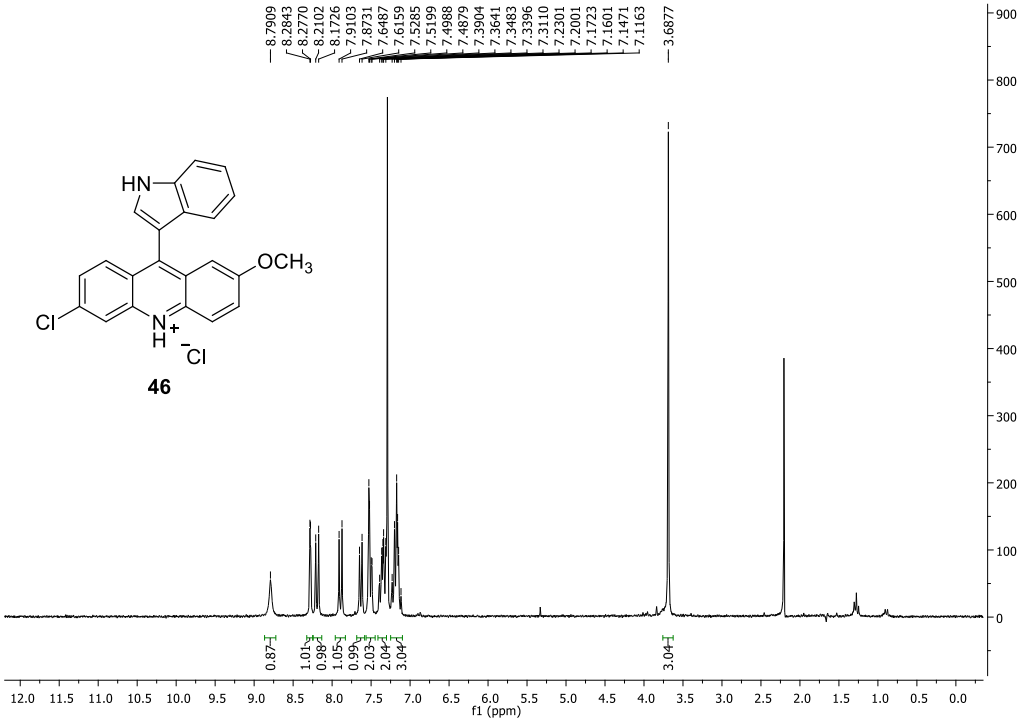
8.7909
8.2843
8.2770
8.2102
8.1726
7.9103
7.8731
7.6487
7.6159
7.5285
7.5199
7.4988
7.4879
7.3904
7.3641
7.3483
7.3396
7.3110
7.2301
7.2001
7.1723
7.1601
7.1471
7.1163
3.6877
HN
OCH3
Cl
N+
H
Cl
46
0.87
1.01
0.98
1.05
0.99
2.03
2.04
3.04
3.04
f1 (ppm)

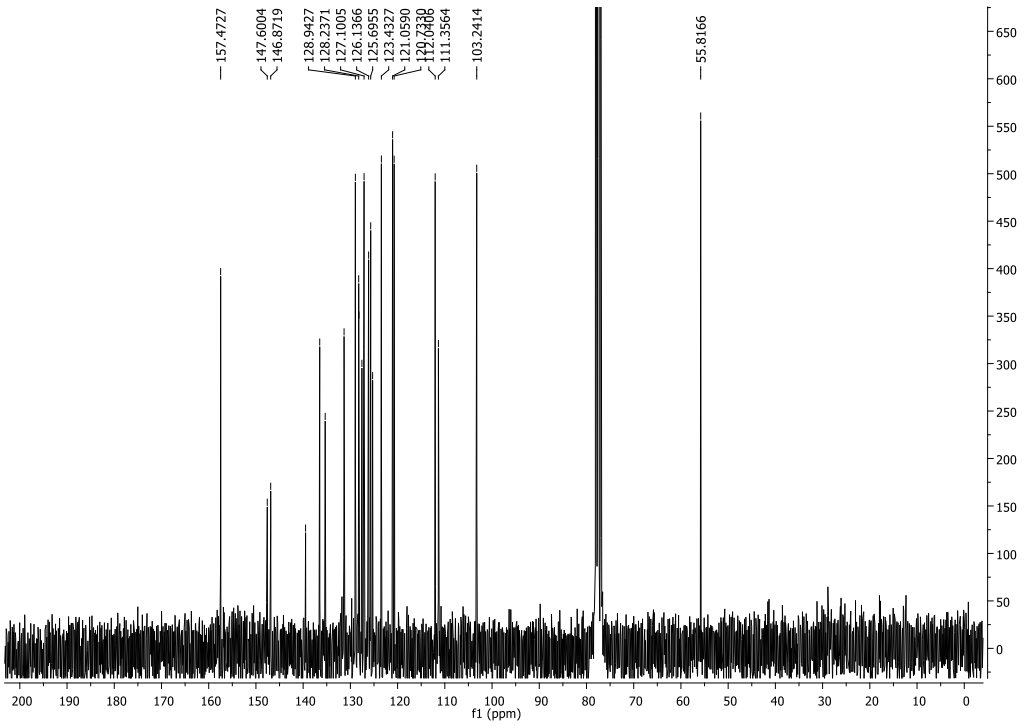
157.4727
147.6004
146.8719
128.9427
128.2371
127.1005
126.1366
125.6955
123.4327
121.0590
120.7330
112.0406
111.3564
103.2414
55.8166
f1 (ppm)

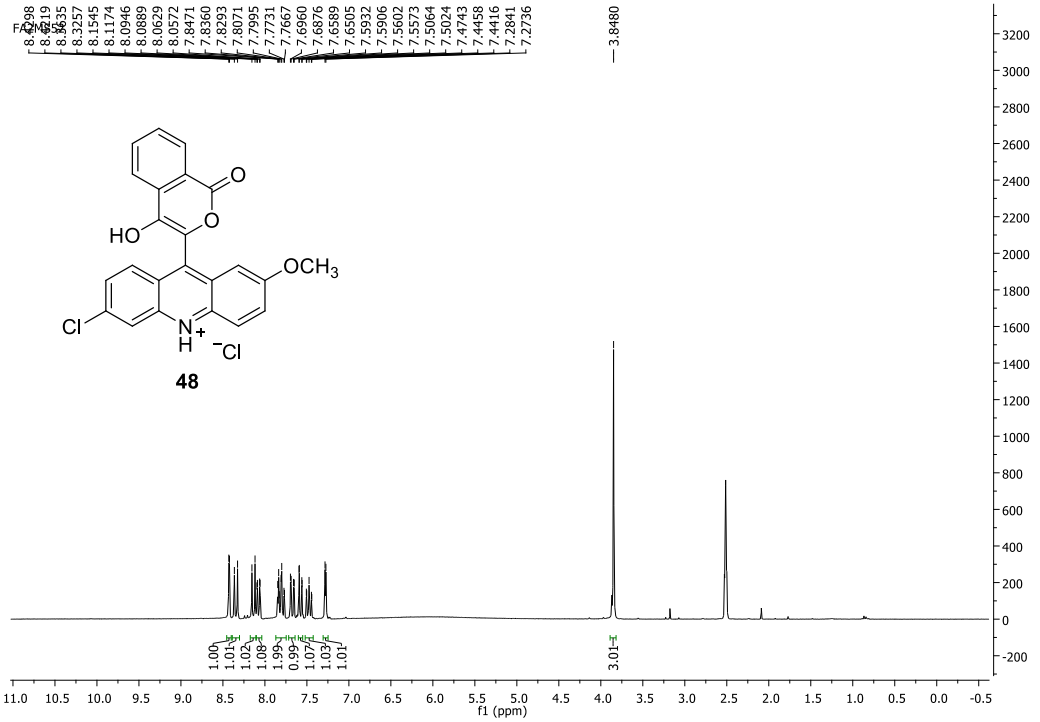
FA2MS52
8.4698
8.4519
8.3635
8.3257
8.1545
8.1174
8.0946
8.0889
8.0629
8.0572
7.8471
7.8360
7.8293
7.8071
7.7995
7.7731
7.7667
7.6960
7.6876
7.6589
7.6505
7.5932
7.5906
7.5602
7.5573
7.5064
7.5024
7.4743
7.4458
7.4416
7.2841
7.2736
3.8480
HO
O
O
OCH3
Cl
N+
H
−Cl
48
1.00
1.01
1.02
1.08
1.99
0.99
1.07
1.03
1.01
3.01
f1 (ppm)

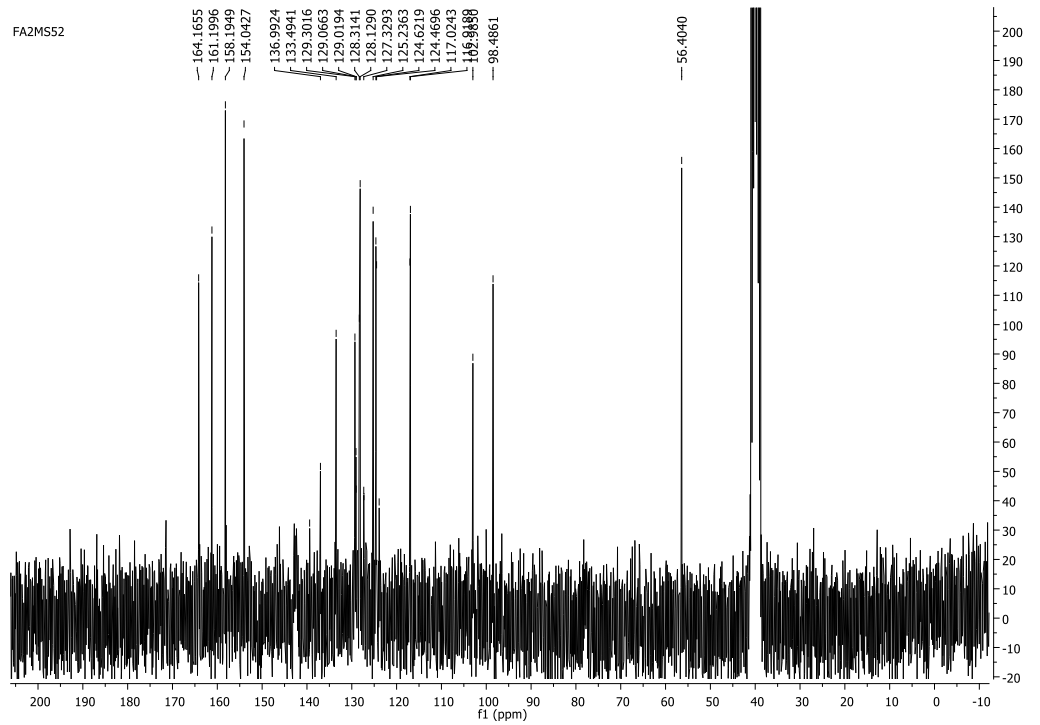
FA2MS52
164.1655
161.1996
158.1949
154.0427
136.9924
133.4941
129.3016
129.0663
129.0194
128.3141
128.1290
127.3293
125.2363
124.6219
124.4696
117.0243
98.4861
56.4040
f1 (ppm)

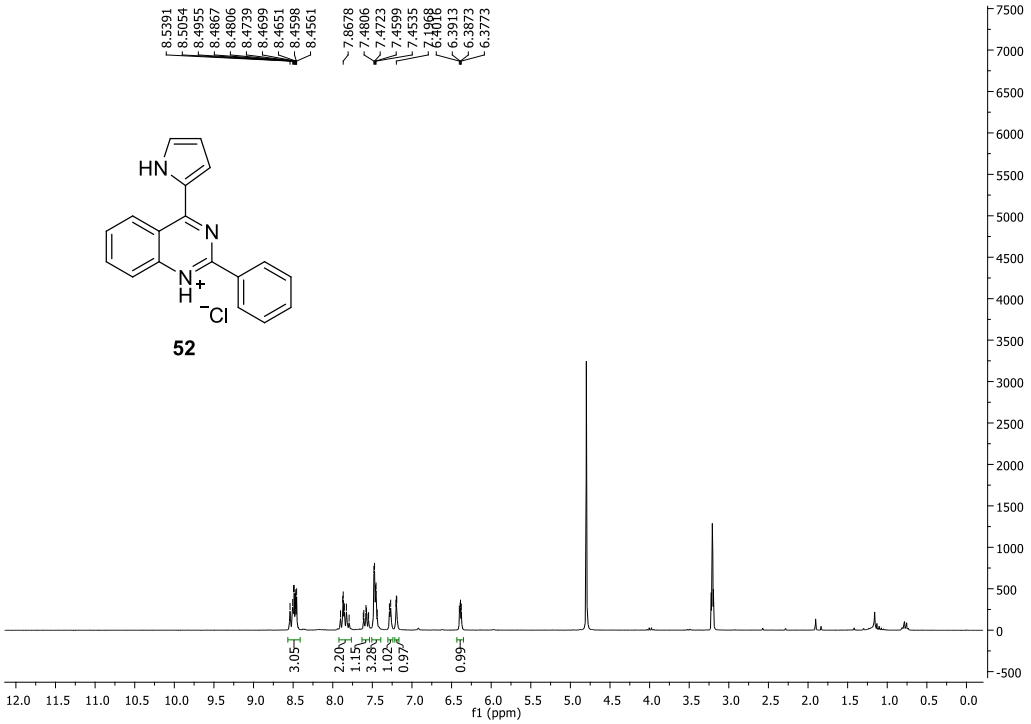
8.5391
8.5054
8.4955
8.4867
8.4806
8.4739
8.4699
8.4651
8.4598
8.4561
7.8678
7.4806
7.4723
7.4599
7.4535
6.3913
6.3873
6.3773
HN
N
N
H
Cl
52
3.05
2.20
1.15
3.26
1.02
0.97
0.99
f1 (ppm)

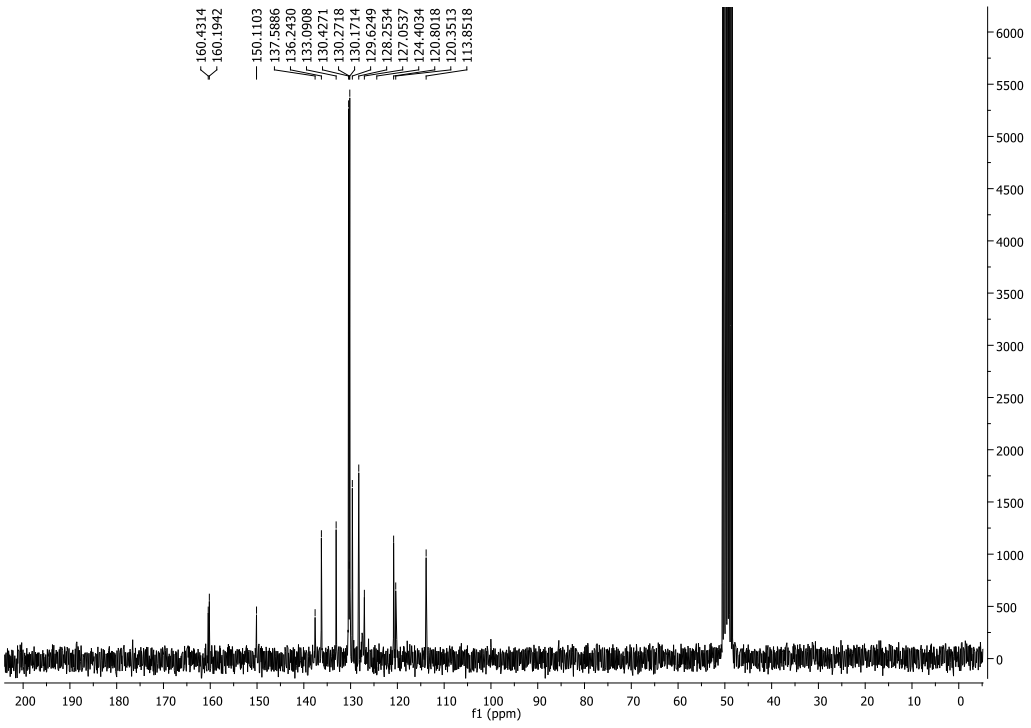
160.4314
160.1942
150.1103
137.5886
136.2430
133.0908
130.4271
130.2718
130.1714
129.6249
128.2534
127.0537
124.4034
120.8018
120.3513
113.8518
f1 (ppm)

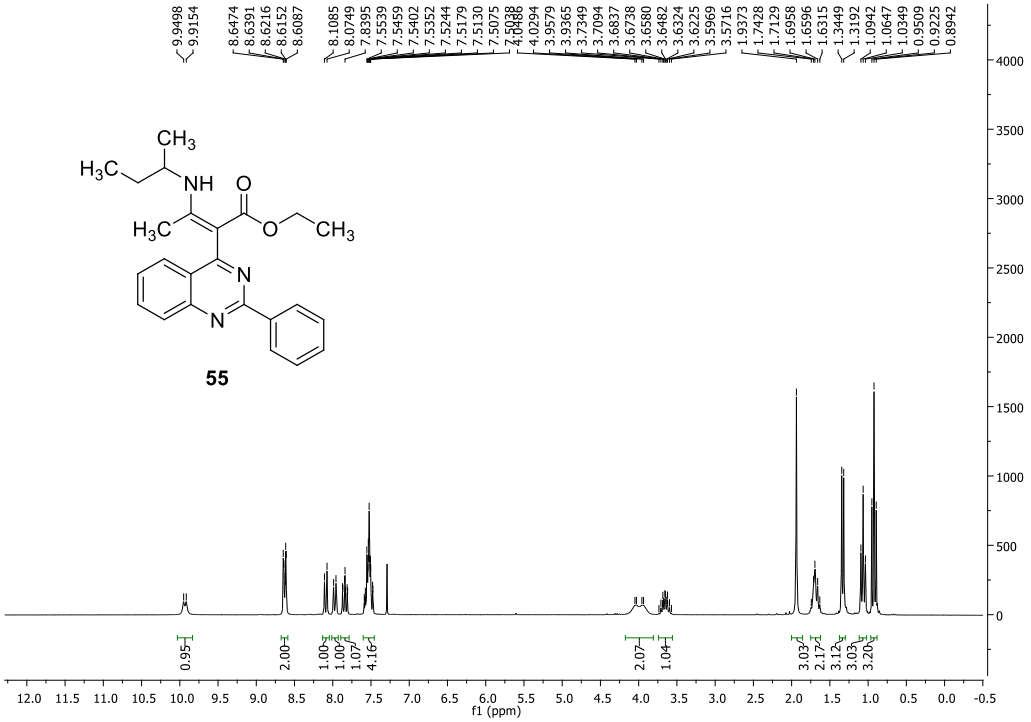
9.9498
9.9154
8.6474
8.6391
8.6216
8.6152
8.6087
8.1085
8.0749
7.8395
7.5539
7.5459
7.5402
7.5352
7.5244
7.5179
7.5130
7.5075
4.0294
3.9579
3.9365
3.7349
3.7094
3.6837
3.6738
3.6580
3.6482
3.6324
3.6225
3.5969
3.5716
1.9373
1.7428
1.7129
1.6958
1.6696
1.6315
1.3449
1.3192
1.0942
1.0647
1.0349
0.9509
0.9225
0.8942
0.95
2.00
1.00
1.00
1.07
4.16
2.07
1.04
3.03
2.17
3.12
3.03
3.20
f1 (ppm)

55

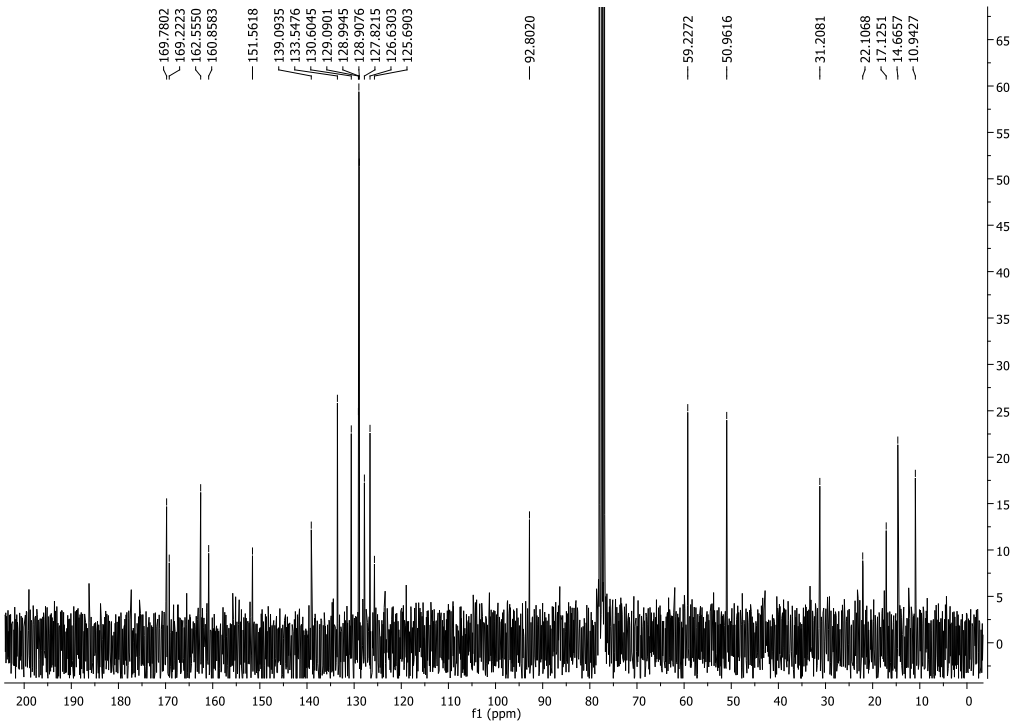
169.7802
169.2223
162.5550
160.8583
151.5618
139.0935
133.5476
130.6045
129.0901
128.9945
128.9076
127.8215
126.6303
125.6903
92.8020
59.2272
50.9616
31.2081
22.1068
17.1251
14.6657
10.9427
f1 (ppm)

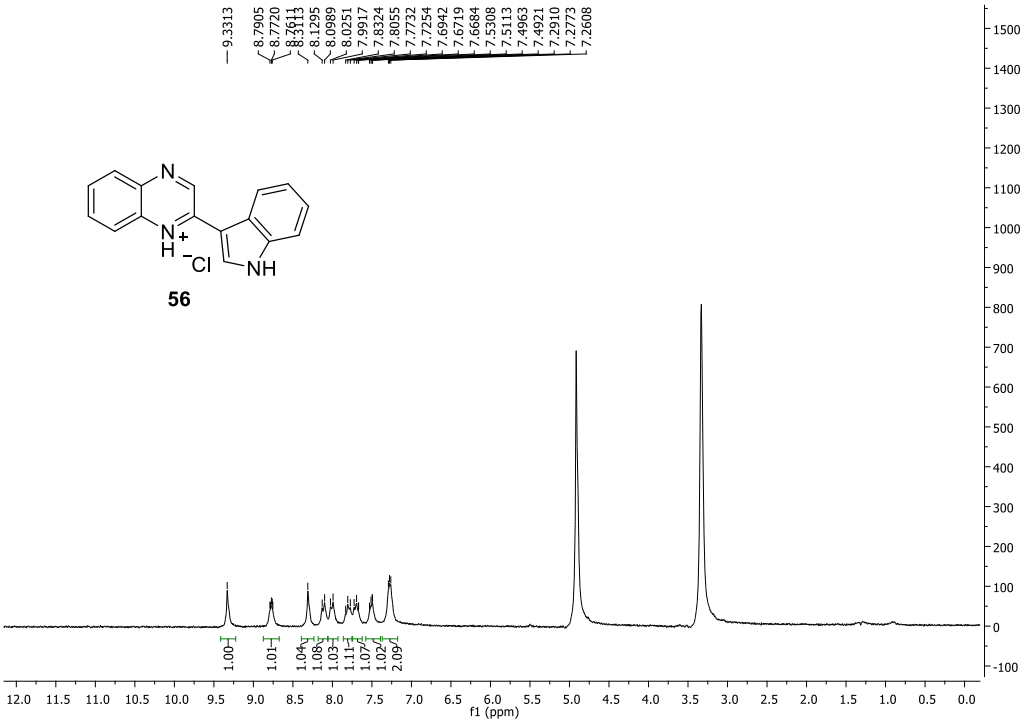
9.3313
8.7905
8.7720
8.3611
8.3313
8.1295
8.0989
8.0251
7.9917
7.8324
7.8055
7.7732
7.7254
7.6942
7.6719
7.6684
7.5308
7.5113
7.4963
7.4921
7.2910
7.2773
7.2608
N
N+
H
Cl
NH
56
1.00
1.01
1.04
1.08
1.03
1.11
1.07
1.02
2.09
f1 (ppm)

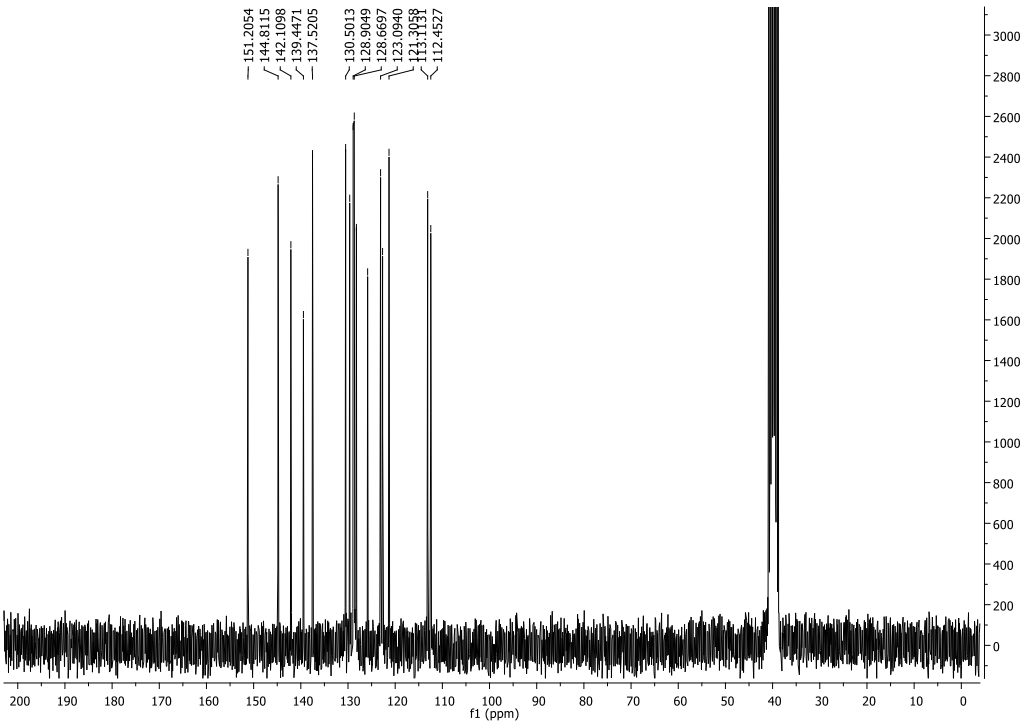
151.2054
144.8115
142.1098
139.4471
137.5205
130.5013
128.9049
128.6697
123.0940
112.4527
f1 (ppm)

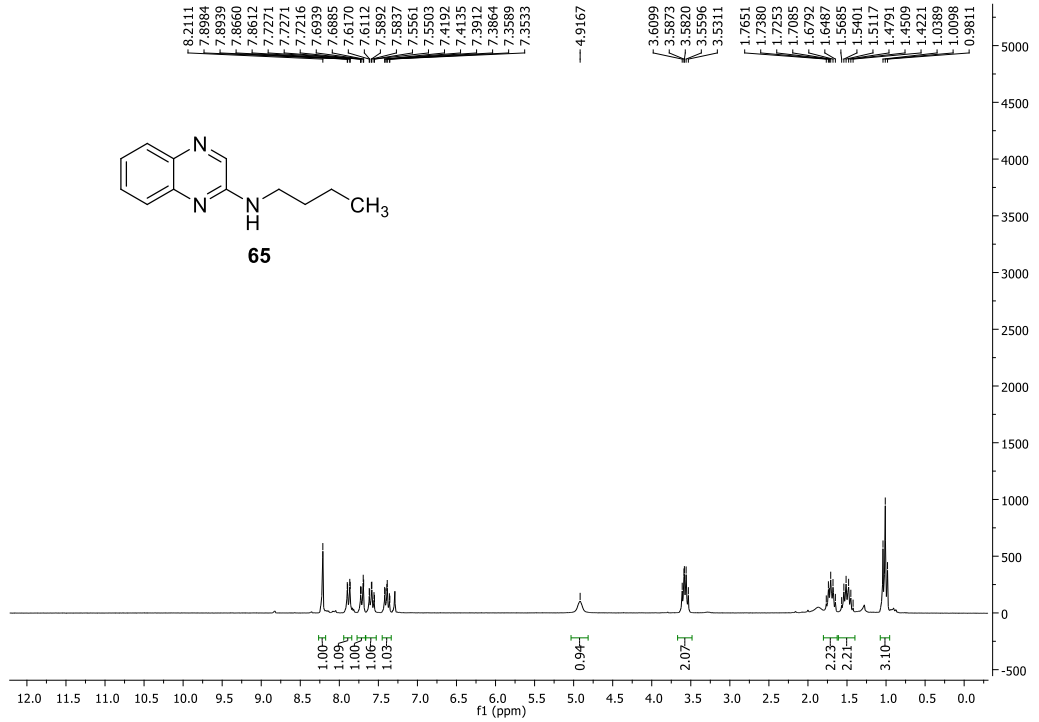
8.2111
7.8984
7.8939
7.8660
7.8612
7.7271
7.7271
7.7216
7.6939
7.6885
7.6170
7.6112
7.5892
7.5837
7.5561
7.5503
7.4192
7.4135
7.3912
7.3864
7.3589
7.3533
4.9167
3.6099
3.5873
3.5820
3.5596
3.5311
1.7651
1.7380
1.7253
1.7085
1.6792
1.6487
1.5685
1.5401
1.5117
1.4791
1.4509
1.4421
1.0389
1.0098
0.9811
N
N
N
H
CH3
65
1.00
1.09
1.00
1.06
1.03
0.94
2.07
2.23
2.21
3.10
f1 (ppm)

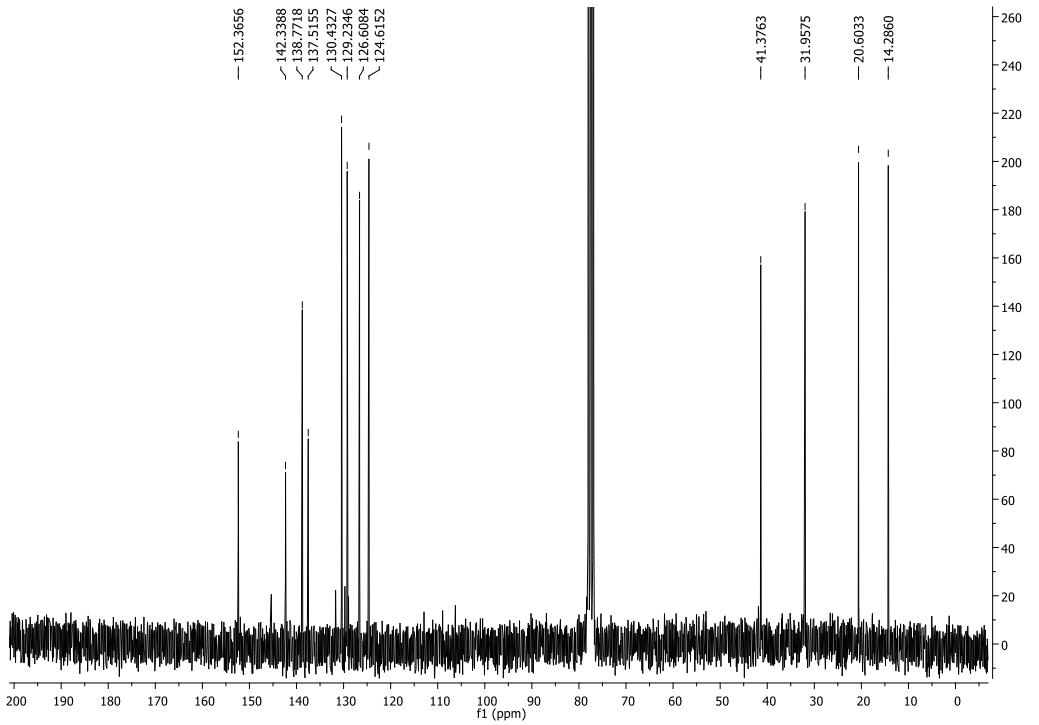
152.3656
142.3388
138.7718
137.5155
130.4327
129.2346
126.6084
124.6152
41.3763
31.9575
20.6033
14.2860
f1 (ppm)

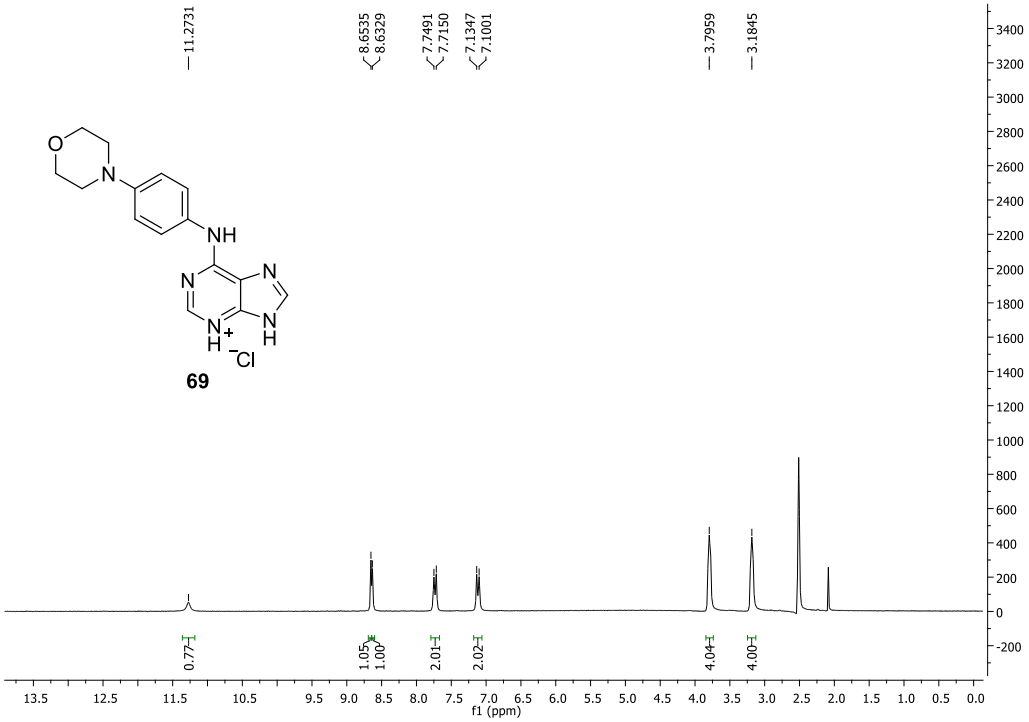
11.2731
8.6535
8.6329
7.7491
7.7150
7.1347
7.1001
3.7959
3.1845
0.77
1.05
1.00
2.01
2.02
4.04
4.00
f1 (ppm)

69

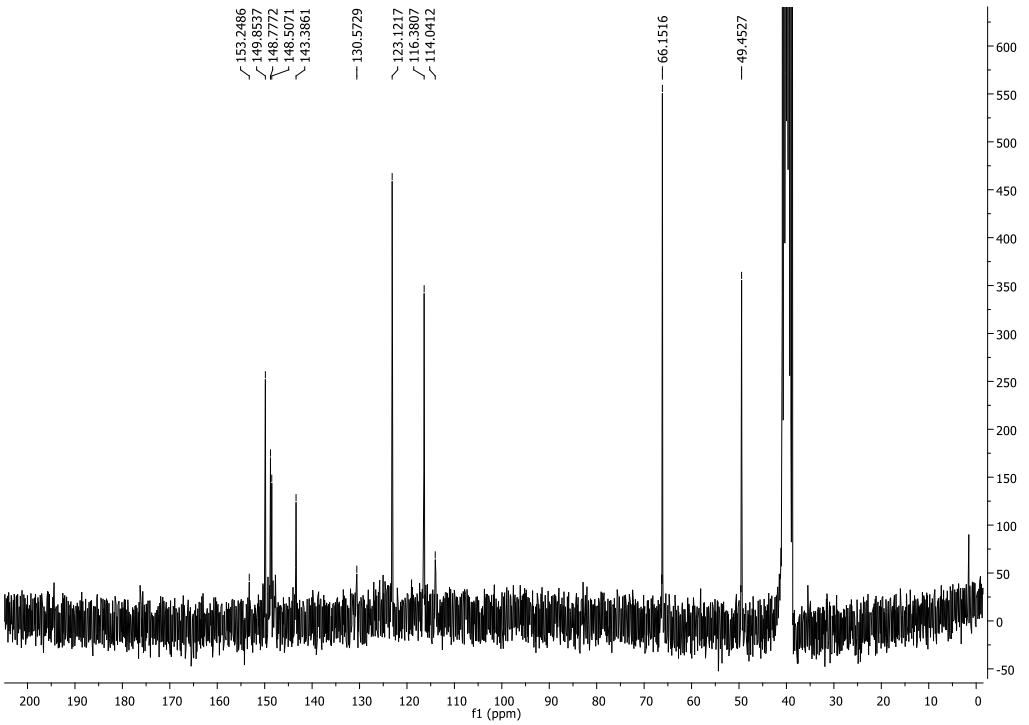
153.2486
149.8537
148.7772
148.5071
143.3861
130.5729
123.1217
116.3807
114.0412
66.1516
49.4527
f1 (ppm)

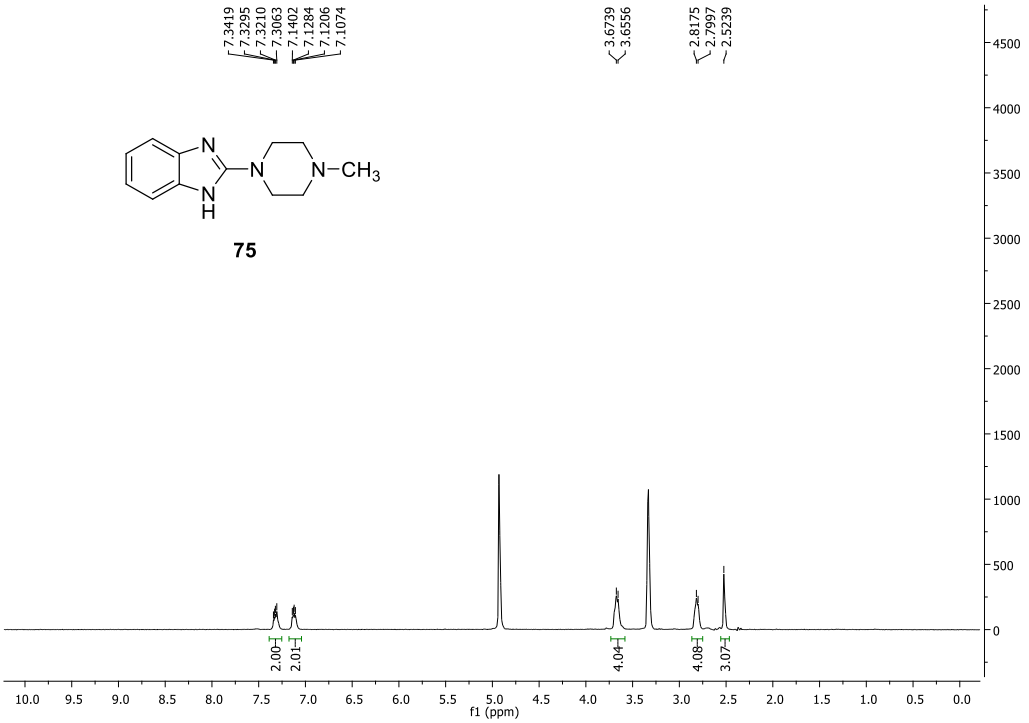
7.3419
7.3295
7.3210
7.3063
7.1402
7.1284
7.1206
7.1074
3.6739
3.6556
2.8175
2.7997
2.5239
2.00
2.01
4.04
4.08
3.07
f1 (ppm)

75

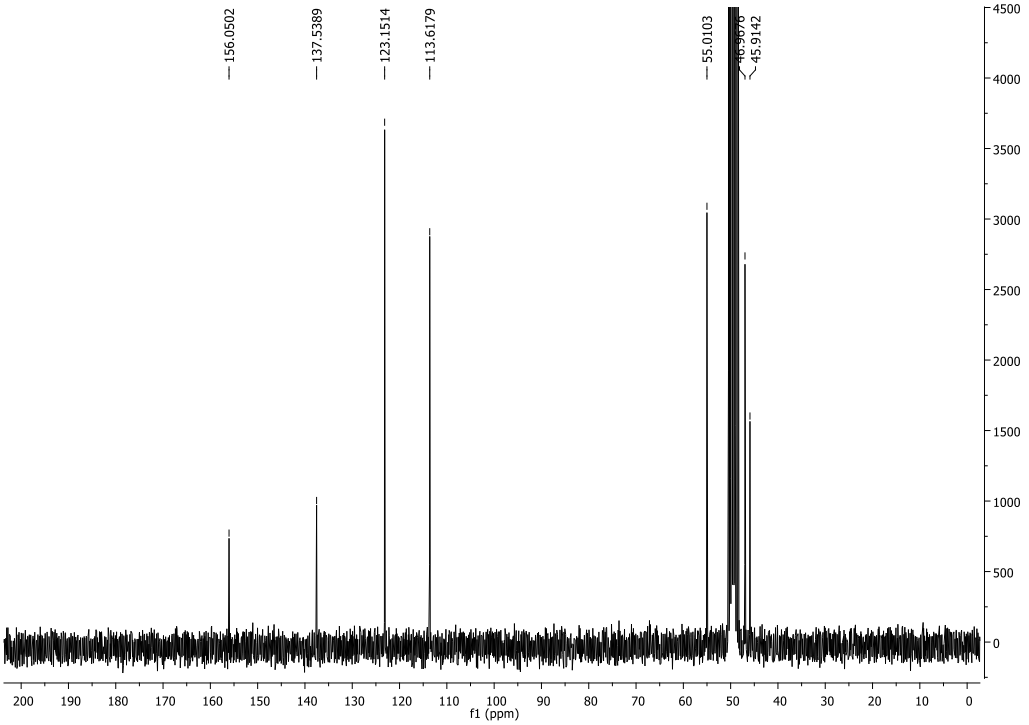
156.0502
137.5389
123.1514
113.6179
55.0103
46.3076
45.9142
f1 (ppm)

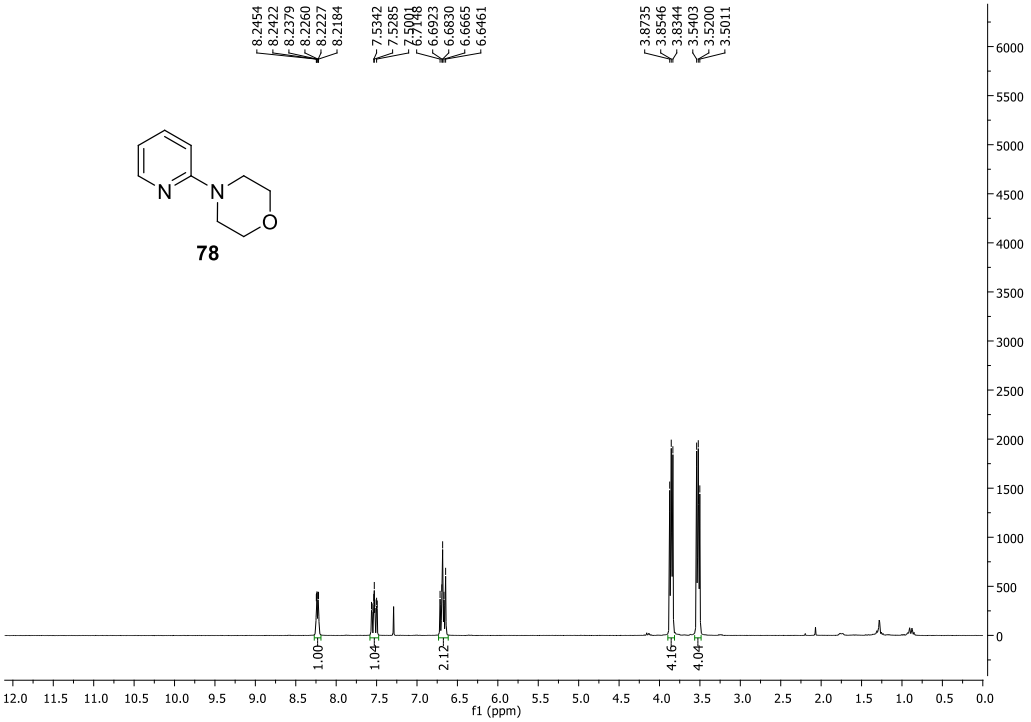
8.2454
8.2422
8.2379
8.2260
8.2227
8.2184
7.5342
7.5285
7.5001
6.7148
6.6923
6.6830
6.6665
6.6461
3.8735
3.8546
3.8344
3.5403
3.5200
3.5011
N
N
O
78
1.00
1.04
2.12
4.16
4.04
f1 (ppm)

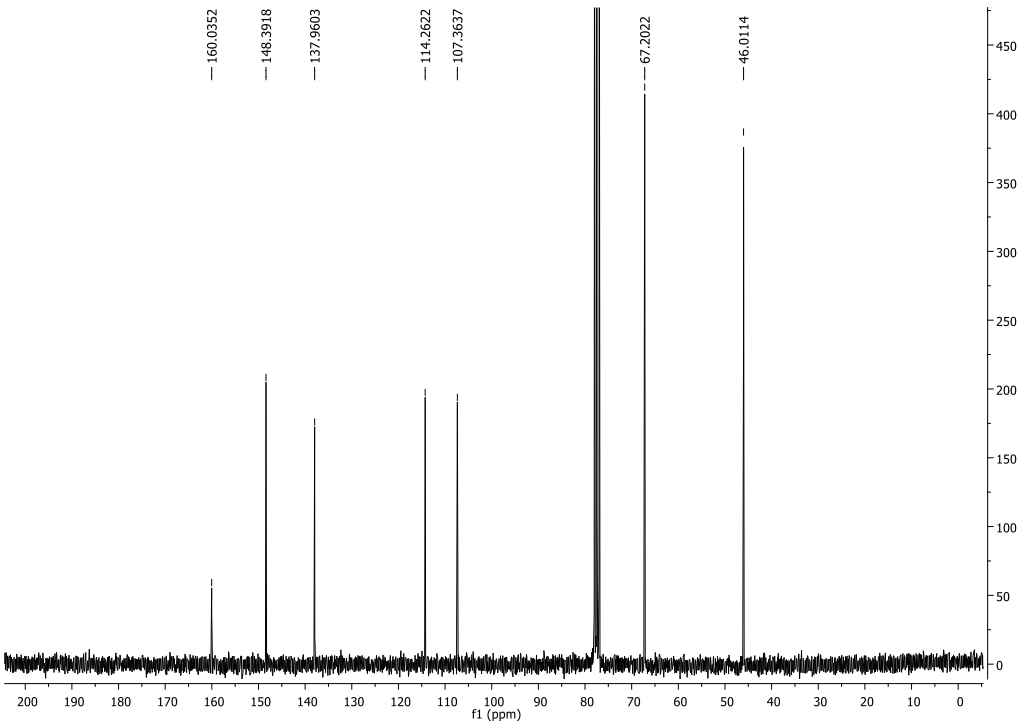
160.0352
148.3918
137.9603
114.2622
107.3637
67.2022
46.0114
f1 (ppm)

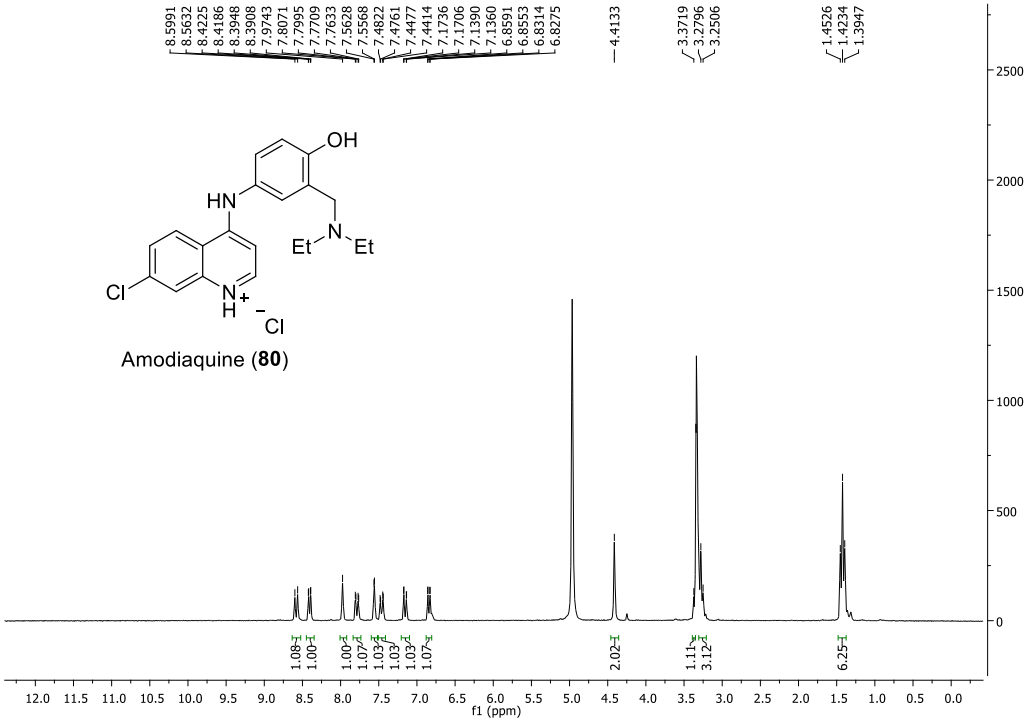
8.5991
8.5632
8.4225
8.4186
8.3948
8.3908
7.9743
7.8071
7.7995
7.7709
7.7633
7.5628
7.5568
7.4822
7.4761
7.4477
7.4414
7.1736
7.1706
7.1390
7.1360
6.8591
6.8553
6.8314
6.8275
4.4133
3.3719
3.2796
3.2506
1.4526
1.4234
1.3947
OH
HN
N
Et
Et
Cl
N+
H
−
Cl
Amodiaquine (**80**)
1.08
1.00
1.00
1.07
1.03
1.03
1.07
2.02
1.11
3.12
6.25
f1 (ppm)

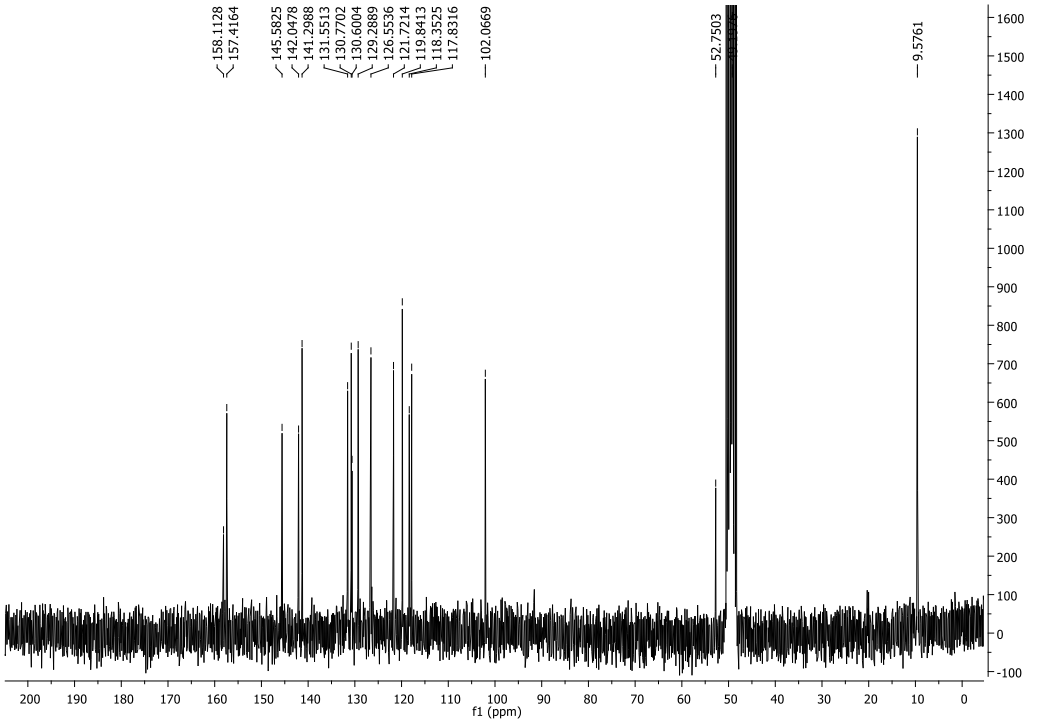
158.1128
157.4164
145.5825
142.0478
141.2988
131.5513
130.7702
130.6004
129.2889
126.5536
121.7214
119.8413
118.3525
117.8316
102.0669
52.7503
9.5761
f1 (ppm)

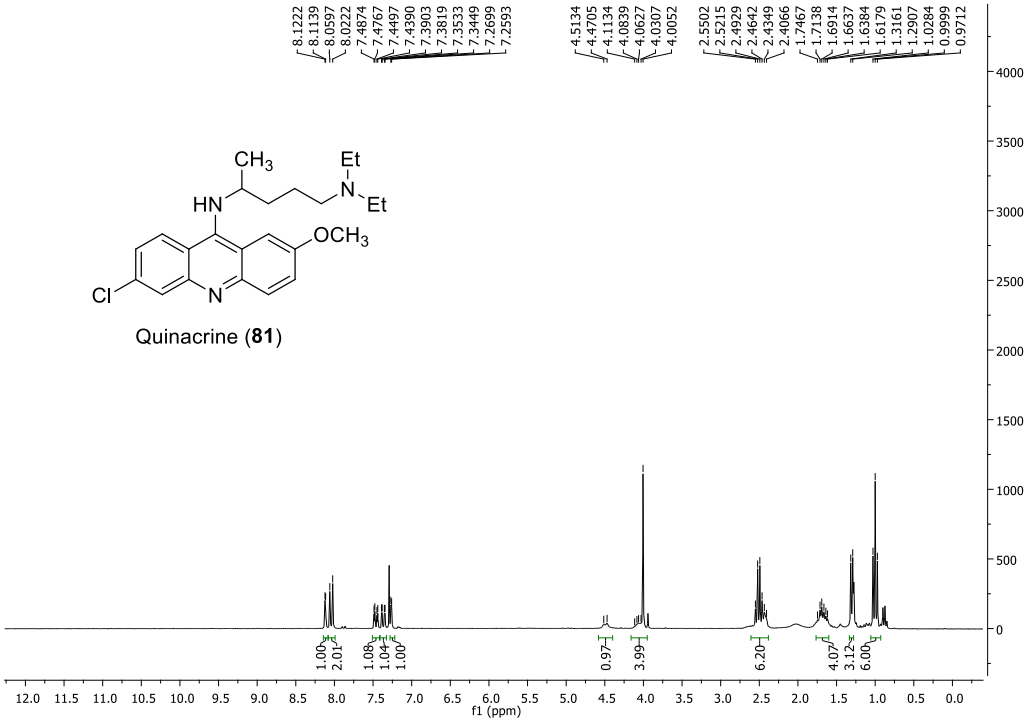
8.1222
8.1139
8.0597
8.0222
7.4874
7.4767
7.4497
7.4390
7.3903
7.3819
7.3533
7.3449
7.2699
7.2593
4.5134
4.4705
4.1134
4.0839
4.0627
4.0307
4.0052
2.5502
2.5215
2.4929
2.4642
2.4349
2.4066
1.7467
1.7138
1.6914
1.6637
1.6384
1.6179
1.3161
1.2907
1.0284
0.9999
0.9712
CH3
Et
N
Et
HN
OCH3
Cl
N
Quinacrine (81)
1.00
2.01
1.08
1.04
1.00
0.97
3.99
6.20
4.07
3.12
6.00
f1 (ppm)

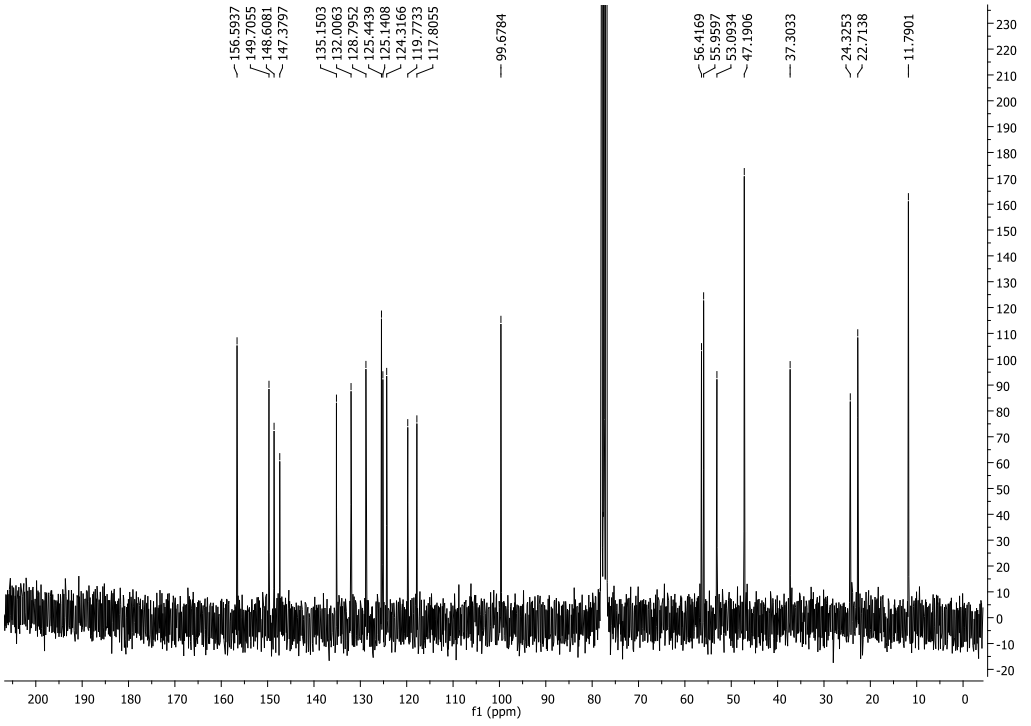
156.5937
149.7055
148.6081
147.3797
135.1503
132.0063
128.7952
125.4439
125.1408
124.3166
119.7733
117.8055
99.6784
56.4169
55.9597
53.0934
47.1906
37.3033
24.3253
22.7138
11.7901
f1 (ppm)

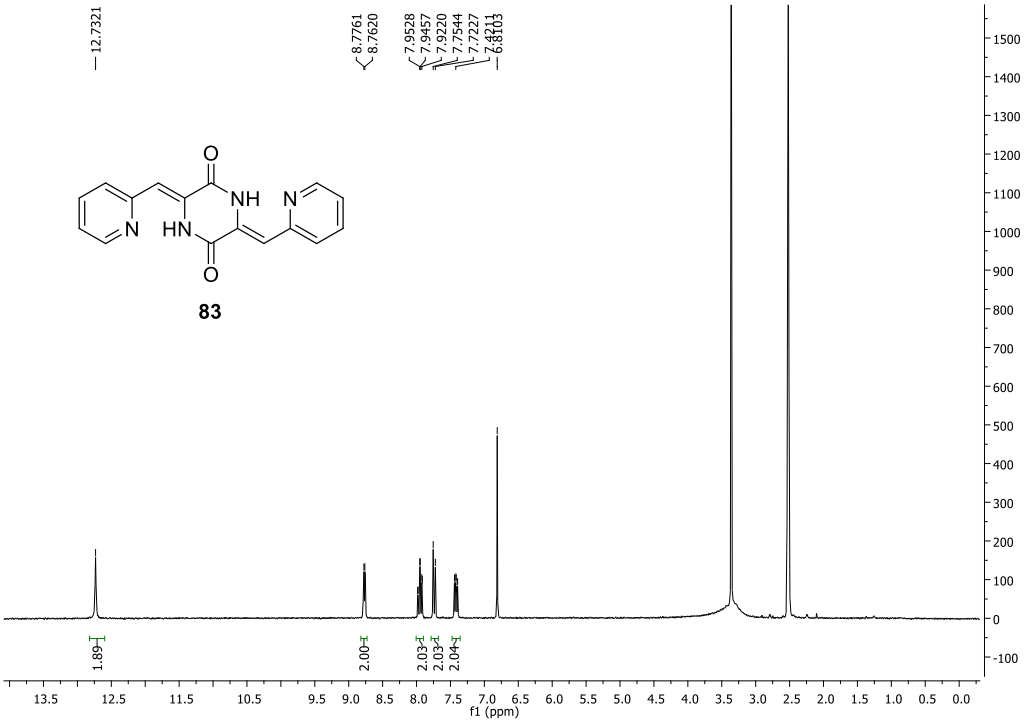
12.7321
8.7761
8.7620
7.9528
7.9457
7.9220
7.7544
7.7227
7.4211
6.8103
O
NH
N
HN
N
O
1.89
2.00
2.03
2.03
2.04
f1 (ppm)

83

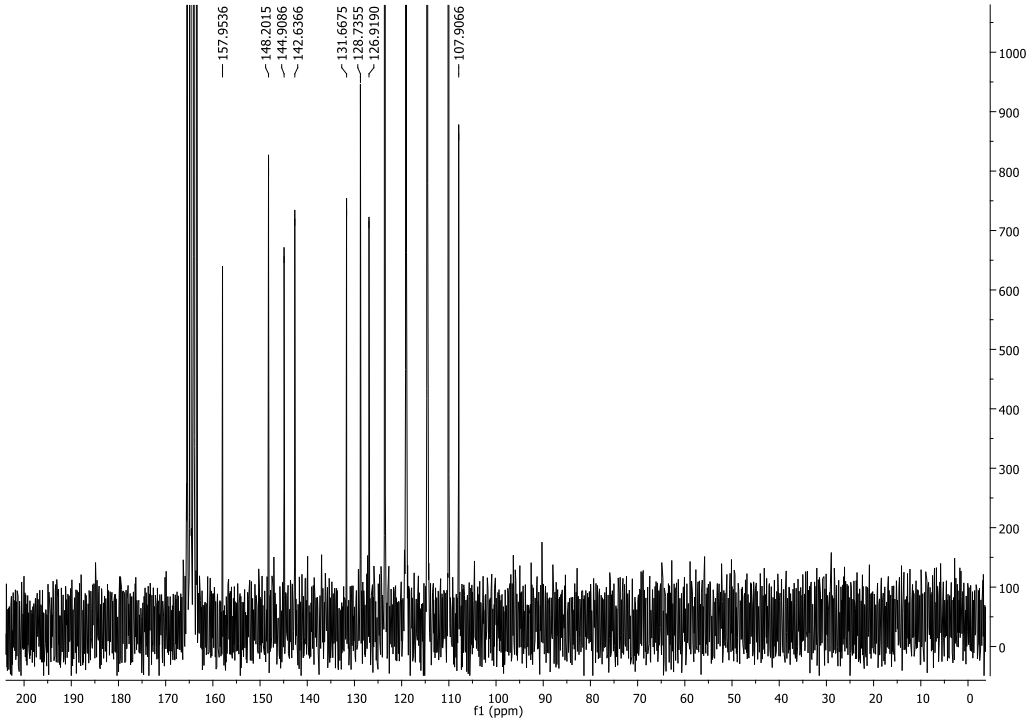
157.9536
148.2015
144.9086
142.6366
131.6675
128.7355
126.9190
107.9066
f1 (ppm)

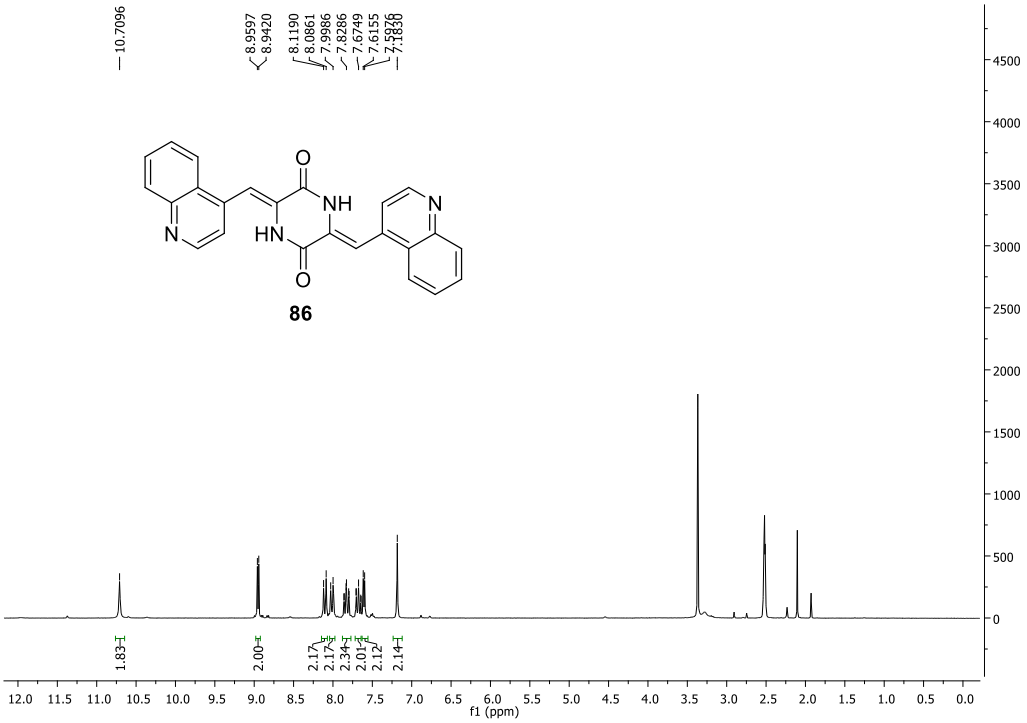
10.7096
8.9597
8.9420
8.1190
8.0861
7.9986
7.8286
7.6749
7.6155
7.5826
7.1830
O
NH
N
HN
N
O
86
1.83
2.00
2.17
2.17
2.34
2.01
2.12
2.14
f1 (ppm)

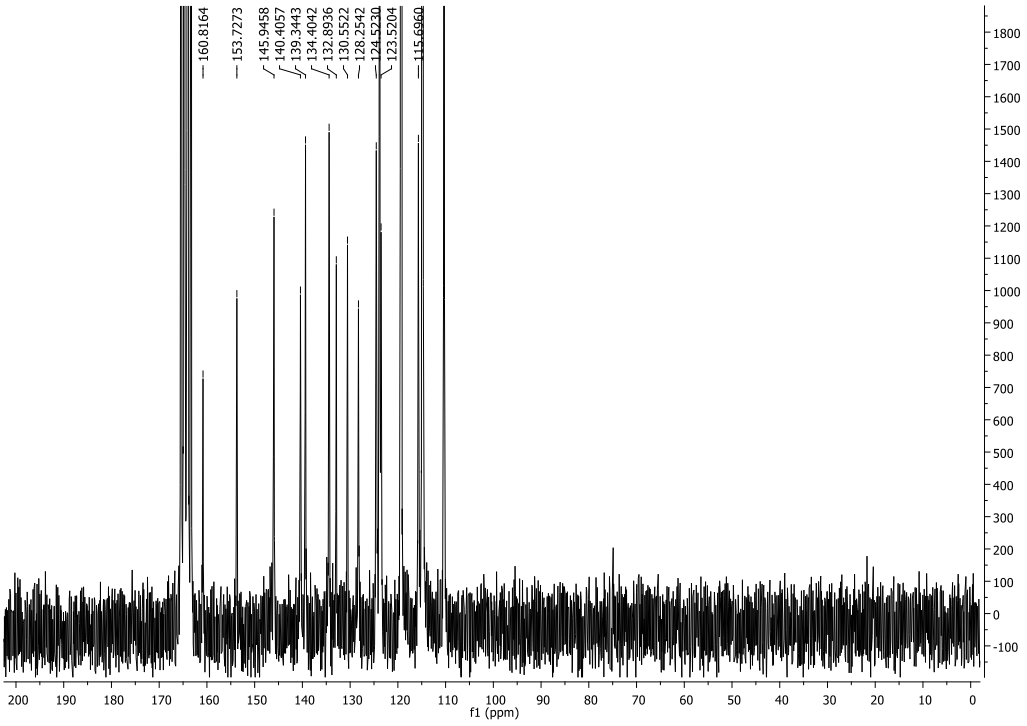
160.8164
153.7273
145.9458
140.4057
139.3443
134.4042
132.8936
130.5522
128.2542
124.5230
123.5204
115.6960
f1 (ppm)

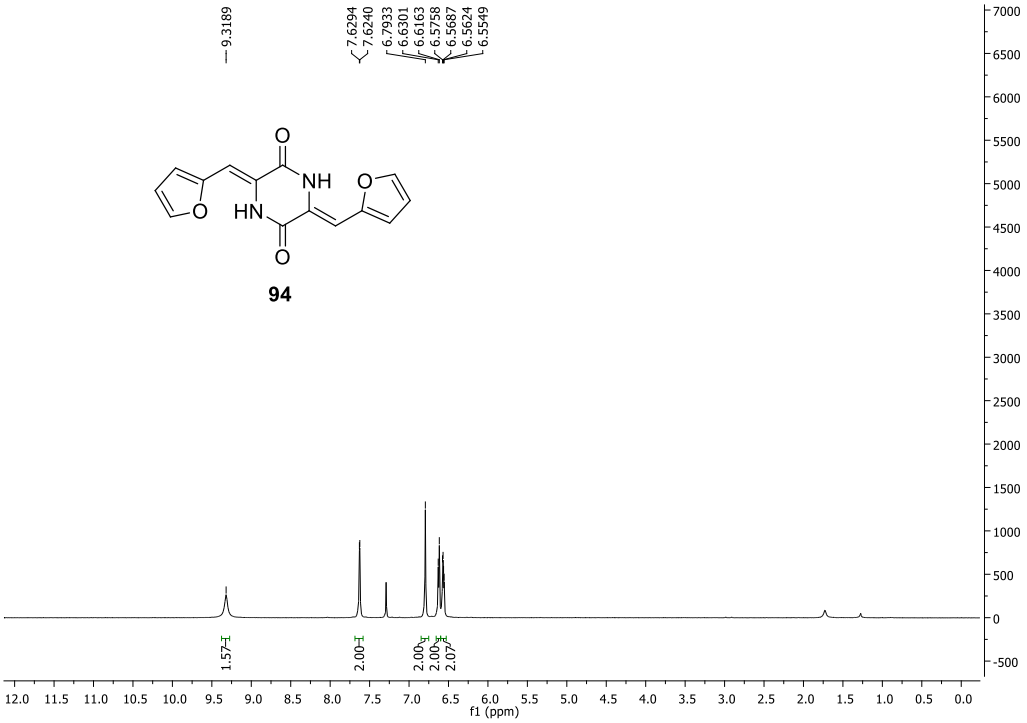
9.3189
7.6294
7.6240
6.7933
6.6301
6.6163
6.5758
6.5687
6.5624
6.5549
O
NH
O
HN
O
1.57
2.00
2.00
2.00
2.07
f1 (ppm)

94

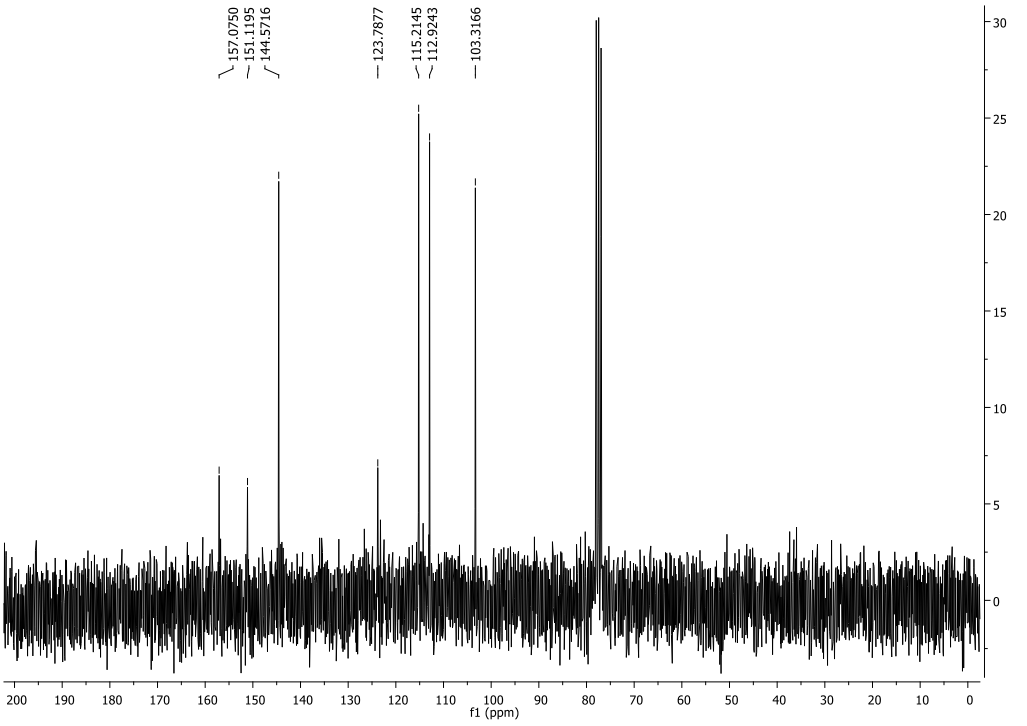
157.0750
151.1195
144.5716
123.7877
115.2145
112.9243
103.3166
f1 (ppm)

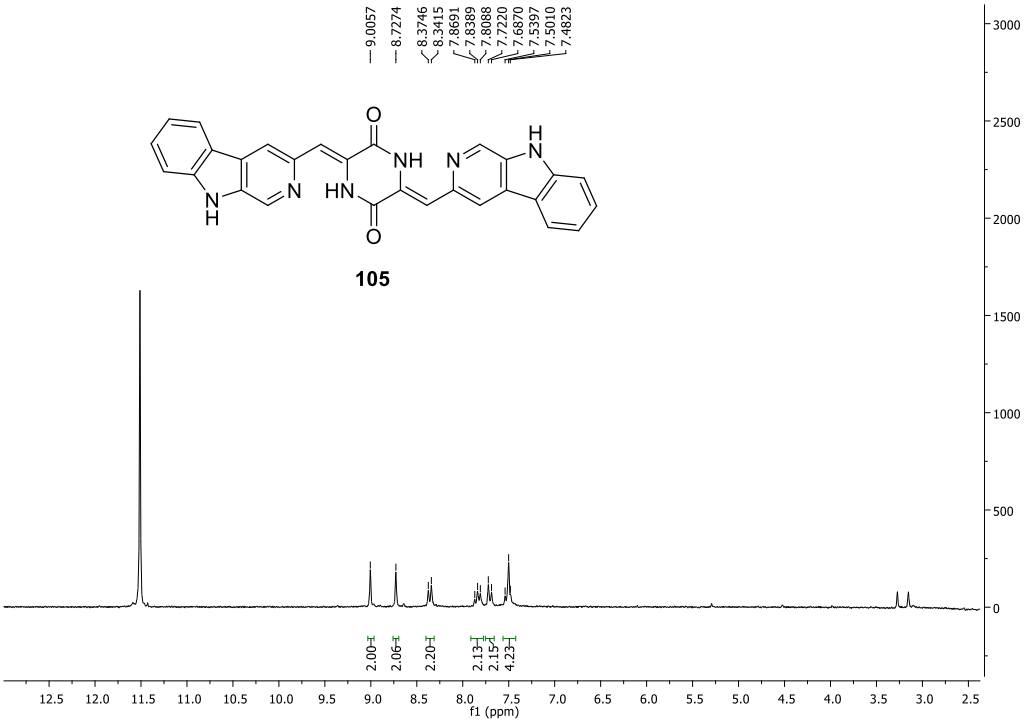
9.0057
8.7274
8.3746
8.3415
7.8691
7.8389
7.8088
7.7220
7.6870
7.5397
7.5010
7.4823
O
NH
N
H
N
HN
N
H
O
105
2.00
2.06
2.20
2.13
2.15
4.23
f1 (ppm)

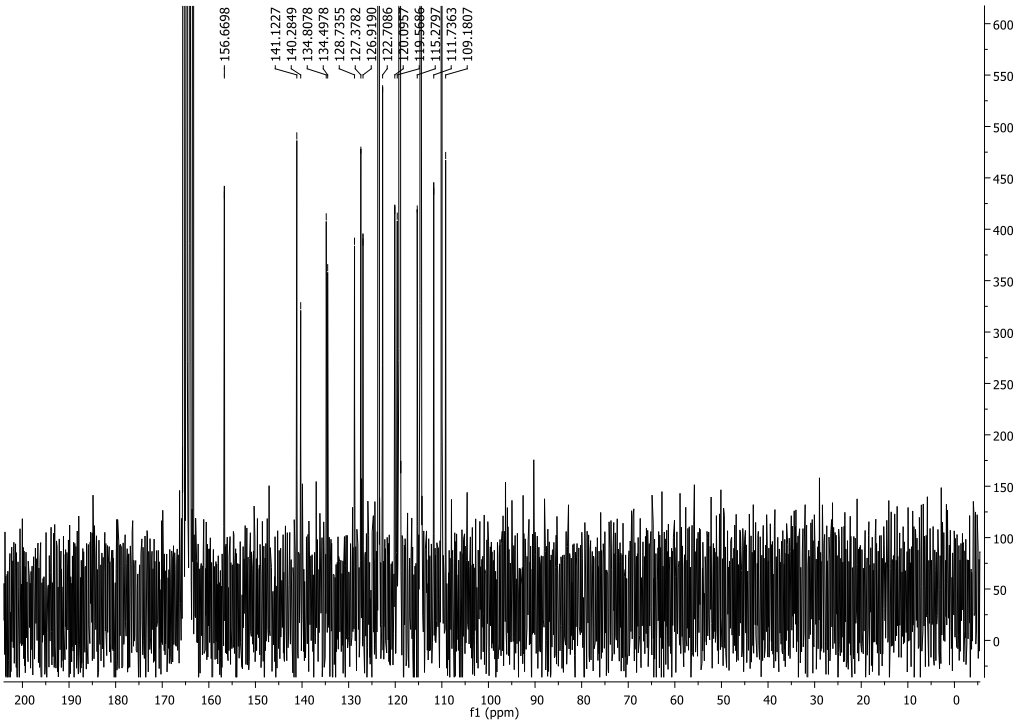
156.6698
141.1227
140.2849
134.8078
134.4978
128.7355
127.3782
126.9190
122.7086
120.0957
119.5686
115.2797
111.7363
109.1807
f1 (ppm)

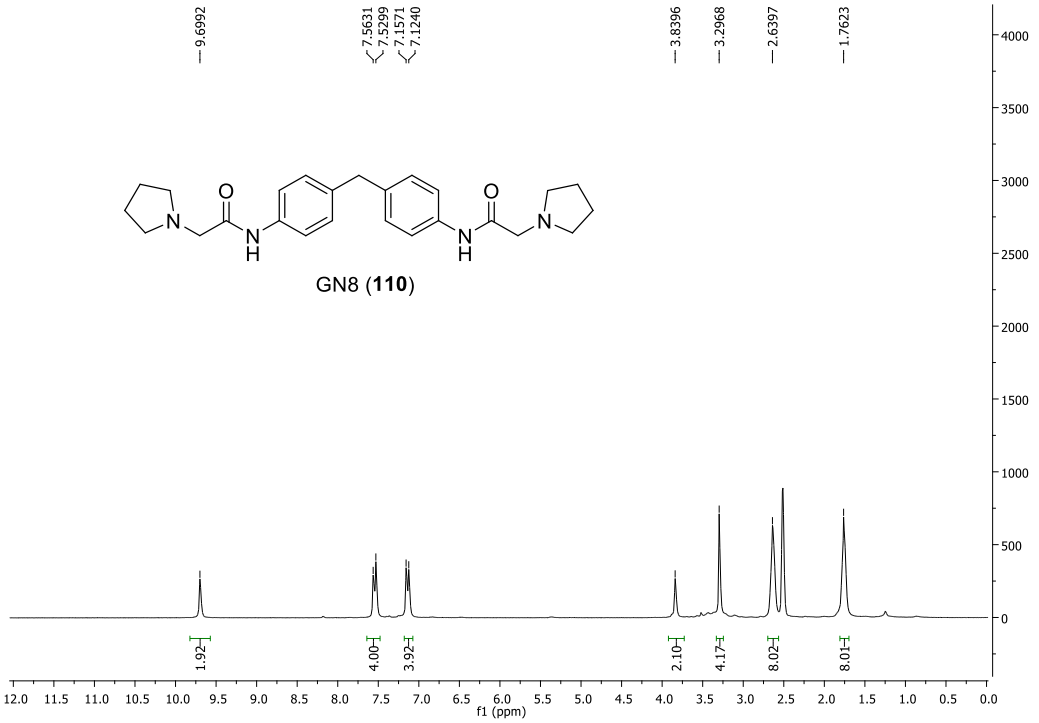
9.6992
7.5631
7.5299
7.1571
7.1240
3.8396
3.2968
2.6397
1.7623
1.92
4.00
3.92
2.10
4.17
8.02
8.01
f1 (ppm)

GN8 (**110**)

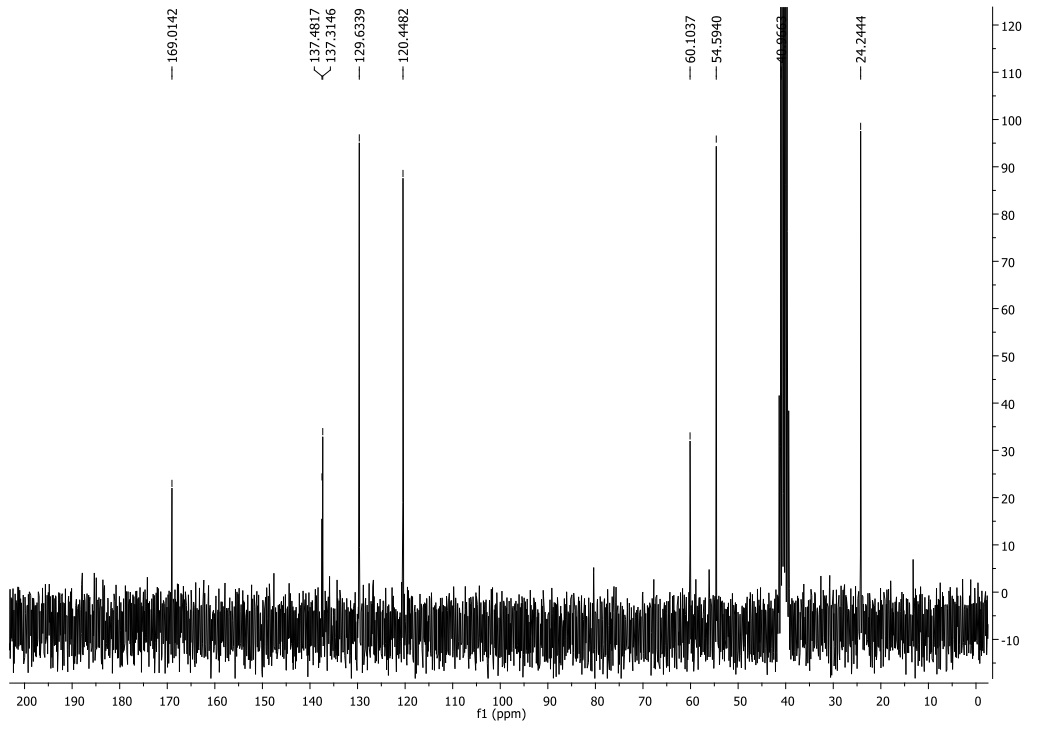
169.0142
137.4817
137.3146
129.6339
120.4482
60.1037
54.5940
40.9663
24.2444
f1 (ppm)

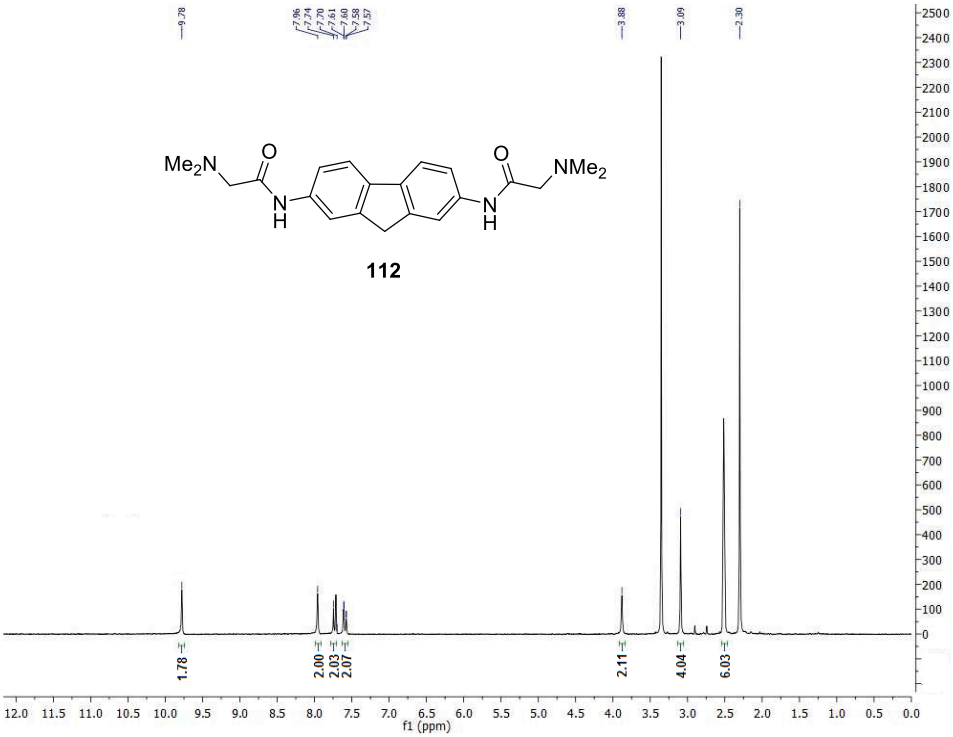
9.78
7.96
7.74
7.70
7.61
7.60
7.58
7.57
3.88
3.09
2.30
Me2N
O
N
H
O
N
H
NMe2
112
1.78
2.00
2.03
2.07
2.11
4.04
6.03
f1 (ppm)

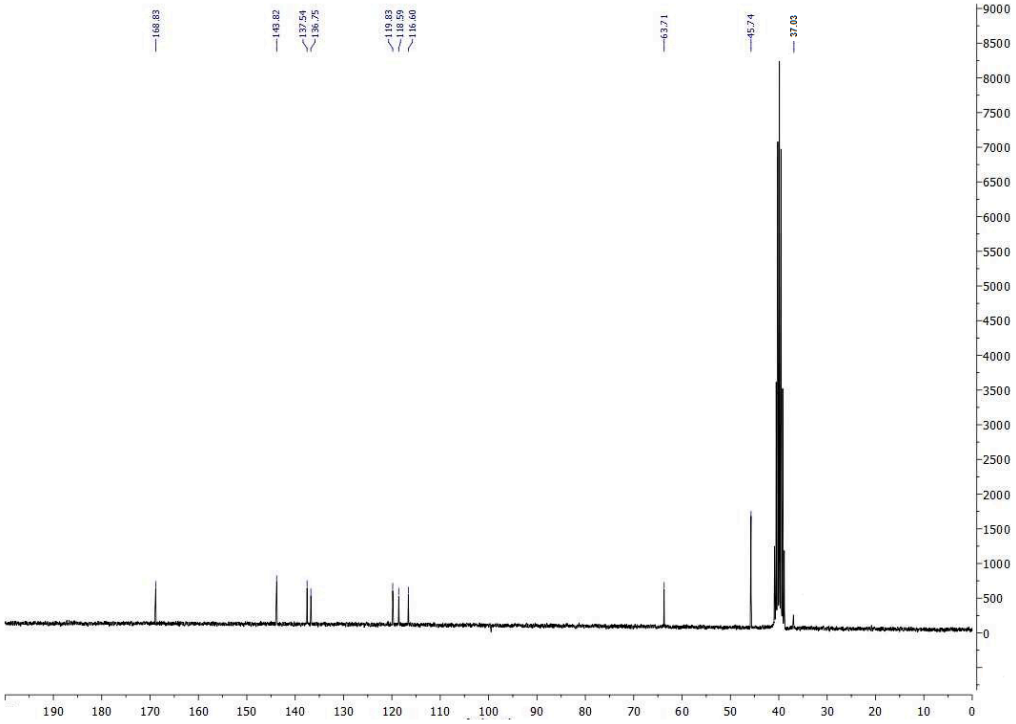
168.83
143.82
137.54
136.75
119.83
118.59
116.60
63.71
45.74
37.03

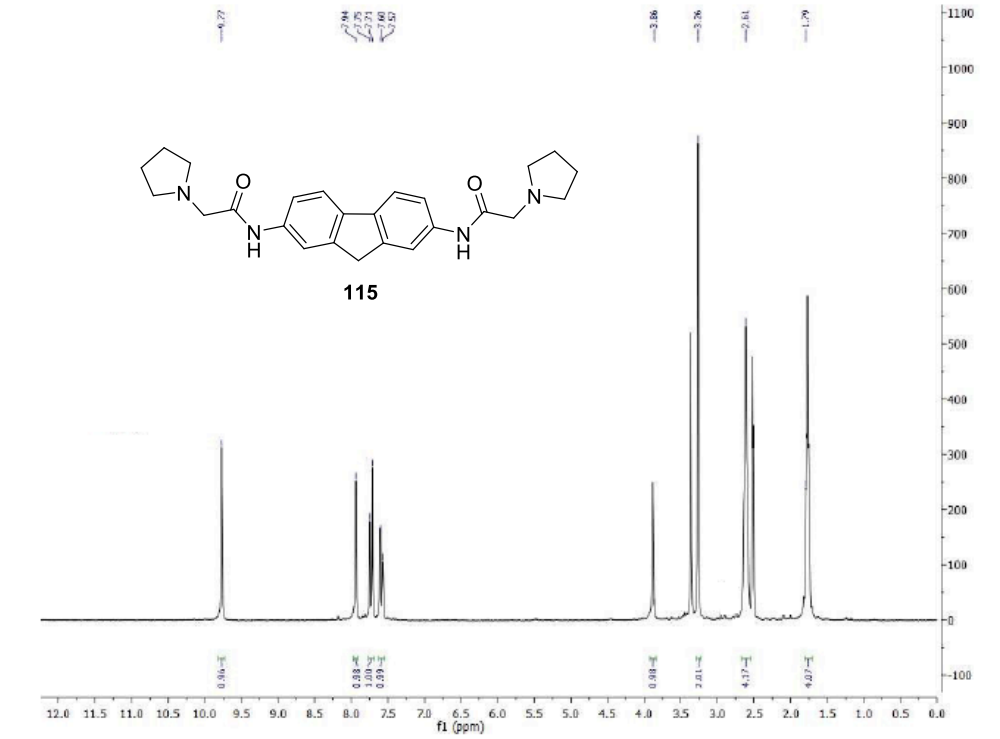

115

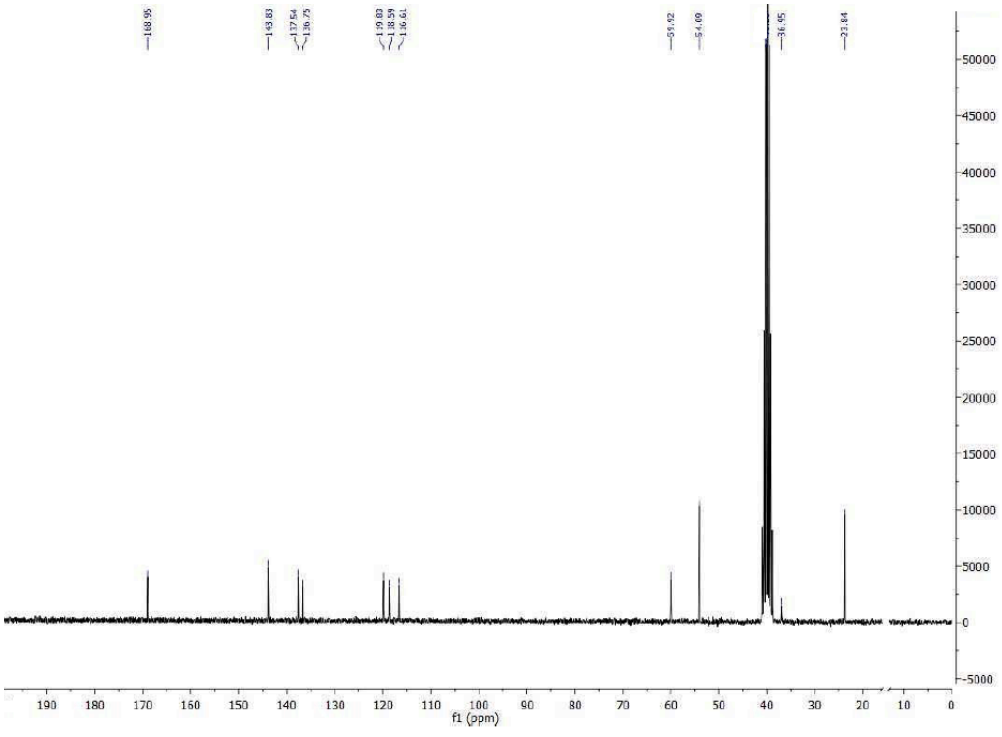

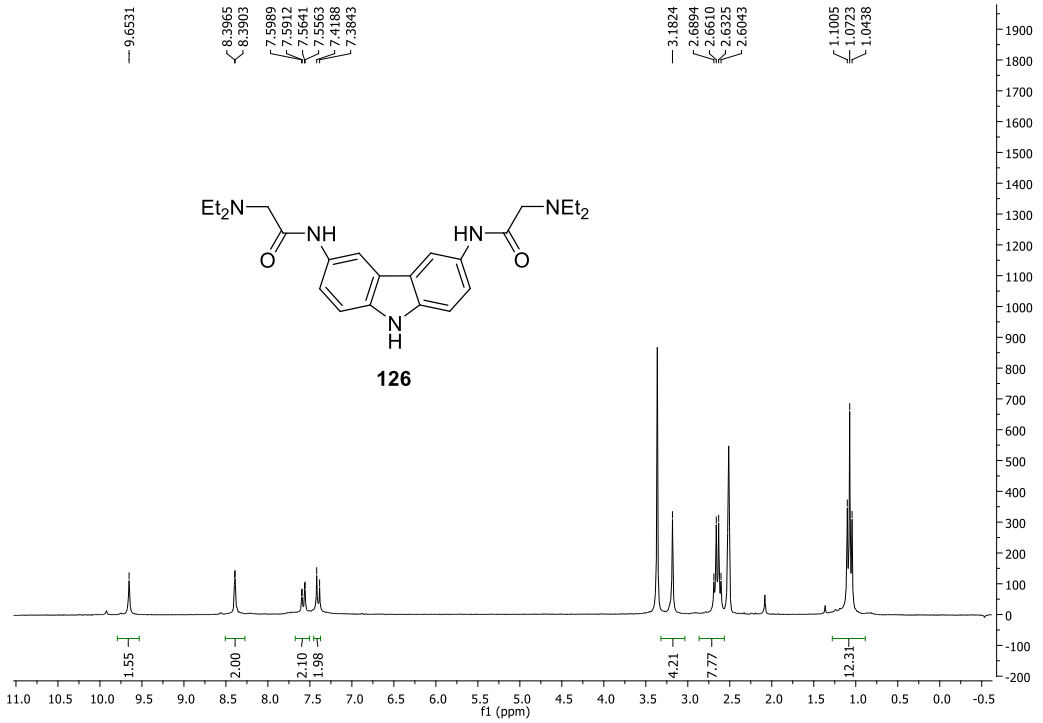
9.6531
8.3965
8.3903
7.5989
7.5912
7.5641
7.5563
7.4188
7.3843
3.1824
2.6894
2.6610
2.6325
2.6043
1.1005
1.0723
1.0438
Et2N
NH
HN
NEt2
O
O
N
H
1.55
2.00
2.10
1.98
4.21
7.77
12.31
f1 (ppm)

126

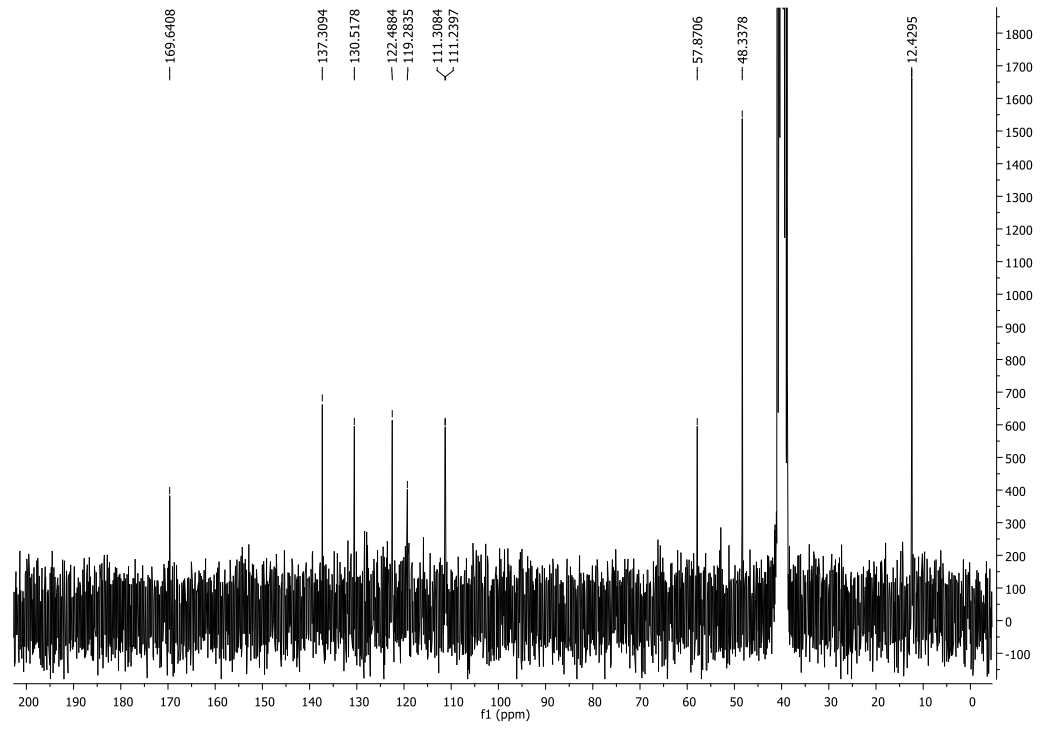
169.6408
137.3094
130.5178
122.4884
119.2835
111.3084
111.2397
57.8706
48.3378
12.4295
f1 (ppm)

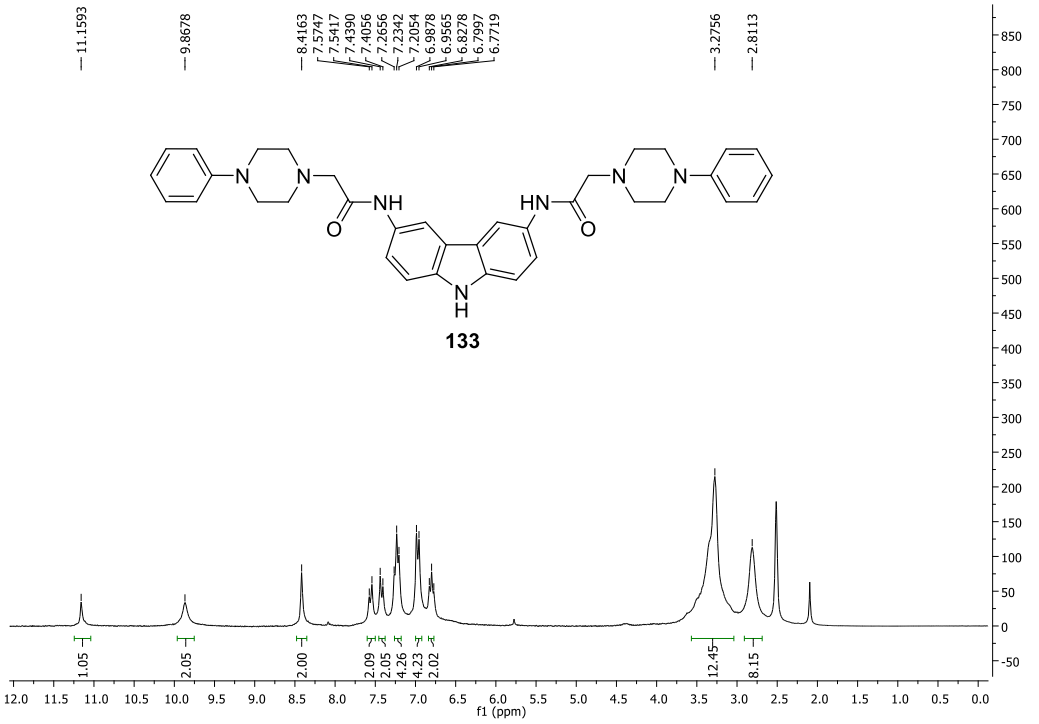
11.1593
9.8678
8.4163
7.5747
7.5417
7.4390
7.4056
7.2656
7.2342
7.2054
6.9878
6.9565
6.8278
6.7997
6.7719
3.2756
2.8113
1.05
2.05
2.00
2.09
2.05
4.26
4.23
2.02
12.45
8.15
f1 (ppm)

133

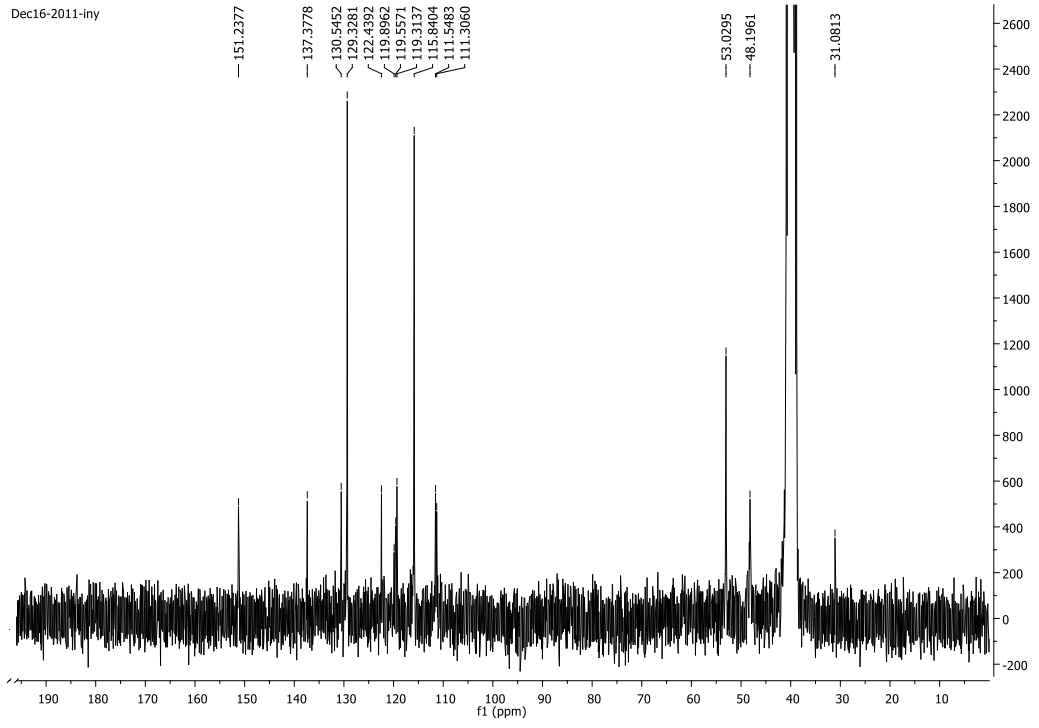
Dec16-2011-iny
151.2377
137.3778
130.5452
129.3281
122.4392
119.8962
119.5571
119.3137
115.8404
111.5483
111.3060
53.0295
48.1961
31.0813
f1 (ppm)

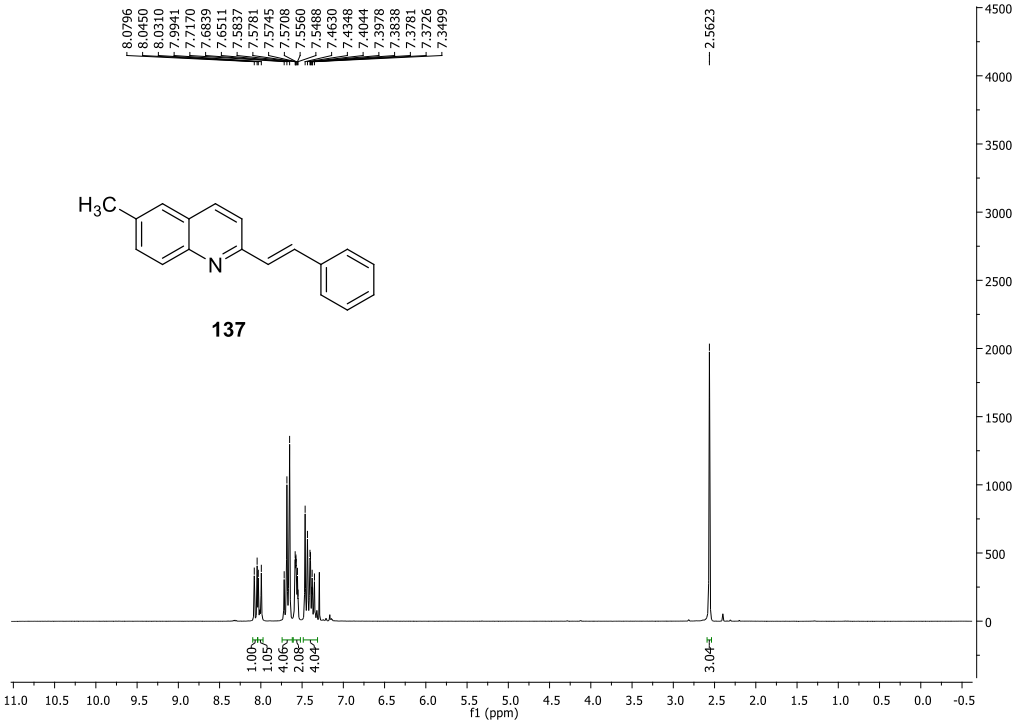
8.0796
8.0450
8.0310
7.9941
7.7170
7.6839
7.6511
7.5837
7.5781
7.5745
7.5708
7.5560
7.5488
7.4630
7.4348
7.4044
7.3978
7.3838
7.3781
7.3726
7.3499
2.5623
H3C
N
137
1.00
1.05
4.06
2.08
4.04
3.04
f1 (ppm)

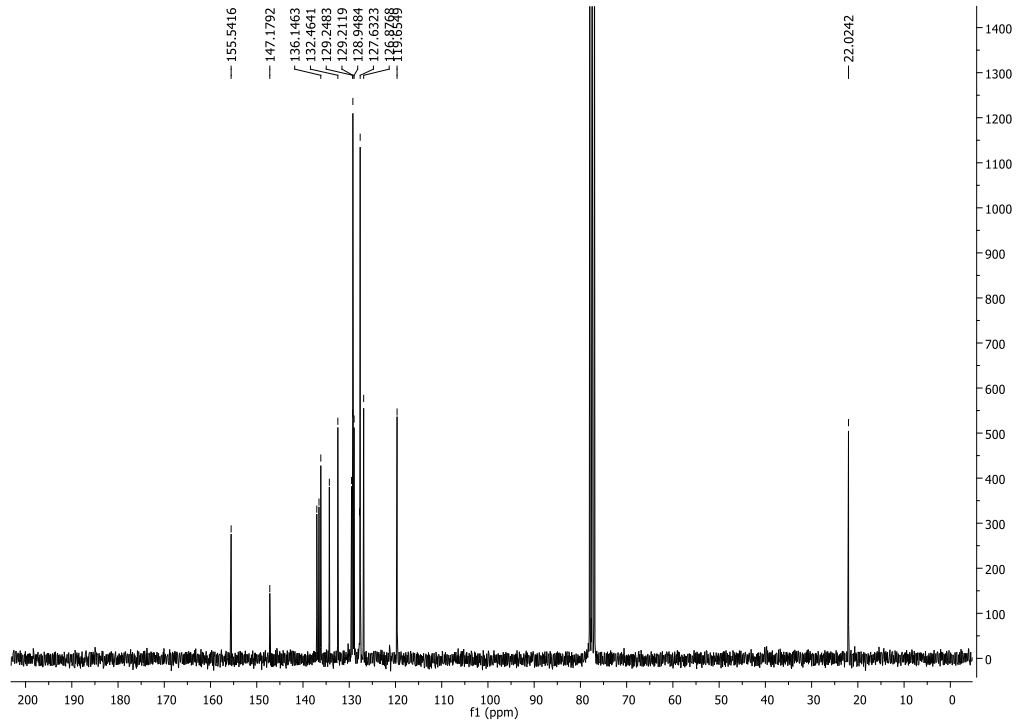
155.5416
147.1792
136.1463
132.4641
129.2463
129.2119
128.9484
127.6323
126.8768
119.6549
22.0242
f1 (ppm)

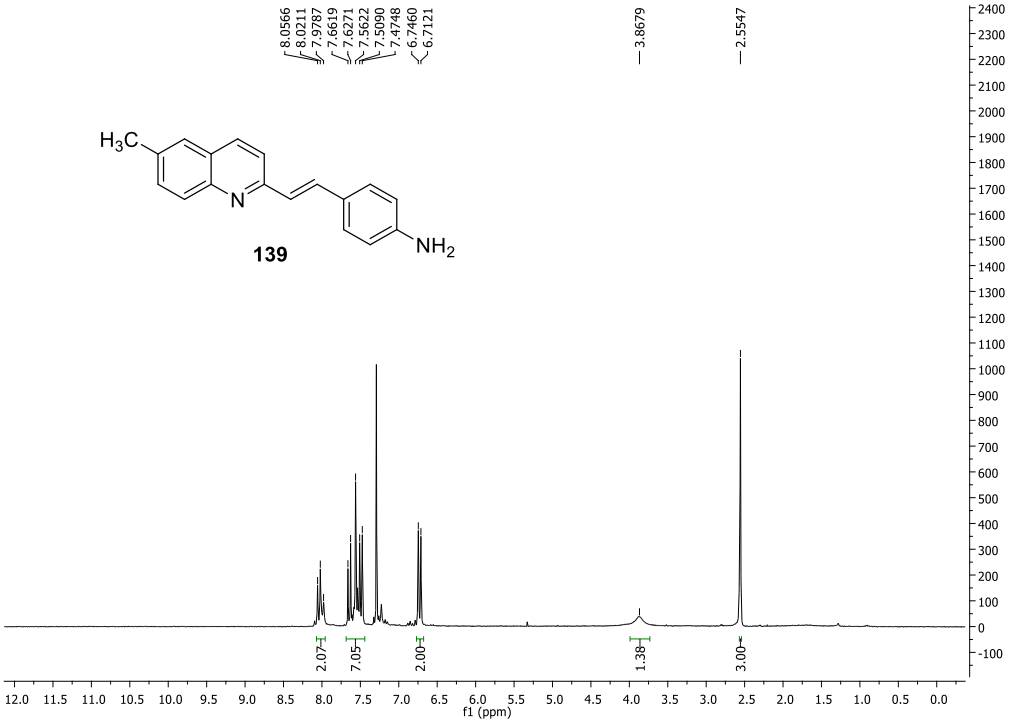
8.0566
8.0211
7.9787
7.6619
7.6271
7.5622
7.5090
7.4748
6.7460
6.7121
3.8679
2.5547
H3C
N
NH2
139
2.07
7.05
2.00
1.38
3.00
f1 (ppm)

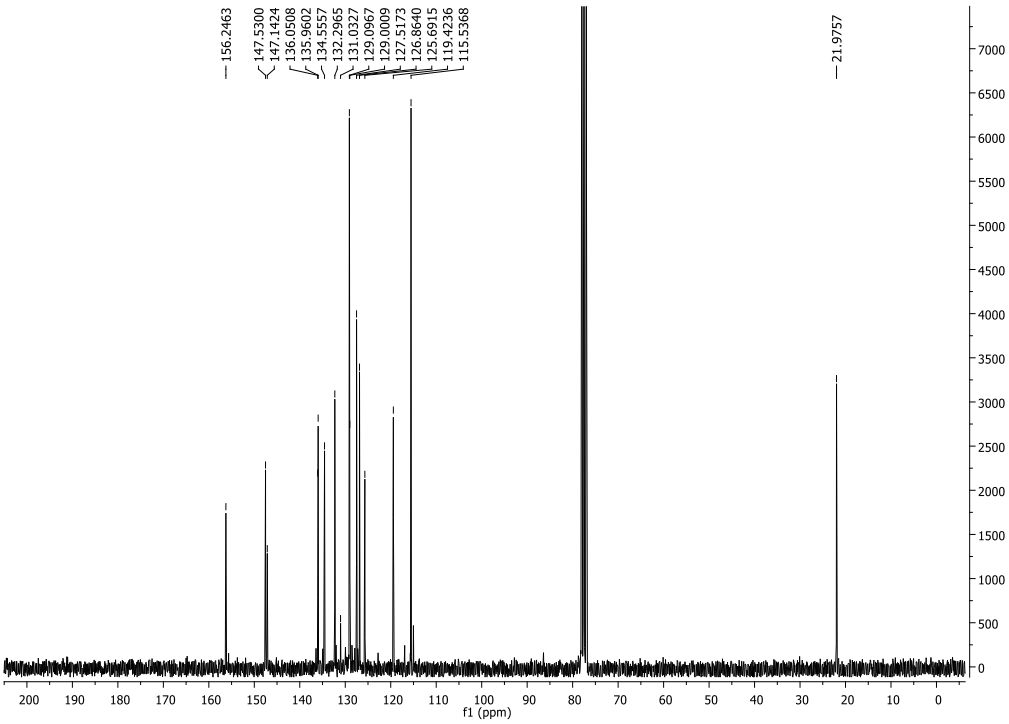
156.2463
147.5300
147.1424
136.0508
135.9602
134.5557
132.2965
131.0327
129.0967
129.0009
127.5173
126.8640
125.6915
119.4236
115.5368
21.9757
f1 (ppm)

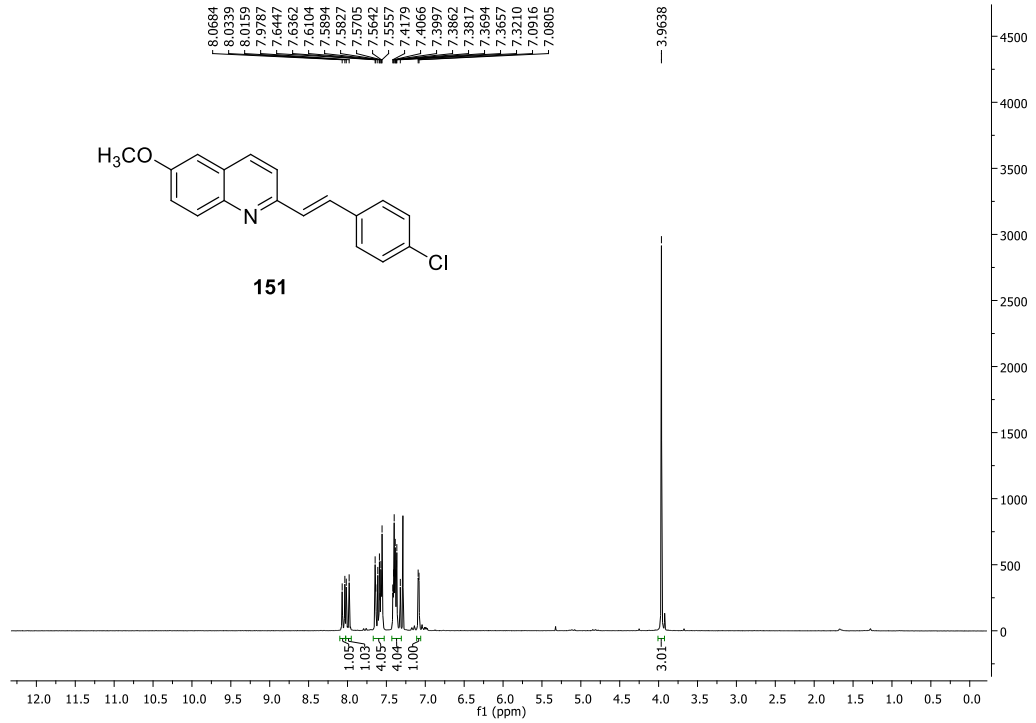
8.0684
8.0339
8.0159
7.9787
7.6447
7.6362
7.6104
7.5894
7.5827
7.5705
7.5642
7.5557
7.4179
7.4066
7.3997
7.3862
7.3817
7.3694
7.3657
7.3210
7.0916
7.0805
3.9638
H3CO
N
Cl
151
1.05
1.03
4.05
4.04
1.00
3.01
f1 (ppm)

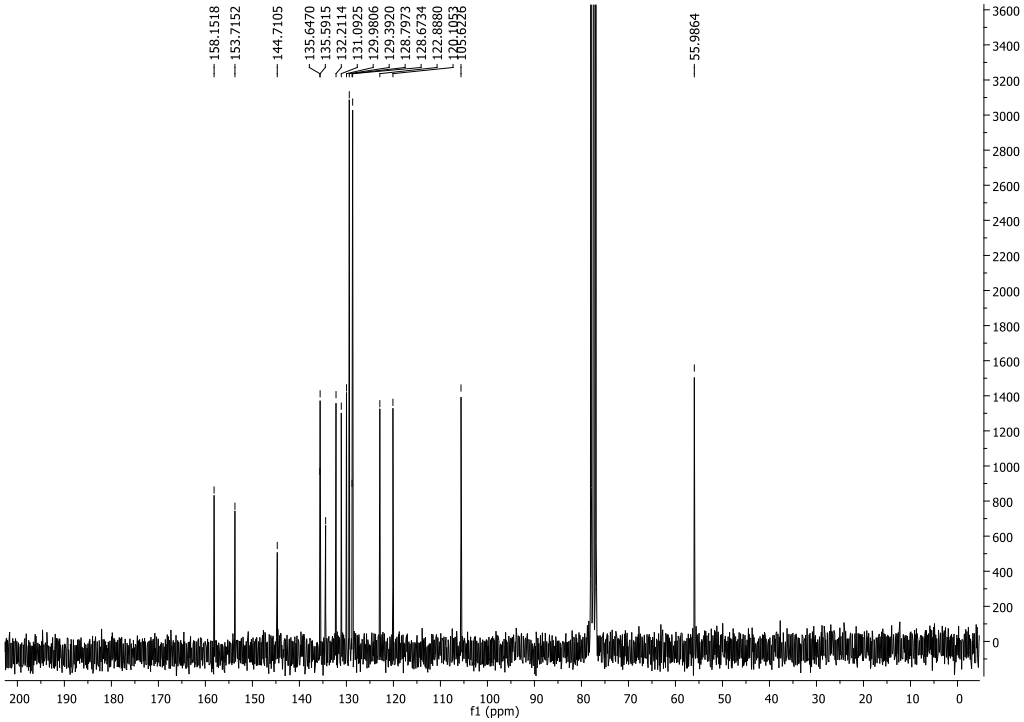
158.1518
153.7152
144.7105
135.6470
135.5915
132.2114
131.0925
129.9806
129.3920
128.7973
128.6734
122.8880
120.1953
105.6228
55.9864
f1 (ppm)

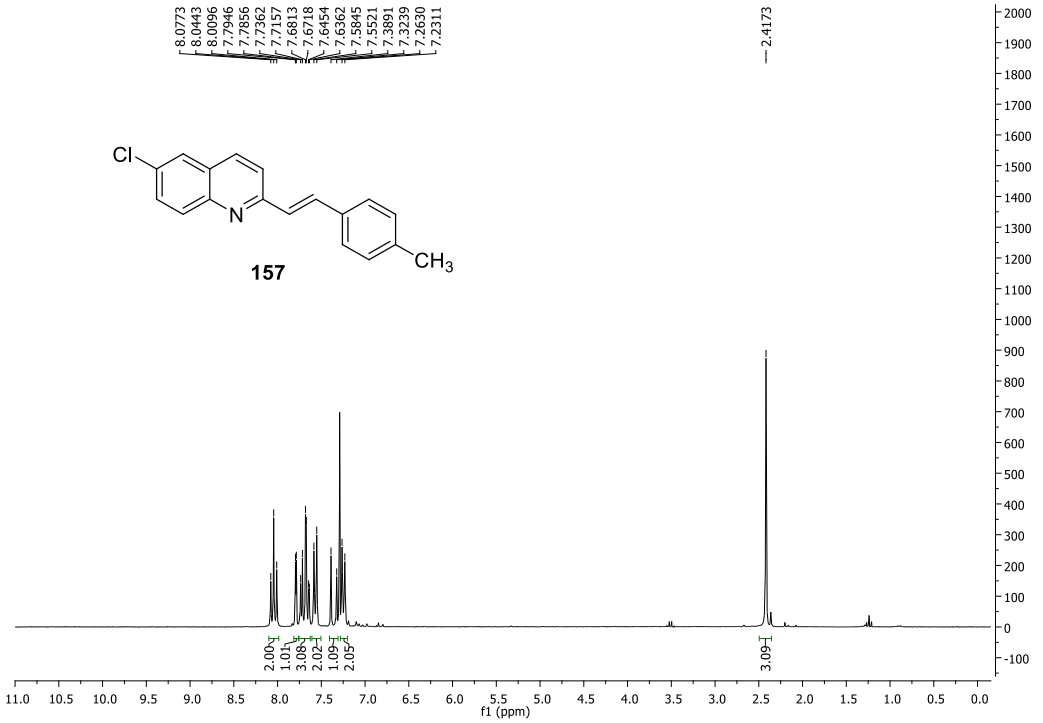
8.0773
8.0443
8.0096
7.7946
7.7856
7.7362
7.7157
7.6813
7.6718
7.6454
7.6362
7.5845
7.5521
7.3891
7.3239
7.2630
7.2311
2.4173
Cl
N
CH3
157
2.00
1.01
3.08
2.02
1.09
2.05
3.09
f1 (ppm)

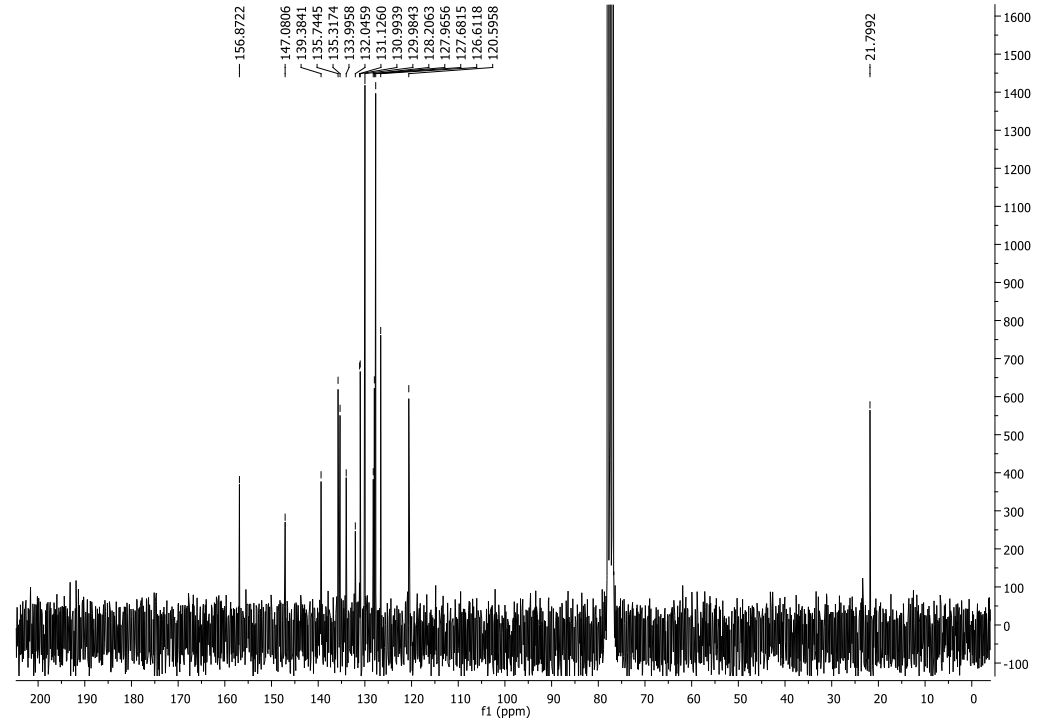
156.8722
147.0806
139.3841
135.7445
135.3174
133.9958
132.0459
131.1260
130.9939
129.9843
128.2063
127.9656
127.6815
126.6118
120.5958
21.7992
f1 (ppm)

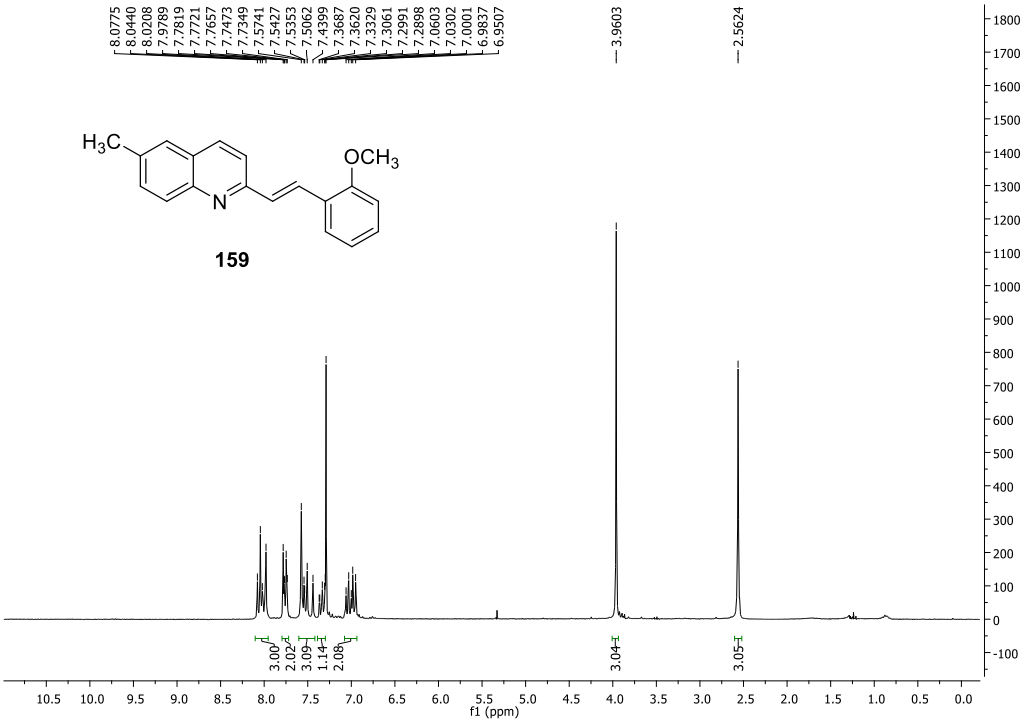
8.0775
8.0440
8.0208
7.9789
7.7819
7.7721
7.7657
7.7473
7.7349
7.5741
7.5427
7.5353
7.5062
7.4399
7.3687
7.3620
7.3329
7.3061
7.2991
7.2898
7.0603
7.0302
7.0001
6.9837
6.9507
3.9603
2.5624
H3C
OCH3
N
159
3.00
2.02
3.09
1.14
2.08
3.04
3.05
f1 (ppm)

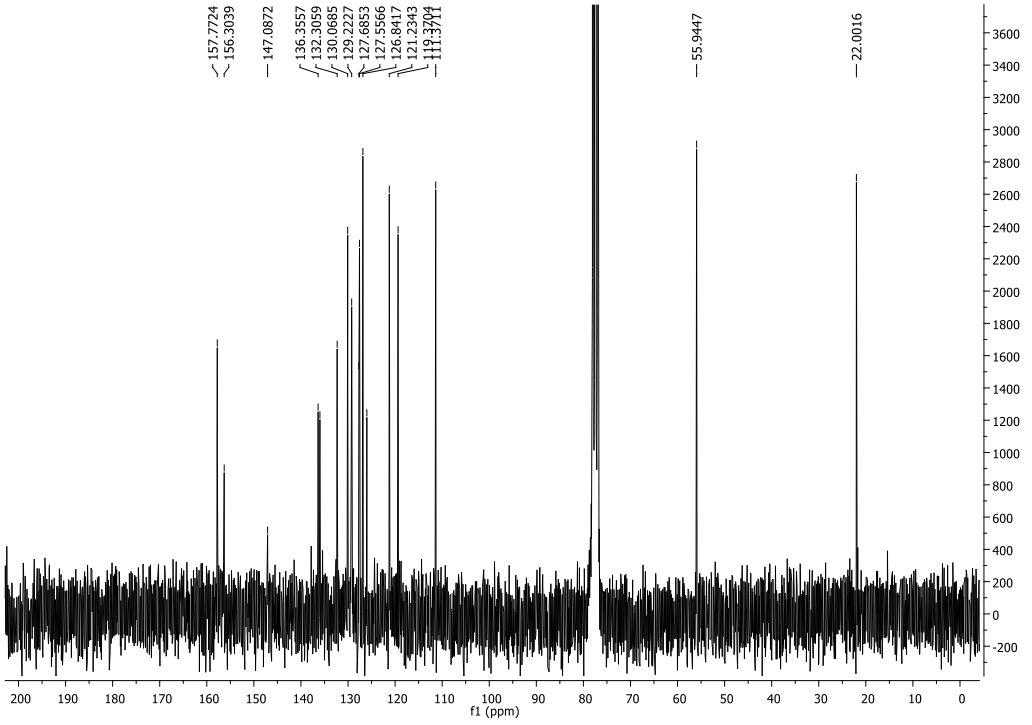
157.7724
156.3039
147.0872
136.3557
132.3059
130.0685
129.2227
127.6853
127.5566
126.8417
121.2343
111.3711
55.9447
22.0016
f1 (ppm)

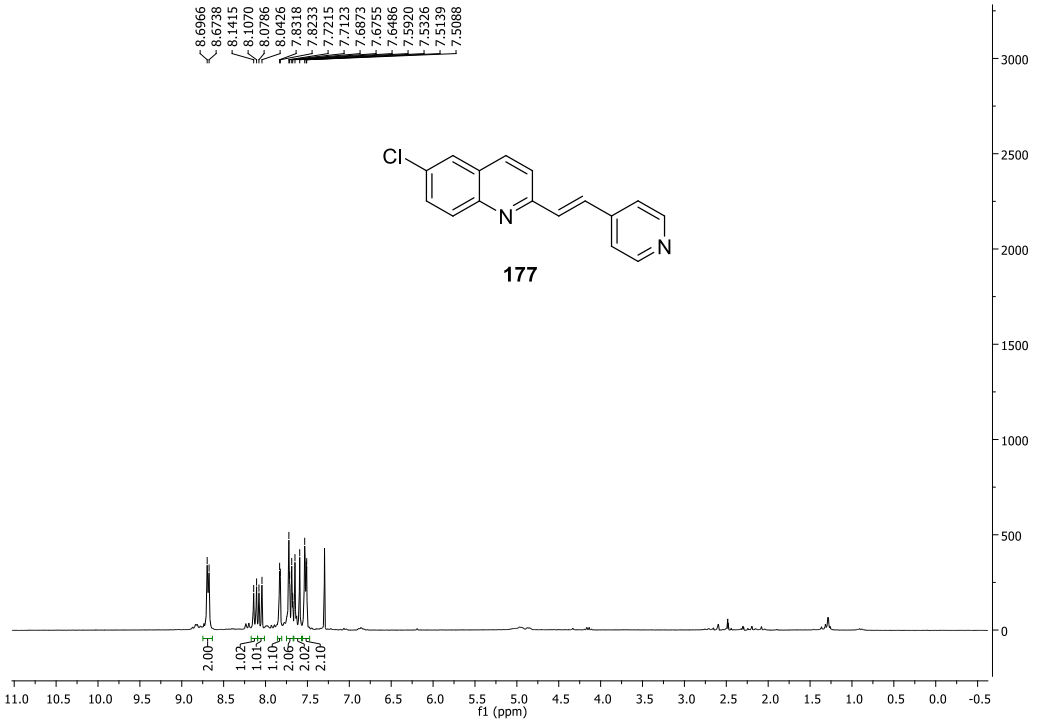
8.6966
8.6738
8.1415
8.1070
8.0786
8.0426
7.8318
7.8233
7.7215
7.7123
7.6873
7.6755
7.6486
7.5920
7.5326
7.5139
7.5088
Cl
N
N
177
2.00
1.02
1.01
1.10
2.06
2.03
2.10
f1 (ppm)

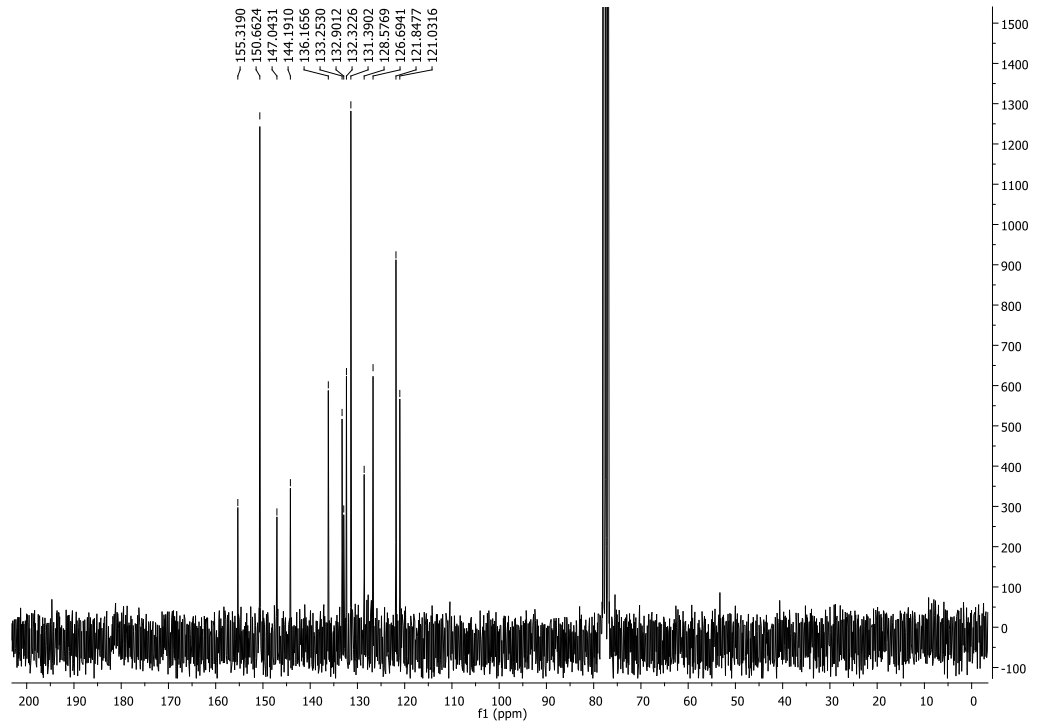
155.3190
150.6624
147.0431
144.1910
136.1656
133.2530
132.9012
132.3226
131.3902
128.5769
126.6941
121.8477
121.0316
f1 (ppm)

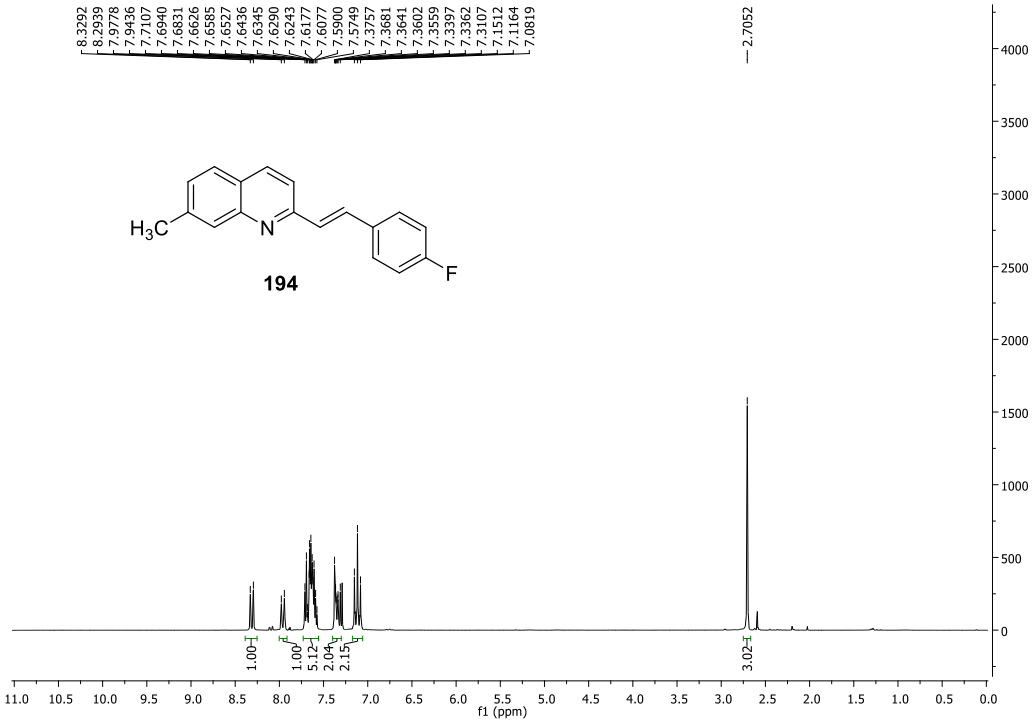
8.3292
8.2939
7.9778
7.9436
7.7107
7.6940
7.6831
7.6626
7.6585
7.6527
7.6436
7.6345
7.6290
7.6243
7.6177
7.6077
7.5900
7.5749
7.3757
7.3681
7.3641
7.3602
7.3559
7.3397
7.3362
7.3107
7.1512
7.1164
7.0819
2.7052
H3C
N
F
194
1.00
1.00
5.12
2.04
2.15
3.02
f1 (ppm)

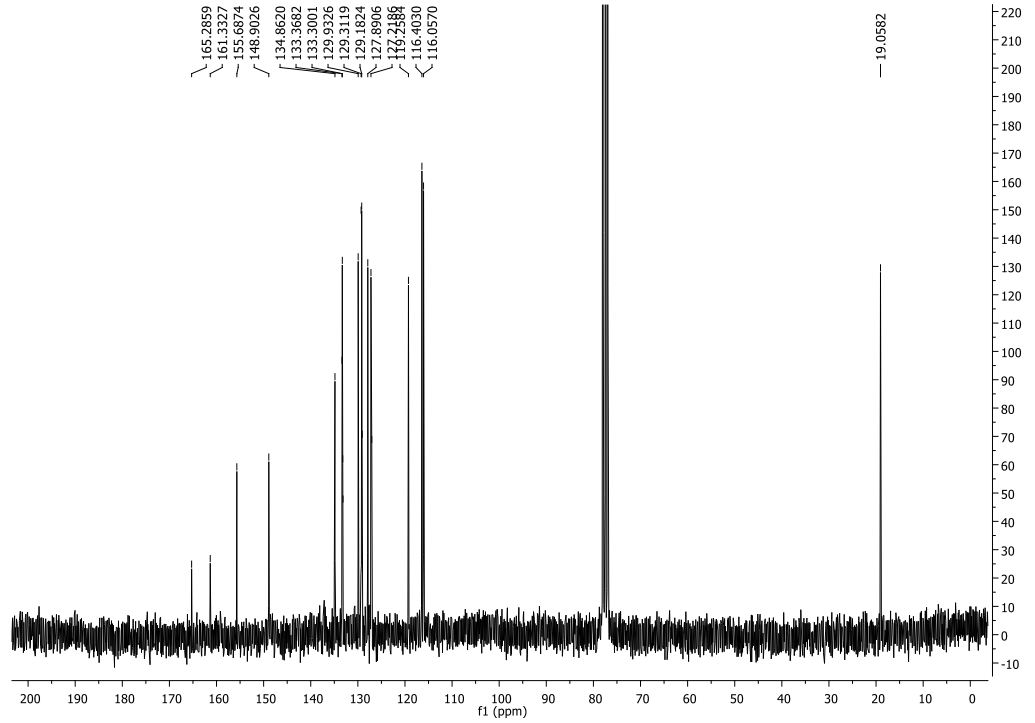
165.2859
161.3327
155.6874
148.9026
134.8620
133.3682
133.3001
129.9326
129.3119
129.1824
127.8906
116.4030
116.0570
19.0582
f1 (ppm)

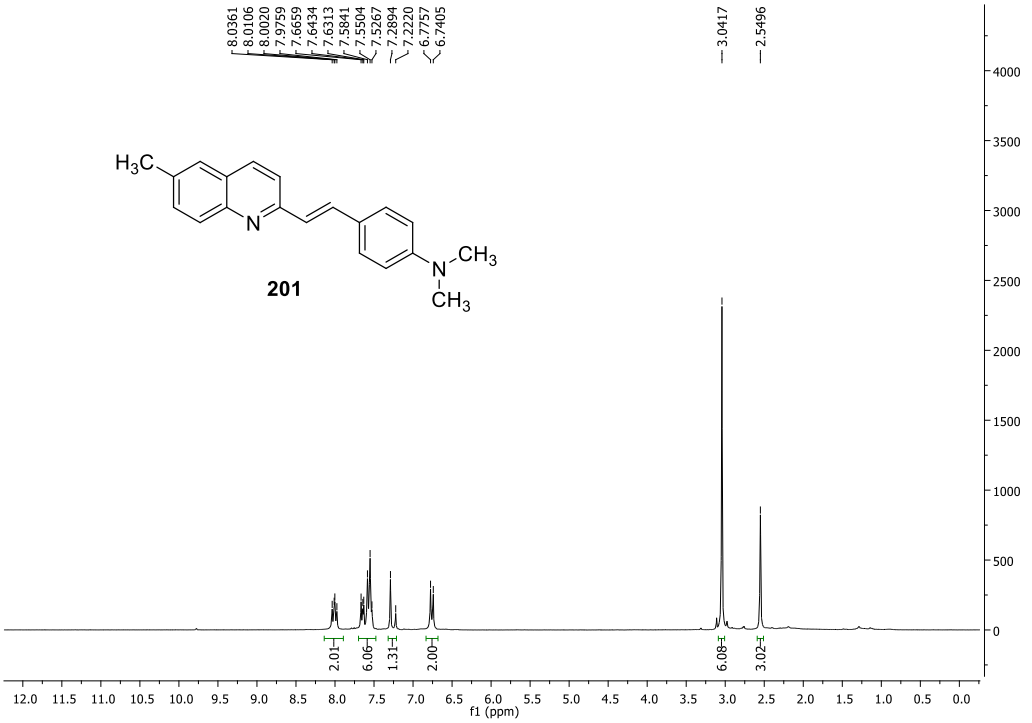
8.0361
8.0106
8.0020
7.9759
7.6659
7.6434
7.6313
7.5841
7.5504
7.5267
7.2894
7.2220
6.7757
6.7405
3.0417
2.5496
H3C
N
N
CH3
CH3
201
2.01
6.06
1.31
2.00
6.08
3.02
f1 (ppm)

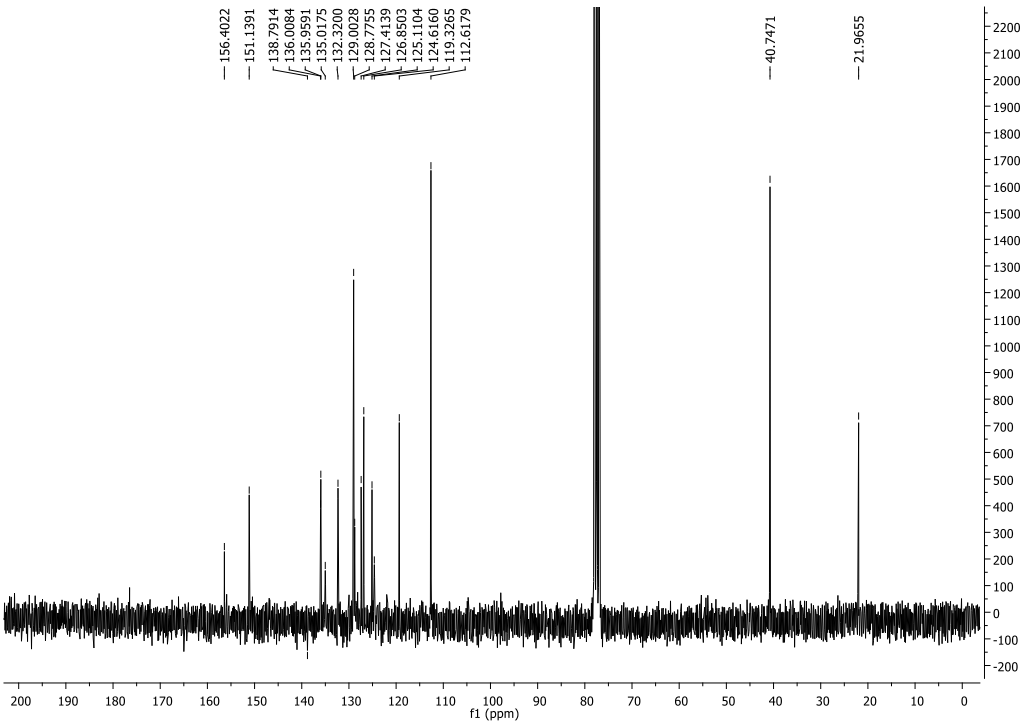
156.4022
151.1391
138.7914
136.0084
135.9591
135.0175
132.3200
129.0028
128.7755
127.4139
126.8503
125.1104
124.6160
119.3265
112.6179
40.7471
21.9655
f1 (ppm)

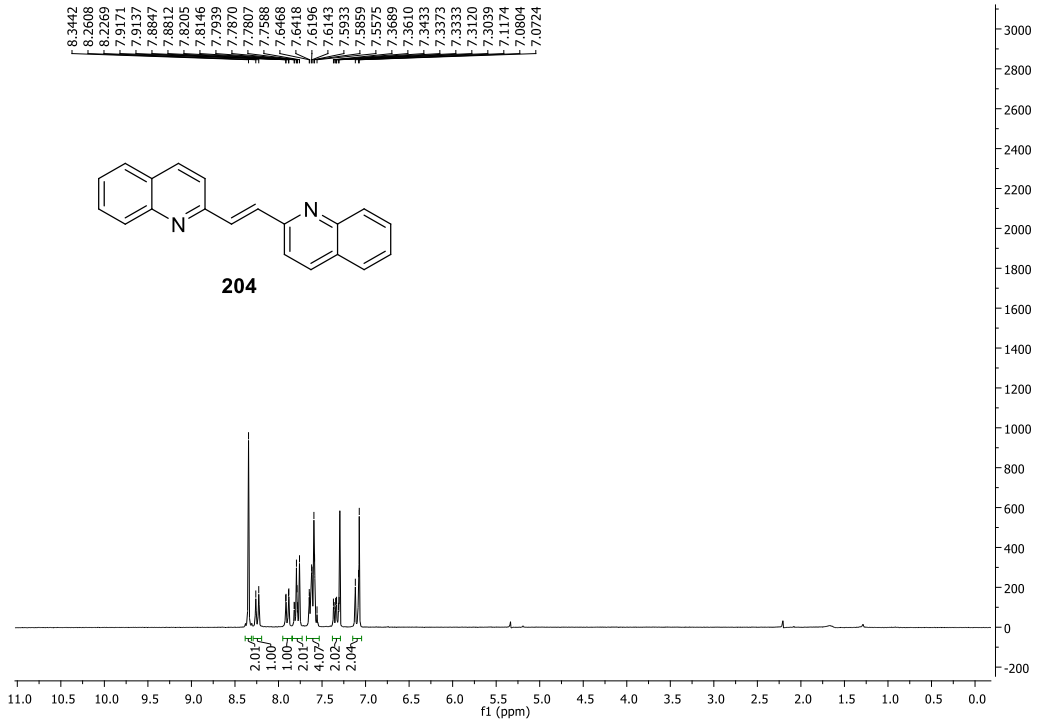
8.3442
8.2608
8.2269
7.9171
7.9137
7.8847
7.8812
7.8205
7.8146
7.7939
7.7870
7.7807
7.7588
7.6468
7.6418
7.6196
7.6143
7.5933
7.5859
7.5575
7.3689
7.3610
7.3433
7.3373
7.3333
7.3120
7.3039
7.1174
7.0804
7.0724
N
N
204
2.01
1.00
1.00
2.01
4.07
2.02
2.04
f1 (ppm)

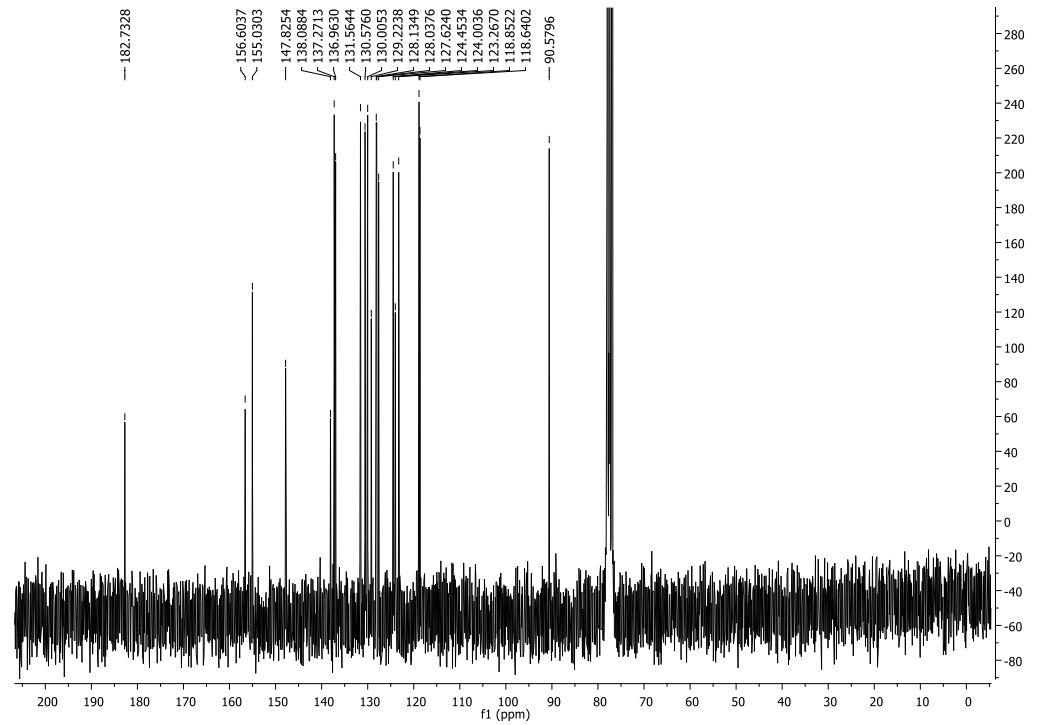
182.7328
156.6037
155.0303
147.8254
138.0884
137.2713
136.9630
131.5644
130.5760
130.0053
129.2238
128.1349
128.0376
127.6240
124.4534
124.0036
123.2670
118.8522
118.6402
90.5796
f1 (ppm)

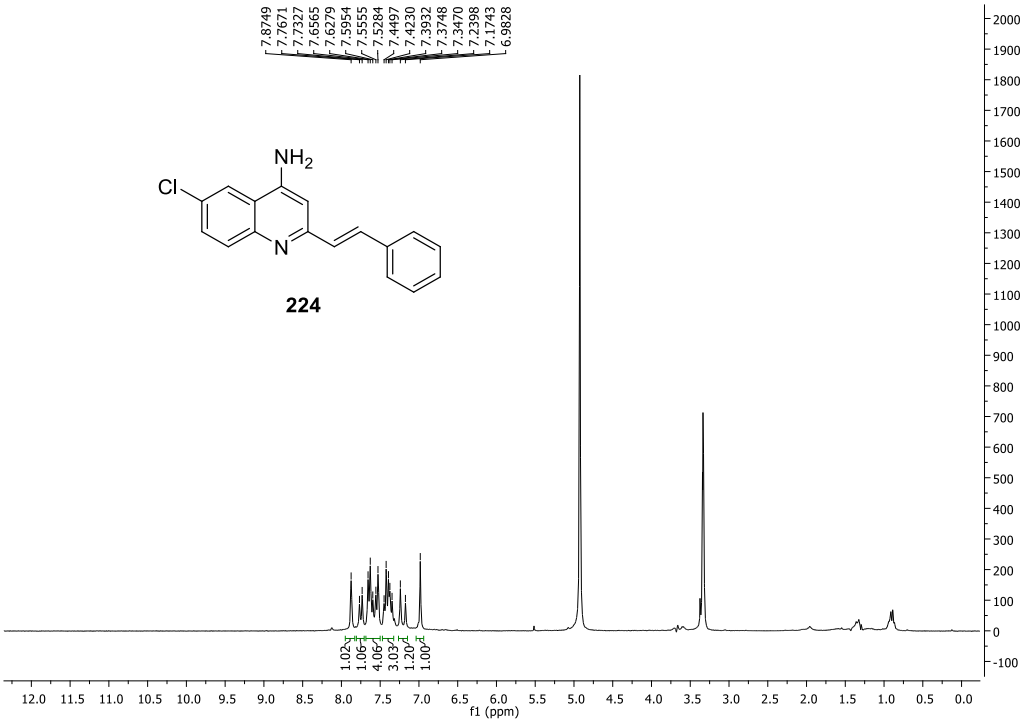
7.8749
7.7671
7.7327
7.6565
7.6279
7.5954
7.5555
7.5284
7.4497
7.4230
7.3932
7.3748
7.3470
7.2398
7.1743
6.9828
NH2
Cl
N
224
1.02
1.06
4.06
3.03
1.20
1.00
f1 (ppm)

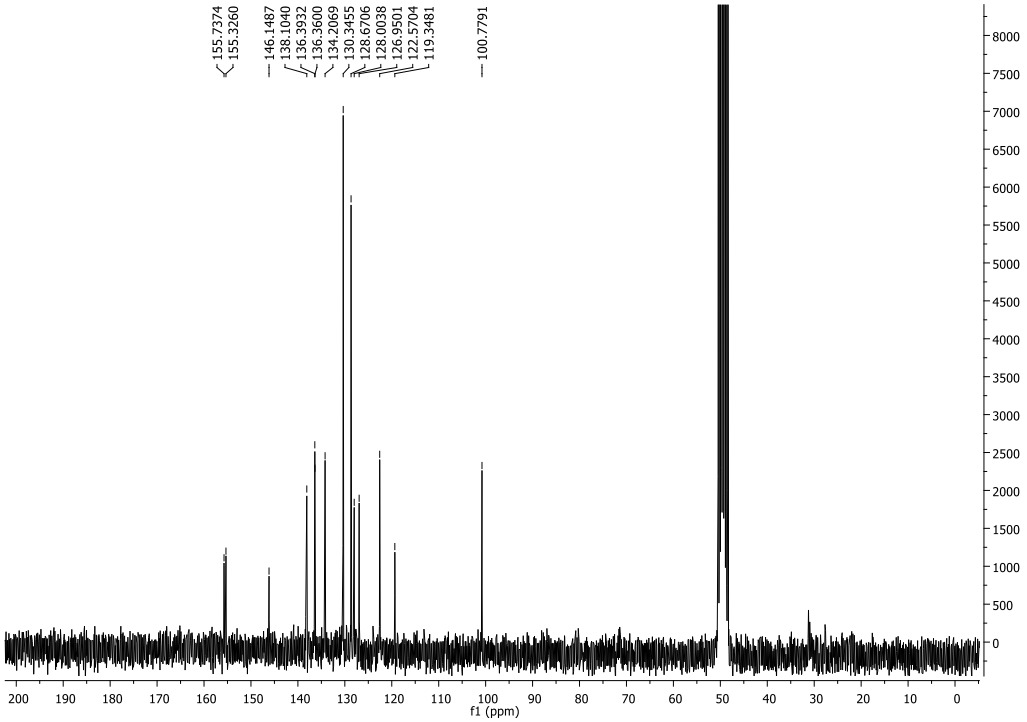
155.7374
155.3260
146.1487
138.1040
136.3932
136.3600
134.2069
130.3455
128.6706
128.0038
126.9501
122.5704
119.3481
100.7791
f1 (ppm)

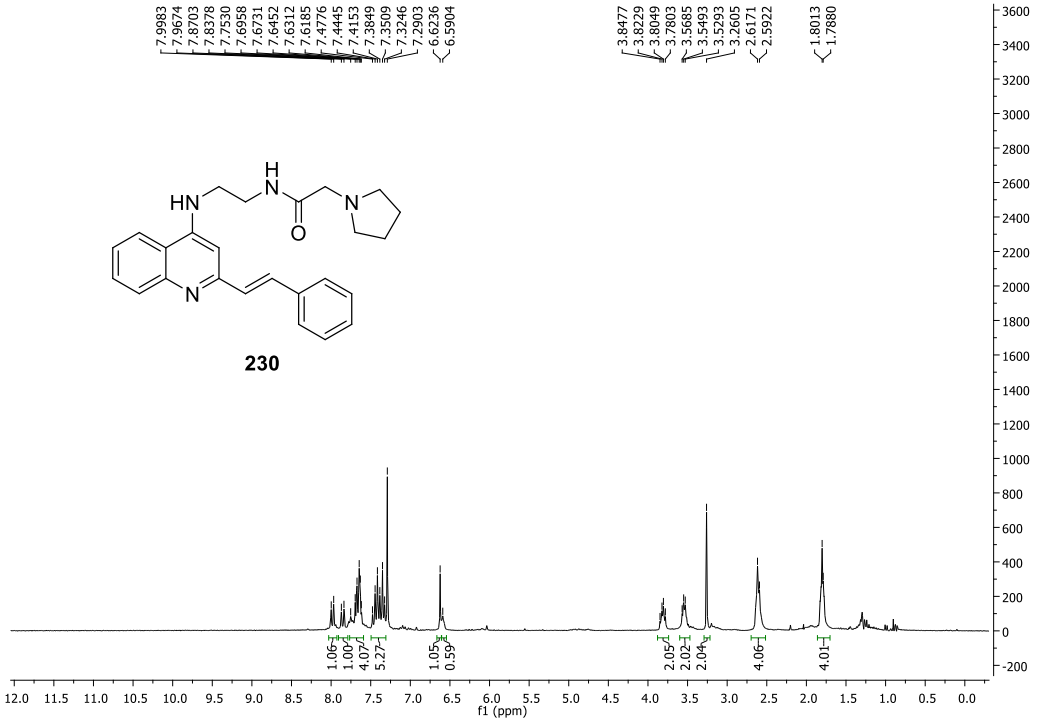
7.9983
7.9674
7.8703
7.8378
7.7530
7.6958
7.6731
7.6452
7.6312
7.6185
7.4776
7.4445
7.4153
7.3849
7.3509
7.3246
7.2903
6.6236
6.5904
3.8477
3.8229
3.8049
3.7803
3.5685
3.5493
3.5293
3.2605
2.6171
2.5922
1.8013
1.7880
HN
H
N
N
O
N
1.06
1.00
4.07
5.27
1.05
0.59
2.05
2.02
2.04
4.06
4.01
f1 (ppm)

230

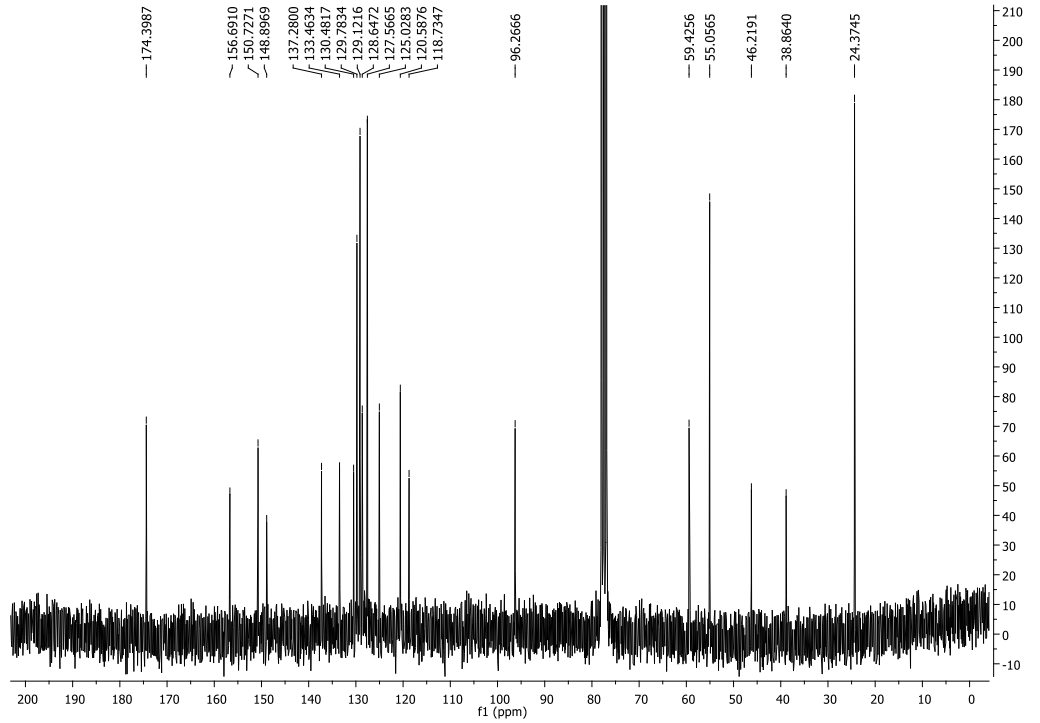
174.3987
156.6910
150.7271
148.8969
137.2800
133.4634
130.4817
129.7834
129.1216
128.6472
127.5665
125.0283
120.5876
118.7347
96.2666
59.4256
55.0565
46.2191
38.8640
24.3745
f1 (ppm)

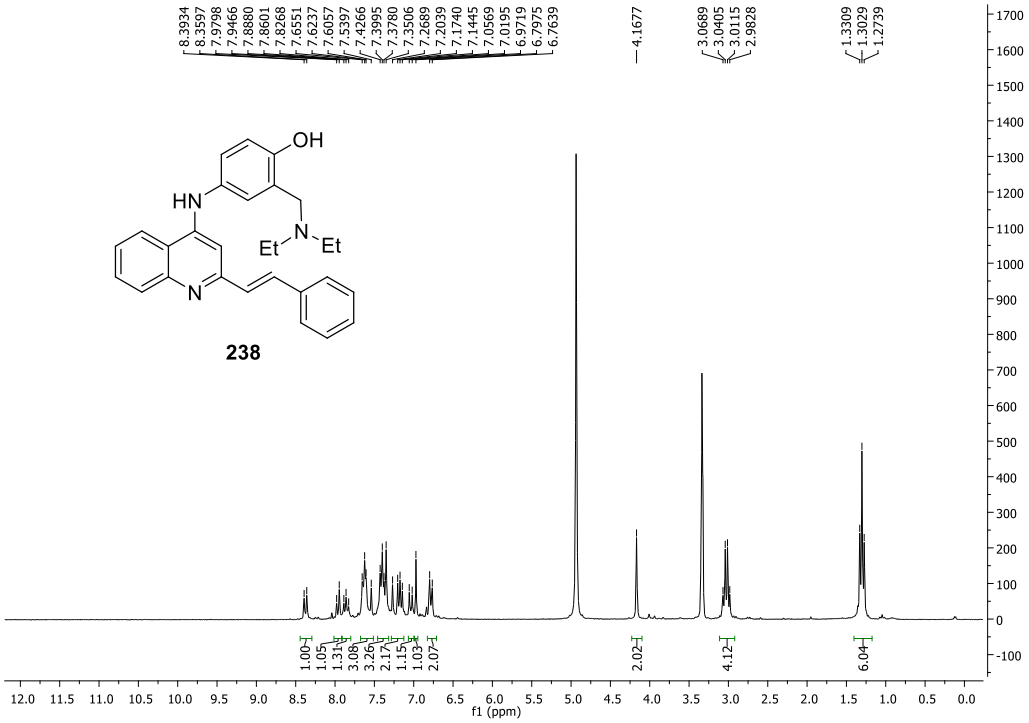
8.3934
8.3597
7.9798
7.9466
7.8880
7.8601
7.8268
7.6551
7.6237
7.6057
7.5397
7.4266
7.3995
7.3780
7.3506
7.2689
7.2039
7.1740
7.1445
7.0569
7.0195
6.9719
6.7975
6.7639
4.1677
3.0689
3.0405
3.0115
2.9828
1.3309
1.3029
1.2739
OH
HN
N
Et
N
Et
238
1.00
1.05
1.31
3.08
3.26
2.17
1.15
1.03
2.07
2.02
4.12
6.04
f1 (ppm)

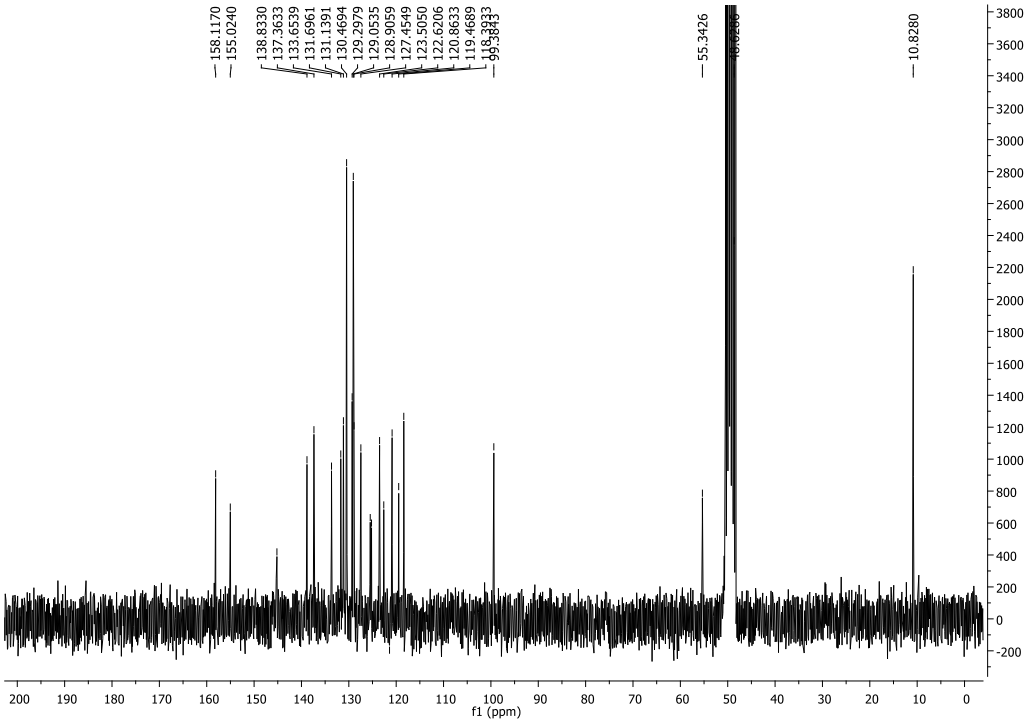
158.1170
155.0240
138.8330
137.3633
133.6539
131.6961
131.1391
130.4694
129.2979
129.0535
128.9059
127.4549
123.5050
122.6206
120.8633
119.4689
55.3426
10.8280
f1 (ppm)

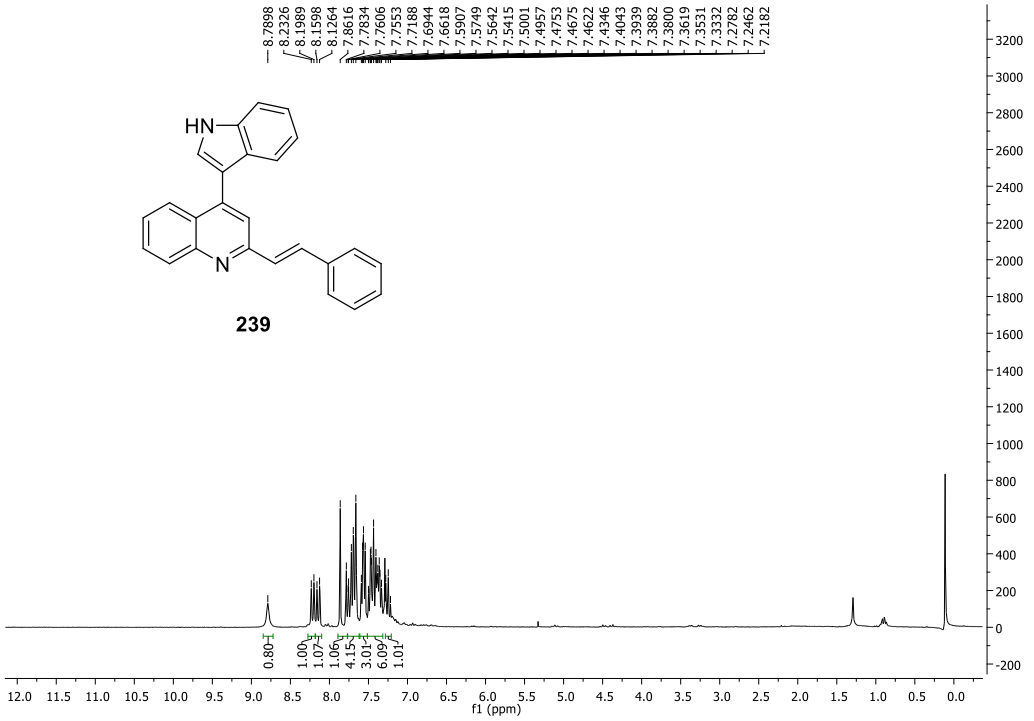
8.7898
8.2326
8.1989
8.1598
8.1264
7.8616
7.7834
7.7606
7.7553
7.7188
7.6944
7.6618
7.5907
7.5749
7.5642
7.5415
7.5001
7.4957
7.4753
7.4675
7.4622
7.4346
7.4043
7.3939
7.3882
7.3800
7.3619
7.3531
7.3332
7.2782
7.2462
7.2182
HN
N
239
0.80
1.00
1.07
1.06
4.15
3.01
6.09
1.01
f1 (ppm)

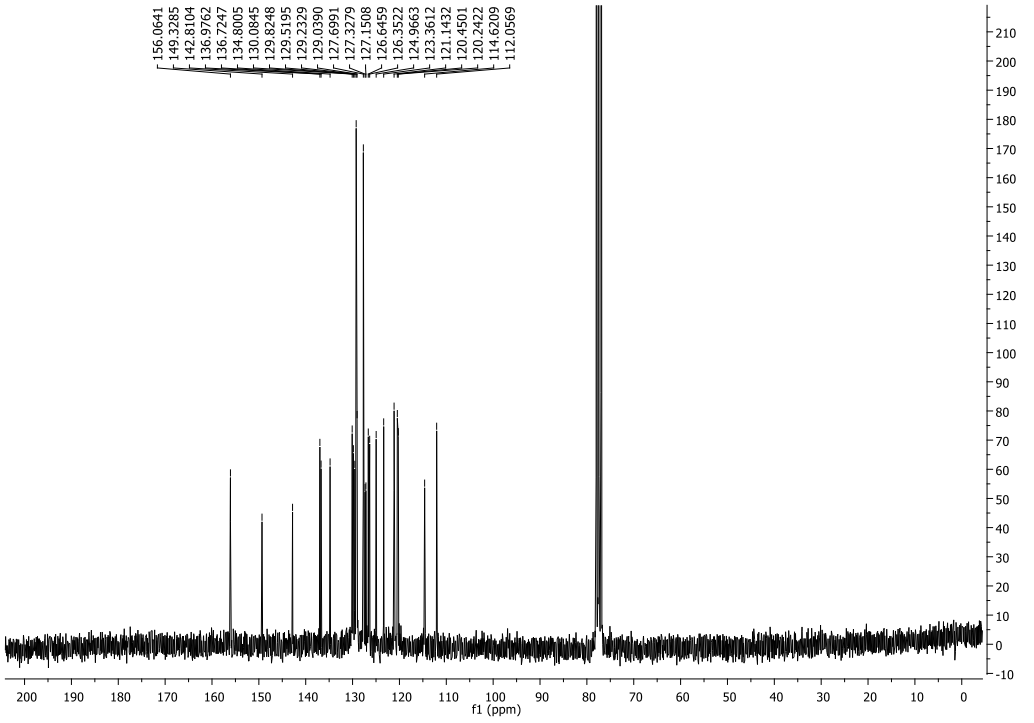
156.0641
149.3285
142.8104
136.9762
136.7247
134.8005
130.0845
129.8248
129.5195
129.2329
129.0390
127.6991
127.3279
127.1508
126.6459
126.3522
124.9663
123.3612
121.1432
120.4501
120.2422
114.6209
112.0569
f1 (ppm)

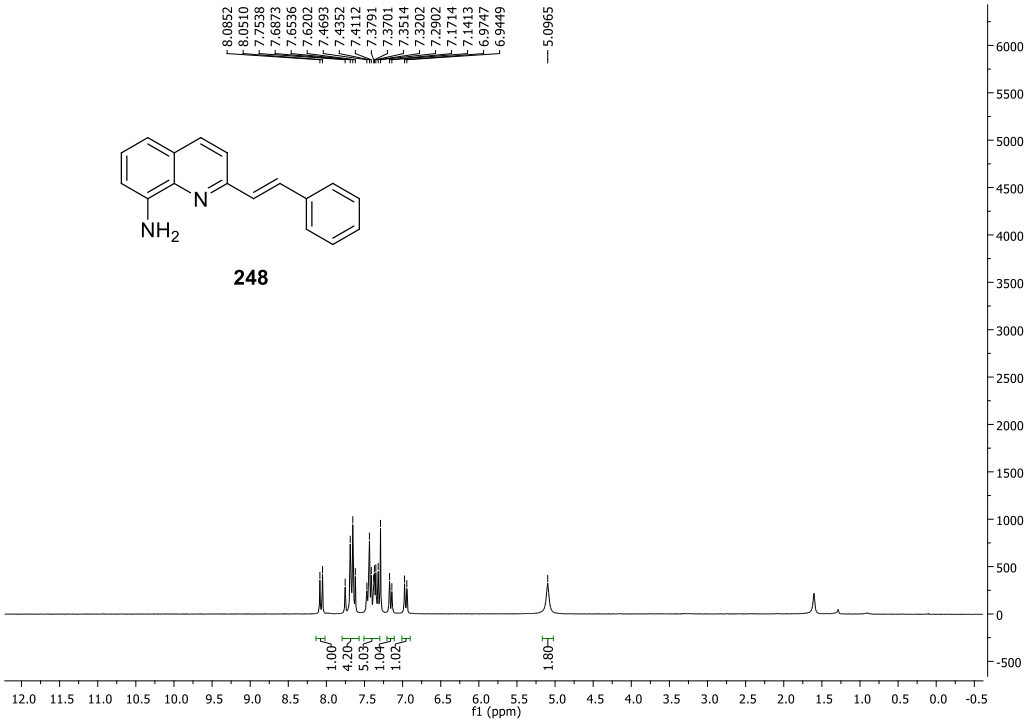
8.0852
8.0510
7.7538
7.6873
7.6536
7.6202
7.4693
7.4352
7.4112
7.3791
7.3701
7.3514
7.3202
7.2902
7.1714
7.1413
6.9747
6.9449
5.0965
N
NH2
1.00
4.20
5.03
1.04
1.02
1.80
f1 (ppm)

248

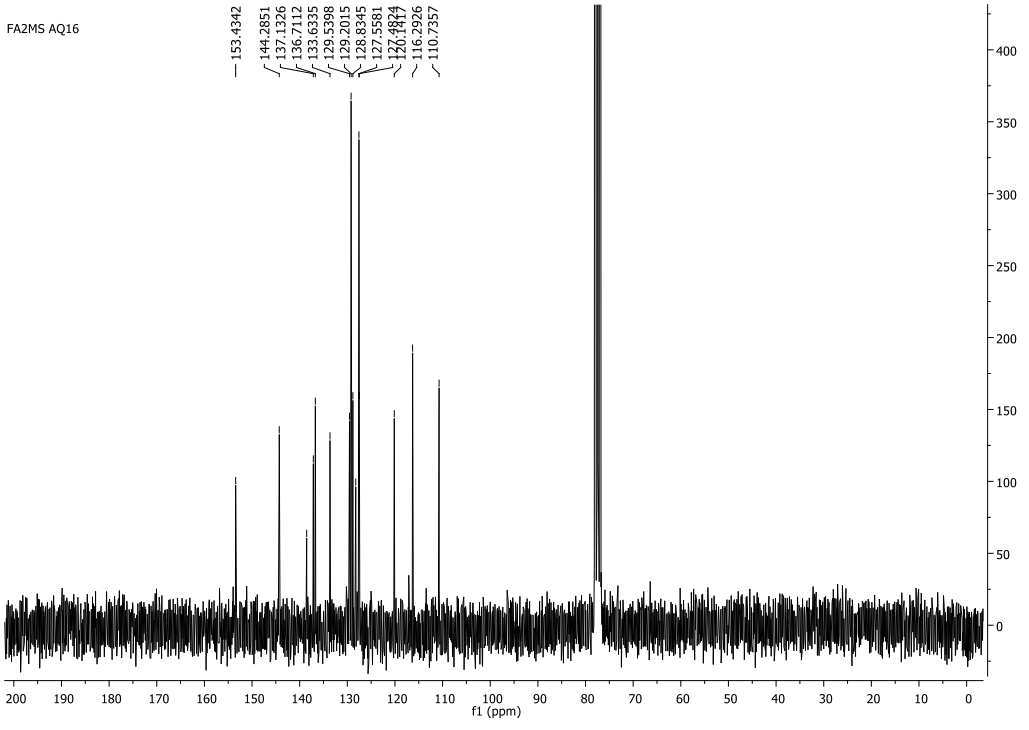
FA2MS AQ16
153.4342
144.2851
137.1326
136.7112
133.6335
129.5398
129.2015
128.8345
127.5581
127.4824
120.1417
116.2926
110.7357
f1 (ppm)